A study of the effects of Ki-Ras inhibition by antisense deoxyoligonucleotides in a rat model of renal fibrosis

Wang, Joe

Awarding institution:
King's College London

Title: A study of the effects of Ki-Ras inhibition by antisense deoxyoligonucleotides in a rat model of renal fibrosis

Author: Jia-hui Wang

A study of the effects of Ki-Ras inhibition by antisense deoxyoligonucleotides in a rat model of renal fibrosis

A thesis submitted for the degree of Doctor of Philosophy

By Dr Jia-hui Wang

Guy's, King's College and St Thomas' School of Medicine

King's College London

University of London

Abstract

Ras monomeric GTPases are key molecules in the signalling pathway of renal fibrogenesis and exist in three isoforms (Kirsten, Harvey and Neural). The aim of this thesis was to determine whether inhibition of Ki-Ras expression by ASOs could ameliorate the process of renal fibrosis.

All isoforms of Ras were expressed in rat renal fibroblasts (primary culture and cell line (NRK-49F)) and in a rat epithelial cell line (NRK-52E). *In vitro* administration of Ki-Ras ASOs resulted in a specific knockdown of the isoform mRNA in all cells. An associated rise in Ha-Ras mRNA was noted in fibroblast cells but absent in epithelial cells.

ASOs administration in non-diseased male Wistar rats resulted in specific renal Ki-Ras mRNA knockdown and an associated decrease in Ras protein expression. Oligo accumulation was seen in the renal proximal tubular cells with extra-renal deposition seen in the liver, heart and wound-tissue. Significant hepatic Ki-Ras mRNA knockdown and inflammation was also demonstrated in ASO treated subjects.

In a rat model of unilateral ureteric obstruction (UUO) a significant rise in both Ki-Ras and N-Ras mRNA expression in the obstructed kidneys compared to non-obstructed kidney samples was demonstrated.

Ki-Ras ASOs administration to models of UUO significantly reduced the isoform mRNA expression, when compared to vehicle-only and scrambled-oligos (SO), and resulted in a significant decrease in renal fibrosis scores, based on trichrome and picrosirius red staining, and interstitial collagen I and α-SMA expression, based on immunohistological staining and western blotting.

ASO administration resulted in an increase in interstitial cell expression of FSP-1, Ki-67 and ED-1. These findings were absent in vehicle-only and control oligo groups.

In summary, administration of ASOs specifically and significantly reduce Ki-Ras mRNA expression and ameliorate fibrosis in a rat model of renal fibrosis in the presence of increased interstitial cell proliferation and inflammation.

Acknowledgements

Firstly I would like to thank my supervisors Dr Claire Sharpe and Professor Bruce Hendry not only for providing me with the opportunity to undertake this project but for their constant encouragement, wise direction and unshakable faith in me (often when I had lost my own!). Claire especially has always been on hand with great advice, incisive ideas and morale boosting talks whenever needed.

Thanks also goes to the other members of our renal research group (Andi Cove-Smith, Qin Hu, Alex Rankin & Fei Wong) who made my time at King's so rewarding, intellectually stimulating and fun. Particular thanks goes to Lucy Newbury for her help in later experiments and to Maz Noor who taught me the basics of many lab techniques before moving on to the more advance lessons of the best places for lunch! More than just colleagues, I am proud to call them friends.

This thesis would also not have been possible without the help of the KCH histopathology department (especially Jane Moorhead), the haematology research group, led by Professor Swee Lay Thein, and Greta Sawyer and Neil Sheerin, who oversaw my anaesthetic and surgical techniques, and Dr Alex Kniseley for his help in interpreting our liver data. A special mention must be made for Dr N. Dutt who analysed the majority of the renal samples in this project but sadly passed away before this work was completed. Incredibly diligent, generous and committed she will be missed greatly as a doctor and even more so as a person.

I am eternally grateful to my parents who have always been there for me and provided me with a world of opportunities they did not have. I would also like to thank my wonderful wife, Nicoletta, for all her love and support and for providing me with our beautiful daughter Sofia-a small being who has changed our world.

Finally I thank both the King's Renal Research Fund and Kidney Research UK without whose generous funding none of this work would have been possible.

Publications & Prizes arising from this work

Publications

2012: Wang JH, Newbury LJ, Knisely AS, Monia B, Hendry BM, Sharpe CC. 'Antisense knockdown of kras inhibits fibrosis in a rat model of unilateral ureteric obstruction.' *Am J Pathol. 2012 Jan;180(1):82-90. Epub 2011 Nov 7.*

2011: Denby L, Ramdas V, McBride MW, Wang J, Robinson H, McClure J, Crawford W, Lu R, Hillyard DZ, Khanin R, Agami R, Dominiczak AF, Sharpe CC, Baker AH. 'miR-21 and miR-214 are consistently modulated during renal injury in rodent models.' *Am J Pathol. 2011 Aug;179(2):661-72. Epub 2011 May 31.*

2008: J.H. Wang, N. Dutt, B.M. Hendry and C.C. Sharpe. 'A study of the effects of Antisense Inhibition of Ki-Ras monomeric GTPase in a rat model of renal fibrosis'. *JASN; ASN 2008 Abstract Supplement*.

2008: Wang JH, Hendry BM, Sharpe CC. Editorial Comment: 'Silencing genes in the kidney: antisense or RNA interference?'. *Nephrology, Dialysis, Transplantation 2008 23(7): 2115-2118.*

2007: J.H. Wang, N. Dutt, B.M. Hendry and C.C. Sharpe. 'A study of the effects of Antisense Inhibition of Ki-Ras monomeric GTPase in a rat model of renal fibrosis'. *JASN; ASN 2007 Abstract Supplement.*

Awards

2008: Royal Society of Medicine Bursary [Nephrology section]

2008: Award for Best Oral Presentation, Kidney Research UK Fellows Day

2006: Kidney Research UK Clinical Training Fellowship Award

Contents

List of figures and tables

Figures

Chapter 1

Chapter 2

Chapter 3

Chapter 4

Chapter 5

Chapter 6

Chapter 7

Tables

Abbreviations

ABC

αSMA	alpha-smooth muscle actin
Ang II	angiotensin II
ASO	antisense oligonucleotide
CRD	cysteine-rich domain
CTGF	connective tissue growth factor

DEF

DEPC	diethylpyrocarbonate
DMEM	Dulbecco's Modified Eagle's Medium
DNA	deoxyribonucleic acid
ECM	extracellular matrix
EGF	epidermal growth factor
EMT	epithelial mesenchymal transdifferentiation
ERK	extracellular signal related kinase
ET-1	endothelin-1
FAK	focal adhesion kinase
FCS	foetal calf serum
FGF	fibroblast growth factor
FITC	fluorescein isothiocyanate
FSP-1	fibroblast-specific protein 1
FTI	farnesyl transferase inhibitor
FTS	farnesylthiosalicylic acid

GHIJ

GAP	GTPase-activating protein
GDP	guanidine diphosphate
GGTI	geranylgeranyltransferase inhibitor
GNEF	guanine nucleotide exchange factor
GTP	guanidine triphosphate
HBSS	Hank's balanced salt solution

Ha-Ras	Harvey-Ras
HMG-CoA	hydroxymethylglutaryl co-enzyme A
ICAM	intercellular adhesion molecule
IGF	insulin-like growth factor
IL	interleukin
JNK	jun N-terminal kinase

KLM

Ki-Ras	Kirsten-Ras
MAPK	mitogen-activated protein kinase
MEK(K)(K)	mitogen activated protein kinase (kinase)(kinase)
MMP	matrix metalloproteinase
mRNA	messenger RNA

NOP

N-Ras	Neural-Ras
NRK	normal rat kidney
Oligo	oligonucleotide
PBS	phosphate-buffered saline
PI3K	phosphatidylinositol 3-kinase
PAI	plasminogen activator inhibitor
PAGE	polyacrylamide gel electrophoresis
PDGF	platelet-derived growth factor
PKB	protein kinase B
PKC	protein kinase C

QRST

QPCR	quantitative polymerase chain reaction
RBD	Ras-binding domain
RNA	ribonucleic acid
RNAi	RNA interference
siRNA	short interfering RNA

SOS	son-of-sevenless
SQ-PCR	semi-quantative polymerase chain reaction
TIMP	tissue inhibitors of metalloproteinases
TGF-beta	transforming growth factor-beta

UVW

UUO	unilateral ureteric obstruction

XYZ

Statistical Annotation

*	$p<0.05$
**	$p<0.01$

Chapter 1: Introduction

1.1 Chronic kidney disease and end-stage renal failure

Renal failure is a growing worldwide problem. The expanding rates of diabetes, hypertension and obesity in the western world coupled with a longer life expectancy has seen the prevalence of chronic kidney disease (CKD) increase in developed nations. A systematic review of 26 studies revealed a prevalence of CKD in patients of over 30 years of 7.2% and of 23-36% in those over 64 years of age (Zhang and Rothenbacher 2008). Though studies suggest that less than 2% of the CKD population progresses to end-stage renal failure (ESRF) requiring renal replacement therapy (RRT) (Coresh, Selvin et al. 2007), this still represents significant numbers.

Data from the 13th annual UK Renal Registry in December 2010 (http://www.renalreg.com/Reports/2010.html) showed the prevalence of renal replacement therapy (RRT) within the adult population at the end of 2009 was 794 pmp compared to 694pmp at the end of 2005. This represents a 3.2% annual increase from 2008 and though this is a more modest measure than the 7% global annual increase predicted by Moeller in the early part of the decade (Moeller, Gioberge et al. 2002) it still reflects the lack of development in the field of prevention of CKD progression to ESRF. The registry also reported an improvement of age-adjusted (adjusted to age 60) one-year survival rate of 85% in 2000 to 89% in 2008 for those on RRT. Though this is an improvement, these figures still represent an age-standardized mortality rate at the age of 30-34 years for those on RRT of 19 times greater than the general population. To put this into perspective this translates to a median life expectancy of 20 years for a 25-29 year old on RRT and 4 years for those over 70 years old on RRT compared to the national average of 79.8 years at birth and 18.9 years at age 65 (Office of National Statistics 2010). The 5-year survival of a dialysis patient of 60 years is about 45% and is comparable to that of patient with colonic or ovarian cancer, with the risk of cardiovascular death estimated at about 100 times higher in ESRF patients on haemodialysis (Bleyer, Russell et al. 1999). Thus a 40 year-old dialysis patient has the same risk of a cardiovascular event as an 80 year-old without renal disease (Foley, Parfrey et al. 1998).

Apart from the medical aspects of CKD and ESRF, there is also a significant socio-economic impact of CKD. Data from the United States Renal Data System (USRDS) show that though CKD patients make up less than 10% of the total Medicare over-65

years population, they account for up to 28% of total Medicare expenditure. For the UK, at present an expenditure of 2% of the total NHS budget is required for the 0.05% of the population with chronic renal failure. Based on values in 2003 and a predicted doubling of the renal failure population, the National Kidney Federation predicted that 4% of the NHS budget would be required for renal treatment by 2013.

1.2 Progression of Chronic Kidney Disease

Irrespective of the initial aetiology of renal insult the progression of widespread destruction of the renal parenchyma by scarring leads to chronic kidney disease (CKD) and ultimately to ESRF. Studies have shown that the natural progression of CKD towards ESRF occurs at a steady rate even if the initial "insult" to the kidney has been removed (Mitch, Walser et al. 1976; Rutherford, Blondin et al. 1977). ESRF is characterized by both tubulointerstitial fibrosis and glomerulosclerosis resulting in renal fibrosis or "scarring" (Figure 1.1). It has long been established that the decline in renal function best correlates to the degree of tubulointerstitial fibrosis as opposed to glomerulosclerosis. (Mackensen-Haen, Bohle et al. 1992; Nath 1992; Bohle, Wehrmann et al. 1994; Muller, Zeisberg et al. 2000). Considering the major impact that ESRF has upon society much work has been undertaken to understanding the process of tubulointerstitial fibrosis with an aim to providing strategies for delaying progression.

Figure 1.1: Histological difference between normal and fibrosed kidney. Trichrome staining of human kidney biopsy sections with areas of fibrosis staining blue.

1.3 Tubulointerstitial fibrosis and fibrogenesis

The process of renal fibrosis or 'scarring' begins with an initial insult to the kidney, which may be from a variety of causes (Figure 1.2). This initial injury results in the release of numerous growth factors, cytokines and chemokines, which initiate inflammation and subsequent fibrogenesis. Fibrogenesis is a complex process involving several steps: (i) the infiltration of inflammatory cells, (ii) increased proliferation and activation of fibroblasts, (iii) tubular epithelial cell apoptosis and subsequent tubular atrophy, (iv) capillary loss and (v) production and deposition of excessive extracellular matrix (ECM) (Fine, Ong et al. 1993; Norman and Fine 1999). The phenomenon of epithelial-to-mesenchymal transition (EMT) has been described which is believed by many to be fundamental in the process of renal fibrogenesis (Iwano, Plieth et al. 2002).

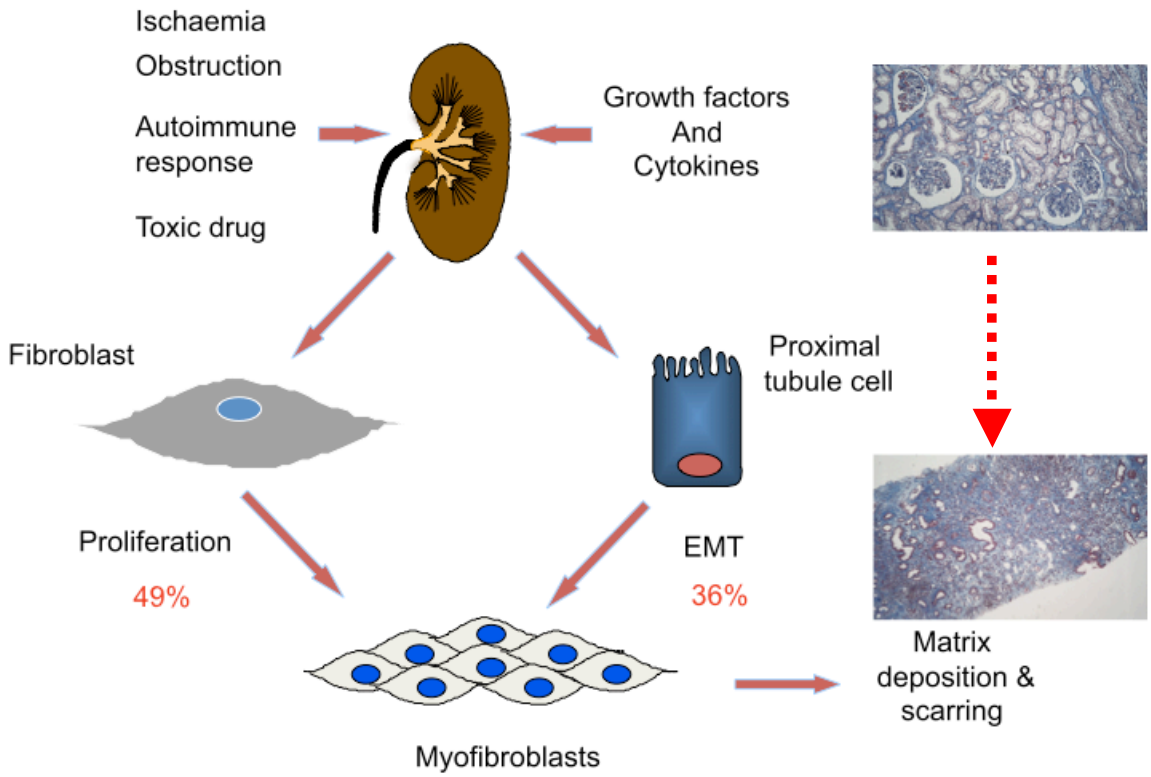

Figure 1.2: Schematic of the process of renal fibrosis depicting postulated cellular mechanisms (Adapted from Iwano, Plieth et al. 2002).

The current model of renal fibrogenesis reflects an inappropriate wound healing response to injury (Kuncio, Neilson et al. 1991; Eddy 2000; Wynn 2008). After an initial insult, tissue attempts to repair and recover from the damage. These recovery

processes involve production of pro-inflammatory cytokines and activation of resident cells. In acute inflammatory reactions subsequent vascular changes and inflammatory infiltration rapidly resolve but persistent chronic inflammation leads to fibrosis. The innate repair process is thought to be composed of two phases: a regenerative phase where injured cells are replaced by viable ones with no obvious lasting sequelae of damage and a "fibroplasia" phase in which connective tissue replaces normal parenchymal tissue. Following tissue injury both epithelial and endothelial cells may release inflammatory mediators which initiate recruitment and activation of inflammatory cells. The secretion of pro-fibrotic cytokines by infiltrating leukocytes stimulates an increase in the myofibroblast population, the cell responsible for matrix deposition, and initiates the process that allows for wound contraction and repair. Subsequently, collagen fibres become organised, angiogenesis takes place, scar tissue is eliminated by matrix metalloproteinases (MMPs) and viable epithelial/endothelial cells proliferate and migrate across the wound to regenerate damaged tissue. Whilst initially this repair process is beneficial, the problem arises in the presence of a continuing and persistent insult where there is loss of control of fibrogensis and excess matrix deposition occurs in areas of normal tissue resulting in permanent scarring (Wynn 2007).

In her review (Eddy 2000), Eddy divided the process of renal fibrogenesis into four arbitrary phases which is a helpful and logical way to approach the complex pathophysiology of fibrosis and has been adapted for this thesis:

(i) Cellular injury, activation and inflammation

(ii) Fibrogenic signalling

(iii) The Fibroblast and Epithelial Mesenchymal Transition

(iv) Parenchymal destruction

1.3.1 Cellular injury, activation and inflammation

It is postulated that bioactive molecules of the plasma not normally filtered by the glomerulus appear in the ultrafiltrate in chronic renal disease (Wang, Lapage et al. 1999; Zoja, Benigni et al. 1999; Hirschberg and Wang 2005). Exposure of tubular cells to these molecules such as albumin, transforming growth factor-β (TGF-β) and hepatocyte growth factor (HGF), in the "proteinuria of disease" results in tubular cell activation and the subsequent release of injurious molecules that may facilitate

inflammation or themselves directly contribute to fibrogenesis (Burton and Walls 1994; Burton and Harris 1996; Abbate, Zoja et al. 2006). *In vitro* studies have shown that many of these proteins may induce "tubular cell activity" and overexpression of pro-inflammatory molecules. These molecules include monocyte chemoattractant protein-1 (MCP-1) (Wang, Chen et al. 1997; Donadelli, Abbate et al. 2000), RANTES (Zoja, Donadelli et al. 1998) and IL-8 (Tang, Leung et al. 2003). Furthermore there is evidence of generation of hydrogen peroxide (Morigi, Macconi et al. 2002; Tang, Leung et al. 2003), which leads to upregulation of chemokine expression by a signalling pathway thought to involve mitogen-activated protein kinase/ extracellular signal regulated kinase 1 and 2 [MAPK/ERK 1/2] (Dixon and Brunskill 1999; Dixon and Brunskill 2000; Donadelli, Zanchi et al. 2003). *In vivo* studies have also confirmed the role of proteinuria in inducing inflammation via upregulation of various chemokines and transcription factors including NF-κB and MCP-1(Eddy and Giachelli 1995; Gomez-Garre, Largo et al. 2001; Eardley, Zehnder et al. 2006).

There is also evidence that renal tubular cells can synthesize factors of the complement cascade (Zhou, Marsh et al. 2001) and PTECs themselves have been found to be able to activate serum complement via the alternative pathway (Biancone, David et al. 1994) resulting in pro-inflammatory activity including production of hydrogen peroxide and cytokines (David, Biancone et al. 1997). Complement is an important mediator of interstitial inflammation and fibrogenesis as can be seen from the significant attenuation of injury in a C3-deficient mouse model (Abbate, Zoja et al. 2008). Epithelial cells have also been demonstrated to be a source of macrophage colony stimulating factor (M-CSF). There is now evidence that this growth factor may be vital for tubular cell survival and regeneration following injury (Menke, Iwata et al. 2009). However M-CSF-1 remains an important macrophage mitogen (Lan, Nikolic-Paterson et al. 1995; Isbel, Hill et al. 2001) and induces macrophage interstitial infiltration.

This release of inflammatory mediators by the tubular epithelial cells results in infiltration by mononuclear cells including macrophages, lymphocytes, eosinophils and plasma cells. Traditionally it has been well accepted that macrophage infiltration as part of the inflammatory process was detrimental in the process of fibrogenesis and may induce renal cell death both directly, by inducing apoptosis of tubular cells (Tesch, Schwarting et al. 1999; Duffield, Erwig et al. 2000; Kipari, Cailhier et al. 2006), or indirectly via the release of cytokines that suppress VEGF expression

(Kang, Joly et al. 2001) that leads to diminished peritubular capillary cell proliferation and subsequent epithelial cell ischemia and hypoxia (Khan, Cleveland et al. 1999). Much of the evidence for this theory was derived from animal models of macrophage depletion or knockout of macrophage recruitment proteins (Holdsworth, Neale et al. 1981; Tesch, Maifert et al. 1999; Tesch, Schwarting et al. 1999; Lange-Sperandio, Cachat et al. 2002). Although macrophage infiltration as part of assumed acute inflammation usually precedes development of, and is believed to contribute to fibrosis, a variety of studies have shown that this is not always the case and that the two processes may actually be distinct mechanisms. In fact it is now thought that inflammation may, under certain circumstances, be beneficial depending on the phenotype of inflammatory cell. Nishida et al. found that wild-type mice reconstituted with angiotensin II type I receptor (Agtr1)-negative bone marrow possessed reduced numbers of peripheral-blood monocytes/macrophage progenitors in bone marrow and had decreased renal interstitial macrophage numbers but exhibited more severe fibrosis following unilateral ureteric obstruction when compared to Agtr1(+/+) controls (Nishida, Okumura et al. 2005). They postulate that the benefits of active macrophage infiltration are derived from their ability to phagocytose dead cells and debris which may be pro-fibrotic. One study employing pharmacological inhibition of the CSF-1 receptor c-fms (Ma, Liu et al. 2009) found that treated groups had significantly attenuated accumulation of the macrophage population following obstruction but there was no difference in either the early or late renal fibrosis score when compared to controls. In addition macrophages have now also been shown to be a source of hepatocyte growth factor (HGF) (Chen, DeFrances et al. 1996), a molecule which is thought to have a role in the inhibition of EMT (Mizuno, Matsumoto et al. 2001; Yang and Liu 2002; Mizui, Isaka et al. 2004), as well as Wnt ligand Wnt7b, which has been shown to promotes tubular cell regeneration following ischemia-reperfusion injury .

Interstitial fibrosis is characterized by tubular destruction that may in part be due to tubular ischemia from matrix-associated loss of interstitial capillary network. It is well recognized that hypoxia induces macrophages recruitment and release of angiogenic factors (Kuwabara, Ogawa et al. 1995; Murdoch, Giannoudis et al. 2004; Murdoch, Muthana et al. 2005; Elbarghati, Murdoch et al. 2008) and as a result these cells may be influential in maintaining or regenerating capillaries in the face of renal fibrosis. These paradoxical roles for the macrophage in fibrosis has now led to another theory:

it is not just the absolute degree of macrophage infiltration within tissue that is associated with severity and progression of fibrosis but actually the "phenotype" and "degree of activation" of the macrophage which is involved and also the time phase of injury, acute or recovery (Lange-Sperandio, Cachat et al. 2002; Duffield 2003). It is now recognized that circulating monocytes have a high degree of cellular plasticity and following recruitment to site of injury may differentiate into specific subsets of macrophages with differing functions depending on cytokines and cell signals of the microenvironment (Geissmann, Auffray et al. 2008; Ricardo, van Goor et al. 2008). Broadly speaking there are two recognized definitive macrophage subsets: classically activated (M1) and alternatively activated (M2). Classical activation results in a pro-inflammatory phenotype M1, whereas the M2 phenotype is recognized as being anti-inflammatory and may secrete trophic factors involved in angiogenesis and wound healing by matrix remodeling (Mosser and Edwards 2008). However though the M2 phenotype is associated with wound resolution, it is also associated with promotion of fibrosis in chronic disease states. Lin et al. demonstrated that following UUO, initially high Ly6C expressing monocytes were recruited to the kidney which subsequently divided into low, intermediate or high expressing Ly6C phenotypes (Lin, Castano et al. 2009) and that the high Ly6C expressing M2 macrophages assumed a pro-fibrotic expressing-profile compared to the other phenotypes. Anders et al. employed RANTES antagonists in a murine model of glomerulonephritis and found that despite decreased macrophage infiltration there was a significant increase in glomerular injury. They noted that the RANTES analogs reduced macrophage infiltration but increased activation state as characterized by morphology and inducible nitric oxide (NO) synthetase expression (Anders, Frink et al. 2003). The importance of timing of infiltration in the process of fibrosis was illustrated by Duffield et al. Using a carbon tetrachloride murine model of liver fibrosis, which has distinct injury and recovery phases, they developed a transgenic mouse that allowed selective depletion of macrophages. They discovered that macrophage depletion in advanced liver fibrosis resulted in reduced scarring but depletion during recovery led to a failure of matrix degradation (Duffield, Forbes et al. 2005). A study depleting macrophages using cyclophosphamide in models of UUO showed no effect on early fibrosis but increased degree of fibrosis at later time points suggesting a role for macrophages with regards to repair at a later stage of injury (Nishida, Okumura et al. 2005). These studies suggest functionally distinct subpopulations of macrophages may play critical roles in

both the injury and recovery phases of inflammatory scarring and that the "degree" of macrophage infiltration alone may not provide the whole answer. Furthermore M1 and M2 states do not appear to be terminally committed and they may actually revert between these phenotypes based on the microenvironment (Duffield 2003; Arnold, Henry et al. 2007). These findings are supported by work by Lee et al. demonstrating that macrophages may switch phenotype *in vivo* following renal ischemic-reperfusion (I/R) injury (Lee, Huen et al. 2011). The group also demonstrated that the timing and subclass of macrophage recruited dictated both the degree of initial renal injury as well as the subsequent degree of renal repair following I/R injury.

Thus distinct processes of inflammation and fibrosis are now being increasingly recognized (Wynn 2004; Ricardo, van Goor et al. 2008) and may also explain the lack of efficacy of non-specific anti-inflammatory therapy in preventing the progression of fibrosis. In fact complete macrophage depletion may be detrimental and selective depletion may be far more beneficial (Ricardo, van Goor et al. 2008).

Furthermore there is now evidence that bone marrow derived cells normally reconstitute renal mesangial and interstitial cells as part of normal cellular turnover (Imasawa, Utsunomiya et al. 2001; Li, Truong et al. 2007) and though the majority of renal regeneration is from intra-renal cells (Lin, Moran et al. 2005), these bone marrow derived cells are thought to contribute to tubular epithelial cell regeneration by a process of cell fusion (Li, Truong et al. 2007; Lin 2008). The haematopoietic cell type involved has been elusive but there is now increasing focus, at least in liver repair, on macrophages (Willenbring, Bailey et al. 2004; Thorgeirsson and Grisham 2006). This is supported by the facts that fetal macrophages play a trophic role in kidney development (Rae, Woods et al. 2007), macrophages have the ability to undergo cell fusion with self or other cell types in response to inflammation (Ovchinnikov 2008) and have been shown to transform in to vascular elements including endothelial and smooth muscle cells (Zhao, Glesne et al. 2003; Bailey, Willenbring et al. 2006). Thus macrophages may play a significant role in organ regeneration and not just in injury.

1.3.2 Fibrogenic signalling

Injured epithelial cells and activated leukocytes secrete a host of pro-fibrotic mediators that contribute to the process of fibrogenesis. In addition, several have both proliferative and apoptotic effects depending on cell type and model of injury. To go into detail about each of these elements is beyond the realms of this thesis, however Table 1.1 aims to provide a summary of mediators of fibrogenesis that have been more widely studied. The single cytokine that is widely accepted to be the most potent pro-fibrogenic stimulus is transforming growth factor β1 (TGFβ1) which will be discussed later in more detail.

Mediator	**Role & mechanism of action**	***In vitro* evidence of role in fibrosis**	***In vivo* evidence of role in fibrosis**
Platelet Derived Growth Factor PDGF	1) Chemotactic & mitogenic for mesenchymal cells 2) Stimulates TGFβ paracrine expression	(Tang, Ulich et al. 1996) (Klahr and Morrissey 2000) (Knecht, Fine et al. 1991)	(Taneda, Hudkins et al. 2003; Boor, Konieczny et al. 2007) (Eitner, Bucher et al. 2008)
Fibroblast Growth Factor FGF-2	1) Mitogen for fibroblasts 2) No effect on matrix deposition 3) Downstream effector of TGFβ 4) Potential role in EMT	(Strutz, Zeisberg et al. 2000) (Strutz, Zeisberg et al. 2002) (Strutz, Zeisberg et al. 2001) (Rosenbaum, Blazejewski et al. 1995)	(Shinozaki, Kawara et al. 1997)
Angiotensin II Ang II	1) Stimulate TGFβ production 2) Direct effects on collagen gene expression 3) Regulation of macrophage infiltration and function	(Wolf, Kalluri et al. 1999) (Ruiz-Ortega and Egido 1997) (Scheidegger, Butler et al. 1997)	(Yu, Wu et al. 2000) (Yu, Gong et al. 2007) (Ishidoya, Morrissey et al. 1995) (Gilbert, Cox et al. 1998) (Kelly, Cox et al. 2002)

Mediator	**Role & mechanism of action**	***In vitro* evidence of role in fibrosis**	***In vivo* evidence of role in fibrosis**
Endothelin-1 ET-1	1) Vasoconstrictive 2) Upregulates TGFβ expression 3) Potentially pro-inflammatory 4) Direct stimulation of matrix production 5) Downregulates collagenase activity	(Yard, Chorianopoulos et al. 2001) (Helset, Sildnes et al. 1993) (Helset, Sildnes et al. 1994) (Zoja, Morigi et al. 1995)	(Hocher, Thone-Reineke et al. 1997) (Benigni, Zoja et al. 1999) (Seccia, Maniero et al. 2008)
Tumour Necrosis Factor-α TNF-α	1) Pro-inflammatory 2) Mitogenic for fibroblasts 3) Induction of matrix metallo-proteinase 4) Inhibition of tissue inhibitors of metallo-protinases	(Wolf, Aberle et al. 1993) (Nee, McMorrow et al. 2004)	(Kaneto, Morrissey et al. 1993) (Guo, Morrissey et al. 1999) (Khan, Cook et al. 2005)
Connective Tissue Growth Factor CTGF	1) Downstream effector of TGF-β [TGF-β responsive element in CTGF promoter] 2) Induces cyclin A upregulation in fibroblasts and subsequent induction of S-phase 3) Induction of collagen production	(Grotendorst, Okochi et al. 1996) (Kothapalli and Grotendorst 2000) (Daniels, Schultz et al. 2003) (Gore-Hyer, Shegogue et al. 2002) (Gao, Li et al. 2008) (Phanish, Wahab et al. 2005)	(Gupta, Clarkson et al. 2000) (Luo, Lu et al. 2008) (Yokoi, Mukoyama et al. 2004) (Uchio, Graham et al. 2004)

Mediator	**Role & mechanism of action**	***In vitro* evidence of role in fibrosis**	***In vivo* evidence of role in fibrosis**
Bone Morphogenic Protein-7 BMP-7	1) Inhibits EMT 2) Anti-inflammatory 3) Antagonistic effects to TGF-β1 4) Antifibrotic 5) ?? Reverses fibrosis	(Zeisberg, Shah et al. 2005) (Zeisberg, Hanai et al. 2003) (Gould, Day et al. 2002)	(Morrissey, Hruska et al. 2002) (Sugimoto, Grahovac et al. 2007) (Wang, de Caestecker et al. 2006) (Lin, Patel et al. 2005)
Hepatocyte Growth Factor HGF	1) Increased production in areas of tubular damage 2) Inhibits myofibroblastic activation 3) Antagonistic effects to TGF-β1 4) Inhibits EMT 5) Anti-inflammatory 6) Inhibits apoptosis and promotes proliferation of tubular epithelial cells 7) Induction of MMPs and suppression of PAI expression	(Dai and Liu 2004) (Yang, Dai et al. 2005) (Yang, Dai et al. 2003) (Gong, Rifai et al. 2008) (Gong, Rifai et al. 2003)	(Taniguchi, Yorioka et al. 1997) (Gong, Rifai et al. 2004) (Dworkin, Gong et al. 2004) (Dai, Yang et al. 2004) (Mizuno, Kurosawa et al. 1998) (Mizuno and Nakamura 2004)

Table 1.1: Mediators of fibrosis

Transforming Growth Factor-β (TGFβ)

Transforming growth factor β (TGFβ) is the best studied of all pro-fibrotic growth factors and it is widely recognised to be vital in the process of fibrosis in many organs including the kidney. TGFβ is a founding member of the TGFβ superfamily which consists of nearly 30 mammalian proteins that regulate a diverse range of physiological processes which include wound healing, cell cycle control, chemotaxis and development. Other family members include activins, inhibins and BMPs. TGFβ itself is a 25kD dimeric protein which has three isoforms in mammals (TGFβ1-3). All three isoforms share significant sequence homology and appear to be functionally similar. TGFβ is initially secreted as a latent precursor bound to a latency-associated peptide (LAP) (Annes, Munger et al. 2003) that inhibits binding to the TGFβ receptor. This complex is then bound to Latent TGFβ binding protein (LTBP1-3). The importance of the latent complex in development of renal fibrosis has been demonstrated (Huang, Chung et al. 2008). Following proteolytic cleavage TGFβ becomes active and may bind to its heteromeric receptor complex consisting of TGFβ type I/type II receptors (Nunes, Munger et al. 1998) that possess serin-threonine kinase activity. The TGFβ-activators responsible for LTBP cleavage and release include plasmin, proteases MMP-2 and MMP–9 and thrombospondin-1 (Border and Noble 1993; Daniel, Wiede et al. 2004). Furthermore a non-proteolytic mechanism of TGFβ-LAP inactivation has been recognized involving integrins. αvβ6 integrin and it's role in fibrogenesis was first identified in the process of lung fibrosis (Munger et al. 1999). Expressed at low levels in normal alveolar epithelial cells, there was up-regulation of expression in disease models such as the lung fibrosis induced by bleomycin (Munger et al. 1999). However it is now been demonstrated that αvβ6 integrin is also overexpressed in human kidney epithelium in disease states such as IgA nephropathy and membranous glomerulonephritis (Trevillian et al. 2004). αvβ6 integrin acts as a receptor for RGD (argining-glycine-aspartate) sites in components of fibrosis such as fibronectin and vitronectin but also for TGFβ-LAP 1 and 3. The binding of αvβ6 is thought to induce a conformational change in TGFβ-LAP thus allowing TGFβ to bind to its receptors (Annes 2004). Moreover the knockout of this integrin appeared to protect against both bleomycin-induced pulmonary fibrosis and renal fibrosis induced by obstruction (Munger et al. 1999, Ma et al. 2003). In addition administration of monoclonal antibodies against this integrin were found to attenuate

fibrosis in a mouse model (Col4A3-/-) of Alport's syndrome and the mechanism of protection correlatated with decreased TGFβ activity and expression (Hahm et al. 2007). Thus αvβ6 integrin appears to be a have a role in in the initiation of fibrosis and is a potential therapeutic target in this process. Interestingly these proteins that appear to be involved in liberating TGFβ from it's binding protein are also fundamentally involved in the processes of wound healing and fibrosis. The best-recognised intracellular pathway of TGFβ signalling involves the 'small mothers against decapentaplegic' (Smad) family of transcriptional activators (Massague 1998). The final steps of this pathway involves the nuclear translocation of a Smad 2/3-Smad 4 complex and subsequent binding to the Smad-binding element of the target gene to alter transcription. However it is now clear that TGFβ biological activity involves several Smad-independent pathways including the MAPK/Erk, p38 and Jun-kinase and integrin-linked kinase cascades (Li, 2009; Siegel, 2003). Furthermore following secretion by both resident renal cells and infiltrating leukocytes, TGFβ may also auto-induce its own expression. TGFβ expression has been found to increase through the course of chronic kidney injury and activation of the latent protein is enhanced in pathological conditions (Bissell, Roulot et al. 2001; Daniel, Wiede et al. 2004). The pro-fibrotic effects of TGFβ were first realised in the 1980s with *in vitro* work showing an association of TGFβ levels and increased matrix synthesis, decreased matrix degradation and modulation of receptors mediating matrix deposition (Ignotz and Massague 1986; Edwards, Murphy et al. 1987; Ignotz and Massague 1987; Laiho, Saksela et al. 1987; Heino, Ignotz et al. 1989). TGFβ is thought to trigger fibrogenic processes including: EMT, chemotaxis of fibroblasts, activation of fibroblasts to myofibroblasts, transcription of matrix encoding gene and matrix binding integrins. In addition TGFβ may also activate inhibitors of matrix metalloprotinases (MMPs) such as tissue inhibitor of metalloprotinases (TIMP) (Ma and Chegini 1999) or plasminogen activator inhibitor (PAI) (Overall, Wrana et al. 1989; Rerolle, Hertig et al. 2000) leading to reduced matrix degradation.

The central role of TGFβ in fibrosis is supported by several *in vivo* experiments demonstrating exogenous TGFβ-promoted wound closure and scarring (Mustoe, Pierce et al. 1987; Lin, Sullivan et al. 1995; Sullivan, Lorenz et al. 1995) while inhibition of TGFβ signalling pathways suppressed extracellular matrix synthesis and scarring (Shah, Foreman et al. 1995; Cordeiro, Mead et al. 2003) in animal models of

renal fibrosis such as subtotal nephrectomy, diabetic and obstructive nephropathy (Wu, Cox et al. 1997; Shihab, Bennett et al. 2002; Lan, Mu et al. 2003; Russo, del Re et al. 2007; Huang, Chung et al. 2008). Thus TGFβ remains an important and viable target for the treatment of progressive renal fibrosis.

1.3.3 The Fibroblast & the Myofibroblast

The fibroblast is central to the process of fibrosis. Though first described in the 19th century, the most recent accepted definition of an interstitial fibroblast is a "non-vascular, non-epithelial, non-inflammatory cell of the connective tissue and is its principal cell component" that possesses a "fusiform or spindle –like shape in profile" with "a stellate nucleus and abundant rough endoplasmic reticulum, collagen secreting granules and actin filaments"(Kalluri and Zeisberg 2006). The persistence of ambiguity in defining this cell type is due to the lack of reliable specific cell markers. Though there are now several well accepted and established indicators of fibroblast phenotype-such as vimentin and fibroblast specific protein-1 (Strutz, Okada et al. 1995), these are in no way specific to the fibroblast nor are they present in all fibroblasts, with expression possibly varying with degree of fibroblast maturity. Matters are further complicated as it has now been shown that fibroblasts in mammals are highly heterogenous and fibroblasts isolated from different anatomical sites show highly divergent gene-expression patterns (Chang, Chi et al. 2002; Sorrell and Caplan 2009). Furthermore the environment in which the fibroblast exists also has a major impact upon its activity: fibroblasts from fibrotic kidneys exhibiting a much higher capacity for proliferation and matrix production when compared to their counterparts from normal non-fibrotic kidneys (Muller and Rodemann 1991; Strutz, Zeisberg et al. 2000).

The main functions of fibroblasts are 1) the deposition of extracellular matrix including the synthesis of the major components such as Collagen I and III and fibronectin, 2) regulation of epithelial differentiation, 3) regulation of inflammation and 4) involvement in wound healing (Tomasek, Gabbiani et al. 2002). It is widely accepted that to perform many of these functions the quiescent fibroblast must adopt an "active" fibroblast phenotype deemed the "myofibroblast". This phenotype describes the fibroblast that possesses contractile properties (Tomasek, Gabbiani et al. 2002) and was originally identified as the cell responsible for wound contraction

(Gabbiani, Hirschel et al. 1972). Visualized under electron microscopy they are characterized by bundles of actin microfilaments associated with contractile proteins and the presence of a well-developed rough endoplasmic reticulum (Gabbiani 1992; Ina, Kitamura et al. 2002; Qi, Chen et al. 2006). αSMA is a major component of this contractile apparatus (Darby, Skalli et al. 1990), is up regulated during wound healing (Desmouliere, Geinoz et al. 1993) and is now widely used as a marker of the myofibroblast to differentiate it from the relatively more "quiescent" fibroblast phenotype. However αSMA expression is not exclusive to myofibroblasts nor is it expressed by all myofibroblasts (Hinz, 2010). With regards to renal fibrosis the myofibroblast is believed to be the phenotype of the cell responsible for ECM deposition and fibrosis within the tubulointerstitium (Qi, Chen et al. 2006) and their presence directly correlates to the subsequent progression of renal failure (Zeisberg, Strutz et al. 2000). In the setting of tubulointerstitial fibrosis, fibroblasts appear to maintain their active phenotype despite the removal of the initial stimulus, a situation that mirrors the clinical phenomenon of progressive renal failure in patients despite treatment/removal of initial cause (Strutz and Muller 1995). How the maintenance of this active state is achieved remains unclear.

1.3.4 Origin of the myofibroblast and Epithelial-Mesenchymal Transition

Though it is now generally accepted that fibroblasts/myofibroblasts are responsible for renal fibrosis the origin of fibroblasts in the kidney, especially in the diseased state, is far more controversial. In the 1800s Cohnheim stated that these "contractile cellular elements" were direct descendents of migrating leukocytes. This theory was largely disregarded when Ross et al. showed that fibroblasts were mainly of local origin and not derived from blood-borne cells (Ross, Everett et al. 1970). The conclusion from this set of experiments using radioactive labelling was supported by a series of subsequent studies demonstrating that adult fibroblasts localized to sites of embryonic mesenchymal cells and arise locally during embryogenesis from mesenchymal progenitor cells via a process of differentiation (Ekblom and Weller 1991; Lang and Fekete 2001). However this issue has become more complicated as not only is the original theory that some fibroblasts are of bone marrow lineage being revisited (Poulsom, Forbes et al. 2001; Forbes, Poulsom et al. 2002) but other possible

sources are being implicated including periadventitial/pericytes (Wiggins, Goyal et al. 1993; Lin, Kisseleva et al. 2008) and tubular epithelial cells via the phenomenon of epithelial-mesenchymal transition (EMT) (Strutz, Okada et al. 1995; Iwano, Plieth et al. 2002). With regards to bone marrow derived precursors of renal cells more recent studies have confirmed that transition of bone marrow derived cells to tubular epithelial cells may exist and could contribute a small but significant part of parenchymal regeneration following injury (Fang, Alison et al. 2005; Yen, Alison et al. 2007). The role that bone marrow derived cells, fibrocytes, play in the process of renal fibrogenesis is more controversial. Grimm et al. examined biopsies of chronic allograft rejection from patients who had received grafts from opposite sex donors (Grimm, Nickerson et al. 2001). Using immunohistological techniques and *in situ* hybridization they suggested that upto 30% of interstitial mesenchymal cells were of bone marrow origin. However this was disputed by Iwano and Neilson using genetic tagging techniques who concluded that only 12% of the interstitial population derived from the bone marrow, 36% derived from EMT and the remaining 52% from a variety of sources including resident interstitial cell proliferation (Iwano, Plieth et al. 2002). However a distinction between the origin of the fibroblast and the activity of the fibroblast has been made by Roufosse et al (Roufosse, Bou-Gharios et al. 2006). Using bone marrow transplantation from transgenic mice in a model of fibrosis they concluded that though 8.6% of αSMA-positive interstitial cells were of bone marrow origin, none of these cells were collagen producing. The true significance of contribution to fibrosis by bone marrow-derived fibroblasts remains unclear.

Epithelial-mesenchymal transition (EMT) was first described by Greenburg and Hay during their observation of epithelial cells from anterior lens suspended in collagen gels (Greenburg and Hay 1982). They found that "…Elongated cells derived from the apical surface develop pseudopodia and filopodia characteristic of migratory cells and acquire a morphology and ultrastructure virtually indistinguishable from that of mesenchymal cells in vivo." and concluded that the collagen gel can "…promote dissociation, migration, and acquisition of secretory organelles by differentiated epithelial cells, and can abolish the apical-basal cell polarity characteristic of the original epithelium." The phenomenon of EMT is a dynamic process by which terminally differentiated epithelial cells undergo a conversion to adopt a mesenchymal phenotype. This process involves the loss and gain of several cellular markers and characteristics, which are summarised in Table 1.2 and in Figure 1.3. To date there are

now three accepted variations of EMT. Type 1 is classified as developmental EMT as seen in biological circumstances, type 2 refers to adult epithelial and endothelial cells transition to fibroblasts and type 3 involves metastases associated with cancer.

Table 1.2: Cellular changes associated with EMT

Loss of	Gain of
1) Expression of E-Cadherin 2) Expression of ZO-1 3) Epithelial cell adhesion 4) Integrity of basement membrane 5) Cell polarity	1) Expression of αSMA 2) Expression of FSP-1 3) Expression of vimentin 4) Enhanced migratory activity

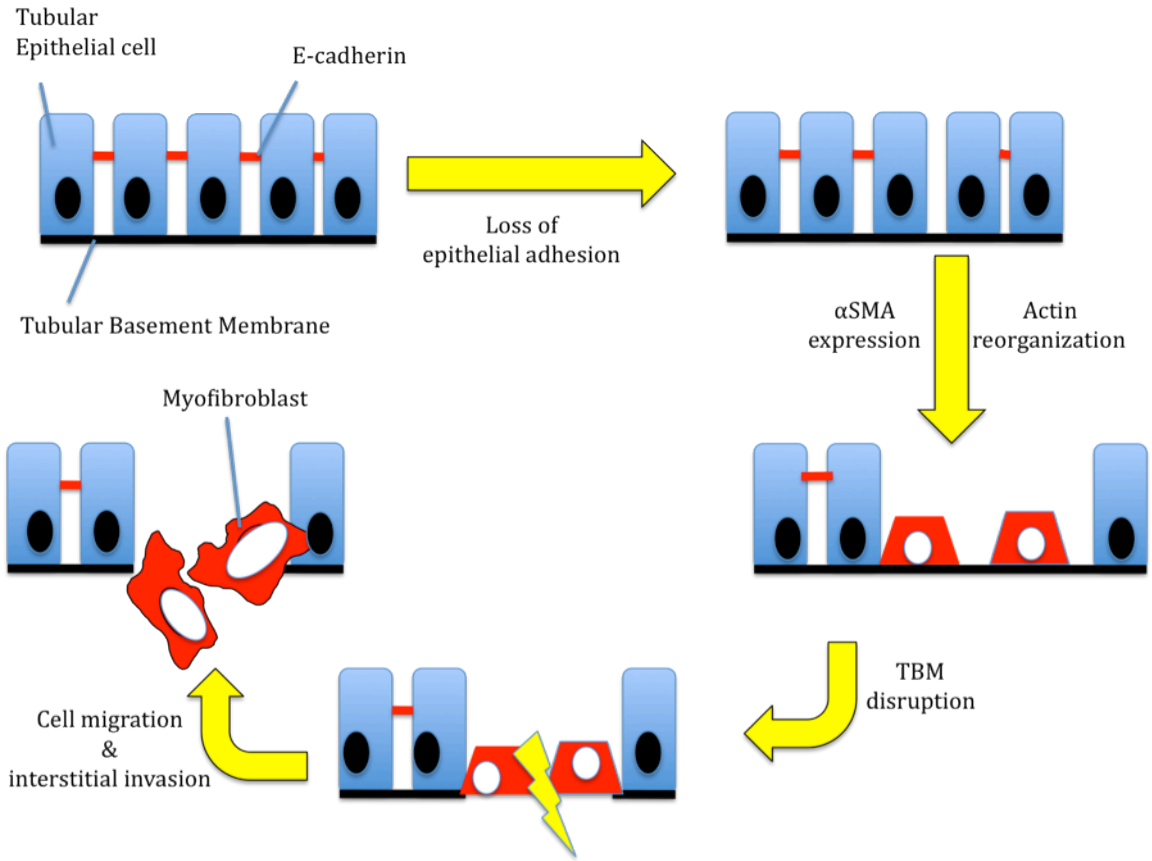

Figure 1.3: Schematic illustrating the key events of the process of EMT (Adapted from Liu 2004)

EMT has been observed to occur in cells from different organs including hepatic, lung and skin (Chaudhuri, Zhou et al. 2007; Ikegami, Zhang et al. 2007; Jain, Shaul et al. 2007; Zeisberg, Yang et al. 2007; Kim, Wei et al. 2009). In addition the process has been of particular interest to the oncology field since EMT is believed to be fundamental for the metastases of malignant cells in cancer (Thiery 2003; Tse and Kalluri 2007; Yilmaz and Christofori 2009). With regards to the kidney and its embryonic development, EMT should not be a completely surprising phenomenon. The mammalian kidney develops from two embryonic tissues: the ureteric bud and the metanephric mesenchyme, which form the collecting system and the nephrons and interstitial cells respectively (Herzlinger, Abramson et al. 1993; Herzlinger 2002). During this differentiation multipotent nephron progenitors of the metanephric mesenchyme develop into glomerular and tubular epithelial cells (Herzlinger, Abramson et al. 1993; Oliver, Barasch et al. 2002), representing mesenchymal to epithelial transdifferentiation (MET). It now appears feasible that in pathological conditions there is a "reverse embryogenesis" reflecting renal cell plasticity. There is compelling evidence that EMT occurs in disease states of the kidney. Strutz et al. first demonstrated the existence of EMT within the kidney by demonstrating the expression of FSP-1 by tubular epithelial cells in a murine model of renal fibrosis (Strutz, Okada et al. 1995). The presence of EMT has now also been shown in models of renal fibrosis including remnant kidney post 5/6 nephrectomy (Ng, Huang et al. 1998) and unilateral ureteric obstruction (Yang and Liu 2001) with the latter study able to show co-expression of both mesenchymal and epithelial cell markers within a high proportion of cells. Other renal disease models in which EMT appears to play a major role include diabetic nephropathy, anti-glomerular basement membrane disease and nephrotoxic nephritis (Ng, Fan et al. 1999; Oldfield, Bach et al. 2001; Li, Yang et al. 2003). Iwano et al. used an elegant genetic technique to demonstrate EMT in a model of UUO. Using transgenic mice that expressed LacZ in tubular cells they were able to demonstrate that these LacZ cells adopted a different morphology and were able to migrate to the interstitium under conditions of ureteric obstruction. Furthermore they reported that these same cells expressed FSP-1 and HSP47, a stress-induced collagen chaperone protein, indicating that interstitial mesenchymal collagen producing cells can derive from tubular epithelial cells (Iwano, Plieth et al. 2002). EMT has also been observed in human renal tissue. Using techniques of immunohistochemistry and *in situ* hybridization these studies support the theory that

EMT occurs in clinical renal disease and is associated with deteriorating renal function (Jinde, Nikolic-Paterson et al. 2001; Rastaldi, Ferrario et al. 2002). Further evidence for EMT contributing to renal fibrogenesis comes from studying potential anti-fibrotic molecules. Both BMP-7 and hepatocyte growth factor have been shown to prevent or even reverse renal fibrosis and in both cases their effects appear to involve inhibition of EMT (Yang and Liu 2002; Klahr 2003; Zeisberg, Hanai et al. 2003).

However various factors regarding the demonstration of EMT have recently called into question the true role of EMT and even its existence in renal fibrosis. Firstly, though EMT has been demonstrated *in vitro*, evidence of *in vivo* existence has being less convincing. Histological demonstration of EMT has relied on catching an 'intermediate transitional' state showing co-localization of both epithelial and myofibroblastic cell markers in addition to expression of transcriptional signals of EMT (Snail, Twist) and possibly use of lineage tags. Many of the cell markers such as FSP-1 and αSMA are non-specific for fibroblasts and may be expressed by other cell types including macrophages, as can the expression of the EMT markers. Though Iwano et al used lineage tagging to demonstrate existence of EMT *in vivo* (Iwano, Plieth et al. 2002), there has been a lack of reproducibility of these results using similar methods in other models of renal injury (Humphreys, Lin et al. 2010; Koesters, Kaissling et al. 2010; Li, Zepeda-Orozco et al. 2010). Interestingly one of these genetic lineage studies though unable to demonstrate EMT *in vivo* did show that epithelial cells readily underwent EMT *in vitro* as primary cultures (Humphreys, Lin et al.2010). However it must be remembered that these fate-mapping studies are all completed in murine models and the lack of lineage tags within human epithelial cells means that advanced stages of EMT cannot be detected in humans. Finally the presence and degree of EMT does not necessarily correlate with myofibroblastic activity, thus the clinical significance of EMT is called into doubt. The failure of a number of studies to confirm the tubular epithelial origin of myofibroblasts has led to increasing emphasis upon other cells as being the source of myofibroblasts. Using methods including fate-tracing other cells that have been considered to be the source of the myofibroblastic population include perivascular cells (pericytes) (Humphreys, Lin et al. 2010; Faulkner, Szcykalski et al. 2005; Lin, Kisseleva et al. 2008), circulating fibroblast precursors (fibrocytes) (Sakai, Furuichi et al. 2010; Wada, Sakai

et al. 2007) and endothelial cells (Wiggins, Goyal et al. 1993; Zeisberg, Potenta et al. 2008). Though many of these studies admit to not being able to completely distinguish between infiltration by circulating fibrocytes and true perivascular pericytes as a source of fibroblasts they do dispute the significance of the role of EMT.

Though EMT has now been widely perceived to exist *in vitro*, the debate regarding its existence and clinical significance in the process of renal fibrogenesis continues. Conceptually the idea of reversal of embryonic pathway at sites of injury is attractive. Furthermore many of the transcriptional pathways of EMT are also anti-apoptotic (Snail, Twist) for tubular epithelial cells thus may drive this process. However the lack of specific markers of fibroblasts and EMT has meant that its existence *in vivo* in humans cannot be conclusively proven. In addition the lack of real-time technology to demonstrate true cell transition and the absence of true human epithelial cell lineage tags means current methodology relies on demonstrating cells co-expressing epithelial and mesenchymal markers at static time points which may rely upon luck as much as ability and may explain the numerous conflicting studies. Advocates of EMT and its contribution to renal fibrosis add that EMT represents a dynamic spectrum of change and that the transition of the epithelial cell does not necessarily need be completed. Thus not all epithelial cells will become fibroblasts and not all cells undergoing EMT will co-express all markers of epithelial/mesenchymal cells in transitional state at one time, making not only timing of tissue analysis critical but also selection of markers vital. Furthermore, though not all epithelial cells may transition to fibroblasts, those that do complete EMT may further proliferate. Thus, in the absence of lineage tags, in theory, a significant number of fibroblasts in the human fibrotic kidney may have been derived from a few fibroblasts of EMT origin. Despite the controversy there remains much focus upon epithelial-mesenchymal transition in renal fibrosis.

Though the true origin of the myofibroblast is in dispute, the cell signalling pathways involved in regulating EMT appear to be more clearly delineated. At present the main protagonists are TGFβ, Smad-dependent and independent pathways, integrin-linked kinase signalling and Wnt/β-catenin signalling. TGFβ Smad-dependent pathways have previously been discussed but non-Smad signalling of TGFβ is also thought to regulate EMT via Rho (Masszi, Di Ciano et al. 2003), MAPK (Janda, Lehmann et al.

2002; Erdogan, Pozzi et al. 2007) and phosphatidylinositol-3-kinase/Akt (Docherty, O'Sullivan et al. 2006; Zeng, Yao et al. 2008) cascades.

Integrin-linked kinase (ILK) is an intracellular kinase that interacts with cell matrix integrins and phosphorylates intracellular proteins such as Akt and glycogen synthase kinase 3β (GSK-3β). This allows for stabilisation of β-catenin and expression of genes required for EMT (Hannigan, Troussard et al. 2005). Studies have demonstrated both the importance of ILK and the benefits of inhibiting this molecule in renal fibrosis (Li, Yang et al. 2003; Li, Tan et al. 2009). Furthermore many members of the ILK-signalling pathway (including ILK and PINCH-1 itself) are up regulated by TGFβ in a Smad-dependent manner (Li, Dai et al. 2007).

Wnt/β-catenin signalling is well recognised in regulating EMT at least in organogenesis and metastasis (Huber, Kraut et al. 2005; Pulkkinen, Murugan et al. 2008). However there is now evidence that this pathway plays a significant role in EMT in renal disease. Interacting via Frizzled receptors, Wnt protein binding results in dephosphorylation of β-catenin thus allowing escape from ubiquitin-mediated degradation. Subsequent accumulation of β-catenin leads to translocation to the nuclei where it binds to T cell factor/lymphoid enhancer binding factor-1 (LEF1) to induce transcription of target genes involved in EMT, including Twist, c-myc, Snail and fibronectin (Surendran, Schiavi et al. 2005; He, Dai et al. 2009). Data is now emerging that inhibition of this cascade may also ameliorate renal disease (Hwang, Seo et al. 2009).

1.3.5 Parenchymal destruction and dysfunction of matrix degradation

Fibrosis occurs as a result of excessive matrix accumulation but also an accompanying decrease in degradation. The matrix "scar" is made up of normal interstitial proteins such as collagen (I, III, V, VII and XV) and fibronectin. However it is now believed that the excessive matrix produced in the development of interstitial fibrosis is not a mere passive end-product but actually actively contributes to the process of fibrosis and cell survival (Eckes, Kessler et al. 1999; Marastoni, Ligresti et al. 2008). These constituents of matrix include proteoglycans, polysaccharides and glycoproteins. For example thrombospondin accumulation has been seen to predict

the development of interstitial fibrosis (Hugo, Shankland et al. 1998; Hugo, Kang et al. 2002), which may in part be due to the protein's observed ability to activate TGFβ both *in vitro* and *in vivo* (Crawford, Stellmach et al. 1998). Interstitial fibrosis has been viewed as a dynamic process where initially the 'scaffold' is thought to be unstable and susceptible to degradation perhaps as part of the healing process. However with time a persistent fibrogenic process results in the formation of non-reversible interstitial scarring due to enzymic modification by glycoslylation, oxidation or transglutamination (Johnson, Skill et al. 1999) leading to formation of cross bridges that conveys both stability and a resistance to proteases. Studies have shown that inhibition of these processes (Johnson, Fisher et al. 2007) may also reduce fibrosis and protect renal function. The ongoing fibrotic process also leads to changes in the composition of matrix such as the increase in the ratio of collagen I to collagen III that may also add to the stability of the "scar". The process of pathological fibrosis not only depends on the increase in matrix production and stability in disease but also on a decrease in the ability to degrade and remodel matrix. The normal kidney produces several proteases with the potential to degrade ECM. Of these, the two groups that have been best studied are the matrix metalloproteinase [MMP] and serine protease family. MMPs are zinc-containing endopeptidases that have a role in renal development (Lelongt, Trugnan et al. 1997) and homeostasis and are now widely implicated in renal pathophysiology. Regulation of MMPs is by a series of tissue inhibitors of metalloprotinases (TIMP), endogenous specific inhibitors that bind to the active catalytic domain of the MMP. Many non-ECM proteins also act as substrates for MMPs and these include cell adhesion molecules (such as cadherins and integrins) and growth factors (TGFβ and FGF) and their receptors (Yu and Stamenkovic 2000; Nagase, Visse et al. 2006). MMPs are classified into six groups: collagenases, gelatinases, stromolysins, matrilysins, membrane-type MMPs and other MMPs while four TIMPs have been identified in vertebrates. Within the kidney expression of both MMPs and TIMPs appear to vary both spatially and temporally and between species (McMillan, Riordan et al. 1996; Suzuki, Miyazaki et al. 1997; Eddy, Kim et al. 2000; Ogbureke and Fisher 2005). The most abundant and the best-studied MMPs in the kidney are MMP-2 and MMP-9 from the gelatinase group. Originally these gelatinases have been seen as protective molecules but more recent studies have forced this view to be re-addressed. In the unilateral ureteric obstruction

model an early rise in MMP-2 expression with a decrease in both MMP-1 and MMP-9 activity (Gonzalez-Avila, Iturria et al. 1998; Iimura, Takahashi et al. 2004) has been demonstrated. This was accompanied by an increase in TIMP expression (especially TIMP-1) (Duymelinck, Dauwe et al. 2000). It is now recognised that TIMPs may have cellular effects outside of inhibition of MMPs that include inhibition of apoptosis, growth promotion, induction of changes in cell morphology and inflammation (Gomez, Alonso et al. 1997; Cai, Zhang et al. 2008). The development of a transgenic mouse that overexpresses MMP-2 which progresses to chronic renal disease with associated histological changes of glomerulosclerosis and tubulointerstitial fibrosis further highlights the role of MMP-2 in CKD (Cheng, Pollock et al. 2006). MMP-2 is required for TGFβ-driven EMT possibly by its ability to cleave LAP of TGFβ (Cheng and Lovett 2003). However, whereas overexpression of MMP-2 appears to accentuate fibrosis, an increase in MMP-9 levels appears to attenuate both glomerular and interstitial scarring (Dworkin, Gong et al. 2004; Uchio-Yamada, Manabe et al. 2005; Bauvois, Mothu et al. 2007; Hultstrom, Leh et al. 2008). The difference in effects of MMP-2 and MMP-9 expression may be less to do with degradation of ECM proteins than with activation/degradation of non-ECM pro-fibrogenic molecules (Lelongt, Bengatta et al. 2001; Catania, Chen et al. 2007). As yet the role of the various MMPs in fibrogenesis has to be clearly delineated. The other major family of proteinases is the serine proteinases that include plasmin and cathepsin G. Plasmin not only may degrade some elements of matrix such as fibronectin but also has a role in activating collagenase precursors (Hu, Yang et al. 2006). In turn active plasmin is a result of proteolytic activation of latent plasminogen by either tissue-type or urokinase-type plasminogen activator [tPA or uPA]. Both tPA and uPA are inhibited by Plasminogen Activator Inhibitors (PAI). Not normally expressed by the kidney, PAI-1 levels are induced by numerous cytokines and growth factors released in a variety of renal diseases (Tomooka, Border et al. 1992; Eddy and Giachelli 1995; Tang, Friess et al. 1998; Duymelinck, Dauwe et al. 2000). PAI-1-inducing elements include pro-fibrotic interleukin-1β, TNF-α, angiotensin II and TGFβ (Wilson, Reid et al. 1995; Wilson, Haites et al. 1996; Kanalas and Hopfer 1997; Nakamura, Nakamura et al. 2000). *In vivo* studies demonstrate a protective outcome in models of obstructive and protein overload nephropathy using PAI-1 null mice (Oda, Jung et al. 2001) while PAI-1 overexpression leads to worse fibrosis

(Matsuo, Lopez-Guisa et al. 2005). A further interesting observation in these studies was a significant delay in interstitial macrophage recruitment in PAI-1 deficient mice (Oda, Jung et al. 2001). Hence the fibrosis protective effects of PAI-1 deficiency may lie not only in the increase in ECM turnover by plasmin activation (and subsequently activated MMPs) but perhaps also in the blunting of the acute inflammatory response in these disease models (Ha, Oh et al. 2009). Though it is predicted plasmin should enhance MMP activity and ECM degradation, it is also recognised that plasmin may activate TGFβ and promote EMT (Zhang, Kernan et al. 2007) and in fact a deficiency of plasminogen activation may be protective (Yang, Shultz et al. 2002). These studies suggest that PAI-1 inhibition of plasmin induction could be beneficial and the protective effects of PAI-1 deficiency may involve mechanisms independent of plasmin formation (Hu, Lin et al. 2008).

The accumulation of matrix and expansion of interstitial space results in parenchymal destruction of the kidney and tubular atrophy. The renal tubules comprise up to 80% of the total kidney volume and subsequent loss leads to “atubular” glomeruli and subsequent renal failure. Tubular cell loss occurs mainly by apoptosis and possibly autophagy and EMT (Yang, Johnson et al. 2001). The circumstances as to whether a tubule regenerates or degenerates are unclear though the duration and extent of insult must be an important factor. Though fibrosis has been assumed to “cause” tubular atrophy this has yet to be conclusively proven and at present the most accurate conclusion is that fibrosis correlates with tubular loss. The most widely accepted link is that of hypoxia. (Norman, Orphanides et al. 1999; Nangaku 2006; Fine and Norman 2008). Tubular cells are highly metabolically active and have a fragile blood supply. Progressive fibrosis leads to progressive capillary loss, microvascular rarefaction and resulting oxidant stress and generation of ROS may lead to both tubular damage and promote further interstitial fibrosis (Orphanides, Fine et al. 1997). The lack of angiogenesis in such conditions has yet to be explained.

In summary the process of renal fibrogenesis is complex and its progression is dependent upon the balance and expression of a whole plethora of cytokines and growth factors- some of which drive the process and others which aim to inhibit it.

1.4 Ras monomeric GTPases

The discovery of Ras dates back to 1964 when Jennifer Harvey identified that a preparation of a murine leukaemia virus from a leukaemic rat induced sarcomas in newborn rodents (Harvey 1964). In 1967, in the laboratory of Werner Kirsten, the Kirsten isoform of the murine sarcoma virus was discovered (Kirsten and Mayer 1967). The *ras* gene was identified as the transforming element in the respective Harvey and Kirsten rat sarcoma viruses (Scolnick, Rands et al. 1973). Ha-*ras* and Ki-*ras* are mammalian counterparts of the viral Harvey and Kirsten genes. In 1983 a third member of the *ras* gene family was discovered, Neural *ras* (N-*ras*), derived from a human neuroblastoma cell line (Hall, Marshall et al. 1983; Shimizu, Goldfarb et al. 1983). Furthermore splice variants of Ki-*ras* are now recognised: Kirsten *ras* 4A (Ki-*ras* 4A) and Kirsten *ras* 4B(Ki-*ras* 4B) which differ in their terminal fourth exon. Ki-Ras 4B is the predominant Ki-Ras variant in mammals (Chen, Otto et al. 2000). The Ha-*ras* gene is on the short arm of chromosome 11(11p15.1-15.5), Ki-*ras* on the short arm of chromosome 12 (12p12.1-pter) and N-*ras* on the short arm of chromosome 1 (1p22-p32).

Ras monomeric GTPases became of particular interest in the early 1980s when the laboratories of Weinberg, Cooper, Barbacid and Aaronson showed that mutations of *ras* were the dominant oncogene in various forms of cancers (Der, Krontiris et al. 1982; Parada, Tabin et al. 1982; Shimizu, Goldfarb et al. 1983) and they play a vital role in the control of cell proliferation (Barbacid 1987). Their importance as a regulator of cell proliferation is reflected by the fact that mutations of *ras* are found in 20-30% of all human cancers (Bos 1989).

The Ras proteins are however only the initial members of a larger "Ras superfamily" of closely related monomeric GTPases. This family is comprised of over 150 GTPases which include Rho, Rac and Rab proteins. All these small G proteins are monomeric molecules ranging from 20 to 40 kDa and all possess a structurally conserved GTP binding domain capable of hydrolytic activity (Bourne, Sanders et al. 1991). The Rho sub-family consists of about 20 members including Rho, Rac and Cdc42 and share 30% homology with Ras proteins and 80-90% homology between each other. Whereas Ras has been identified as being involved in the process of cell proliferation it appears that Rho proteins are involved in formation of the cell cytoskeleton, cell-cell interaction and cellular motility (Hall 1992; Ridley 1995;

Mackay and Hall 1998). While Rho appears to regulate contractile actin-myosin filament formation, Cdc42 induces filopodia formation, a process involving finger-like extensions consisting of actin bundles and probably associated with recognition/regulation of the microenvironment. Rac regulates lamellipodia formation and membrane extension during phagocytosis (Heasman and Ridley 2008).

1.4.1 Ras genes and protein structure

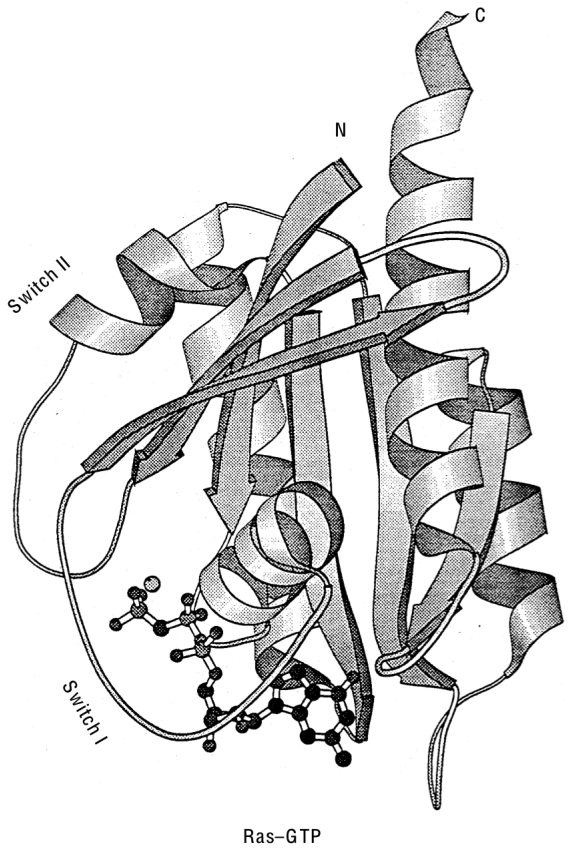

Figure 1.4: Molecular structure of Ras-GTP (Kim, S.-H., Prive, G. G. and Milburn, M. V. (1993) Handb. Exp. Pharmacol. 108).

The Ras proteins are 188-189 amino acids in length and have a molecular weight of 21 kilodaltons (Figure 1.4). There is a high degree of homology within the first 165 amino acids between the isoforms and this region contains the major effector and GTP binding regions. However the remaining 24 amino acids are highly dissimilar between the isoforms of the proteins and are termed the "hypervariable region" (Figure 1.5).

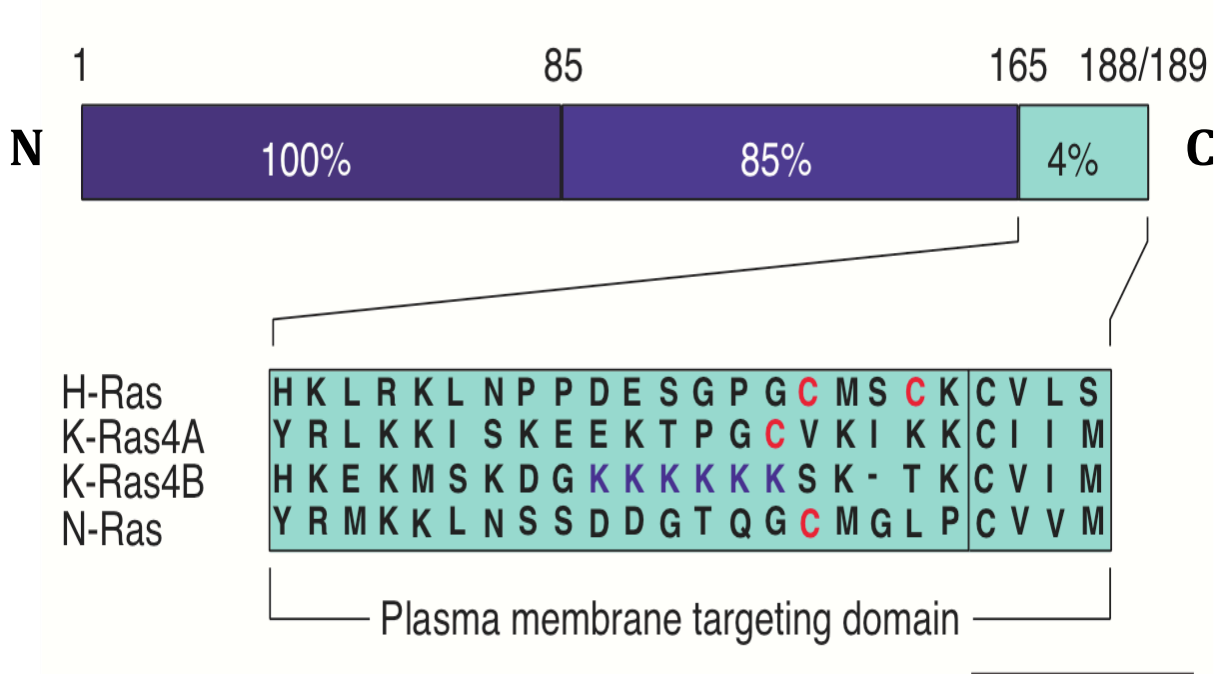

Figure 1.5: The 'Hypervariable region' of human Ras isoforms (Figure taken from (Shields, Pruitt et al. 2000)). Ras molecules demonstrate 85% homology in the amino-terminal residues but significant divergence in the final 24 carboxy-terminal residues, the hypervariable region.

Ras is a central cellular component in the signalling pathway of numerous cell surface receptors and acts as a convergent point for a variety of effector molecules. The protein can be seen as a molecular switch that allows transduction of upstream signals to downstream effector molecules resulting in end cell response (Figure 1.6) (Wittinghofer and Pai 1991).

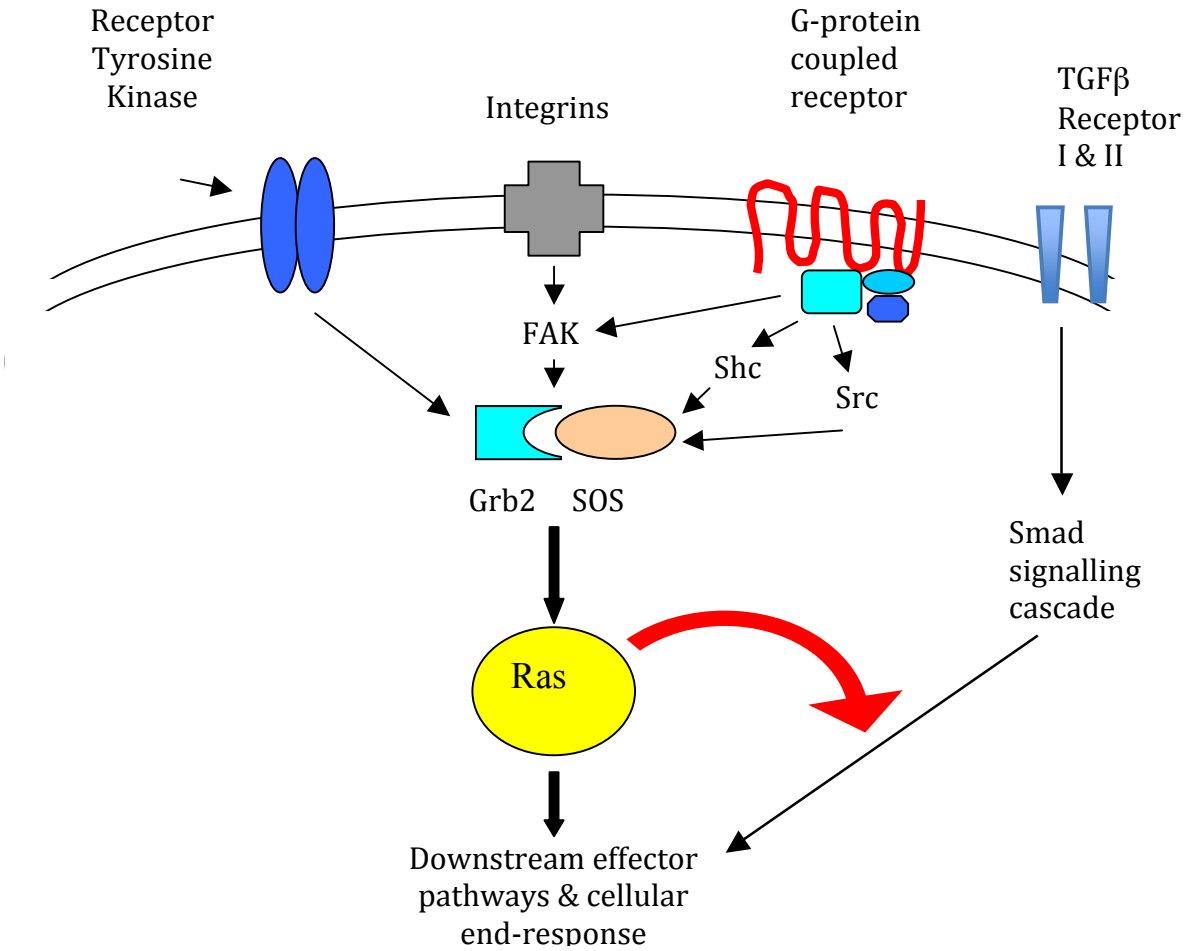

Figure 1.6 : Upstream cell activation of Ras pathways.

Regulation of Ras protein activity is by binding with guanine nucleotides (Wittinghofer 1998), the nature of which, whether triphosphate (GTP) or diphosphate (GDP), determine the ability of Ras to interact with downstream proteins. In the "dormant" form Ras is highly bound to GDP. Activation of Ras results in the release of the GDP molecule and binding of GTP (Figure 1.7). This results in a conformational change in the Ras molecule allowing it to interact with downstream effectors. Due to high affinity of Ras to GDP, molecules known as Guanine Nucleotide Exchange factors (GNEFs) are required to accelerate GDP disassociation. One of the most vital Ras GNEFs is son-of-sevenless (SOS) which interacts with Ras via the adapter molecule Grb2. Activation of cell surface tyrosine receptors depends on binding of the Grb2/SOS complex to Ras. Grb2 and SOS interact via Src

homology-2 (SH2) and phosphotyrosyl domains. These are common binding domains which are well preserved in nature (Campbell 1998). The formation of this adapter molecule complex allows translocation of cytosolic SOS to the plasma membrane where the GNEF can interact with Ras. The disassociation of GDP and subsequent binding of GTP allows Ras to interact with downstream effector molecules (Sundaram 2006; McKay and Morrison 2007).

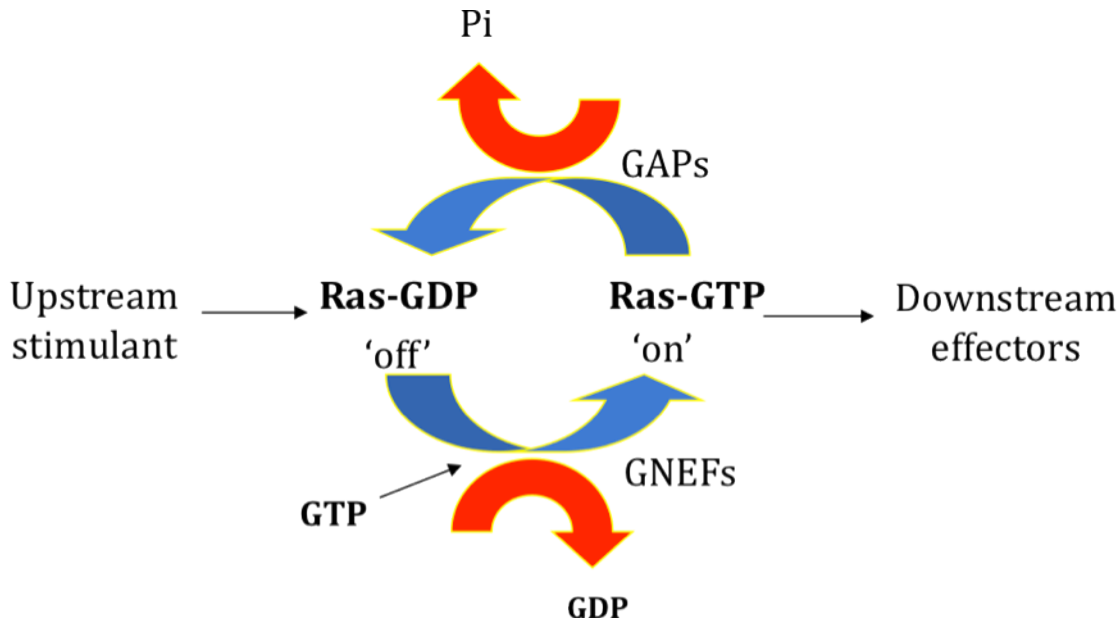

Figure 1.7: Ras GTPase molecule activation & deactivation-a 'molecular on/off switch'. GNEF, guanine nucleotide exchange factor, GAP, GTPase activating protein.

Initially Ras was found to be a signalling component downstream of a variety of tyrosine kinase receptors (a family of receptors for agonists that include EGF, FGF and PDGF) (Buday and Downward 1993; van der Geer, Hunter et al. 1994; Howe and Juliano 1998) but it has now been demonstrated that Ras can also act downstream from other cell surface receptors. G-protein coupled receptors, including those for Angiotensin II and Endothelin-1, possess seven membrane-spanning domains and were originally thought to signal via Ras–independent pathways. However it is now known that theses receptors may involve Ras GTPases via two mechanisms (Luttrell, Daaka et al. 1997). The first involves interaction of the activated receptor with a docking protein, either focal adhesion kinase (FAK) or SHC (Src homology 2 domain containing) transforming protein 1 (Della Rocca, van Biesen et al. 1997). Following phosphorylation this then binds to the Grb2/SOS complex bringing the GNEF to the plasma membrane to interact with Ras. Alternatively a non-receptor proto-oncogenic

tyrosine kinase, Src, may be activated by G-Protein receptor with subsequent binding of the Grb2/SOS complex in the membrane (Luttrell and Luttrell 2003; Luttrell 2003). Cell-cell and cell-matrix interactions via the integrin family of proteins may also activate the Ras pathway (Schlaepfer, Hanks et al. 1994). The signalling pathway is similar to that of Ras activation by G-Proteins which involves activated integrins utilizing FAK to recruit the Grb2/SOS to the membrane (Ramos 2008; Yee, Weaver et al. 2008). There is also evidence now that Ras may be involved in TGFβ signalling in fibroblasts (Axmann, Seidel et al. 1998; Janda, Lehmann et al. 2002; Zavadil 2009). The relationship between TGFβ and Ras is complex, not fully understood and will be discussed later. From current evidence it can be appreciated that Ras is a downstream convergent point for many cell surface receptors and their ligands, acting as an "on/off switch" to allow transduction of upstream signals to an array of downstream effectors. Hence targeting Ras may circumvent the relative redundancy in the multitude of signalling events involved in the process of fibrogenesis.

1.4.2 Ras activation and molecular conformational change

Upon exchange of GDP for GTP, there are two highly mobile regions of the Ras molecule that change conformation termed Switch I (residues 30-38) and Switch II (residues 60-76) (Polakis and McCormick 1993). Residues 32-40 of the molecule have been identified as the effector binding and transforming element (Sigal, Gibbs et al. 1986; Marshall, Davis et al. 1991) and this region overlaps with Switch I and alters conformation of GTP binding. In addition it has now been shown that residues surrounding this region are also vital for effector binding though do not undergo conformational change. This region has been termed the 'activator' or 'constitutive effector' region (Marshall 1993; Fujita-Yoshigaki, Shirouzu et al. 1995; Nassar, Horn et al. 1995) and may be important for the binding of GTPase-activating proteins (GAP) (Schaber, Garsky et al. 1989). The switch II region has also been shown to be vital to Ras function and blocking this region abolished Ras transforming capabilities (Milburn, Tong et al. 1990). Subsequently it has been discovered that this region was required for direct interaction with GNEFs such as SOS (Quilliam, Hisaka et al. 1996). SOS has also been shown to exert its effect via the switch I domain in addition to switch II. There are distinct functional roles to switch I and switch II: switch II mediates the anchoring of Ras to SOS, whereas the interaction with switch I leads to

disruption of the nucleotide-binding site and GDP dissociation via a catalytic mechanism (Hall, Yang et al. 2001). The displacement of GDP and subsequent binding of GTP catalysed by GNEFs such as SOS leads to a conformational change of the Ras molecule and allows for interaction with downstream effector proteins.

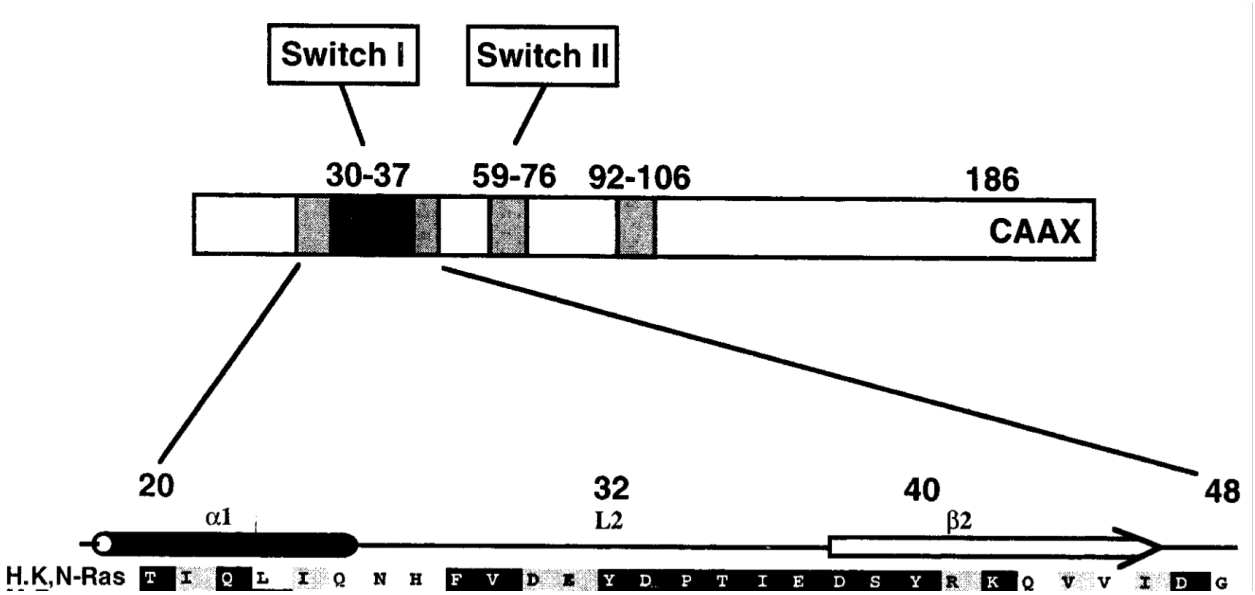

Figure 1.8: Ras-effector regions (Figure taken from Campbell et al., Oncogene (17) 1998). Effector interaction residues of Ras molecule occur within the highly homologous region of the molecule. CAAX motif required for post-translational modification (C, cysteine, A, aliphatic amino acid, X, serine or methionine).

1.4.3 Ras deactivation

Activated Ras (bound to GTP) is "turned off" by its own innate ability as a GTPase to hydrolyse GTP to GDP. However this process of GTP-hydrolysis is intrinsically slow and requires another group of proteins, known as GTPase-activating proteins or GAPs, to accelerate the reaction (Cales, Hancock et al. 1988). These proteins include RASAL1, neurofibromin (NF1) and p120 GAP (Garrett, Self et al. 1989; Martin, Viskochil et al. 1990) and have been found to share conserved residues with which they interact with Ras (Miao, Eichelberger et al. 1996; Scheffzek, Lautwein et al. 1996). The binding of GAPs to Ras allows the stabilization of the transition state of the GTPase reaction and increases the reaction rate by more than one thousand-fold (Ahmadian, Stege et al. 1997; Scheffzek, Ahmadian et al. 1997).

Ras mutations are the single most common abnormality of human proto-oncogenes and occur in 30% of all human cancers and up to 90% in specific tumour types. (Bos 1989). The most common mutation found is at residue 12 where there is a substitution of glycine for valine resulting in reduced binding of and response to GAPs (Trahey and McCormick 1987; Hall 1992; Wittinghofer, Scheffzek et al. 1997) and constitutively active Ras.

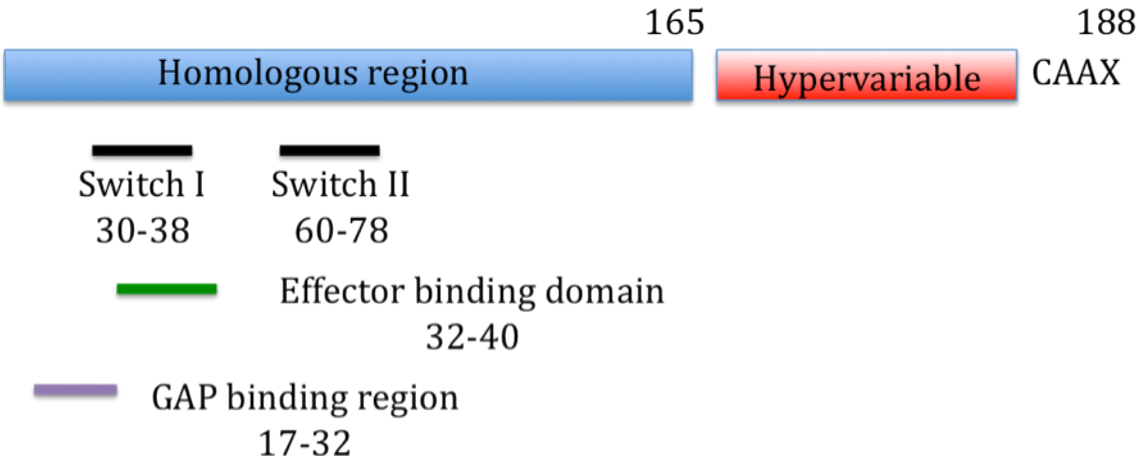

Figure 1.9: Schematic of Ras molecule illustrating residue sequences involved in Ras function. (C, cysteine, A, aliphatic amino acid, X, serine or methionine).

1.5 Posttranslational processing of Ras

It was well-recognized for some time that the activity of Ras is critically dependant upon correct localization to the inner surface of the plasma membrane (Willumsen, Christensen et al. 1984; Magee, Gutierrez et al. 1989) despite the fact that Ras proteins per se do not themselves possess any hydrophobic sequences which could mediate this (Barbacid 1987). It is thought that differential localization of the Ras isoforms allows for specific signalling and function by bringing respective isoforms into contact with distinct pools of effectors and activators (Prior and Hancock 2001). The effect of differential microdomain localization was only first noted in 1999 in studies that disrupted the integrity of the lipid raft microdomain of the plasma membrane which resulted in inhibition of Ha-Ras activation of Raf but not that of Ki(B)-Ras (Roy, Luetterforst et al. 1999). The ability of Ras to be membrane-associated is achieved via a complex series of posttranslational modifications resulting in the prenylation of the protein. Despite a high degree of homology between the isoforms there is a significant difference in the C-terminal hypervariable

region (HVR) of 23-24 amino acids. However in all Ras HVR there is a highly conserved CAAX motif (C being cysteine, A any aliphatic amino acid and X any amino acid) (Hancock, Cadwallader et al. 1991). The initial step involves prenylation of the cysteine residue by farnesyl protein transferase to generate S-farnesyl cysteine thioester, allowing for binding to the endoplasmic reticulum (ER) and golgi apparatus (Zhang and Casey 1996; Choy, Chiu et al. 1999). Subsequently at the ER, the AAX motif is cleaved off by the endopeptidase Ras converting enzyme Rce1 (Otto, Kim et al. 1999) and the farnyslated cysteine is methylated by isoprenyl cysteine carboxymethyl transferase (ICMT) (Gutierrez, Magee et al. 1989; Wright and Philips 2006). Both Rce1 and ICMT are ER-localized proteins that have been shown to be vital for development with knockout of either enzyme leading to late embryonic lethality in mice at between 10.5 to 15.5 days (Kim, Ambroziak et al. 1999; Bergo, Leung et al. 2001). There is now increasing focus on these enzymes as potential therapeutic targets to Ras activation (Svensson, Casey et al. 2006). The inability of Ras to be activated in the absence of farnesylation also led to the promotion of farnesyl transferase inhibitors (FTI) as potential anti-Ras therapies. However the use of the FTIs have not been as effective as predicted and led to the discovery that both Ki(B)-Ras and N-Ras could be alternatively prenylated by geranylgeranyl transferase in the absence of farnesylation (Whyte, Kirschmeier et al. 1997). Though this farnesyl group is essential, farnesylation itself provides only a weak membrane binding affinity and stabilization of association is obtained by a second motif signal that allows for correct trafficking and microlocalisation of each isoform (Hancock, Paterson et al. 1990). For Ha-Ras, N-Ras and the splice variant Ki(A)-Ras this involves palmitoylation of cysteine residues adjacent to the farnesylated cysteine residue. The cysteine residues that undergo palmitoylation are C181 and C184 in Ha-Ras, C181 in N-Ras and C180 in Ki(A)-Ras and augment localization to the plasma membrane (Smotrys and Linder 2004; Magee and Seabra 2005). Ki(B)-Ras however does not undergo palmitoylation but instead a polybasic chain of six lysine residues (K175-K180) that provides a net positive charge to the HVR domain and allows it to interact electrostatically with the negatively charged phospholipids of the internal membrane leaflet (Figure 1.11) (Hancock, Magee et al. 1989; Hancock, Paterson et al. 1990).

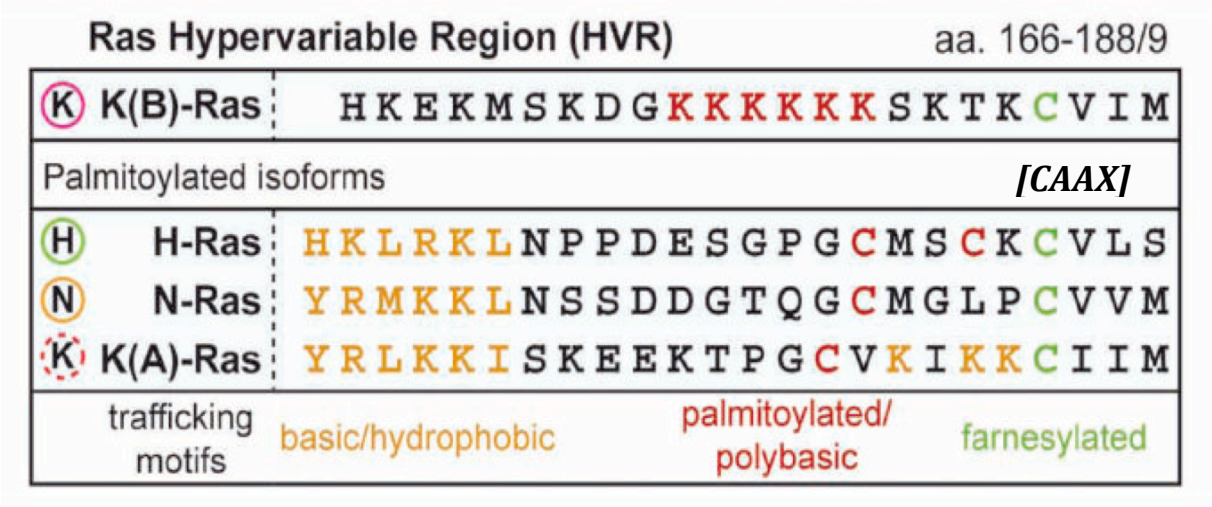

Figure 1.10: Hypervariable regions of Ras isoforms demonstrating combinations of posttranslational lipid modifications and membrane interacting polybasic motifs (Figure taken from (Henis, Hancock et al. 2009)). [The terminal four residues represent the CAAX motif, C being Cysteine, A any aliphatic aminio acid and X, serine or methionine. K, lysine.]

The essential nature of these posttranslational modifications became evident with mutagenic studies that rendered Ras-GTP cytosolic thus inhibiting membrane interaction and activation of downstream effectors (Hancock, Paterson et al. 1990; Jackson, Cochrane et al. 1990). The enzyme responsible for palmitoylation is also thought to be ER bound though as yet has not been fully characterized (Apolloni, Prior et al. 2000). Non-palmitoylated Ha-/N-Ras mutants and Ki-Ras mutants lacking the polybasic sequence highlight the importance of the second signalling motif. In both cases the mutants accumulated in the ER suggesting these sequences and modifications were vital for Ras protein trafficking from the ER to the plasma membrane. It is now recognised that the palmitoylated isoforms of Ras access the plasma membrane by vesicular trafficking through the classical exocytic pathway via the Golgi body whereas polybasic Ki-Ras appears to be excluded from this pathway and is transported to the membrane via an uncharacterized Golgi-independent route (Choy, Chiu et al. 1999; Apolloni, Prior et al. 2000). Data now indicates that the vesicular form of transportation of palmitoylated Ras may not be the sole pathway (Zheng, McKay et al. 2007). With regards to Ki-Ras, transportation has been thought to involve association with microtubules (Thissen, Gross et al. 1997). This hypothesis is supported by the finding that the polybasic domain of Ki-Ras mediates microtubule binding (Chen, Otto et al. 2000). However subsequent electron microscopic and

immunofluorescent analysis has failed to find a close relationship between Ki-Ras and microtubules though an accumulation in endosomes has been observed (Apolloni, Prior et al. 2000; Lu, Tebar et al. 2009). The high affinity electrostatic interaction between Ki-Ras and the membrane has led others to postulate that there may be no specific transport mechanism but Ki-Ras reaches the membrane by simple passive diffusion. In fact it has been shown that mutations to the polybasic domain of Ki-Ras to allow for the same overall net charge and amphiphilic character to be retained, do not prevent the protein associating with the plasma membrane (Jackson, Li et al. 1994; Roy, Leventis et al. 2000). At present the pathway of Ki-Ras trafficking to the plasma membrane has yet to be fully identified.

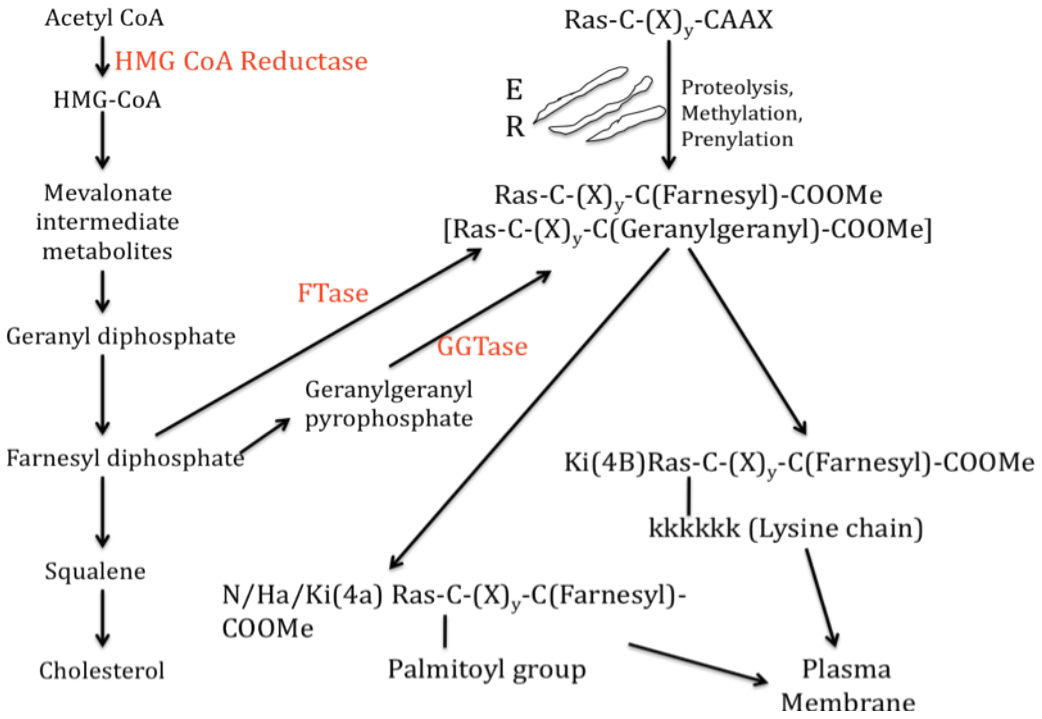

Figure 1.11: Post-translational modification and trafficking of Ras. ER, endoplasmic reticulum. FTase, Farnesyl transferase. GGTase, Geranylgeranyltransferase. C-$(X)_y$-C indicates two cysteine residues separated by an amino acid sequence.

A difference in microlocalizations within the plasma membrane may provide a basis for their different roles and interactions with downstream effectors. The lipid raft of the membrane is a liquid-ordered structure consisting of sphingolipids and glycosphingolipids packed with cholesterol where proteins are anchored via long, saturated acyl chains. Proteins with only farnesylated or geranylgeranylated groups

and lacking fatty acid chains are excluded from this region. Ki-Ras, lacking in a palmitoylated chain, has been shown to reside in the disordered non-raft plasma domain while Ha-Ras has been shown to target both the caveolae and non-caveolar lipid rafts (Prior and Hancock 2001). Furthermore the Ha-Ras microlocalization is more complex than previously thought. In GDP-bound form Ha-Ras has been shown to be equally distributed between the lipid raft and cholesterol-independent domain but the binding of GTP leads to majority translocation to the non-raft domains (Prior, Harding et al. 2001; Prior, Muncke et al. 2003). It appears that this translocation is critically dependent on the hypervariable "linker region" of Ha-Ras: the sequence of amino acids of the hypervariable region of Ras which is not involved in farnesylation or palmitoylation (Jaumot, Yan et al. 2002; Rotblat, Prior et al. 2004). Differential localization of the isoforms clearly has important consequences for downstream effector interactions. This is supported by the observation that Raf, though recruited equally well to lipid raft or non-raft domains of the plasma membrane, is much less efficiently activated in the former localization (Prior and Hancock 2001). Apart from the plasma membrane there is now increasing interest in other intracellular platforms for Ras activation. Effectors and facilitators of Ras signalling have been localized to the ER, the Golgi apparatus and endosomes (Chiu, Bivona et al. 2002; Arozarena, Matallanas et al. 2004; Mitin, Ramocki et al. 2004). However many of these studies involve Ras-overexpression and the significance of these findings in untransformed cells is unclear.

1.6 Ras Effectors

Effectors of Ras may be defined as molecules that can bind preferentially to the GTP-bound state of Ras as opposed to the GDP-bound state. Over the last decade there has been much evidence to show that multiple signalling pathways are activated by Ras. However the individual cellular response resulting from Ras activation may differ considerably between different cell types and different environmental contexts despite the identical effector protein downstream of Ras being activated (Cowley, Paterson et al. 1994). The first identified effector protein was Raf and it is through the examination of the Ras-Raf interaction that the subsequent binding regions between the molecules were discovered. Mutational analysis revealed that the effector-binding region of Ras consisted of residues 32-40, crossing over with switch I domain (Sigal,

Gibbs et al. 1986; Marshall, Davis et al. 1991; Shirouzu, Koide et al. 1994). Switch II was not seen to be directly involved in binding of Raf but appeared to contribute to selectivity of binding (Nassar, Horn et al. 1995). The effector binding region of Ras, termed the Raf-Binding Domain (RBD), residues 51-131, interacts with the Raf molecule via a mechanism involving formation of antiparallel β sheets (Scheffler, Waugh et al. 1994; Herrmann, Martin et al. 1995; Nassar, Horn et al. 1995). Affinity studies show that the affinity of the RBD of Raf to GTP-bound Ras is 1000 fold higher than to GDP-bound Ras (Herrmann, Martin et al. 1995) and allows translocation of the normally cytoplasmic Raf to the plasma membrane where phosphorylation possibly by non-receptor kinases, such as src, takes place. In this way GTP-bound Ras acts as a membrane-anchor for Raf (Leevers, Paterson et al. 1994; Stokoe, Macdonald et al. 1994). However the process of Raf activation is more complex and may involve several other proteins, in particular 14-3-3 protein which also regulates Raf activity (Li, Janosch et al. 1995; Luo, Zhang et al. 1995). The process of Raf activation is now thought to involve both dephosphorylation and phosphorylation of target residues. Active Ras displaces 14-3-3 from its binding site, via dephosphorylation of a phosphoserine residue by protein phospahatase 2A, to allow membrane localization (Jaumot and Hancock 2001; Kubicek, Pacher et al. 2002). Accumulation of Raf to the plasma membrane and subsequent phosphorylation leads to a marked increase in the molecule's own kinase properties with the major phosphorylation sites identified forming a high affinity MEK-binding epitope (Marais, Light et al. 1995; King, Sun et al. 1998; Xiang, Zang et al. 2002). The activation of Raf following Ras-GTP binding is the first step of the well-recognized mitogen-activated protein kinase (MAPK) signalling cascade (Figure 1.10). Once activated, Raf (or MAPK kinase kinase) phosphorylates two downstream MAPK kinases (also called MAP/Erk Kinase: MEK1 and MEK2) that subsequently phosphorylate tandem threonine and tyrosine residues in two downstream MAPK, also known as extracellular signal related kinases, Erk1 and Erk2 (Avruch, Zhang et al. 1994; Robinson and Cobb 1997). Activated ERK1/2 translocate to the cell nucleus where they phosphorylate and activate the family of E-twenty six (ETS) transcription factors including Elk-1 to induce gene expression (Deng and Karin 1994; Gille, Kortenjann et al. 1995; Janknecht, Ernst et al. 1995). Elk-1 is a ternary complex factor protein. Activation of Elk-1 and formation of a complex with the serum response

factor (SRF) at the serum response DNA element domain of many promoters of gene expression leads to induction of expression of immediate early genes such as c-fos. In addition ERK also phosphorylates c-Jun leading to activation of the AP1 transcription factor made up of fos-jun heterodimers (Yordy and Muise-Helmericks 2000). These pathways mediate such diverse functions as cell growth, proliferation, survival and differentiation, though the end cell response appears to depend not only on the cell type and the cellular context/environment but also on the intensity and duration of ERK activity (Weber, Raben et al. 1997; Woods, Parry et al. 1997; Kerkhoff and Rapp 1998; Xue, Murray et al. 2000).

Though the MAPK pathway is the best characterized of signalling pathways downstream to Ras, there are now an increasing number of other candidate effectors. These alternative signalling networks first became apparent when it was noted that certain point mutations of Ras within the effector domain led to an inability to bind Raf but were still able to exert biological effects within cells (Campbell, Khosravi-Far et al. 1998) and appear to have a far more complex relationship to Ras as compared to Raf/MEK/ERK pathway.

Phosphatidylinositol 3-kinase (PI3-K) is an important regulatory protein in cell signalling and has a vital role in the processes of cell growth, apoptosis and malignant transformation (Krasilnikov 2000). The enzyme consists of a regulatory p85 subunit and a catalytic p110 subunit. Upon stimulation the p85 subunit is recruited to the membrane while the p110 mediates phosphorylation of phosphoinositides at position three of the inositol ring (Kapeller and Cantley 1994). Ras has been shown to interact with the p110 subunit leading to an increase in PI3-kinase activity (Kodaki, Woscholski et al. 1994; Rodriguez-Viciana, Warne et al. 1994). This rise in PI3-kinase activity has been linked to protection from apoptosis via a protein kinase B/Akt (PKB/Akt) mechanism in epithelial cells (Khwaja, Rodriguez-Viciana et al. 1997). However the relationship between Ras and PI3-kinase is more complicated than a simple linear signaling pathway. Firstly there is data that shows that PI3-kinase may actually be responsible for activation of small GTP-binding proteins such as Rho and Rac, two members of the Ras GTPase superfamily (Reif, Nobes et al. 1996). Furthermore a subsequent study has indicated that PI3-kinase itself may be an activator of Ras (Hu, Klippel et al. 1995). The Ras-PI3-kinase relationship has yet to be clearly delineated.

On the basis that effector proteins are those that bind to Ras in a GTP-dependant manner, several other candidate proteins have been identified. These include Ral–Guanine nucleotide dissociation simulator (Ral-GDS), which acts as a guanine nucleotide exchange factor for the Ras-related GTPases RalA and RalB (Kikuchi, Demo et al. 1994). The exact functions of Ral GTPases have been elusive but they appear to be components of Src-mediated activation of phospholipase D (PLD) and subsequent lipid second messengers including diacylglycerol (Jiang, Luo et al. 1995). Furthermore there appears to be an association between Ral GTPases and the Rho network, which is involved in cytoskeleton regulation (Jullien-Flores, Dorseuil et al. 1995). In this way Ras binding of Ral-GDS may be the initial step in bridging Ras activation to Rho signalling via Ral GTPase and PLD. Ral may be involved in c-fos promoter regulation and contribute to regulation of cyclin D1 through activation of NF-κB and so be involved in mitogenesis and survival signalling (Murai, Ikeda et al. 1997; Henry, Moskalenko et al. 2000). Mitogen-activated protein kinase kinase kinase 1 (MEKK1) is a serine-threonine kinase that regulates the kinase pathway involving stress-activated protein kinase Jun-N-terminal kinase (JNK) and has been found to directly interact with Ras-GTP (Derijard, Hibi et al. 1994; Russell, Lange-Carter et al. 1995). JNK activation occurs in stressful environmental conditions such as UV radiation and heat and may also be activated in response to cytokines such as nerve growth factor and epidermal growth factor in a Ras-dependant manner (Minden, Lin et al. 1994). JNK cascade activation leads to phosphorylation and activation of c-jun transcription factor and is implicated in apoptosis, oncogenic transformation and inflammatory responses in various cell types (Hagemann and Blank 2001).

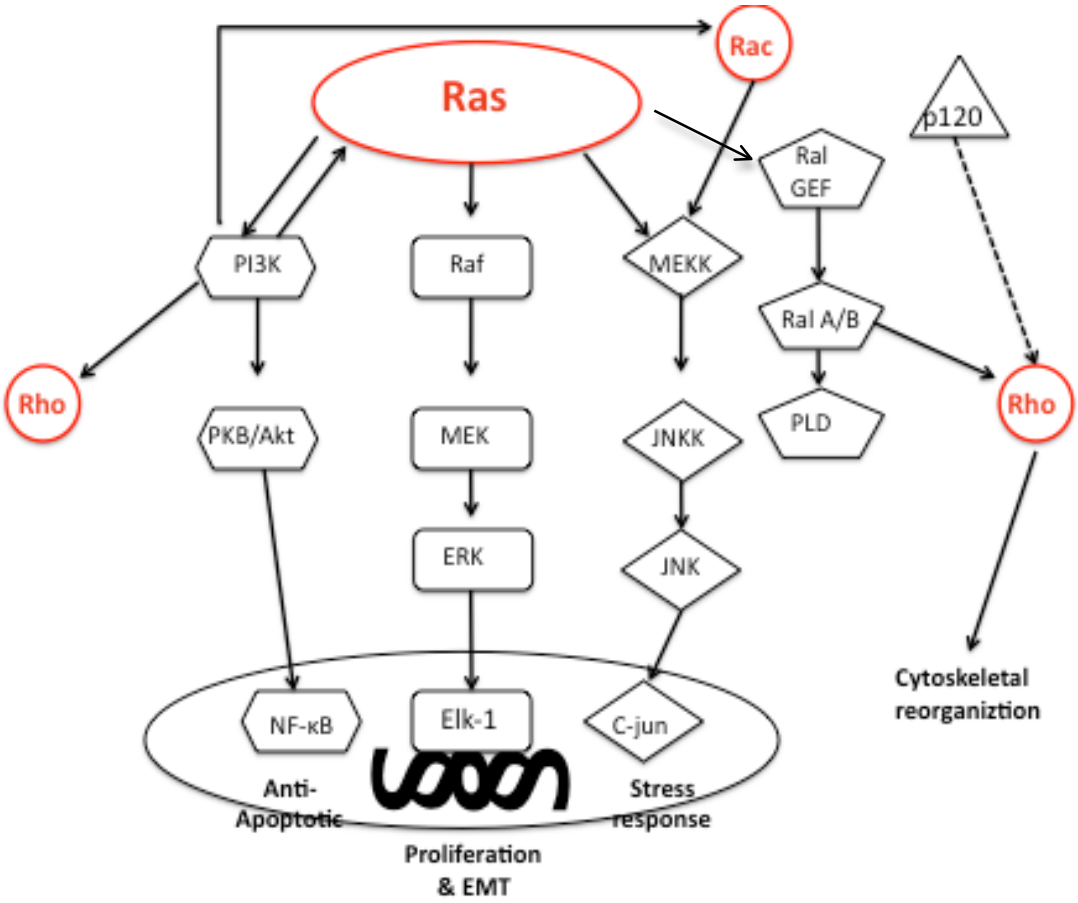

Figure 1.12: Ras effector pathways. Solid lines are activating and dashed are inhibiting actions. Members of the Ras superfamily are represented in red. Degree of activation of each phosphorylation cascade and the degree of cross-talk is dependent on initial stimulus.

1.7 Ras isoforms and differential cellular function

There is now increasing evidence that Ras isoforms may have distinct roles within the cell and the hypervariable region may be vital to this function. Firstly there is significant variation in the levels of expression of isoforms not only between tissues types but also at different time points of development in mice. Ha-*ras* transcripts are most highly expressed in the brain, muscle and skin while Ki-*ras* levels are highest in the gut, lung and thymus of mice (Leon, Guerrero et al. 1987). Furthermore during murine pre-natal development there is differential expression with time points: N-*ras* transcripts being highest at day 10 and Ki-*ras* lowest towards the end of gestation (Muller, Slamon et al. 1983). Though these findings suggest that the isoforms possess distinct cellular functions, at least in development, the fact that all three isoforms are

concurrently expressed in most murine and human tissues and share high degree of homology suggests that there may be a degree of functional overlap and potentially compensatory alterations in expression (Chesa, Rettig et al. 1987; Furth, Aldrich et al. 1987). Following the analysis of various human tumours it was found that 80% of pancreatic adenocarcinomas harboured a mutated Ki-*ras* gene while in acute myeloid leukaemia, N-*ras* was the most frequently mutated (Bos 1989). In addition it was found that different oncogenic isoforms of Ras resulted in different effects. In a mouse model of colon cancer Ki-Ras overexpression resulted in hyperproliferation of colonic epithelium. Though this was not observed with N-Ras overexpression, a resistance to apoptosis was demonstrated (Haigis, Kendall et al. 2008). More compelling evidence comes from the use of knockout mice. Knockout of N-Ras, Ha-Ras or the splice variant Ki(A)-Ras produced phenotypically normal mice (Umanoff, Edelmann et al. 1995; Esteban, Vicario-Abejon et al. 2001; Plowman, Williamson et al. 2003). However the absence of Ki-Ras, in particular Ki(B)-Ras variant, led to embryonic lethality with defects of haematopoeisis, myocardial cell proliferation and neuronal cell survival (Johnson, Greenbaum et al. 1997; Koera, Nakamura et al. 1997). However the relationship between Ras isoforms and development is more complex than this. Potenza et al. generated genetic mice in which Ki-Ras was replaced by Ha-Ras so that neither splice variant of the Ki-Ras protein was expressed. Unlike previous experiments involving null-Ki-Ras models, these mice reached adulthood with normal development during embryogenesis but did develop cardiomyopathy (Potenza, Vecchione et al. 2005). This study suggests that during embryogenesis there is a degree of redundancy in the roles of the isoforms yet specific Ras isoform functions are required for certain aspects of normal developmental homeostasis. Further support for specific roles of each isoform comes from the observation that Ha-Ras and Ki-Ras localize to distinct microdomains within the plasma membrane (Roy, Luetterforst et al. 1999). Ki-Ras is localized predominantly to the disordered plasma membrane, whereas Ha-Ras localizes mainly to the cholesterol-rich lipid rafts (Prior and Hancock 2001; Hancock 2003). Subsequently it has been shown that the different platforms within the plasma membrane in which the different isoforms of Ras reside may provide novel spatial and dynamic differences that Ras may utilize for differing signal transduction (Hancock and Parton 2005). In addition it was discovered that Ha-Ras and Ki-Ras signalling are differently dependent on the process of endocytosis (Roy, Wyse et al.

2002) with Ha-Ras, but not Ki-Ras, signalling through the Raf/MEK/MAPK cascade requiring endocytosis and endocytic recycling. Carozzi *et al.* also showed that a natural mutant of caveolin-3, C71W, specifically inhibited activated Ha-Ras signalling but not that by Ki-Ras thus indicating that different isoforms localizing to different microdomains provide different cell signals (Carozzi, Roy et al. 2002). Knockdown of Ha-Ras using antisense oligonucleotides (ASO) in mouse mesangial cells resulted in an increase in apoptosis not observed in ASOs to control, Ki-Ras or N-Ras. However in human mesangial cells, ASOs to both Ha-Ras and Ki-Ras but not N-Ras reduced proliferation but not apoptosis. This suggests not just a distinct role of isoforms but also a distinct role between species (Hendry, Khwaja et al. 2006). Within the kidney Kocher *et al.* showed distinct cellular distribution of Ras isoforms in samples of normal and diseased human kidney tissue. Using isoform specific monoclonal antibodies, staining for Ha-Ras and Ki-Ras was widespread but was absent in podocytes whereas N-Ras staining appeared to be localized to the collecting duct cells in normal kidney(Kocher, Moorhead et al. 2003)and the expression and distribution of each isoform differed significantly in diseased samples. The same group also employed immunogold labeling and EM to study Ras isoform distribution in normal human kidney samples and demonstrated distinct subcellular localization within the kidney. The affinity of Ras isoform for downstream effectors also differs. Studies have shown that activation of Raf was most efficient by Ki-Ras followed by N-Ras then Ha-Ras (Hamilton and Wolfman 1998; Voice, Klemke et al. 1999). However with regards to PI3K activation Ha-Ras was found to be more potent (Yan, Roy et al. 1998).

In conclusion Ras isoforms appear to have distinct subcellular distribution which may be related to the individual functional aspects of the isoform. The different isoforms appear to have distinct roles both in development and homeostasis that may also be related to this localization and the affinity of each isoform to downstream effectors. There appears to be a degree of redundancy or potential compensatory change between the three isoforms in certain circumstances but there is also a large body of evidence towards distinctive roles of each isoform especially with regards to renal disease.

1.8 Ras and TGFβ

Though Ras does not appear to be directly downstream of TGFβ there is now increasing evidence of crosstalk and interaction between the two signalling cascades. Atfi et al. used a prostate cancer cell line to show signals, initiated by receptor of TGFβ, could downregulate Src family kinases resulting in an accumulation of its substrate, non-phosphorylated SHC (Atfi, Drobetsky et al. 1994). The group postulates the decreased affinity of binding to the Grb/SOS complex may inhibit Ras activation. Other studies have shown a less direct link, with Ras pathway influencing the Smad signalling cascade downstream of TGFβ. Mulder demonstrated, in proliferating TGFβ-sensitive epithelial cells, that TGFβ signalling involved rapid activation of the Ras pathway for growth inhibitory effects and autoinduction and these effects involved the Ras-mediated phosphorylation of Smad 1 (Mulder 2000). However the role of Ras in TGFβ signalling appears to differ in transformed cells as well as in cell type. Overexpression of Ras in transformed lung epithelial cells conveyed a resistance to TGFβ (Kretzschmar, Doody et al. 1999). The constitutively active Ras cascade results in inhibition of nuclear accumulation of Smad 2 and Smad 3 and inhibition of transcriptional activation. This may explain the resistance to growth inhibitory response to TGFβ in oncogenic cells. Paradoxically the overexpression of Ras in renal mesangial cells promotes Smad 3-dependent processes including collagen I synthesis (Hayashida, Decaestecker et al. 2003). The reason for the differing response of sustained Erk activation between the different cell types is unknown.

In untransformed epithelial cells the administration of TGFβ has been observed to result in a transient activation of the Ras/MEK/Erk pathway (Mulder and Morris 1992). Crosstalk between the Ras and TGFβ pathways has also been demonstrated in mesangial and fibroblastic cells. Some of the TGFβ downstream effects in fibroblasts, including growth inhibition, have been shown to be Ras dependent (Hu, Shen et al. 1999; Kivinen and Laiho 1999). Martinez-Salgado et al. were also able to demonstrate involvement of Ras isoforms in TGFβ-induced proliferation and associated collagen and fibronectin synthesis using fibroblasts from double knockout (KO) Ha- and N-Ras mice (Martinez-Salgado, Fuentes-Calvo et al. 2006). Ras activity also appears to be involved in the expression of the TGFβ downstream effector molecule connective tissue growth factor (CTGF). Chen et al. showed that

CTGF expression in cultured mesangial cells required synergy between Smad and Ras/MEK/ERK signalling (Chen, Blom et al. 2002) while Leask et al. were able to demonstrate that Ras activation is of equal importance in TGFβ-induced CTGF expression in fibroblasts (Leask, Holmes et al. 2003). Leask's group further demonstrated both *in vitro* and *in vivo* that prostacyclin derivatives prevent the fibrotic response to TGFβ by inhibiting the Ras/MEK/ERK pathway. They further concluded that the Ras pathway did not directly affect Smad activity but may be of importance in a promoter-specific manner (Stratton, Rajkumar et al. 2002). Phanish et al. used antisense oligonucleotides to demonstrate that TGFβ-induced expression of CTGF in human proximal tubular epithelial cells was N-Ras dependent. The group also observed that N-Ras inhibition diminished TGFβ-autoinduction (Phanish, Wahab et al. 2005).

The growing interest in EMT has also led to further investigation into TGFβ activation of Ras especially in the field of cancer. Janda et al. examined the role of hyperactive Ras/MAPK pathway on TGFβ-induced EMT in a combined *in vitro/in vivo* carcinogenesis model of polarized Ha-Ras-transformed mammary epithelial cells (EpRas) (Janda, Lehmann et al. 2002). They concluded that a hyperactive Raf/MAPK pathway is required for 'full' EMT involving change in both phenotypic and cellular markers. In contrast TGFβ alone induces "scattering"-a spindle-like cell phenotype which is fully reversible after factor withdrawal and does not involve sustained marker changes. This suggests that EMT seems to be a close *in vitro* correlate of metastasis and requires synergism between TGFβ and Ras/Raf/MAPK signalling. The group also found that activation of phosphatidylinositol 3-kinase (PI3K) induces "scattering" and protects from TGFβ-induced apoptosis. The expression of the transcription factor Snail is also induced by TGFβ and subsequent overexpression represses E-cadherin expression and induces EMT (Peinado, Olmeda et al. 2007) while silencing of Snail, at least in tumour cells, reduces capacity for invasion by down regulating EMT (Olmeda, Jorda et al. 2007). Horiguchi et al. demonstrated that Snail is a key regulator of TGFβ-induced EMT in pancreatic tumor cells (Horiguchi, Shirakihara et al. 2009) and that Snail induction by TGFβ was highly dependent on co-operation with active Ras signals. Furthermore using Ki-Ras siRNA to silence Ki-Ras activity they were able to abolish Snail induction by TGFβ in pancreatic cancer Panc-1 cells. Safina et al. found that TGFβ induces EMT but limits cell migration and

motility by increasing cell-matrix adhesions. Conversely Ras hyperactivation does not appear to cause EMT per se but enhances cell migration through matrigel via a method of high molecular weight-tropomyosins suppression (Safina, Varga et al. 2009). Thus activated Ras alters the TGFβ response, conferring a tumorgenic and invasive potential to cells, a major aspect of EMT in metastases. Though the majority of investigations regarding TGFβ and Ras activation involve transformed cell lines there is now an increasing interest in this phenomenon outside the field of oncology. Xie et al. used both normal murine mammary gland (NMuMG) epithelial cells and mouse cortical tubule (MCT) epithelial cells to demonstrate increased gene expression of Ras, Raf, MEK1/2, and Erk1/2, as shown by microarray analysis and real-time polymerase chain reaction, in a model of TGFβ-induced EMT (Xie, Law et al. 2004). In a TGFβ 1-driven *in vitro* EMT model using primary human tubular epithelial cells (HUTEC), Campanaro et al. employed large-scale oligonucleotide microarrays, to show an excess of up-regulated proteins involved in biological processes, such as "morphogenesis", "cell fate determination" and "regulation of development" with the most up-regulated genes belonging to these categories. They found that Smad signalling was not the major effector for these genes but instead the RAS/MAPK signalling pathway seemed to be the main regulator involved in the cell cycle and proliferation/apoptosis (Campanaro, Picelli et al. 2007). Shimizu et al. have utilized siRNA against MAPK1 to demonstrate amelioration of glomerular disease in a murine model of lupus nephritis (Shimizu, Hori et al. 2010). As part of their studies they found that knockdown of MAPK1, a downstream effector molecule of Ras, significantly decreased TGFβ expression. More recently, one group has demonstrated a direct link between Ras signalling pathway and EMT. Bozic et al. showed that the glutamate receptor, N-methyl-D-aspartate (NMDAR), present on proximal epithelial cells was critical in maintaining the normal epithelial phenotype and modulating TGFβ-induced EMT in HK-2 cells (Bozic, de Rooij et al. 2011) and the mechanism of this antagonistic effect involves decreased activation of Ras-GTPase and subsequent inhibition of the Ras-MEK pathway. The group further demonstrated that administration of NMDA in UUO models significantly attenuated fibrosis. From these studies there appears to be increasing evidence for TGFβ and Ras crosstalk in EMT and possibly subsequent fibrogenesis.

1.9 Ras and Renal disease

There is a large body of evidence that supports a role for Ras and even individual isoforms of Ras in renal disease. Our group has previously employed ASOs to demonstrate that the pre-dominantly expressed isoform in human renal fibroblasts was Kirsten (95% of total Ras) (Sharpe, Dockrell et al. 1999) and that this Ras isoform played a pivotal role in EGF and serum-induced fibroblast proliferation. In addition, Ha-Ras, though expressed at a lower level than Ki-Ras, was also seen to contribute significantly towards fibroblast proliferation while N-Ras knockdown did not (Sharpe, Dockrell et al. 2000). Mesangial cell proliferation and subsequent matrix deposition has also been shown to be Ras dependant. An increase in membrane associated Ras was observed in the presence of mesangial cell proliferation induced by high glucose (Danesh, Sadeghi et al. 2002) while Chen *et al.* also found that in mesangial cells CTGF induction required Smad and Ras/MEK/ERK synergy (Chen, Blom et al. 2002). Furthermore there appears to be distinct roles for Ras isoforms in the homeostasis of mesangial cells (Hendry, Khwaja et al. 2006).

Further evidence for the role of Ras in renal disease is provided by studies inhibiting Ras and its downstream effectors. Farnesylthiosalicylic acid (FTS) is a compound that displaces prenylated Ras from its site of action at the plasma membrane. Khwaja *et al.* showed that FTS reduced PDGF-driven human mesangial cell proliferation but had no effect on serum induced proliferation despite both Ras and phospho-MAPK activation being inhibited in both conditions (Khwaja, Sharpe et al. 2005). Furthermore PDGF-stimulated activation of the survival protein Akt was inhibited by FTS while serum-stimulated activation of Akt was unaffected by FTS resulting in increased HMC apoptosis in the former condition. *In vivo* effects of FTS on the kidney have also been observed. In a rat model of Thy-1 nephritis an increase in glomerular expression of Ki-Ras and N-Ras isoforms was observed and was almost fully prevented by FTS. Intraperitoneal administration of FTS resulted in both a reduction of glomerular cellular proliferation and inflammation as well as a decrease in proteinuria by day 10 (Clarke, Kocher et al. 2003). These results indicate that this model of cytokine-driven glomerular cell proliferation and invasion is likely to involve Ras signalling pathways and Ras inactivation by FTS ameliorates this damage. Masterson *et al* used farnesyltransferase and geranylgeranyltransferase inhibitors (FTI and GGTI respectively) to target the post-translational process of prenylation of Ras. The group

reported a significant decrease in rat renal fibroblast proliferation and CTGF expression with both agents. However there was a far more significant decrease in collagen production with FTI while GGTI administration alone resulted in a decrease in collagen lattice contraction (Masterson, Kelynack et al. 2006). It is now recognized that Ras proteins (or at least the Kirsten and Neural isoforms) are preferentially farnyslated though, like Rho proteins, may be alternatively geranylgeranylated. This study indicates the distinct roles between these two members of the Ras superfamily.

Statins have also been used to target the prenylation pathway (Fried 2008). Inhibition of HMG-CoA reductase inhibits the first step of prenyl group formation and in this way reduces the degree of achievable Ras prenylation. These agents are known to be safe in humans and in various models of renal disease studies report an attenuation of progression of renal disease though the majority used doses of statin far greater than that administered in the clinical environment (Vrtovsnik, Couette et al. 1997; Yokota, O'Donnell et al. 2003; Li, Yang et al. 2004; Sabbatini, Pisani et al. 2004). Though the above studies all demonstrate an important role for Ras in renal disease progression the treatments are non-specific and have a generalized effect on all members of the Ras 'superfamily' of GTPases so one cannot delineate the actual role of the Ras proteins in disease. Furthermore they do not and cannot differentiate between the Ras isoforms, which are now thought to have distinct cellular roles.

Several studies have focused on the downstream effectors of the Ras superfamily and demonstrated a role for the Ras signalling pathway in renal disease. Choudhury *et al.* demonstrated the importance of both the MAPK and PI3K pathway in PDGF-driven mesangial cell proliferation (Choudhury, Karamitsos et al. 1997) while Xu et *al*. observed that the co-activation of Ki-Ras and Erk by advanced glycation end products in mesangial cells was PI3K-dependant (Xu and Kyriakis 2003). Rodriguez-Pena *et al.* reported an increased ratio of activated Ras and increased levels of phosphorylated ERK 1/2 and Akt/PKB in a model of unilateral ureteric obstruction (Rodriguez-Pena, Grande et al. 2008) Inhibition of these downstream effectors resulted in a decrease of myofibroblastic phenotype, fibroblast proliferation and matrix deposition indicating a role for Ras in tubulointerstitial fibrosis.

However only in 2010, a direct link between Ras activation and renal fibrogenesis has been conclusively demonstrated by a seminal paper from the group of Michael Zeisberg (Bechtel, McGoohan et al., 2010). The group elegantly demonstrated that hypermethylation of *RASAL1* gene, resulting in the decreased expression of the Ras

GAP RASAL1, correlated with Ras hyperactivity and a subsequent increase in fibrosis in a number of murine models of renal fibrosis. They also demonstrated that the administration of FTS significantly reduced fibrosis when compared to control groups though this was thought to be by a RASAL1 hypermethylation-independent mechanism. The group concludes that "hyperactive Ras contributes to fibroblast activation and fibrosis" and "that the antifibrotic capacity of Ras inhibitors should be further explored."

1.10 RNA interference and Gene silencing

The term gene therapy was conceived in the 1980s and originally referred to the insertion of a 'normal' functioning gene into a cell that possessed a defective form of the gene. However more recently a subset of gene therapy has developed which involves the inactivation of specific genes that are involved in disease process. This strategy has been termed 'Gene Silencing'. Now the human genome has been mapped this technique offers huge potential for research into elucidating gene function and pathways of cellular signalling. The two methods of gene silencing that have been most widely used are: Antisense oligodeoxynucleotides (ASO) and short-interfering RNA (siRNA) also known as RNA interference (RNAi). The mechanism of action of siRNA was determined by Fire & Mello in 1998 (Fire, Xu et al. 1998). It involves the initial cleavage of double stranded RNA by the enzyme Dicer into short RNA duplexes which are incorporated into a ribonucleoprotein-endonuclease complex termed 'RNA Induced Silencing Complex' (RISC). Once incorporated into RISC, the antisense strand of unwound siRNA binds to the specific endogenous RNA target sequence. The target RNA transcript is then bound and degraded by endonulease activity of RISC. The precise mechanism of target RNA recognition and degradation by RISC remains unclear. However the use of siRNA has been shown to be over ten times more potent than either sense or antisense RNA use alone and has been proved to be a powerful tool for target mRNA knockdown *in vitro*. The major problems associated with the use of this technology have been related to short half-life, efficiency of transfection and side effects, especially involving interferon mediated systemic inflammatory responses, their use *in vivo* has been restricted though it appears only a matter of time before these obstacles are overcome (Fire 2007; Wang, Hendry et al. 2008).

Zamecnick and Stephenson were the first to recognize the potential of ASO in 1978 when studying inhibition of Rous sarcoma virus replication (Stephenson and Zamecnik 1978). Since then antisense technology has developed into a powerful research tool and has begun to make its mark in the world of clinical therapy.

ASO consist of a single strand of 12 to 22 oligodeoxynucleotides which are complementary to the target mRNA sequence (Loke, Stein et al. 1989). Binding of the ASO to target mRNA transcript via Watson-Crick hybridization results in steric inhibition of translation by the ribosomal complex but more importantly the induction of RNase H, which cleaves the 3'-O-P-bond of the RNA molecule (Figure 1.13). This mechanism of action theoretically provides 100% specificity for the target gene; an unachievable goal for most conventional pharmacological agents.

Since the 1970s ASO have been used widely as research tools used to investigate mechanisms of disease pathogenesis *in vitro*, particularly in the field of nephrology. The use of ASO to target the kidney *in vivo* has been both challenging and highly rewarding. Unmodified, single-stranded oligonucleotides are rapidly broken down in serum by endogenous nucleases greatly limiting cellular uptake. To overcome this, ASO have a modification of the phosphate backbone whereby non-bridging oxygen molecules are replaced by sulphur molecules, greatly enhancing resistance to nuclease activity. These phosphorothioate ASO have a half-life in serum in the region of 10 hours (in comparison to 30-60 minutes of unmodified forms) and, following parenteral administration, have a systemic bioavailability as high as 90% (Crooke and Bennett 1996). Further modifications of the sugar-phosphate backbone of the oligonucleotides can be made to increase their stability and RNA affinity without compromising binding selectivity. Unfortunately, complete 2'-O-modification of the molecule results in the loss of its ability to activate RNAase H. This has led to the development of chimeric oligonucleotides or 'Gapmers' that are formed by combining 2'-O-modified oligonucleotides with regions of 2'-deoxy phosphorothioates. The resulting second generation ASO supports both RNAase H activity and demonstrates enhanced nuclease resistance and RNA affinity. Following parenteral administration, these ASO distribute to all peripheral tissues with the highest accumulation being in the liver and kidneys, which have a concentration ratio to plasma of 20:1 and 80:1 respectively after 2 hr (Sands, Gorey-Feret et al. 1994). Within the kidney ASO are filtered freely by the glomerulus and reabsorbed by proximal tubule epithelial cells (Rappaport, Hanss et al. 1995) making antisense

technology a very attractive tool for the investigation and possibly treatment of renal disease.

Although some animal studies have shown that ASO infusions may lead to complement cascade activation (Levin 1999; Farman and Kornbrust 2003), these effects appear to be both dose-dependent and related to rate of administration. Subsequent clinical studies using lower doses of ASO have reported minimal toxic effects. Furthermore subsequent generations of ASO have lower toxicity profiles (Jason, Koropatnick et al. 2004). There has therefore been much interest in pushing forward ASO for clinical therapy. Although currently there is only one ASO licensed for clinical use, Formivirsen (Vitravene®) for AIDS-related CMV retinitis, numerous others are in Phase 2 of clinical development such as ASO to ApoB-100 for the treatment of hypercholesterolaemia, ASO to ICAM-1 in ulcerative colitis and many others. With the publication by Tillman *et al* demonstrating efficacy of oral delivery of ASO in man (Tillman, Geary et al. 2008), comes the potential that this form of gene therapy becoming part of the normal repertoire of therapeutic options open to the physician in the mid to long term future.

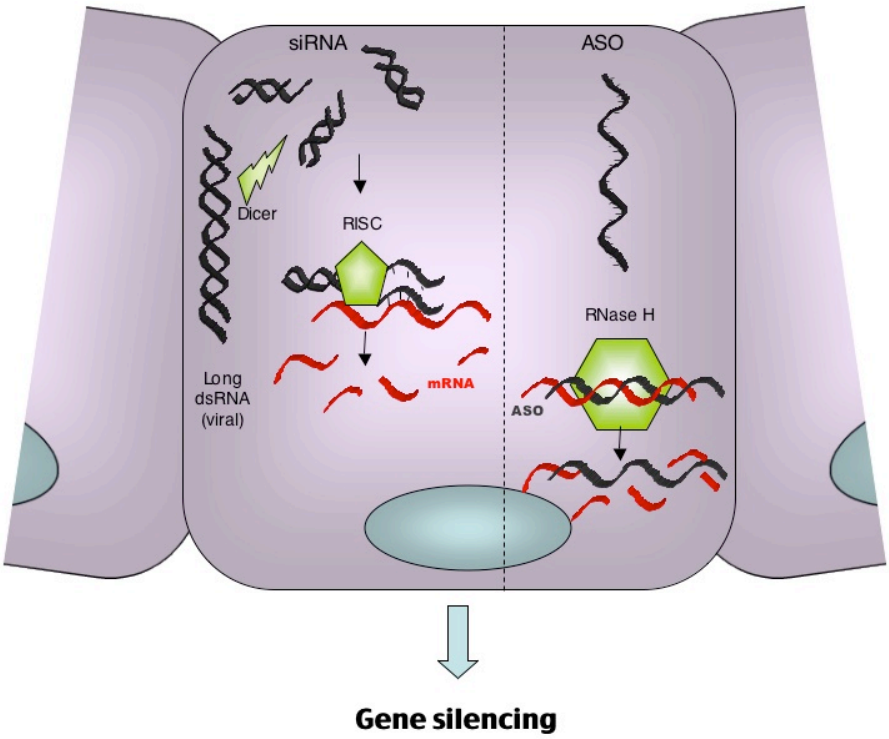

Figure 1.13: Mechanisms of action of siRNA and antisense oligonucleotides (ASO). (Figure from Wang, 2008). Targeted RNA silencing by siRNA is via incorporation into RNA Induced Silencing Complex (RISC) and antisense via RNAse H degradation to target-ASO duplex molecule.

For the purpose of this project and its translational aspect, ASOs have several advantages over siRNA. They have a much longer half-life, are being used at present in a clinical setting and have been proven to be both safe and efficient *in vivo*. Furthermore with regards to renal disease ASOs concentrate in the PTECs of the kidney and so can be seen to be a renal targeting therapy.

1.11 Aims of project

The potential importance of Ras in renal fibrosis has been described above. Our group has previously demonstrated that Ki-Ras is pivotal to renal fibroblast proliferation *in vitro*. Targeting this isoform may ameliorate renal fibrosis. This project aims to further this work by studying the effects of Ki-Ras inhibition with antisense oligonucleotides in a rat model of renal fibrosis induced by unilateral ureteric obstruction.

The specific aims of this project are:

1) To validate the efficacy and specificity of Ki-Ras antisense oligonucleotides *in vitro* in both rat renal fibroblasts and tubular epithelial cells.
2) To develop a model of renal interstitial fibrosis secondary to unilateral ureteric obstruction.
3) To characterise Ras isoform expression within the normal rat kidney and in a rat model of unilateral ureteric obstruction.
4) To determine the effects both in renal and extra-renal tissue of Ki-Ras inhibition by antisense oligonucleotides in a rat model of renal fibrosis.

Chapter 2: Methods and Materials

2.1 Cell culture & passage

Cells were plated and grown in 75cm^2 flasks containing DMEM medium (Gibco) supplemented with penicillin (100IU/ml), streptomycin (100μg/ml), amphotericin (2.5μg/ml) and fetal calf serum (FCS) (Sigma) to give a final concentration of 5-10% FCS by volume. Flasks were incubated in Techne incubators set at 37ºC with 95% O_2 and 5% CO_2. Primary cultures and commercial cell lines were grown in separate incubators. For the purposes of passaging, cells were grown to 70% confluence and washed twice in phosphate-buffered saline (PBS) prior to incubation at 37ºC for five minutes with 1ml of 1x Trypsin-EDTA (Life-Technologies, Paisley, UK). Trypsin was neutralised by re-suspending released cells in 10% FCS/DMEM. For experiments, cells were sub-cultured into either 35mm or 100mm diameter dishes. Only cells of at least three passages were used in experiments.

2.2 Primary culture of adult rat fibroblasts

Kidneys harvested from PVG (Piebald Virol Glaxo) rats were kindly donated by Dr Greta Sawyer, King's College London. PVG rats are inbred to provide a genetic background for production of congenic resistance to autoimmune thyroiditis and allergic encephalitis. The technique of retrieval and culturing of fibroblasts was adapted from a previously published protocol (Johnson, Saunders et al. 1998) and has been previously used in our laboratories. The freshly harvested rat kidneys were placed in a 100mm dish of sterile ice-cold Hank's Balanced Salt solution (HBSS) and decapsulated using forceps. The cortex was removed using scissors and the medulla disposed of. The shaven cortex was further 'minced' under sterile conditions and washed in HBSS to remove any remaining blood. Excess HBSS was removed and the kidney cortex 'mince' was re-suspended in 50-100ml Collagenase XI solution (0.5mg/ml made up in HBSS). The suspension was placed in a water bath at 37ºC for 30-40 minutes and a magnetic sterile stirrer was used to aid enzymatic digestion. The digestion process was terminated by the addition of an equal volume of ice-cold 2% FCS/HBSS solution. The suspension was decanted into a sterile 50ml falcon tube, with any residual cortex discarded, then centrifuged at 1000G at 4ºC for 5 minutes. The supernatant was discarded and the pellet re-suspended in 50ml ice-cold 2%

FCS/HBSS and re-spun at 1000G at 4ºC for 5minutes. The supernatant was disposed of and pellet retained. The pellet was then re-suspended in 30ml sterile 50% Percoll solution (50% Percoll/50% HBSS containing mannitol (0.82g in 30ml Percoll/HBSS solution pH7) and centrifuged at 30,000G at 4ºC for 30 minutes to create a density gradient. In an accompanying falcon tube density beads in an identical 50% Percoll solution were used as a reference for density distribution. Following centrifugation, the cellular layer in the sample correlating to the top band (F1) layer of density beads were harvested and re-suspended in a new sterile falcon tube in 50ml of DMEM/10%FCS medium and centrifuged at 1000G at 4ºC for 5 minutes. The supernatant was removed and pellet re-suspended again in medium and again centrifuged at 1000G at 4ºC for 5minutes. The supernatant was disposed off and the remaining pellet weighed. The pellet was then once again re-suspended in medium in a volume sufficient to allow plating of 100mg of cellular material per 100mm dish. These initial plated cells were allowed to attach for 2 days before medium was changed. After 10 days growth, cells were trypsinized and replated. Following two passages, cultures of cells were phenotypically fibroblastic in 95% of cases.

2.3 Commercial cell lines

Normal adult rat fibroblast (NRK-49F) and epithelial (NRK-52E) cells were obtained from the European Collection of Cell Cultures (ECACC no: 86101301 and 87012902 respectively). Cells were resuscitated according to accepted guidelines and sub-cultured 1:10-1:20 when grown to 70-80% confluence. Only cells that had undergone at least three passages were utilized in experiments. These cells were employed in this project as they were seen to as closely mimic as possible ‘normal’ rat renal cells physiologically and with regards to response to treatment.

2.4 Antisense Oligonucleotides

Antisense oligonucleotides (ASOs) were supplied by ISIS Pharmaceuticals, Carlsbad, California. In total, six different oligonucleotides were used throughout the duration of this project: two targeting Ki-Ras in the rat (ASO 1 and ASO 2) and four as control. Two of the controls (CO 1 and CO 2) have no recognised target in the rat, while the other two are scrambled oligos of ASO 1 and ASO 2, named SO 1 and SO 2 respectively. All were 20-mer second generation gapmers consisting of a ten nucleotide phosphorothioate backbone with the addition of five 2'-methoxyethyl modified nucleotides at either end. These alterations provide resistance against degradation and decreased toxicity while maintaining a high target binding affinity in comparison to non-modified oligos. Table 2.1 summarises the properties of each oligo including the NIH accession number of the target gene when base sequence is interrogated.

TARGET	ISIS NUMBER	SEQUENCE [5'→3']	NIH ACCESSION NUMBER OF TARGET
Ki-Ras (ASO 1)	104440	ATTCACATGACTATACACCT	BC126086 NM_031515
Ki-Ras (ASO 2)	104419	CACACTTATTCCCTACTAGG	BC126086.1 NM031515.3
Human HIV promoter sequence (CO 1)	15167	TCAGTAATAGCCCCACATGG	AC145070.10 AL139296.4
CO 2	141923	CCTTCCCTGAAGGTTCCTCC	CP000855.1 NG_000008.7
SO 1 (Scramble of ASO 1)	417230	ATTAACACGCCTACATACTT	EF363480.1
SO 2 (Scramble of ASO 2)	417226	CCCACTAAATCCGTTCTATG	NM_148126.3

Table 2.1: Oligonucleotides employed in project

2.5 *In vitro* transfection of oligonucleotides

Methods of cell transfection with oligonucleotides varied depending on cell type used. Initially oligonucleotides were diluted with OptiMEM (Gibco BRL, Life Technologies Paisley, UK) to form a 10μM stock.

Primary cell cultures and NRK-49F cell lines: Cells were grown in 100mm dishes to a confluence of 50-70% and washed with PBS prior to transfection. Oligos were transfected into cells using a cationic liposomal system, either Lipofectin or Oligofectamine (Invitrogen).

For Lipofectin, 1.25μl of Lipofectin per 100nM oligo per 100μl final transfection volume was used as advised by ISIS and as for previous published protocol (Sharpe, Dockrell et al. 1999). The final volume for a 100mm dish was 2ml with a final oligo concentration of 200nM. To ensure maximum transfection efficiency an initial solution of Lipofectin in five-times its volume of Opti-MEM transfection medium was vortexed and incubated at room temperature for 45 minutes. The appropriate amount of oligo was then added to this solution and left at room temperature for a further 15 minutes before being made up to its final volume with Opti-MEM and added to the cells for transfection. In later experiments Oligofectamine liposomal transfection system (Invitrogen) was used as a result of literature stating higher efficiency of oligo transfection. For each 1ml of a final transfection volume, 4μl Oligofectamine was diluted in 15μl Opti-MEM and rota-mixed and allow to stand at room temperature for 10 minutes. Specific oligo was then added as required to achieve a final transfection concentration of 200nM-400nM. The solution was gently mixed and allowed to stand for 20 minutes at room temperature. Opti-MEM was then added to make a final transfection volume of 2 ml per 100mm dish.

Cells were incubated in transfection medium at 37ºC for 6-18 hours followed by immediate RNA extraction. For protein retrieval, cells were incubated in transfection medium at 37ºC for 18-20 hours followed by addition of 2% FCS/DMEM medium and allowed to grow for further 48 hours prior to lysis.

NRK-52E cell line: The normal rat renal epithelial cell line obtained from ECACC proved to be difficult to transfect using the standard protocol above. As a result an adaptation of the technique of "reverse transfection" using Lipofectamine LTX reagent (Invitrogen) was employed. Initially developed as a method of high-output analysis of genetic function in cells using microarray, it appears that cells may be

more receptive to transfection via the reverse as opposed to standard protocol (Erfle, Neumann et al. 2007). The basis of the process involves detachment of target cells that are then subsequently re-plated at higher cell density into a dish containing pre-prepared transfection complexes. The combination of increased cell:complex ratio and the cell detachment may increase efficiency of transfection. In summary, cells were grown to 80-90% confluence, washed twice in sterile PBS and 1ml of trypsin added and incubated at 37°C for 3-5mins with intermediate shaking to detach cells. They were then transferred and resuspended in 4mls 10% FCS/DMEM medium and centrifuged at room temperature for 5mins at 13000rpm. The supernatant was discarded and the cells were resuspended in 500µl of Opti-MEM. Transfection medium was made up using 6.25µl of Lipofectamine LTX for every 500µl Opti-MEM. Specific Oligo was added at a dose so that final transfection medium concentration would be 200nM. This solution was vortexed and stood at room temperature for 30min before being transferred to cell plate. The cell suspension was subsequently added to the transfection medium. For higher cell density, amalgamation of two dishes post-trypsin treatment was used. Final volume in our studies was 2ml in 100mm dish with a final oligo concentration of 200nM.

As for standard protocol, cells were incubated at 37ºC for 6-18 hours followed by immediate RNA extraction.

2.6 LDH Cytotoxicity assay

CytoTox 96 non-radioactive cytotoxicity assay (Promega) was used to assess the presence of cytotoxicity secondary to oligonucleotide transfection at varying concentrations. CO 1, ASO 1 and ASO 2 were used at concentrations of 50nM, 100nM, 200nM, 500nM and 1000nM. The protocol used was as according to manufacturer's instructions outlined as follows: for test samples, each well contained 50µl of approximately 5000 NRK-49F cells, 100µl of medium (10% FCS DMEM) and 50µl of Control Oligo/ASO in OptiMem (at 4x target concentration to allow for dilutional effect).

Baseline control wells were as follows:

a) Baseline: Culture Medium Only control (150µl Medium + 50µl OptiMem)

b) Baseline LDH Cell Release: Positive control (100µl Medium + 50µl OptiMem + 50µl of approximately 5000 NRK-49F cells)

c) Target Cell Volume Correction Control: (100µl Medium + 50µl OptiMem+ 50µl Lysis Buffer)

d) Target Cell Maximum LDH Release Positive control: (50µl Medium + 50µl OptiMem + 50µl Lysis Buffer +50µl of approximately 5000 NRK-49F cells).

Both control and test samples were run in quadruplet per plate. Once samples were plated they were incubated overnight at 37°C. Subsequently 45mins prior to harvesting supernatant 10µl of lysis solution (10x) was added per 100µl well volume to test samples, Target Cell Volume Correction Control samples and Target Cell Maximum LDH Release Positive Control samples. The plate was further incubated for 60mins then 50µl aliquots of supernatant from each well were transferred to a fresh 96 well plate. 50µl of activated substrate mix was added to each well. The plate was covered with foil to prevent light exposure and left at room temperature for 30 mins. 50µl of 'Stop Solution" was then added to each well to terminate enzymatic reactions. Any large bubbles in individual wells were popped with a sterile needle and the absorbance recorded at 492nm.All values were normalized for Baseline culture medium only control.

Absorbance for Maximum LDH release = (Target Cell Maximum LDH Release Positive Control -Target Cell Volume Correction Control).

Percentage cytotoxicity for each sample compared to non-treated cells was calculated as follows:

$$\% \text{ Cytotoxicity} = \frac{\text{Abs (sample)} - \text{Abs (Baseline LDH Cell Release)}}{\text{Abs (Maximum LDH release)}} \times 100$$

(Abs is absorbance at a wavelength of 492nm).

2.7 Total RNA isolation

All solutions were made up using water pre-treated with 0.1% diethyl pyrocarbonate (DEPC) (See Appendix I). All materials used in this section were either purchased pre-treated to be RNAse free or treated to be RNAse free using the following protocol:

a) Soak in 0.1M Sodium Hydroxide solution (made up with 0.1% DEPC water) for 60mins then,
b) Soak in 1mM EDTA solution (made up with 0.1% DEPC water) for 60mins then,
c) Soaked and rinsed in 0.1% DEPC water overnight

Bench surfaces were treated with RNAse-free spray (Qiagen) pre-procedure.

RNA isolation and purification was performed using a Qiagen RNeasy Mini kit. The principle involves initial lysis and homogenization of biological samples in the presence of highly denaturing chaotropic agent guanidine isothiocyanate (GITC) containing buffer that also inactivates RNases. Addition of ethanol provides optimal conditions for RNA to bind to the silica membrane of columns to allow for efficient removal of contaminants. Pure RNA can subsequently be eluted from the membrane using RNase free water. The process isolates RNA molecules longer than 200 nucleotides and excludes most RNA below this length (such as 5S RNA and tRNA), thus also providing enrichment of target mRNA.

From cell cultures: Cells grown on a monolayer were washed in PBS and total RNA extracted using the Qiagen RNeasy mini-kit® (Qiagen Ltd) using the manufacturer's protocol. This process involved direct lysis of cells by addition of 600µl of GITC lysis buffer to each 100mm cell dish followed by disruption of cell membranes by traumatic needle lysis. The cell lysates were then homogenized by passing through a QIAshredder® sitting in a 2ml-collection tube that was subsequently centrifuged at 15,000 rpm for 2 minutes. Equal volumes of 70% ethanol was added to the lysates and mixed by pipetting. Samples (upto 700µl) were then transferred to RNeasy spin columns for adsorption of RNA to RNA-binding MinElute membrane. Contaminants were removed by sequential spin washes in wash buffers and mRNA was eluted with 30-50µl of RNAse-free water per sample. RNA was stored at –80^{o}C.

For tissue samples: 30mg of sample was initially homogenized in 600µl lysis buffer using a Potter homogenizer. This suspension was then transferred to a QIAshredder and above protocol subsequently followed. Glassware and homogenizer were initially made RNase free by above protocol.

Quantification of the isolated RNA was achieved using a spectrophotometer. An absorbance of 1 unit at a wavelength of 260nm corresponds to 40µg of RNA per ml and all calculations were based on this. To determine purity, absorbance was also measured at 280nm. The A260:A280 ratio provides an estimate of purity with pure RNA having a ratio of 2. All samples used in this study had a ratio of 1.8-2.3. RNAse-free water was used for all dilutions of RNA samples for quantification. For later samples a Nanodrop 2000 spectrophotometer (Thermo Scientific) was used for RNA quantification. The principle of measurement is identical but far less volume of sample is used and the automated process reduces both operator and processing error while being technically easier.

2.8 Protein extraction

From cell cultures: Cell were washed twice in ice-cold PBS and then lysed by the addition of ice-cold PBSTDS lysis buffer containing protease inhibitors (1x PBS, 1% Triton-X 100, 0.5% sodium deoxycholate, 0.1% SDS, leupeptin 0.5µg/ml, pepstatin 1.0µg/ml, EDTA 1.0mM, PMSF 0.2mM). 1ml of PBSTDS lysis buffer was used per 100mm dish and 250µl per 35mm dish. Cells were left in lysis buffer on ice for 10 minutes then scraped off dish surface and transferred to an eppendorf tube on ice. Further traumatic cell lysis was achieved by pipetting cell suspension in eppendorf via a 22G needle and syringe. The lysate was left on ice for 30-40minutes prior to centrifugation at 13,000G for 20 minutes at 4^{o}C. The resulting cellular precipitate was discarded and the supernatant collected and stored at - 80^{o}C.

From tissue: This protocol was adapted from a published protocol (Yang and Liu 2002). 100-200mg of tissue was placed in a thick-bottomed glass tube containing 1ml PBSTDS lysis solution and homogenized using a potter homogenizer on ice for 30 seconds or until a homogenous suspension was obtained. The suspension was then transferred to an eppendorf on ice and further traumatic cell lysis was achieved via a 22G needle and syringe. Subsequent steps were identical to that of protein extraction from cell cultures as described above.

The concentration of protein was determined by a colorimetric protein assay (BCA Protein Assay kit, Pierce) based on the reactions:

1) Peptide + Cu^{2+} → Tetradentate- Cu^{1+} complex

2) Cu^{1+} + 2 Bicinchoninic Acid (BCA) →BCA-Cu^{1+} complex (purple)

Concentration of protein was read at a wavelength of 540nm at an absorbance of A_{562}. A standard curve for analysis was made using serial dilutions of Bovine Serum Albumin.

2.9 Semi-quantative PCR Primer design

Semi-quantative polymerase chain reaction (SQ-PCR) primer pairs targeting the isoforms of Ras in the rat were designed initially by studying the cDNA sequences provided by the National Center for Biotechnology Information GenBank using the Basic Local Alignment Search Tool (BLAST). Using these as source sequences for the 'Primer 3' web based design program (Massachusetts Institute of Technology) optimum primer pair sequences were suggested. Selected primer sequences were 17-20 base pairs in length, at least 50% G-C rich, were non-palindromic and had similar melting temperature to it's opposite pair. The selected sequences were then re-analysed using BLAST to confirm specificity of primer to target product. Primers were purchased from Genosys based on the following template.

Gene	Accession Number	Primer Sequence (5'-3')	Product Length (bp)	Melting Temp. (ºC)
Ki-Ras	NM_031515	F:AGAGTGCCTTGACGATACAGC R: TCCCTCATTGCACTGTACTCC	159	63.3 64.0
N-Ras	NM_080766	F: AAGCGGGTGAAAGACTCTGA R: CATCCGGTACTGGCGTATCT	204	63.9 63.7
Ha-Ras	BC099130	F: TGCCATCAACAACACCAAGT R: TAGAAGGCATCCTCCACACC	224	64.1 64.0
β-Actin	NM_031144	F: CCCACACTGTGCCCATC R: TGATCCACATCTGCTGGA	593	64.0 63.9

Table 2.2: SQ-PCR primer pair sequences

2.10 Semi-Quantative [Standard] PCR (SQ-PCR)

The single step system Promega's Access SQ-PCR kit (Promega, Southampton, UK) was used for semi-quantative PCR analysis of sample RNA. This allows both reverse transcription and DNA amplification to occur in a single test tube and so minimizes pippetting errors and contamination. The kit uses thermosensitive AMV reverse transcriptase (AMV-RT) from Avian Myeloblastosis Virus for first strand DNA synthesis, and the thermostable Tfl DNA Polymerase from Thermus flavus for second strand cDNA synthesis and amplification. The Access SQ-PCR System buffer permits activity of both polymerases therefore negating the need for buffer additions between the reverse transcription and PCR amplification steps. AMV reverse transcriptase works at 48°C which minimizes problems encountered with secondary structures in RNA.

In all SQ-PCR reactions 0.5µg of total RNA and 50pmol of each primer was used. The number of nanograms of primer in 50pmol was derived from the following formula: 50pmol=16.3ng x b (where b= number of bases in the primer).

Each tube contains a final volume of 50µl reaction mixture consisting of:

10µl AMV/Tfl 5x reaction buffer

2µl Magnesium Sulphate (25mM)

1µl AMV RT

1µl Tfl DNA polymerase

1µl dNTP mix (10mM each dNTP)

1µl Upstream Ras primer (50µM)

1µl Downstream Ras primer (50µM)

1µl Upstream β-actin primer (50µM)

1µl Downstream β-actin primer (50µM)

10µl Total RNA sample (1pg-1µg total RNA)

21µl Nuclease free water

Magnesium is required as a co-factor for both AMV transcriptase and Tfl DNA polymerase. β-actin was used as an internal control.

The reaction protocol is outlined below:

First strand cDNA synthesis

1 cycle	48°C for 45mins	Reverse transcription

↓

1 cycle	94°C for 2mins	AMV RT inactivation RNA/cDNA/Primer denaturation

↓

Second strand cDNA synthesis and PCR amplification

27-40 cycles	94°C for 30sec	Denaturation
	56-59°C for 1min	Annealing
	68°C for 2mins	Extension

↓

1 cycle	68°C for 7mins	Final extension

↓

1 cycle	4°C	Soak

Figure 2.1: Semi-quantative PCR reaction protocol.

The annealing temperature for each reaction was calculated at 4-5^{o}C below the melting temperature of each primer and averaged between the forward and reverse primer. For initial detection of Ras isoform mRNA, maximum amplification using 40 cycles of PCR was used. However, in order to assess the effects of the ASOs on mRNA levels a semi-quantitative approach was needed. To achieve this, the exponential phase of the amplification reaction was determined by varying the cycle number from 20 to 35. Cycle numbers 22 to 30 were demonstrated to be in the exponential phase for Ras products. To minimize pipetting error and allow quantification by comparison, an internal standard was used in the form of β-actin mRNA. This form of RNA is relatively stable in cells regardless of experimental conditions. 20% of the final reaction product volumes were analysed on a 1.5% agarose gel containing 1μl/100ml ethidium bromide. TAE buffer containing

1µl/100ml ethidium bromide was used for electrophoresis. A 50bp DNA Step ladder (Promega, G452A) was used as a product size marker. The gel was subsequently viewed in a UV light box.

2.11 Real-Time (Quantitative)-Polymerase chain reaction (QPCR)

There are several advantages of QPCR compared to traditional SQ-PCR. The process of PCR consists of three main phases: Exponential, Linear and Plateau. During the exponential phase PCR is efficient, specific and precise and slows through linear phase before stopping in plateau phase. Ideally samples should be analysed in the exponential phase of PCR where differences between samples are amplified compared as opposed to plateau phase. Furthermore end-point results for SQ-PCR are obtained from running samples on an agrose gel with ethidium bromide. Gel resolution may be poor thus making it difficult to differentiate changes below 5-10 fold. The use of a loading control is required to normalize the starting copy number of each target in each sample but may further add operator and interpretation error. Furthermore the use of ethidium bromide does not provide a quantative, numerical result. As opposed to SQ-PCR, QPCR allows for the monitoring of PCR as it occurs so reactions are characterized by the point during cycling when amplification of target is first detected rather than the amount of target that has accumulated after a set number of cycles thus ensuring PCR is analysed in exponential phase. Compared to SQ-PCR, QPCR is far less time consuming, has fewer practical techniques thus reducing operator error, is highly sensitive as analyses samples in exponential phase and allows detection of a two-fold change and provides a numerical interpretable result. QPCR in this project employed TaqMan chemistry (Applied Biosystems).

TaqMan chemistry: The TaqMan sequence detection system developed by Applied Biosystems utilizes a fluorgenic probe and the 5' nuclease activity of Taq DNA polymerase. The system allows the detection of a specific PCR product as it accumulates during PCR-that is in "real time".

Step Process

1. An oligonucleotide probe is constructed containing a reporter fluorescent dye on the 5´ end and a quencher dye on the 3´ end. While the probe is intact, the proximity of the quencher dye greatly reduces the fluorescence emitted by the reporter dye by fluorescence resonance energy transfer (FRET) through space.
2. If the target sequence is present, the probe anneals downstream from one of the primer sites and is cleaved by the 5´ nuclease activity of Taq DNA polymerase as this primer is extended.
3. This cleavage of the probe:

. • Separates the reporter dye from the quencher dye, increasing the reporter dye signal.

. • Removes the probe from the target strand, allowing primer extension to continue to the end of the template strand. Thus, inclusion of the probe does not inhibit the overall PCR process.

4. Additional reporter dye molecules are cleaved from their respective probes with each cycle, resulting in an increase in fluorescence intensity proportional to the amount of amplicon produced.

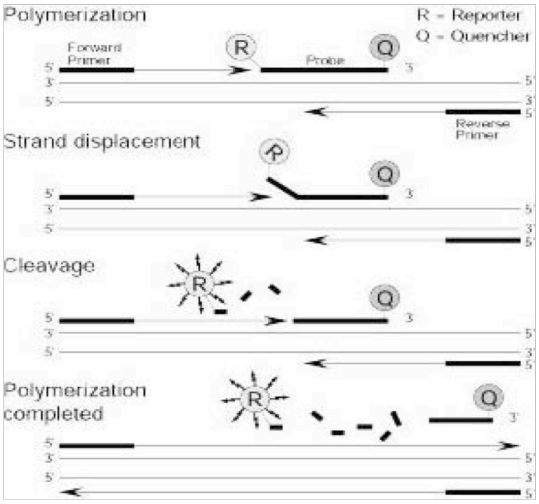

Figure 2.2: Summary of the Taqman sequence detection system (from "Essentials of Real Time PCR", Applied Biosystems). R, reporter dye, Q, quencher dye.

Quantitation assay: Quantitation of target in QPCR using TaqMan chemistry relies on the increase of fluorescence with each cycle of PCR. Initially there is little change in fluorescent signal and this defines the baseline for the amplification plot. An increase above this baseline implies detection of accumulation of target. A fixed fluorescent threshold may be set above baseline. The fractional cycle number for which fluorescence reaches this threshold for any target is defined as the parameter Ct (threshold cycle).

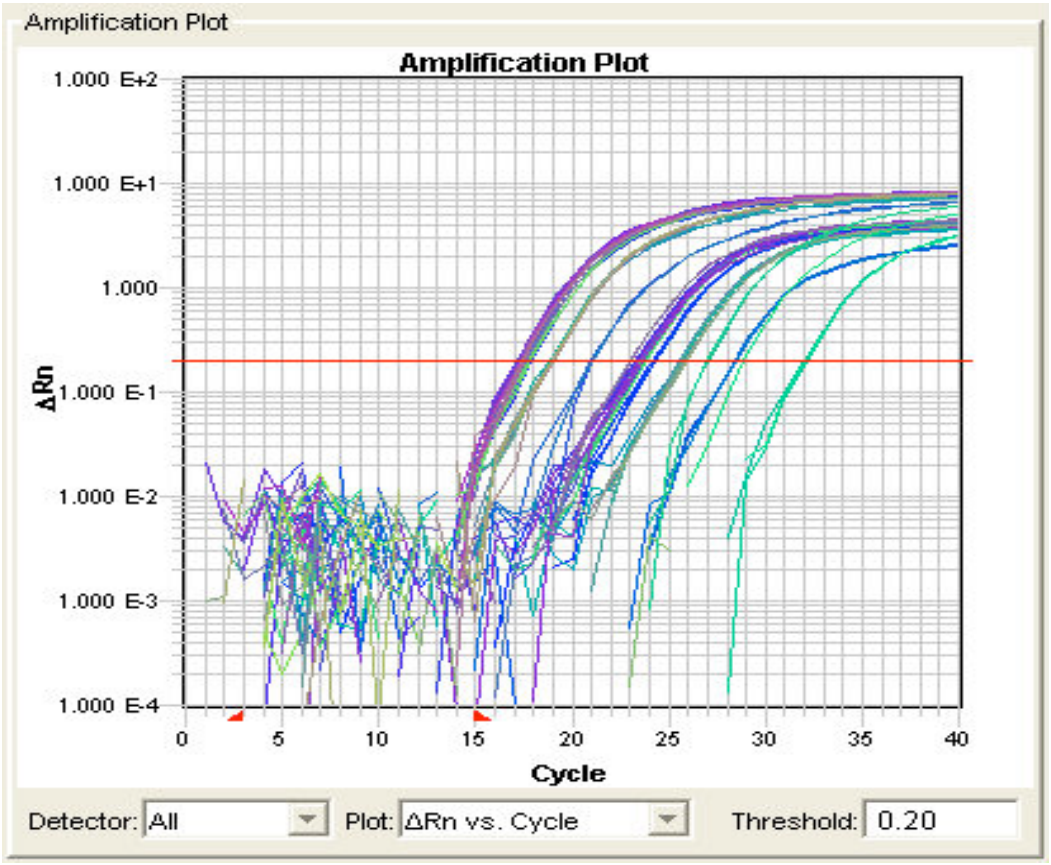

Figure 2.3: Amplification plot obtained by QPCR. Red line represents threshold from which Ct can be deduced.

Quantitation may be absolute or relative. The former involves determining values by use of a standard curve. Relative quantitation is used for analyzing changes in target expression between a given sample and a control sample and was utilized in this project using the comparative Ct method. The comparative Ct method of relative quatitation requires the measurement of an endogenous control gene in addition to target gene. One can standardize the amount of target gene to endogenous control gene for any given sample. Thereafter by comparing standardized values a relative quantitation of target between samples may be derived. The comparative Ct method has the benefit of eliminating need for a standard curve however it is necessary to assess the validity of the endogenous control. For this method to be valid the control gene must not significantly alter in experimental conditions and both target and control gene must have similar efficiency of amplification.

The arithmetic formula that is derived to give the amount of target, normalized to an endogenous control, in a sample and relative to a calibrator sample is

$$2^{-\Delta\Delta Ct}$$

where ΔΔCt is the difference between the normalized values of target Ct between sample and calibrator sample.

QPCR in this project was a two-step process involving initial reverse transcription and then subsequent measurement of target cDNA.

Reverse Transcription step

Reverse transcription of total RNA was performed using Omniscript kit (Qiagen) following product protocol. Oligo-dT (Qiagen, 82840865) was not included in the kit. Omniscript Reverse Transcriptase is a recombinant heterodimeric enzyme expressed in E. coli. An outline of the protocol per tube is below:

2 μl 10x Buffer RT

2 μl dNTP Mix (5 mM each dNTP)

2 μl Oligo-dT primer (10 μM)

1 μl per 20 μl reaction Omniscript Reverse Transcriptase

5μl RNA containing (50ng-2 μg RNA)

RNase-free water added to make a final volume of 20μl

The final 20μl reaction mixture was incubated at 37^{o}C for 1 hour. Following incubation mixture was diluted to 75-100μl volume with RNase-free water and used in QPCR or stored at -80°C.

QPCR Step

QPCR was performed on an ABI Prism 7900HT using the Applied Biosystems Taqman chemistry system. The housekeeping gene GAPDH was used as an endogenous control. QPCR was performed on 96 well and 384 well plates. Measurement of target and endogenous control levels for each sample was performed in triplicate. Each well consisted of the components as shown in Table 2.3:

Reagents	96 wells (Final volume of 25µl/well)	384 well (Final volume of 10µl/well)
(2x) Taqman Mastermix	12.5µl	5µl
Taqman Gene Expression Assay Primer (Final concentration 250nM)	1.75µl	0.7µl
Water	5.75µl	2.3µl
RT Product	5µl	2µl

Table 2.3: Taqman gene expression assay reagent volumes

Target	Accession Number	Assay ID	Product size (bp)
Ki-Ras	NM_031515	Rn00580460_m1	125
N-Ras	NM_080766	Rn00821645_g1	82
H-Ras	BC099130	Rn01479665_g1	106
GAPDH	NM_017008	Rn99999916_s1	87

Table 2.4: Taqman gene expression assay identification. TaqMan gene expression assays and TaqMan mastermix were purchased from Applied Biosystems. The process of QPCR was performed with an ABI Prism 7900HT. The thermal cycling conditions were as follows:

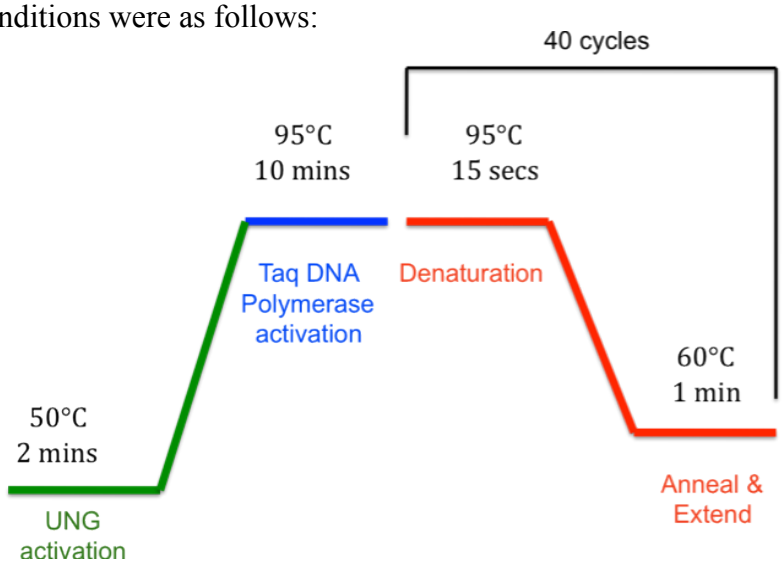

Figure 2.4: Taqman gene expression assay cycle

2.12 Validation of QPCR and reference control

Quantitative PCR allows the monitoring of the progress of PCR as it occurs so that data is collected throughout the process instead of at the end, as in semi-quantitative SQ-PCR, and allows for detection of changes as small as two-fold. Two step SQ-PCR using Taqman chemistry and the comparative (Ct) method of relative quantitation were employed in this project. In order for this method to be employed a suitable reference control is required.

Ideally when using the comparative (Ct) method of analysis, the Ct value for each gene target should be between 18 and 30 cycles, as this correlates to exponential phase of PCR, in addition to being of similar range with regards to Ct value of reference house-keeping or control gene. This avoids analysing samples that have either low abundance or supersaturation of target, both of which may lead to unreliable Ct values.

In addition the reference control gene target must be stable in the model of UUO, that is that their mRNA levels should not alter as a result of experimental conditions. The two gene reference controls that were examined were β-actin and GAPDH. Using kidney samples from three sham kidneys and five obstructed kidneys (12 days duration), the Ct value was compared for the two gene targets in samples standardized to 1μg total RNA.

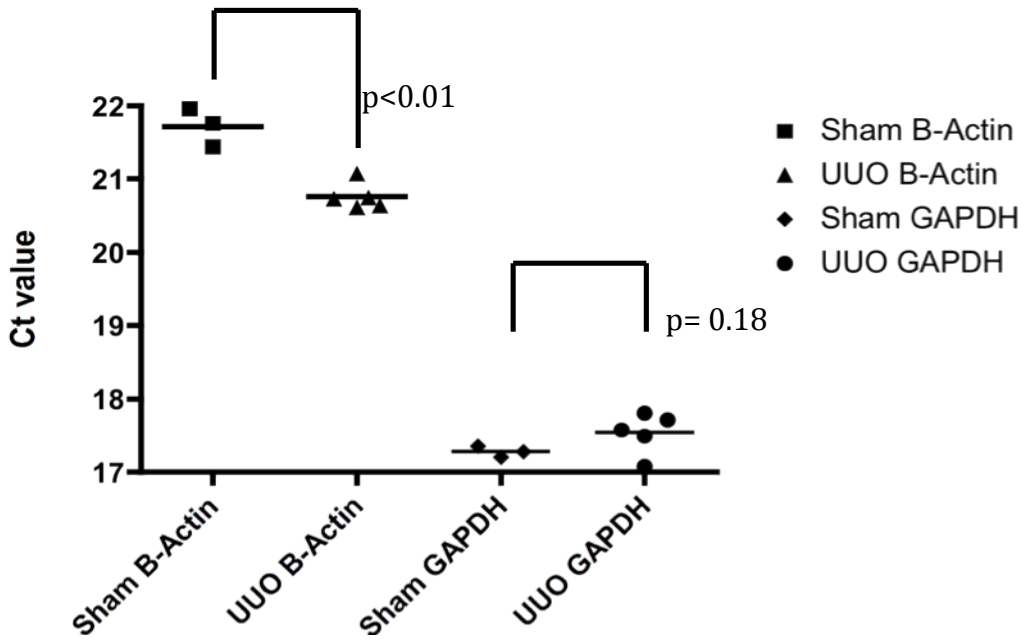

Figure 2.5: Ct values for β-actin and GAPDH in sham and obstructed samples standardised to 1μg total RNA.

From the above figure it appears that the Ct value of β-actin significantly falls, which translates to an increase in β-actin mRNA levels in the condition of experimental obstruction. GAPDH mRNA levels however appear to be stable in this setting when compared to sham. As a result GAPDH was used as the 'housekeeping' reference control gene target for QPCR. However it must be taken into consideration that the above validation of reference controls was completed in models of UUO at 12-days whereas majority of experimental groups were assessed at 16-days.

For calculations to be valid, the efficiency of target and reference amplification during QPCR must be approximately equal. A sensitive method of assessing this is by a calibration curve & observing how ΔCt varies with template dilution.

Serial dilutions of rat renal RNA obtained from two samples of whole kidney tissue was analysed for Ki-Ras and GAPDH levels.

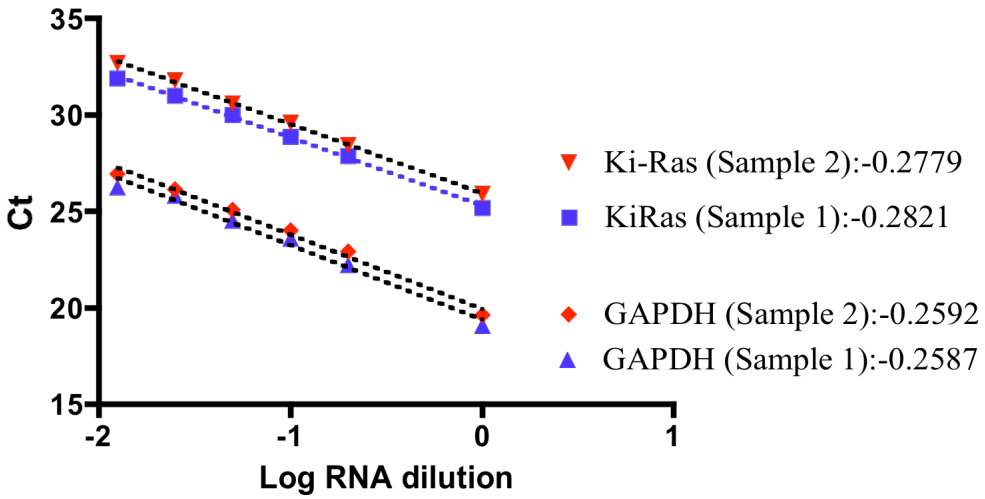

Figure 2.6: Graph of log of serial dilution of RNA obtained from whole rat kidney against absolute Ct cycle numbers. Results from two separate experiments. Slope of line of best-fit are shown along each lone of best-fit.

The above figure shows that the slope of corresponding Log RNA vs. Ct lines of regression of Ki Ras and GAPDH are near identical suggesting equivalent amplification.

PCR percentage efficiency can be determined by the formula:

$$10^{-1/\text{slope}} - 1 \times 100$$

From the above analysis, the mean PCR amplification efficiencies for Ki-Ras and GAPDH are similar at 91% and 82% respectively

To further validate the use GAPDH as a housekeeping gene reference for Ki-Ras comparative QPCR, ΔCt vs. Log RNA dilution was plotted (Figure 2.7). The slope in both cases is <0.1, which fulfils the required criteria for a pair of target and reference sequences to be used in comparative Ct method of QPCR.

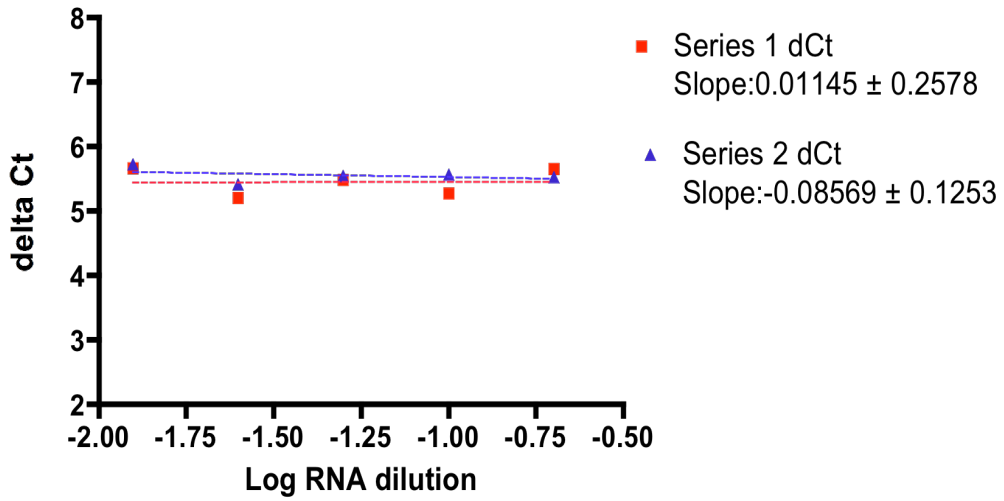

Figure 2.7: Plot of log input amount versus ΔC_t of serial dilution of rat kidney RNA.A summary of two separate experiments.

2.13 Western Blotting [Polyacrylamide Gel Electrophoresis]

Immunoprecipitation: Due to relatively low abundance of Ras within the cell, Ras was concentrated from crude protein lysates using immunoprecipitation. The total protein concentrations of cell lysates were assayed as previously described and equal amounts of total protein (0.5–1 mg) from each sample were used. All volumes were normalised to 1ml with PBSTDS. 15µl of anti-Ras-agarose conjugate (anti-v-H-Ras rat monoclonal antibody (Y13-259) agarose conjugate (OPO1A), Calbiochem) was added per ml volume of lysate and all samples were left rotating at 4°C overnight. Samples were then centrifuged at 2,500G at 4°C for 3 minutes and the supernatant discarded. The pellets were further re-suspended in 1ml of PBSTDS and centrifuged again as above before being washed in 1ml of PBS and again centrifuged as above. Following a further wash in 1ml of 50mM Tris solution (pH6.5) and centrifugation as above supernatant was discarded and the pellets were re-suspended in 40µl x3-4 western sample buffer containing 5% 2-mercaptoethanol and heated to 100°C for 3

minutes. The agarose beads were removed by pulse centrifugation for 15 sec and 30-35 µl of final supernatant was used for both mini and large gel SDS electrophoresis.

SDS polyacrylamide gel electrophoresis: For non-Ras proteins that are relatively abundant, immunoprecipitation was not required prior to western blotting. For these samples 10-20 µg of total protein was used per sample. A volume of 40µl x3-4 western sample buffer containing 5% 2-mercaptoethanol was added and final volume made up to 50 µl with PBSTDS. Each sample was heated to 100^{o}C for 3 minutes to fully denature the proteins. 30 µl of each sample was then loaded on to either a SDS polyacrylamide mini gel or loading gel. The gel concentrations used ranged from 8%, 10%, 12% or 15%. Both biotinylated and colour molecular weight markers were used as reference ladders. Mini-gels were run at a constant voltage of 200v for a period of time according to desired weight band of colour marker ('Colorburst', Sigma). Large resolving gels were run at a constant current of 70-80mAmps at ph6.8 for a duration according to colour marker for desired weight band of target.

Following electrophoresis, gels were blotted onto nitrocellulose membranes (Hybond-C, Amersham Biopscience, RPN203G) at 100V for 45–60 minutes. The membranes were then blocked and detected as below.

Membrane Blocking and Immunodetection: Following blotting, nitrocellulose membranes were blocked for 1 hour at room temperature in either 5% dried skimmed milk/0.1% PBST for non-phospho-specific primary antibodies or in 5% bovine serum albumin/TBST for phospho-specific primary antibodies. The membrane was then incubated at 4^{o}C overnight in a heat-sealed bag containing the primary antibody [diluted in blocking solution]. Primary antibodies and their dilutions are provided below.

2.14.3 Immunodetection: Following incubation, the nitrocellulose membrane was washed three times for 10 mins each either in 0.1% PBST or, for phospho-specific antibodies, in 0.05% TBST. The membrane was then incubated in a heat sealed bag with secondary antibody conjugated with horseradish peroxidase for 30 mins. The membrane was then subsequently washed three times, for 10mins each, either in 0.1% PBST or, for phospho-specific antibodies, in 0.05% TBST. The membrane was then developed using a chemiluminescence ECL system (Pierce 32106) and exposed to X-Ray film for 5 sec to 10 mins. Film was then fixed and washed. A biotinylated protein ladder detection system (New England Biolabs) was used to determine molecular weight of protein bands. GAPDH was used as a loading control.

Antibody target	Dilution 1° antibody	Company	Dilution 2° antibody	Molecular Weight
Ki-Ras Mouse mAB	1/200	Calbiochem (OP24)	1/1000	20-21kDa
N-Ras Mouse mAB	1/500	Santa Cruz (sc-31)	1/2000	20-21kDa
Ha-Ras Mouse mAB	1/500	Santa Cruz (sc-29)	1/2000	20-21kDa
Pan Ras Mouse mAB	1/1000	Calbiochem (OP40)	1/2000	20-21 kDa
GAPDH Mouse mAB	1/1000	Millipore (MAB374)	1/1000	36 kDa
αSMA Mouse mAB	1/1000	Sigma (A2547)	1/2000	42 kDa
Collagen I Mouse mAB	1/100	Santa Cruz (sc-59772)	1/1000	70-90 kDa (Mature) 140-210 kDa (Precursor)

Colour marker: 'Colorburst' electrophoresis marker (8-220 kDa) (Sigma C1992)

Biotinylated protein ladder detection kit (Cell Signaling #7727S)

Table 2.5: Primary Antibodies used in Western Blotting

2.14 Model of unilateral ureteric obstruction

Adult male Wistar male rats (mean initial weight 200 grams) were used for *in vivo* models of renal fibrosis. Pre-op all instruments (including ties) were cleaned thoroughly and autoclaved.

Anaesthesia: Inhaled anaesthesia was preferred over the injected for several reasons. Induction is rapid and recovery post anaeasthesia is equally quick. One avoids the use of injections, which may result in tissue injury and furthermore as the dose of anaesthesia may be rapidly adjusted the dose per animal can be more tightly controlled. Each animal was placed in an induction chamber and exposed to 3-4% Isoflurane at an oxygen flow rate of 4 litres/minute. Induction was confirmed by 1) loss of righting reflex, 2) loss of both pinch and tail reflex and 3) a decrease in rate but increase in depth of respiration. The abdomen of each animal was shaved prior to transfer to a heated mat. Isoflurane delivery was maintained by a facemask and concentration was reduced 2-2.5% for maintenance and oxygen flow rate was reduced to 0.5-2 l/min.

Procedure: Once maintenance of anaesthetization was reconfirmed, abdominal region was cleaned using chlorhexidine solution. A midline laparotomy incision was made using aseptic technique and the contents of intestinal cavity were wrapped in moist sterile gauze and gently removed to the side. The contents were periodically moistened with sterile saline. Using a magnifying lamp, the left kidney was exposed and the left ureter identified. The left ureter was isolated by blunt dissection and two 6/0 silk ligatures were used as ties to cause obstruction. The ureter was NOT ligated. Abdominal contents were replaced and incision was re-sutured in two stages using a deep muscle layer continuous suture followed by a continuous skin suture. Buprenorphine was administered subcutaneously (s/c) at a dose of 30μg/kg. Any first dose of treatment (oligo or vehicle) was also administered subcutaneously at this point. Rats were placed in an incubator at 30°C to recover.

For rats acting as controls, a sham operation was performed involving a laparotomy and manipulation and blunt dissection of the ureter only.

Harvesting: Rats were sacrificed at various time points by a schedule one method. Some groups received an intraperitoneal injection of BrdU (25mg/kg) 1hour pre sacrifice. Both left obstructed kidneys and contralateral non-obstructed kidneys were cut in half longitudinally with one half placed in liquid nitrogen for storage at -80°C. The remaining half was placed in formalin for blocking in paraffin. Extra-renal tissue consisting of heart, liver and laparotomy wound tissue were also harvested and placed in liquid nitrogen before storage at -80°C.

2.15 *In vivo* administration of oligonucleotides

Oligonucleotides were administered by subcutaneous injection either in the nape of the neck or rear limbs as variation of injection points prevented tissue damage. Oligonucleotides were dissolved in sterile water and administered on alternate days at doses of 5mg/kg, 12.5mg/kg or 20mg/kg during this project. Time length of experiment until sacrifice was 5, 6, 12 or 16 days.

2.16 Histology:

2.16.1 Paraffin embedded:

Preparation of tissue: Tissue was fixed in 40% neutral buffered formalin solution for 24-48 hours then subsequently embedded ("blocked") in paraffin wax to enable sectioning. The process of blocking was an automated process performed in the Histopathology department, King's College Hospital, London. Blocks were cut into 4μm tissue sections using a microtome (Reichert Jung 2030). Sections were floated in a water-bath (Raymond A Lamb mounting water bath) containing distilled water at a temperature of 42-45°C. The sections were then lifted from water surface on glass or polysine slides and allowed to drip dry for 5mins. The slides were then placed on a heating block (Raymond A Lamb hotplate) at a temperature of 60-80°C for at least 5 mins to allow wax melting and adherence of section to slide. Prior to staining, slides were required to be de-waxed and rehydrated as per protocol used below. Distilled water was used for final rehydration.

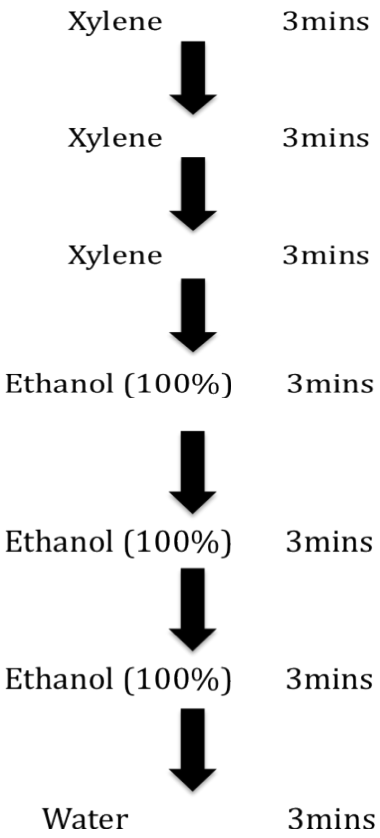

Mounting: Following staining of paraffin embedded tissue, section was again dehydrated and cleared before subsequent mounting in a synthetic medium (Mountex mounting medium, Cellpath)

2.16.2 Cryosection:

Preparation of tissue: Tissue for cryosectioning was placed in liquid nitrogen immediately on harvesting and was stored at -80°C until use. The tissue was not fixed in formalin. For sectioning, tissue was removed from storage and placed on a cryostat chuck and embedded in OCT, a tissue support medium. The medium and tissue were frozen immediately by placing chuck in a dish of liquid nitrogen allowing conductive freezing. The block was then transferred to a cryostat for sectioning. The cryostat chamber was set at -18 to -23°C with the blade temperature set at -18°C. Sections of 5μm were cut employing an anti-roll plate and transferred on to a polysine slide. The sections may then be stored non-fixed or may be fixed in acetone. For the latter, sections were placed in acetone at room temperature for 10 mins then allowed to air dry. All cryosections were stored at -20°C.

2.17 Basic & special stains:

Only paraffin embedded samples were used for basic and special stains.

Positive control slides of human placental tissue were used for basic and special staining procedures.

2.17.1 Haematoxylin & Eosin stain: In this project H&E staining was an automated process and allowed for viewing of general, non-specific tissue structure under light microscopy. Nuclei are stained by oxidized haematoxylin and tissue counterstained with eosin, which differentially stains cytoplasm and tissue constituents varying shades from red to pink.

The outline of the automated procedure is as follows:

Dewax & rehydrate tissue as above.	
Stain in Mayer's haematoxylin	10mins
Rinse in running water	
Differentiate in 1% acid-alcohol	2-4secs
Wash & blue sections in running water	
Counterstain in 1% eosin	3 mins
Wash in running water	
Dehydrate, clear & mount	

2.17.2 Picrosirius Red: This technique is a variation of one used for staining of amyloid fibres. Sirius red is a strong anionic dye and stains collagen by a reaction between the sulphonic acid groups of the dye with the basic groups of the collagen molecule. The dye molecules attach to the collagen fibres in such a way as to allow enhanced birefringence under cross-polarized light. Picrosirius red solution was made up as described in *Appendix I*. A concentration of 0.02% was used if sections were to be viewed under bright light, to remove background stain, and 0.1% for viewing under cross-polarized light.

Picrosirius red protocol:

Dewax & rehydrate tissue	
Rinse in water	10 mins
Picrosirius Red solution	120 mins
Wash in 0.05% Acetic Acid (x 2)	2 mins per wash
Dehydrate, clear & mount	

Under bright field white light collagen fibres appears red on a yellow-red background. Under cross-polarized light larger collagen fibres appear yellow or orange while the thinner ones (including reticular fibres) appear green.

2.17.3 Picro-Mallory Trichrome: Trichrome stains are widely used for the differential differentiation of connective tissues and there are several different variations of this technique. PMT staining, a variant of Masson's trichrome staining, was used in this project. Due to acidic staining solutions, hematoxylin was unable to be used as a counterstain and a combination of Celestine blue-hematoxylin was used instead:

Picromallory trichrome protocol:

Dewax & rehydrate tissue	
Celestine Blue-haemalum sequence	
Wash and blue sections in running water	
Rinse in 70% Industrial Methylated Spirit	
Stain in Picro-Orange	10 mins
Rinse in distilled water	
Stain with Ponceau fuchsin	2 mins
Differentiate in 1% Phosphomolybdic Acid	
Rinse in distilled water	
Counterstain in Aniline Blue	2 mins
Rinse in distilled water	
Treat sections with 1% Acetic Acid as required	
Dehydrate, clear & mount	

Of note, the differentiation step is vital and requires microscopic examination of section while preventing dehydration. At this stage red blood cells should appear yellow but fibrin remain red. Cell nuclei appear blue-black, red blood cells yellow, muscle and fibrin red and collagen and reticulin blue.

2.18 Immunohistological staining:

Both paraffin embedded and cryosections were used for immunohistohemistry (IHC). Sections were mounted on polysine slides and baked overnight at 40-45°C prior to use. The process of IHC techniques fundamentally relies on whole or fragments of antibodies. The use of antibodies allows for selective identification of target epitopes via antigen-antibody interaction. Both polyclonal and monoclonal antibodies were employed as part of this project.

2.18.1 Antigen retrieval: In tissues that have been fixed in formalin, the formation of formaldehyde cross-links may result in the loss of immunoreactivity of certain antigens. To overcome this and to unmask the epitope for antibody binding several antigen retrieval techniques (see *Appendix II*) were trialled in this project and the optimal method was:

	Pressure cook in citrate buffer (pH 6)	3mins
followed by	Placement in distilled water	5mins

This method of antigen retrieval gave the most homogenous and consistent results with regards to immunohistological staining. It was vital that tissue section drying was avoided at any point in this process. In addition not all immunohistological staining required antigen retrieval.

2.18.2 Immunodetection: For the majority of IHC tissue analysis the indirect method of detection was employed. This involves the use of a labelled secondary antibody directed towards the primary antibody that also allows for the amplification of signal. Primary antibodies used are shown in Table 2.6. Instead of a secondary antibody, DAKO REAL Envision detection system (Dako, K5007) was used for signal generation. This synthetic dextran polymer system

allows for far more sensitive binding thus requires less incubation time and results in a decrease in non-specific antibody binding and improved amplification of signal and is a system which is now regularly used in clinical medicine. The secondary antibodies of the polymer were raised in goat and directed against both mouse and rabbit. Signal detection used 3',3'-diaminobenzidine (DAB) as a chromagen. Oxidation of DAB by peroxidase resulted in a brown end product.

2.18.3 Peroxidase block: Peroxidase activity in tissue sections was blocked. by treating sections with 2% Hydrogen peroxide (30 parts) in methanol solution prior to incubation with primary antibody.

2.18.4 Serum block: In order to reduce non-specific binding of secondary labeled antibody or polymer, sections were also serum blocked using serum from host of secondary antibody. As secondary antibody component of the Envision polymer system were raised in goat, goat serum (at a concentration of 1 in 10 made up in wash solution) was used in the blocking step. This solution of serum block was also used to make up the primary antibody solution.

2.18.5 Counterstain: For DAB substrate, counterstaining with haematoxylin was employed:

Hematoxylin	3mins
Rinse in running water	
1% Acid alcohol	3 dips
Rinse in running water	

Paraffin embedded protocol: The protocol for each antibody was essentially similar. There are variations in incubation time and wash solutions which are noted in Table 2.6. Both positive and negative controls for each antibody were used to ensure optimum staining and to assess non-specific staining and background non-specific staining.

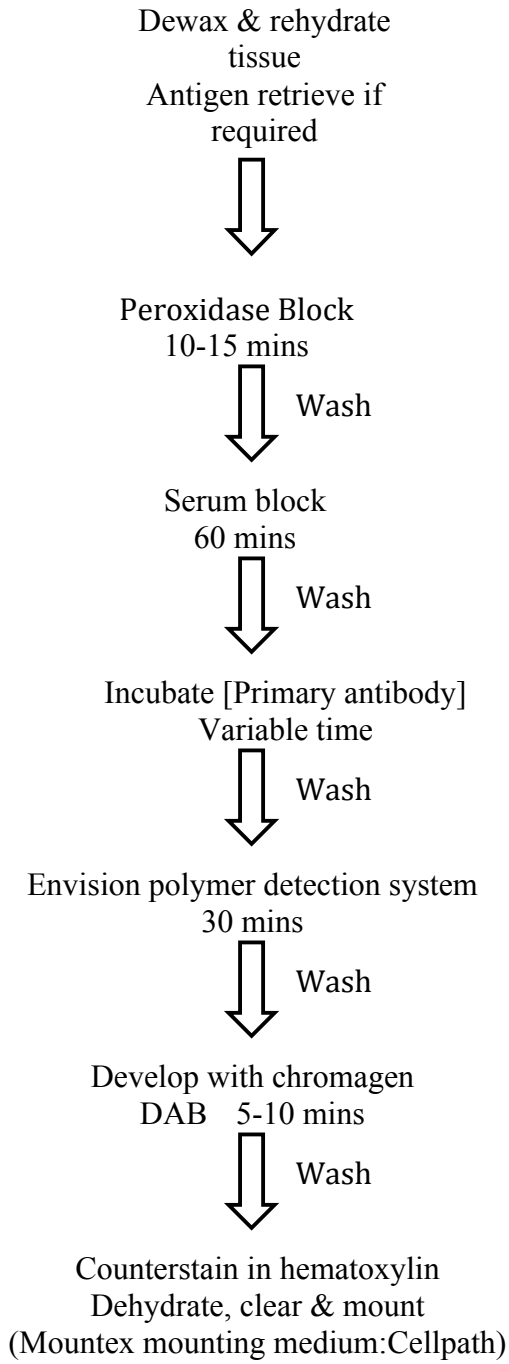

Figure 2.8: Immunohistological staining protocol for paraffin embedded samples

Cryosection IHC: The protocol for frozen tissue staining differed from that of paraffin embedded samples. No antigen retrieval step is required. All washes in TBS solution.

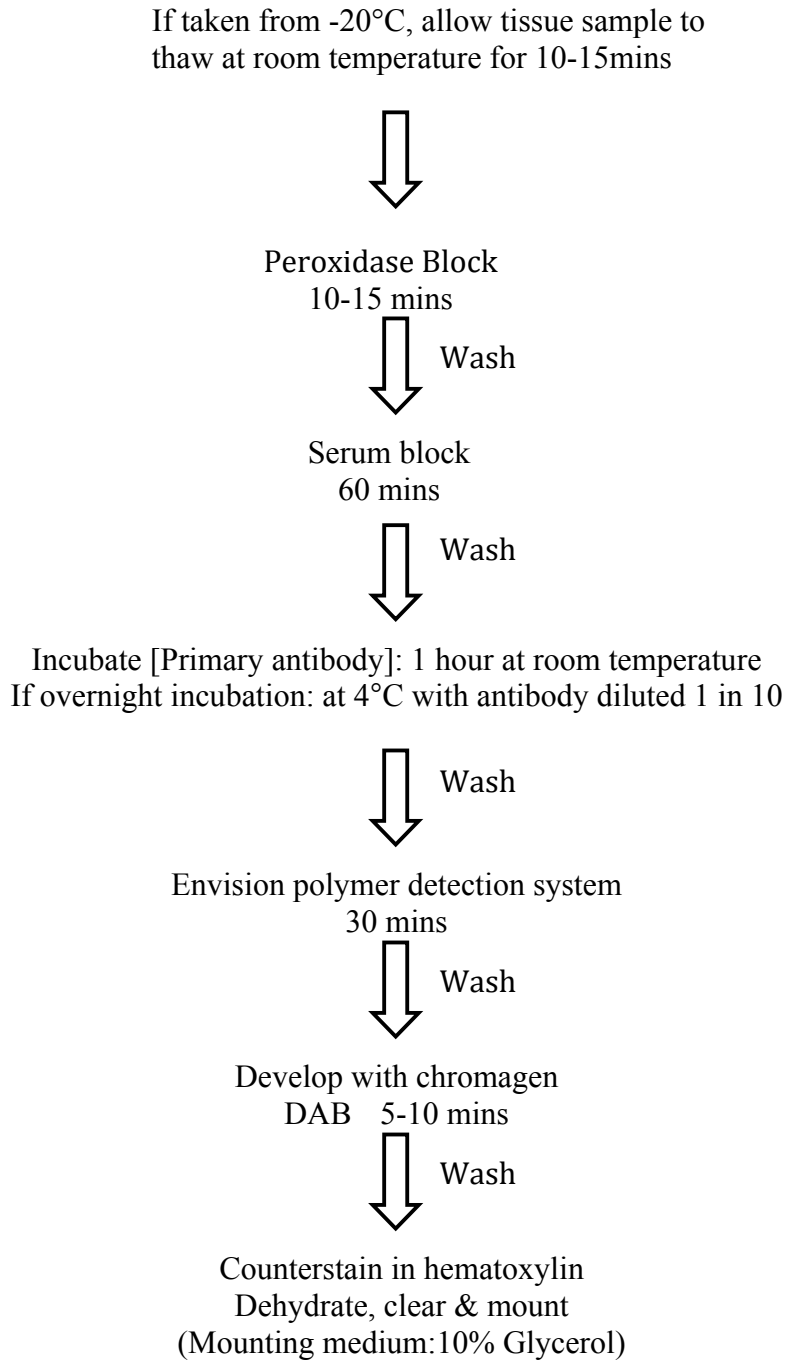

Figure 2.9: Immunohistological staining protocol for frozen samples

Primary Antibodies used in IHC: The table below gives the various parameters of antibodies used in IHC. All antibodies were made up in serum blocking solution. Colour development was with chromagen DAB (1part in 50) from DAKO.

Antibody target	**Dilution**	**Company**	**Incubation**	**Wash solution**	**Antigen Retrieval**
αSMA Mouse mAB	1/200	Sigma clone 1A4 (A2547)	60 mins Room Temp	0.05% TBST	None
Collagen I Rabbit polyAB	1/4000	Chemicon (AB755P)	Overnight 4°C	0.05% TBST	None
Ki-67 Mouse mAB	1/100	Novocastra (NCL-L-Ki67-MM1)	60 mins Room Temp	PBS	(HIER) PC Citrate buffer pH6
ED1 (CD68) Mouse mAB	1/100	Serotec (MCA341R)	Overnight 4°C	PBS	(HIER) PC Citrate buffer pH6
S100A4 (FSP-1) Rabbit polyAB	1/1000	Dako (A5114)	60 mins Room temp	PBS	(HIER) PC Citrate buffer pH6
Ki-Ras Mouse mAB	1/10	Calbiochem (OP24)	Overnight 4°C	0.05% TBST	Various
Pan-Ras Mouse mAB	1/200-1/2000	Calbiochem (OP40)	Overnight 4°C	0.05% TBST	Various
Oligo-AB Rabbit polyAB	1/4000	ISIS (Unspecified)	60 mins Room temp	PBS	Protinase K
Aquaporin-1 Rabbit polyAB (Aqp1)	1/4000	Millipore (AB2219)	60 mins Room temp	0.1% TBST	(HIER) PC Citrate buffer pH6
Aquaporin-2 Rabbit polyAB (Aqp2)	1/2000	Millipore (AB3066)	60 mins Room temp	0.1% TBST	(HIER) PC Citrate buffer pH6

Table 2.6: Primary Antibodies used in IHC; HIER Heat induced epitope retrieval, PC: Pressure cook,

Control samples for αSMA and Collagen I: Placental tissue

Control samples for Ki-67 and ED1: Lymph node tissue

Control samples for Ki-Ras and Pan Ras: Skin tissue

Negative controls used for all staining.

2.20 Laser microdissection and pulsed capture (LMPC)

The rationale behind PALM and subsequent RNA analysis was to attempt to localize mRNA knockdown to renal cellular compartments. Thus measurement of Ras mRNA within isolated cellular compartments in samples would indicate location of mRNA knockdown effect. The principle of laser microdissection involves restricted dissection of target area from tissue mounted on a special membrane slide. The process was performed using P.A.L.M. Microlaser Technologies that allows for microdissection and micro-manipulation systems using LMPC (Laser Microdissection and Pressure Catapulting). PALM microlaser technology consists of a robo-stage under the control of PALM microbeam software. Cutting is via a solid-state laser that is passed via the microscope and focused through the microscope and focused through an objective to a beam diameter of under 1μm. Following dissection the target region is "pulsed" upwards into the specialized adhesive cap of an RNAse free eppendorf container. This avoids any physical contact for tissue transfer and so reduces contamination risk. Following collection of several target regions, tissue could be lysed and RNA retrieved. In this project the protocol of tissue preparation, cell recognition and laser microdissection was adapted from a protocol kindly provided by Dr Catherine Kielar, Department of Neuroscience, Institute of Psychiatry, King's College London.

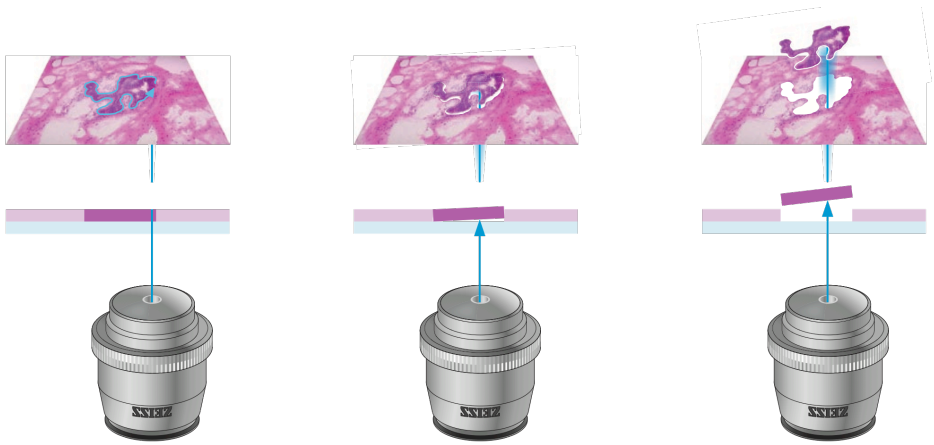

Figure 2.10: Schematic of PALM depicting laser dissection and 'pulsing' of dissected section upwards to container. (Taken from PALM user manual).

2.20.1 Tissue preparation for PALM:

Frozen tissue sections were used for PALM microdissection. 10μm cryosection were cut using a Microm microtome cryostat cryo-star HM 560 MV. The chamber and blade were cleaned with RNAse Zap (Qiagen) prior to cryosectioning. Tissue was prepared as mentioned in histology section. Chamber was set at -20°C and the blade at -18°C. The section was then mounted on 1mm Polyethylene (PEN)-membrane covered slides (PALM microlaser technology, Cat 1440-1000). Sections were then stained to allow cellular identification and microdissection as follows: All solutions were made up with DEP-C treated water and all steps were performed at room temperature unless specified. The cryosections were dehydrated in ascending concentration of ice cold ethanol from 75%, 90 % and 100%-at 1 min in each. The sections were subsequently stained with ice-cold 1% Nissl stain for 90 seconds. The section was then washed in ascending concentrations of ice-cold ethanol (of 75%, 90% and 100%) for 20 seconds in each then mounted on a PEN-membrane slide prior to loading on the robo-stage. A PALM adhesive cap RNAse-free eppendorf was loaded into the collection arm. Using PALM Microbeam HT software, one was able to navigate across the section under x10 to x60 magnification. The software allowed manual outlining of target regions or cells for microdissection. Microdissection was on performed at x20 to x40 magnification. The PALM microbeam laser would automatically cut sequential targeted regions. For the purpose of tubular cell microdissection, the settings were speed of 23, laser energy 68, laser focus 56, catapulting energy 90 and catapulting focus 68, all of arbitrary units. Microdissected regions were collected in RNase-free eppendorf containers and immediately underwent RNA retrieval. The whole process from tissue cryosection to initiation of RNA retrieval was to be restricted to a maximum of 30 minutes per section to reduce RNA degradation. The number of tubules collected on each sitting ranged from 30 to 120 (with on average of 8-10 cells per tubule).

2.20.2 RNA retrieval of microdissected cells

RNA retrieval from collected microdissected tissue was performed using the RNeasy Micro kit from Qiagen (Qiagen, 74004). This kit is designed to purify RNA (maximum of 45μg) from small amounts of tissue and even from single cells. The principle of the kit is similar to RNeasy Mini kit used for whole tissue RNA retrieval (see Section 2.7). Protocol was as for manufacturer's instructions and summarized as follows: Microdissected cells catapulted on to the adhesive cap were disrupted by addition of 75μl of lysis buffer RLT followed by vortex mixing. The lysate was transferred to a QIA-shredder for further homogenization by centrifuging at 2 mins at >10,000 rpm at room temperature. Further lysate disruption was achieved by needle lysis. An equal volume of 70% ethanol was added to the sample before transfer to an RNeasy MiniElute column. The tube was centrifuged for 15 seconds at >10,000 rpm and the flow through discarded. 350μl of Buffer RW1 (wash solution) was added to the sample and tube was centrifuged once again for 15 seconds at >10,000 rpm and the flow through discarded. 80μl of DNase I incubation mix was added to the sample and gently mixed by tube inversion and incubated at 20-30°C for 15 mins. The DNase mix allows for digestion of contaminating DNA in the RNA solutions prior to RNA clean up. Following digestion by DNase, 350μl of Buffer RW1 was added to the sample and tube was centrifuged once again for 15 seconds at >10,000 rpm and the flow through discarded. 500μl of Buffer RPE was then added to the sample and centrifuged once again for 15 seconds at >10,000 rpm and flow through discarded. 500μl of 80% ethanol was then added and column was centrifuged for 2 minutes at >10,000 rpm and flow through discarded. The column was then further centrifuged at >10,000 rpm for 5 minutes and flow through discarded. The column was then transferred to a new collecting column and RNA eluted by addition of 10-14μl of RNase-free water and centrifuging for 1 minute. RNA quantitation was performed as previously described. In order to reduce tissue temperature related damage, the process from staining until completion of microdissection took no longer than 20 minutes in total.

2.21 *In situ* hybridization (ISH):

ISH was performed on paraffin embedded tissue using a non-radioactive ISH Hybriprobe® Triseq kit purchased from Biognostik. All glassware and materials was made RNAse-free (See Appendix I). All solutions were made up with DEP-C treated water. Hybriprobes are fluorescein-isothio-cyanate (FITC) labeled single stranded phosphodiester DNA oligonucleotides. Each probe is double labeled with FITC groups at 5' and 3' end nucleotides. The Triseq kit provides three different probes directed at three different regions of the same target mRNA to enhance signal intensity and assay sensitivity and so is of benefit in targeting mRNA with low or normal expression. 5μm paraffin embedded sections were cut, mounted on polysine slides and oven baked overnight at 45°C. Protocol was as for manufacturer's instructions: Sections were dewaxed and rehydrated then underwent Proteinase K digestion (freshly made, 20-50μg/ml) at 37°C for 15-20 mins in a humid chamber to increase accessibility of mRNA in formalin fixed tissue. Following a wash in PBS, sections were taken through a prehybridization step. This step allows equilibration with the hybridization buffer (Hybribuffer) and reduces background staining. Prehybridization was carried out in tightly sealed boxes containing humidifying box buffer (50% formamide/ 4 x SSC). Hybribuffer was activated by heating up to 95°C before cooling to 35°C and being added to sections. Sections were incubated in hybribuffer at 30°C for 2-4 hours. Subsequently prehybridization was drawn off and hybridization solution (activated hybribuffer containing each probe at a concentration of 60pmol/1000μl hybribuffer) added. Sections were incubated overnight at 30°C in humidified boxes. Sections were then washed twice for 30 seconds in 1 x SSC, followed by a wash in 1 x SSC for 5mins then a two 15 minutes (stringent) washes in 0.1 x SSC at 40°C for prior to detection of hybriprobes. Sections were washed in PBS then serum blocked for 30 mins in goat serum (1 in 10) prior to incubation with goat anti-FITC antibody conjugated to alkaline phosphatase (Vector MB-2100) at a dilution of 1/100 for 1 hour at room temperature. Visualization of signal was obtained by addition of NBT/BCIP substrate (Vector SK5400) to produce a blue stain. Section was then counterstained using neutral fast red (1 min) before rinsing in distilled water, dehydration and mounting. Poly-d(T) hybriprobes were used as a positive control. Hybriprobes for Ki-Ras were designed by Biognostik. The sequences for the hybriprobes are as below:

Sequence	Biognostik number	Gene match
CCTGCTGTGTCGAGAATATCCAAGAGACAG	H11554	BC141051.1 Mus musculus v-Ki-ras2
CTAGGACCATAGGCACATCTTCAGAGTCCT	H11555	BC126086.1 Rattus norvegicus v-Ki-ras2
ATGTATAGAAGGCATCGTCAACACCCTGTC	H11556	BC126086.1 Rattus norvegicus v-Ki-ras2

Table 2.7: ISH hybriprobe sequences

Several alterations to the above manufacturers protocol were performed and are documented in Appendix II. The basis of variation in steps originated from published literature, in particular that of Dr JH Pringle (Bailey et al. 1999), and current ISH protocol utilized for clinical samples by the Department of Histopathology, King's College Hospital, London.

2.22 TUNEL Assay:

Detection of apoptosis in tissue sections was performed using a TACS TdT (terminal deoxynucleotidyl transferase) kit (R&D systems TA4625). The TACS kit detects DNA fragmentation resulting from apoptosis through a combination of enzymatic and immunohistological techniques. The incorporation of biotinylated nucleotides into the 3'-OH ends of DNA fragments by terminal deoxynucleotidyl transferase (TdT) is subsequently followed by their detection using streptavidin-horseradish peroxidase conjugate and development of signal using DAB substrate. The enzyme reaction generates colour precipitate where DNA fragmentation has occurred. The sections are subsequently counterstained to allow for morphological identification. Paraffin sections of 4μm were used. Tissue was initially dewaxed and rehydrated. Following incubation in 1x PBS for 10 mins at room temp, tissue was permeabilized with Protinase K solution (15 mins at 21°C). Samples were washed twice in distilled water before endogenous peroxidase activity was quenched using 10% Hydrogen Peroxide solution (5 mins at room temp). Following a wash in PBS for 1 min, samples were incubated in TdT labeling buffer (5 mins at room temp) before transfer to TdT labeling reaction mix for 1 hr at 37°C. The reaction was terminated by addition of Stop buffer (5 mins at room temp). Samples were washed x 2 in 1xPBS for 2mins per

wash prior to incubation with Streptavidin HRP solution (10 mins at room temp). Colour preciptation with DAB (2-10 mins at room temperature) was completed following a further wash in distilled water. Finally samples were counterstained with hematoxylin. Positive controls were provided by incubation of samples with TACS nuclease solution provided.

2.24 Summary of method of scoring system used for histological evaluation within this project

Fibrosis Parameter/Marker	Method of assessment (All blinded assessments)
Picromallory Trichrome (PMT)	Histological: Overall degree of fibrosis in renal cortex assessed by a consultant histopathologist under bright light. Degree of tubulointerstitial fibrosis was provided as a percentage.
Picrosirius Red (PSR)	Histological: Overall degree of fibrosis in renal cortex assessed by a consultant histopathologist under bright light. Degree of tubulointerstitial fibrosis was provided as a percentage.
α-SMA	Histological: Overall degree of expression in renal cortex assessed by a consultant histopathologist under bright light. Degree of expression was provided as a percentage. Immunoblotting: α-SMA & GAPDH expression in renal cortical samples were measured by densitometry. α-SMA expression (relative to GAPDH) for each treatment group was then normalised to sham-operated control group.
Collagen I	Histological: Overall degree of fibrosis in renal cortex assessed by a consultant histopathologist under bright light. Degree of tubulointerstitial fibrosis was provided as a percentage.
FSP-1	Histotological: Mean number of FSP-1+ cells across ten random cortical views per section (at x40 magnification). FSP-1+ cells were divided into glomerular, tubular and interstitial compartments.
Ki-67	Histotological: Mean number of Ki-67+ cells across ten random cortical views per section (at x40 magnification). Ki-67+ cells were divided into glomerular, tubular and interstitial compartments.
ED-1	Histological: Overall degree of expression in renal cortex assessed by Nikon Elements BR software package. Mean score was derived by assessment across five random cortical views per section at x20 magnification. Degree of expression was provided as a percentage.

Table 2.8: Summary of histological evealuation used in this project

The table above summarises the methods used for assessment of fibrosis and markers of fibrosis and inflammation used in this project. Assessments made by a consultant histopathologist, would include interpretation of staining thought to be non-specific and oedema-related with views of the whole sample taken over magnifications ranging from x10 to x40 with assessment. Evaluationof FSP-1 and Ki-67 was less complex due to low non-specific background staining and the discrete nature of the stain. ED-1 staining was performed using Nikon Elements BR software package which allows measurement of area measured relative to section seen. All samples were assessed with operators blinded to treatment of sample.

2.25 Statistics

Statistical analysis of data was performed using Prism 4 software package (Graphpad software). For pairs of data, an unpaired t-test was used. For group data, an ANOVA (Analysis of variance) was initially performed. Subsequently Bonferroni adjustment was used to correct for multiple testing in this case. A linear regression model was used for multiple variances in analysis of data of unbalanced design.

Chapter 3: Characterization of Ki-Ras antisense oligonucleotides *in vitro and in vivo*

Previous screening work performed by our group, using primary culture rat renal fibroblasts, identified two antisense oligonucelotides out of a series of twenty Ki-Ras ASOs supplied by ISIS Pharmaceuticals that were deemed highly efficient when transfected *in vitro* (unpublished data). Preliminary data from administration of these two ASOs, ASO 1 & ASO 2, in rat models of UUO showed a decrease in αSMA expression and collagen IV deposition compared to a sham-treated control group (unpublished data). ISIS Oligo 15167 (CO 1), targeting the human HIV promoter sequence, was used as a control oligo in *in vitro* experiments unless otherwise specified.

In vitro models employed in this project consisted of primary culture of adult PVG rat renal fibroblasts, obtained from freshly discarded kidneys at time of sacrifice, and commercial cell lines were obtained. NRK-49F fibroblasts and the equivalent tubular epithelial cell line, NRK-52E, were used. The cell lines represent fibroblastic and epitheloid clones isolated from a mixed cell growth of Normal Rat Kidney cells. Thus they best represent non-transformed rat cells and are expected to possess similar physiology and allow the undertaking of comparative studies between different cell types from the same species.

3.1 Ras mRNA expression in rat renal fibroblasts following ASO transfection

3.1.1 Primary cell cultures

Following transfection with CO 1 and Ki-Ras ASOs, total RNA from cells was extracted and Ras mRNA expression compared using SQ-PCR. Subsequent SQ-PCR products were run on a DNA gels. Results are representative of duplicate experiments. There was an observable decrease in Ki-Ras mRNA expression with an accompanying increase in Ha-Ras expression following transfection with ASO 1 & ASO 2 compared to CO 1. Due to limited amounts of RNA extracted from primary cells, expression of N-ras was unable to be examined.

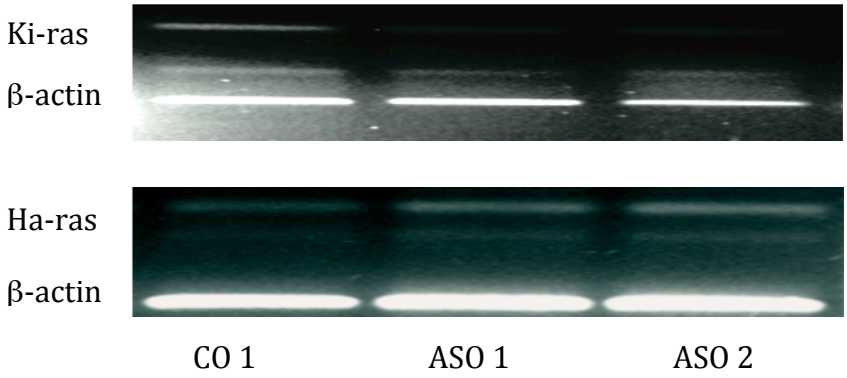

Figure 3.1: SQ-PCR expression of Ki-ras & Ha-ras mRNA in primary cultures of rat renal fibroblasts following transfection by control and Ki-Ras antisense oligonucleotides.. Products of reactions completed in the linear phase of amplification using 27 cycles of PCR. Upper bands represent isoforms of Ras as indicated, the lower bands represent amplification product of β-actin.
(n=2 for Ki-Ras, n=1 for H-Ras)

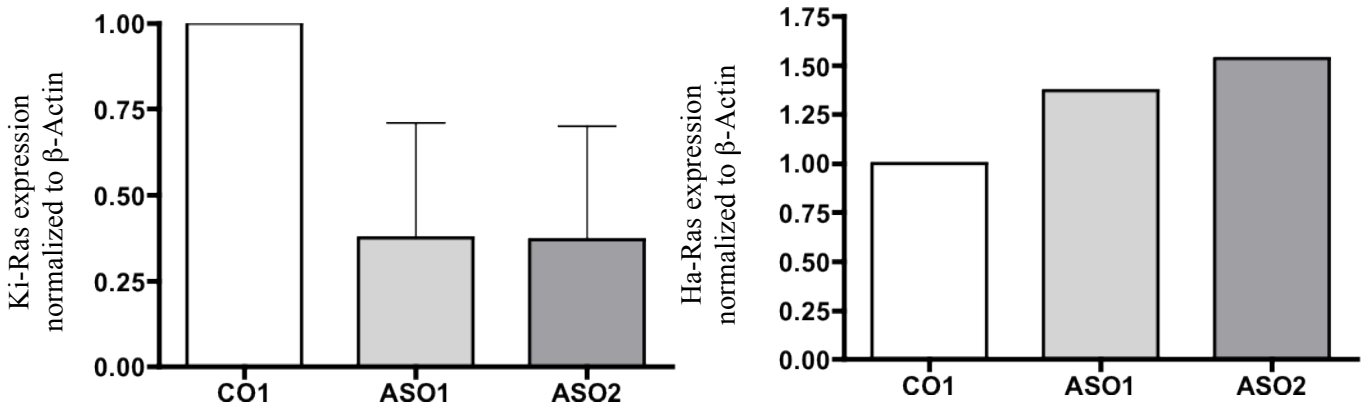

Figure 3.2: Densitometry analysis of Ki-Ras and Ha-Ras cDNA expression relative to β-actin in primary cultures of rat renal fibroblasts following transfection by control and Ki-Ras antisense oligonucleotides. (n=2 for Ki-Ras, n=1 for H-Ras)

3.1.2 Fibroblast cell line (NRK-49F)

Following transfection with oligonucleotides and RNA extraction, SQ-PCR was initially employed to analyse expression of Ras. However despite using a low number of cycles of PCR, a significant difference in Ki-Ras expression was not observed. This may have been due to an issue of technique, a failure of transfection of NRK-49F cells, a failure of knockdown of target mRNA or significantly higher Ras expression in NRK-49F cells as compared to primary cell cultures. The knockdown results observed in primary cell cultures suggested that the Ki-Ras ASOs were active and the absence of observable mRNA knock down in NRK-49F cells was thought to be due in part to the amplifying nature of semi-quantitative SQ-PCR and possible insensitive method of assessing any changes. Subsequently real time PCR (QPCR) was employed. QPCR is specific and sensitive, being able to detect differences as small as two-fold. However, more importantly, QPCR provided an objective quantitative end-point that was not available for semi-quantitative PCR. The QPCR comparative measurement of Ras mRNA (See *Methods & Materials)* from NRK-49F cells transfected with Ki-Ras ASOs and CO 1 were analysed for mRNA expression of the various isoforms of Ras. GAPDH was used as an internal reference gene.

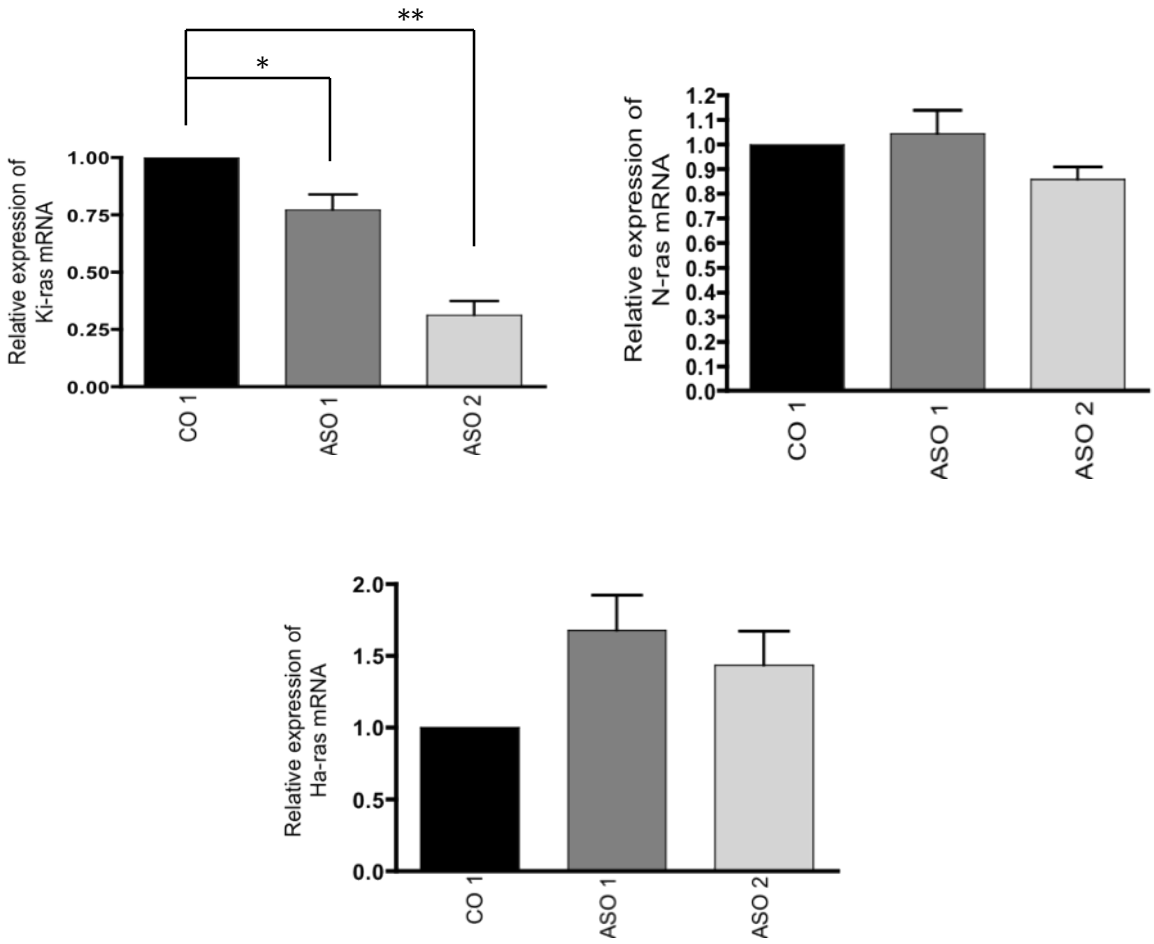

Figure 3.3: Quantitative PCR determination of expression of Ras mRNA isoforms in NRK-49F cells transfected with Ki-Ras ASO at 200nM. Following RNA retrieval samples were run on 96 well plates in triplicate and Ras mRNA expression relative to CO 1 group was calculated using the comparative method of analysis with GAPDH as an internal reference gene. Each graph is a representation of three separate QPCR analyses with samples run in triplicate on each analysis.
[*denotes p value <0.05, ** p < 0.01]

The above figures show that both Ki-Ras ASOs reduced expression of Ki-Ras mRNA by 35% (ASO 1) and 70% (ASO 2) in comparison to CO 1 administration. In addition the knockdown effect of ASOs was specific for the Ki-Ras isoform, with no knockdown of either N- or Ha-Ras, though an up-regulation of the latter isoform was noted on administration of both ASO 1 (64%) and ASO 2 (45%).

3.2 Ras mRNA expression in rat renal epithelial cell line (NRK-52E)

It has been proposed that the increase in the population of fibroblasts in the process of renal fibrogenesis, is as a result of the phenomenon of epithelial-mesenchymal transition (EMT). Since oligonucleotides have been shown to be actively taken up by the tubular epithelial cells of the nephron, their effect in normal rat renal epithelial cells was investigated. Figure 3.3 show that there is no significant difference in mRNA expression of N- and Ha-Ras in NRK-52E cells following transfection with Ki-Ras ASOs when compared with either transfection with control oligos or vehicle-only (OptiMem). There was a decrease in Ki-Ras mRNA expression in the ASO 1 group by 32% and by 57% in the ASO 2 group in comparison to vehicle-only control. Though no significant statistical difference was seen between control and antisense oligo groups, a definite trend towards decreased Ki-Ras mRNA levels following ASO administration was observed.

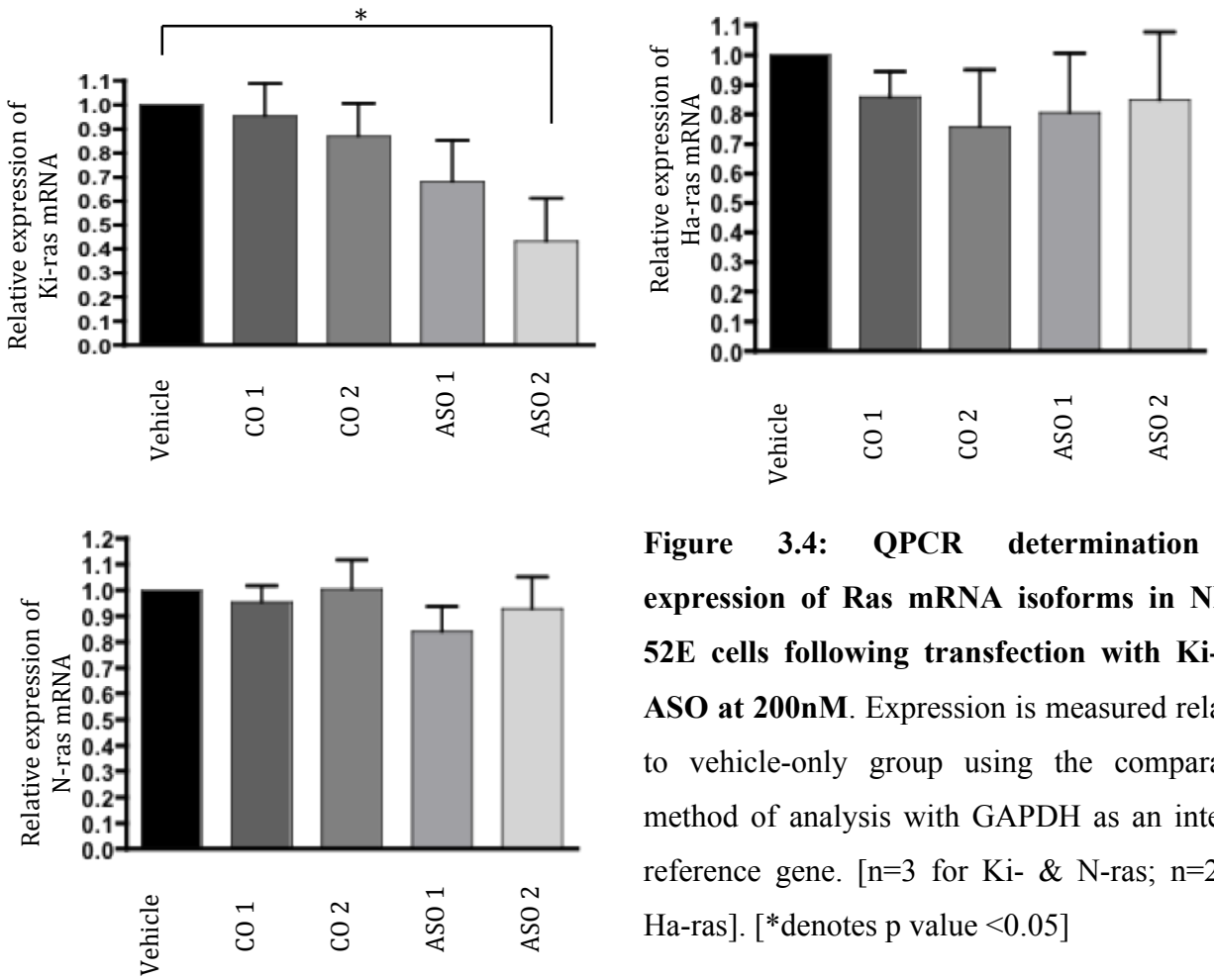

Figure 3.4: QPCR determination of expression of Ras mRNA isoforms in NRK-52E cells following transfection with Ki-Ras ASO at 200nM. Expression is measured relative to vehicle-only group using the comparative method of analysis with GAPDH as an internal reference gene. [n=3 for Ki- & N-ras; n=2 for Ha-ras]. [*denotes p value <0.05]

3.3 ASOs and cytotoxicity

CytoTox 96 (Promega) non-radioactive cytotoxicity assay from Promega was used to assess oligonucleotide toxicity. The assay is based on comparative analysis of lactate dehydrogenase release. Cytotoxicity of oligonucleotides was assessed at different concentrations of oligonucleotides ranging from x0.25 to x5 concentration of that used in *in vitro* experiments (200nM). From figure 3.4 it can be seen that none of the oligonucleotides had any significant cytotoxic effects on NRK-49F up to a dosage of 1μM compared to vehicle only treated cells acting as a negative control

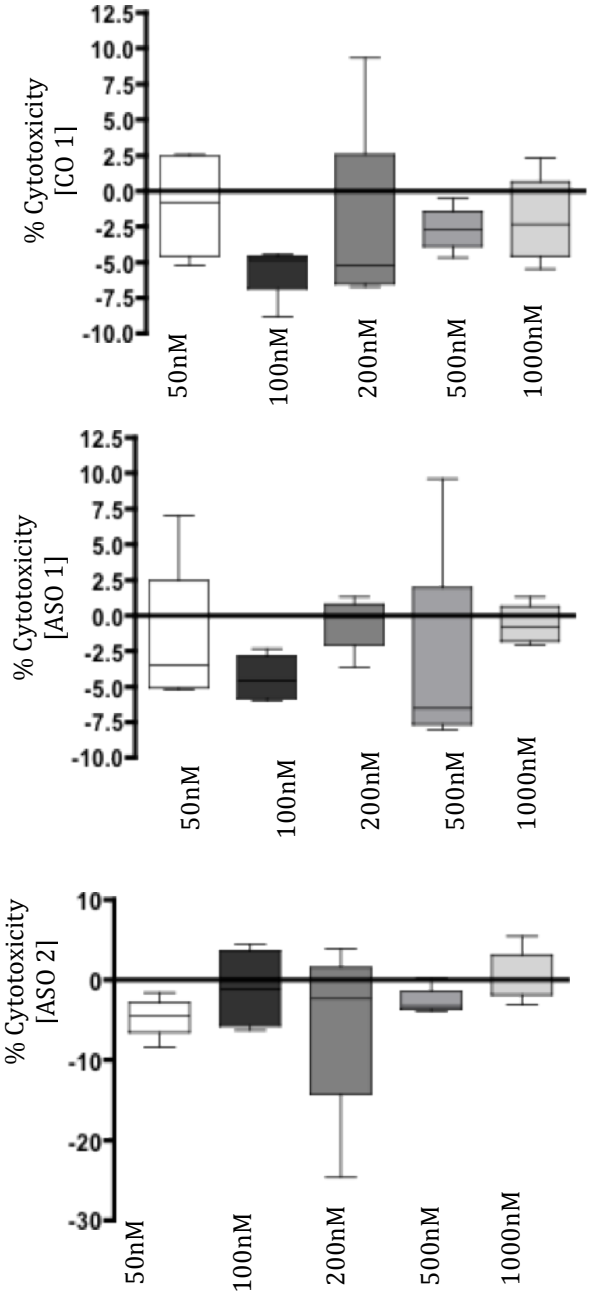

Figure 3.5: Cytotoxicity in NRK-49F cells following oligonucleotide transfection.

A non-radioactive colourmetric LDH assay was employed to assess cytotoxcity. Results are depicted as a mean and spread of degree of cytoxicity in relation to vehicle – only negative control and maximum cell lysis. (n=3 per dose-group with samples run in triplicate per plate)

3.4 Assessment of ASO specificity and effects in non-obstructed rats

Though cell culture studies provide one with the opportunity to establish and investigate the role of certain molecules and mediators in specific cell types, when looking to translate potential therapies from benchside to bedside, this highly controlled environment is not representative of a whole biological organism where a multitude of different cells interact and respond to both local and distant cell signals. In order to achieve a better insight into this, animal models have been used to elucidate disease processes and evaluate potential therapies. Apart from considering the cross-talk of cells, *in vivo* models also allow for the examination of "proof of concept" and restrictions to potential therapies as well as providing information regarding toxicity and side effects. Oligonucleotides employed in this assessment include control oligo CO 2, antisense oligos ASO 1 and 2 and scramble oligos SO 1 and 2.

3.4.1 Ras mRNA and protein expression

The specificity and efficiency of oligos *in vivo* were initially investigated in non-obstructed male Wistar rats. By examining the effects of the oligonucleotides in non-diseased models, changes in Ras expression induced by obstruction can be removed and the specific effects of each oligo both at a molecular and organism level may be analysed. In figure 4.1, QPCR was used to demonstrate that there is a specific and significant knockdown of Ki-ras by ASO 2 compared to CO 2 of 66%. ASO 1 only reduced Ki-Ras expression by 12%. There is no significant Ras knockdown by CO 2 compared to Sham.

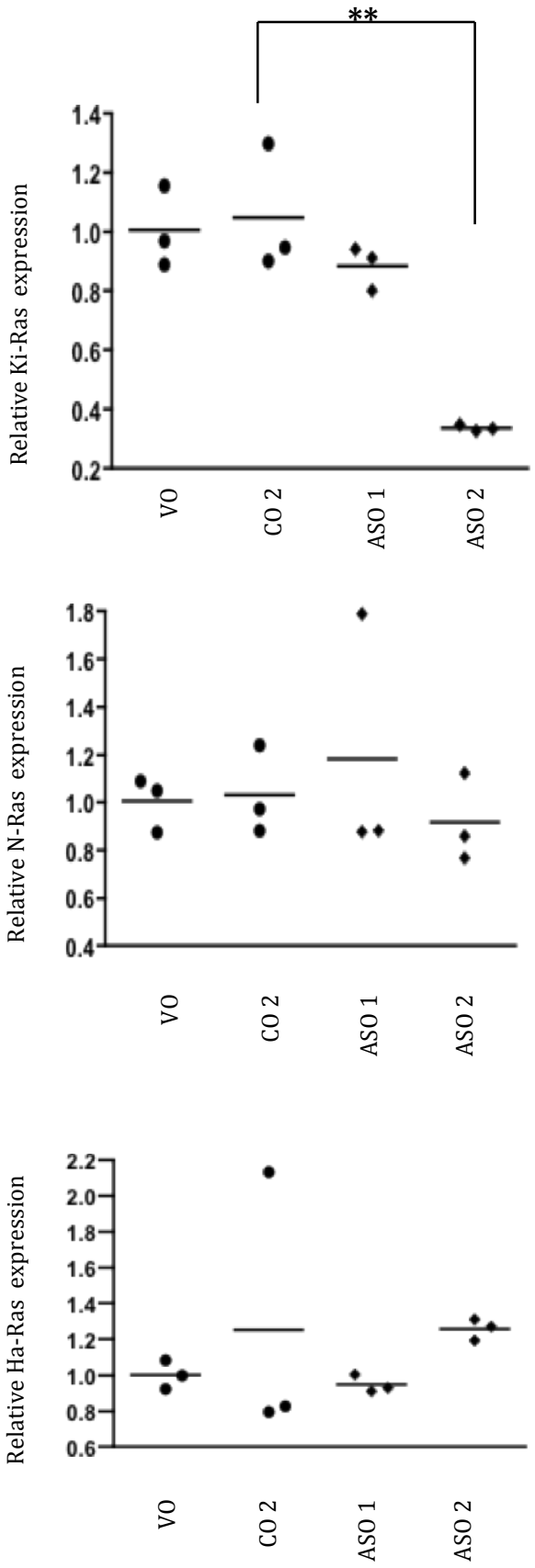

Figure 3.6: Expression of Ras isoform mRNA on administration of oligonucleotides in non-diseased rat models. Real time PCR was used to analyse mRNA expression of Ras isoforms Kirsten (A), Neural (B) and Harvey (C) in retrieved renal tissue. The results are a combination of two separate QPCR analyses, each analysis being composed of three replicates per animal. Thus each point is representative of the mean of six replicates from one single animal. Oligos were administered at a dose of 12.5mg/kg subcutaneously on alternate days over a 6-day period (Three doses in total).

The above RNA analysis indicates that only Ki-Ras mRNA levels are specifically affected by Ki-Ras ASO administration in non-diseased models. Thus it is postulated that any change in pan-Ras protein expression is due to ASO effect on Ki-Ras protein levels and not those of Ha- or N-Ras. Subsequently an immunblot of pan-Ras protein expression and was normalised to GAPDH in solution from the immunoprecipitation step (See *Methods & Materials*).

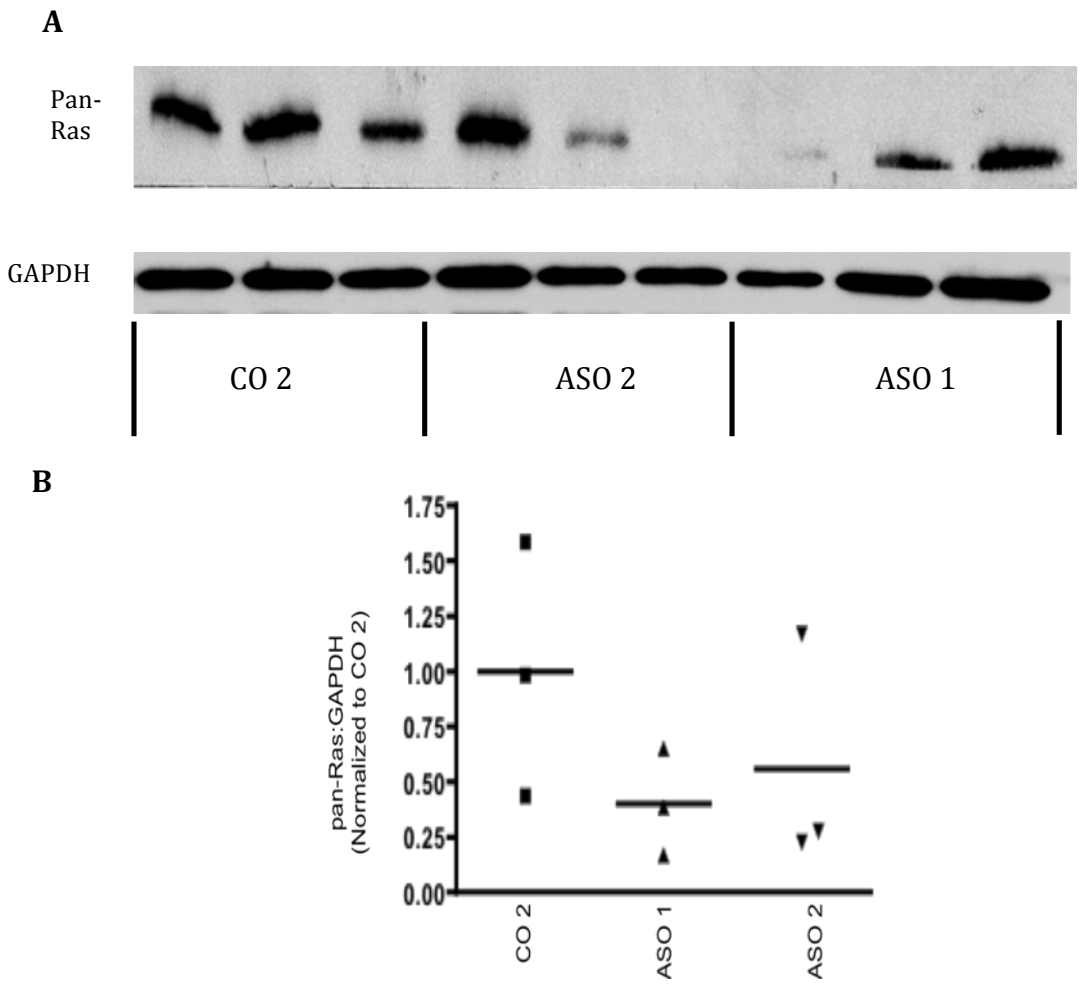

Figure 3.7: Western blot analysis for pan-Ras in oligo-treated non-diseased rat models. **A** Immunoblot for pan-Ras. GAPDH in the supernatant from Ras immunoprecipitation was used as a loading control. This blot is representative of three similar blots. **B** Densitometry of blot bands to quantify Ki-Ras protein expression relative to GAPDH.

The above graph demonstrates that there is a knockdown of Ki-Ras protein by ASO 1 of 60% and ASO 2 of 45% in comparison to CO 2 administration.

3.4.2 Cell proliferation

Ras is known to be a key molecule in the control of cell proliferation, therefore renal tissue was stained for the cell proliferation marker Ki-67 to investigate effects of ASO on this process.

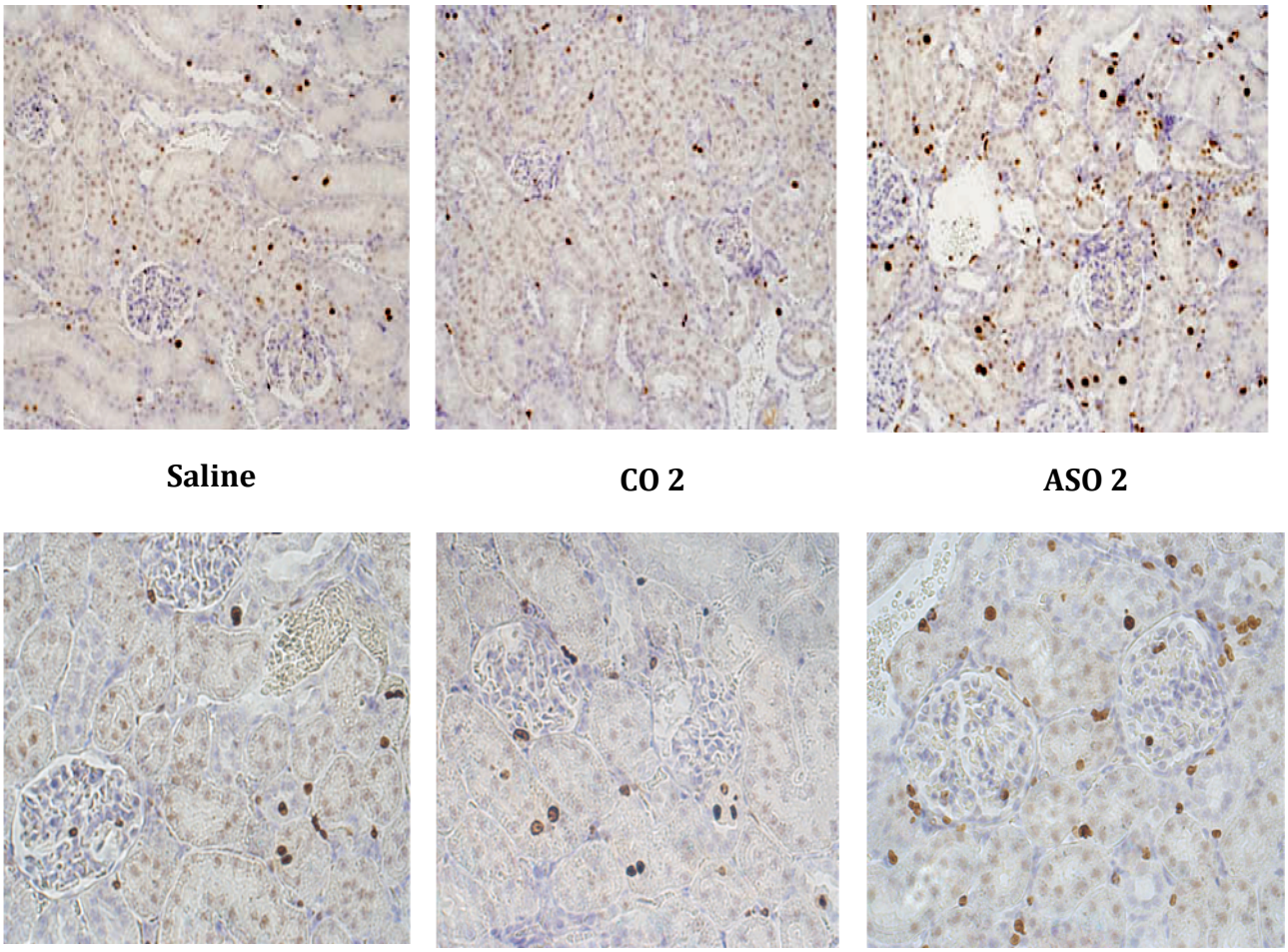

Figure 3.8: Sections of non-diseased rat renal tissue stained for Ki-67 following treatment with saline or oligos (x10 and x40). Representative sections from treatment groups following indirect immunodetection using a Ki-67 monoclonal antibody and signal detection with HRP-DAB.

The mean number of Ki-67 positive cells per section (magnification x20) were compartmentalized into glomeruli, tubules and interstitium. 10 views per section were scored and analysed in a blinded fashion.

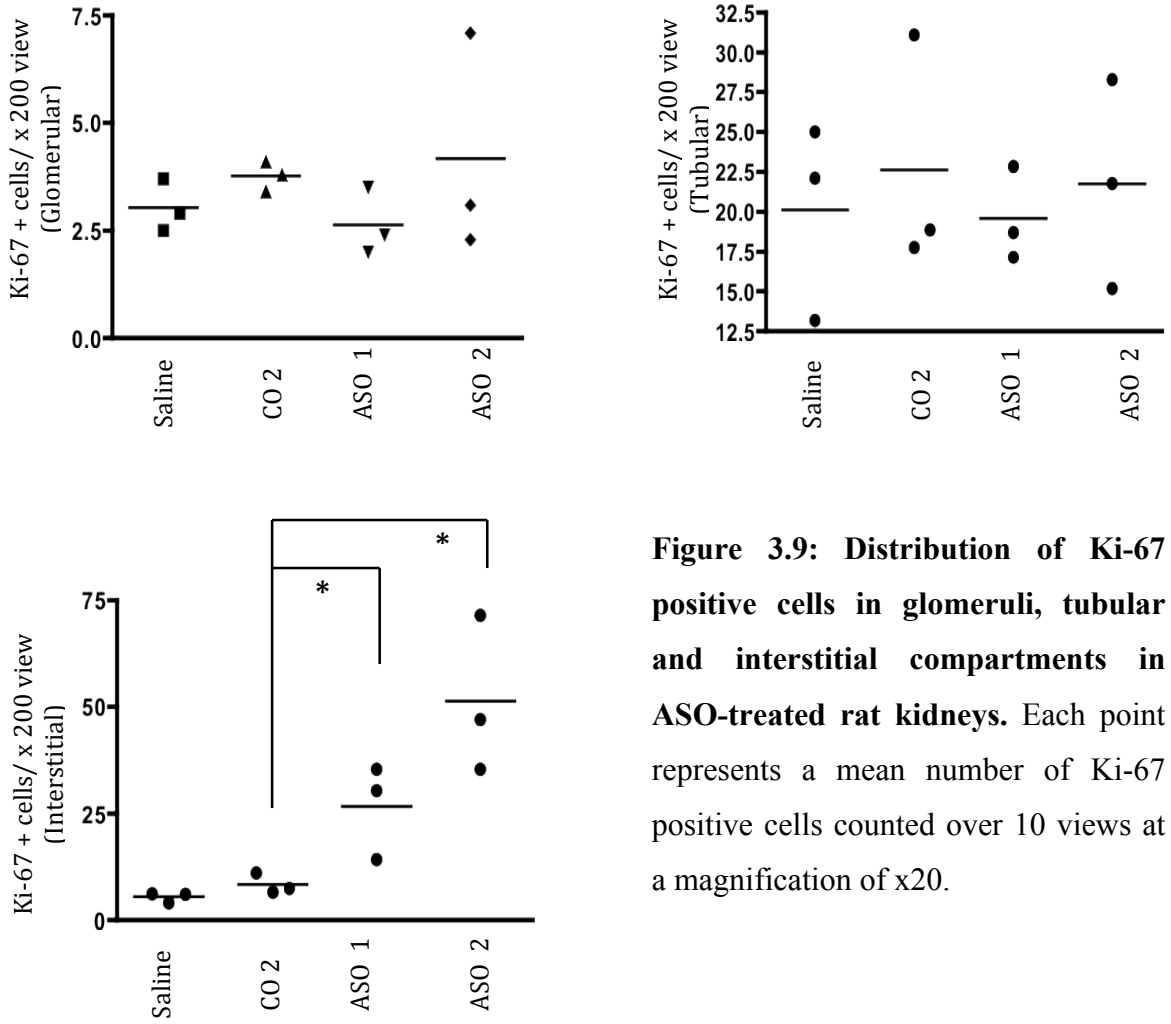

Figure 3.9: Distribution of Ki-67 positive cells in glomeruli, tubular and interstitial compartments in ASO-treated rat kidneys. Each point represents a mean number of Ki-67 positive cells counted over 10 views at a magnification of x20.

There was no significant difference in Ki-67 positive cells within the glomeruli or tubular cells between groups but a significant increase in positive cells in the interstitium in Ki-Ras ASO-treated groups compared to saline and control oligo treated groups.

3.5 Tissue distribution of oligonucleotides following subcutaneous administration

To our knowledge, this project is the first to utilize subcutaneous administration of antisense oligonucleotides in a renal fibrosis model. From published literature and information from ISIS, it is well recognized that paraenteral oligo administration results in active uptake of oligos by proximal tubular cells of the nephron. To investigate if this was also true of subcutaneous administration and to confirm that oligos would reach renal tissue at the dose (12.5mg/kg) that was administered, sections were stained using an antibody against oligonucleotides provided by ISIS Pharmaceuticals. Though the exact epitope target of the antibody was not provided, the fact that it was able to target all oligos suggests that the target epitope was part of the phosphorothioate spine. Antibodies against aquaporin-1 and aquaporin-2 were used to differentiate proximal and distal tubules/collecting ducts respectively and by staining sequential sections ('zero sections'), renal cortical cells in which ASO accumulated could be identified. As part of this experiment the distribution of the antisense oligos both within the kidney and in non-renal tissue was investigated.

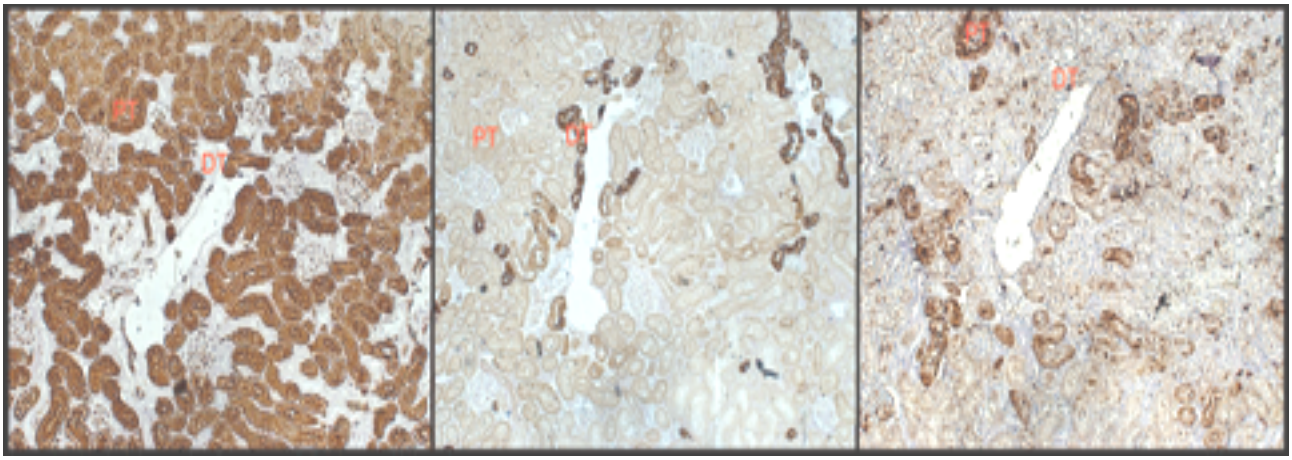

Aquaporin 1 Aquaporin 2 ASO 1

Figure 3.10a: Sequential sections from a single rat kidney immunostained for Aquaporin 1, Aquaporin 2 and oligonucleotide deposits following administration of ASO 1 (12.5mg/kg) (x10). The same proximal convoluted tubule (PT) and distal convoluted tubule (DT) are labeled in each section.

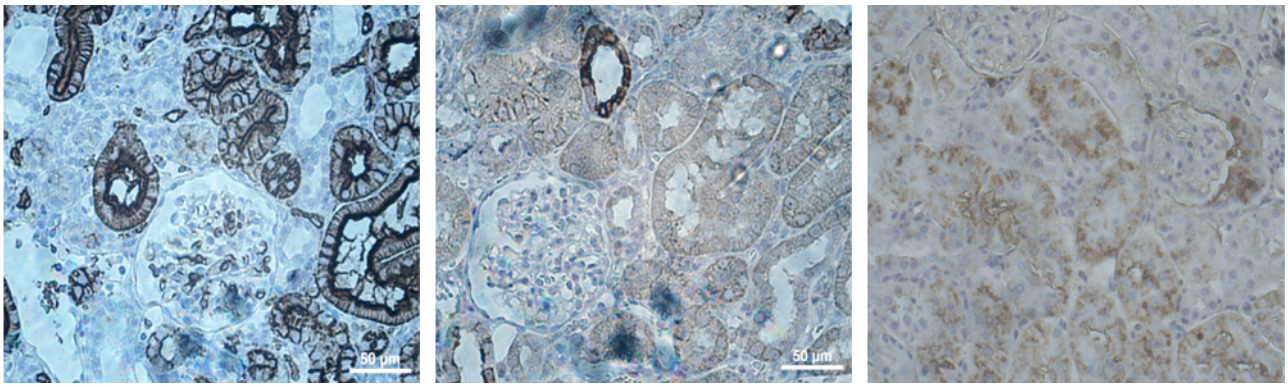

Aquaporin 1 Aquaporin 2 ASO 1

Figure 3.1b: Sequential sections from a single rat kidney immunostained for Aquaporin 1, Aquaporin 2 and oligonucleotide deposits following administration of ASO 1 (12.5mg/kg) (x40).

Immunostaining of sequential sections as demonstrated above revealed that oligos administered via subcutaneous injections were able to accumulate within the kidney. Furthermore oligos accumulated in proximal tubular cells (identified by expression of AQ-1) and the interstitium with virtually no oligo uptake being seen in distal tubular cells (as identified by AQ-2 expression). This suggests that oligonucleotides administered by subcutaneous injection are able to target the kidney, be freely filtered and then appear to be actively taken up by the proximal tubular cells with little reaching the distal nephron in the non-obstructed kidney.

3.6 Distribution of oligo in non-renal tissues

Non-renal tissues harvested included heart, liver and tissue circumventing the laparotomy scar. Tissues was stained for oligo deposition using the specific anti-oligo antibody provided by ISIS Pharmaceuticals.

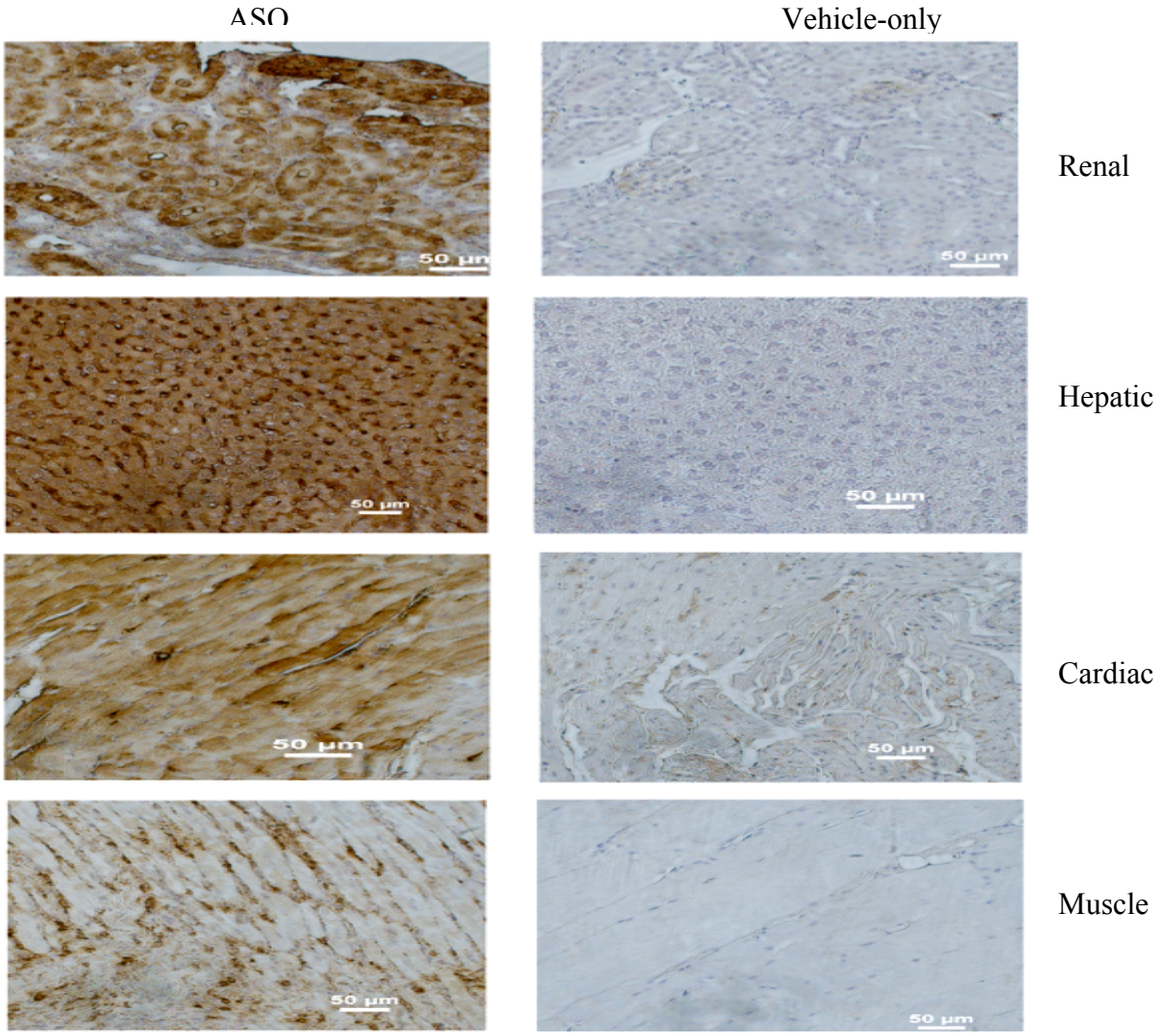

Figure 3.11: Oligonucleotide deposition within renal and non-renal tissue of non-obstructed Wistar rats following subcutaneous administration of ASO 1 at a dose of 12.5mg/kg subcutaneously on alternate days over a 6-day period (Three doses in total). Comparison is made with vehicle only.

The use of anti-oligo antibody confirmed that, following subcutaneous administration, there was a significant accumulation of oligo within both renal and hepatic tissue. However a high degree of deposition of oligo was also observed within both cardiac and muscle tissue.

3.7 Effects of oligonucleotide administration on non-renal tissues

3.7.1 Hepatic tissue

Hepatic tissue is recognized to have a high cellular turnover and has been shown to both actively and specifically take up oligos that are administered parenterally. Hepatic tissue from UUO models that were treated with oligos was retrieved and QPCR for Ki-Ras mRNA expression was undertaken.

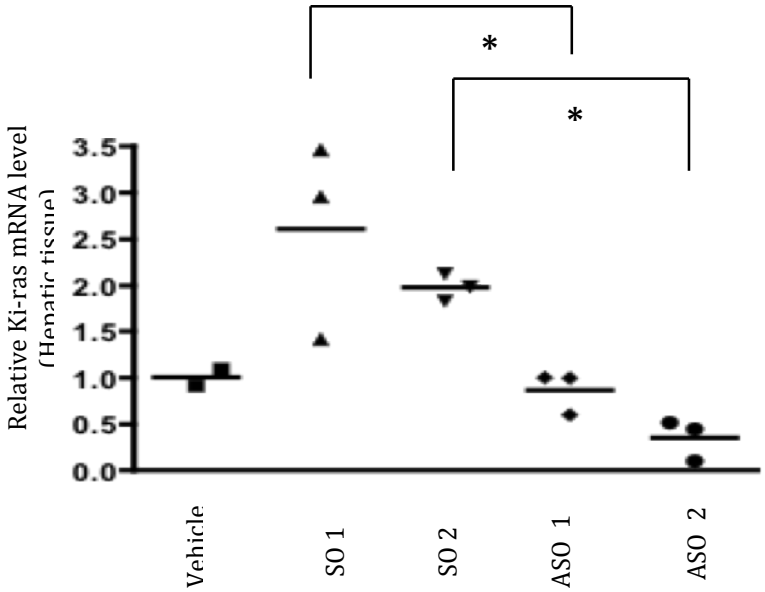

Figure 3.12: Ki-Ras mRNA expression in hepatic tissue of rat models of UUO following oligo administration. Oligos administered at 12.5mg/kg on alternate days over a six day period. Each point is the mean result of six replicates of a single sample. SO 1 and 2 are scrambles of ASO 1 and 2 respectively.

In relation to vehicle-only treated UUO group, there is a significant rise in Ki-Ras expression seen in scrambled oligo groups. ASO 2 reduces Ki-Ras expression by 49% while ASO 1 has no significant effect compared to vehicle-only treated group. Subsequently, hepatic tissue was stained with hematoxylin and eoisin and analysed by a consultant liver histopathologist in a blinded fashion. Unfortunately hepatic tissue treated with scrambled oligos was lost during storage due to freezer malfunction and was not available for analysis.

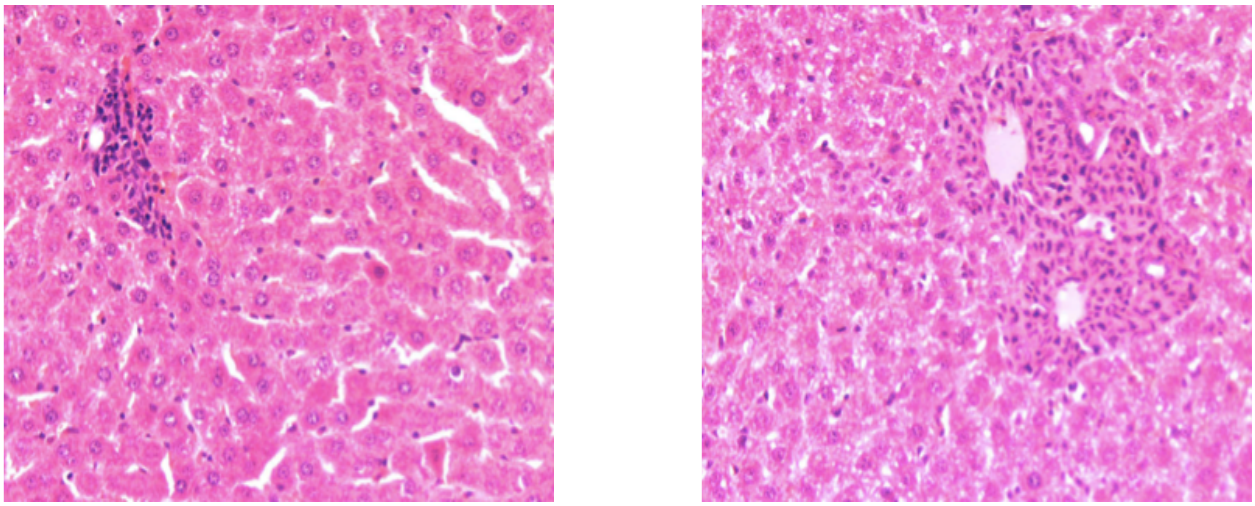

A B

Figure 3.13: Sections of hepatic tissue from UUO model treated with (A) ASO 1 and (B) ASO 2 stained by H&E (x20). Note significant increase in peri-portal inflammation in ASO 2 treated section compared to ASO 1.

Hepatic lobar inflammation was defined by necrosis of individual hepatocytes, mitosis of hepatocytes and increases in numbers of intralobular (intrasinusoidal) leucocytes. It was observed that inflammation was principally a portal-tract phenomenon, with dense cuffs of leucocytes around portal-tract structures. These cuffs appear to be isolated and expand the portal tract itself rather than infiltrating the limiting plate or seeping into the lobule. Ductular reaction was scant and focal and restricted to within the substance of the portal tract. Architecture of the liver was not observed to be disordered with portal tracts and draining venules disposed regularly throughout. The degree of inflammation was given as an arbitrary score with regards to inflammation with 1 being minimal and 4 severe. Inflammation was separated into that affecting lobules and that affecting the portal tract.

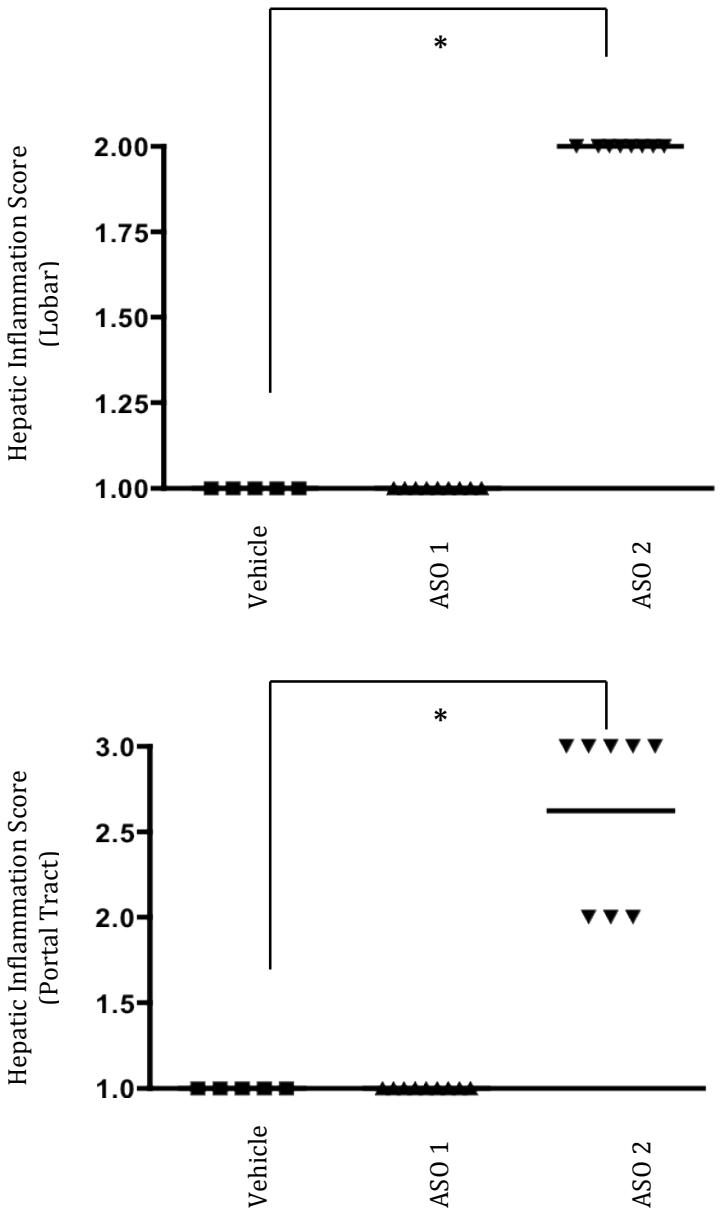

Figure 3.14: Inflammation score for hepatic tissue treated with Ki-Ras ASO. Sections were scored in a blinded fashion by a consultant hepatic histopathologist with an arbitrary score of 1-4 and inflammation divided into lobar and portal tract. Each point represents one animal.

The degree of inflammation within liver tissue was found to be significantly higher in tissue retrieved from ASO 2 treated models as compared to vehicle-only and ASO 1 treated tissue. Liver tissue retrieved from ASO 1 treated models had an inflammation score comparable to vehicle-only-treated.

3.7.2 Cardiac tissue

Following the observation of inflammatory effects in the liver subsequent to ASO administration, cardiac tissue was stained using ED-1 antibody, a macrophage marker.

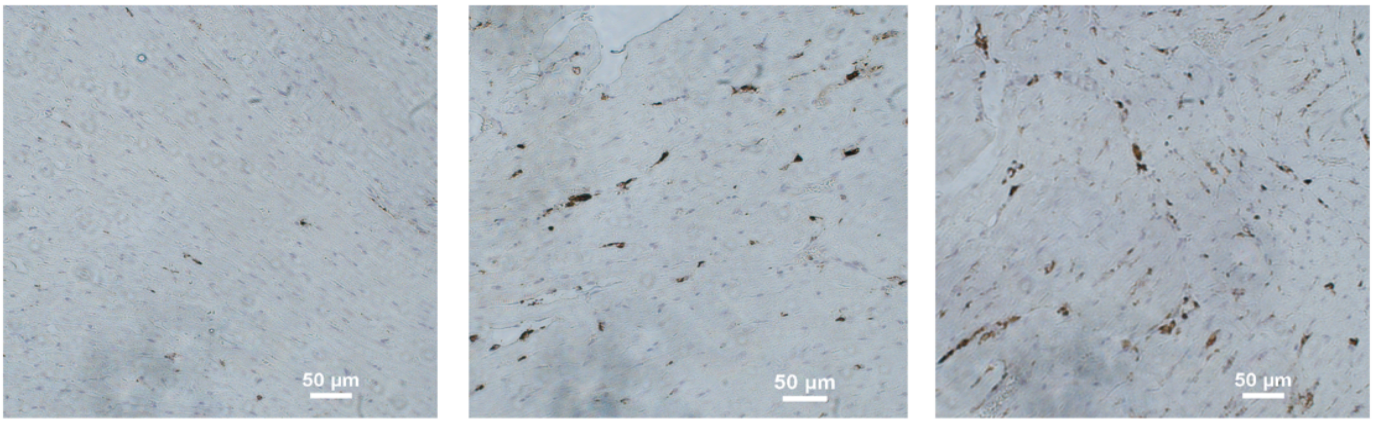

Figure 3.15: ED-1 staining of cardiac tissue retrieved from non-obstructed Wistar rats following administration of vehicle-only or ASOs. Oligos administered at 12.5mg/kg on alternate days over a 6-day period

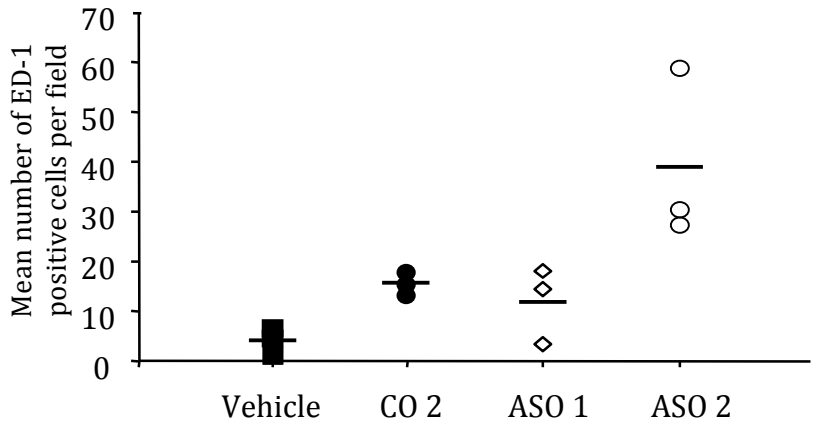

Figure 3.16: Number of positive ED-1 cells per field of view in cardiac tissue retrieved from non-obstructed Wistar rats following administration of oligos. Oligos administered at 12.5mg/kg on alternate days over a 6-day period Each point represents one animal.

The above results demonstrate that, following administration of oligos, the degree of inflammation within the heart is comparable with that of the liver with regards to individual ASO effect. Both CO 2 and ASO 1 result in a doubling of ED-1 positive cells when compared to vehicle-only treated models but ASO 2 treated group results in a near five-fold increase in ED-1 positive cells per view reflecting increased macrophage infiltration and possibly inflammation.

3.8 Summary of results:

1) Transfection of both primary culture fibroblasts and NRK-49F fibroblast cell line with Ki-Ras ASOs at 200nM demonstrated significant and specific knockdown of Ki-ras mRNA expression.
2) Knock down of Ki-ras mRNA resulted in an observed compensatory rise in Ha-ras mRNA expression in primary culture of rat renal fibroblasts and in NRK-49F cell line. There were no observed changes in N-ras expression.
3) Transfection of NRK-52E epithelial with Ki-Ras ASOs at 200nM reduced Ki-ras expression compared to vehicle-only control.
4) Transfection of NRK-52E epithelial with Ki-Ras ASOs at 200nM did not alter either Ha-ras or N-ras mRNA expression when compared to vehicle-only control
5) Transfection of NRK-49F cells at a concentration of 200nM did not induce cytotoxicity based on an LDH assay.
6) Administration of CO 2 in non-diseased Wistar rat models did not significantly alter mRNA levels for any of the isoforms of Ras when compared to vehicle-only group.
7) Administration of Ki-Ras ASO 2 (12.5mg/kg) in non-diseased Wistar rat models resulted in both specific and significant knock down of Ki-Ras mRNA when compared to CO 2 group. These results were comparable to those obtained *in vitro*.
8) Protein expression of pan-Ras was decreased by 60% and 45% on administration of Ki-Ras ASO 1 and ASO 2 respectively in comparison to CO 2.

9) Administration of Ki-Ras ASOs resulted in a significant increase in interstitial cells undergoing active proliferation as detected by Ki-67 expression. There was no observed change in Ki-67 positive cell numbers in either glomerular or tubular compartments following ASO administration.
10) Following subcutaneous administration, accumulation of oligonucleotides within kidney is demonstrated. The proximal tubular cells are the main site of oligo uptake and accumulation within the kidney with no deposition seen in distal tubule cells.
11) Following subcutaneous administration, oligos have a systemic deposition including within cardiac, hepatic and muscle tissue in addition to renal.
12) Both the scramble oligos, SO 1 and SO 2, increase Ki-Ras hepatic expression compared to UUO-VO. Administration of ASO 1 and ASO 2 reduces Ki-Ras mRNA expression in the liver by 14% and 65% respectively compared to UUO-VO.
13) Administration of ASO 2 resulted in significant inflammatory changes in both the lobar and portal tract areas of the liver in comparison to vehicle-only treated group. These changes were not observed on administration of ASO 1.
14) Administration of ASO 2 resulted in a significant increase in ED-1 positive cells in cardiac tissue in comparison to vehicle-only, CO 2 and ASO 1 treated groups.

3.9 Discussion

The main aim of this project was to translate previous *in vitro* work undertaken by our group (Sharpe, Dockrell et al. 1999) to *in vivo* models. However, as the oligos being used for this project were targeted against a different species to those previously used, examination of oligo transfection in rat kidney cells *in vitro* allowed validation of oligo specificity and efficiency in organism-specific cells. The results of this series of experiments indicate that both the Ki-Ras ASOs are effective and specific in knocking down Ki-Ras mRNA expression in rat primary renal fibroblasts and NRK-49F cells.

This knockdown was associated with a possible compensatory up-regulation of Ha-Ras isoform mRNA expression within these mesenchymal cells.

The rat tubular epithelial cells (NRK-52E) cell line was found to be quite resistant to ASO transfection using the simple protocol employed for mesenchymal cells (both primary and NRK-49F). Successful transfection of the epithelial cell line required the technique of 'reverse transfection' which involves addition of detached epithelial cells onto a plate of pre-prepared transfection complexes. Following transfection, NRK-52E cells demonstrated a lesser degree of Ki-Ras mRNA knockdown when compared to their sister NRK-49F cells. This decrease in efficiency may in part be due to difficulties in transfecting this cell line. However, whereas there appears to be a compensatory rise in H-ras expression on Ki-Ras ASO transfection in NRK-49F fibroblast cells, both expression of N- and Ha-Ras mRNA in NRK-52E epithelial cells remained unchanged when Ki-Ras mRNA was knocked down. This difference in 'compensatory' response may indicate different roles for the isoforms of Ras in different cell types.

Using a LDH-based cytotoxicity assay, it was demonstrated that the relative decrease in Ki-Ras mRNA following transfection with ASOs was not as a result of increased cell death from cell toxicity. In fact there was no significant difference in cytotoxicity at increasing concentrations of ASO.

Analysis by QPCR for Ras mRNA expression *in vivo* from oligo treated non-diseased rat models reflected results obtained *in vitro*, demonstrating a significant knockdown of Ki-Ras mRNA expression by ASO 2 (67%), with minimal Ki-Ras mRNA knockdown (12%) by ASO 1. Both ASOs were specific to Ki-Ras with no significant affects on either N- or Ha-Ras levels. Since the ASO effects in non-obstructed kidneys were seen to be specific for Ki-Ras mRNA, in this context one can assume that the decrease in pan-Ras protein expression reflects mainly Ki-Ras protein knockdown. Immunoblot analysis revealed a significant decrease in pan-Ras protein following Ki-Ras ASO administration and moreover it was noted that despite low-level Ki-Ras mRNA knock down by ASO 1, this antisense appeared to produce a greater degree of protein level knockdown overall. However there was significant variability in the immunoblot results and this is likely to represent inaccuracies with regards to immunoprecipitation and normalization to GAPDH of the residual supernatant following immunoprecipitation which may be highly variable and inaccurate.

There was no observable difference in the number of Ki-67 positive cells within the glomeruli or tubular compartments between groups. However there was a significant increase in Ki-67 positive cells in the interstitium of sections taken from both the active Ki-Ras ASO groups in comparison to vehicle and CO 2 treated groups. The lack of increase in Ki-67 cells in the CO 2 group indicates that this observation is due either to Ki-Ras knockdown per se or possible specific attributes of Ki-Ras antisense oligo. Since Ki-Ras is pivotal to cell proliferation the increase in interstitial proliferation is surprising, though the identity of the proliferating cells is unknown and may represent non-mesenchymal cells.

Employing antibodies to oligonucleotides and aquaporin-1 and 2 allowed for identification of proximal tubular cells as the cells in which oligos were deposited within the renal cortex following subcutaneous administration. The lack of any correlation of oligo-positive cells with those expressing aquaporin-2 suggests that that following systemic administration, oligos are freely filtered at the glomerulus and actively reabsorbed at the proximal tubule. This appears to be an efficient process since minimal oligo appears to reach the distal nephron for reabsorption as reflected by lack of accumulation of oligo in distal tubular cells.

Analysis of non-renal tissues also confirms that subcutaneous administration of ASO results in systemic distribution with evidence of oligo deposition in cardiac, hepatic and muscle tissue.

As a site of significant oligo accumulation, the extra-renal effects of ASOs on hepatic tissue was investigated. QPCR of hepatic tissue revealed a significant increase in Ki-Ras mRNA levels on administration of scrambled oligos compared to vehicle-only treatment. Though administration of ASO 1 did not significantly reduce hepatic Ki-Ras mRNA levels, ASO 2 reduced expression by 49% compared to vehicle-only treated tissue. These results of mRNA knockdown reflect the ASO potency observed in renal tissue with more potent knockdown effects observed with administration of ASO 2. It is well recognized that oligonucleotides are actively taken up by liver cells, in particular the Kupffer cells, and these results confirm this. Histological analysis of liver samples was limited by the loss of tissue treated by scrambled oligos due to storage malfunction. However analysis of remaining samples revealed significant inflammation both in lobules and portal tracts of models treated by ASO 2 compared to vehicle-only. Inflammation with ASO 1 administration was minimal and on par with the vehicle-only group.

Cardiac tissue from oligo treated models was also investigated for inflammation by staining for ED-1 expression, a cell marker of macrophages. It was found that though there was an increase in ED-1 positive cells seen in ASO 1 and CO 2 treated samples a much greater increase in cell numbers was observed on administration of ASO 2. This demonstrates that subcutaneous administered oligos may be widely deposited throughout peripheral tissues. Furthermore that the oligos themselves may induce a inflammatory reaction within the tissue they are deposited in and that the make-up of individual oligos, perhaps in terms of which bases they are composed of or the binding site of target mRNA, may dictate the degree of inflammatory response.

The above results demonstrate that subcutaneous administration of ASOs is able to target both the kidney and liver and that uptake of these molecules may potentially lead to significant knock down of both Ki-Ras mRNA and protein levels. The observed reduction in Ki-Ras expression was not associated with any decrease in cell proliferation within the kidney. The uptake of certain oligos may lead to increased inflammation within various tissues depending on the oligo make-up. This point was discussed with ISIS pharmaceuticals and it was confirmed that oligos had been recognised to induce inflammation but they are now able to design newer oligos that avoid this effect.

Chapter 4: Expression & characterization of Ras isoforms in a rat model of unilateral ureteric obstruction

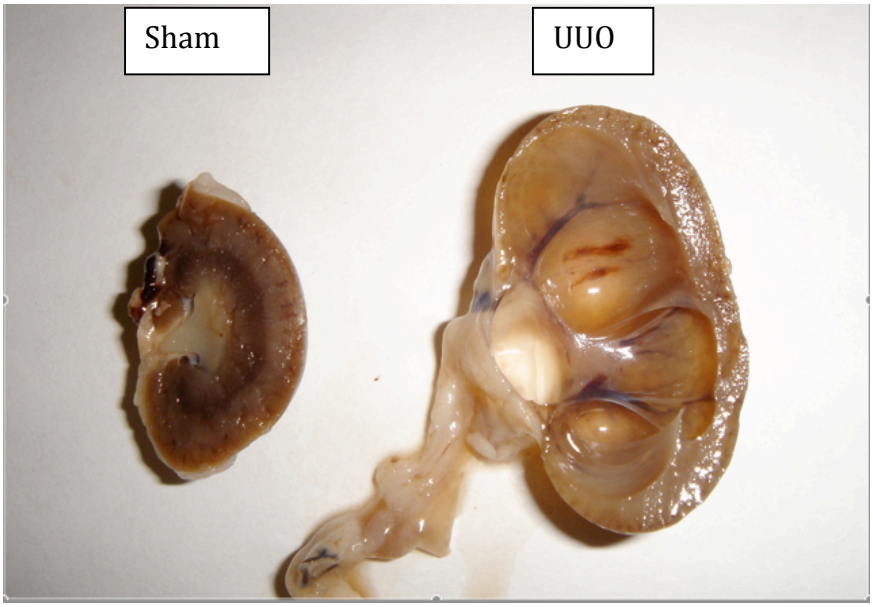

Figure 4.1: Gross appearance of an obstructed kidney compared to a kidney from a sham-operated model following 12-days obstruction.

As part of this project a model of renal fibrosis secondary to unilateral ureteric obstruction was set up (see *Methods & Materials*). An assessment of fibrosis and the process of fibrogenesis was made using both histological staining and molecular markers. The time periods for the length of obstruction examined were 5, 12 and 16 days. Following assessment of fibrosis, made by a consultant renal histopathologist, at these various time points, it was concluded that the optimum time period for observing both a significant degree of interstitial fibrosis and a rise in fibrogenic molecular parameters was 12 to16 days.

4.1 Fibrosis in UUO kidney samples compared to sham at different time points

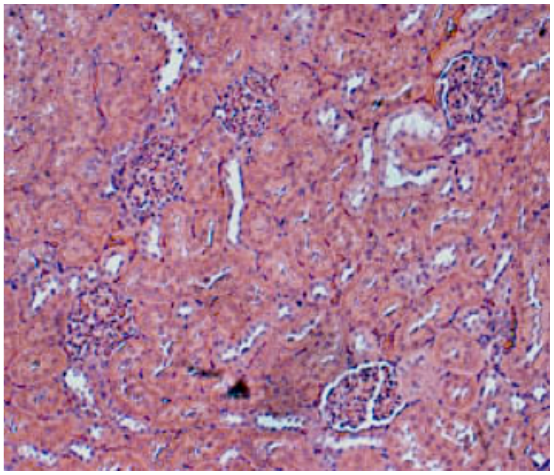

Sham

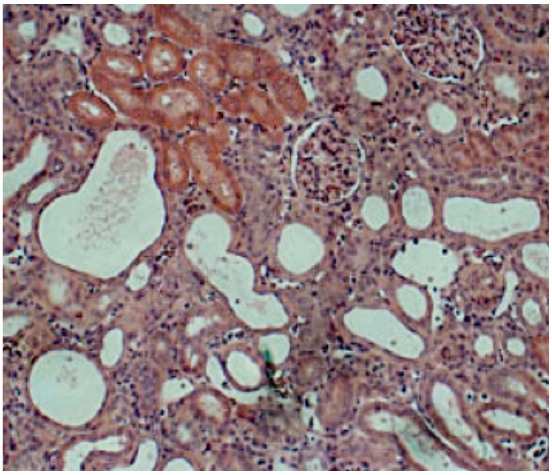

UUO Day 5

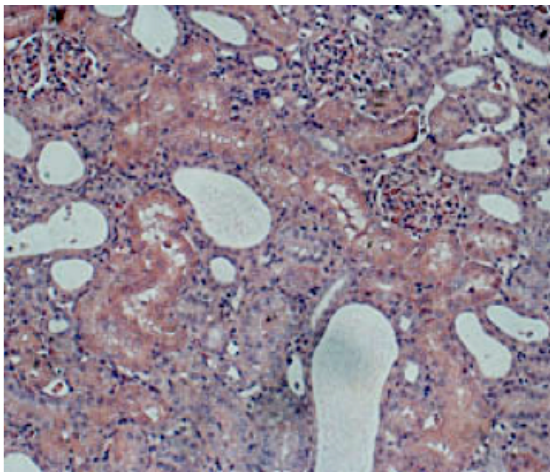

UUO Day 12

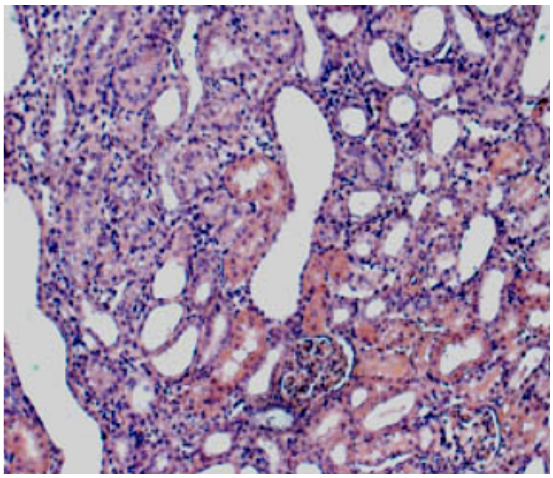

UUO Day 16

Figure 4.2: H&E stained sections from sham and UUO kidneys Day 5, 12 & 16 (x10). Note dilated tubules, flattened tubular cells, increased interstitial area and inflammatory infiltrate in obstructed samples.

Various stains, both special and immunohistological, were used to examine tissue for fibrosis and parameters of fibrogenesis:

1) Fibrosis & matrix deposition: Picromallory trichrome (PMT) and Picrosirius Red
2) Myofibroblastic activity: alpha smooth muscle actin (αSMA) & collagen I
3) Fibroblast marker: Fibroblast specific protein 1 (FSP-1)

4.1.1 Picromallory Trichrome

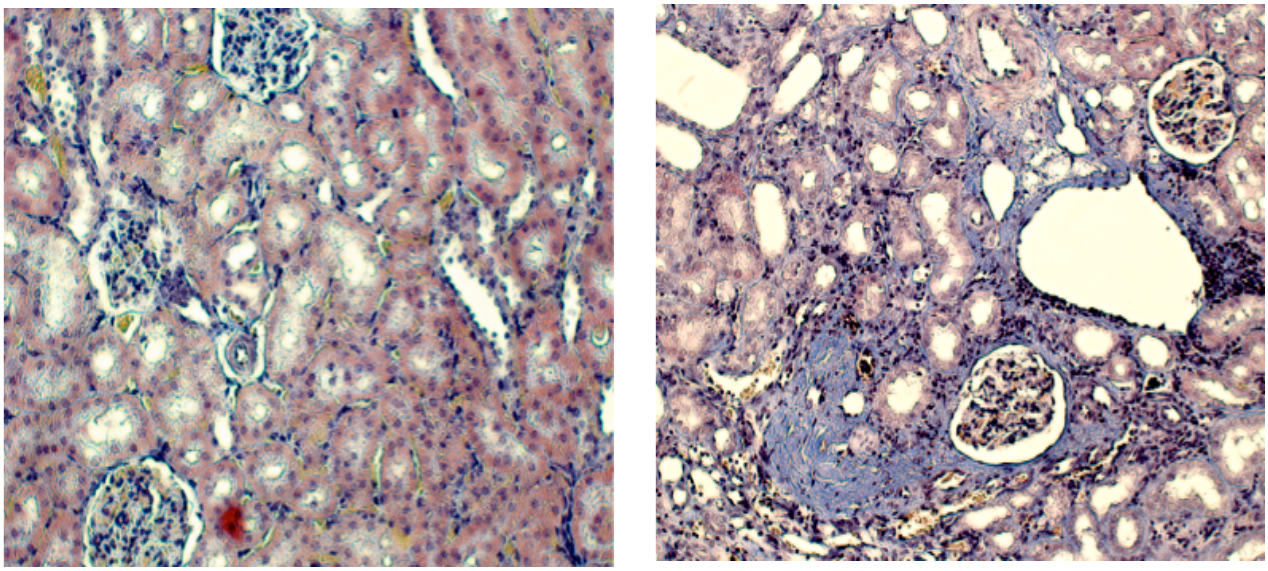

Sham **UUO**

Figure 4.3: Picromallory trichrome (PMT) staining of kidney sections from Sham and UUO kidneys at day 12 (x20). Fibrin & muscle stain red, collagen & reticulin stain blue, nuclei stain blue/black & red blood cells stain yellow. The sham section demonstrates normal perivascular collagen staining. The UUO section demonstrates dilated tubules with flattened epithelial cells, expansion of interstitial space with increased interstitial collagen deposition & inflammatory infiltration.

4.1.2 Picrosirius Red

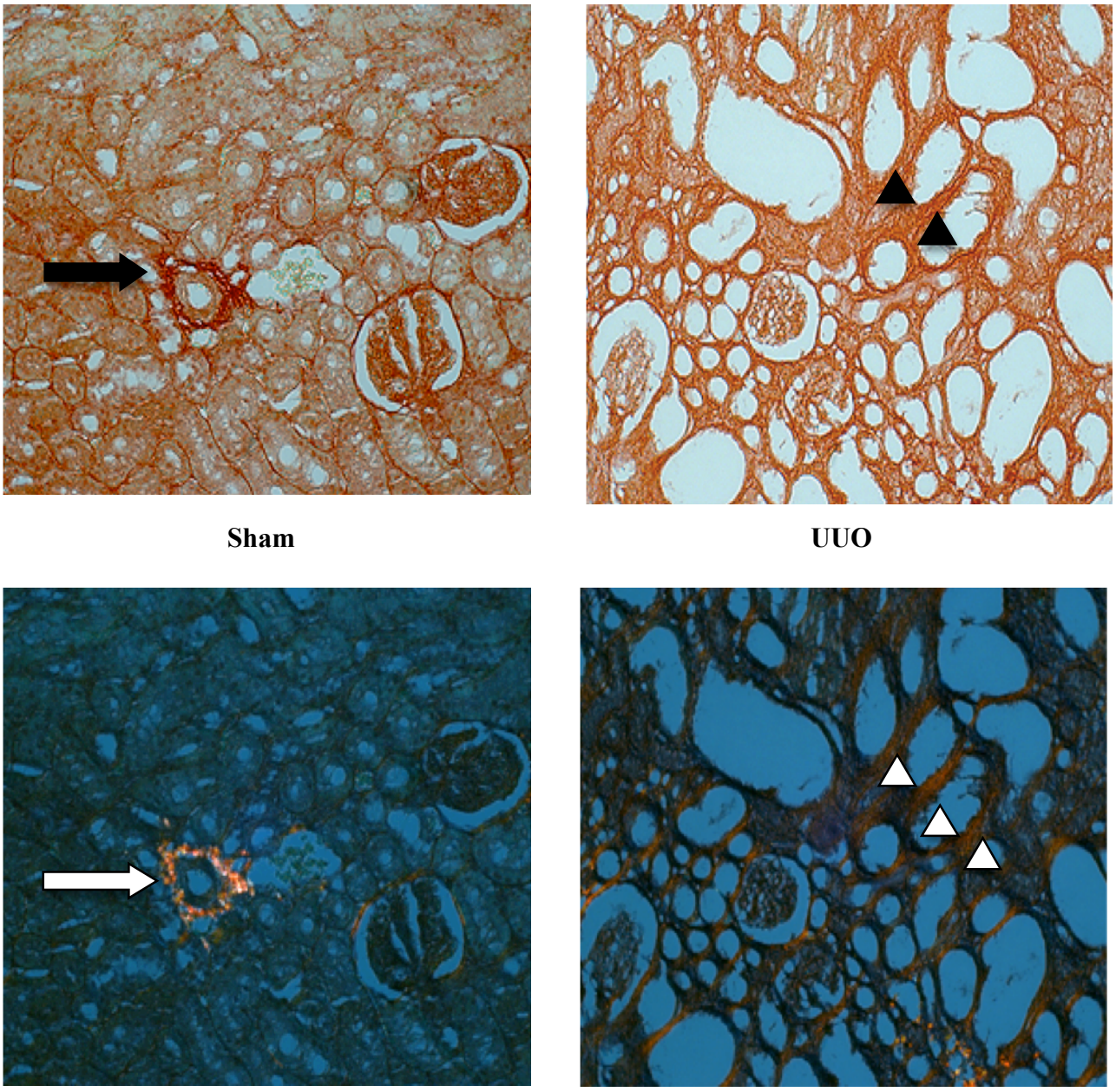

Figure 4.4: Sections of sham and UUO kidney at day 16 stained using 0.1% picrosirius red (x20). (A) Bright light: collagen fibres appear red on yellow-rose background. Note normal perivascular (arrow) staining in sham sample around an artery & increased interstitial staining (arrowheads) in UUO section. **(B) Cross-polarized light:** Larger collagen fibres (I & III) appear orange-yellow while thinner fibres appear green. Note normal perivascular collagen deposition in sham sample (arrow) and interstitial deposition within UUO samples (arrowheads) that are widespread as compared to viewing under bright light.

4.2 αSMA staining

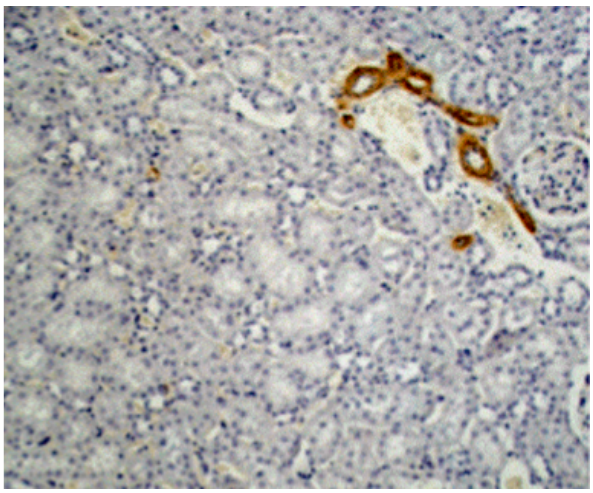

Sham

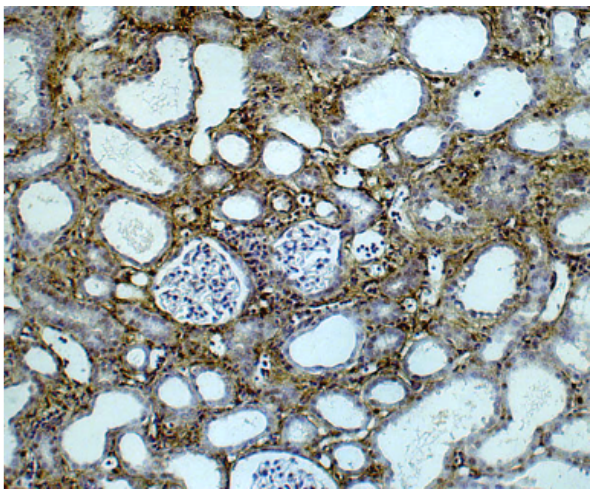

UUO

Figure 4.5: αSMA staining of kidney sections from Sham and UUO at day 12 (x10). Note normal perivascular staining for αSMA expression in sham section but lack of interstitial staining. There is widespread interstitial αSMA expression detected on UUO sample.

4.3 Collagen I staining

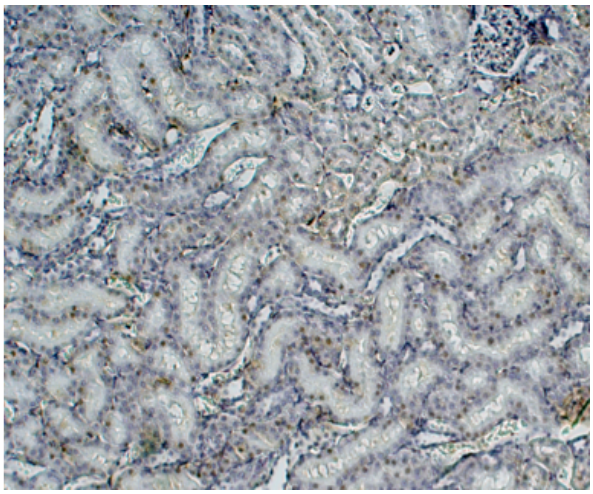

Sham

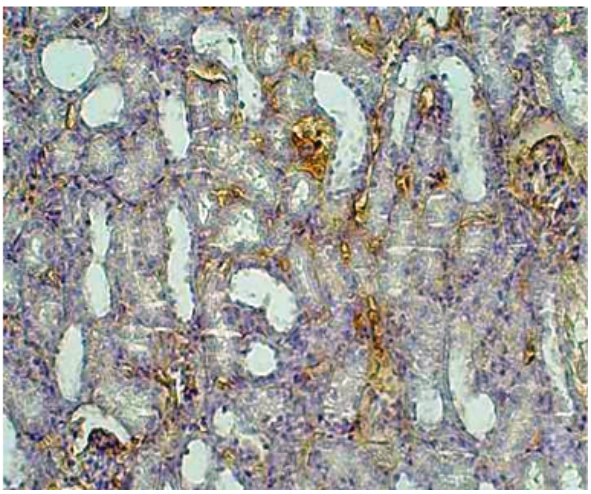

UUO

Figure 4.6: Collagen I staining of kidney sections from Sham and UUO at day 12 (x10). Polyclonal antibody to collagen I shows widespread interstitial collagen expression (arrowheads) detected on UUO sample that is absent in sham sample.

The previous figures are representative of renal tissue from sham and UUO models. Sections from both groups were scored by a consultant renal histopathologist for degree of tubulointerstitial fibrosis, collagen I and α-SMA expression.

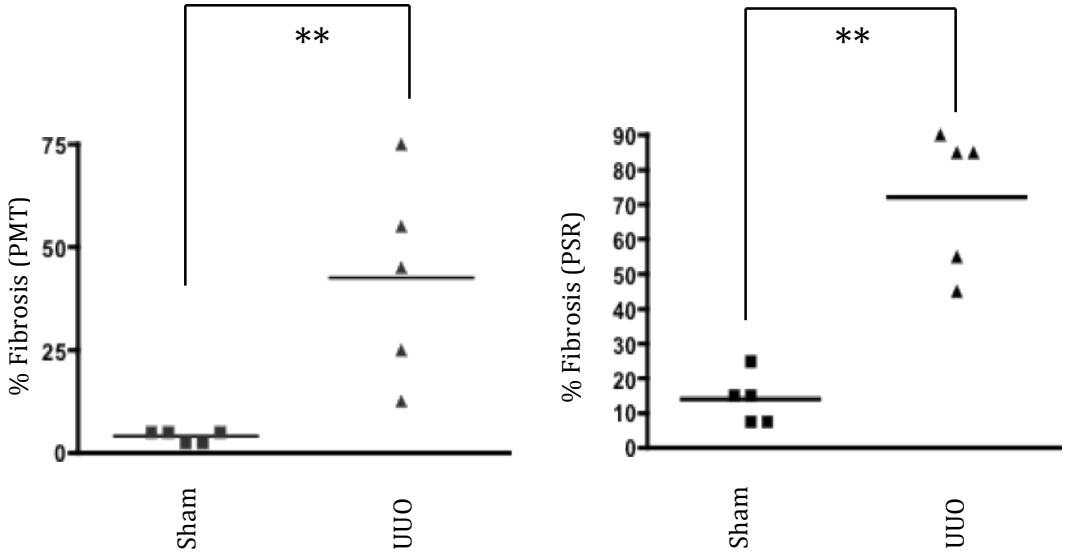

Figure 4.7: Renal cortical tubulointerstitial fibrosis based on picromallory trichrome and picrosirius red staining in sham and UUO kidneys at day 16 [p<0.01].**

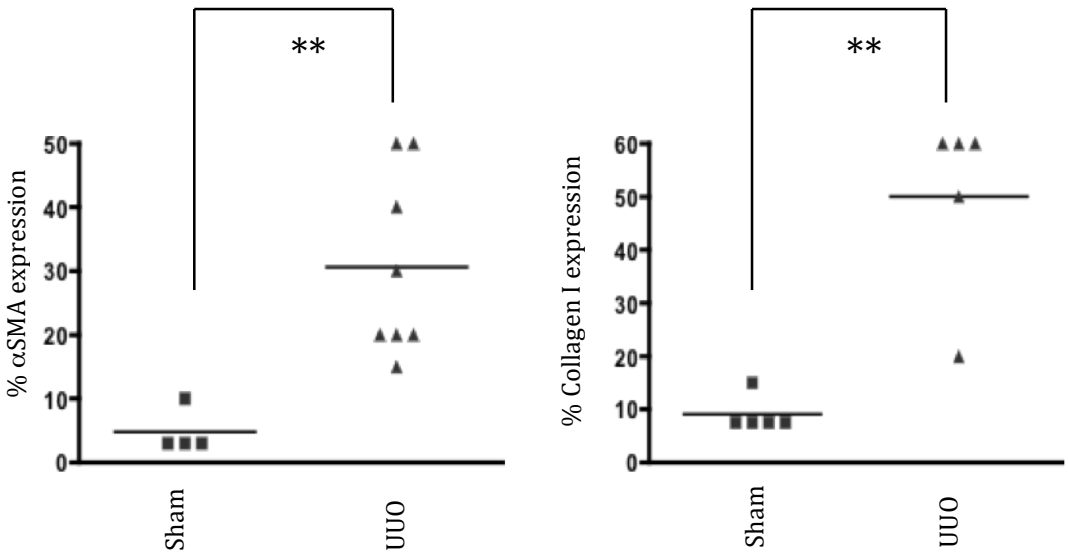

Figure 4.8: Cortical tubulointerstitial αSMA and collagen I expression in sham and UUO kidneys at day 12 [p<0.01].**

4.4 FSP-1

Staining and scoring of FSP-1 in three sham-operated and nine obstructed kidney samples was performed with score based on the mean of ten views per section at a magnification of x 40.

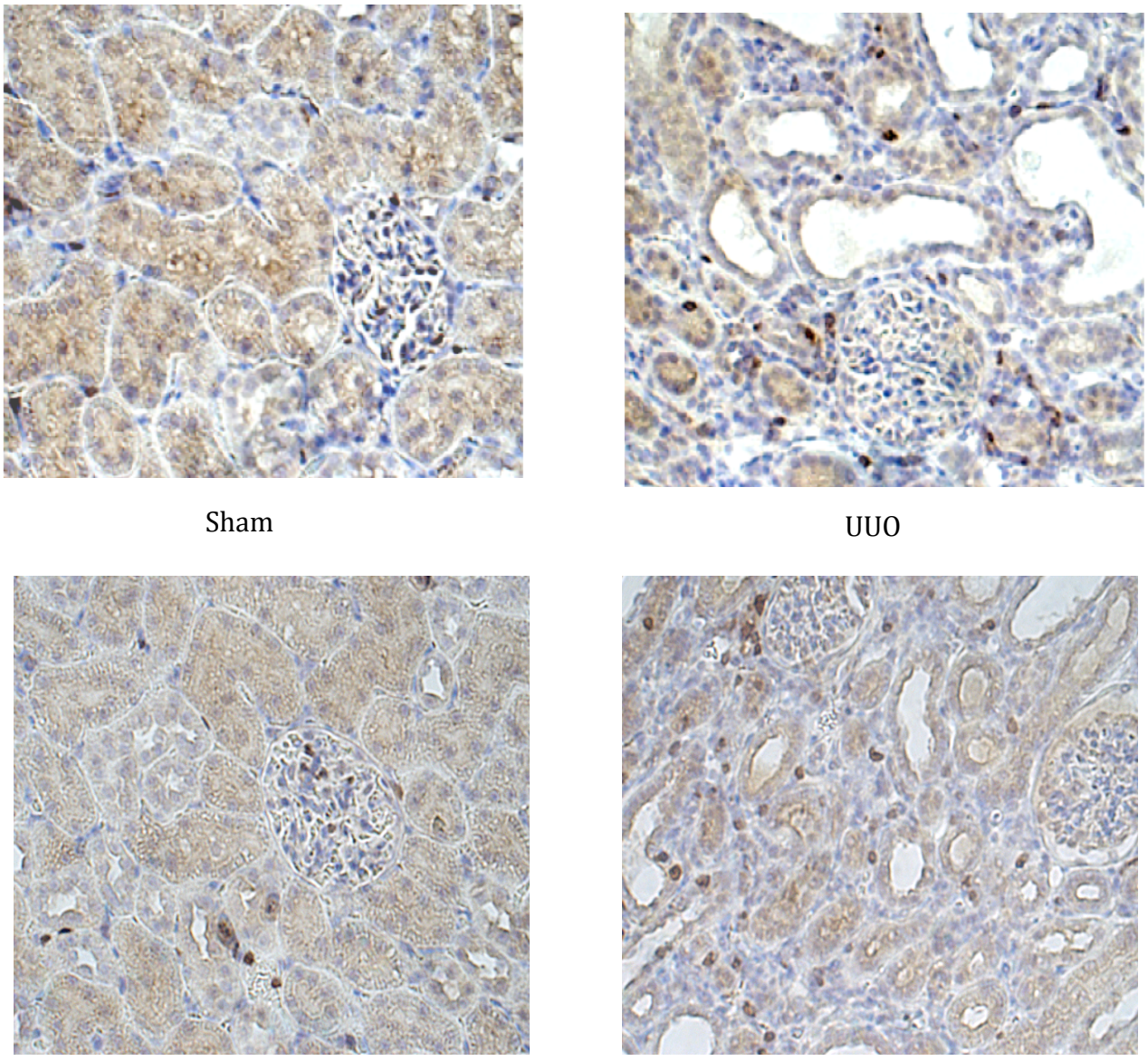

Figure 4.9: FSP-1 staining of kidney sections from two Sham and two UUO at day 16 (x40). Note scant staining in sham section but increased expression was detected on UUO sample.

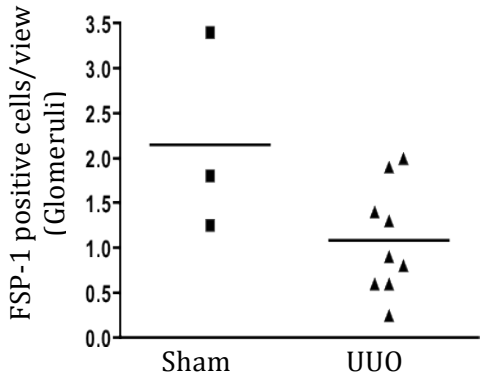

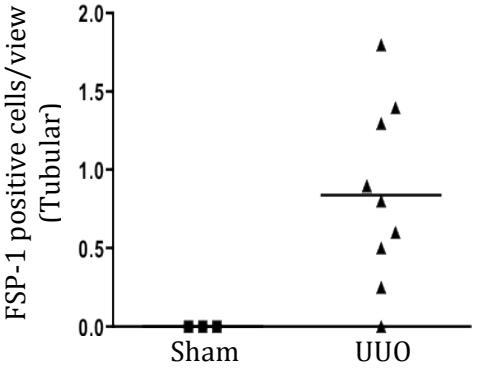

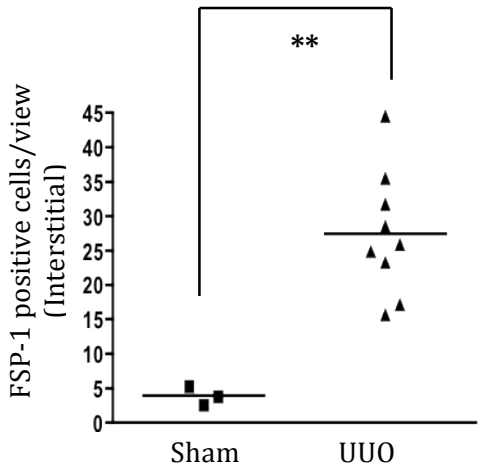

Figure 4.10: FSP-1 positive cells per view (x 40) in day 16 sham-operated and obstructed kidneys. Cell count compartmentalized in to glomerular, tubular and interstitial compartments.

Staining for FSP-1 demonstrated an increase in tubular expression in obstructed kidneys when compared to sham. Though this difference was statistically significant, in absolute terms the mean difference was one positive cell. However obstruction resulted in a mean five-fold increase in FSP-1 expression within the interstitium of obstructed kidneys when compared to sham-operated samples.

4.5 Ras isoform mRNA expression in a rat model of UUO

4.5.1 Semi-quantative PCR

Semi-quantative reverse transcriptase polymerase chain reaction (SQ-PCR) was used to examine mRNA expression. Primers were designed using published sequences for the different isoforms (see *Methods & Materials*). β-actin was used as reference gene. The figures below are representative examples of SQ-PCR results comparing Ras expression between sham and UUO renal specimens.

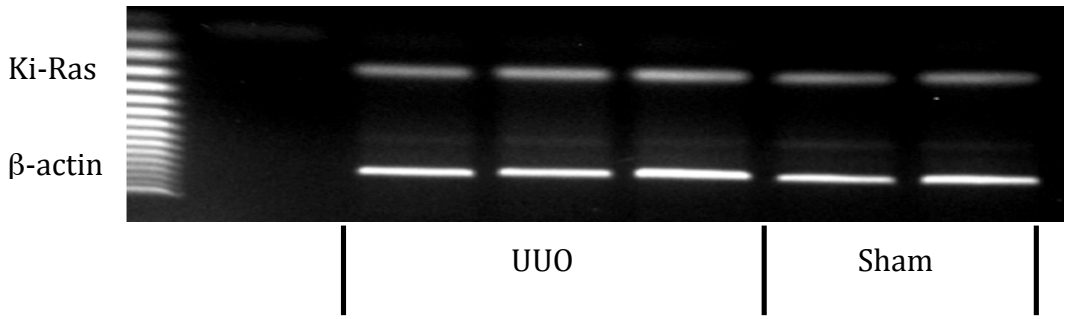

Figure 4.11: DNA gel of SQ-PCR of Ki-ras (159bp) from renal tissue of sham-operated rats and the obstructed kidney of UUO 12 day models. The SQ-PCR reaction was carried out using 26 cycles of PCR. The figure is representative of 3 separate SQ-PCR experiments using identical renal samples of UUO at 12 days. β-actin (593bp) was used as a loading control.

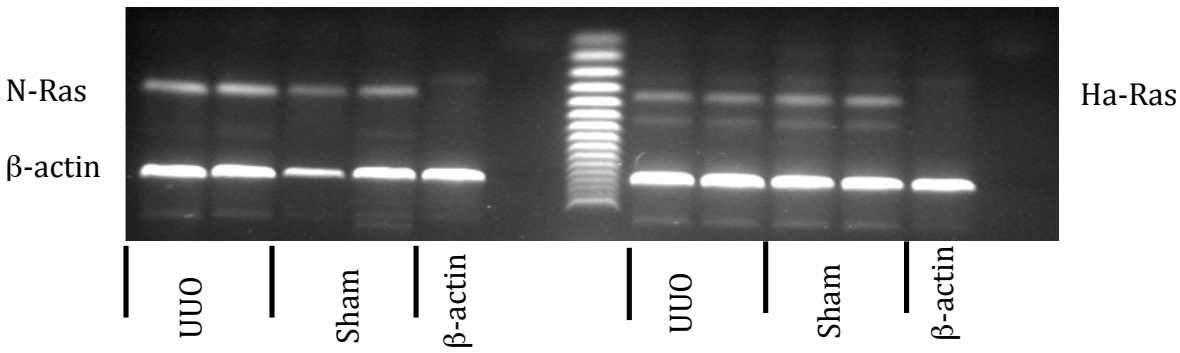

Figure 4.12: DNA gel of semi-quantative SQ-PCR of N-ras (204bp) and Ha-ras (224bp) from renal tissue of sham-operated rats and the obstructed kidneys of 12 day UUO models. The SQ-PCR reaction was carried out using 25 cycles of PCR. The figure is representative of 3 (Ha-Ras) and 4 (N-Ras) separate SQ-PCR experiments using identical renal samples. β-actin was used as a loading control.

When Ras isoform mRNA expression was normalised to β-actin expression there was found to be no significant difference between Ras isoform expression in sham as compared to obstructed kidney cortical tissue.

Previous studies have observed a difference in both total and isoform Ras protein expression in both human and animal models of renal disease (Kocher, Moorhead et al. 2003; Grande, Fuentes-Calvo et al. 2009). It was thought that the lack of observation in difference in Ras mRNA expression may be in part due to lack of sensitivity secondary to high amplification of SQ-PCR and the relative inability to adequately discriminate between bands on gel electrophoresis. Furthermore, the potential of change in expression of β-actin mRNA levels in obstructed kidneys was also considered to be a possible factor in a result that was inconsistent compared to previous other studies. Subsequently real-time PCR (or QPCR) was employed. QPCR is highly sensitive and can detect differences as low as x2 to x10. In addition GAPDH mRNA levels were shown to be more stable in the context of UUO than β-actin levels (see *Methods & Materials*) and thus GAPDH was used as a reference gene.

4.5.2 Real-time PCR

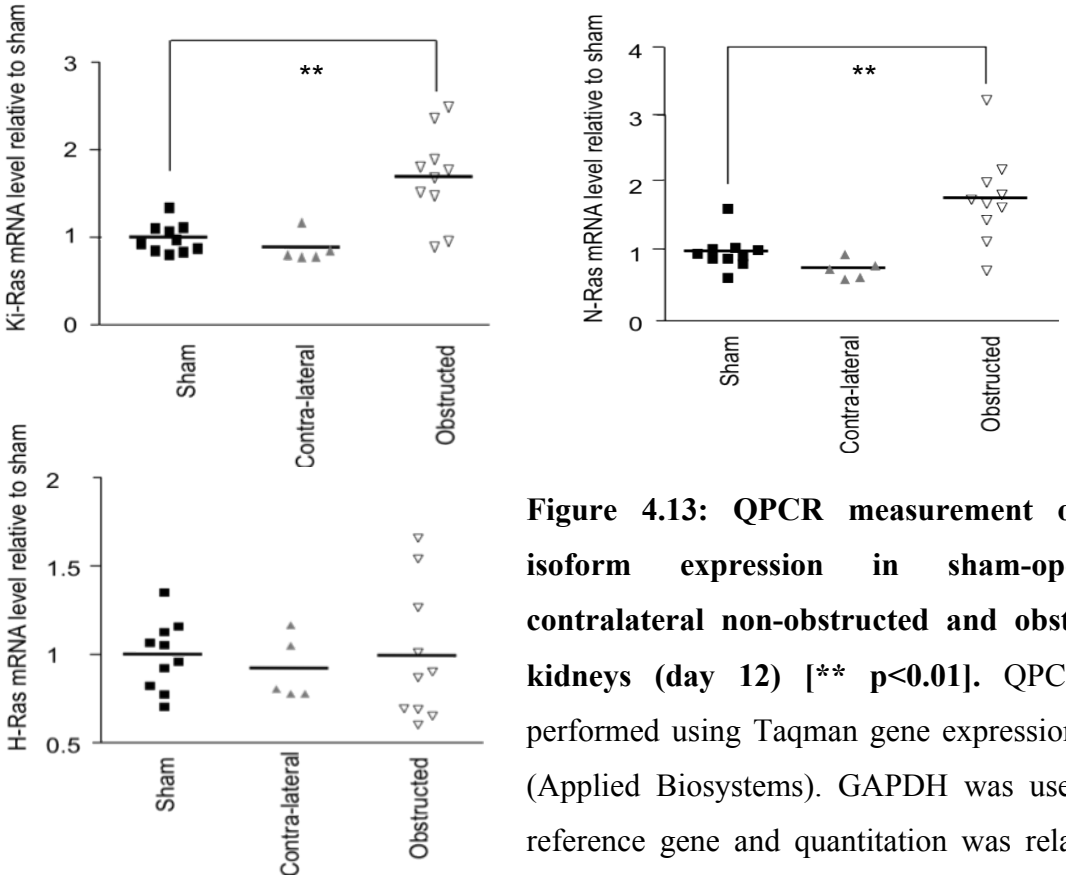

Figure 4.13: QPCR measurement of Ras isoform expression in sham-operated, contralateral non-obstructed and obstructed kidneys (day 12) [p<0.01].** QPCR was performed using Taqman gene expression assay (Applied Biosystems). GAPDH was used as a reference gene and quantitation was relative to expression in sham group.

Results from QPCR analysis of Ras isoforms show no difference in Ha-Ras mRNA expression between UUO and sham kidneys. However there was a significant increase in Ki-Ras mRNA expression of 71% and in N-Ras mRNA expression of 80% observed in UUO samples compared to sham (both p value <0.001). The rise in these isoforms of Ras mRNA expression is localised to the obstructed kidney alone with measurement of Ras isoform expression in the contralateral non-obstructed kidney being comparable to sham for all Ras isoforms.

4.6 Ras isoform protein expression in a rat model of UUO

Due to relatively low abundance in the cell, Ras protein isolation required overnight immunoprecipitation from protein lysates of kidney samples *(See Methods & Materials)*. Western blotting for Ras isoforms as well as for Pan-Ras was performed. There was strong non-Ras band at 25-27kD of unknown origin that was constantly detected. This protein band was not further investigated in this project. Comparison of Ras protein expression was measured using area and densitometry. The following results are representative of at least three experiments.

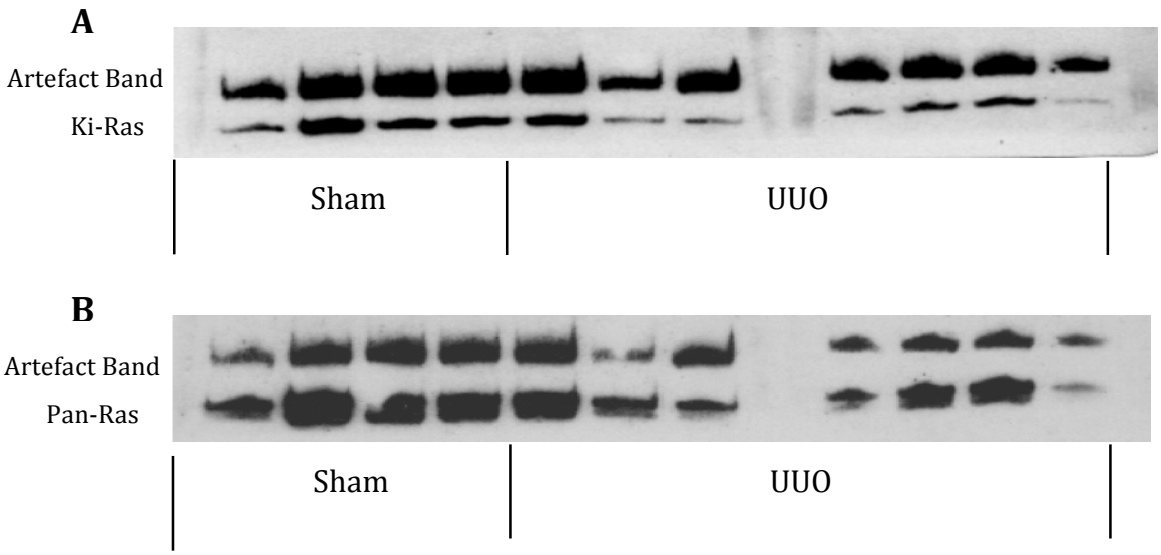

Figure 4.14: Western blot for Ki-Ras (A) and Pan-Ras (B) in Sham and UUO kidney (day 12). Note consistent heavy artefact 26kD band. Ras protein detected at 21-22kD with high intra-group variability in band density. Immunoblots are representative of three experiments.

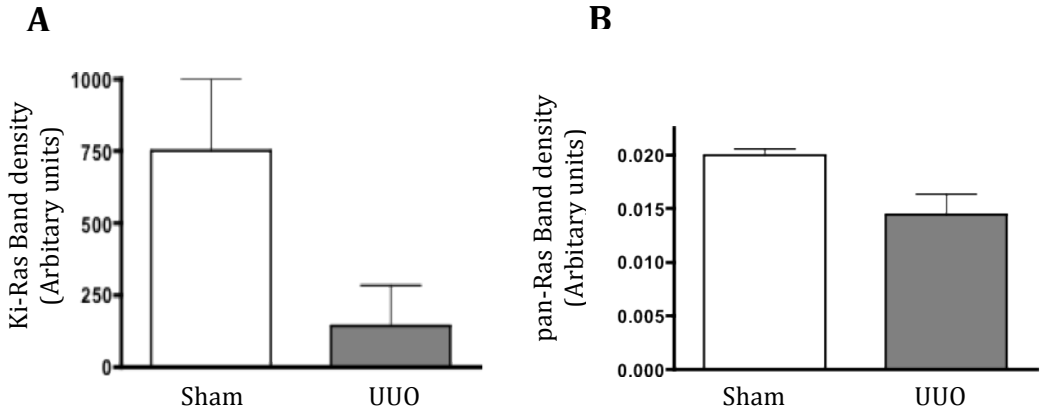

Figure 4.15: Comparison of band density for Ki-Ras (A) and pan-Ras (B) for Sham and UUO kidneys (day 12).

The results obtained from western blotting for Ras proteins were highly variable and lacked consistency despite using identical samples and materials, with band density for a single sample varying significantly between experiments. The mean measurement of band density/area demonstrated an overall decrease in Ras protein in UUO samples when compared to sham. This contradicts both previous published studies and results obtained from analysis of mRNA levels using QPCR in this project.

4.7 Ras immunohistochemistry

Histological staining for Ras protein allows assessment of abundance and localization of Ras as a whole and its various isoforms both in sham and UUO kidney and how expression changes during the process of renal fibrosis secondary to obstruction.

As mentioned in *Methods & Materials* the actual practical process of obtaining satisfactory immunohistological staining for Ras was difficult and required the trial of several antigen retrieval techniques (see *Appendix I*). Poor antibody specificity with high isoform crossover resulted in an inability to differentiate isoforms and a high non-specific background. The procedure of immunohistochemistry, though occasionally successful, was in by no means consistent, homogenous or reliable enough to interpret comprehensively.

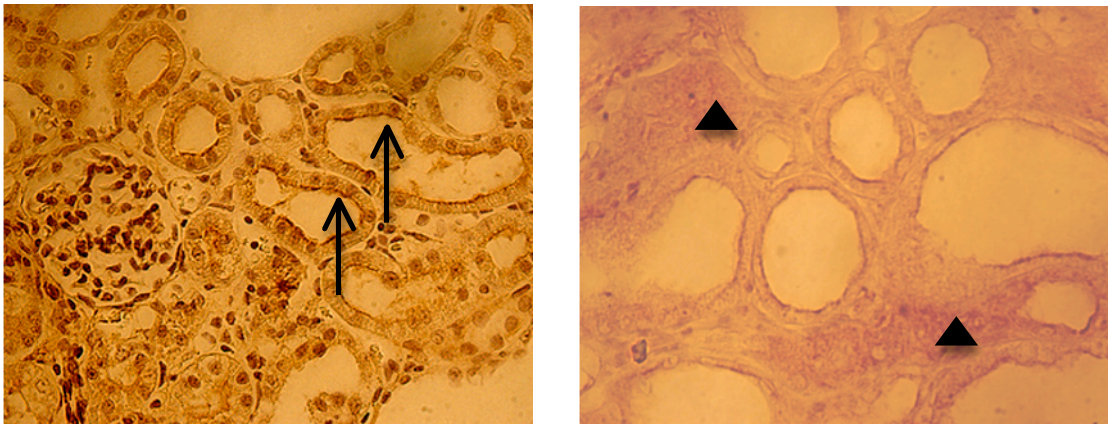

A B

Figure 4.16: Immunohistological staining for Ki-Ras (A) Section of UUO kidney [x20]. In both above figures, note once again occasional non-specific apical tubular epithelial stain (arrows) but lack of cytoplasmic or interstitial staining. **(B) Section of UUO kidney [x40].** Note increased staining of apical border of tubular cells and a degree of increase on interstitial staining (arrowhead).

4.8 Localization of Ki-Ras mRNA expression

Whole renal cortex tissue lysate is used for analysis of Ras expression thus there may actually be an underestimate of ASO knockdown effects on renal cells alone as there may be a contribution from infiltrating inflammatory cells to the overall Ras expression within the kidney sample. In addition, oligonucleotides have been shown to be actively taken up by proximal tubular cells with interstitial infiltration being more problematic. Though overall knockdown of Ki-ras mRNA expression in whole tissue lysate has been seen on administration of ASOs (see *Chapter 3*), the compartment which is affected, be it glomerular, tubular or interstitial, is not identified. We attempted to localize the cellular compartments in which Ki-Ras mRNA is expressed and assess how expression in these cells altered in UUO and by treatment with ASOs by employing laser microdissection and *in situ* hybridization.

4.8.1 Laser microdissection and pulsed collection

This technique allows for exclusive dissection of tubular cells and thus removes the possible confounding factor of target gene contribution from infiltrating inflammatory cells. The microdissection process was performed using P.A.L.M. Microlaser Technologies incorporating a micromanipulation systems using laser microdissection and pressure catapulting [LMPC] (see *Methods & Materials*). Laser microdissection has previously been used in mRNA analysis of renal tissue. Nagasawa *et al.* used LMPC to confirm upregulation of TGFβ mRNA in glomeruli of an anti-Thy1.1 rat models (Nagasawa, Takenaka et al. 2000). Cohen *et al.* also used PALM microdissection technology from human renal transplant rejection biopsy tissue (Cohen, Grone et al. 2002) and were able to employ both paraffin embedded samples as well as cryosections.

From my initial trials, dissection of 10 proximal tubules (each tubule consisting of a mean of 15-20 epithelial cells) from sham kidney samples only resulted in a mean RNA retrieval of 0.4 ng/µl. For adequate RNA reverse transcription a minimum of 50ng of RNA was required. Subsequently up to 120 tubules were dissected from various tissue samples including UUO vehicle-treated tissue. RNA retrieval unfortunately only produced a maximum of 3.8ng/ µl RNA-still significantly too low for RNA RT by this method.

Thus though LMPC isolation of Ki-Ras knockdown is still potentially possible, the process is restricted by time limits for each section, high number of cells required for adequate RNA retrieval and may be influenced by low Ras expression generally in cells. Furthermore adequate RNA retrieval from sham kidneys may not reflect UUO samples where tubules are distended and tubular cells are flattened and atrophic. Though this work focused mainly on tubular retrieval (since oligos have been shown to actively be taken up by these cells), future attempts should also consider glomerular and interstitial compartments.

4.8.2 *In situ* hybridization

In situ hybridization (ISH) provides an ideal method for localizing mRNA expression within tissue samples. However it is a difficult technique and in the case of renal Ras expression there are the further complicating factors:

1) Ras is expressed at low levels
2) the fact that Ras mRNA is a relatively small molecule
3) identification of Ras isoforms means probes are required to be directed to the nucleotides coding for the hypervariable region- which is only 20% of the whole sequence of which not all may be spatially available for probe binding.

A commercial non-radioactive ISH kit was used to attempt to localize Ki-Ras (Hybriprobe® Triseq kit purchased from Biognostik). This kit was designed for detecting RNA which has a low level of expression.

Unfortunately the results from using this kit were highly variable and inconsistent. Though the positive control, Poly dT probes, was successful experiments employing probes for Ki-Ras were never successful despite over six attempts with variation in probe concentration and stringency of experiment. In part this is due to the points mentioned above. In addition of the three actual probes provided in the kit only two were directed towards *rattus norvegius* Ki-Ras and it is unclear from manufacturer's data whether these probes have been designed with regards to spatial character of molecule. ISH is still of great potential in localizing Ki-Ras mRNA expression within tissue. However there must be particular aspects of the technique that must be addressed including design of probes, use of multiple probes to amplify detection and possibly use of radioactive probes.

4.9 *In vivo* TUNEL staining for apoptosis

Ras has a significant role in cell proliferation and survival. A TACS TdT (terminal deoxynucleotidyl transferase) kit (R&D systems TA4625) was used to detect apoptosis. 10 views per section were analysed for positive TUNEL staining at magnification of x40.

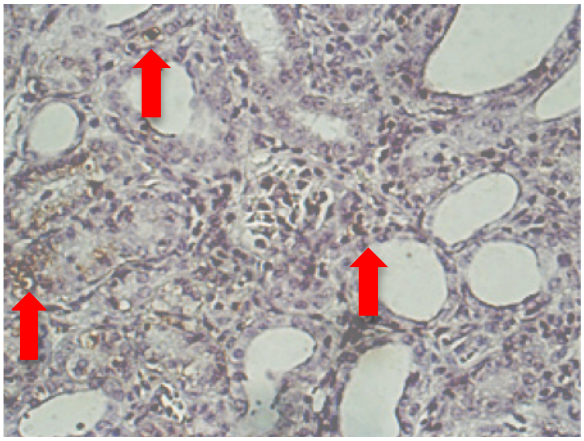

Figure 4.17: UUO vehicle only treated section stained with TUNEL assay. Positive TUNEL cells marked by arrows.

Unfortunately the staining of tissue sections was not always consistent and several sections were not adequately stained for scoring. This process will require repeating to improve the number of samples for each condition. Another method to look at degree of *in vivo* apoptosis is to analyse expression of caspase-3 on SDS PAGE and immunoblotting though this does not have the advantage of localizing apoptotic cells.

4.10 Summary of results of characterization of UUO model:

1) A model of renal fibrosis based on unilateral ureteric obstruction over a 12-16 day period was set up and characterized by using a histological fibrosis score based on PMT & PSR staining.
2) There is a significant increase of molecular markers of fibrogenesis including αSMA, FSP-1 and collagen 1 in the UUO model when compared to sham-operated kidneys.
3) Both Ki-Ras and N-Ras mRNA expression was increased by 71% and 80% respectively in obstructed kidneys compared to sham-operated kidneys. There was no change in Ha-Ras mRNA levels.

4) Changes in Ras isoform mRNA levels was localized to obstructed kidney and did not extend to the non-obstructed contralateral kidney of UUO models.
5) Attempts at measurement of Ras protein expression by western blotting and immunohistological methods were inconsistent and severely restricted by poor antibody specificity and the lack of an appropriate loading control due to requirement for immunoprecipitation.
6) Attempts at localisation of Ras isoform mRNA expression and up-regulation employing laser microdissection and *in situ* hybridization were unsuccessful in this project

The table below summarises changes observed in Ras expression and fibrosis markers in the rat kidney following ureteric obstruction when compared to a sham-operated kidney at 12 and 16 days.

Duration of UUO	**Ras Isoforms mRNA expression measured by QPCR in obstructed kidneys in comparison to sham-operated kidney samples**	**Fibrosis & fibrotic markers in obstructed kidneys in comparison to sham-operated kidney samples**
12 days	1) Kras upregulated by 71% 2) Nras upregulated by 80% 3) Hras expression equivalent to sham *All Ras isoform expression in the contralateral kidney was equivalent to sham*	1) αSMA: Increased tubulointerstitial expression x 6 2) Collagen I: Increased tubulointerstitial expression by x 5
16 days	1) Kras upregulated by 84% 2) Nras upregulated by 87% 3) Hras upregulated by 23%	1) PMT: Increased tubulointerstitial expression x 10 fold 2) PSR: Increased tubulointerstitial expression x 7 fold 3) FSP-1:Interstitial: x 5 fold 4) Collagen 1: Increased tubulointerstitial expression by x 5 fold 5) αSMA: Increased by x 8 fold

Table 4.1: Changes in Ras & fibrosis markers expression following UUO at 12 & 16 days

4.11 Discussion

The development of an animal model of renal fibrosis was central to this project. The model of unilateral ureteric obstruction was chosen for several reasons. It is a model of tubulointerstitial fibrosis that is widely employed and provides significant quantifiable molecular and histological changes over a short time span. It is a robust model and so often used to evaluate potential therapies. Furthermore the contralateral non-obstructed kidney may provide an internal control to the disease process if so wished and the potential for reversal of obstruction can aid future studies into fibrosis recovery. The initial assessment of the model in this project revolved around determining the duration required to provide significant histological fibrosis with observable differences in the molecular parameters for quantifying fibrogenesis and the subsequent characterisation of Ras expression both at an RNA and protein level. It was found that a duration of obstruction of 12-16 days provided significant fibrosis on staining with PMT and picrosirius red (PSR). This time frame is consistent with other studies looking at Ras expression in murine models of renal fibrosis (Grande, Arevalo et al. 2009). In addition, immunostaining for collagen I and α-SMA expression were also significantly increased in UUO models at this time point. A significant increase in interstitial expression of FSP-1 was also observed in the obstructed renal tissue. This may represent an increase in fibroblast population as part of the fibrotic process induced by obstruction. However FSP-1 expression must be viewed with caution as there is now data showing that FSP-1 is expressed by active mononuclear cells and not exclusively by fibroblasts. Interestingly, there was also a statistically significant rise in tubular expression of FSP-1 following renal obstruction. However in absolute terms this difference was a mean of 1 cell/view only and was a reflection mainly of the complete absence of FSP-1 positive tubular cells in sham kidneys. However the presence of FSP-1 positive tubular cells may be argued to represent a phase of EMT, though the non-specificity of this cell marker and the fact that detection for co-expression with cell markers of tubular cells was not undertaken must be taken into consideration.

With regards to Ras RNA expression, use of SQ-PCR showed that all three isoforms are expressed in the kidney. However unlike cell culture studies (see *Chapter 3*), the use of this technique was unable to reliably discriminate between the levels of expression of isoforms of Ras *in vivo*. Furthermore, β-actin was used as a house-

keeping gene but subsequent analysis demonstrated that this gene expression appeared upregulated in obstructed when compared to sham-operated kidney samples. Ras, though ubiquitous, is normally expressed at low levels *in* vivo, thus small increments in the level of Ras expression may have significant cellular effects but may be difficult to detect. Subsequently QPCR was employed and showed that there was a significant increase in Ki-Ras and N-Ras mRNA expression in obstructed kidney when compared to sham kidney samples ($p<0.01$). Furthermore the increase in both Ki-Ras and N-Ras expression appeared to be localised to the obstructed kidney while expression in the contralateral non-obstructed kidney was comparable sham. To investigate whether these changes in mRNA expression were translated to protein level SDS PAGE was employed.

Western blotting for Ras protein from whole kidney lysate was technically difficult. Due to low abundance of Ras protein, immunoprecipitation of protein was required and so a loading control was unable to be employed. In addition the sensitivity of western blotting itself is very much dependent on the affinity of antibodies used and the antibodies for the Ras isoforms are recognized to have a high degree of cross-reactivity. Thus results were highly variable and lacked consistency despite using identical samples and materials on repeated experiments. Apart from the technical difficulty of the process and the lack of antibody specificity, the inconsistent results obtained from western blotting may be due to a relative difficulty in the extraction of a low abundant target protein, such as Ras, from fibrotic kidneys compared to non-fibrotic sham samples due to a combination of cell atrophy, matrix deposition and fibrosis. The fact that our experiments tend to demonstrate a decrease in Ras protein in UUO samples, which contradicts previous published studies and our results obtained from analysis of mRNA levels using QPCR, supports the idea that Ras isoform protein analysis was unreliable when employing current available antibodies to Ras isoforms and SDS PAGE techniques in this project. In addition there was the presence of a heavy slower running artefact band with a molecular weight of 28-30kD near that of Ras. The significance of this band with regards to Ras is unknown. With regards to the molecular weight of this molecule, it was not possible that the band represented dimers or polymers of Ras. A possibility may be the detection of heavy or light chains of the Raf-binding antibody of the agarose beads used for immunoprecipitation. These antibody components (generated in Sprague-Dawley rats) may have broken off to form aggregates which are subsequently bound to Ras.

The heavier complex is then detected in immunoblotting. Thus true quantification of Ras protein levels, and its isoforms, was not possible when the amount could not be reliably quantified especially in the absence of a reliable loading control. Immunohistochemical (IHC) methods were employed to assess protein expression. The benefit of such a technique would be not only to provide a quantifiable result but also localisation of Ras isoforms which would be of benefit later in the project when employing ASOs. However IHC for Ras also proved to be difficult and gave inconsistent results and non-homogenous staining. Much of the staining appeared to be non-specific uptake and harsh methods of antigen retrieval were required, which in turn may have denatured the target protein. Furthermore on contacting the technical departments of Calbiochem and Santa-Cruz, it was confirmed that the antibodies employed were not completely specific for the various isoforms of Ras and there was a crossover of upto 20-30% between 'isoform-specific' antibodies. The lack of specificity of antibodies against Ras isoforms meant that accurate localisation of specific isoform proteins in renal tissue was not possible and our attention turned to detection of mRNA isoforms of Ras. Initially *in situ* hybridization was attempted. Due to normally low abundance of Ras mRNA, a non-radioactive assay composed of three probes to allow for signal amplification was employed. Unfortunately, despite some success using the control poly-dT probe, no significant signal was successfully achieved either with the control α-Tubulin or Ki-Ras probes despite numerous variation in experimental conditions. In part this may be due to probe sequences: only two of the three were directed at rat (the other being mouse directed) and it was unclear if the target sequences of the probe were spatially available for binding. However since the control poly-dT probe did show some degree of success, the possibility arises that there was insufficient RNA preservation in the tissue or insufficient amplification of signal. *In situ* hybridization must still be considered a potential option for localizing Ras isoform expression, though the relative short sequence in base variability between isoforms would mean probe design would be difficult and a cocktail of several probes directed against the hypervariable region of individual isoforms and subsequent amplification would be required. It may be that the use of a radioactive probe may provide a more distinct picture by removal of background signal and the use of fresh frozen samples may remove potential issue of rapid RNA degradation. An alternative approach to localising Ras expression differences was by use of laser microdissection and subsequent QPCR. The

technology of PALM allows for single cells to be dissected out of tissue sections, collected and RNA retrieved. The rationale for use of this was to dissect out specific cortical regions or cells and analyse them for Ras isoform mRNA expression using QPCR in sham, UUO and ASO treated kidneys. Unfortunately, though this procedure was seen to work, insufficient amounts of RNA was retrieved to provide adequate reverse transcription and subsequent QPCR. This may be in part that the tissue used, though snap-frozen at retrieval, had been stored for a significant period of time before cryosection and freshly retrieved tissue should be used instead. Furthermore it was seen that a lower amount of RNA was retrievable from obstructed kidneys as opposed to sham-operated for a comparable number of cells dissected. It has been recognosed that more RNA can be retrieved from more active cells. In this way, possible decreased tubular activity in UUO may result in decreased retrievable RNA. This may mirror the results seen on western blotting for Ras protein in UUO samples where the apparent lower amounts of protein seen on immunoblots may reflect increasing difficulty in retrieving protein as opposed to 'absolute' low levels of protein. The same may apply for retrieval of RNA from individual cells by microdissection. Though neither *in situ* hybridization nor laser microdissection was successful within the scopes of this project, they still hold potential to be of success in localising Ras isoform expression and should be revisited in the future.

Chapter 5: Administration of Ki-Ras antisense oligonucleotides to a rat model of unilateral ureteric obstruction: ASO dose determination & Ras mRNA analysis

5.1 Experiment I: Administration of low dose (5mg/kg) Ki-ASO in a model of UUO

Low dose Ki-Ras ASO 1 at 5mg/kg was administered on alternate days over a 12-day period to a rat model of UUO. This dose was initially selected on the advice of ISIS Pharmaceuticals and on the basis of preliminary experiments performed by Dr Helen Clarke (unpublished). Both ASO 2 and control oligo CO 2 were not used due to lack of stock at the time of experiment. Saline was used for the control group. There were seven animals in each group.

5.1.1 Ras mRNA expression in low dose ASO administration

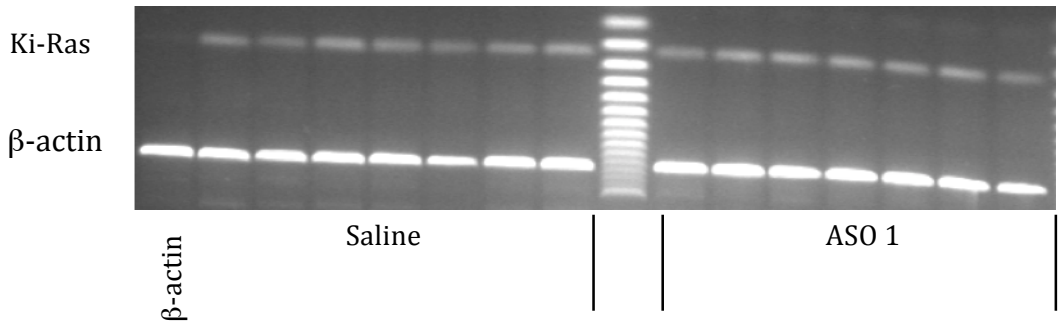

Figure 5.1: DNA gel of semi-quantitative PCR (25 cycles) products from kidney tissue of saline and ASO 1 (5mg/kg) treated UUO rats at day 12. Gel is representative of four separate PCR runs.

Semi-quantitative PCR using RNA retrieved from whole kidney tissue from both groups failed to show any significant knockdown of Ki-Ras mRNA following ASO 1 administration. This was a similar finding when characterizing the model of UUO

(see *Chapter 4)* and it was believed that SQ-PCR in this setting was not sensitive enough to discriminate between samples. Subsequently QPCR was again employed.

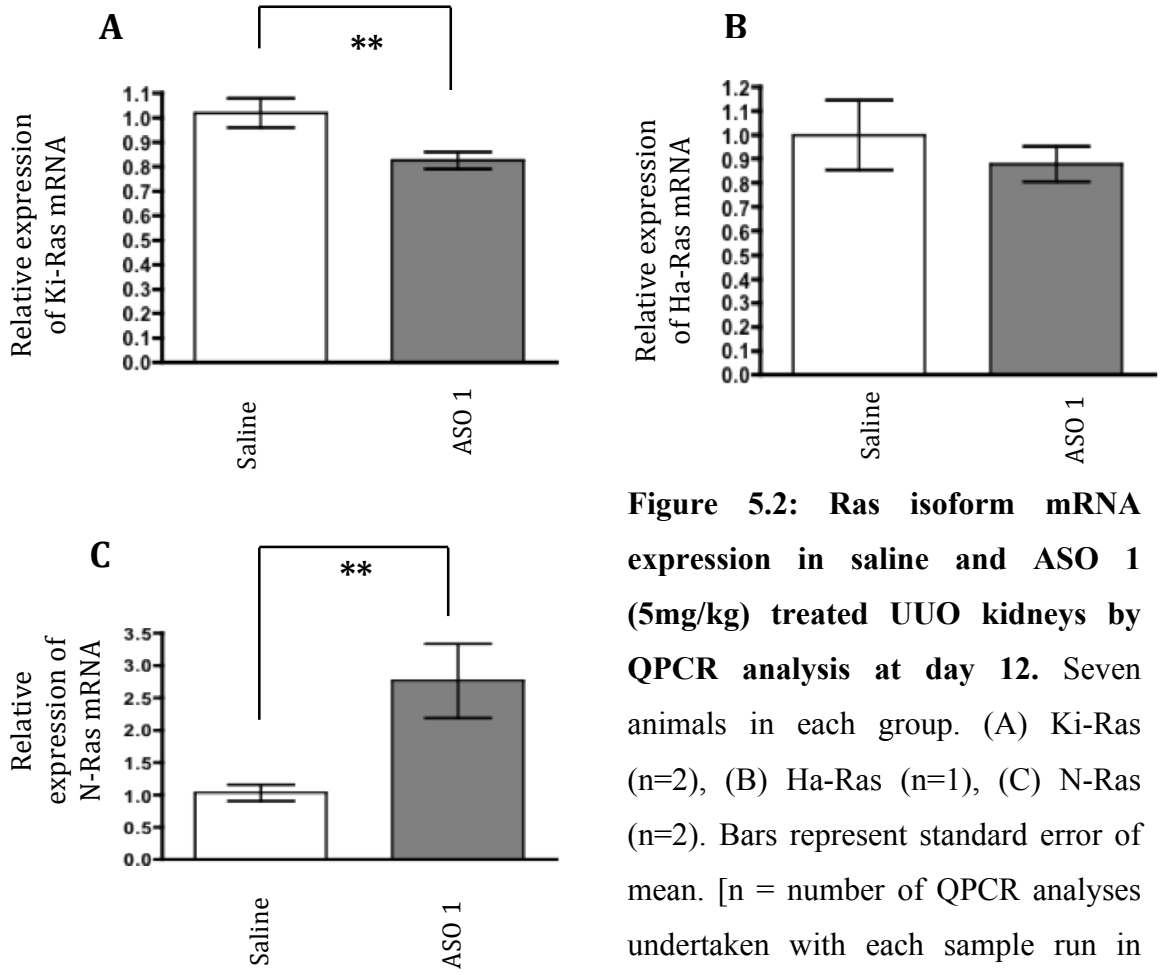

Figure 5.2: Ras isoform mRNA expression in saline and ASO 1 (5mg/kg) treated UUO kidneys by QPCR analysis at day 12. Seven animals in each group. (A) Ki-Ras (n=2), (B) Ha-Ras (n=1), (C) N-Ras (n=2). Bars represent standard error of mean. [n = number of QPCR analyses undertaken with each sample run in triplicate per analysis]

There was an 18% decrease in Ki-Ras mRNA expression in ASO 1 treated group as compared with saline treated controls that was statistically significant ($p<0.01$). There was no significant difference in H-Ras expression between groups but there was a significant rise in N-Ras mRNA expression by 176% in the ASO group ($p<0.05$) compared to saline-control.

5.1.2 Protein expression in low dose ASO administration

Cortical kidney tissue lysed and western blotting performed to analyse Ras isoform protein expression. As previously described, due to relative paucity of Ras protein immunoprecipitation was required, thus there was a lack of a loading control, though equal amount of protein (600μg) was loaded per sample.

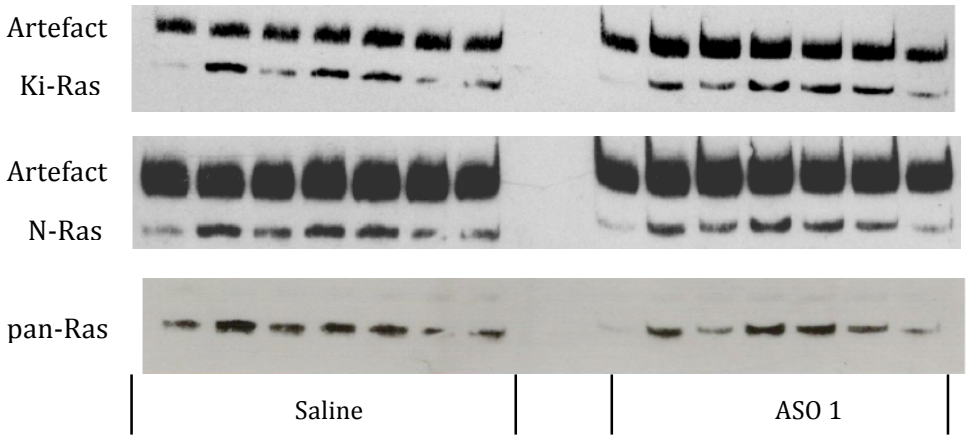

Figure 5.3: Representative immunoblots for (A) Ki-Ras, (B) N-Ras and (C) pan-Ras protein in saline and low-dose (5mg/kg) ASO 1 treated UUO kidneys following 12 days of treatment. 600μg of protein from each sample protein lysate was loaded for immunoprecipitation with 20μl of anti-Ras agarose beads. Note significant artefact band and high intra-group variability in band density.

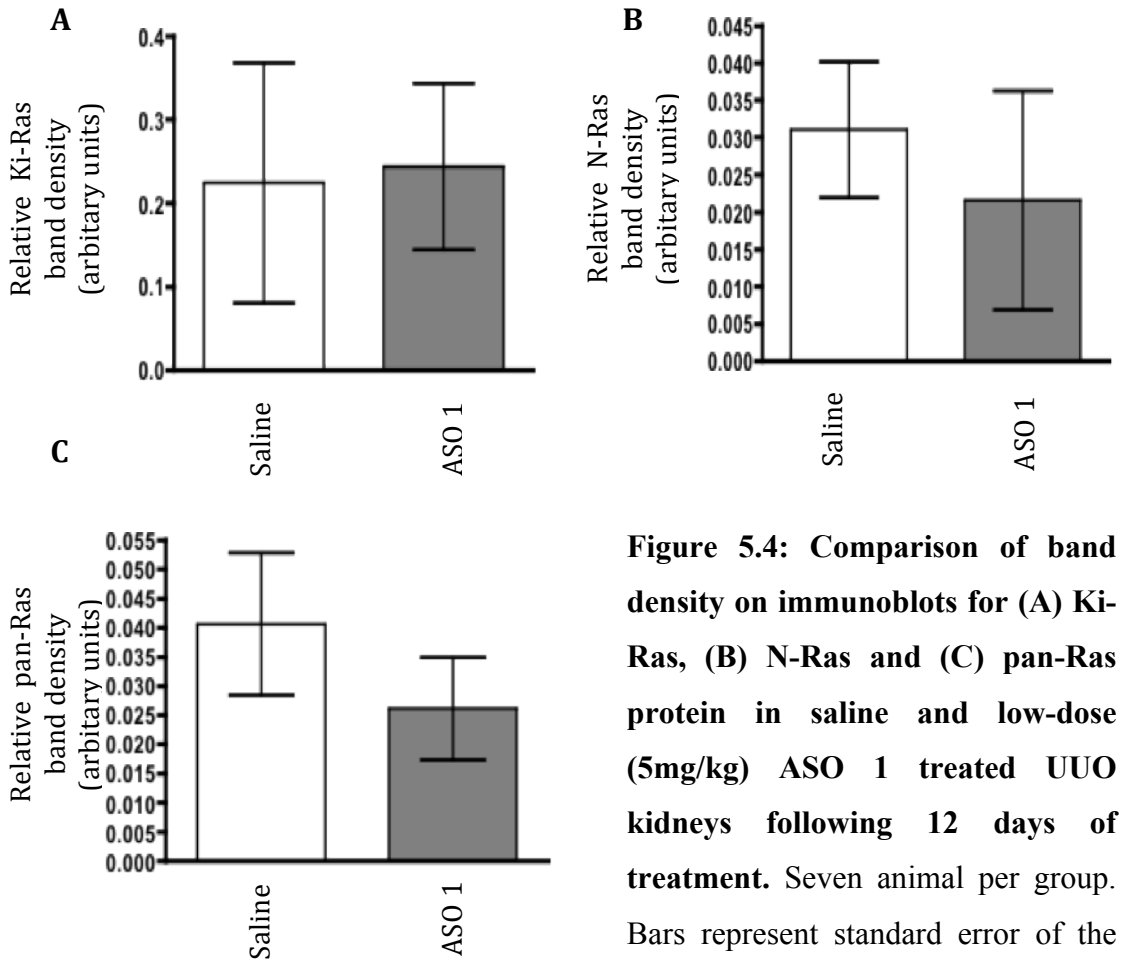

Figure 5.4: Comparison of band density on immunoblots for (A) Ki-Ras, (B) N-Ras and (C) pan-Ras protein in saline and low-dose (5mg/kg) ASO 1 treated UUO kidneys following 12 days of treatment. Seven animal per group. Bars represent standard error of the mean.

QPCR had shown a decrease in Ki-Ras mRNA levels in ASO 1 group compared to saline-control but there was no significant difference at a protein level. Furthermore the significant near three-fold increase in mRNA expression in N-Ras actually appeared to translate to a decrease in N-Ras expression at a protein level. Immunoblotting of pan-Ras showed a decreased protein expression in the ASO 1 group. Results obtained from Ras protein analysis demonstrated high intra-group variability and it is difficult to interpret the significance of these highly variable results, especially with the technical issues associated protein retrieval and immnuoblotting as previously mentioned (see *Chapter 4*).

5.1.3 Fibrosis scores in low dose ASO administration

Fibrosis was assessed by staining with PMT and Picrosirius Red. αSMA staining was used to assess myofibroblastic activity. Following staining the sections were scored in a blinded fashion by a consultant renal histopathologist.

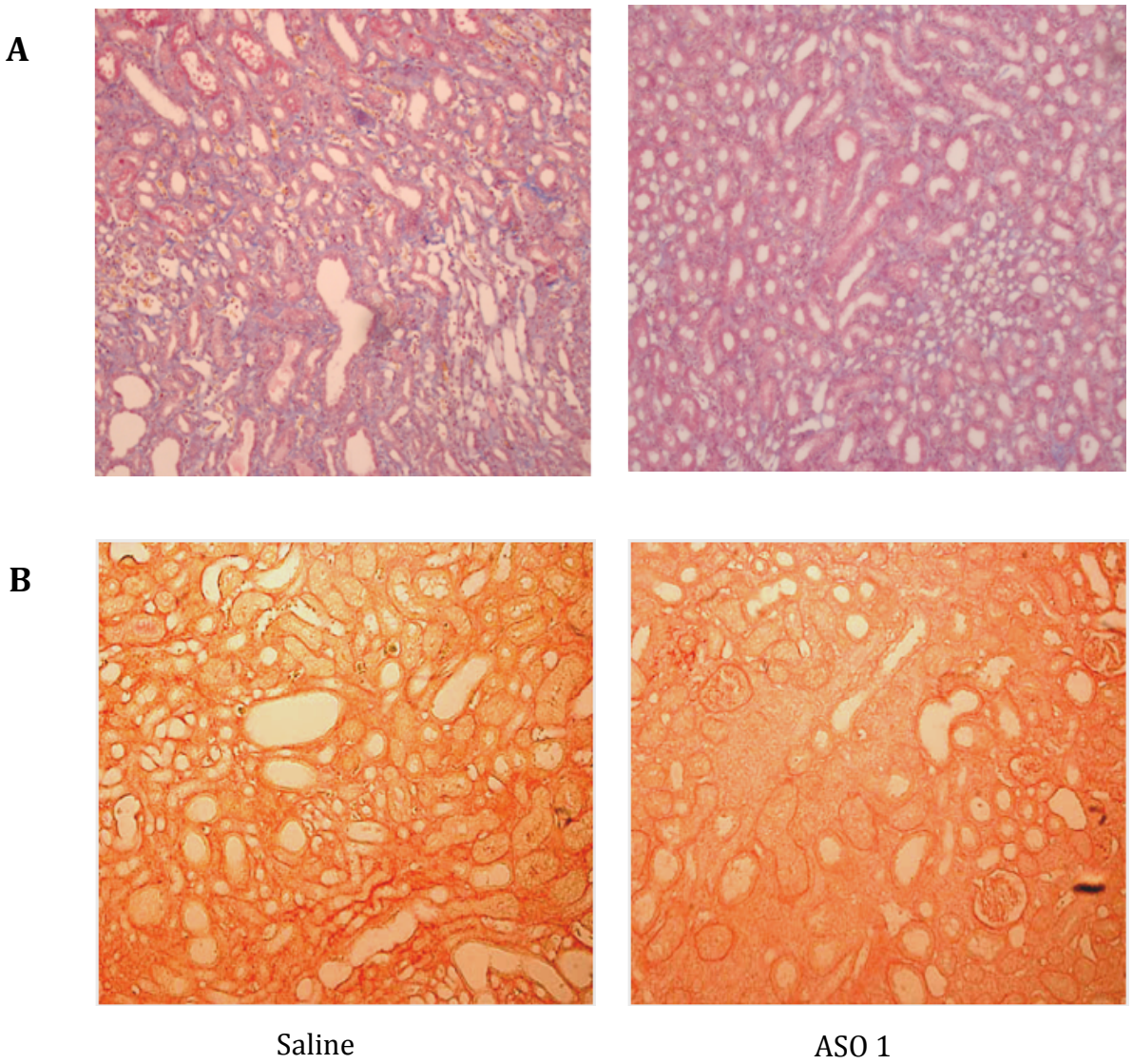

Figure 5.5: Sections of UUO kidneys from saline-control and low-dose (5mg/kg) ASO 1 treated rat models at day 12 stained for fibrosis with (A) PMT and (B) 0.02% Picrosirius red at low-magnification.

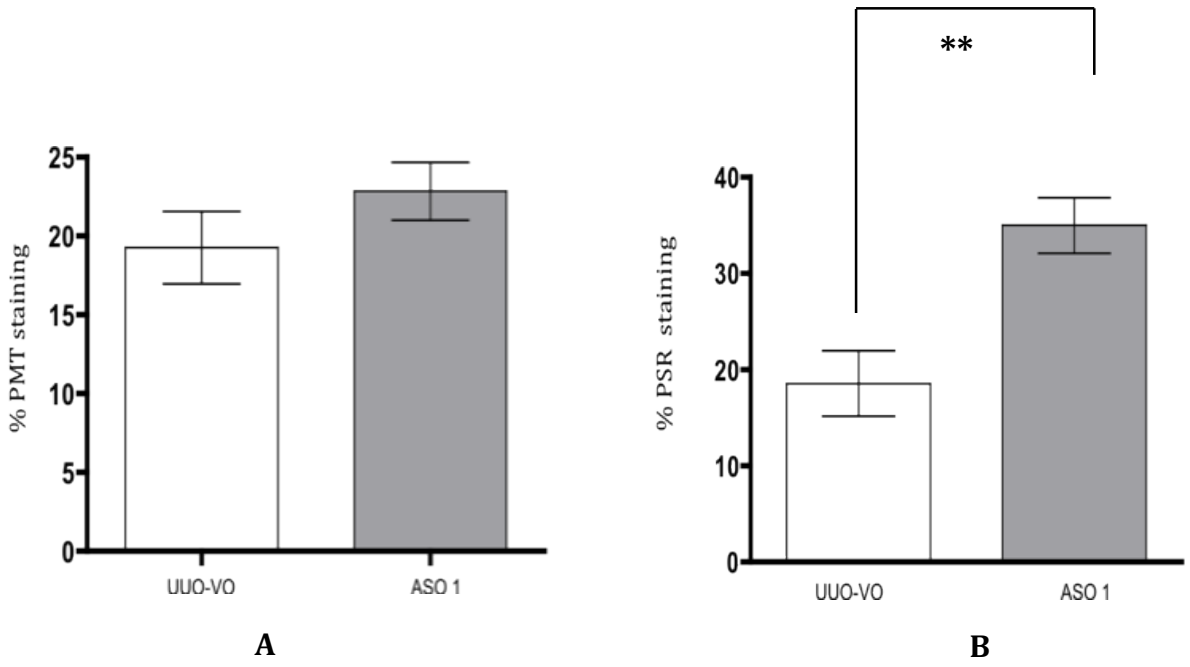

Figure 5.6: Renal fibrosis scores for saline-control and low-dose (5mg/kg) ASO 1 treated models based on (A) PMT and (B) Picrosirius red staining

5.1.4 αSMA expression in low-dose ASO administration

A

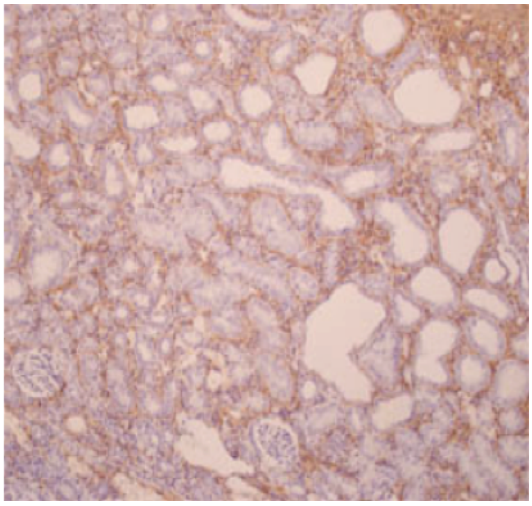

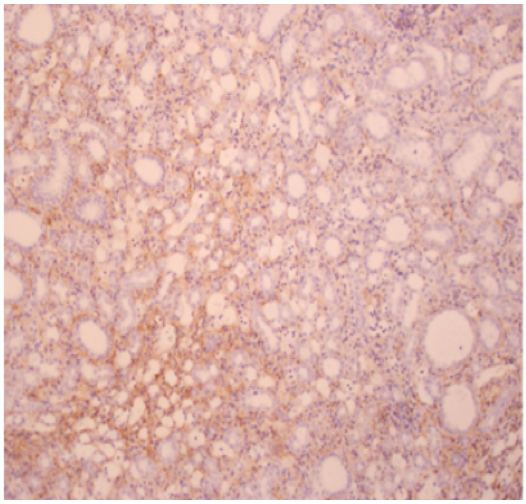

Saline

ASO 1

B

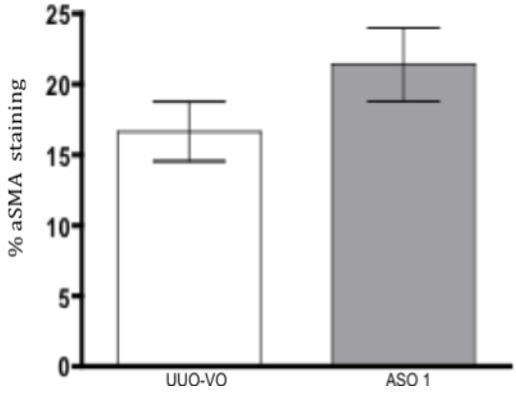

Figure 5.7: (A) Sections of UUO kidneys from saline-control and low-dose (5mg/kg) ASO 1 treated rat models at day 12 for αSMA expression [x10]. (B) αSMA expression scores for saline treated and ASO 1 treated models.

Analysis of tissue demonstrated no difference in fibrosis score by PMT staining on administration of ASO 1 compared to saline-controls but an increase in fibrosis score by 16% on picrosirius red staining in ASO 1 treated group was noted. Staining for αSMA expression by immunohistochemistry did not demonstrate any differences in αSMA expression between the groups.

5.2 Experiment II: Administration of high-dose (12.5mg/kg) Ki-ASO in a model of UUO

Following these preliminary results with low dose ASO (5mg/kg), high dose ASO (12.5mg/kg) was subsequently administered to rat models of UUO subcutaneously on alternate days over a 16-day period. Initially CO 2 (ISIS 141923), which has no known gene target within the specie of *rattus norvegius*, was administered as a control oligo. Sterile water was administered using an identical protocol for a baseline vehicle-only control group.

Following these initial experiments, scramble oligos of ASO 1 (ISIS 104440) and ASO 2 (ISIS 104419) , SO 1 (ISIS 417230) and SO 2 (ISIS 417226) were used for control groups. Tissue retrieved at day 16 included: Obstructed kidney, contra-lateral non-obstructed kidney, heart, liver and wound (scar tissue from laparotomy) tissue.

5.2.1 Oligo uptake within the obstructed kidney

As part of this project, it has been demonstrated that subcutaneous administration of ASO is taken up by the proximal tubules of the kidney (see *Chapter 3)*. To investigate if this was also true of subcutaneous administration in a model of obstructive nephropathy and to confirm that oligos would reach renal tissue at the high dose (12.5mg/kg) that was administered, our group stained sections using a polyclonal antibody against oligonucleotides provided by ISIS Pharmaceuticals.

ASO 1 (Sham)

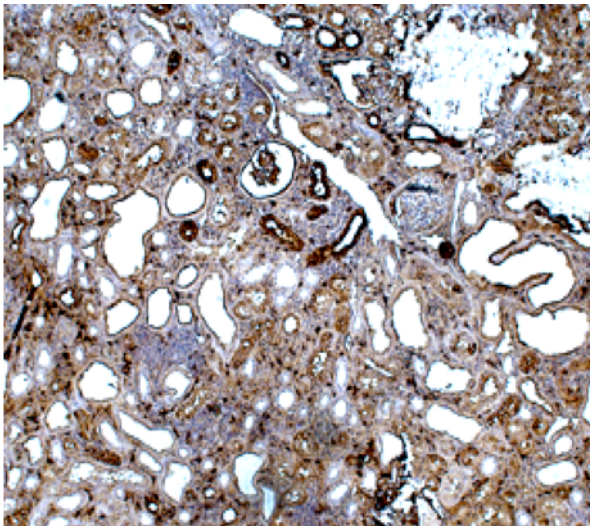

ASO 1 (UUO)

Figure 5.8: Sections of cortex from (A) a non-obstructed and (B) a UUO models both following ASO-1 administration (12.5mg/kg) and subsequent staining for oligo deposition. Both demonstrate oligo deposition within the cortex with accumulation in proximal tubules. However oligo deposition within the in UUO section also includes the interstitium and appears to be of greater intensity compared to the sham sample.

The above sections demonstrate that, following UUO, there is an overall increase in oligo deposition seen in the renal cortex with oligo presence seen within the interstitial department that was largely absent in non-obstructed kidneys. This suggests the possibility of increased oligo concentration in UUO kidneys and affects on cells not targeted in the non-diseased model where deposition was restricted to the proximal tubules (see *Chapter 3*).

5.2.2 Ras mRNA expression in high-dose ASO administration

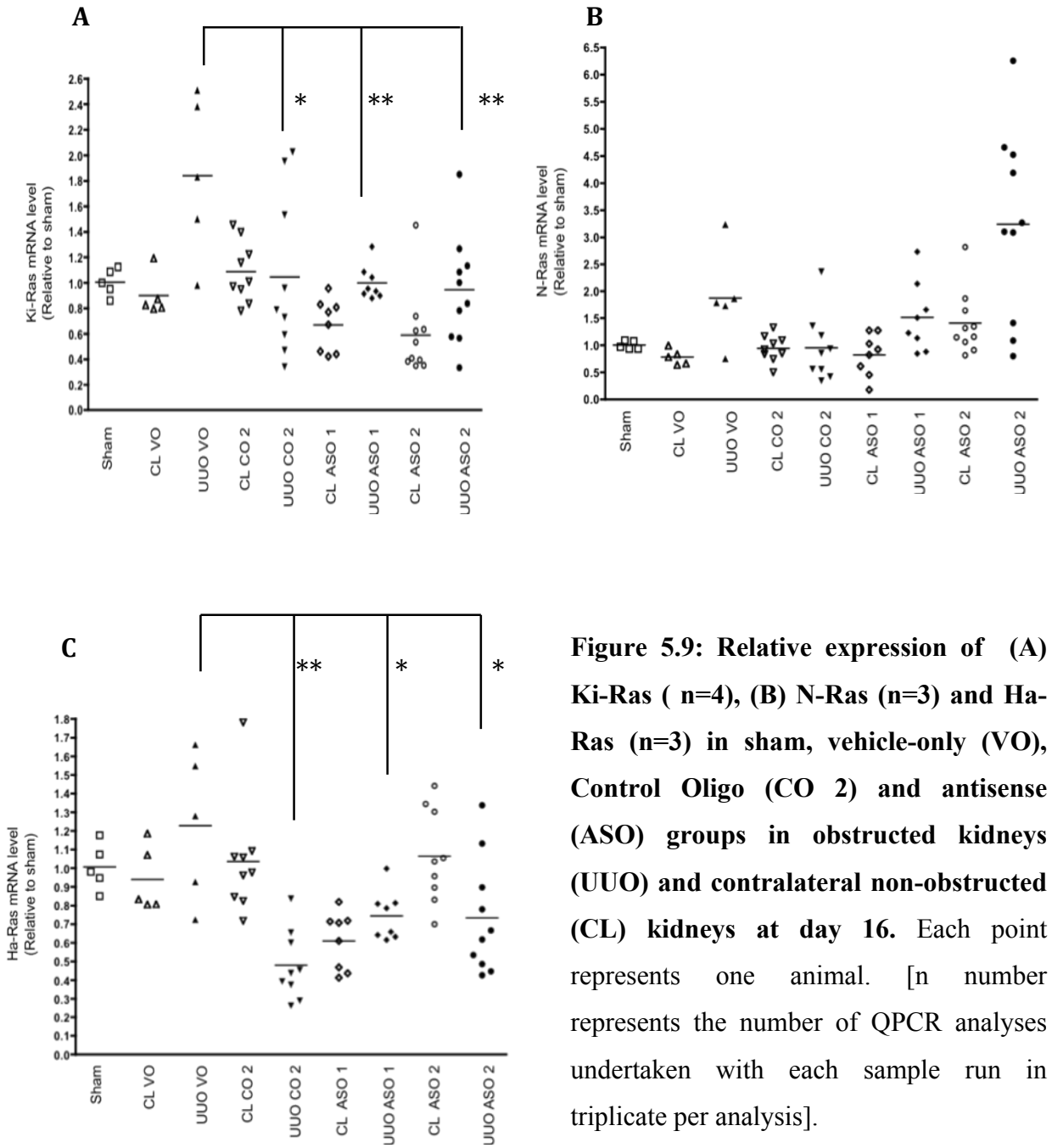

Figure 5.9: Relative expression of (A) Ki-Ras (n=4), (B) N-Ras (n=3) and Ha-Ras (n=3) in sham, vehicle-only (VO), Control Oligo (CO 2) and antisense (ASO) groups in obstructed kidneys (UUO) and contralateral non-obstructed (CL) kidneys at day 16. Each point represents one animal. [n number represents the number of QPCR analyses undertaken with each sample run in triplicate per analysis].

As seen with characterization of UUO model, there is a significant increase in Ki-Ras mRNA levels (by 84%) by day 16 in vehicle-only obstructed kidney (UUO VO) compared to sham which localised to the obstructed kidney with levels in the contralateral kidney (CL VO) being equivocal to sham. Administration of ASO 1 and 2 significantly downregulated Ki-Ras mRNA expression in the obstructed kidney (UUO ASO 1 and UUO ASO 2) by 45% and 49% respectively to a level of Ki-Ras mRNA expression comparable to sham-operated kidneys. Again it was noted that ASO 1 has a much greater Ki-Ras knockdown affect in the obstructed kidney than has been predicted from experiments of administration to non-obstructed models. As noted previously, there was an increase in N-Ras mRNA expression by 87% in obstructed kidneys (UUO-VO) as compared to a sham-operated kidneys and this again was localized to the obstructed kidney. Administration of ASO 2 appeared to further increase N-Ras mRNA expression by 72% in the obstructed kidney and 60% in the contralateral group when compared to the respective vehicle-only groups. ASO 1 administration did not result in any significant difference in N-Ras expression when compared to vehicle-only controls. Obstruction resulted in a 23% rise in Ha-Ras mRNA expression but administration of ASO 1 and 2 significantly reduced expression by 40% and 41% of this isoform. Furthermore within the contralateral kidney, administration of ASO 1 further reduced Ha-Ras mRNA levels by 32%. CO 2 was used as a control oligo. This oligo has no known target within the rat and has previously been used in this capacity (see *Chapter 3*) in non-obstructed rat models. In this experiment, administration of CO 2 to UUO models led to significant pan-Ras mRNA knockdown in all obstructed kidney samples with a knockdown of Ki-Ras by 43%, N-Ras by 49% and Ha-Ras by 61%. The effects of CO 2 were isolated to the obstructed kidney of UUO models and the levels of all Ras isoforms in the contralateral kidneys of CO 2 treated UUO models were comparable to sham-operated kidneys.

5.3 Experiment III: Administration of high-dose (12.5mg/kg) Scrambled Oligos in a model of UUO

Results obtained from administration of CO 2 in UUO models led to a request for a new control oligo from ISIS Pharmaceuticals. Scrambled oligos of the active Ki-Ras ASO SO 1 (417230) and SO 2 (ISIS 417226) were subsequently employed as controls. Initially these oligos were interrogated in models of UUO to examine effects on Ras expression.

Following administration of SO 1 and SO 2 subcutaneously on alternate days over a 16 days time period, tissue was retrieved and analysed using QPCR in comparison to vehicle-only and sham-operated samples from previous experiments. There were ten animals in each SO group and the following results represent two separate QPCR analyses using sham-operated renal tissue as reference control with each sample run in triplicate on each QPCR analysis.

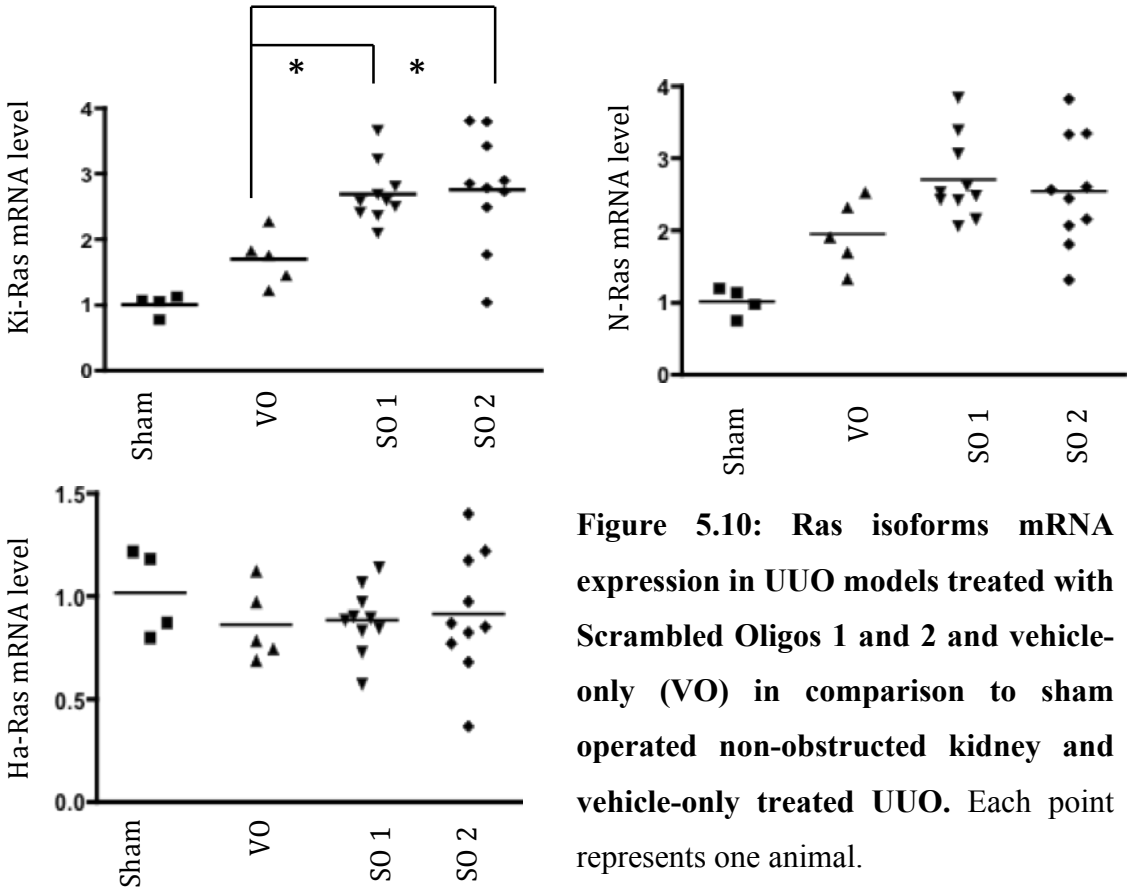

Figure 5.10: Ras isoforms mRNA expression in UUO models treated with Scrambled Oligos 1 and 2 and vehicle-only (VO) in comparison to sham operated non-obstructed kidney and vehicle-only treated UUO. Each point represents one animal.

QPCR analysis shows a 70% rise in Ki-Ras expression in obstructed kidneys which is consistent with previous findings. The administration of SO 1 and SO 2 led to an upregulation of Ki-Ras expression by 169% and 175% respectively compared to sham-operated kidneys. N-Ras expression rose by 95% secondary to obstruction alone but a further rise SO groups was observed with SO 1 causing a 170% and SO 2 a 154% mean increase in N-Ras mRNA expression in relation to sham-operated kidneys. There was a trend to decrease in Ha-Ras expression in all UUO groups compared to sham-operated though none were significant. There was no difference in Ha-Ras expression upon administration of SO 1 or 2 when compared to vehicle-only UUO.

5.4 Experiment IV: Contemporaneous *in vivo* experiment employing scrambled oligos

The results obtained above from the combination of QPCR analyses was supported by a subsequent contemporaneous *in vivo* experiment involving subcutaneous administration of vehicle only (UUO VO), SO 2 and ASOs 1 and 2 at a dose of 12.5mg/kg on alternate days over 16-day time period. The lack of suitable amounts of SO 1 meant this group was omitted for this experiment. Tissue was subsequently harvested for Ras mRNA expression analysis.

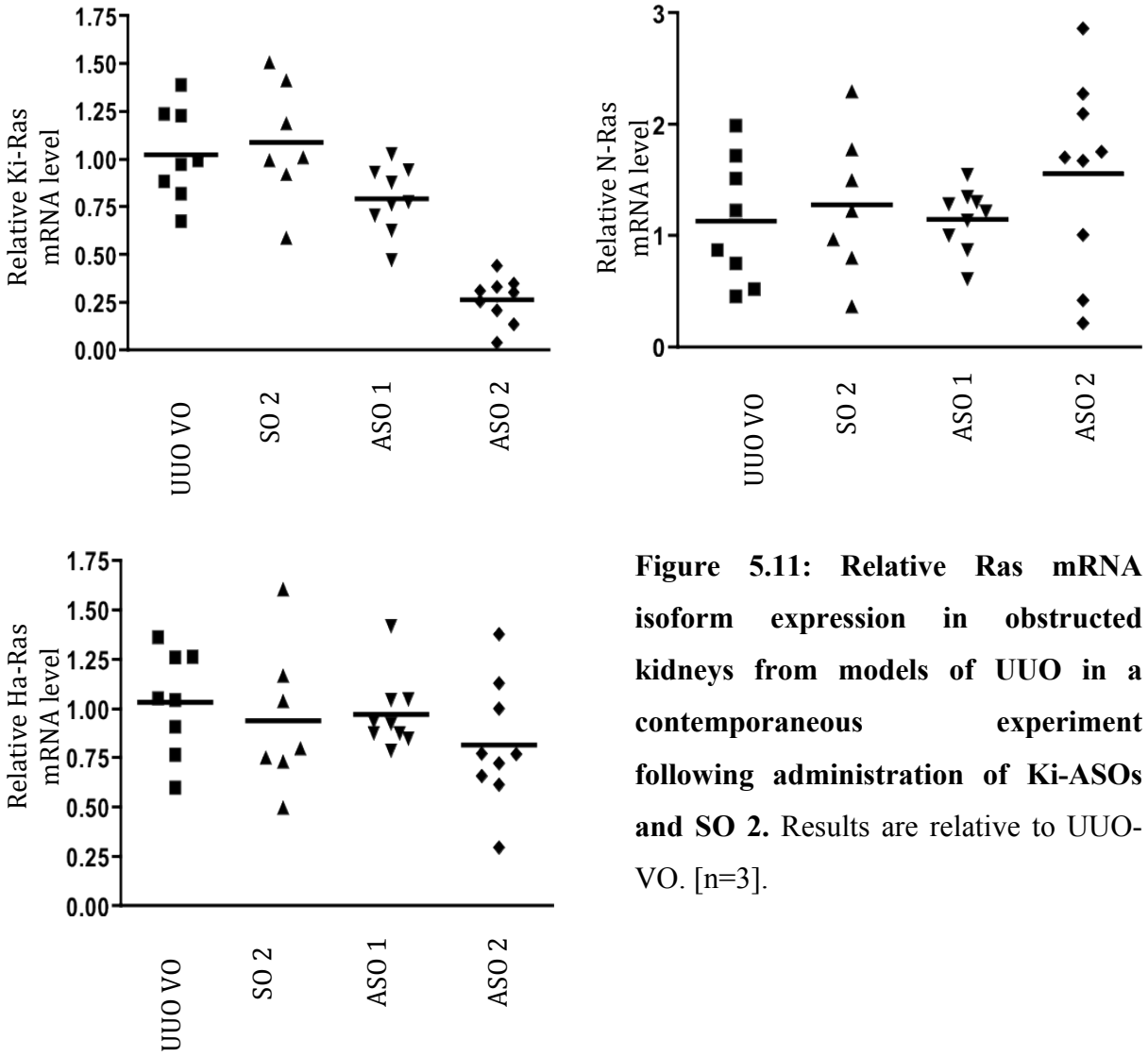

Figure 5.11: Relative Ras mRNA isoform expression in obstructed kidneys from models of UUO in a contemporaneous experiment following administration of Ki-ASOs and SO 2. Results are relative to UUO-VO. [n=3].

There was no significant difference in mRNA expression levels of any of the isoforms of Ras following administration of SO 2 in comparison to UUO VO kidneys. Administration of ASO 1 and ASO 2 led to Ki-Ras knockdown of 27% and 76% respectively when compared to SO 2. These results mirror those previously obtained *in vitro* both with mesenchymal and epithelial cell lines and in *in vivo* experiments in non-obstructed animal models (see *Chapter 3*).

There were no observable knockdown effects in N-Ras or Ha-Ras mRNA expression though the administration of ASO 2 led to an increase of N-Ras expression by 22%. This was not statistically significant but is consistent with previous experiments and observations of N-Ras expression increase associated with ASO 2 administration.

5.5: Combined data from *in vivo* experiments

The results of the contemporaneous experiment (Experiment IV) revealed that Ki-Ras mRNA was specifically knocked down on administration of ASOs in comparison to SO 2. Since the process of comparative method of QPCR analysis involves measurement against a sample's own internal 'housekeeping' gene, in order to assess effects in relation to SO 1 in addition to increasing numbers in both the vehicle-only and SO2 treated control groups, the raw data from the above contemporaneous *in vivo* experiment was combined with raw data from previous *in vivo* Experiment III involving UUO vehicle only, SO 1, SO 2 and ASO administration. Further support for the rationale for using pooled data was the fact that the experiments were performed by a single operator using identical reagents and species, age and sex of animal (male Wistar rats of 200g) under identical operative conditions. Thus experiments were performed under consistent and reproducible circumstances though at different time points. Though this method cannot be seen to be a substitute to a true contemporaneous experiment, since there may be variations in animal batches, animal feed, tissue fixation and processing and reagents, it was seen as the best possible process logistically to obtain a more comprehensive overview of effects of ASOs in comparison to SOs on the expression of Ras isoforms. All raw QPCR data was collated and reanalyzed relative to UUO VO group. This additional data from the groups vehicle-only, SO 1 and SO 2 in Experiment III was obtained from a mean of three separate QPCR analyses. In order to assess comparability of data from this contemporaneous experiment with those that had been performed previously, delta Ct

values for Ki-Ras analysis from the Vehicle-only and SO 2 groups in the both the contemporaneous experiment (Experiment IV) and from the previous Experiment III were compared. Figure (5.12) shows that the mean delta Ct values of Ki-Ras were not significantly different when either vehicle-only (p= 0.6) or SO 2 group (p= 0.09) from Experiment III were compared to their respective groups in Experiment IV using unpaired t-tests.

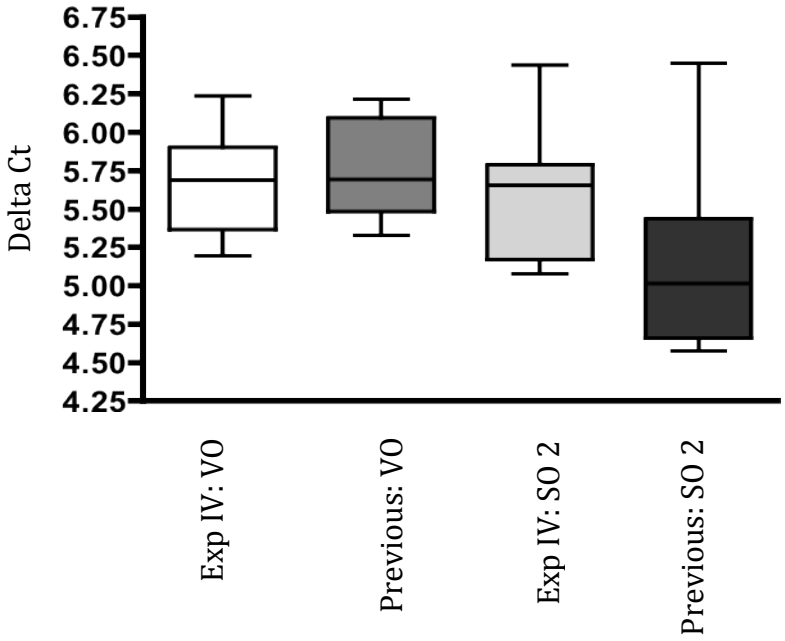

Figure 5.12: Comparison of variation in delta Ct values for relative measurement of Ki-Ras expression in a contemporaneous experiment (Experiment IV) compared to previous experiments (Previous) for the groups vehicle-only (VO) and scrambled oligo 2 (SO 2).

In addition, statistical analysis via a linear regression model using Ki-Ras delta Ct as the dependent variable with 'Treatment with SO 2' and 'Time of experiment' as the two variable factors was performed using statistical package SPSS IX to see if there was any observable significant measurement differences between the two experimental environments. Tables 5.1 & 5.2 below are results from this analysis demonstrating that though there was a significant difference (p=0.012) observed in the data with relation to treatment (that is, given SO 2 or not), there was no difference (p=0.178) with regards to time point of experiment.

Pairwise Comparisons-Treatment

Dependent Variable:Ras

(I) Group	(J) Group	Mean Difference (I-J)	Std. Error	Sig.[a]	95% Confidence Interval for Difference[a]	
					Lower Bound	Upper Bound
1	2	.344*	.127	.012	.083	.605
2	1	-.344*	.127	.012	-.605	-.083

Based on estimated marginal means

a. Adjustment for multiple comparisons: Least Significant Difference (equivalent to no adjustments).

Table 5.1:Results obtained from comparison of Ki-Ras delta Ct results obtained from Experiment III and IV using a linear regression model with variation in treatment (1=Vehicle-only, 2= SO 2) of experiments.

Pairwise Comparisons-Time

Dependent Variable:Ras

(I) Time	(J) Time	Mean Difference (I-J)	Std. Error	Sig.[a]	95% Confidence Interval for Difference[a]	
					Lower Bound	Upper Bound
1	2	-.176	.127	.178	-.437	.086
2	1	.176	.127	.178	-.086	.437

Based on estimated marginal means

a. Adjustment for multiple comparisons: Least Significant Difference (equivalent to no adjustments).

Table 5.2:Results obtained from comparison of Ki-Ras delta Ct results obtained from Experiment III and IV using a linear regression model with variation time point (1=Experiment 3, 2= Experiment 4) of experiments.

Combining the data from both experiments meant an increase in ‘n’ numbers for the different groups. This resulted in an increase of number of animals in Vehicle-only group from eight to thirteen animals and SO 2 from ten to seventeen animals. Ten

animals from SO1 were added to analysis while both ASO group numbers remained the same at nine though change in Ras expression was recalculated relative to new VO mean.

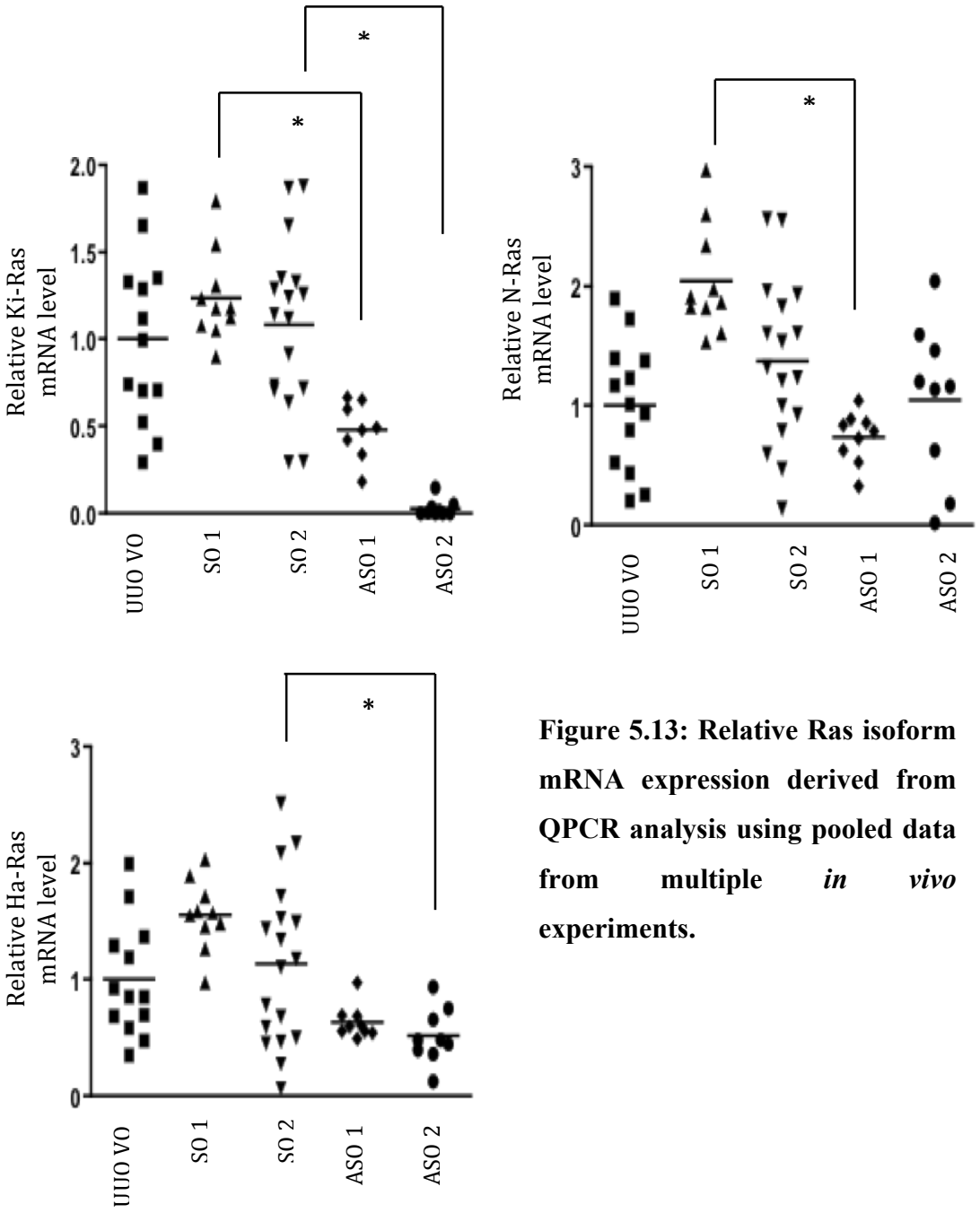

Figure 5.13: Relative Ras isoform mRNA expression derived from QPCR analysis using pooled data from multiple *in vivo* experiments.

The preceding graphs show that there is no significant difference in Ki-Ras expression between UUO-VO group and either SO groups. However there is a significant knock-down of Ki-Ras mRNA expression by administration of ASO 1 and ASO 2 by 53% and 97% respectively compared to UUO-VO. ASO 1 decreased Ki-Ras mRNA expression by 61% when compared to its scramble (SO 1) while ASO 2 decreased expression by 97% compared to SO 2. With regards to N-Ras both scrambled oligos increased N-Ras mRNA expression compared to UUO-VO. SO 1 increased N-Ras mRNA expression by 100% and SO 2 by 37% when compared to UUO-VO control. There was a no significant difference in N-Ras expression observed with ASO 1 and ASO 2 when compared to UUO-VO. Both SO 1 and SO 2 administration increased Ha-Ras expression in comparison to UUO-VO by 55% and 14% respectively. However, as previously seen in *in vivo* administration of ASOs (see *Chapter 4*) there was also a decrease in Ha-Ras mRNA levels of 37% (ASO 1) and 48% (ASO 2) compared to UUO-VO group though this was not statistically significant.

5.6 Summary of results of administration Ki-Ras ASO to model of UUO: RNA analysis

1) Low dose (5mg/kg) administration of ASO 1 in a 12-day rat model of UUO resulted in a specific knockdown in Ki-Ras mRNA expression in the obstructed kidney, a significant increase in N-Ras mRNA expression and no change in Ha-Ras mRNA expression compared to saline-control group.
2) Low dose (5mg/kg) administration of ASO 1 in a 12-day rat model of UUO resulted in an increase in fibrosis score both on PMT and picrosirius red staining and a trend towards increased αSMA expression compared to saline-control group.
3) Following unilateral ureteric obstruction in a 16-day rat model there was an increase in Ras mRNA expression localized to the obstructed kidney of 84% in Ki-Ras, 72% in N-Ras expression and 23% in Ha-Ras compared to sham-operated controls.
4) Oligo deposition was seen to be in the proximal tubules and the interstitium of the obstructed kidney following high dose (12.5mg/kg) administration of ASO in a 16-day rat model of UUO.

5) High dose (12.5mg/kg) administration of ASO 1 or ASO 2 in a 16-day rat model of UUO resulted in a specific knockdown of Ki-Ras mRNA expression in the obstructed kidney to levels comparable to sham-operated controls. ASO 1 and ASO 2 administration also reduced Ki-Ras mRNA expression in the contralateral non-obstructed kidneys when compared to vehicle-only and control oligo, CO 2, groups.
6) High dose (12.5mg/kg) administration of ASO 2 in a 16-day rat model of UUO resulted in a further increase of 72% in N-Ras mRNA expression above the increase seen in vehicle-only group. These observations were localized to obstructed kidney only.
7) High dose (12.5mg/kg) administration of ASO 1 or ASO 2 in a 16-days rat model of UUO resulted in a reduction in Ha-Ras mRNA by 40% and 41% respectively when compared to vehicle-only treated group.
8) High dose (12.5mg/kg) administration of CO 2 in a 16-day rat model of UUO resulted in pan-Ras mRNA knockdown. These changes were localized to the obstructed kidney only.
9) High dose (12.5mg/kg) administration of SO 1 and SO 2 in a 16-day rat model of UUO resulted in an increase in both Ki- and N-Ras mRNA expression in obstructed kidneys in comparison to vehicle-only group. There was no difference in Ha-Ras mRNA expression.
10) A contemporaneous *in vivo* experiment demonstrated significant knockdown of Ki-Ras mRNA in obstructed kidneys on administration of ASO 1 and ASO 2 compared to SO 2. There was no difference between these groups or with vehicle-only group with regards to N- or Ha-Ras mRNA expression.
11) Analysis of pooled data from *in vivo* experiments demonstrated that administration of high dose (12.5mg/kg) administration of ASO 1 and ASO 2 in a 16-days rat model of UUO resulted in significant and specific knockdown of Ki-Ras mRNA in obstructed kidneys compared to both vehicle-only and sister scrambled oligo control groups. There was no significant difference in N-Ras expression upon ASO administration when compared to vehicle-only. ASO administration was associated with a decrease in Ha-Ras mRNA expression when compared to vehicle-only group.

5.7 Discussion

Low dose (5mg/kg) administration of Ki-Ras ASO

Initially low dose Ki-Ras ASO 1 was administered at 5mg/kg on alternate days subcutaneously over a 12-day period in models of UUO. The choice of this dose arose from discussions with ISIS Pharmaceuticals and from preliminary work performed by Dr Helen Clarke from our group (unpublished) as part of her doctorate thesis. Dr Clarke had administered a Ki-Ras ASO at a dose of 5mg/kg intravenously in a rat model of UUO and was able to demonstrate a decrease in parameters of fibrosis. For this experiment, Ki-Ras ASO 2, which appears more potent in *in vitro* studies, was omitted due to a lack of availability at the time of the experiment. Semi-quantitative PCR analysis failed to identify any significant difference in Ras isoform expression between ASO 1 and saline-control groups and this is believed to be due to reasons previously mentioned (see *Chapter 4*). Subsequent QPCR showed that there was a significant decrease of 18% in Ki-Ras mRNA expression in the ASO 1 treated group and an associated rise in N-Ras mRNA expression of 290% when compared to saline-control group. Due to a lack of a control oligo group, one cannot exclude the fact that administration of an oligo per se had caused the observed changes in Ras mRNA levels. Though the knock down effect on Ki-Ras mRNA expression at this dose was statistically significant, in absolute terms the reduction may be insufficient to have effects clinically. Indeed Ras protein analysis by western blotting showed no significant difference in Ki-Ras protein levels between ASO 1 and saline-control groups. In fact there was a trend towards a decrease in N-Ras and pan-Ras protein levels in the ASO 1 group. The results from SDS PAGE and protein analysis are paradoxical to those that would be expected from mRNA analysis from QPCR. The previously mentioned difficulties with Ras protein retrieval and analysis (see *Chapter 4*) may explain the apparent incongruous results between QPCR and western blotting. It was decided at this stage that future western blotting for Ras isoforms would be difficult to interpret in the absence of highly specific antibodies and the focus of the project should be on mRNA expression and histological end-points.

Fibrosis scores by PMT and picrosirius red staining demonstrated an increased degree of fibrosis in the ASO 1 group. However when the absolute values are looked at, it can be seen that there is only a difference in fibrosis of 3% by PMT staining and 16% by picrosirius red staining, neither of which may be clinically significant. Maximum

fibrosis by any method of staining was 40%, which is surprisingly lower than expected for the duration of experiment (12-days). Thus, though the differences in fibrosis scores between the ASO 1 and saline-control groups can be seen to be statistically significant, with regards to absolute fibrosis the differences may be viewed as 'clinically' insignificant. This idea is supported by the lack of difference in αSMA expression between groups. From previous experiments and literature one would expect a greater degree of fibrosis and myofibroblastic activity (as reflected by αSMA expression) at this time point of obstruction. From the results of this preliminary low-dose (5mg/kg) ASO experiment it was felt that the following changes should be made to subsequent *in vivo* experiments:

1) A more active fibrotic model be employed by extending length of experiment time from 12 to 16 days and using a double tie for obstruction.
2) Increasing the total dose of ASO to be administered from 30mg/kg to 100mg/kg. This decision was made following discussions with ISIS Pharmaceuticals who suggested a three-fold increase in dosage.
3) Using a control oligo to isolate effects of targeting Ki-Ras as opposed to those effects associated to the administration of an oligo per se.
4) Employing additional histological analysis parameters including those of fibrosis, proliferation and inflammation.

High dose (12.5mg/kg) administration of Ki-Ras ASO

QPCR analysis of Ras isoform expression in this series of experiments confirmed that Ki-ras mRNA expression was upregulated by 84% within the obstructed kidney with levels within the non-obstructed contralateral kidney being equivalent to that of sham-operated kidney. N-Ras mRNA expression was also noted to increase by 87% while Ha-Ras expression did not significantly alter from sham-operated kidneys. These results are consistent with those obtained in characterizing the model of UUO (see *Chapter 4*).

In Experiment II, following administration of 12.5mg/kg Ki-Ras ASOs, using an anti-oligo antibody provided by ISIS Pharmaceuticals, it was demonstrated that ASO clearly deposits within the renal cortex. Though there is significant accumulation within the proximal tubules, as is seen with non-obstructed kidneys (see *Chapter 3*) there also appears to be a significant degree of deposition within the interstitium of

the obstructed kidney when compared to the non-obstructed kidney. It is unclear whether this increased deposition within this renal compartment has arisen from trans- or paracelluar transport of the oligos following glomerular filtration or as a result of drug delivery via renal capillaries on the background of renal injury and inflammation. It is also not clear whether the deposition within the interstitium lies within the matrix only or if the oligos have been taken up by specific cell types, though the likelihood is that both has occurred. However there appears to be overall a much higher degree of ASO accumulation within the obstructed kidney compared to the non-obstructed. It may be that in the obstructed kidney, the active tubular cell uptake and decreased clearance of oligos results in an increase in oligo deposition within the cortex. Administration of both ASO 1 and 2 resulted in knockdown of Ki-Ras mRNA expression within the obstructed kidneys from the UUO upregulated state to a level comparable with normal sham-operated kidneys. Previous *in vitro* and *in vivo* experiments have revealed poor knock down effect by ASO 1 (see *Chapter 3*) but in this model of UUO, ASO 1 had a knockdown efficiency comparable to ASO 2. This may reflect the increased deposition and accumulation of ASO 1 within the obstructed kidney by aforementioned processes that leads to a greater degree of RNA hybridization and inhibitory effect. Ki-Ras mRNA expression was observed to be down-regulated in the contralateral non-obstructed kidneys of ASO treated models of UUO. The degree of knockdown is in keeping with previous results obtained with knockdown of Ki-Ras mRNA (12% by ASO 1, 66% by ASO 2) observed in non-obstructed kidneys (see *Chapter 3*) and reflects true systemic effects of Ki-Ras ASOs following subcutaneous administration. There was a significant increase in N-Ras mRNA expression in obstructed kidneys following administration of ASO 2 that was absent on treatment with ASO 1. This difference was localized to the obstructed kidneys of ASO 2 group, with no significant difference in the expression of N-Ras mRNA within contralateral kidneys of all UUO groups. It was postulated whether the change in N-Ras expression was associated with Ki-Ras knockdown, either as a compensatory upregulation in presence of Ki-Ras knockdown or possibly representing a mechanism by which Ki-Ras induced suppression of N-Ras expression is removed. Another explanation may be that the compensatory rise in N-Ras observed with administration of ASO 1 and 2 may actually be involved in a protective cell-signaling pathway in a response to profibrotic process of obstruction. However when examining data, it appears unlikely that the change in N-Ras expression is

directly linked to Ki-Ras expression. Firstly when low-dose (5mg/kg) results are reviewed one can observe a significant increase in N-Ras expression (176%) in the absence of a significant Ki-Ras knockdown (only 18%). In this experiment, Experiment II, the degree of Ki-Ras knock down in ASO 1 group was comparable to that seen in ASO 2 but there was an absence of an increase in N-Ras mRNA expression in the former. Furthermore the experiments validating scrambled oligos SO 1 and SO 2 (Experiment III) demonstrated both a significant rise in Ki-ras mRNA expression upon administration of scrambled oligos with an associated rise in N-Ras mRNA expression. This suggests that the rise in N-Ras is independent of Ki-Ras mRNA knockdown, either as a compensatory or non-suppressed response. From the characterization of the UUO model, a rise in N-Ras was noted which may represent an inflammatory infiltration with cells that predominantly express N-Ras. The subsequent further increase in this isoform upon administration of ASO 2 is likely to represent further increase in inflammatory infiltration and may represent a pro-inflammatory nature of ASO 2.

Ha-Ras mRNA expression was also decreased upon administration of both ASO 1 and ASO 2 by 40% and 41% respectively. Again these changes are mainly localized to the obstructed kidney and are inconsistent with previous experiments. *In vitro* experiments employing cell lines demonstrated a rise in Ha-Ras expression (NRK-49F) or no significant difference (NRK-52E) following ASO transfection when compared to vehicle-only group (see *Chapter 3*). *In vivo* experiments involving ASO administration in both non-obstructed (see *Chapter 3*) and obstructed (5mg/kg) models also both failed to demonstrate a difference in Ha-Ras mRNA expression on administration of ASOs when compared to vehicle-only groups. In addition, the contemporaneous experiment involving SO 2 and ASOs in this chapter (Experiment IV) also failed to demonstrate a significant difference in Ha-Ras mRNA expression. Previous validation of the Ki-Ras ASOs has shown that there is high specificity and effect of action with no obvious, significant direct targeting of other isoforms of Ras. From the above-mentioned experimental results and the fact that 20mer oligos, which are highly specific, were employed and the lack of Ha-Ras reduction in contralateral kidneys of ASO groups, it can be assumed that Ki-Ras ASOs do not target Ha-Ras via an antisense mechanism, be it full or partial complementary. This issue highlights the limitations of *in vitro* experiments compared to *in vivo*. In the latter situation there are a multitude of cells involved organ maintenance and function and the administration

of oligos in such an environment may stimulate changes (such as inflammation, cell infiltration or EMT) within both a non-diseased and a diseased model. This may result in a relative lower level of Ha-Ras mRNA expression within the total kidney samples analysed. Another possibility is that the observed knockdown of Ha-Ras may represent non-hybridization effects in association with increasing ASO levels in an environment of poor ASO clearance, in a way that ASO 1 has increased potency in UUO. There is now good evidence that oligos may interact with proteins themselves and affect their expression directly via an aptameric effect [Bennett et al. 2010]. From this series of experiments it is not possible to say if the observed result of Ha-Ras reduction in this case reflects the accumulation of ASO in an obstructed kidney or is an artefact, nor what the clinical significance of this observation is.

The results of Ras expression in the CO 2 group were highly inconsistent with previous experiments. In this experiment, CO 2 administration resulted in a reduction of all Ras isoforms. This observation was localized to the obstructed kidney only with Ras mRNA expression in the contralateral kidney of CO 2 treated models being comparable to sham. Previous interrogation of the CO 2 oligo sequence did not reveal any recognized target within the rat. Furthermore, this oligo has previously been used as a control in both *in vitro* experiments employing renal epithelial cells (NRK-52E) and *in vivo* in non-obstructed rat models (see *Chapter 3*). In both cases there was no observable knockdown or up-regulation in any of the Ras isoforms on administration of CO 2. The generalized, non-specific Ras knockdown effects seen in this group suggests that the results are not particular to the 'oligo sequence' but may reflect a cellular response to CO 2 per se. Whereas obstruction appeared to increase ASO 1 potency to enable Ki-Ras mRNA knock down of 4-fold greater than that observed in non-obstructed models, it may be that the same mechanism has resulted in CO 2 becoming cell toxic. It is possible that CO 2, on the background of increased levels, may suppress mRNA expression of a number of proteins including Ras, but only Ras was examined in this project. In this way CO 2 may also have significant aptameric effects at high concentration. The argument that CO 2 does not cause a 'true' specific Ras knockdown is further supported by the absence of Ras knockdown in the contralateral kidneys of CO 2 group compared to UUO-VO thus excluding a systemic antisense effect that is demonstrated by Ki-Ras ASO administration. In summary it is postulated that the pan-Ras knockdown resulting from CO 2 administration reflects accumulation of the oligo in an environment of decreased clearance secondary to

obstruction leading to non-specific effects by a non-antisense mechanism of action on Ras (and possibly other proteins) related to the base constituency of CO 2.

In order to dissect the effects of Ki-Ras ASOs administration from the effects of oligo administration per se two new oligos were requested from ISIS Pharmaceuticals. To allow for more specific examination of Ki-Ras knockdown effects of ASOs, theses new control oligos were 'scrambles' of the active ASO's: SO 1 being a scramble of ASO 1 and SO 2 a scramble of ASO 2. Being scrambles of the ASOs, these oligos are made up of identical base composition with an aim to remove the artefactual/ toxic effects observed with CO 2 administration and effects that may result from different base sequence binding. The scrambled oligos have no known target in the rat and were subsequently used as controls in two separate *in vivo* experiments: 1) the contemporaneous administration of SO 1 and SO 2 into UUO models for validation of these oligos as controls (Experiment III) and 2) a contemporaneous experiment of administration of vehicle, SO 2, ASO 1 and ASO 2 in UUO models (Experiment IV). Due to a lack of sufficient amounts of SO 1, this oligo was omitted from the latter experiment. Administration of scrambled controls in a model UUO led to an observed rise in both Ki- and N-Ras mRNA expression in the obstructed kidneys when compared to vehicle-only samples. There was no difference in Ha-Ras mRNA levels between vehicle-only and scrambled oligo groups. The rise in the expression of N-Ras in the presence of a concurrent rise in Ki-Ras mRNA upon administration of an oligo suggests that the increase in N-Ras is secondary to oligo presence per se and not a result of effects of Ki-Ras expression. An increase in N-Ras mRNA following Ki-Ras ASO administration has been previously observed both *in vitro* and *in vivo* (see *Chapter 3*).

Analysis of tissue from Experiment IV showed that there was no knockdown of any Ras isoform following administration of SO 2 when compared to UUO-VO, while administration of ASO 1 and 2 led to specific knock down of Ki-Ras mRNA expression consistent with results obtained both *in vitro* and *in vivo* in non-obstructed animal models (*Chapter 3*).

Ideally to obtain a true picture of effect of ASO and scrambled oligos, a contemporaneous 'master' experiment consisting of groups of at least eight animals treated as follows- sham, UUO vehicle-only, CO 2, SO 1, SO 2, ASO 1 and ASO 2- would need to be undertaken. Due to the logistics of such a large experiment, lack of

reagents, time constraints and respect for 3R's of animal experimentation this 'master' experiment was not possible in this project. However since all experimental conditions were consistent (apart from oligos administered) with operations and tissue analysis performed by a single operator using data that consisted of internal controls, it was felt that the pooling of data from experiments performed at different time points to obtain an overall picture of the effects of oligo was justified. Raw QPCR data obtained from the above contemporaneous experiment was combined with raw QPCR data from previous individual experiments involving administration of SO 1 and SO 2 in addition to vehicle-only and ASO administration experiments. To assess if the mean data from these different time points were statistically different the delta Ct values for Ki-Ras from vehicle-only and SO 2 groups from Experiment IV were compared to those obtained from previous vehicle-only and SO 2 experiments. T-tests between paired results showed that there was no significant difference between the mean delta Ct values for the identical experiments performed at different time points. From this combined data, there was no difference in mRNA expression in any of the isoforms of Ras was seen following administration of either SO 1 or SO 2. Treatment with ASO 1 and ASO 2 significantly reduced Ki-Ras mRNA expression with the latter reducing expression by 97%. Though a rise in N-Ras in ASO groups had previously been noted, on this combined analysis there was no statistically significant change in either N- or Ha-Ras mRNA levels in either of the ASO groups compared to vehicle-only. This may reflect the removal of the effect of outliers by including a far higher number of analyses in each group by pooling of data. In summary, from this pooled data, the administration of scrambled oligos did not result in any reduction in mRNA of any isoform of Ras while administration of ASO 1 and 2 both specifically and significantly reduced Ki-Ras mRNA expression in comparison to both vehicle-only and scrambled oligo control groups.

Chapter 6: Administration of Ki-Ras antisense oligonucleotides to a rat model of unilateral ureteric obstruction: Assessment of fibrosis & molecular biomarkers

6.1 Effects of Ki-Ras antisense oligonucleotides administration *in vivo* on weight gain

Ras is a significant molecule in the signaling pathway for cell proliferation, thus there was concern that inhibition of this molecule may be associated with systemic effects. The higher dose of ASO (12.5 mg/kg) did not obviously affect animals phenotypically or with regards to gross behaviour. Models in the ASO groups gained weight in a manner comparable to control groups.

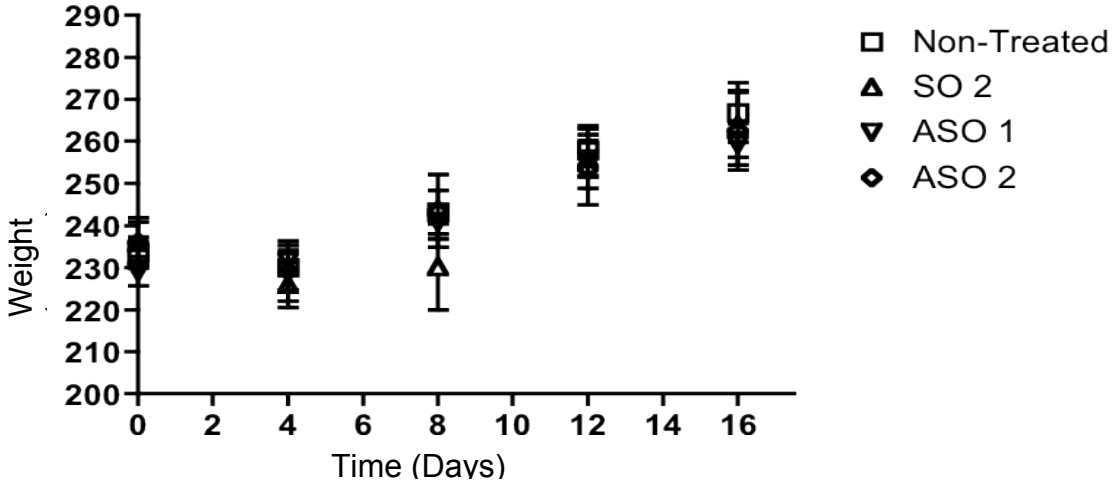

Figure 6.1: Weight chart for control and ASO groups over 16-days duration of Experiment IV.

The effects of Ki-Ras knockdown upon renal fibrogenesis was investigated by 1) the analysis of tissue samples stained by special stains and 2) immunohistological techniques for fibrosis and 3) markers of fibrogenesis and inflammation including αSMA, FSP-1 and CD68 (ED1). Although experiments providing tissue were not completed at identical time points, all staining was contemporaneous. These sections were then subsequently either scored by a consultant renal histopathologist or by

using a computer imaging software package (Nikon Elements BR package). All slides were scored in a blinded fashion.

6.2 Effects of Ki-Ras antisense oligonucleotides administration *in vivo* on renal fibrosis

Despite accurate assessment of parenchymal fibrosis being one of the most important parameters of evaluation of chronic kidney injury, definitions and methods of assessment of fibrosis in the clinical setting vary considerably and consistency between assessors is often difficult to achieve. The main stains used for analysis of degree of fibrosis in this project were picromallory trichrome (PMT) and picrosirius red (PSR). For PMT, areas of fibrosis would stain blue, while in picrosirius red collagen fibres would appear red. In addition, for PSR staining, under cross-polarized light, areas of fibrosis (characterized by excessive collagen type I and III deposition) would appear orange or red. However formal scoring for PSR slides undertaken by a consultant histopathologist was completed under bright-light to avoid inconsistencies with inadequate settings for cross-polarized light.

6.2.1 Picromallory trichrome stain

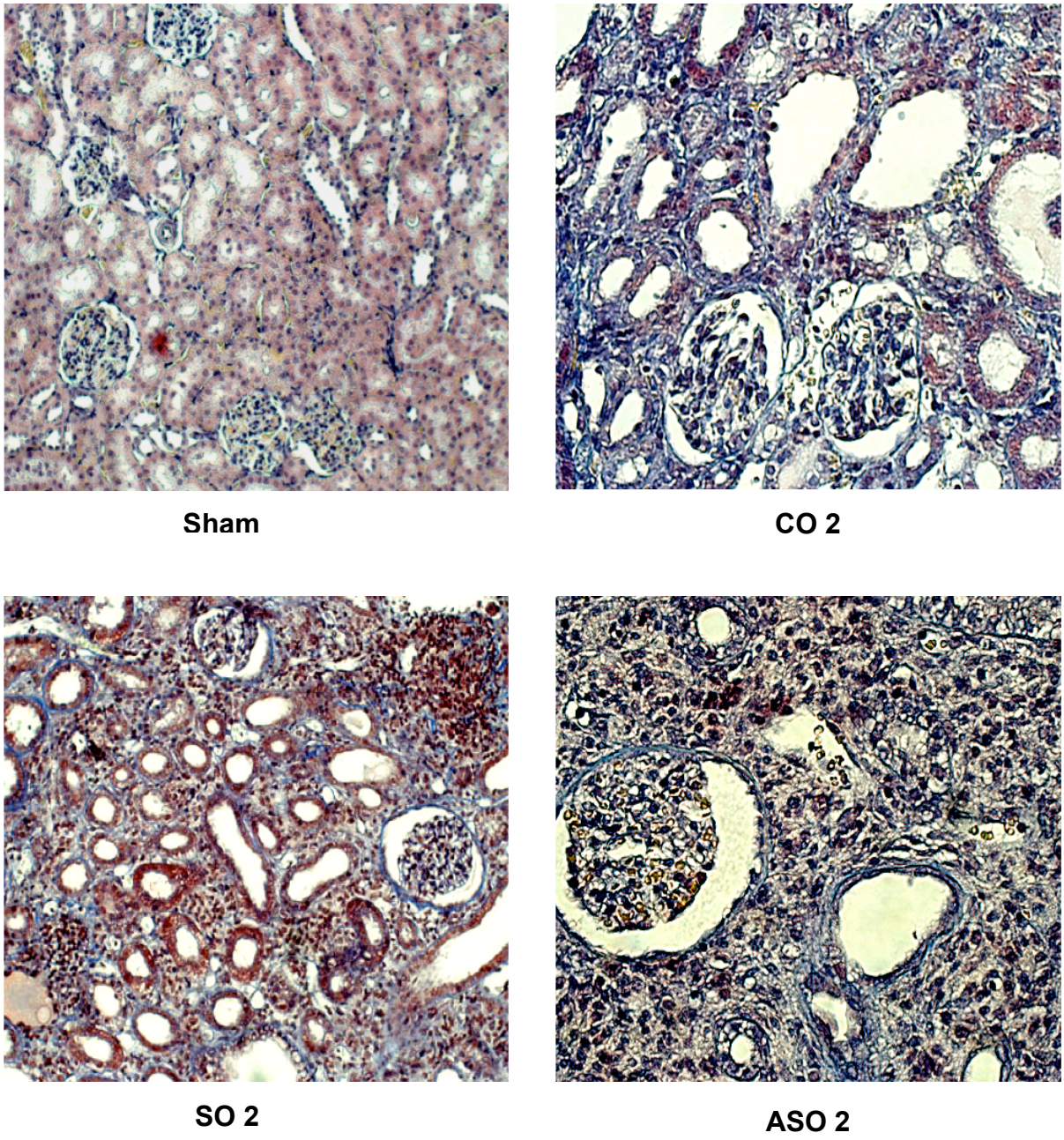

Figure 6.2: Representative sections of obstructed kidneys treated with control oligos (CO 2 & SO 2) and ASO 2 stained by PMT. Areas of fibrosis appear blue. (Sham and SO 2 x10, CO 2 and ASO x 20). Note interstitial inflammatory infiltration in section from ASO 2 treated sample, but the lack of staining for fibrosis.

6.2.2 Picrosirius Red

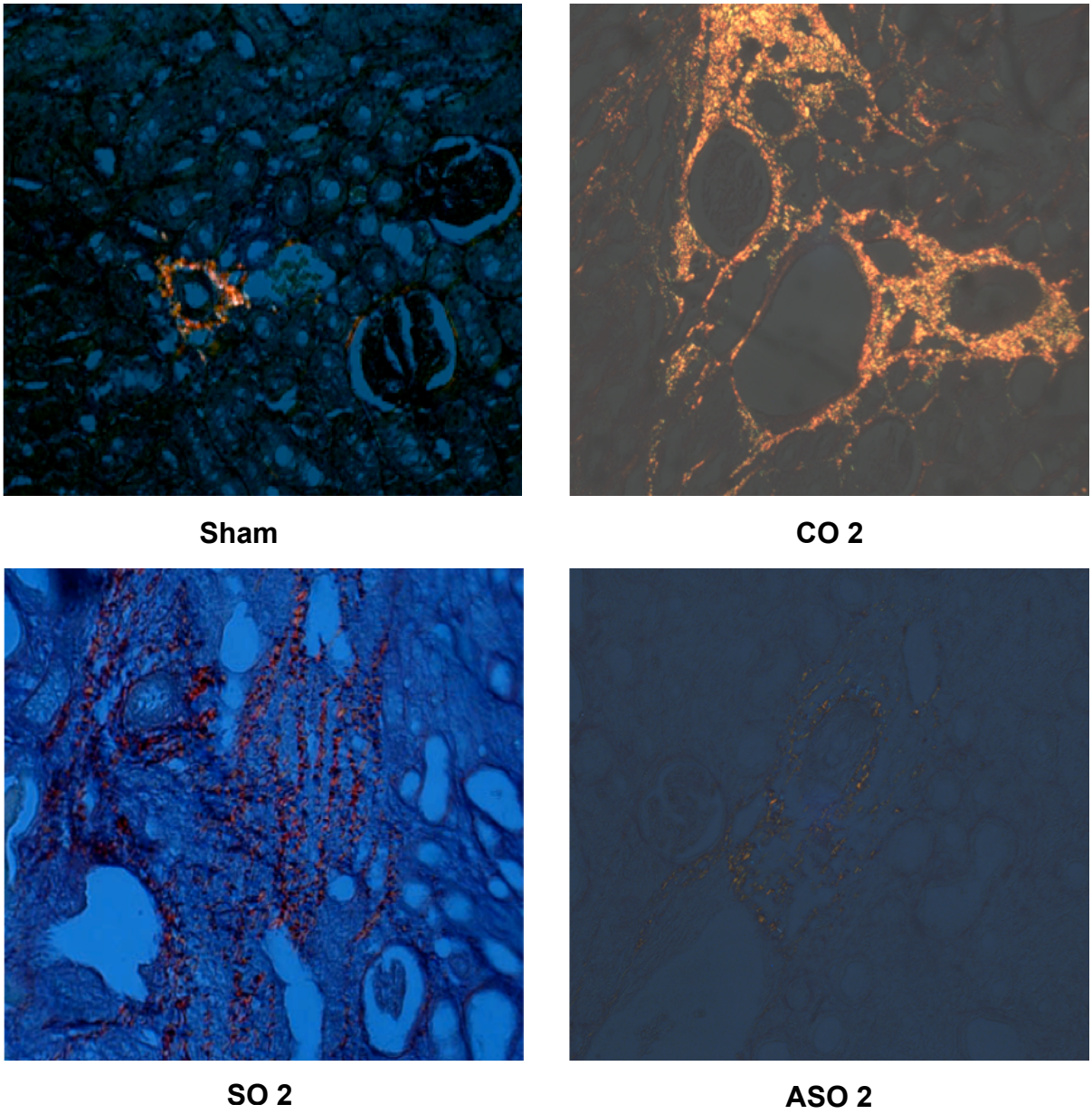

Figure 6.3: Representative sections of obstructed kidneys treated with CO 2, SO 2 and ASO 2 stained by picrosirius red viewed under cross-polarized light [x20]. Collagen type III and I appear orange. Fibronectin appears green. Note normal high perivascular staining for collagen within sham sample but absence of interstitial collagen deposition.

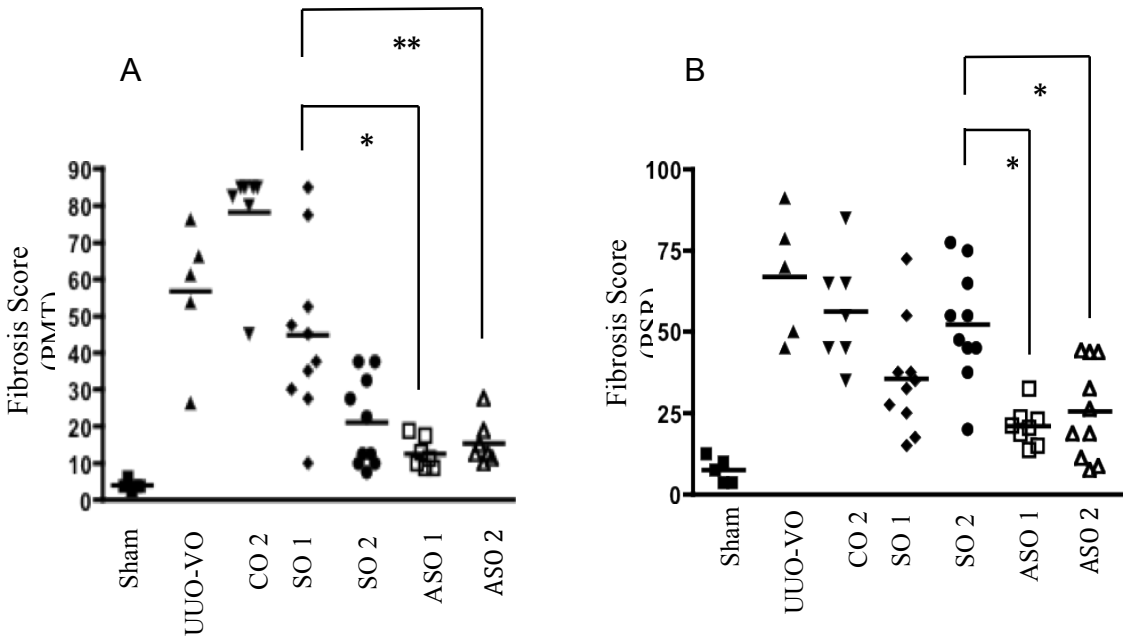

Figure 6.4: Fibrosis score of renal cortex based on (A) PMT and (B) picrosirius red staining (both assessed under bright-light).

Staining by both PMT and PSR showed a significant increase in fibrosis score from a background of 4% in sham kidneys to 57% on UUO-VO sections by PMT and 62% by picrosirius red. Fibrosis scores in CO 2 treated group were comparable to UUO-VO treated group with scores of 78% and 52% based on PMT and PSR respectively. Treatment with ASO 1 and 2 significantly reduced the amount of fibrosis present on PMT staining to 13% and 15% and on picrosirius red to 21% and 26% respectively. Thus administration of Ki-Ras antisense reduced fibrosis scores to levels near comparable with sham-operated kidneys. However PMT and PSR staining of tissue from SO groups produced incongruous results depending on stain used. Administration of SO 2 appeared to reduce fibrosis score on PMT staining to 21%, but on PSR staining there was a fibrosis score in this group comparable to UUO-VO. In contrast, fibrosis score on PMT following administration of SO 1 was comparable to UUO-VO treated group, but on assessment by PSR staining appeared to reduce fibrosis score to 35%. In summary, there appears to be discrepancies in fibrosis score following administration of scrambled oligos depending on staining methods employed and validates our use of two staining methods for assessment of overall fibrosis. Despite these inconsistencies in fibrosis scores seen with scrambled oligos, the administration of either ASO 1 or ASO 2 was still found to significantly reduce

fibrosis on both methods of histological fibrosis assessment. However in order to obtain an overall view of effects of oligo administration on fibrosis, the data obtained from both PMT and PSR scoring was combined for each sample and the mean value was taken as a 'definitive' fibrosis score.

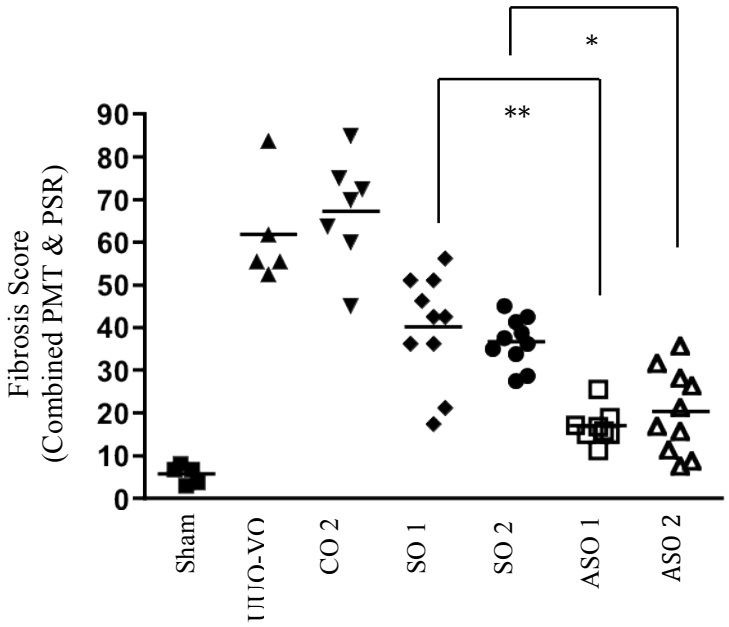

Figure 6.5: Combined fibrosis score of renal cortex based on mean of PMT and picrosirius staining scores. Both ASOs significantly reduced fibrosis in comparison to sister scrambled oligo administration in models of UUO. Each point represents one animal.

Combined PMT and PSR scores demonstrated an increase in fibrosis score of over ten-fold following ureteric obstruction (UUO-VO) compared to sham (62% vs. 6%). Administration of CO 2 did not significantly change the fibrosis score (67%) compared to UUO-VO. However administration of SO 1 and 2 resulted in a significant reduction of fibrosis score to 40% and 37% respectively when compared to UUO-VO treated group. These scrambled oligos have previously been shown to have no active target in the rat or to target any of the Ras isoforms (see *Chapter 5*). Despite this observed reduction in fibrosis score following administration of SOs, the administration of ASO 1 and 2 consistently resulted in a significant further reduction in the combined fibrosis score when compared to scrambled oligo groups with ASO 1 further reducing fibrosis score by 56% in relation to SO 1 ($p<0.01$) and ASO 2 reducing score by 46% compared to SO 2 ($p<0.05$).

6.3 Effects of Ki-Ras antisense oligonucleotides administration *in vivo* on collagen deposition

Collagen type I has been shown to be the collagen isoform which has the greatest relative increase in renal fibrotic disease.

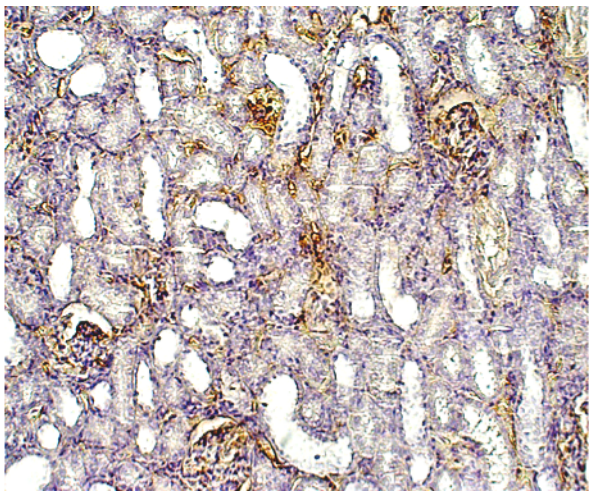

CO 2

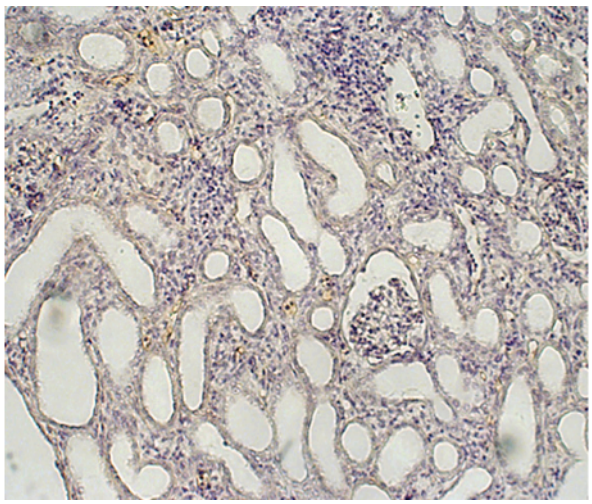

ASO 2

Figure 6.6: Representative sections of obstructed kidneys treated with control oligo and ASO 2 immunohistologically stained for Collagen I. Interstitial collagen I expression is represented by DAB-peroxidase staining which appears brown.

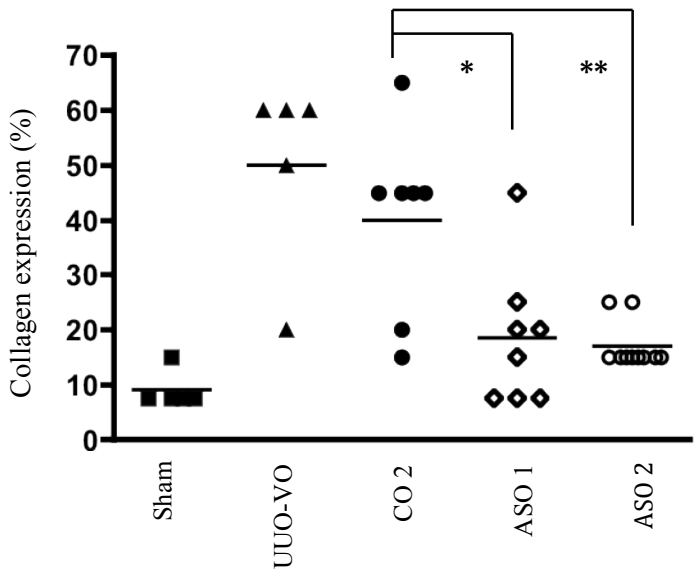

Figure 6.7: Collagen I expression score of renal cortex based on intensity & percentage area of staining of section in sham, vehicle-only and oligo treated sections.

Collagen I expression in the interstitium increased from a background of 9% in sham-operated kidneys to 50% in UUO-VO kidneys. Administration of CO 2 did not significantly alter expression (40%) compared to UUO vehicle-only group. Collagen I expression was seen to decrease by up to 58% in ASO treated groups in comparison to CO 2 group to 18% (ASO 1) and 17% (ASO 2).

6.4 Effects of Ki-Ras antisense oligonucleotides administration *in vivo* on FSP-1 expression

To assess the effects of Ki-Ras knockdown on fibroblast expression, renal tissue was stained for fibroblast specific protein-1 (FSP-1 or S100A4 protein). Cells labeled by the FSP-1 antibody display nuclear, cytoplasmic and membrane staining and in normal tissues the cells positively labeled by the antibody include fibroblasts, T-lymphocytes, plasma cells, macrophages and Kupffer cells (DAKO A5114 datasheet)(Le Hir, Hegyi et al. 2005). Following staining, sections were scored for FSP-1 expression. Due to discrete nature of cellular staining, assessment could be divided into glomerular, tubular and interstitial compartments. The results are the mean of 10 views per section at a magnification of x 40.

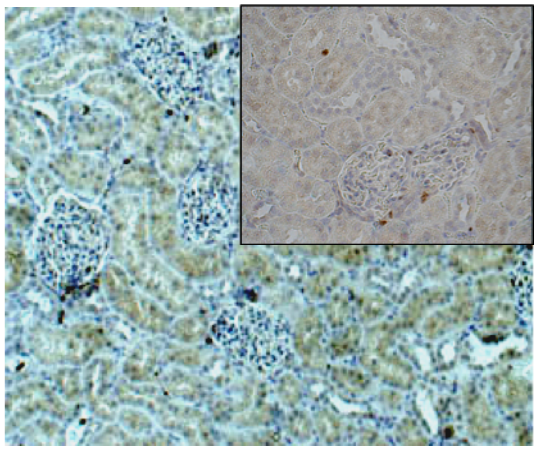

Sham

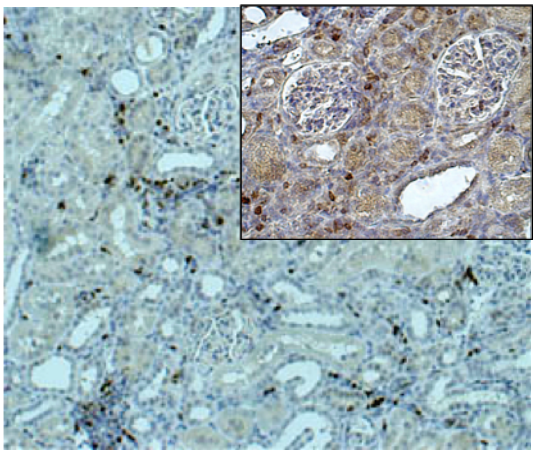

UUO-VO

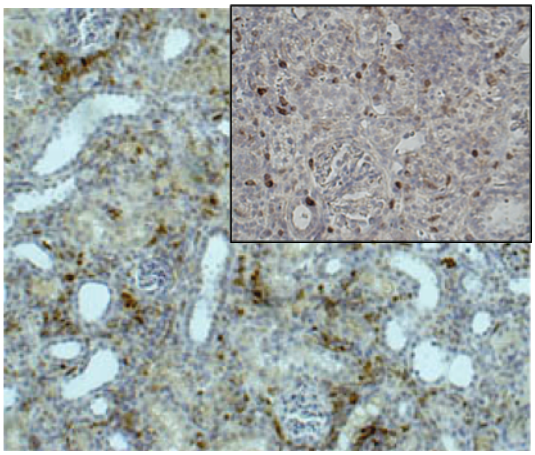

SO 1

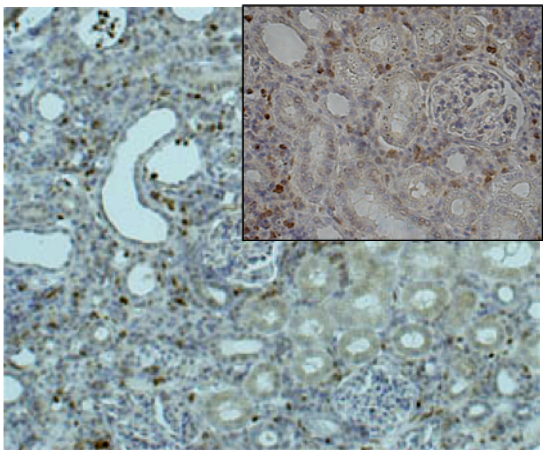

SO 2

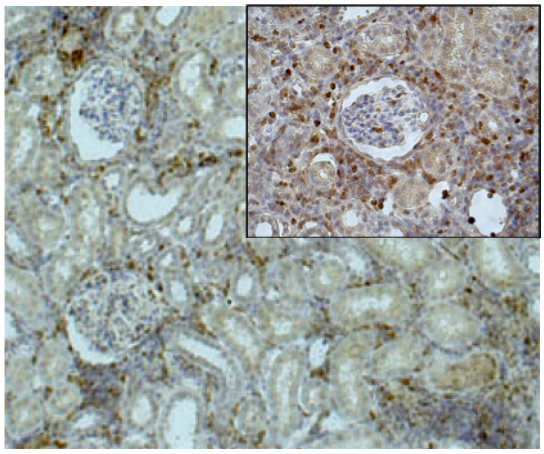

ASO 1

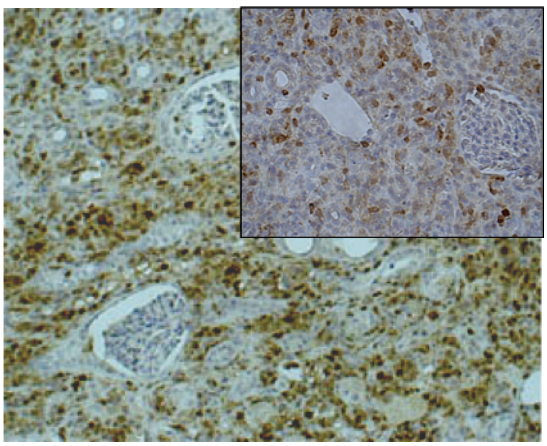

ASO 2

Figure 6.8: FSP-1 staining of kidney tissue from sham and UUO models treated by vehicle-only, scrambled oligos and ASOs. FSP-1 positive cells appear brown. (x20 and inset x 40)

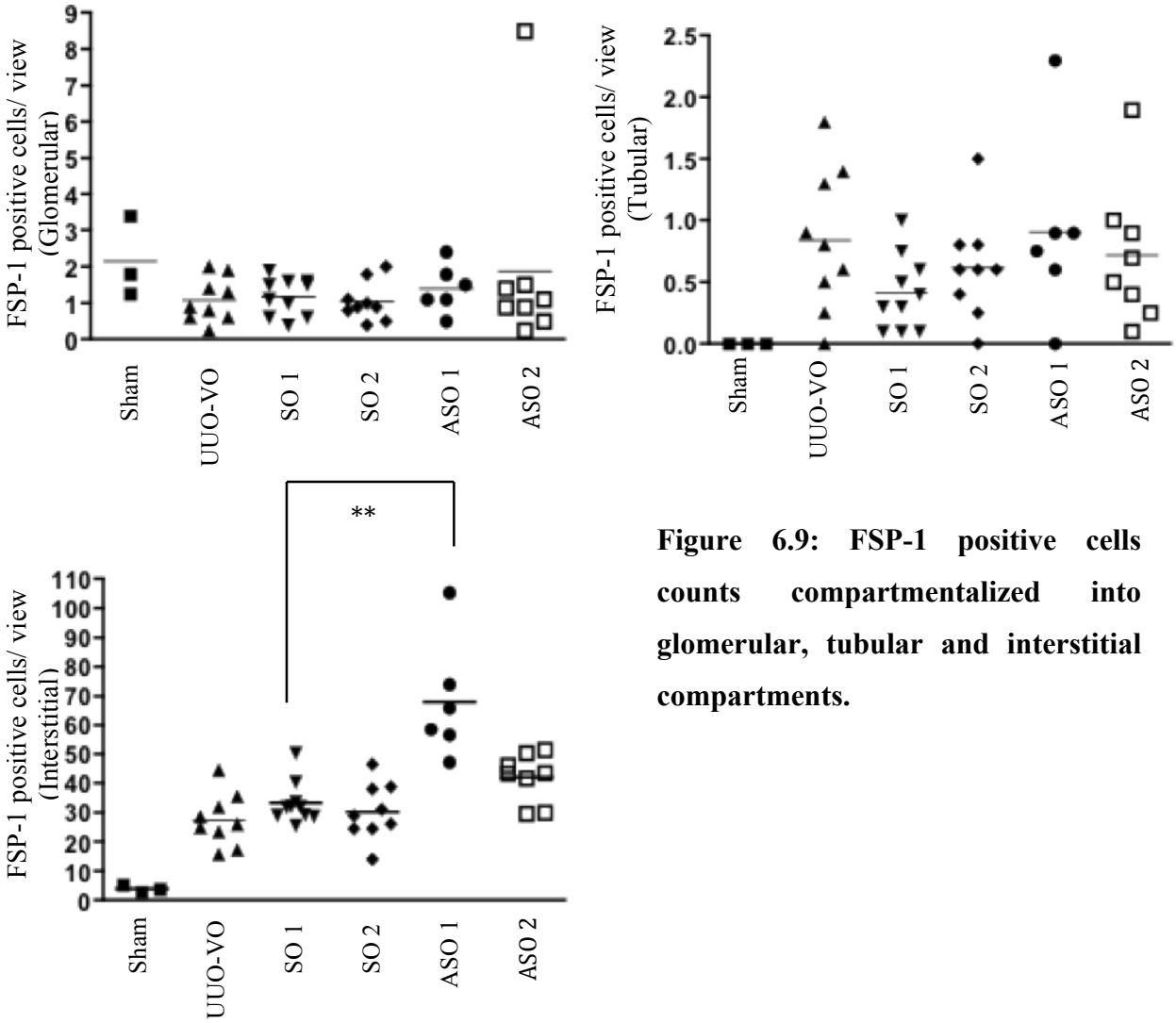

Figure 6.9: FSP-1 positive cells counts compartmentalized into glomerular, tubular and interstitial compartments.

The administration of oligonucleotides, either scrambled or antisense, did not affect FSP-1 glomerular or tubular cell expression in comparison to vehicle-only treated renal samples. There were very few positive FSP-1 cells in the interstitium of sham samples as expected. Obstruction led to a seven-fold increase in interstitial FSP-1 expression compared to sham-operated kidneys and there was no change in expression following administration of SO 1 or 2. However administration of ASO 1 and 2 resulted in a trend towards increased FSP-1 interstitial expression in comparison to SO treated groups, though this was only statistically significant in ASO 1 treated group when compared to scrambled oligos where numbers of FSP-1 positive cells doubled.

6.5 Effects of Ki-Ras antisense oligonucleotides administration *in vivo* on αSMA expression

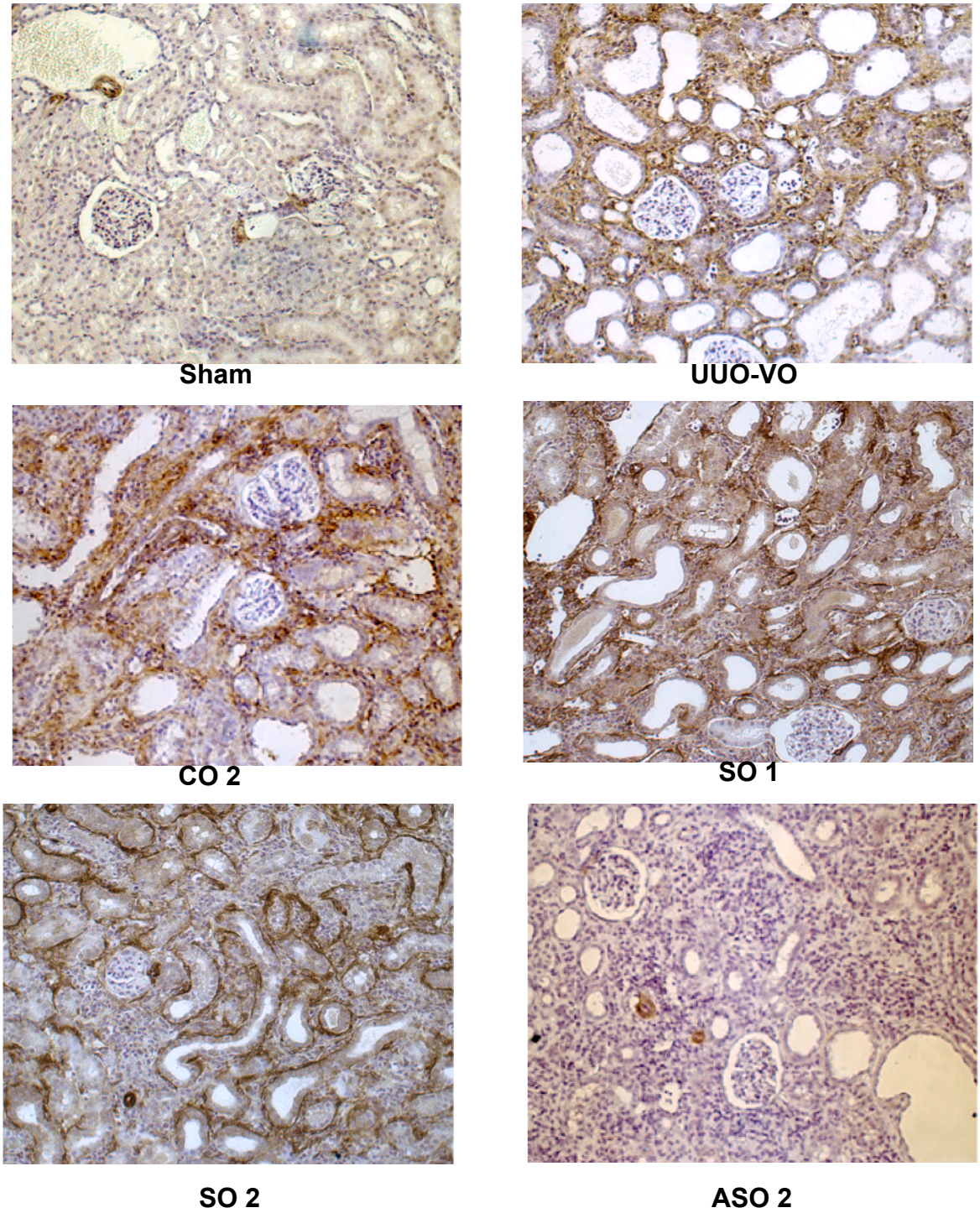

Figure 6.10: Representative sections of obstructed kidneys treated with CO 2, scrambled oligos and ASO 2 and stained for αSMA expression [x10]. Note peri-vascular staining in ASO 2 section comparable to sham but complete absence of interstitial expression.

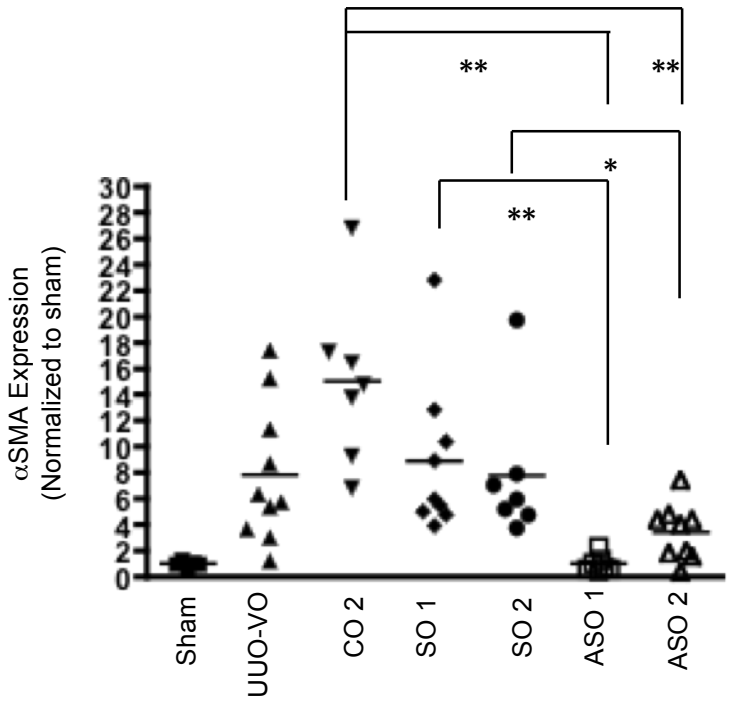

Figure 6.11: αSMA expression score of renal cortex based on intensity & percentage area of staining of section relative to sham kidneys.

α-smooth muscle actin is widely accepted to be a marker of myofibroblastic activity and expression is seen to correlate to degree of matrix deposition. Renal sections were stained for this protein (Figure 6.10).

Staining for αSMA showed an eight-fold increase in expression in UUO-VO compared to sham-operated kidneys. Administration of CO 2 doubled interstitial expression of αSMA. Scrambled oligo groups demonstrated a degree of αSMA expression comparable to UUO-VO with αSMA expression being nine-fold higher in SO 1 group and eight-fold higher in SO 2 group compared to sham-operated kidneys. Administration of ASOs led to a significant decrease in αSMA expression in comparison to both vehicle-only, control and scrambled oligo (CO 2, SO 1, SO 2) groups with ASO 2 reducing expression by three-fold compared to UUO-VO and ASO 1 reducing αSMA expression within obstructed kidneys to a level comparable with sham-operated kidneys. Samples were also examined for αSMA protein expression by western blotting using GAPDH as a loading control. The following blots are representative of at least three separate experiments using three samples from both sham-operated and UUO vehicle-only treated groups and five samples from the oligo treated groups.

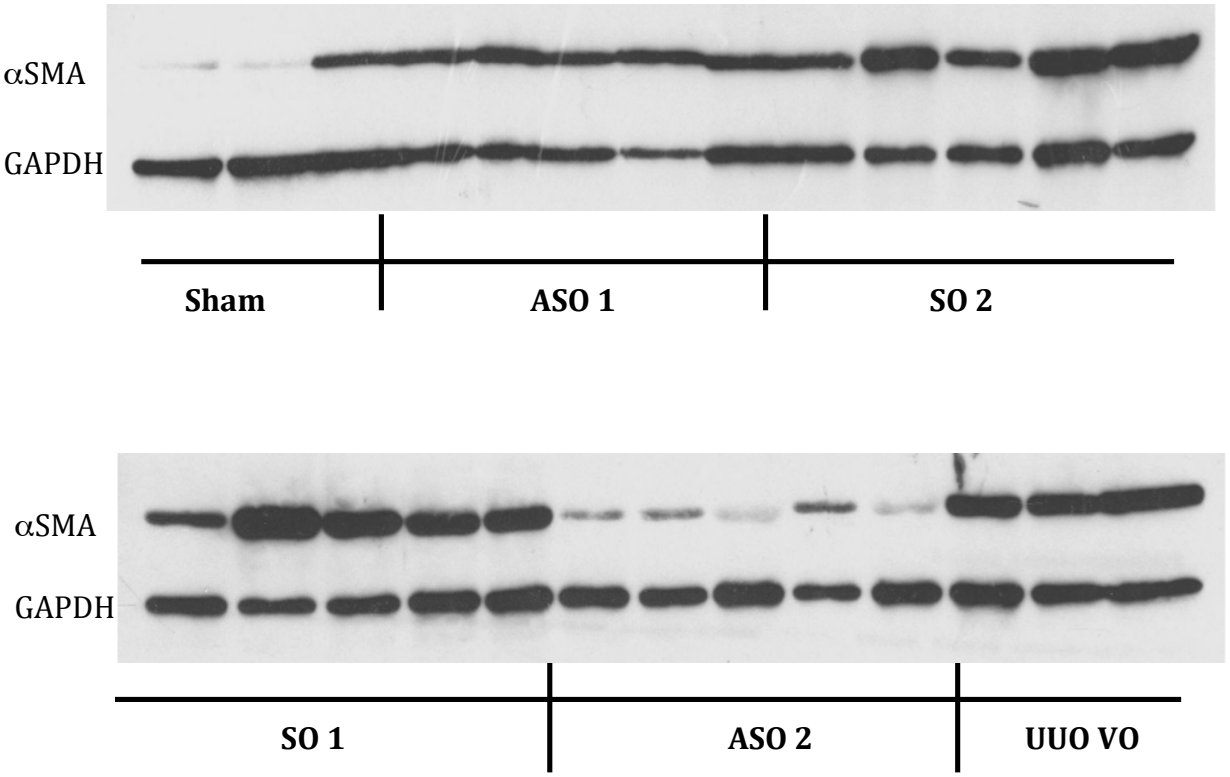

Figure 6.12: Western blots demonstrating αSMA and GAPDH expression for various oligo treated UUO groups. Note significant decrease in band density for ASO 2 group to a level comparable with sham.

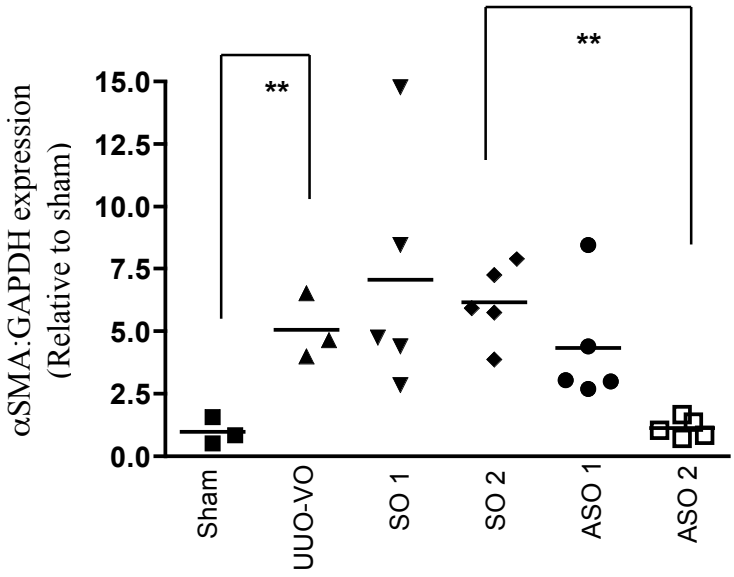

Figure 6.13: αSMA expression relative to GAPDH expression and normalized to sham-operated samples.

Western blotting demonstrated that UUO-VO samples have a five-fold increase in αSMA expression relative to sham-operated kidneys. The administration of scrambled oligos does not reduce αSMA expression relative to UUO-VO group. However the administration of ASO 1 and ASO 2 reduced αSMA expression by 43% and 83% relative to their sister scrambled oligos. The administration of ASO 2 reduced protein expression of αSMA in obstructed kidneys to a level comparable with sham-operated kidneys.

6.6 Effects of Ki-Ras antisense oligonucleotides administration *in vivo* on Ki-67 expression

Ras monomeric GTPase is a well-recognized pivotal molecule involved in the process of cellular proliferation, therefore it was postulated that the use of ASOs to down-regulate Ras mRNA expression may potentially affect proliferation. Ki-67 is a cell proliferation marker that is expressed in the nucleus by cells in the active phases of the cell cycle (G_1, S, G_2 and M phases) but is absent in resting cells (G_0). Renal sections were stained for Ki-67 and expression was subsequently compartmentalized into glomerular, tubular and interstitial areas. 10 views per section were scored to provide a mean expression score for each section.

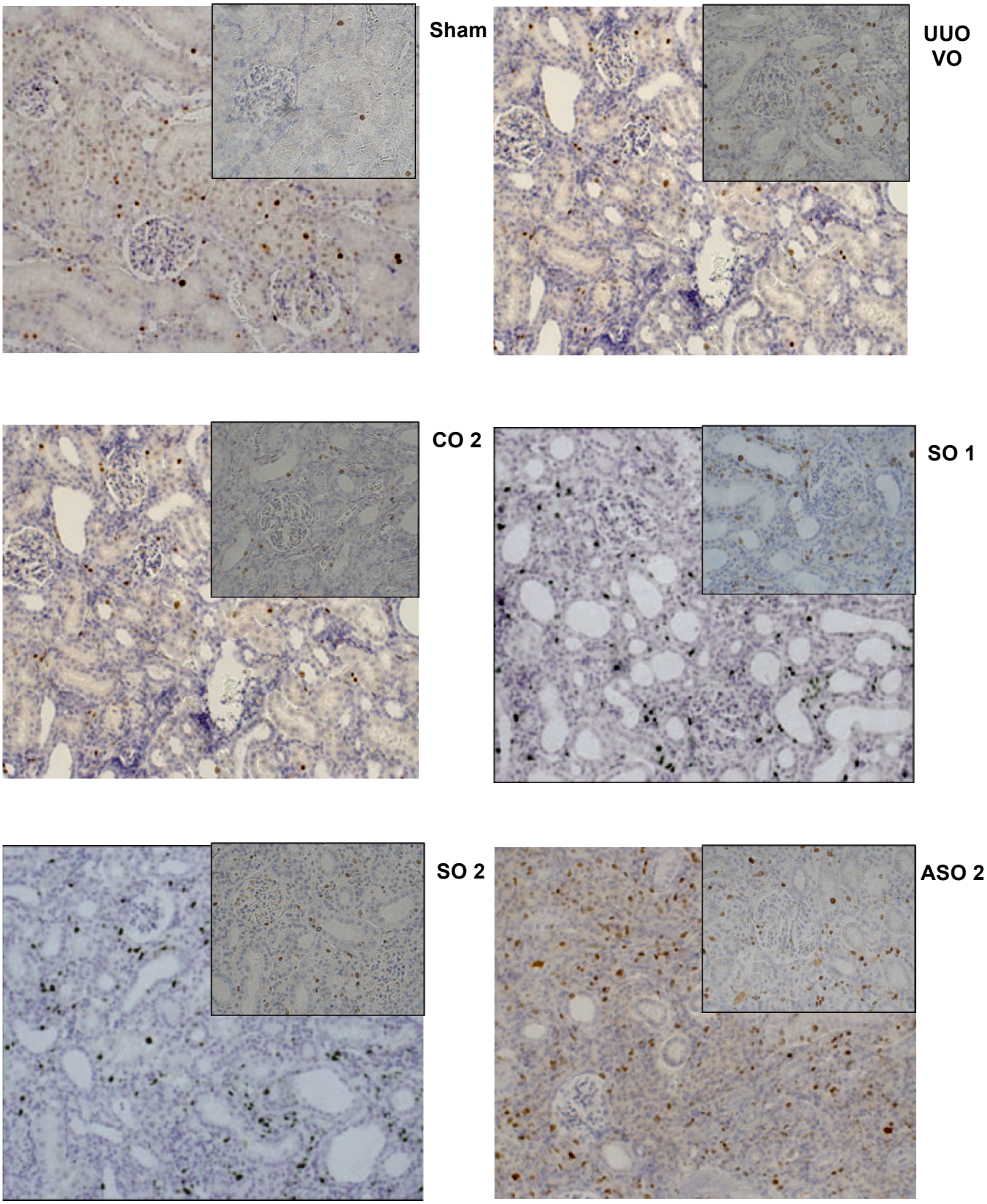

Figure 6.14: Ki-67 expression in renal cortex in Sham and Control Oligo, Scramble Oligo and ASO treated UUO kidney (x 20 and inset x 40)

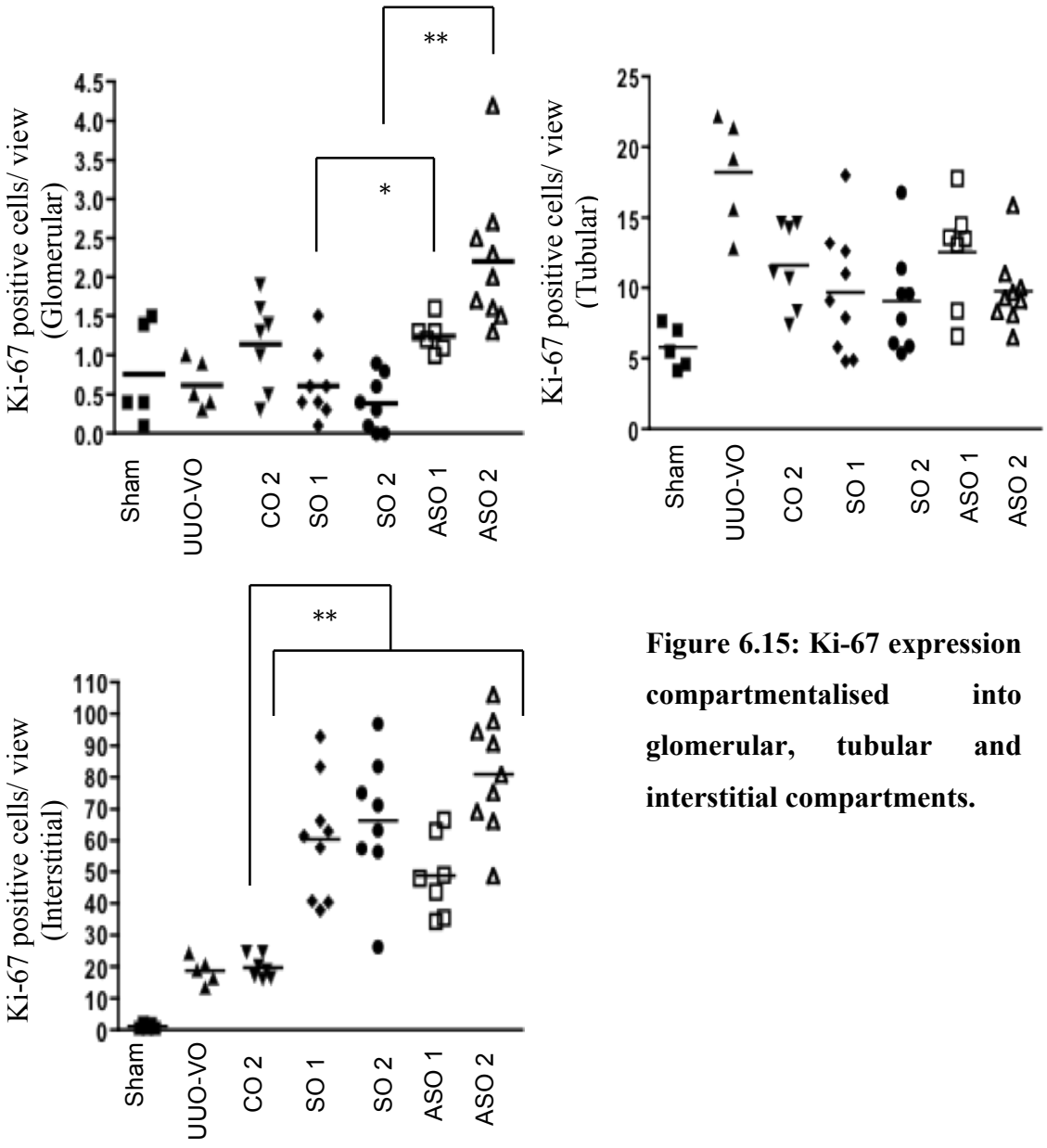

Figure 6.15: Ki-67 expression compartmentalised into glomerular, tubular and interstitial compartments.

Following kidney obstruction there was no significant change in Ki-67 expression within the glomeruli but there was a significant increase in tubular and interstitial expression when compared to sham-operated groups. Administration of either CO 2, scrambled oligos did not alter glomeruli expression compared to UUO-VO group but ASOs administration resulted in an increase in expression within this compartment, though in absolute terms this was an increase of only 1 cell/view. Administration of an oligo per se (CO 2, scrambled or antisense) did result in decreased tubular cell

expression by a mean of 42% compared to UUO-VO. Administration of CO 2 did not affect interstitial Ki-67 expression compared to vehicle-only treated group, but the administration of either scrambled or antisense oligos resulted in an increase of expression of interstitial Ki-67 by about 3-fold when compared to UUO-VO or CO 2.

6.7 Effects of Ki-Ras antisense oligonucleotides administration *in vivo* on monocyte infiltration

On analysis of sections for fibrosis it was noted that some sections, in particular those from ASO treated groups, had significantly more pronounced inflammatory infiltration of the interstitium.

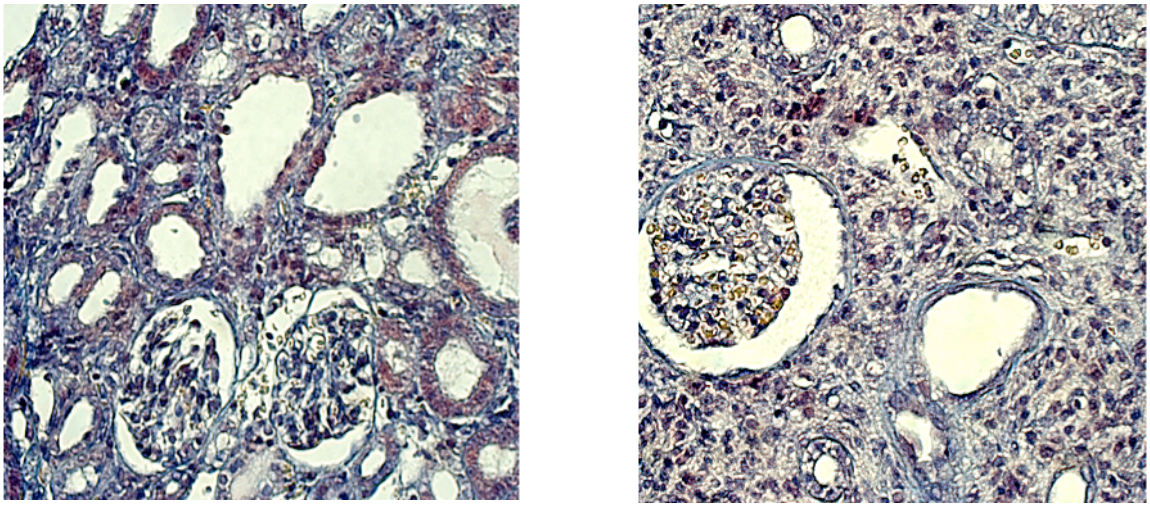

Figure 6.16: PMT staining of obstructed kidneys showing decreased fibrosis in ASO treated section but also increased interstitial inflammatory cell infiltration.

Following this observation, sections were subsequently stained for CD 68, recognised by ED-1 antibody. ED-1 antigen is expressed by the majority of tissue macrophages and weakly by peripheral blood granulocytes. Positive staining by ED-1 antibody was scored using Nikon Elements BR software package on x20 magnification based on 5 fields of view per section. Scoring was completed in a blinded fashion.

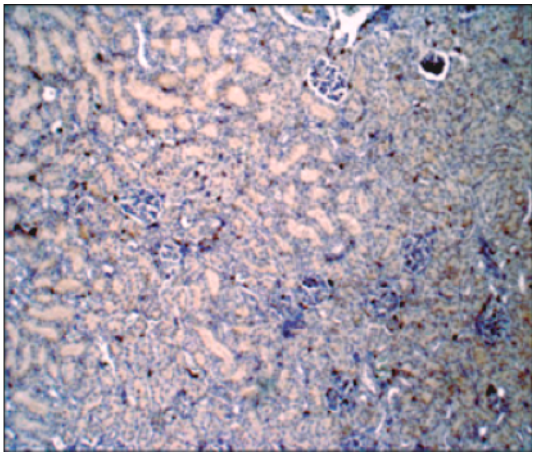

Sham

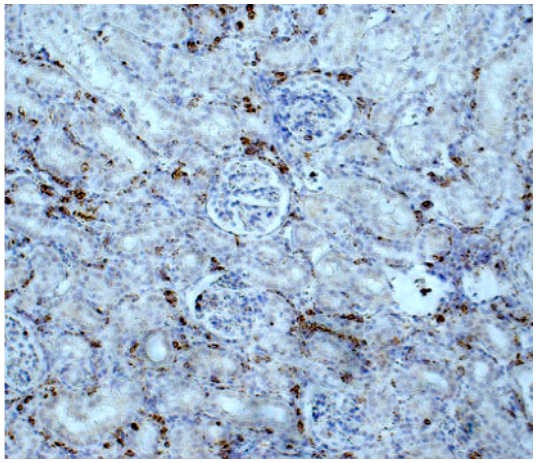

UUO
VO

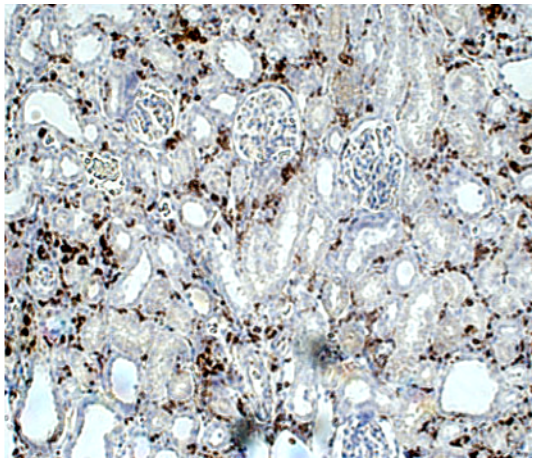

CO 2

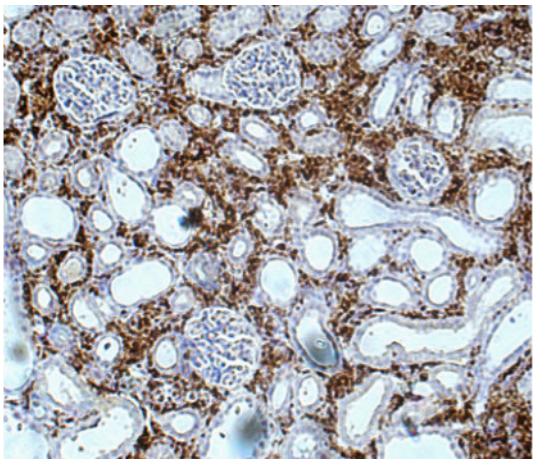

SO 1

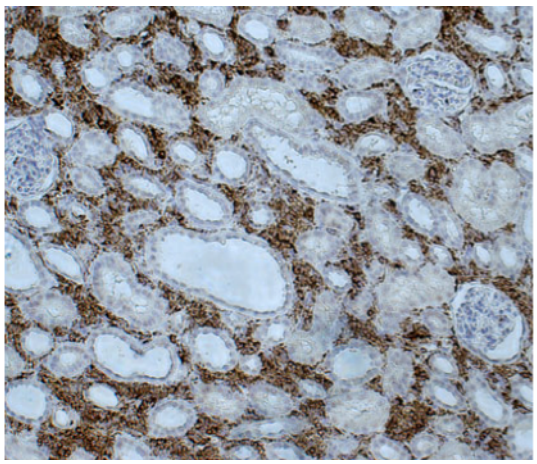

SO 2

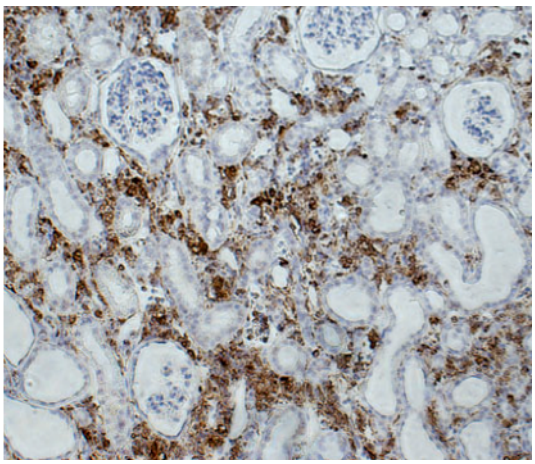

ASO 1

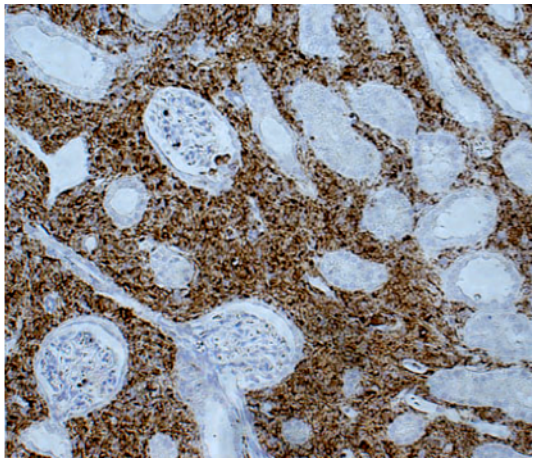

ASO 2

Figure 6.17: Representative sections sham and obstructed kidneys from vehicle-only and oligo treated models stained by ED-1.

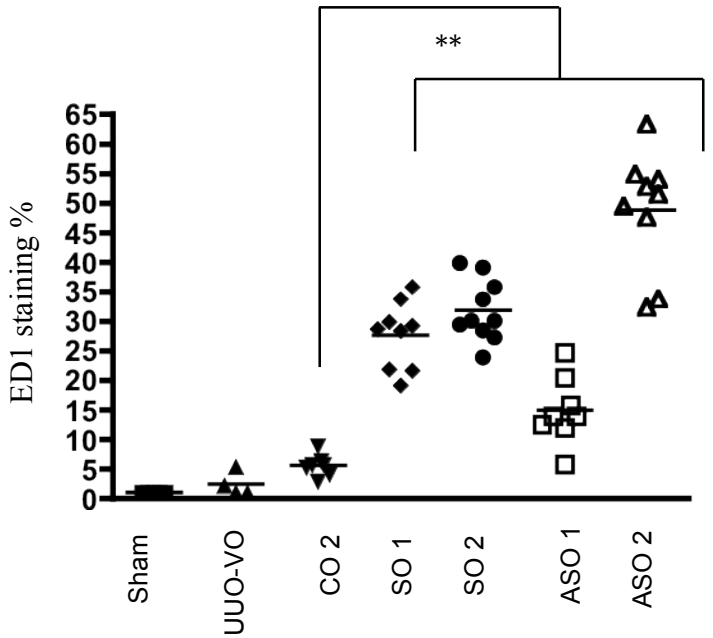

Figure 6.18: Interstitial ED-1 staining of sham and obstructed kidneys from non-treated and oligo treated models.

Staining for tissue macrophages showed they were in scarce number (1%) in sham-operated, non-obstructed kidneys. Numbers doubled to 2.4% on obstruction. Administration of CO 2 led to further increase in expression to 5.5%. However the administration of either scrambled or antisense oligonucleotides resulted in a significant increase in macrophage tissue infiltration peaking in the ASO 2 treated group which demonstrated a 20-fold increase to 49% when compared to UUO-VO alone.

6.8 Summary of results of administration Ki-Ras ASO in a model of UUO: Endpoint analysis

1) Administration of oligos did not appear to grossly affect either behaviour or weight gain of animal models compared to vehicle-only treated group.
2) Ureteric obstruction resulted in an increase of combined mean fibrosis score by 62% which is consistent with previous results.
3) There was no significant difference in combined mean fibrosis score on administration of CO 2 when compared to UUO-VO (67% v 62%).
4) Administration of SO 1 and SO 2 reduced combined mean fibrosis score by 35% and 40% respectively compared to UUO-VO.
5) Administration of ASO 1 and ASO 2 reduced combined mean fibrosis score by 73% and 68% compared to UUO-VO.
6) Administration of ASO 1 and ASO 2 reduced combined mean fibrosis score by 56% and 46% compared to sister scrambled oligo groups SO 1 and SO 2 respectively.
7) Administration of ASO 1 and ASO 2 significantly reduced Collagen I expression by 58% compared to CO 2 group.
8) There was no significant difference in glomerular or tubular FSP-1 expression between UUO-VO, scrambled oligos or ASO groups.
9) There was an increase in interstitial FSP-1 expression in UUO-VO group compared to sham-operated kidney group but no difference between SO treated groups compared to UUO-VO.
10) Administration of ASOs resulted in a trend towards increase in interstitial FSP-1 expression compared to scrambled oligo treated groups.
11) Ureteric obstruction led to an increase in αSMA expression in UUO-VO compared to sham-operated group based on immunohistology. There was no significant difference in expression on administration of SO 1 or SO 2 compared to UUO-VO.
12) Administration of ASO 1 and ASO 2 significantly reduced αSMA cortical expression compared to UUO-VO and sister SO treated groups based on immunohistology. ASO 1 group reduced renal cortical αSMA expression score to a level comparable to sham-operated group.

13) Ureteric obstruction resulted in a significant increase in αSMA protein expression compared to sham-operated group based on western blotting. There was no significant difference in αSMA expression between UUO-VO and SO 1 and SO 2 groups.
14) Administration of ASO 1 and ASO 2 reduced αSMA protein expression compared to sister SO groups based on western blotting. ASO 2 reduced αSMA expression to levels comparable with sham-operated kidneys.
15) There was no significant difference in Ki-67 glomerular expression between sham-operated, UUO-VO and scrambled oligo treated groups. Administration of ASO 1 and ASO 2 resulted in an increase in glomerular Ki-67 expression when compared to their sister scrambled oligo treated.
16) Ureteric obstruction led to a significant increase in tubular Ki-67 expression. There was a decrease in Ki-67 tubular expression in all oligo (CO 2, SOs or ASOs) treated groups when compared to UUO-VO.
17) There was an increase in interstitial Ki-67 expression following ureteric obstruction. Though administration of CO 2 did not alter interstitial expression compared to UUO-VO, administration of SO 1, SO 2, ASO 1 or ASO 2 resulted in a significant increase in interstitial Ki-67 expression.
18) There was no significant difference in ED-1 staining score between UUO-VO or CO 2 groups. There was a significant increase in ED-1 staining on administration of SO 1, SO 2, ASO 1 or ASO 2 in comparison to CO 2 or UUO-VO.

6.9 Discussion

Ras is a ubiquitous cell molecule and plays a central role in cell proliferation, thus it was of a concern that the systemic administration of an ASO targeting Ki-Ras may result in significant decrease in cellular proliferation and significant clinical side effects. However following administration of oligos, animals gained weight at an identical rate and were of an identical endpoint mass compared to vehicle-only treated models. There were no observable significant differences either in macroscopic appearance or general behaviour in oligo treated models though neither parameter was formally assessed. The stains chosen for assessment for interstitial fibrosis were picromallory trichrome and picrosirius red. Trichrome staining is a widely used staining method in clinical medicine especially in the assessment of degree of fibrosis in renal biopsies in the clinical setting mainly due to the distinctive degree of staining of fibrotic areas. Picrosirius red was employed for the stains targeting of collagen fibres in particular collagen type I and III. A further advantage was the unique red/orange appearance of stained fibres under cross-polarized light allowing for better differentiation of collagen from background. One publication (Farris, Adams et al. 2011) compared different staining methods and techniques with regards to assessment of renal fibrosis and concluded that, when considering efficiency, reproducibility and best correlation with estimated GFR the best current techniques include visual assessment of trichrome-stained slides and morphometric assessment of unpolarized picrosirius red stains. In comparison to sham-operated models there was a significant increase in fibrosis score following ureteric obstruction as measured both on PMT and PSR staining and these results were comparable to those previously seen (see *Chapter 4*). Administration of CO 2 did not result in any significant change in fibrosis score as compared to vehicle-only treated group despite pan-Ras mRNA knockdown. Administration of scrambled oligos resulted in a significant discrepancy in fibrosis score depending on staining method, that is either PMT or picrosirius red, used to assess fibrosis. For fibrosis score based on PMT, there was no significant difference for SO 1 treated group when compared to UUO-VO but there appeared a significant reduction in fibrosis on administration of SO 2. However, when picrosirius red staining was used to assess fibrosis, the reverse was seen with SO 1 administration significantly reducing degree of fibrosis compared to UUO-VO whereas fibrosis score in SO 2 group was comparable to vehicle-only treated group. This observed

inconsistency in scoring based upon staining method is thought to be due to different degrees of oedema within the tissue and uptake of stains thus highlighting the degree to which tissue response to different oligos, timing of retrieval and treatment post-harvesting may affect degree of staining. Other factors include animal batch, antigen retrieval, fixation time and stain penetration. Since quantification of fibrosis is not standardized and there is no widely accepted method of assessment, in order to overcome variables such as oedema, it is preferable to have an objective assessment by a single expert observer rather than a software-based model of measurement. This allows assessment of staining based on intensity, area and distribution allowing for more accurate exclusion of non-specific staining as opposed to assessment on colour difference alone. The inconsistency seen with the fibrosis scores in this project validates the decision to use two different methods to assess the degree of fibrosis within tissue samples. In order to obtain a more robust reflection of degree of fibrosis between treated groups, the fibrosis scores achieved by PMT and PSR were combined to provide an overall 'combined mean fibrosis score'. Results showed that there was a significant increase in fibrosis score following ureteric obstruction from 6% (sham) to 62% (UUO-VO) and that CO 2 administration did not significantly change this score. Administration of both SO 1 and SO 2 appeared to reduce fibrosis scores by about 20% though it is uncertain how true this knockdown in fibrosis score really is in the absence of a true contemporaneous experiment. Ideally to remove all confounders, a 'master' experiment would need to be performed using identical animal batches with all ureteric obstruction and treatments performed at exactly the same time points and identical harvest and fixation times with same-day sectioning and staining. This was logistically impossible in the scope of this project. There was an insufficient amount of reagents, the limit of time constraints and only a single operator. Additionally a large repeated experiment could not be justified with respect to the 3 'R's (replacement, reduction and refinement) of *in vivo* work. Thus groups compared were from different time points and may have varied to a degree with regards to animal batch and tissue treatment and staining post-harvest that may lead to a degree of discrepancies in results as seen in SO groups, however all experiments were performed by a single operator using an identical protocol with scoring performed as much as possible by a single assessor for each parameter with an aim to ensure results were as consistent and reproducible as possible.

Despite the discrepancy between stains observed with administration of scrambled oligos, it was demonstrated that administration of either ASO 1 or 2 consistently halved the fibrosis score when compared to either SO group on both PMT and PSR staining. The consistent reduction in fibrosis score on administration of Ki-Ras ASO in comparison to scrambled oligo groups independent of staining method implies that active Ki-Ras knockdown, not just oligo per se, administration, contributes to decreased end-point fibrosis scores.

Interstitial collagen I expression was also seen to increase following ureteric obstruction as expected. CO 2 administration did not significantly alter the expression. Administration of ASO 1 or ASO 2 both significantly reduced collagen I expression. Again this suggests the active knockdown of Ki-Ras mRNA expression and not the presence of an oligo per se has an active role in reducing collagen deposition within the interstitium in a model of UUO. The attempts to stain samples from the scrambled oligo groups using our protocol employing a collagen I polyclonal antibody proved to be more inconsistent and less successful and may in part reflect the difference in the nature of the renal tissue that has been eluded to in the above discussion regarding PMT and picrosirius red staining.

To determine if the ASOs had an effect on fibroblast numbers, sections were stained for FSP-1 and compartmentalized into glomerular, tubular and interstitial expression. Ureteric obstruction led to an increase in both interstitial and tubular expression of FSP-1, though in the case of the latter, in terms of absolute numbers this was an increase of only 1 cell/view. Though the expression of interstitial FSP-1 was similar in SO 1 and SO 2 compared to UUO-VO, there was a trend to increased FSP-1 expression in the interstitium of ASO treated models which was statistically significantly following administration of ASO 1. As an expression of the fibroblast population, this is unexpected especially in the light of decreased fibrosis and collagen I scores in the ASO treated groups compared to both UUO-VO and SO groups. Furthermore, previous data from our group had demonstrated that Ki-Ras knockdown reduced stimulated fibroblast proliferation *in vitro*. However it must be considered that there is debate regarding the degree to which FSP-1 is fibroblast specific and expression of this protein has also been demonstrated to be present in other cell types including T-lymphocytes, macrophages, Kupffer cells and plasma cells (Le Hir, Hegyi et al. 2005). Thus the increase observed in interstitial FSP-1

expression in ASO treated groups may not solely represent a fibroblast population but also an inflammatory one.

Immunohistological staining for αSMA demonstrated a significant increase in interstitial expression following obstruction that may represent increased myofibroblastic activity. Administration of either CO 2 or scrambled oligos did not alter expression compared to UUO-VO but both ASO 1 and ASO 2 treatment resulted in significantly reduced αSMA expression compared to sister scrambled oligos with ASO 1 treated group reducing immunohistological expression of αSMA to a level comparable to sham-operated kidneys. The expression of αSMA protein was also analysed using SDS PAGE. Densitometry analysis of immunoblots revealed that there was a 5-fold increase in αSMA expression following ureteric obstruction. Neither administration of SO 1 or SO 2 resulted in a significant difference but both ASOs reduced αSMA expression compared to UUO-VO on western blotting with ASO 2 administration resulting in complete knockdown of αSMA protein expression to a level comparable to sham-operated kidneys. Thus using two differing techniques of αSMA expression anaylsis, it has been demonstrated that administration of Ki-Ras ASO results in decreased αSMA expression in obstructed kidneys compared to both vehicle-only and scrambled oligo treated samples and may reflect a downregulation in myofibroblastic activity. Why ASO 1 should appear more potent on immunohistological assessment but ASO 2 more potent on western blotting is unknown, but may be associated with the degree of ease of either staining or extraction of protein from the individual ASO treated group. Furthermore the presence of one outlier within the ASO 1 group following SDS PAGE may also have led to a higher than expected mean protein expression of αSMA than expected. If one takes into context the decrease in αSMA expression on the background of increased FSP-1 expression in ASO treated groups, it could be postulated that Ki-Ras inhibition does not reduce fibroblast population but does reduce myofibroblastic activation thus resulting in decreased matrix deposition and scarring despite increased fibroblast numbers. However since both αSMA and FSP-1 are not cell specific, in the absence of identification of αSMA/FSP-1 positive cells, this cannot be confirmed from this work.

The effects of Ki-Ras inhibition on the proliferation of fibroblasts *in vitro* (Sharpe, Dockrell et al. 1999) suggests a potential mechanism for decreased fibrosis in ASO

treated groups *in vivo*. Tissue was stained for the cell nuclear proliferation marker Ki-67 with expression compartmentalized into glomerular, tubular and interstitial areas. There was no significant difference in glomerular expression between sham, UUO-VO, CO 2 or SO. However administration of Ki-Ras ASOs led to a trend towards upregulation of glomerular expression. The nature of these proliferating cells was undetermined. Ureteric obstruction alone (UUO-VO) led to a significant increase in tubular expression of Ki-67 and this observation may reflect an attempt at 'healing' of damaged tubules following obstruction. However administration of an oligo (either CO 2, scrambled or ASO) led to a decrease in tubular Ki-67 expression compared to UUO-VO. As this phenomenon was observed in all oligo groups, it can be assumed that this may be a result of oligo uptake by tubular cells per se and is not specific to the oligo sequences or antisense targeting effects. The recognized preferential uptake of and concentration of oligos within tubular epithelial cells (see *Introduction*) may affect tubular cell proliferation in a non-specific manner. Within the interstitium there is a sixteen-fold increase in Ki-67 expression upon obstruction compared to sham-operated kidneys. Administration of CO 2 did not alter this level of expression. However there was a subsequent four-fold increase in interstitial Ki-67 expression upon administration of either ASOs or scrambled oligos compared to UUO-VO and CO 2 treated groups. Thus this observed difference in interstitial Ki-67 expression appears to be related to the base make up of the oligo (not the sequence) and is unlikely to be related to Ki-Ras inhibition. It is unclear at present which cells are actively undergoing proliferation.

Despite decreased fibrosis scores, some sections from ASO treated groups appeared to have a noticeable increase in inflammation. To assess this more accurately, ED-1 antibody against CD68, a cell surface antigen expressed by mononuclear cells, was used to stain sections. ED-1 staining showed that as expected there was an increase in monocyte presence in obstructed kidney sections as compared to sham-operated ones. Administration of CO 2 resulted in increased ED-1 staining that may reflect the administration and uptake of a foreign molecule by renal tubular cells. However the administration of both SOs and ASOs resulted in a further significant increase in ED-1 staining over and above that seen with CO 2 treatment. Again, as for interstitial Ki-67 expression, the degree of monocyte infiltration and inflammation appears to be related to base representation of the oligo and not the sequence. In addition a greater degree of inflammation was seen with ASO 2 administration and this appears to be

consistent with previous results (see *Chapter 3*). Previously assessment of ASOs found that ASO 2 appeared to be a more potent for Ki-Ras mRNA knockdown (see *Chapter 3*). However, in a model of UUO, the measurement of the endpoints of fibrosis showed that there was no significant difference between groups treated with ASO 1 or ASO 2. It may be that, in the case of UUO, ASO 1 may ameliorate fibrosis to the same degree as ASO 2 but with fewer systemic inflammatory effects. Following discussions with ISIS Pharmaceuticals we were informed that inflammation was a recognized effect of this generation of oligos, though new oligos that caused minimal inflammatory response were now in development. The correlation in the degree of interstitial Ki-67 expression and ED-1 staining between SOs and ASO groups suggest that the interstitial proliferating cells may in fact be inflammatory cells and not mesenchymal. However of particular interest is the fact that although there is a similar degree of inflammation between SOs and ASOs there remains a significant difference in end-point parameters of fibrosis and fibrogenic activity in the presence of a significant difference in Ki-Ras mRNA knockdown.
These results suggest that there may be a dissection between the processes of inflammation and fibrosis. It can also be postulated that there may be different sub-populations of inflammatory cell infiltration in SO and ASO groups. Different subpopulations of macrophages (M1 and M2) are now recognized with differing properties. This may explain why equal degree of inflammation may be pro-fibrotic in one condition (scrambled oligos) and anti-fibrotic in another (ASOs). As both SOs and ASOs are identical with regards to length and base representation, the difference in inflammation and fibrotic response is postulated to be related to the effect of Ki-Ras knockdown.

In conclusion these results suggest that antisense inhibition of Kirsten-Ras ameliorates interstitial fibrosis in a rat model of unilateral ureteric obstruction despite increased inflammation and interstitial proliferation. In addition it is possible that Ki-Ras may have a role with regards to inflammatory infiltration and also suggests that the degree of inflammation per se may not directly correlate to the degree of fibrosis.

Chapter 7: Discussion

7.1 Summary of findings

The work presented in this thesis combined both *in vitro* and *in vivo* experiments to demonstrate that specific Kirsten-Ras mRNA knockdown by antisense oligonucleotides ameliorates interstitial fibrosis in a rat model of unilateral ureteric obstruction.

Transfection of primary rat renal fibroblasts and normal rat kidney fibroblastic and epithelial cell lines with Ki-Ras ASOs employing a cationic liposomal transfection system resulted in specific knockdown of Ki-Ras mRNA expression. The efficiency of knockdown was seen to be far greater with ASO 2 transfection than ASO 1. A 'compensatory' rise in Ha-Ras mRNA was associated with Ki-Ras knockdown within fibroblasts but this observation was absent in epithelial cells following administration of ASOs. None of the oligos were demonstrated to cause significant cytotoxicity in NRK-49F cells when compared to vehicle-only controls.

Administration of these Ki-Ras ASOs in wild-type, non-diseased Wistar rats demonstrated uptake and concentration of oligos within the proximal convoluted tubules of the kidney with no uptake within the interstitium or distal tubules and collecting ducts. Oligo was also seen to be deposited in cardiac, liver and muscle tissue following subcutaneous administration. Within the kidneys, ASO administration resulted in specific knockdown of Ki-Ras mRNA to a degree comparable to that seen *in vitro*. Though ASO 2 again appeared more potent than ASO 1 with regards to mRNA knockdown of Ki-Ras, subsequent analysis of total Ras protein expression demonstrated a comparable decrease in protein levels by both Ki-Ras ASOs when compared to CO 2. The administration of Ki-Ras ASOs was associated with a significant increase in interstitial expression of the cellular proliferation marker Ki-67 when compared to CO 2 group. This observation was absent in glomerular and tubular cell compartments. Analysis of liver tissue revealed that hepatic Ras expression following ASO administration reflected trend of results achieved in the kidney with comparable efficiency of knockdown by ASO 1 and ASO 2. Examination of both cardiac and liver tissue revealed significant increase in inflammation following administration of ASO 2 that was absent on ASO 1 administration.

A rat model of unilateral ureteric obstruction was set-up and characterized with regards to fibrosis and Ras expression as part of this project. With regards to histological fibrosis score and expression of fibrogenic markers, an optimal experimental time-period of 16 days was employed. A significant rise in both Ki-Ras and N-Ras mRNA was noted in the obstructed kidney compared to sham-operated kidneys. This observation was localized to the obstructed kidney only and not the contra-lateral non-obstructed kidney. No significant difference in Ha-Ras mRNA levels was observed. Protein analysis was limited by the lack of specific Ras isoform antibodies, a limitation observed by other groups (Fuentes-Calvo, Blazquez-Medela et al. 2010).

Low dose (5mg/kg) administration of ASO 1 in UUO models over a 12-day period did not significantly decrease Ki-Ras mRNA expression or affect fibrosis parameters but a rise in N-Ras mRNA was noted in comparison to a saline-only treated group.

Administration of high dose (12.5mg/kg) Ki-Ras ASO to models of UUO over a 16-day period resulted in increased deposition within the proximal tubules when compared to non-obstructed models. In addition there was deposition of oligo in the interstitium of obstructed kidneys that is absent in non-obstructed kidneys. Following administration of ASOs a decrease of Ki-Ras mRNA from up-regulated levels seen with vehicle-only treated UUO models to a level comparable with sham-operated kidneys within the obstructed kidney was noted. A decrease in Ki-Ras mRNA expression within the contralateral kidney was also noted. In UUO models the potency of ASO 1 was found to be comparable to ASO 2 with regards to Ki-Ras mRNA knockdown. N-Ras mRNA expression within ASO treated groups was also found to increase while Ha-Ras mRNA expression decreased. Administration of CO 2 in UUO models led to pan-Ras isoform knockdown effect that was isolated to the obstructed kidney. This was not previously seen following CO 2 administration in non-obstructed models and was thought to be an artefact related to accumulation of CO 2 on the background of obstruction. Analysis of end-point data demonstrated both a significant increase in fibrosis scores and expression of αSMA and collagen I following ureteric obstruction comparable or greater than that observed in vehicle-only. Administration of both ASO 1 and ASO 2 resulted in a significant decrease in histological fibrosis score, αSMA and collagen I expression compared to CO 2

treated groups. There were no obvious gross adverse effects on animal growth or behaviour following oligo administration.

Validation experiments showed that administration of scrambled oligos (SO 1 and SO 2) in UUO models did not result in knock down of any isoform of Ras when compared to UUO-VO group and this data was supported by a contemporaneous experiment. These results suggest that Ki-Ras mRNA knockdown was specific to Ki-Ras ASO administration and not due to oligo administration per se. However administration of SO 1 and SO 2 resulted in inconsistencies in fibrosis scores dependent on stain used to assess fibrosis. It is postulated that these discrepancies are the result of dissimilarities in tissue treatment and reaction. However the administration of either ASO 1 or ASO 2 resulted in further reduction in fibrosis score when compared to SOs treated groups suggesting an anti-fibrotic effect associated with antisense Ki-Ras knockdown. Both ASO 1 and ASO 2 administration resulted in a significant decrease in αSMA expression in the obstructed kidney, assessed by both immunohistological and western blotting analysis, to a level comparable with sham-operated kidneys when compared with SOs groups.

FSP-1 expression was increased following obstruction as expected. Though expression was the same between UUO-VO and SO groups in the interstitium, there was a trend to increased interstitial FSP-1 expression in ASO treated groups. Ureteric obstruction also led to a significant increase in tubular Ki-67 expression but the administration of any oligo (control, scrambled or antisense) led to a significant decrease in Ki-67 expression in this compartment compared to UUO-VO. Both the administration of either scrambled oligos or ASOs resulted in a significant increase in interstitial Ki-67 expression when compared to UUO-VO and CO 2 treated groups.
Staining for CD 68 (using ED-1 antibody), a macrophage marker, also demonstrated a significant increase in expression within renal tissue of SO and ASO treated groups when compared to UUO-VO and CO 2 groups. The parallel results obtained from Ki-67 and ED-1 staining suggests that these differences may be determined by the specific nucleotides representation (not the actual sequence) of the scramble and antisense oligo make up.

However, despite a heavy degree of inflammatory infiltrate there was a significant decrease in fibrosis score and expression of molecular markers of fibrogenesis in ASO treated groups compared to SO treated groups. This is surprising as it is widely accepted that the degree of interstitial inflammation correlates with the degree of fibrosis, yet findings in this project appear to contradict this idea.

In summary the work presented in this thesis has shown that subcutaneous administration of Ki-Ras antisense oligonucleotides in a rat model of renal fibrosis significantly reduces the degree of interstitial fibrosis both on a histological and molecular level. The amelioration of fibrosis by Ki-Ras ASOs appears to be independent of the degree of interstitial cellular proliferation and inflammatory cell infiltration.

7.2 Choice of cell models

The aim of this project was to examine the effect of inhibition of wild type Ras in the process of renal fibrosis. To this end, in order to best extrapolate a cell model to that of a living organism, the former must be as closely related to the latter as possible. We initially used primary cell lines derived directly from rat renal tissue. Though this has the benefit of being a cell model that most closely correlates to the organism being studied, there are several restrictions. Retrieval is time consuming, primary cells are less robust and they have a shorter life span and are usually unable to undergo multiple passages compared to cell lines. Due to the method of retrieval, the 'purity' of cells may also be limited and there may be several different cell types in each retrieval batch and these cells may also change phenotype after only a few passages. Both these effects will result in inconsistent results. Immortal cell lines do not possess these issues. They have the advantage of availability, reproducibility and they retain their phenotype through multiple passages. Their robustness allows for increased survival following various treatments and possibly a decreased vulnerability to infection. However in attaining these attributes, certain physiological changes may take place and this transformation can significantly alter cell characteristics and their response when compared to cells of true wild-type parentage, though these changes may not always be immediately obvious. Thus there is a risk that observations in these cell lines may not be truly reflective of response in wild-type scenario.

Furthermore it must be remembered that cells are grown and treated in non-physiological buffers and reagents that may induce a different response from that which is deemed normal in man.

For our purposes of validating ASO characteristics, we employed both a fibroblast and epithelial cell line in addition to primary cell cultures. NRK-49F is a fibroblast cell line derived from a mixed normal rat kidney cell culture and exhibits contact-inhibition and possesses a mesenchymal cell morphology. The lack in specific fibroblast markers makes differentiation from other cell types difficult but they have been observed to have distinctly different characteristics to their sister epithelial cell line. NRK-52E is an epithelial cell line cloned from the same mixed culture of normal rat kidney cells as NRK-49F, but has epithelial-like morphology. These epithelial cells have distinct growth and transforming characteristics distinct from NRK-49F cells. Both cell lines are robust and retain their phenotype following multiple passages but may transform spontaneously especially if not maintained in a sub-confluent state.

7.3 Choice of *in vivo* models

It is well established that the degree of renal dysfunction best correlates to the degree of tubulointerstitial fibrosis (Bohle, Strutz et al. 1994). There are several models of renal tubulointerstitial fibrosis including diabetic nephropathy, cyclosporine-induced and hypertensive. However these models will also have concurrent glomerular changes and involve either administration of disease inducing compounds or genetic mutations with specific end-points occurring only after a relatively long time period. One of the most widely accepted experimental models of renal tubulointerstitial injury and fibrosis is that of obstructive nephropathy. This model was created by Hinman and Morion in 1926 and has several advantages compared to the aforementioned ones. Firstly a wild-type animal may be used and so no additional compounds or genetic manipulation is required which may better reflect the "real" state and is of added value when assessing new therapeutic compounds. Secondly the rate at which fibrosis occurs is far more rapid than other methods. Thirdly the model provides both histological changes (essentially in the tubulointerstitium) and quantifiable molecular changes that have been shown to reflect fibrogenesis. This includes increased capillary permeability, inflammatory cell infiltration, *de novo* myofibroblasts production and increased matrix production with progressive tubular loss. Finally

unilateral ureteric obstruction (UUO) allows for the use of the contralateral non-obstructed kidney as a control if appropriate. Unfortunately in the classical UUO model, functional data is not available. This model has not previously been used in our laboratory and part of this project was the development and characterization of this model of renal fibrosis.

Despite the benefits of animal models in studying disease and potential therapies, one must be very aware of the shortfalls in results obtained. Firstly it is highly unlikely that any one model will adequately represent the true entity of 'renal fibrosis' and data obtained from one experiment may not be wholly applicable to another model. Thus a therapy deemed successful in one model of fibrosis must always be evaluated in at least one other. In addition in various models, especially those models of toxicity or secondary cause (adriamycin, cisplatin, Thy-1), it is difficult to distinguish treatment effects on fibrogenesis as opposed to amelioration or removal of underlying cause or stimulating factor and natural organ recovery. The timing of treatment is also important. Majority of experimental treatment is provided early, whereas in the human clinical scenario interventions are usually at medium to late stage of fibrosis progression when disease is clinically apparent. Early administration also implies that treatment results are focused on fibrosis development as opposed to fibrosis modulation or reversal. Furthermore in the clinical setting patients tend to be on multiple medications (such as ACE inhibitors) that are absent in the animal model. The lack of a good molecular marker of fibrosis means that results are not standardized, with fibrosis being assessed by different techniques and parameters, thus quantification of fibrosis may vary considerably in different hands. Finally one must be aware that there may be considerable variability in outcomes for even well defined models in part due to animal strain variability but also in regards to their diet and care. More importantly the translation of therapeutic interventions in animal models must be translated to humans with the utmost care as they may potentially be ineffective or worse, harmful.

7.4 Targeting Ras signaling

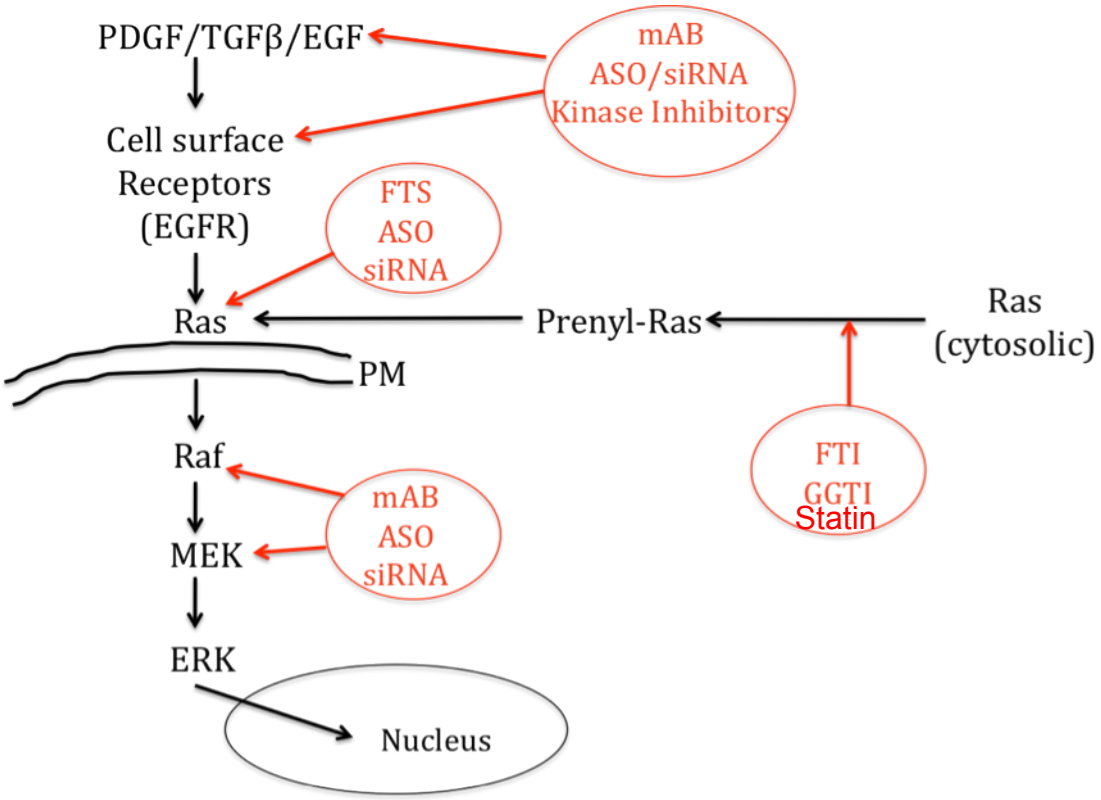

Figure 7.1: Potential targets of the Ras signaling pathway. PM, Plasma membrane. FTS, farnesylthiosalicylic acid. FTI, Farnesyltransferase inhibitor. GGTI, Geranylgeranyl transferase inhibitor. mAB, neutralizing monoclonal antibody. ASO, Antisense oligonucleotide. siRNA, short-interfering RNA.

The above figure summarizes the potential targets along the Ras signaling pathway which may be of therapeutic value in renal disease. Since Ras appears to be a convergent point for a plethora of cytokines and growth factors, the use of monoclonal antibodies or agents to any single one of these upstream molecules may be redundant with regards to inhibition of Ras activation (Stadler 2005; Gagliardini and Benigni 2006). Inhibitors of prenylation in the form of statins and prenylation inhibitors, such as farnesyl- and geranylgeranyl transferase inhibitors (FTI and GGTI), have shown more promise. However these agents are not specific for Ras proteins and may affect other members of the Ras GTPase superfamily such as Rho and Rac. In addition one must consider that at least Ki-Ras and N-Ras can be alternatively geranylgeranylated so possibly in order for a significant therapeutic

effect both FTI and GGTI may be required to achieve significant clinical effect and of the subsequent complete inhibition of prenylation of Ras (or other molecules) may be toxic. Statins have been widely used in clinical medicine and have been shown to be promising in animal models of renal disease. However statins are also non-specific with regards to their actions on Ras signaling and, though statins have been shown to be safe and are now widely used for their benefits in cardiovascular disease, the dose at which they have been employed with regards to Ras inhibition in animal studies have tended to be extremely high (30-40mg/kg) and likely to cause side effects such, as myopathy, if translated into humans (Laezza, Mazziotti et al. 2006; Trebicka, Hennenberg et al. 2007). Furthermore, since 40% of all human cancers are associated with a mutation in Ras, clinical trials utilizing statins to inhibit Ras activity have been undertaken mainly within the oncology community and have not as yet proved beneficial (Jakobisiak and Golab 2003), though this may in part be due to the background oncogenic nature of Ras in these settings.

S-trans, trans-farnesylthiosalicylic acid (FTS) is a synthetic prenyl derivative of a rigid carboxylic acid which structurally resembles the carboxy-terminal farnesylcysteine group common to all Ras proteins (Marciano, Ben-Baruch et al. 1995). FTS has been shown to interfere with the anchoring process of the Ras protein to the plasma membrane which is vital to the molecule's function. Dislodgement of Ras from its plasma membrane domains both removes it from proximity to downstream effectors and facilitates its degradation and has been shown to be effective both *in vitro* and *in vivo* (Gana-Weisz, Haklai et al. 1997; Reif, Weis et al. 1999; Clarke, Kocher et al. 2003; Khwaja, Sharpe et al. 2005; da Silva Morais, Saliez et al. 2008). FTS was administered daily via intra-peritoneal route in these studies though now an oral compound of FTS, Salirasib, has been developed (Haklai, Elad-Sfadia et al. 2008). However recent results from a phase II trial of Salirasib in patients with lung adenocarcinomas with Ki-Ras mutations have been disappointing (Riely, Johnson et al. 2011). It is uncertain if these poor results are due to the dose of Salisirab employed, resistance to therapy of mutated Ki-Ras or whether it is related to the mechanism of FTS action and its non-specific effects on the Ras GTPase family of molecules. Many of the studies in which FTS inhibition of prenylated Ras have shown promise have involved transformed/malignant cells but in non-transformed cells there is now evidence that prenylation may not be essential for Ras activation (Khwaja, Dockrell et al. 2006). This suggests that the benefits of FTS in non-

oncogenic circumstances may involve a mechanism of action other than simple Ras membrane dislocation.

An alternative approach to inhibiting Ras activity has been to target the downstream effectors of the Ras pathway. The majority of these studies have been undertaken in the field of cancer and have employed monoclonal antibodies, small-molecule kinase inhibitors (such as BAY 43-9006 against Raf and PD98059 and PD184352 against MEK) and antisense oligonucleotides against kinases of the Ras pathway (Monia 1997; Lyons, Wilhelm et al. 2001; Arslan, Kutuk et al. 2006). Though they have shown promise in cell and animal models, clinical trial have been of variable success (Stevenson, Yao et al. 1999; Lorusso, Adjei et al. 2005; Strumberg, Richly et al. 2005). The degree to which these results can be translated to renal disease in the context of non-malignant cells has yet to be answered. However the importance of Ras in renal disease, and in particular in the process of fibrogenesis, has recently been highlighted by a seminal paper (Bechtel, McGoohan et al. 2010) which reported that the removal of inhibition of Ras activity by hypermethylation of Ras inhibitor RASAL 1 resulted in the perpetuation of fibrogensis in murine fibrosis induced by folate injections. Ras activation results in the activation of numerous downstream effector pathways, not just the pro-proliferative Raf/MEK/Erk cascade and several, such as the anti-apoptotic PI3K pathway, are potentially of equal importance in the process of progressive renal fibrosis. Furthermore, as well as the majority of previous studies being conducted on the background of transformed cells or states, the compounds employed to inhibit Ras function have not been isoform specific. In view that distinct roles of isoforms of Ras are now recognized, this now appears to be a very crude approach and numerous laboratories are now studying the targeting of individual Ras isoforms. One group has examined the role of Ras isoforms in H- and N-Ras knockout mice and concluded that there was no significant role for either isoform in early renal damage by UUO (3 days) (Grande, Arevalo et al. 2009). However they found that after 15 days of obstruction there was significantly lower degree of fibrosis and expression of inducers of EMT in H-Ras knockout mice compared to wild-type (Grande, Fuentes-Calvo et al. 2009). These studies reveal a significant role for Ras in progressive fibrosis induced by UUO and also imply that isoforms of Ras may have different roles in the process of fibrogenesis at different time points. However the use of knockout mice, which may have a different Ras mediated developmental profile than wild type, and the non-viability of Ki-Ras

knockout mice coupled with a degree of functional cross-over of isoforms of Ras means that the role of Ras isoforms in non-genetically modified conditions remains unclear.

Though other groups have previously employed RNAi in animal models of renal disease, none have targeted Ras isoforms and their success has been limited by delivery of drug to target sites within the kidney, which have required techniques that would be difficult to translate to a clinical setting. From our knowledge, this project is the first to utilize systemic subcutaneous delivery of antisense oligonucleotides to a specific isoform of Ras in a model of interstitial renal fibrosis.

7.5 Antisense oligodeoxynucleotides

Zamecnick and Stephenson first recognised the potential of ASOs in 1978 when studying the inhibition of Rous sarcoma virus replication (Stephenson and Zamecnik 1978). Since then antisense technology has developed into a powerful research tool and has begun to make it's mark in the world of clinical therapy. ASOs consist of a single strand of 20 to 22mer oligodeoxynucleotides which are complementary to the target mRNA sequence. The binding of the ASO to its target mRNA induces RNase H, a non-specific [endo-]ribonuclease, that cleaves the 3'-O-P-bond of RNA in the DNA/RNA duplex to produce 3'-hydroxyl and 5'-phosphate terminated products and results in target mRNA hydrolysis and 'gene silencing'. For specific knock down effect appropriate choice of mRNA target sequence must be made. By considering potential folding patterns and inter-chain hybridization within any given RNA sequence single stretches which are most accessible to ASO may be chosen. Sequences of 20-22mers are used as 20 or more nucleotides occur only once in the human genome, thus decreasing non-specificity effects, and cellular uptake decreases with sequences over 25 bases (Loke, Stein et al. 1989).

However more recently the knowledge regarding mechanism of oligo action has expanded. There is now evidence that oligos that do not induce RNase H may still affect gene expression via non-cleavage mechanisms. These include translational arrest where the oligo may inhibit mRNA translation by hybridizing to target mRNA and blocking binding and scanning by ribosomes but does not initiate RNase H degradation [Baker et al. 1997]. This mechanism has also been developed to target microRNA (miRNA) function [Davis et al. 2009]. Thus a single oligo may affect

numerous gene expression targets by inhibiting miRNA activity. ASOs have also been developed that are complementary to telomere sequences of RNA in telomerase. By binding to these sequences and inhibiting telomerase activity, these ASOs can promote telomere shortening and cell proliferation [Hochreiter et al. 2006]. ASOs may also intefere with RNA intermediary metabolism by binding to pre-mRNA and modulating the splicing of the molecule by masking splicing enhancer and repressor sequences. This 'splice-switching' may realign the translational reading frame which may be of benefit in conditions such as Duchenne muscular dystrophy and β-thalassaemia [Dominski et al. 1993; Roberts et al. 2006]. Oligos have also been shown to disrupt secondary and tertiary structures of RNA molecules upon binding that may affect the activity of the transcript [Ivanova et al. 2007]. Finally, there is now evidence that ASOs may also target promoter sequences of gene expression. This may result in either promotion or inhibition of gene transcription and is thought to involve targeting of short RNA transcripts at the promoter sites of the gene. It may be that these short RNA transcripts control gene expression by affecting histone methylation patterns [Schwartz et al. 2008; Janowski et al. 2005].

7.5.1 ASOs: *In vitro*

Within the realms of renal medicine antisense technology has been a useful research tool in determining gene function *in vitro* and over the last few years has become increasingly prolific in *in vivo* experiments. Our group has previously employed ASOs targeting Ras isoforms (Sharpe, Dockrell et al. 2000) to demonstrate that growth factor induced proliferation of HRF and Vero cells was dependent on Kirsten and, to a lesser extent, Harvey isoforms. Zhang et al. used an ASO targeting connective tissue growth factor (CTGF) (Zhang, Meng et al. 2004) in an *in vitro* model of EMT to demonstrate that CTGF could promote transdifferentiation while Okado et al. demonstrated that Smad 7 has a role in TGFβ induced apoptosis in mesangial cells via activation of caspase-3 using antisense technology (Okado, Terada et al. 2002). Though the use of ASO has been taken up enthusiastically within the renal community, there has been great variability in the doses employed and the methods of cell transfection. Concentrations of ASO used have varied from 200nM to 3μM with duration of transfection time varying from 6hrs to 24hrs. This variation in dose and transfection protocols may in part be a result of the variation in the ease of

transfection of various renal cell types. Cellular uptake of ASOs involves a combination of pinocytosis, absorptive and possibly receptor-mediated endocytosis (Akhtar and Juliano 1992). Naked ASOs have been shown to be inefficient and results in a low yield of internalization and methods employed to increase cellular uptake include the use of cationic liposomes, electroporation and microinjection techniques. (Regnier, Tahiri et al. 2000), (Williams and Buzby 2000). Despite these technical differences overall the use of ASO *in vitro* can be seen as successful.

In this project, transfection of ASOs into cells also appeared to require different protocols depending on cell type. For primary rat fibroblastic cell cultures and fibroblast cell lines (NRK-49F) using a simple liposomal cationic system for transfection was sufficient, but transfection of epithelial cell line (NRK-52E) proved resistant to this protocol and reverse-transfection technique was required. Though transfection of Ki-Ras ASOs resulted in specific Ki-Ras knockdown in both fibroblastic and epithelial cell lines, there appeared to be a compensatory rise in Ha-Ras in fibroblasts that was absent following treatment of epithelial cells. Previous work in primary human fibroblast cell cultures by our group have suggested that Ha-Ras may have a role in stimulated fibroblast proliferation (Sharpe, Dockrell et al. 2000) thus the observed rise in Ha-Ras on administration of Ki-Ras ASOs may reflect a compensatory response to maintain fibroblastic cell proliferation. It may be that whereas Ha-Ras has a role in proliferation in fibroblasts, this may not hold true for epithelial cells thus further supporting different roles for Ras isoforms in different cell types. Previous studies have demonstrated different roles of Ras isoforms in different cells. *In vitro* cell culture studies using renal mesenchymal cells have not demonstrated a role for N-Ras in fibroblast proliferation (Sharpe, Dockrell et al. 2000), however those employing PTEC's suggest a role in downstream signaling upon TGFβ stimulation (Phanish, Wahab et al. 2005; Dockrell, Phanish et al. 2009).Furthermore these discrepancies also indicate that investigation of the role of Ras in cell cultures alone may not be sufficient and use of animal models where multitudes of cell types interact is vital to further understanding of the role of physiological Ras in renal fibrosis.

7.5.2 ASOs: *In vivo*

In general, administration of ASOs in *in vivo* models has been more challenging than that of *in vitro* and therapeutic development has been hindered by non-specific toxicity, short biological half-life of ASOs and heterogeneous distribution and poor targeted cell uptake on systemic administration. Side effects arising from antisense oligonucleotide administration can be divided into hybridization-dependent and hybridization-independent effects. Hybridization effects include exaggerated pharmacologiocal effects upon binding of oligo to target RNA which can be addressed by altering dose of administration and carful characterization of pharmacology. More pertinent is the hybridization of oligo to non-target RNA or 'off-target' effects. This describes hybridization of the ASO to and RNA strand that may differ in sequence from the target by a few base-mismatches. Though 20mer oligonucleotides will demonstrate a 100% complementality match to the targeted RNA, it may exhibit partial complementality to several other genes. Both siRNA and miRNA will demonstrate more off-target effects than those seen by ASOs due to shorter sequences and the intergration of RISC which allows for fewer nucleotides to induce activity and numerous off-target effects.

The observed H-ras knockdown in UUO models by Ki-Ras ASOs could be explained by off-target effects except that previous interrogation of the validity and specificity of both ASO 1 and 2 both *in vitro* and *in vivo* (in non-obstructed models) did not demonstrate any H- or N-ras knockdown when ASOs where administered. Furthermore H-ras knockdown was not demonstrated in contemporaneous experiment IV. This would suggest that the H-ras knockdown seen in UUO models in the prior experiments was not via a mechanism of hybridization-dependent mechanism.

Off target hybridization-dependent effects can be minimized by performing careful analysis of oligo and potential targets with up to three mismatches. Analysis of only up to three mismatches has been chosen as further mismatches have been seen to be associated with loss of activity (Monia et al. 1995).

Hybridization-independent effects are believed to be due to interaction of oligos with various proteins. These 'aptameric' effects may be sequence-dependent or independent. Sequence-dependent effects are initiated via interaction with Toll-like receptors (Krieg et al. 2006) that may result in inflammation, complement activation and development of constitutional symptoms such as fevers, chills and headaches.

Non-sequence specific effects may depend on the chemistry of the oligo in question and the proteins with which they interact and can cause thrombocytopenia, prolongation of APTT, liver transaminitis and injection site reactions. Second generation ASOs appear to be better tolerated than first though clinical effects are hard to predict for each specific oligo. Previous studies in animal models have shown that infusions of ASO may lead to complement cascade activation resulting in haemodynamic instability, neutropenia, prolonged activated partial thromboplastin times and a rise in hepatic transaminases (Farman and Kornbrust 2003)(Levin 1999). These effects appeared to be both dose dependent and related to rate of administration.

The anti-cancer drug Oblimersen targeting the anti-apoptotic gene B-cell Lymphoma-2 (bcl2) underwent numerous clinical trials since it's development. However a study looking at Oblimersen's effect in melanoma cells demonstrated non-specific downregulation of several proteins including cancer markers involved in apoptotic resistance and endoplasmatic reticulum (ER) stress such as the 78 kDa glucose regulated protein (GRP 78), protein disulfide isomerase A3 (PDIA3, GRP 58), calumenin, and galectin-1, as well as the glycolytic enzymes triose phosphate isomerase, glyceraldehyde phosphodehydrogenase, and phosphoglycerate mutase (Winkler et al. 2010). This was believed to be a result of the oligonucleotide's aptemeric effect.

The pan-Ras and H-Ras knockdown in UUO models noted on administration of CO 2 and ASOs respectively in this project may be a result of such hybridization-independent effects from increased oligo levels on the background of obstruction and decreased oligo clearance.

Subsequent clinical studies involving various other antisense oligos have shown that non-specific side effects do occur with increasing dose but the majority of trials now use lower doses of ASO and report minimal toxic effects. In addition recent developments in antisense technology has resulted in subsequent generations of ASO with lower toxicity profiles (Jason, Koropatnick et al. 2004).

Though ASOs are not degraded by RNAse H activity, they are, in unaltered form, rapidly degraded by endogenous nucleases. The modification of the phosphate backbone whereby one oxygen molecule is substituted for a sulphur molecule greatly enhances resistance to nuclease activity. These first generation phosphorothioate ASOs have a half-life in humans in the region of 10 hours in comparison to 30-60

minutes of the original unmodified phosphodiester agents (Crooke and Bennett 1996). However these phosphorothioate ASOs are comparably more toxic and have lower affinity to complementary RNA target. Second generation ASOs contain nucleotides with alkyl modifications, most commonly the addition of 2'-O-methyl group. These ASOs are less toxic and have higher affinity to RNA target. However they cannot induce RNAse (Kurreck 2003). This has led to the development of chimeric ASOs ('gapmers') consisting of phosphorothioate oligodeoxynuclotides backbone with 2'-O-methyl nucleotides at either end (Figure 7.2).

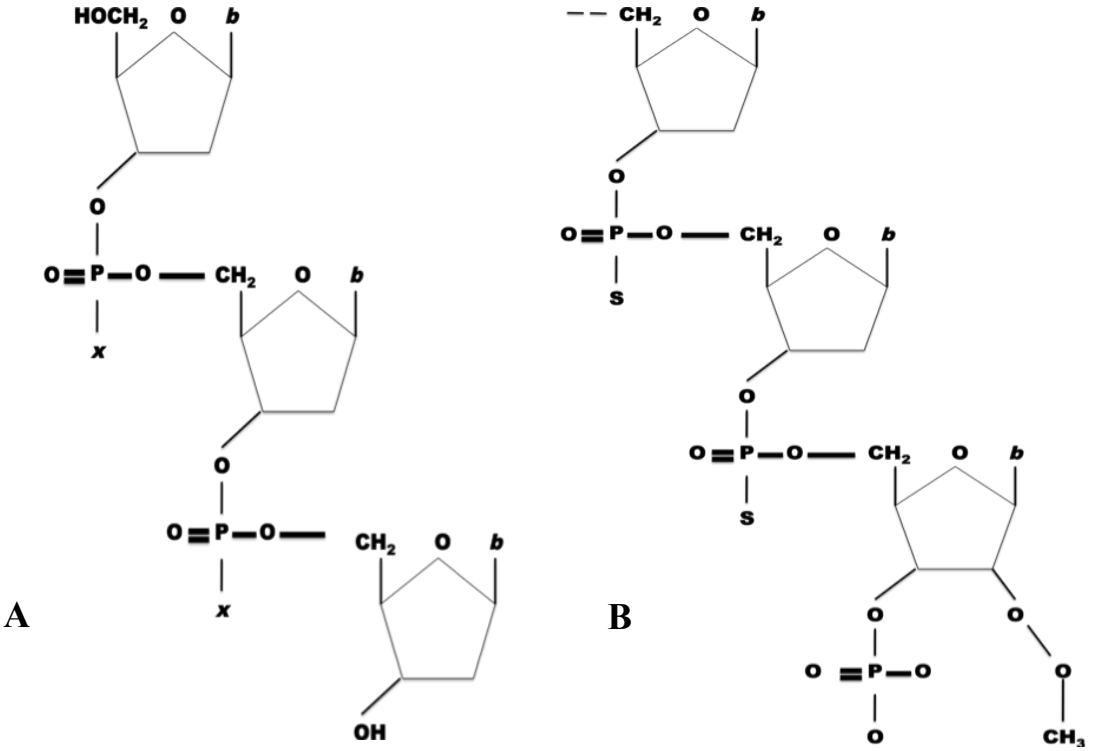

Figure 7.2: (A) Structure of oligonucleotide. *b = base* [adenine, guanine, cytosine, or thymine]. When *x= O*, a phosphodiester oligmer is formed. When *x=S*, a phosphorothioate oligomer is formed. **(B)** Structure of second-generation phosphorothioate oligonucleotide with 2'-O-methoxy-ethyl (MOE) cap, *b = base* [adenine, guanine, cytosine, or thymine].

Further numerous modifications of nucleotides have led to a third generation of ASOs. These molecules include peptide nucleic acids, addition of phosphoroamidate groups and intranucleotide bridging to decrease toxicity, enhance affinity and increase stability (Kurreck 2003)(Hughes, Hussain et al. 2001). Though these modifications

appear to affect the oligos RNAse H inducution ability, these modified molecules are now thought to affect RNA metabolism via non-cleavage mechanisms as mentioned above. Studies into systemic administration via parenteral routes other than intravenous show that phosphorothioate ASOs are rapidly and extensively absorbed, with a systemic bioavailability as high as 90% (Crooke and Bennett 1996). They distribute to all peripheral tissues with sites of highest accumulation being in the liver and kidney resulting in concentration ratios to plasma of up to 20:1 and 80:1 respectively after 2 hours (Sands, Gorey-Feret et al. 1994). Clearance is via a mechanism of slow metabolism mediated by exo- and endonucleases. Within the kidney autoradiographic assays have shown labelled ASOs within cells of Bowman's capsule and the proximal tubule after systemic administration (Rappaport, Hanss et al. 1995). The size and structure of phosphorothioate ASOs allows for free filtration at the glomerulus yet only a small percentage of ASO are excreted in the urine in non-metabolised form, hence the accumulation in PTECs can be explained in part by high reabsorption rate by tubular cells.

This project utilized antibodies to oligonucleotides and aquaporin channels to demonstrate uptake of oligos by proximal tubular cells with no accumulation within glomeruli or distal tubules or collecting ducts of the nephron following subcutaneous administration in non-obstructed Wistar rats. These results are compatible with the above literature and demonstrate that oligos of this size are freely filtered and actively taken up and concentrated within the PTEC, with little reaching the distal nephron. The high concentration of oligo within the kidney has made antisense technology an attractive potential therapy for renal disease. Deposition of oligo to a lesser extent was also seen within cardiac, liver and muscle tissue reflecting the true systemic distribution of oligonucleotides following subcutaneous administration.

There has been much interest in pushing forward ASO for clinical therapy especially in the field of infection and oncology. However results of clinical trials have been variable and currently there is still only one ASO licensed for clinical use, Formivirsen for AIDS related CMV retinitis. However there are several other ASOs at phases II and III of clinical trials. Mipomersen is an ASO to apolipoprotein B (apoB) administered subcutaneously on a weekly basis and has been shown to reduce LDL-C in patients with high cholesterol and cardiovascular risk. Phase III clinical trials in patients with familial hypercholesterolaemia in 2009 have so far been

positive. The advanced stage of Mipomersen development demonstrates that ASOs are effective when administered systemically at a relatively low frequency. Other ASOs in clinical trials at present include Alicaforsen, targeting ICAM-1, for the treatment of ulcerative colitis and LY2181308 targeting the protein survivin in patients with relapsed/refractory acute myeloid leukemia and hormone refractory prostate cancer [www.isispharm.com]. Furthermore the development and successful administration of an oral compound of ASO further enhances the translational potential of this therapy (Tillman, Geary et al. 2008).

7.6 Model of unilateral ureteric obstruction

Unilateral ureteric obstruction (UUO) is a well-accepted model of interstitial fibrosis. It is now clear that obstructive nephropathy is not a simple result of mechanical impairment to urine flow but a complex process resulting in alterations of both glomerular heamodynamics and tubular function caused by the interaction of a variety of vasoactive factors and cytokines that are activated in response to obstruction. These cytokines include PDGF and TGFβ, the mRNA levels of which have been shown to parallel the increasing tubulointerstitial damage seen with obstruction (Walton, Buttyan et al. 1992; Liapis, Nag et al. 1994). Experimental hydronephrosis appears to reflect the changes observed on obstruction in human kidneys where TGFβ has also been seen to be upregulated (Kaneto, Ohtani et al. 1999). Following urinary tract obstruction and tubular dilatation, there is an upregulation of the intrarenal renin-angiotensin system, tubular apoptosis and macrophage infiltration of the interstitium leading to destruction of renal parenchyma and fibrosis that correlates with length of time of obstruction (Himmelstein, Coffman et al. 1990). Acute ureteric obstruction leads to an initial increase in interstitial volume of the renal cortex while prolonged obstruction eventually leads to tissue loss, tubular atrophy and fibrosis. Within a the obstructed kidney of a rat, the change in renal function occurs within 24 hours, with GFR falling to 52% at 4 hours, 23% at 12 hours and 4% at 24 hours (Harris and Gill 1981; Capelouto and Saltzman 1993). Within this project it was concluded that the time point which provided the optimum endpoint results for fibrosis, both from a histological and molecular viewpoint, was 16-days. This time length of obstruction in our studies was comparable to previous studies of Ras in murine models of UUO (Grande, Fuentes-Calvo et al. 2009).

QPCR, a technique that is currently used in the clinical setting for detection of Ki-Ras mutations as a predictive factor for metastatic colorectal cancer (Santini, Galluzzo et al. 2011), was employed and demonstrated that all three isoforms of Ras are expressed in the obstructed kidney. From previous *in vitro* studies from our group an increase in Ki-Ras expression in the presence of fibrogenesis was expected, as a potential reflection of increased fibroblast proliferation, and this was observed to be true within this model of UUO with a rise of 71% compared to sham-operated kidneys. The role of Ha-Ras in stimulated fibroblast proliferation suggested that this isoform may also be up regulated in this context but this was not the case. However a significant increase in N-Ras mRNA expression (80%) in obstructed kidneys was observed when compared to sham-operated samples. The spectrum of Ras isoform expression demonstrated in this project using rat UUO models is significantly different from data published by Grande et al. showing an increase in all Ras isoforms in kidneys from mice that had undergone UUO (Grande, Arevalo et al. 2009). This may reflect species variation. However the group did use an antibody mediated ELISA assay to measure Ras expression and from our experience antibodies against specific Ras isoforms have had high-crossover binding and were unreliable in differentiating between isoforms. Both Ki- and N-Ras up-regulation in our model of UUO was localised to the obstructed kidney while expression in the contralateral non-obstructed kidney was comparable to sham-operated samples. N-Ras is known to be expressed in inflammatory conditions and to play a role in suppressing T-regulatory cell numbers and function (Mor, Keren et al. 2008) as well as potentially having a role in both granulocyte and macrophage proliferation (Skorski, Szczylik et al. 1992). More recently it has also been shown that N-Ras is required for expression of TGFβ induced messenger CTGF in human tubular epithelial cells (Dockrell, Phanish et al. 2009). Thus in an environment of fibrogenesis with significant inflammation, N-Ras mRNA expression can be expected to be upregulated and the observed rise seen in obstructed kidneys may reflect the degree of tissue inflammatory cell infiltration or increased TGFβ induced CTGF activation. These findings support the idea that different Ras isoforms may have different distribution and function within different cell types. The results obtained also reflect the differences between *in vitro* and *in vivo* studies. The role of Ha-Ras observed in fibroblast cell cultures may hold true for fibroblasts in the *in vivo* setting, but the multitudes of other cells present in renal

tissue and the use of whole kidney cortex for analysis may result in the dilution of any changes in the mRNA levels of this isoform. In order to localize the cellular compartments in which Ki-and N-Ras were up-regulated several techniques were employed. Unfortunately results obtained from both immunohistochemistry and SDS PAGE were restricted by conditions and reagents previously mentioned (see *Chapter 4*).

Other methods used to attempt to localize Ras isoform expression include *in situ* hybridization and laser microdissection. In principle the use of ISH would be ideal for exactly localizing Ras mRNA knockdown but it is a difficult technique and in the context of localizing isoform specific Ras mRNA there are further challenges. The difficulty lies in discriminating between the isoforms of Ras and being able to amplify the detection and probe design. Ras isoforms share 80% homology with the remaining 24 amino acids being within the hypervariable region. Thus in designing probes to be isoform specific there is only a sequence of about 72 bases that can be targeted. Not all bases of the sequence may be available for probe hybridization when the molecule's tertiary spatial structure is taken into account. In addition Ras is expressed at low levels in renal tissue and detection would require signal amplification. Probe construction is restricted by several factors and a balance between hybrid stability, specificity and tissue penetration must be met. Following a discussion with Dr James Howard Pringle (Department of Cancer Studies and Molecular Medicine, University of Leicester) and taking into account the above factors, a cocktail of Ki-Ras probes would need to be designed and fully assessed prior to utilization. Furthermore the harsh retrieval techniques may need significant refinement to optimize antigen exposure and limit RNA damage or destruction. It was felt that this work would be beyond the scope and time scale within this project but does however remain a possibility for the future. Focus was then moved towards utilizing the success obtained with QPCR by employing the pulsed microdissection (Hudkins, Gilbertson et al.) and microcapture system that allows for even individual cells to be analysed with regards to mRNA expression. The hypothesis was that by dissecting out specific areas of renal cortex from samples (such as tubular cells and glomeruli), one could localize the cells in which Ras mRNA expression had changed using QPCR and thus localize Ras isoform up- or down regulation to specific cells. The process required strict working conditions and a time constraint in order to preserve RNA and restrict degradation and contamination. The technique was seen to be successful in isolating

renal tubular epithelial cells but the amount of RNA retrieved from obstructed tissue samples was insufficient for analysis. It may be that in the UUO model where tubular cells appear flattened with altered morphology, RNA retrieval from atrophic tubules on the background of obstruction is difficult and limited and a higher number of tubules may be required for resection as compared to sham-operated samples. This poor return may also be due to other factors including the use of stored frozen tissue as opposed to freshly harvested, poor technique by operator or requirement of refinement of parameters of procedure. Though this technique did not yield any interpretable results in this project, it remains one with the most potential in terms of isolating Ki-Ras ASO effect. Thus though both ISH and pulsed microdissection techniques were unsuccessful during this project, both still have great potential and could be revisited in the future.

7.7 Renal targeting by antisense oligonucleotides

The fact that PTECs actively take up oligonucleotides administered systemically, makes ASO therapy attractive for targeting kidney disease. However though PTECs readily take up ASOs following systemic administration, delivery to mesangial and interstitial cells has proved far more difficult. Several groups have looked at the potential of antisense therapy in animal models of renal disease using a variety of delivery methods. Cheng et al. administered ASO to Intracellular Adhesion Molecule 1 (ICAM-1) intravenously via the tail vein in a mouse model of unilateral ureteric obstruction (UUO) and found decreased inflammatory infiltration and extracellular matrix accumulation compared to control ASO. (Cheng, Chen et al. 2000). Isaka et al also used the UUO model of tubulointerstitial fibrosis and targeted interstitial cells with a TGFβ ASO using an artificial viral envelope (AVE) of hemagglutinating virus of Japan (HVJ) (Isaka, Tsujie et al. 2000). Using retrograde ureteric administration of the AVE /ASO liposome, the group successfully targeted interstitial fibroblasts and showed treated models expressed less collagen I and α-smooth muscle actin as well as decreased fibrosis area on trichrome staining. Yokoi et al (Yokoi, Mukoyama et al. 2002) administered naked CTGF ASO to the kidney by way of a hydrodynamics-based technique to target the interstitium. The technique involves clamping off both the renal vein and artery while ASO is injected under high pressure via the renal vein with the kidney being reperfused within 2 seconds (Yazawa, Murakami et al. 2006).

The group reported that CTGF ASO administration using the hydrodynamic method reduced interstitial fibrotic areas in UUO. Antisense has also proved effective in other models of renal disease. Akagi et al. also used the HVJ liposome method to introduce TGFβ ASO in rat anti-Thy 1.1 antibody models of mesangial proliferation (Akagi, Isaka et al. 1996) and demonstrated a role for TGFβ suppression in the treatment of progressive glomerulosclerosis. In a model of anti-GBM, Yamada et al used ASOs to examine the role of CK2 (casein kinase II) in disease progression (Yamada, Katsuma et al. 2005). Using a cationic liposome transfection reagent the ASO was subsequently infused by osmotic pump into the peritoneum. They reported that by day 14 the ASO treated group had significantly less proteinuria and lower blood urea nitrogen levels. From these studies one can appreciate that there is a potential role for ASO therapy in renal disease. However there are multiple techniques involved in delivery ranging from use of naked ASO to HVJ-complexed liposomes and in administration (from simple iv injection to use of electroporation) in order to target specific renal cells. Some methods of administration, such as the hydrodynamic model, may itself induce cytokine release and damage the kidney and the use of liposomal delivery systems are themselves toxic (Rudin, Marshall et al. 2004). Therefore though many of the techniques appear successful it is difficult to see how they will be directly translated to a human clinical setting.

In this project Ki-Ras ASOs were administered by alternate day subcutaneous injection of naked ASO to a model of renal fibrosis. Immunohistological results from this project demonstrated that the ASOs were deposited within the PTECs of both obstructed and non-obstructed kidneys at day 16. In addition, there was evidence of accumulation of oligos within the interstitium of obstructed kidney samples that was absent in their non-obstructed counterparts. The mechanism of interstitial deposition in a model of UUO following subcutaneous injection is unknown and may involve either transcellular or paracellular routes. However in view that oligos are normally filtered prior to uptake by PTEC, within the obstructed model where GFR rapidly drops off, another route of uptake must exist. In this model oligos may possibly reach the interstitium via the increased vascular permeability associated with inflammation as part of the model.

The oligos appeared non-toxic and safe for the dose and time interval used for this experiment with no group demonstrating any difference in weight gain, endpoint mass or gross behaviour.

7.8 ASO targeting of renal Ki-Ras in a model of UUO

7.8.1 Ras expression

Initial administration of ASOs (12.5mg/kg) in non-obstructed Wistar rats demonstrated a specific knockdown of Ki-Ras mRNA levels in correlation with results achieved *in vitro*, with ASO 2 having a potency of five-fold greater than ASO 1. At a protein level, administration of ASOs translated to a significant decrease in pan-Ras expression by up to 90%. In view that the ASOs appeared specific in targeting Ki-Ras, it was assumed this total Ras knock-down at a protein level reflected decrease in the Kirsten isoform. The discrepancy in results between mRNA and protein Ras assessment in the ASO 1 group is most likely explained by the logistical challenges of western blotting leading to result inconsistencies as mentioned previously.

Following administration of ASO 1 at a low dose (total experimental dose of 30mg/kg), discussions were held with ISIS Pharmaceuticals and a higher dose of ASOs (total experimental dose of 100mg/kg) was administered over a longer time period of obstruction in the presence of a control oligo (CO 2) group. High dose administration resulted in efficient knockdown of Ki-Ras mRNA by 80% compared to UUO-VO group by both ASO 1 and 2 to levels comparable with sham-operated kidneys. The observed equivalent potency of ASO 1 to ASO 2 in UUO models contradicts previous *in vitro* and *in vivo* experiments in non-obstructed models. This can be explained if one considers the accumulation of oligo in the PTECs and interstitium of obstructed renal sections and is compatible with the known pharmacodynamics of oligo distribution and clearance. The reduction of ASO 1 clearance on the background of UUO has potentially led to accumulation within the obstructed kidney and increased therapeutic knockdown effect on Ki-Ras expression. Ki-Ras expression was also decreased to a lesser degree within the contralateral kidneys following administration of ASOs which suggests that subcutaneous injections of ASOs results in systemic distribution and effects which may be outside of target organ. The distribution and deposition of oligos in extra-renal tissue has been

demonstrated by immunohistology and the analysis of hepatic tissue from animals treated with antisense demonstrated knockdown of Ki-Ras on par with that seen within the non-obstructed kidney. These results provide evidence that these ASOs, when administered subcutaneously may have true systemic effects. Cardiac and muscle tissue has not as yet been analysed and it is uncertain whether the hepatic Ki-Ras knockdown effects of ASOs would be replicated in these tissues at this dose of ASO or whether the hepatic effects are a response to the accumulation of oligo within this organ that is absent in cardiac or muscle. Ureteric obstruction results in the increase of N-Ras mRNA expression within the obstructed kidney, however the administration of ASO 2 further increased these levels when compared to UUO-VO and ASO 1. In addition there was an observable increase in N-Ras in the contralateral kidney of ASO 2 group suggesting that the rise in this isoform expression is a systemic response and associated with the administration of ASO 2 per se. Prior to use, both ASO 1 and ASO 2 had both been validated with regards to their specificity and efficacy in knocking down Ki-Ras mRNA both *in vitro* and *in vivo*, so it was unexpected to observe that ASO administration in UUO models resulted in a decrease in Ha-Ras expression. This observation was localized to the obstructed kidney only, thus suggesting this is not a true systemic antisense or off-target effect on Ha-Ras mRNA by ASOs but associated with oligo accumulation. The observed reduction in Ha-Ras expression is likely to be due to non-specific effects of the ASOs, perhaps by inducing a change in the cell population. By stimulating inflammatory cell infiltration, the level of total Ha-Ras within the whole cortex may be 'diluted' and thus expression appears to be decreased in comparison to UUO-VO samples where cell influx or turnover may be less prominent. CO 2 administration resulted in a knock down of pan-isoforms of Ras in a model of UUO again with knock down effects being localized to the obstructed kidney. This control oligo had also been previously tested and demonstrated no Ras targeting effects. It is postulated that the decreased clearance of CO 2 in the obstructed kidney resulted in accumulation to a level that caused non-specific cellular effects that include a decrease in Ras expression. One could argue that administration of CO 2 in obstructive nephropathy may affect other cell signaling molecules, but these were not measured in this project. However the precise nature of CO 2 effects on Ras mRNA expression and downstream effects in UUO remain unknown and were not further investigated in this project but it is postulated that this may involve a non-hybridization effect.

Following further discussions with ISIS Pharmaceuticals, two new controls oligos were provided. These were scrambled oligos of ASO 1 and 2, thus they had the advantage of being made up of the same respective bases, contained the equal number of hydrogen and covalent bonds and were of the same length and generation of oligodeoxynucleotides as the active Ki-Ras ASOs though the secondary or tertiary structure may differ. These scrambled oligos were initially validated in separate experiments against five sham-operated and five UUO-VO models to demonstrate that neither targeted any of the isoforms of Ras. A subsequent contemporaneous experiment confirmed that SO 2 did not have any knockdown effect on Ras isoforms while confirming the specific knockdown potency of both the ASOs. Ideally a master contemporaneous experiment should be performed to compare SOs and ASOs effect but for reasons previously outlined (see *Chapter 5*) this was not deemed possible or appropriate. Subsequently data from this experiment was pooled with data from the previous validation experiments of the scrambled oligos and vehicle-only groups (Experiment III). This was to increase 'n' numbers for VO and SO 2 groups as well as allowing for incorporation of analysis of SO 1, which was lacking from the contemporaneous experiment due to insufficient amounts at the time of the experiment. The rationale for pooling of the data was that all QPCR results were derived from experiments performed by a single operator in circumstances employing reagents, substrates and animal models that were as identical as possible, though they were performed at different time points. Furthermore data obtained for each animal was based on an internal control (that is, relative to GAPDH) thus results were relatively comparable. This idea was supported by the examination of the delta Ct levels for Ki-Ras between the contemporaneous and validation experiments for UUO-VO and SO 2 groups which showed no significant difference in dCt values between identical groups at different time points. Pooled data confirmed that both SOs appeared inert with regards to Ki-Ras knockdown but both ASO 1 and 2 administration resulted in specific and significant Ki-Ras knockdown effects.

7.8.2 Cell proliferation and inflammation

Previous evidence demonstrating a role for Ki-Ras in stimulated fibroblast proliferation gave rise to the hypothesis that inhibition of this isoform may reduce fibroblast population expansion in a model of fibrosis. However administration of ASOs even in non-obstructed models resulted in a significant increase in interstitial expression of the cell proliferation marker Ki-67. This increase was further amplified in UUO models. Administration of SO 1 and 2 in UUO models gave a response equal to that of ASOs that was absent in UUO-VO and CO 2 groups. This suggests that the increase in interstitial Ki-67 expression is related to the base make up of the oligo in question and not due to the presence of any oligo per se. Since the cells expressing Ki-67 have not been characterized it is not possible to comment on the effects of ASOs on interstitial fibroblasts themselves, the proliferation of which may still be suppressed in the presence of proliferation of other interstitial cell types.

There was also significant increase staining using the ED-1 antibody in both SOs and ASOs treated group over and above that observed in UUO-VO and CO 2 treated. This suggests that inflammatory infiltration within tissue samples, like Ki-67 expression, relys very much on the base make up of the oligo in question. Administration of ASO 2 resulted in the most significant rise in ED-1 expression and this correlates to results in extra-renal tissues. Examination and scoring of cardiac tissue for ED-1 staining demonstrated that ASO 2 administration resulted in the highest score in this tissue also. Furthermore H&E staining of hepatic tissue demonstrated significant lobar and peri-portal tract inflammation in the ASO 2 group that was absent in UUO-VO and ASO 1 treated groups. Taking into account that ASO 2 administration also results in a significant rise in N-Ras mRNA expression, it is postulated that ASO 2 is highly pro-inflammatory and the high N-Ras and interstitial Ki-67 expression along with the high interstitial ED-1 scores reflect significant inflammatory cell infiltration and proliferation in response to ASO 2 interstitial deposition. On discussion with ISIS Pharmaceuticals, they stated that the pro-inflammatory nature of ASOs has been well-recognised and less inflammatory ASOs are currently in development. Of interest, ASO 1 appears to have Ki-Ras knockdown effects equal to ASO 2 in a model of UUO but not such potent pro-inflammatory effects. This property of ASO 1 could be taken advantage of in a clinical setting.

7.8.3 Fibrosis and fibrogenic markers

Though *in vivo* experiments were performed at different time points, the actual staining of sections was performed contemporaneously and, where possible, to maintain comparative consistency, each staining run was comprised of sections from different treated groups for a single experiment.

Employing PMT and picrosirius red staining, it was demonstrated that administration of ASO 1 and ASO 2 (12.5mg/kg) reduced fibrosis scores on obstructed kidneys to a level comparable with sham-operated samples. Despite the pan-Ras knockdown observed with CO 2 administration, there was no difference seen in fibrosis scores between this group and vehicle-only. This result supports the belief that mRNA knockdown effects seen with CO 2 are not truly Ras specific and are a due to non-specific effects associated with the accumulation of the oligo per se. The discrepancies in fibrosis scores seen in SO 1 and SO 2 groups were thought to be due to tissue response to treatment, method of staining and tissue oedema. However the significant further decrease in fibrosis scores in ASO groups when compared to their scrambled oligo counterparts suggest that Ki-Ras mRNA knockdown has a role in fibrosis inhibition. The inhibitory role of Ki-Ras mRNA knockdown in fibrosis is further supported by the decrease in αSMA expression and collagen I interstitial deposition following ASO administration compared to control and scrambled oligos. From previous work by our group demonstrating *in vitro* inhibition of fibroblast proliferation upon Ki-Ras knockdown, it was though that this mechanism could explain fibrosis inhibition *in vivo*. However staining for FSP-1 expression showed an increase in the interstitial expression of this cell marker following administration of ASOs when compared to control and scrambled oligos. However FSP-1 expression has been shown not to be exclusive to fibroblasts (Lin, Kisseleva et al. 2008) and has been demonstrated to co-localize with macrophage markers (Inoue, Plieth et al. 2005) in addition to lymphocytes, plasma cells and Kupffer cells. Hence up-regulation of FSP-1 seen in the interstitium in this case may represent mononuclear cells in presence of heavy inflammation as opposed to fibroblasts and thus the true effect of the Ki-Ras ASOs upon fibroblast cell proliferation *in vivo* is masked.

However despite equivocal interstitial inflammation between scrambled and antisense oligo treated samples, the significant decrease in fibrosis and fibrogenic markers in Ki-Ras ASO treated groups compared to SO treated groups suggests that the degree of

inflammation per se may not directly correlate to degree of fibrogenesis and this finding of reduced fibrosis in the presence of significant monocyte infiltration is of interest. Traditionally renal interstitial disease is characterized by inflammation, macrophage accumulation and subsequent promotion of fibrogenesis. However there is now a growing belief that a sustained macrophage presence may not be a detrimental condition and may actually be a beneficial process with regards to phagocytosis of dead cells and removal of foreign bodies (Ricardo, van Goor et al. 2008). This theory is supported by studies demonstrating distinct macrophage subpopulations that may be distinguished by differential expression of cell surface antigens and proteins (Sunderkotter, Nikolic et al. 2004). These macrophage sub-populations have been termed M1 (pro-inflammatory) and M2 (pro-fibrotic) (Martinez, Sica et al. 2008). Whereas the M1 population appears to be pro-inflammatory, a higher expression of the M2 population is associated with a predominant anti-inflammatory response (Sunderkotter, Nikolic et al. 2004) thought to be associated with endocytic clearance, expression of trophic factors and decreased production of pro-inflammatory cytokine release compared to M1 (Kluth 2007; Wang, Wang et al. 2007). The expression of IL-1 receptor antagonist and arginase 1 (an inhibitor of NO) are also thought to contribute to the anti-inflammatory actions of M2 (Wilson, Walbaum et al. 2004). However, though the M2 phenotype is recognized to be anti-inflammatory and associated with wound healing, in pathological circumstances it is thought to be profibrotic. Interestingly the same cytokines (IL-4 and IL-13) appear to drive monocyte differentiation to a M2 phenotype as drive fibrocytes to become fibroblasts *in vitro* (Shao et al. 2008). Though the macrophage is widely believed to be terminally differentiated and non-proliferative, there is evidence of a M1/M2 phenotypic switch, which may be dictated by the cellular microenvironment (Duffield 2003). Furthermore, there is now increasing interest in the role of macrophages in promoting tissue healing. Macrophages are now thought to have an ability to fuse or transdifferentiate into epithelial and mesenchymal cells including myofibroblasts (Havemann, Pujol et al. 2003; Zhao, Glesne et al. 2003; Vignery 2005). Once again this process and end-point result may be prompted by the surrounding microenvironment and various as yet unidentified cell signals.

Within the kidney, two groups of such macrophage markers that have been studied include the S100 proteins (myeloid related protein MRP8 and MRP14) and cell surface marker Ly6c (lymphocyte antigen 6 complex) (Frosch, Vogl et al. 2004; Lin,

Castano et al. 2009). Frosch et al. demonstrated that MRP8/MRP14 complex expressing monocytes prevailed in glomerulonephritides (GN) associated with a high degree of cellular proliferation such as systemic lupus erythematosus GN while in chronic types of inflammatory reaction the majority of macrophages in the renal interstitium expressed MRP8 and MRP14 without concomitant formation of their complex. They conclude that distinct macrophage subpopulations prevail in the different forms of GN and reflect differences in the inflammatory mechanisms underlying the various forms of GN (Frosch, Vogl et al. 2004). More pertinent to our model of renal fibrosis are the recent findings from Lin et al. Their group used a model of UUO to identify three subset populations of macrophages/monocytes differentiated by the expression of Ly6c-high, medium and low. Using mRNA transcription profiling, they found that these subpopulations had differential functional roles in kidney injury. Furthermore the low Ly6c expressing macrophage subpopulation was associated with transcribing genes consistent with profibrotic function. In addition they demonstrated that native kidney macrophages, contrary to popular belief, had the ability to proliferate and make up to 40% of the final inflammatory macrophage population though they did not appear to contribute to the process of fibrosis (Lin, Castano et al. 2009).

It may be that in this project, though both scrambled and antisense oligos induce a quantitatively equal degree of tissue inflammation, the qualitative nature of the infiltrate may be significantly different between macrophage subpopulations resulting in different endpoints of fibrosis & potential cell transdifferentiation. These studies show that there is a clear distinction between inflammation and monocyte/macrophage infiltration and subsequent fibrogenesis.

From data presented in this thesis, a postulated mechanism of action for Ki-Ras inhibition in fibrogenesis is as follows: An initial insult to the kidney results in an inflammatory response. Monocyte infiltration with either a macrophage M1 or M2 sub-population majority occurs depending on the microenvironment. Ki-Ras inhibition may skew macrophage sub-population towards pro-inflammatory M1 phenotype thus explaining significant inflammatory infiltration on administration of ASOs. The relative decrease in M2 phenotype allows for adequate wound healing but decreased pro-fibrotic signalling with subsequent inhibition of myofibroblastic activity as reflected by decreased αSMA expression. There may also be reduced fibroblast proliferation in this setting. In combination this leads to a reduced fibrosis

endpoint. The increased Ki-67 expression within the interstitium may be associated with inflammatory cell proliferation as a response to M1 phenotype or perhaps cell regeneration via macrophage repair mechanisms.

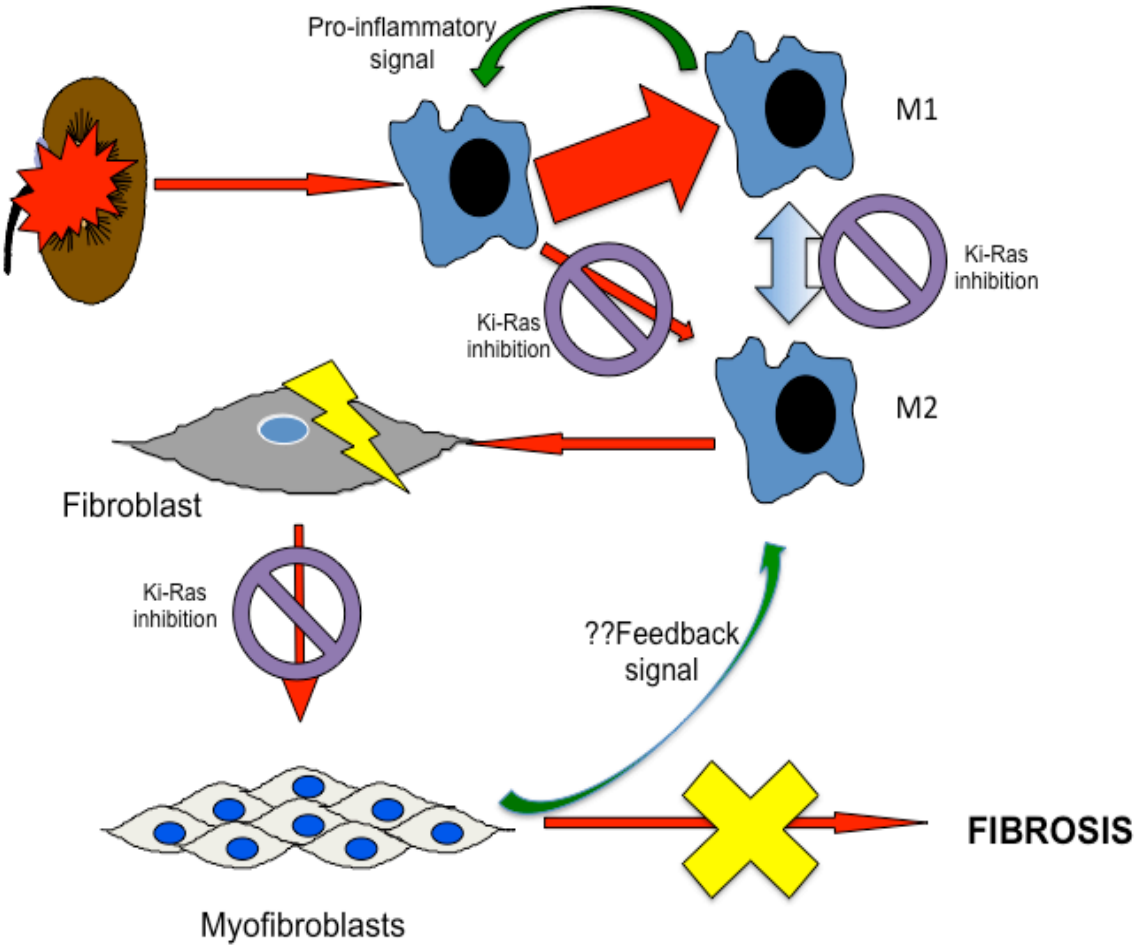

Figure 7.3: Postulated role of Ki-Ras in renal fibrogenesis

Thus the results presented in this thesis show that antisense inhibition of Kirsten-Ras ameliorates interstitial fibrosis in a rat model of unilateral ureteric obstruction despite increased interstitial inflammation and cell proliferation. The process by which Ki-Ras inhibition prevents fibrosis may involve decreased fibroblast population expansion and myofibroblastic activation and different sub-populations of inflammatory cells.

7.9 Future studies

Work in this thesis has shown that Ki-Ras antisense oligonucleotides are both specific and efficient in knocking down the Kirsten isoform of Ras mRNA and their administration in a rat model of UUO ameliorates fibrosis despite increased interstitial inflammation and proliferation. However there are also many questions raised by this project.

One is the location of Ki-Ras knockdown. Whole cortical tissue was used for analysis and thus Ki-Ras knockdown may be underestimated since there is a contribution of Ki-Ras mRNA by inflammatory infiltrative cell population that may not be targeted by ASOs and in fact may be induced by the presence of ASOs. By optimizing techniques of PALM or *in situ* hybridization a more accurate measure of degree of effect, as well as localization, of the knockdown effects of ASOs may be determined.

The cellular location of Ki-Ras knockdown is a step towards investigating the mechanism of anti-fibrotic effect. EMT is an attractive process to examine with regards to antisense technology, as it is believed to play a significant role in renal fibrogenesis and tubular epithelial cells are specific targets for oligo uptake following systemic administration. From cancer studies there appears to be an increasing interest in Ras and TGFβ crosstalk especially concerning the downstream pro-EMT transcription factor Snail (Horiguchi, Shirakihara et al. 2009). More recently, there is convincing evidence that the Ras signaling pathway is involved in TGFβ induced EMT in renal cells. Bozic et al. demonstrated that the N-methyl-D-aspartate receptor (NMDAR) present on proximal tubular epithelial cells is critical in maintaining normal epithelial phenotype and modulating TGFβ induced EMT in HK-2 cells (Bozic, de Rooij et al. 2011) and that the mechanism of TGFβ antagonism involved the inhibition of the Ras-MEK pathway and decreased activation of Ras GTPase. The perceived role of EMT in renal fibrosis, the fact that ASOs uptake in the kidney is primarily by tubular cells and recent literature suggests that further studies into the role of Ki-Ras in this phenomenon should be considered and downstream biomarkers and transcription factors of EMT (such as E-Cadherin, β-catenin and Snail) be examined both *in vitro* and *in vivo* following treatment with Ki-Ras ASOs.

Though this thesis has demonstrated that knockdown of Ki-Ras mRNA expression ameliorates fibrosis in a model of UUO, the actual mechanism and signalling pathways that play a part in this remain unclear. The pivotal role of Ras GTPase in cell signalling with regards to proliferation, apoptosis and differentiation requires that these pathways and their molecular components be examined in the presence of Ki-Ras ASO administration *in vivo*. TUNEL staining was undertaken as part of this project but was unsuccessful. The subject of apoptosis and Ki-Ras mRNA knockdown requires revisiting and examination of apoptotic cell signals such as caspase 3 expression may be of help.

This body of work also supports the fact that different isoforms of Ras may have different expression in different cell types as well as different functions. The observed increase in N-Ras expression following oligo administration *in vivo* in this project is thought to be as a result of high inflammatory cell infiltrate. However the findings that N-Ras is involved in CTGF expression downstream from TGFβ stimulation also raises the question that N-Ras increased expression in the presence of Ki-Ras knockdown may be associated with increased CTGF production. If this is true then there is increased N-Ras and CTGF production in Ki-Ras ASO treated kidneys but a significant decrease in TGFβ-induced CTGF endpoints including fibroblast up-regulation and induction of matrix production. This would suggest a signalling feedback mechanism of some degree from cells active in fibrogenesis to cells expressing CTGF and possibly other fibrogenic cytokines. Could this feedback mechanism involve the active myofibroblast? Does additional knockdown of other Ras isoforms have additional effect to Ki-Ras knockdown alone or would this lead to adverse effects? Future experiments could involve measurement of CTGF in ASO treated and non-treated samples *in vitro* and *in vivo* and possible double knock out of both Ki- and N-Ras expression.

Historically, increased inflammation on human biopsies is seen as detrimental and assumed to be a precursor to increased fibrosis. An important result in this thesis was the paradoxical finding of increased inflammation in ASO treated samples in the presence of decreased fibrosis. Subpopulations of macrophages/monocytes (M1 and M2) are now recognized and some of these are now thought to be wound healing. It

may be that the inflammation seen on ASO and control oligo groups may represent different sub-populations of macrophages and qualifying these sub-populations of macrophages by cell markers such as Ly6c or arginase-1 expression may shed light upon the role of Ki-Ras in inflammation and subsequent fibrosis.

Interstitial Ki-67 expression was also increased in ASO and scrambled oligo treated groups and though it is postulated that this reflects inflammatory cell proliferation, the actual nature of these cells are unknown. Double staining for Ki67 and inflammatory cell markers such as CD3, CD20 or CD68 may identify the proliferating cell population. Unfortunately a true fibroblast specific marker remains elusive.

Though ASO administration demonstrated decreased fibrosis, the *in vivo* experiments were artificial in that treatment was commenced at time of insult. It would be of interest to see if there was differential expression of Ras isoforms at different time points of fibrogensis (early vs. late) and whether administration of Ki-Ras ASOs in the late phase of disease (which is most similar to clinical presentation) has similar anti-fibrotic effects as found in this project. By establishing UUO prior to administration of ASOs with subsequent reversal of ureteric obstruction, effects of Ki-Ras knockdown with regards to regeneration and protection against irreversible renal fibrosis may also be examined.

Though the UUO is a robust model for molecular and histological assessment of potential therapies, it cannot provide adequate data on functional outcome. Employing other models of interstitial fibrosis such as diabetic nephropathy, folic acid, hypertensive nephropathy or chronic allograft nephropathy one may be able to assess the functional benefits of Ki-Ras ASO administration. This would be of particular interest as there is already literature describing different Ras isoform patterns in human glomerulonephritidies (Kocher, Moorhead et al. 2003). Furthermore, though interstitial penetration by oligonucleotides appears difficult from previous literature, the findings presented in this project employing models of UUO demonstrated oligo deposition within the interstitium following simple subcutaneous administration. Whether this finding is isolated to obstructive nephropathy models or is shared between models of progressive fibrotic disease involving tubular injury and atrophy

and whether similar results are obtained on administration of Ki-Ras ASOs is unknown.

Finally the focus of this project has been the kidney. However Ki-Ras ASO systemic administration may affect all organs. From this project there is evidence of hepatic effects from oligonucleotides. Other tissue sources such as cardiac and wound tissue (where there is high cell turnover) need also to be interrogated for a more comprehensive analysis of systemic effects of Ki-Ras knockdown.

Appendix I: Buffers & Solutions

A1.1: Cell culture medium

All culture media were obtained from Gibco BRL, Life Technologies (Paisley, UK). Foetal calf serum (FCS) and goat serum were obtained from Sigma (Poole, Dorset, UK) but dialysed FCS was supplied by Gibco BRL, Life Technologies.

A1.2: Buffers and solutions

DEPC water:

Add 0.1ml DEPC (diethyl pyrocarbonate) to every 100ml water. Incubate for overnight at room temperature. Autoclave for 15 mins prior to use.

1.5% DNA gel:

Add 1.5g agarose to 100ml 1x Tris-acetate-EDTA (TAE) buffer. Microwave at medium power for 2 mins or until agarose melts. Cool to 60°C in a waterbath. Add 1µl ethidium bromide (10µg/ml). Pour onto gel support and allow to set. Equilibrate in gel running buffer prior to use.

HANKS' balanced salts (HBSS):

Obtained from Sigma. Calcium chloride 0.185g/l, magnesium sulphate 0.09767 g/l, potassium chloride 0.4 g/l, potassium phosphate monobasic 0.06 g/l, sodium chloride 8 g/l, sodium phosphate dibasic 0.04788 g/l, D-glucose 1 g/l.

Gels for Tris-glycine SDS polyacrylamide gel electrophoresis:

Resolving gel solution (20ml):

Volume (ml)	**Resolving Gel**		
Gel strength	**10%**	**12%**	**15%**
Water	7.9	6.6	4.6
30% acrylamide mix	6.7	8.0	10.0
1.5M Tris (pH 8.8)	5.0	5.0	5.0
10% SDS	0.2	0.2	0.2
10% ammonium persulfate	0.2	0.2	0.2
TEMED	0.008	0.008	0.008

5% Stacking gel solution (10ml):

Water	6.8ml
30% acrylamide mix	1.7ml
1M Tris (pH 6.8)	1.25ml
10% SDS	0.1ml
10% ammonium persulfate	0.1ml
TEMED	0.01ml

Phosphate buffered saline (PBS) x 10:

80g sodium chloride, 2g potassium chloride, 14.4g disodium hydrogenphosphate, 2.4g potassium dihydrogen phosphate. Titrate with 1M Hydrochloric acid to pH 7.4.

PBST 0.1%:

1x PBS, 0.1% Tween 20 (Bio-Rad Herts, UK),

PBSTDS lysis buffer:

1x PBS, 1% Triton-X 100, 0.5% sodium deoxycholate, 0.1% SDS, leupeptin 0.5µg/ml, pepstatin 1.0µg/ml, EDTA 1.0mM, PMSF 0.2mM.

RNase-free protocol for glassware:

Wash glassware thoroughly. Incubate in 0.1M Sodium Hydroxide solution for 1 hour at room temperature. Rinse in DEPC treated water. Incubate in 1mM EDTA solution for 1 hour at room temperature. Rinse in DEPC treated water.

TAE (Tris-acetate EDTA) Buffer (50 X) per 500ml:

121g Tris base, 28.6ml glacial acetic acid, 14.6g EDTA. Make up with DEPC treated water.

Towbin transfer buffer (1000ml):

200ml methanol, 14.4g glycine, 3.03g Tris base. Make up with deionised water.

Tris-buffered saline (TBS)

50mM Tris-HCL pH 7.5, 150mM NaCl

TBST 0.05% (1000ml):

0.5ml Tween 20 in 1000ml 1xTBS

Western gel running buffer:

0.025M Tris, 0.192M glycine, 0.1% SDS. pH8.3.

For 5000ml of 4x gel running buffer: 60.4g Tris, 288g glycine, 20g SDS. Make up to 5000ml with deionised water.

Western sample buffer (WSB) (6x concentrate):

0.5M Tris pH 6.8, 0.35M SDS, 30% glycerol, 0.6M dithiothreitol, 0.175M bromophenol blue (Bio-Rad, Herts, UK).

A1.3: Standards and ladders

Biotinylated protein ladder detection pack:

For western blotting. Cell Signaling 7727S

ColorBurst electrophoresis marker:

For western blotting. Sigma C1992.

50bp DNA ladder:

For DNA gel. Promega G452A.

A1.4: Histology solutions and sequences

Acid-alcohol (100ml):

70ml industrial methylated spirit, 30ml distilled water, 1 ml 1M Hydrochloric acid

Acidified water:

5ml acetic acid in 1000ml distilled water

1% Aniline blue in 1% acetic acid:

2g aniline blue, 2ml acetic acid, 200ml distilled water.

Celestine blue haemalum sequence:

Dewax and rehydrate sections. Stain in Celestine blue solution for 5 mins. Rinse I distilled water. Stain in Mayer's alum haematoxylin for 5 mins. Differentiate and blue as required. Proceed with staining.

Celestine blue solution:

Dissolve 25g ferric ammonium sulphate in 500ml of distilled water. Add 2.5g Celestine blue B and boil for 3 mins. Filter solution then add and mix 70ml glycerol.

Citrate buffer pH 6.0:

Dissolve 2.1g citric acid monohydrate in 900ml distilled water. Add 26ml 1M sodium hydroxide. Adjust to pH 6 and make up to 1000ml with distilled water.

Harris' haematoxylin:

Dissolve 4g haematoxylin in 40ml IMS. Dissolve 80g aluminum potassium sulphate in 800ml distilled water. Mix the two solutions and bring to boil. Remove from heat and place in fume cupboard and add 2g mercuric oxide. Cool rapidly, add 32ml acetic acid and filter solution.

1% Nissl stain solution:

2g Cresyl violet in 200ml RNase free water.

Nuclear fast red:

Dissolve 0.1g nuclear fast red in 10ml 5% aluminum sulphate solution. Warm solution to dissolve, cool and filter.

Picro-orange solution:

Dissolve 0.25g orange G dye in 100ml picric acid saturated in 80% propan-2-ol.

Picrosirius red solution:

0.1%: Dissolve 100mg Direct dye in 100ml saturated picric acid

Ponceau-acid fuchsin:

Mix equal parts of solutions A and B:

Solution A: 0.5g Acid fuchsin, 1ml acetic acid, 100ml distilled water

Solution B: 0.5g Ponceau de xylidine, 1ml acetic acid, 100ml distilled water.

Appendix II: Additional Methodology for histology and *in situ* hybridization

A2.1 Ras Antigen retrieval

Routine histology requires tissues to be fixed initially in formalin followed by subsequent processing and embedding in paraffin to allow ease of sectioning. This processing can lead to either masking or even destruction of target antigen. There are many antigen retrieval methods used to 'unmask' target epitopes in processed tissue. The most suitable method will vary widely according to epitope.

Initially pre-treatment used was identical to that previously used in our laboratory (Kocher et al, 2005). Though from publications the pre-treatment appeared to provide specific and crisp Ras staining, in this project it was found that there was a very poor signal-to-background ratio using this method.

As a result several antigen retrieval methods were used to optimize immunohistological staining for Ras which are listed below:

1) Wash with saponin 0.05% for 30 mins and subsequent digestion with 0.1% pepsin (pH 2.3) at room temperature for 20 mins. [Original Method]
2) Wash with saponin 0.05% for 30 mins and subsequent digestion with 0.1% pepsin (pH 1.8) at 37°C for 20 mins.
3) Digestion with 0.1% pepsin (pH 1.8) at 37°C for 20 mins only
4) Pressure cook in Tris EDTA (pH 9) for 3 mins
5) Pressure cook in citrate buffer (pH 6) for 3 mins
6) Microwave in citrate buffer (pH 6) for 20 mins and subsequent digestion with 0.1% pepsin (pH 2.3) at room temperature for 20 mins.
7) Microwave in citrate buffer (pH 6) for 20 mins and subsequent digestion with 0.1% pepsin (pH 1.8) at 37°C for 20 mins.
8) Digestion with 0.1% Trypsin (pH 7.8) at 37°C for 10 mins.
9) Pressure cook in Tris EDTA (pH 9) for 3 mins and subsequent digestion with 0.1% pepsin (pH 2.3) at room temperature for 20 mins.
10) Pressure cook in Tris EDTA (pH 9) for 3 mins subsequent digestion with 0.1% pepsin (pH 1.8) at 37°C for 20 mins.

The antigen retrieval methods were repeated for both pan-Ras antibody and for isoform specific Ras. The reason for this is that the monoclonal antibody for pan-Ras is directed against a common epitope sequence in all Ras proteins but isoform specific antibodies will be directed against the terminal twenty amino acid sequence of each Ras isoform. Thus the pre-treatment method which may be optimal for pan-Ras may not necessary be the same for Ras isoforms.
However from the above experiments is was found that the pre-treatment methods that provided optimum staining and signal-background ratio were:

1) Pressure Cooking at in Tris EDTA buffer pH 9 for 3 mins
2) Digestion with 0.1% Trypsin at 37°C for 10 mins.

A2.2 Buffers & Solutions for Antigen retrieval

10 x Tris EDTA buffer:

12g Tris
1g EDTA
10ml 1N HCI
500ml distilled water
Dilute to x 1 and pH 9 prior to use.

Trypsin solution

0.1% Trypsin
0.1% Calcium Chloride
pH 7.8

A2.3 Variations in *in situ* hybridization protocol

In order to optimize the results achieved initially using the manufacturer's protocol for ISH, as outlined in section 2.21, several variations were made in the process based on published literature, in particular that of Dr JH Pringle (Bailey et al. 1999), and the current ISH protocol utilized for clinical samples by the Department of Histopathology, King's College Hospital, London. These changes are highlighted below. It should be noted that the original manufacturer's protocol was attempted twice prior to adjustments.

Experiment	Slides	Proteinase K digestion	Probe Concentration	Hybridization conditions	Post-hybridization wash conditions	Visualization
1 (Original Protocol)	Paraffin	20µg/ml for 15 mins at 37°C	60µl per 1ml buffer (=20 units of probe)	Overnight incubation at 30°C	2 x 30 secs in 1 x SSC at RT 1 x 5mins in 1 x SSC at RT 2 x 15 mins in 0.1 x SSC at 40°C	1/100 Anti-FITC antibody for 1 hour at RT. NBT/BCIP substrate for 30 mins at RT
2		**20µg/ml for 20 mins at 37°C**		**Overnight incubation at 25°C**	**2 x 30 secs in 1 x SSC at RT 1 x 5mins in 1 x SSC at RT 2 x 15mins in 0.1% SSC at 30°C**	
3		**40µg/ml for 20mins at 37°C**				**1/100 Anti-FITC antibody for 2 hours at RT. NBT/BCIP substrate overnight at RT**
4				**Overnight incubation at 34°C**		
5	**Cryosection**		**75µl per 1ml buffer (=25 units of probe)**			
6	**Cryosection**	**10µg/ml for 1 hour at 37°C**			**2x 10 mins SSC/30% Formamide at 37°C 2 x 5mins 1x SSC at RT**	

Table A2.1: *in situ* hybridization experimental variations

References

(1997). "Randomised placebo-controlled trial of effect of ramipril on decline in glomerular filtration rate and risk of terminal renal failure in proteinuric, non-diabetic nephropathy. The GISEN Group (Gruppo Italiano di Studi Epidemiologici in Nefrologia)." Lancet 349(9069): 1857-63.

Abbate, M., C. Zoja, et al. (1998). "In progressive nephropathies, overload of tubular cells with filtered proteins translates glomerular permeability dysfunction into cellular signals of interstitial inflammation." J Am Soc Nephrol 9(7): 1213-24.

Abbate, M., C. Zoja, et al. (2008). "Complement-mediated dysfunction of glomerular filtration barrier accelerates progressive renal injury." J Am Soc Nephrol 19(6): 1158-67.

Abbate, M., C. Zoja, et al. (2006). "How does proteinuria cause progressive renal damage?" J Am Soc Nephrol 17(11): 2974-84.

Ahmadian, M. R., P. Stege, et al. (1997). "Confirmation of the arginine-finger hypothesis for the GAP-stimulated GTP-hydrolysis reaction of Ras." Nat Struct Biol 4(9): 686-9.

Akagi, Y., Y. Isaka, et al. (1996). "Inhibition of TGF-beta 1 expression by antisense oligonucleotides suppressed extracellular matrix accumulation in experimental glomerulonephritis." Kidney Int 50(1): 148-55.

Akhtar, S., M. D. Hughes, et al. (2000). "The delivery of antisense therapeutics." Adv Drug Deliv Rev 44(1): 3-21.

Akhtar, S. and R. L. Juliano (1992). "Cellular uptake and intracellular fate of antisense oligonucleotides." Trends Cell Biol 2(5): 139-44.

An, H. J., O. Maeng, et al. (2006). "Activation of Ras up-regulates pro-apoptotic BNIP3 in nitric oxide-induced cell death." J Biol Chem 281(45): 33939-48.

Anders, H. J., M. Frink, et al. (2003). "CC chemokine ligand 5/RANTES chemokine antagonists aggravate glomerulonephritis despite reduction of glomerular leukocyte infiltration." J Immunol 170(11): 5658-66.

Annes, J. P., J. S. Munger, et al. (2003). "Making sense of latent TGFbeta activation." J Cell Sci 116(Pt 2): 217-24.

Annes, J. P., Y. Chen, et al. (2004). "Integrin alphaVbeta6-mediated activation of latent TGF-beta requires the latent TGF-beta binding protein-1." J Cell Biol **165**(5): 723-34.

Apolloni, A., I. A. Prior, et al. (2000). "H-ras but not K-ras traffics to the plasma membrane through the exocytic pathway." Mol Cell Biol 20(7): 2475-87.

Arnold, D. D. (1966). "The effect of developing experimental open hydronephrosis upon compensatory hypertrophy of the kidney in the rat." Br J Urol 38(1): 9-15.

Arnold, L., A. Henry, et al. (2007). "Inflammatory monocytes recruited after skeletal muscle injury switch into antiinflammatory macrophages to support myogenesis." J Exp Med 204(5): 1057-69.

Arozarena, I., D. Matallanas, et al. (2004). "Activation of H-Ras in the endoplasmic reticulum by the RasGRF family guanine nucleotide exchange factors." Mol Cell Biol 24(4): 1516-30.

Arslan, M. A., O. Kutuk, et al. (2006). "Protein kinases as drug targets in cancer." Curr Cancer Drug Targets 6(7): 623-34.

Atfi, A., E. Drobetsky, et al. (1994). "Transforming growth factor beta down-regulates Src family protein tyrosine kinase signaling pathways." J Biol Chem 269(48): 30688-93.

Avruch, J., A. Khokhlatchev, et al. (2001). "Ras activation of the Raf kinase: tyrosine kinase recruitment of the MAP kinase cascade." Recent Prog Horm Res 56: 127-55.

Avruch, J., X. F. Zhang, et al. (1994). "Raf meets Ras: completing the framework of a signal transduction pathway." Trends Biochem Sci 19(7): 279-83.

Axmann, A., D. Seidel, et al. (1998). "Transforming growth factor-beta1-induced activation of the Raf-MEK-MAPK signaling pathway in rat lung fibroblasts via a PKC-dependent mechanism." Biochem Biophys Res Commun 249(2): 456-60.

Bailey E, Bottomley MJ, Westwell S, Pringle JH, et al. (1999). "Vascular endothelial growth factor mRNA expression in minimal change, membranous, and diabetic nephropathy demonstrated by non-isotopic in situ hybridisation." J Clin Pathol. 1999 Oct;52(10):735-8.

Bailey, A. S., H. Willenbring, et al. (2006). "Myeloid lineage progenitors give rise to vascular endothelium." Proc Natl Acad Sci U S A 103(35): 13156-61.

Baker, B. F., S. S. Lot, et al. (1997). "2'-O-(2-Methoxy)ethyl-modified anti-intercellular adhesion molecule 1 (ICAM-1) oligonucleotides selectively increase the ICAM-1 mRNA level and inhibit formation of the ICAM-1 translation initiation complex in human umbilical vein endothelial cells." J Biol Chem 272(18): 11994-2000.

Bander, S. J., J. E. Buerkert, et al. (1985). "Long-term effects of 24-hr unilateral ureteral obstruction on renal function in the rat." Kidney Int 28(4): 614-20.

Barbacid, M. (1987). "ras genes." Annu Rev Biochem 56: 779-827.

Bartlett, D. W. and M. E. Davis (2006). "Insights into the kinetics of siRNA-mediated gene silencing from live-cell and live-animal bioluminescent imaging." Nucleic Acids Res 34(1): 322-33.

Bass, B. L. (2001). "RNA interference. The short answer." Nature 411(6836): 428-9.

Bauvois, B., N. Mothu, et al. (2007). "Specific changes in plasma concentrations of matrix metalloproteinase-2 and -9, TIMP-1 and TGF-beta1 in patients with distinct types of primary glomerulonephritis." Nephrol Dial Transplant 22(4): 1115-22.

Bechtel, W., S. McGoohan, et al. (2010) "Methylation determines fibroblast activation and fibrogenesis in the kidney." Nat Med 16(5): 544-50.

Benigni, A., C. Zoja, et al. (1999). "Renoprotection by nitric oxide donor and lisinopril in the remnant kidney model." Am J Kidney Dis 33(4): 746-53.

Benigni, A., C. Zola, et al. (1996). "Blocking both type A and B endothelin receptors in the kidney attenuates renal injury and prolongs survival in rats with remnant kidney." Am J Kidney Dis 27(3): 416-23.

Bennett, C. F. and E. E. Swayze "RNA targeting therapeutics: molecular mechanisms of antisense oligonucleotides as a therapeutic platform." Annu Rev Pharmacol Toxicol 50: 259-93.

Bergo, M. O., G. K. Leung, et al. (2001). "Isoprenylcysteine carboxyl methyltransferase deficiency in mice." J Biol Chem 276(8): 5841-5.

Bertrand, J. R., M. Pottier, et al. (2002). "Comparison of antisense oligonucleotides and siRNAs in cell culture and in vivo." Biochem Biophys Res Commun 296(4): 1000-4.

Biancone, L., S. David, et al. (1994). "Alternative pathway activation of complement by cultured human proximal tubular epithelial cells." Kidney Int 45(2): 451-60.

Bissell, D. M., D. Roulot, et al. (2001). "Transforming growth factor beta and the liver." Hepatology 34(5): 859-67.

Bitko, V., A. Musiyenko, et al. (2005). "Inhibition of respiratory viruses by nasally administered siRNA." Nat Med 11(1): 50-5.

Bleyer, A. J., G. B. Russell, et al. (1999). "Sudden and cardiac death rates in hemodialysis patients." Kidney Int 55(4): 1553-9.

Bohle, A., F. Strutz, et al. (1994). "On the pathogenesis of chronic renal failure in primary glomerulopathies: a view from the interstitium." Exp Nephrol 2(4): 205-10.

Bohle, A., M. Wehrmann, et al. (1994). "Pathogenesis of chronic renal failure in primary glomerulopathies." Nephrol Dial Transplant 9 Suppl 3: 4-12.

Boor, P., A. Konieczny, et al. (2007). "PDGF-D inhibition by CR002 ameliorates tubulointerstitial fibrosis following experimental glomerulonephritis." Nephrol Dial Transplant 22(5): 1323-31.

Border, W. A. and N. A. Noble (1993). "Cytokines in kidney disease: the role of transforming growth factor-beta." Am J Kidney Dis 22(1): 105-13.

Boriack-Sjodin, P. A., S. M. Margarit, et al. (1998). "The structural basis of the activation of Ras by Sos." Nature 394(6691): 337-43.

Bos, J. L. (1989). "ras oncogenes in human cancer: a review." Cancer Res 49(17): 4682-9.

Bourne, H. R., D. A. Sanders, et al. (1991). "The GTPase superfamily: conserved structure and molecular mechanism." Nature 349(6305): 117-27.

Bozic, M., J. de Rooij, et al. (2011) "Glutamatergic signaling maintains the epithelial phenotype of proximal tubular cells." J Am Soc Nephrol 22(6): 1099-111.

Braasch, D. A., S. Jensen, et al. (2003). "RNA interference in mammalian cells by chemically-modified RNA." Biochemistry 42(26): 7967-75.

Braasch, D. A., Z. Paroo, et al. (2004). "Biodistribution of phosphodiester and phosphorothioate siRNA." Bioorg Med Chem Lett 14(5): 1139-43.

Brenner, B. M., M. E. Cooper, et al. (2001). "Effects of losartan on renal and cardiovascular outcomes in patients with type 2 diabetes and nephropathy." N Engl J Med 345(12): 861-9.

Brunger, A. T., M. V. Milburn, et al. (1990). "Crystal structure of an active form of RAS protein, a complex of a GTP analog and the HRAS p21 catalytic domain." Proc Natl Acad Sci U S A 87(12): 4849-53.

Buday, L. and J. Downward (1993). "Epidermal growth factor regulates the exchange rate of guanine nucleotides on p21ras in fibroblasts." Mol Cell Biol 13(3): 1903-10.

Burton, C. and K. P. Harris (1996). "The role of proteinuria in the progression of chronic renal failure." Am J Kidney Dis 27(6): 765-75.

Burton, C. J., S. J. Harper, et al. (2001). "Turnover of human tubular cells exposed to proteins in vivo and in vitro." Kidney Int 59(2): 507-14.

Burton, C. J. and J. Walls (1994). "Proximal tubular cell, proteinuria and tubulo-interstitial scarring." Nephron 68(3): 287-93.

Cai, G., X. Zhang, et al. (2008). "Tissue inhibitor of metalloproteinase-1 exacerbated renal interstitial fibrosis through enhancing inflammation." Nephrol Dial Transplant 23(6): 1861-75.

Cales, C., J. F. Hancock, et al. (1988). "The cytoplasmic protein GAP is implicated as the target for regulation by the ras gene product." Nature 332(6164): 548-51.

Campanaro, S., S. Picelli, et al. (2007). "Genes involved in TGF beta1-driven epithelial-mesenchymal transition of renal epithelial cells are topologically related in the human interactome map." BMC Genomics 8: 383.

Campbell, S. L., R. Khosravi-Far, et al. (1998). "Increasing complexity of Ras signaling." Oncogene 17(11 Reviews): 1395-413.

Capelouto, C. C. and B. Saltzman (1993). "The pathophysiology of ureteral obstruction." J Endourol 7(2): 93-103.

Carozzi, A. J., S. Roy, et al. (2002). "Inhibition of lipid raft-dependent signaling by a dystrophy-associated mutant of caveolin-3." J Biol Chem 277(20): 17944-9.

Catania, J. M., G. Chen, et al. (2007). "Role of matrix metalloproteinases in renal pathophysiologies." Am J Physiol Renal Physiol 292(3): F905-11.

Chang, H. Y., J. T. Chi, et al. (2002). "Diversity, topographic differentiation, and positional memory in human fibroblasts." Proc Natl Acad Sci U S A 99(20): 12877-82.

Chaudhuri, V., L. Zhou, et al. (2007). "Inflammatory cytokines induce the transformation of human dermal microvascular endothelial cells into myofibroblasts: a potential role in skin fibrogenesis." J Cutan Pathol 34(2): 146-53.

Chen, L., B. C. Liu, et al. (2006). "Influence of connective tissue growth factor antisense oligonucleotide on angiotensin II-induced epithelial mesenchymal transition in HK2 cells." Acta Pharmacol Sin 27(8): 1029-36.

Chen, Q., M. C. DeFrances, et al. (1996). "Induction of met proto-oncogene (hepatocyte growth factor receptor) expression during human monocyte-macrophage differentiation." Cell Growth Differ 7(6): 821-32.

Chen, Y., I. E. Blom, et al. (2002). "CTGF expression in mesangial cells: involvement of SMADs, MAP kinase, and PKC." Kidney Int 62(4): 1149-59.

Chen, Z., J. C. Otto, et al. (2000). "The C-terminal polylysine region and methylation of K-Ras are critical for the interaction between K-Ras and microtubules." J Biol Chem 275(52): 41251-7.

Cheng, Q. L., X. M. Chen, et al. (2000). "Effects of ICAM-1 antisense oligonucleotide on the tubulointerstitium in mice with unilateral ureteral obstruction." Kidney Int 57(1): 183-90.

Cheng, S. and D. H. Lovett (2003). "Gelatinase A (MMP-2) is necessary and sufficient for renal tubular cell epithelial-mesenchymal transformation." Am J Pathol 162(6): 1937-49.

Cheng, S., A. S. Pollock, et al. (2006). "Matrix metalloproteinase 2 and basement membrane integrity: a unifying mechanism for progressive renal injury." FASEB J 20(11): 1898-900.

Chesa, P. G., W. J. Rettig, et al. (1987). "Expression of p21ras in normal and malignant human tissues: lack of association with proliferation and malignancy." Proc Natl Acad Sci U S A 84(10): 3234-8.

Chiloeches, A., C. S. Mason, et al. (2001). "S338 phosphorylation of Raf-1 is independent of phosphatidylinositol 3-kinase and Pak3." Mol Cell Biol 21(7): 2423-34.

Chiu, V. K., T. Bivona, et al. (2002). "Ras signalling on the endoplasmic reticulum and the Golgi." Nat Cell Biol 4(5): 343-50.

Choi, Y. J., L. Mendoza, et al. (2001). "Role of p53-dependent activation of caspases in chronic obstructive uropathy: evidence from p53 null mutant mice." J Am Soc Nephrol 12(5): 983-92.

Choudhury, G. G., C. Karamitsos, et al. (1997). "PI-3-kinase and MAPK regulate mesangial cell proliferation and migration in response to PDGF." Am J Physiol 273(6 Pt 2): F931-8.

Chow, F. Y., D. J. Nikolic-Paterson, et al. (2006). "Monocyte chemoattractant protein-1 promotes the development of diabetic renal injury in streptozotocin-treated mice." Kidney Int 69(1): 73-80.

Choy, E., V. K. Chiu, et al. (1999). "Endomembrane trafficking of ras: the CAAX motif targets proteins to the ER and Golgi." Cell 98(1): 69-80.

Claperon, A. and M. Therrien (2007). "KSR and CNK: two scaffolds regulating RAS-mediated RAF activation." Oncogene 26(22): 3143-58.

Clarke, H. C., H. M. Kocher, et al. (2003). "Ras antagonist farnesylthiosalicylic acid (FTS) reduces glomerular cellular proliferation and macrophage number in rat thy-1 nephritis." J Am Soc Nephrol 14(4): 848-54.

Clausen, G. and A. Hope (1977). "Intrarenal distribution of blood flow and glomerular filtration during chronic unilateral ureteral obstruction." Acta Physiol Scand 100(1): 22-32.

Coles, H. S., J. F. Burne, et al. (1993). "Large-scale normal cell death in the developing rat kidney and its reduction by epidermal growth factor." Development 118(3): 777-84.

Cook, H. T., S. B. Khan, et al. (2002). "Treatment with an antibody to VLA-1 integrin reduces glomerular and tubulointerstitial scarring in a rat model of crescentic glomerulonephritis." Am J Pathol 161(4): 1265-72.

Cordeiro, M. F., A. Mead, et al. (2003). "Novel antisense oligonucleotides targeting TGF-beta inhibit in vivo scarring and improve surgical outcome." Gene Ther 10(1): 59-71.

Coresh, J., E. Selvin, et al. (2007). "Prevalence of chronic kidney disease in the United States." JAMA 298(17): 2038-47.

Cowley, S., H. Paterson, et al. (1994). "Activation of MAP kinase kinase is necessary and sufficient for PC12 differentiation and for transformation of NIH 3T3 cells." Cell 77(6): 841-52.

Crawford, S. E., V. Stellmach, et al. (1998). "Thrombospondin-1 is a major activator of TGF-beta1 in vivo." Cell 93(7): 1159-70.

Crooke, S. T. and C. F. Bennett (1996). "Progress in antisense oligonucleotide therapeutics." Annu Rev Pharmacol Toxicol 36: 107-29.

da Silva Morais, A., A. Saliez, et al. (2008). "Inhibition of the Ras oncoprotein reduces proliferation of hepatocytes in vitro and in vivo in rats." Clin Sci (Lond) 114(1): 73-83.

Dai, C. and Y. Liu (2004). "Hepatocyte growth factor antagonizes the profibrotic action of TGF-beta1 in mesangial cells by stabilizing Smad transcriptional corepressor TGIF." J Am Soc Nephrol 15(6): 1402-12.

Dai, C., J. Yang, et al. (2004). "Intravenous administration of hepatocyte growth factor gene ameliorates diabetic nephropathy in mice." J Am Soc Nephrol 15(10): 2637-47.

Danesh, F. R., M. M. Sadeghi, et al. (2002). "3-Hydroxy-3-methylglutaryl CoA reductase inhibitors prevent high glucose-induced proliferation of mesangial cells via modulation of Rho GTPase/ p21 signaling pathway: Implications for diabetic nephropathy." Proc Natl Acad Sci U S A 99(12): 8301-5.

Daniel, C., Y. Takabatake, et al. (2003). "Antisense oligonucleotides against thrombospondin-1 inhibit activation of tgf-beta in fibrotic renal disease in the rat in vivo." Am J Pathol 163(3): 1185-92.

Daniel, C., J. Wiede, et al. (2004). "Thrombospondin-1 is a major activator of TGF-beta in fibrotic renal disease in the rat in vivo." Kidney Int 65(2): 459-68.

Daniels, J. T., G. S. Schultz, et al. (2003). "Mediation of transforming growth factor-beta(1)-stimulated matrix contraction by fibroblasts: a role for connective tissue growth factor in contractile scarring." Am J Pathol 163(5): 2043-52.

Darby, I., O. Skalli, et al. (1990). "Alpha-smooth muscle actin is transiently expressed by myofibroblasts during experimental wound healing." Lab Invest 63(1): 21-9.

Daub, M., J. Jockel, et al. (1998). "The RafC1 cysteine-rich domain contains multiple distinct regulatory epitopes which control Ras-dependent Raf activation." Mol Cell Biol 18(11): 6698-710.

David, S., L. Biancone, et al. (1997). "Alternative pathway complement activation induces proinflammatory activity in human proximal tubular epithelial cells." Nephrol Dial Transplant 12(1): 51-6.

Davis, S., S. Propp, et al. (2009). "Potent inhibition of microRNA in vivo without degradation." Nucleic Acids Res 37(1): 70-7.

Della Rocca, G. J., T. van Biesen, et al. (1997). "Ras-dependent mitogen-activated protein kinase activation by G protein-coupled receptors. Convergence of Gi- and Gq-mediated pathways on calcium/calmodulin, Pyk2, and Src kinase." J Biol Chem 272(31): 19125-32.

DeMali, K. A., K. Wennerberg, et al. (2003). "Integrin signaling to the actin cytoskeleton." Curr Opin Cell Biol 15(5): 572-82.

Deng, T. and M. Karin (1994). "c-Fos transcriptional activity stimulated by H-Ras-activated protein kinase distinct from JNK and ERK." Nature 371(6493): 171-5.

Der, C. J., T. G. Krontiris, et al. (1982). "Transforming genes of human bladder and lung carcinoma cell lines are homologous to the ras genes of Harvey and Kirsten sarcoma viruses." Proc Natl Acad Sci U S A 79(11): 3637-40.

Derijard, B., M. Hibi, et al. (1994). "JNK1: a protein kinase stimulated by UV light and Ha-Ras that binds and phosphorylates the c-Jun activation domain." Cell 76(6): 1025-37.

Desmouliere, A., A. Geinoz, et al. (1993). "Transforming growth factor-beta 1 induces alpha-smooth muscle actin expression in granulation tissue myofibroblasts and in quiescent and growing cultured fibroblasts." J Cell Biol 122(1): 103-11.

Diamond, J. R., D. Kees-Folts, et al. (1994). "Macrophages, monocyte chemoattractant peptide-1, and TGF-beta 1 in experimental hydronephrosis." Am J Physiol 266(6 Pt 2): F926-33.

Dixon, R. and N. J. Brunskill (1999). "Activation of mitogenic pathways by albumin in kidney proximal tubule epithelial cells: implications for the pathophysiology of proteinuric states." J Am Soc Nephrol 10(7): 1487-97.

Dixon, R. and N. J. Brunskill (2000). "Albumin stimulates p44/p42 extracellular-signal-regulated mitogen-activated protein kinase in opossum kidney proximal tubular cells." Clin Sci (Lond) 98(3): 295-301.

Docherty, N. G., O. E. O'Sullivan, et al. (2006). "TGF-beta1-induced EMT can occur independently of its proapoptotic effects and is aided by EGF receptor activation." Am J Physiol Renal Physiol 290(5): F1202-12.

Dockrell, M. E., M. K. Phanish, et al. (2009). "Tgf-beta auto-induction and connective tissue growth factor expression in human renal tubule epithelial cells requires N-ras." Nephron Exp Nephrol 112(3): e71-9.

Dominski, Z. and R. Kole (1993). "Restoration of correct splicing in thalassemic pre-mRNA by antisense oligonucleotides." Proc Natl Acad Sci U S A 90(18): 8673-7.

Donadelli, R., M. Abbate, et al. (2000). "Protein traffic activates NF-kB gene signaling and promotes MCP-1-dependent interstitial inflammation." Am J Kidney Dis 36(6): 1226-41.

Donadelli, R., C. Zanchi, et al. (2003). "Protein overload induces fractalkine upregulation in proximal tubular cells through nuclear factor kappaB- and p38 mitogen-activated protein kinase-dependent pathways." J Am Soc Nephrol 14(10): 2436-46.

Downward, J., R. Riehl, et al. (1990). "Identification of a nucleotide exchange-promoting activity for p21ras." Proc Natl Acad Sci U S A 87(15): 5998-6002.

Drumm, K., B. Bauer, et al. (2002). "Albumin induces NF-kappaB expression in human proximal tubule-derived cells (IHKE-1)." Cell Physiol Biochem 12(4): 187-96.

Duffield, J. S. (2003). "The inflammatory macrophage: a story of Jekyll and Hyde." Clin Sci (Lond) 104(1): 27-38.

Duffield, J. S., L. P. Erwig, et al. (2000). "Activated macrophages direct apoptosis and suppress mitosis of mesangial cells." J Immunol 164(4): 2110-9.

Duffield, J. S., S. J. Forbes, et al. (2005). "Selective depletion of macrophages reveals distinct, opposing roles during liver injury and repair." J Clin Invest 115(1): 56-65.

Duymelinck, C., S. E. Dauwe, et al. (2000). "TIMP-1 gene expression and PAI-1 antigen after unilateral ureteral obstruction in the adult male rat." Kidney Int 58(3): 1186-201.

Dworkin, L. D., R. Gong, et al. (2004). "Hepatocyte growth factor ameliorates progression of interstitial fibrosis in rats with established renal injury." Kidney Int 65(2): 409-19.

Eardley, K. S., D. Zehnder, et al. (2006). "The relationship between albuminuria, MCP-1/CCL2, and interstitial macrophages in chronic kidney disease." Kidney Int 69(7): 1189-97.

Eckes, B., D. Kessler, et al. (1999). "Interactions of fibroblasts with the extracellular matrix: implications for the understanding of fibrosis." Springer Semin Immunopathol 21(4): 415-29.

Eddy, A. A. (1995). "Interstitial macrophages as mediators of renal fibrosis." Exp Nephrol 3(2): 76-9.

Eddy, A. A. (1996). "Molecular insights into renal interstitial fibrosis." J Am Soc Nephrol 7(12): 2495-508.

Eddy, A. A. (2000). "Molecular basis of renal fibrosis." Pediatr Nephrol 15(3-4): 290-301.

Eddy, A. A. and C. M. Giachelli (1995). "Renal expression of genes that promote interstitial inflammation and fibrosis in rats with protein-overload proteinuria." Kidney Int 47(6): 1546-57.

Eddy, A. A., H. Kim, et al. (2000). "Interstitial fibrosis in mice with overload proteinuria: deficiency of TIMP-1 is not protective." Kidney Int 58(2): 618-28.

Edwards, D. R., G. Murphy, et al. (1987). "Transforming growth factor beta modulates the expression of collagenase and metalloproteinase inhibitor." EMBO J 6(7): 1899-904.

Eide, I., E. Loyning, et al. (1977). "Mechanism of renin release during acute ureteral constriction in dogs." Circ Res 40(3): 293-9.

Eitner, F., E. Bucher, et al. (2008). "PDGF-C is a proinflammatory cytokine that mediates renal interstitial fibrosis." J Am Soc Nephrol 19(2): 281-9.

Ekblom, P. and A. Weller (1991). "Ontogeny of tubulointerstitial cells." Kidney Int 39(3): 394-400.

Eknoyan, G., N. Lameire, et al. (2004). "The burden of kidney disease: improving global outcomes." Kidney Int 66(4): 1310-4.

Elbarghati, L., C. Murdoch, et al. (2008). "Effects of hypoxia on transcription factor expression in human monocytes and macrophages." Immunobiology 213(9-10): 899-908.

Elbashir, S. M., J. Harborth, et al. (2001). "Duplexes of 21-nucleotide RNAs mediate RNA interference in cultured mammalian cells." Nature 411(6836): 494-8.

Erdogan, M., A. Pozzi, et al. (2007). "Signaling pathways regulating TC21-induced tumorigenesis." J Biol Chem 282(38): 27713-20.

Erfle, H., B. Neumann, et al. (2007). "Reverse transfection on cell arrays for high content screening microscopy." Nat Protoc 2(2): 392-9.

Essig, M., F. Vrtovsnik, et al. (1998). "Lovastatin modulates in vivo and in vitro the plasminogen activator/plasmin system of rat proximal tubular cells: role of geranylgeranylation and Rho proteins." J Am Soc Nephrol 9(8): 1377-88.

Esteban, L. M., C. Vicario-Abejon, et al. (2001). "Targeted genomic disruption of H-ras and N-ras, individually or in combination, reveals the dispensability of both loci for mouse growth and development." Mol Cell Biol 21(5): 1444-52.

Fallowfield, J. A., M. Mizuno, et al. (2007). "Scar-associated macrophages are a major source of hepatic matrix metalloproteinase-13 and facilitate the resolution of murine hepatic fibrosis." J Immunol 178(8): 5288-95.

Fang, T. C., M. R. Alison, et al. (2005). "Proliferation of bone marrow-derived cells contributes to regeneration after folic acid-induced acute tubular injury." J Am Soc Nephrol 16(6): 1723-32.

Fang, T. C., W. R. Otto, et al. (2008). "Exogenous bone marrow cells do not rescue non-irradiated mice from acute renal tubular damage caused by HgCl2, despite establishment of chimaerism and cell proliferation in bone marrow and spleen." Cell Prolif 41(4): 592-606.

Farman, C. A. and D. J. Kornbrust (2003). "Oligodeoxynucleotide studies in primates: antisense and immune stimulatory indications." Toxicol Pathol 31 Suppl: 119-22.

Farris, A. B., C. D. Adams, et al. (2011) "Morphometric and visual evaluation of fibrosis in renal biopsies." J Am Soc Nephrol 22(1): 176-86.

Faulkner, J. L., L. M. Szcykalski, et al. (2005). "Origin of interstitial fibroblasts in an accelerated model of angiotensin II-induced renal fibrosis." Am J Pathol 167(5): 1193-205.

Fernandez-Campo, L., M. T. Grande, et al. (2009). "Effect of different antihypertensive treatments on Ras, MAPK and Akt activation in hypertension and diabetes." Clin Sci (Lond) 116(2): 165-73.

Fine, L. G. and J. T. Norman (1992). "Renal growth responses to acute and chronic injury: routes to therapeutic intervention." J Am Soc Nephrol 2(10 Suppl): S206-11.

Fine, L. G. and J. T. Norman (2008). "Chronic hypoxia as a mechanism of progression of chronic kidney diseases: from hypothesis to novel therapeutics." Kidney Int 74(7): 867-72.

Fine, L. G., A. C. Ong, et al. (1993). "Mechanisms of tubulo-interstitial injury in progressive renal diseases." Eur J Clin Invest 23(5): 259-65.

Fink, R. L., D. T. Caridis, et al. (1980). "Renal impairment and its reversibility following variable periods of complete ureteric obstruction." Aust N Z J Surg 50(1): 77-83.

Fire, A., S. Xu, et al. (1998). "Potent and specific genetic interference by double-stranded RNA in Caenorhabditis elegans." Nature 391(6669): 806-11.

Fire, A. Z. (2007). "Gene silencing by double-stranded RNA." Cell Death Differ 14(12): 1998-2012.

Foley, R. N., P. S. Parfrey, et al. (1998). "Clinical epidemiology of cardiovascular disease in chronic renal disease." Am J Kidney Dis 32(5 Suppl 3): S112-9.

Forbes, S. J., R. Poulsom, et al. (2002). "Hepatic and renal differentiation from blood-borne stem cells." Gene Ther 9(10): 625-30.

Fried, L. F. (2008). "Effects of HMG-CoA reductase inhibitors (statins) on progression of kidney disease." Kidney Int 74(5): 571-6.

Frokiaer, J., L. Knudsen, et al. (1992). "Enhanced intrarenal angiotensin II generation in response to obstruction of the pig ureter." Am J Physiol 263(3 Pt 2): F527-33.

Frokiaer, J., A. S. Nielsen, et al. (1993). "The effect of indomethacin infusion on renal hemodynamics and on the renin-angiotensin system during unilateral ureteral obstruction of the pig." J Urol 150(5 Pt 1): 1557-63.

Frosch, M., T. Vogl, et al. (2004). "Expression of MRP8 and MRP14 by macrophages is a marker for severe forms of glomerulonephritis." J Leukoc Biol 75(2): 198-206.

Fuentes-Calvo, I., A. M. Blazquez-Medela, et al. (2010) "Analysis of k-ras nuclear expression in fibroblasts and mesangial cells." PLoS One 5(1): e8703.

Fujita-Yoshigaki, J., M. Shirouzu, et al. (1995). "A constitutive effector region on the C-terminal side of switch I of the Ras protein." J Biol Chem 270(9): 4661-7.

Fukasawa, H., T. Yamamoto, et al. (2004). "Treatment with anti-TGF-beta antibody ameliorates chronic progressive nephritis by inhibiting Smad/TGF-beta signaling." Kidney Int 65(1): 63-74.

Furth, M. E., T. H. Aldrich, et al. (1987). "Expression of ras proto-oncogene proteins in normal human tissues." Oncogene 1(1): 47-58.

Gabbiani, G. (1992). "The biology of the myofibroblast." Kidney Int 41(3): 530-2.

Gabbiani, G., B. J. Hirschel, et al. (1972). "Granulation tissue as a contractile organ. A study of structure and function." J Exp Med 135(4): 719-34.

Gagliardini, E. and A. Benigni (2006). "Role of anti-TGF-beta antibodies in the treatment of renal injury." Cytokine Growth Factor Rev 17(1-2): 89-96.

Gana-Weisz, M., R. Haklai, et al. (1997). "The Ras antagonist S-farnesylthiosalicylic acid induces inhibition of MAPK activation." Biochem Biophys Res Commun 239(3): 900-4.

Gao, S. Y., C. Y. Li, et al. (2007). "Rho-family small GTPases are involved in forskolin-induced cell-cell contact formation of renal glomerular podocytes in vitro." Cell Tissue Res 328(2): 391-400.

Gao, X., J. Li, et al. (2008). "Connective tissue growth factor stimulates renal cortical myofibroblast-like cell proliferation and matrix protein production." Wound Repair Regen 16(3): 408-15.

Garrett, M. D., A. J. Self, et al. (1989). "Identification of distinct cytoplasmic targets for ras/R-ras and rho regulatory proteins." J Biol Chem 264(1): 10-3.

Gattone, V. H., 2nd, D. A. Sherman, et al. (1992). "Epidermal growth factor in the neonatal mouse salivary gland and kidney." Biol Neonate 61(1): 54-67.

Geissmann, F., C. Auffray, et al. (2008). "Blood monocytes: distinct subsets, how they relate to dendritic cells, and their possible roles in the regulation of T-cell responses." Immunol Cell Biol 86(5): 398-408.

Geissmann, F., M. G. Manz, et al. "Development of monocytes, macrophages, and dendritic cells." Science 327(5966): 656-61.

Ghielli, M., W. Verstrepen, et al. (1998). "Regeneration processes in the kidney after acute injury: role of infiltrating cells." Exp Nephrol 6(6): 502-7.

Giancotti, F. G. (1997). "Integrin signaling: specificity and control of cell survival and cell cycle progression." Curr Opin Cell Biol 9(5): 691-700.

Giancotti, F. G. and E. Ruoslahti (1999). "Integrin signaling." Science 285(5430): 1028-32.

Gil, J. and M. Esteban (2000). "Induction of apoptosis by the dsRNA-dependent protein kinase (PKR): mechanism of action." Apoptosis 5(2): 107-14.

Gil, J., M. A. Garcia, et al. (2002). "Caspase 9 activation by the dsRNA-dependent protein kinase, PKR: molecular mechanism and relevance." FEBS Lett 529(2-3): 249-55.

Gilbert, R. E., A. Cox, et al. (1998). "Expression of transforming growth factor-beta1 and type IV collagen in the renal tubulointerstitium in experimental diabetes: effects of ACE inhibition." Diabetes 47(3): 414-22.

Gille, H., M. Kortenjann, et al. (1995). "ERK phosphorylation potentiates Elk-1-mediated ternary complex formation and transactivation." EMBO J 14(5): 951-62.

Gojo, A., K. Utsunomiya, et al. (2007). "The Rho-kinase inhibitor, fasudil, attenuates diabetic nephropathy in streptozotocin-induced diabetic rats." Eur J Pharmacol 568(1-3): 242-7.

Gomez, D. E., D. F. Alonso, et al. (1997). "Tissue inhibitors of metalloproteinases: structure, regulation and biological functions." Eur J Cell Biol 74(2): 111-22.

Gomez-Garre, D., R. Largo, et al. (2001). "Activation of NF-kappaB in tubular epithelial cells of rats with intense proteinuria: role of angiotensin II and endothelin-1." Hypertension 37(4): 1171-8.

Gong, R., A. Rifai, et al. (2008). "Hepatocyte growth factor suppresses proinflammatory NFkappaB activation through GSK3beta inactivation in renal tubular epithelial cells." J Biol Chem 283(12): 7401-10.

Gong, R., A. Rifai, et al. (2004). "Hepatocyte growth factor ameliorates renal interstitial inflammation in rat remnant kidney by modulating tubular expression of macrophage chemoattractant protein-1 and RANTES." J Am Soc Nephrol 15(11): 2868-81.

Gong, R., A. Rifai, et al. (2003). "Hepatocyte growth factor modulates matrix metalloproteinases and plasminogen activator/plasmin proteolytic pathways in progressive renal interstitial fibrosis." J Am Soc Nephrol 14(12): 3047-60.

Gonzalez-Avila, G., C. Iturria, et al. (1998). "Changes in matrix metalloproteinases during the evolution of interstitial renal fibrosis in a rat experimental model." Pathobiology 66(5): 196-204.

Gore-Hyer, E., D. Shegogue, et al. (2002). "TGF-beta and CTGF have overlapping and distinct fibrogenic effects on human renal cells." Am J Physiol Renal Physiol 283(4): F707-16.

Gould, S. E., M. Day, et al. (2002). "BMP-7 regulates chemokine, cytokine, and hemodynamic gene expression in proximal tubule cells." Kidney Int 61(1): 51-60.

Grande, M. T., M. Arevalo, et al. (2009). "Targeted genomic disruption of H-ras and N-ras has no effect on early renal changes after unilateral ureteral ligation." World J Urol.

Grande, M. T., I. Fuentes-Calvo, et al. (2009). "Deletion of H-Ras decreases renal fibrosis and myofibroblast activation following ureteral obstruction in mice." Kidney Int.

Grassmann, A., S. Gioberge, et al. (2005). "ESRD patients in 2004: global overview of patient numbers, treatment modalities and associated trends." Nephrol Dial Transplant 20(12): 2587-93.

Greenburg, G. and E. D. Hay (1982). "Epithelia suspended in collagen gels can lose polarity and express characteristics of migrating mesenchymal cells." J Cell Biol 95(1): 333-9.

Grimm, P. C., P. Nickerson, et al. (2001). "Neointimal and tubulointerstitial infiltration by recipient mesenchymal cells in chronic renal-allograft rejection." N Engl J Med 345(2): 93-7.

Grotendorst, G. R., H. Okochi, et al. (1996). "A novel transforming growth factor beta response element controls the expression of the connective tissue growth factor gene." Cell Growth Differ 7(4): 469-80.

Guo, G., J. Morrissey, et al. (1999). "Role of TNFR1 and TNFR2 receptors in tubulointerstitial fibrosis of obstructive nephropathy." Am J Physiol 277(5 Pt 2): F766-72.

Gupta, S., M. R. Clarkson, et al. (2000). "Connective tissue growth factor: potential role in glomerulosclerosis and tubulointerstitial fibrosis." Kidney Int 58(4): 1389-99.

Gutierrez, L., A. I. Magee, et al. (1989). "Post-translational processing of p21ras is two-step and involves carboxyl-methylation and carboxy-terminal proteolysis." EMBO J 8(4): 1093-8.

Ha, H., E. Y. Oh, et al. (2009). "The role of plasminogen activator inhibitor 1 in renal and cardiovascular diseases." Nat Rev Nephrol 5(4): 203-11.

Hagemann, C. and J. L. Blank (2001). "The ups and downs of MEK kinase interactions." Cell Signal 13(12): 863-75.

Hahm, K., M. E. Lukashev, et al. (2007). "Alphav beta6 integrin regulates renal fibrosis and inflammation in Alport mouse." Am J Pathol 170(1): 110-25.

Haigis, K. M., K. R. Kendall, et al. (2008). "Differential effects of oncogenic K-Ras and N-Ras on proliferation, differentiation and tumor progression in the colon." Nat Genet 40(5): 600-8.

Haklai, R., G. Elad-Sfadia, et al. (2008). "Orally administered FTS (salirasib) inhibits human pancreatic tumor growth in nude mice." Cancer Chemother Pharmacol 61(1): 89-96.

Hall, A. (1992). "Signal transduction through small GTPases--a tale of two GAPs." Cell 69(3): 389-91.

Hall, A. (1992). "Ras-related GTPases and the cytoskeleton." Mol Biol Cell 3(5): 475-9.

Hall, A., C. J. Marshall, et al. (1983). "Identification of transforming gene in two human sarcoma cell lines as a new member of the ras gene family located on chromosome 1." Nature 303(5916): 396-400.

Hall, B. E., S. S. Yang, et al. (2001). "Structure-based mutagenesis reveals distinct functions for Ras switch 1 and switch 2 in Sos-catalyzed guanine nucleotide exchange." J Biol Chem 276(29): 27629-37.

Hallan, S. I., J. Coresh, et al. (2006). "International comparison of the relationship of chronic kidney disease prevalence and ESRD risk." J Am Soc Nephrol 17(8): 2275-84.

Hamar, P., E. Song, et al. (2004). "Small interfering RNA targeting Fas protects mice against renal ischemia-reperfusion injury." Proc Natl Acad Sci U S A 101(41): 14883-8.

Hamilton, M. and A. Wolfman (1998). "Ha-ras and N-ras regulate MAPK activity by distinct mechanisms in vivo." Oncogene 16(11): 1417-28.

Han, Y. P., Y. D. Nien, et al. (2002). "Recombinant human platelet-derived growth factor and transforming growth factor-beta mediated contraction of human dermal fibroblast populated lattices is inhibited by Rho/GTPase inhibitor but does not require phosphatidylinositol-3' kinase." Wound Repair Regen 10(3): 169-76.

Hancock, J. F. (2003). "Ras proteins: different signals from different locations." Nat Rev Mol Cell Biol 4(5): 373-84.

Hancock, J. F., K. Cadwallader, et al. (1991). "A CAAX or a CAAL motif and a second signal are sufficient for plasma membrane targeting of ras proteins." EMBO J 10(13): 4033-9.

Hancock, J. F., A. I. Magee, et al. (1989). "All ras proteins are polyisoprenylated but only some are palmitoylated." Cell 57(7): 1167-77.

Hancock, J. F. and R. G. Parton (2005). "Ras plasma membrane signalling platforms." Biochem J 389(Pt 1): 1-11.

Hancock, J. F., H. Paterson, et al. (1990). "A polybasic domain or palmitoylation is required in addition to the CAAX motif to localize p21ras to the plasma membrane." Cell 63(1): 133-9.

Hannigan, G., A. A. Troussard, et al. (2005). "Integrin-linked kinase: a cancer therapeutic target unique among its ILK." Nat Rev Cancer 5(1): 51-63.

Harris, D. C., Y. C. Tay, et al. (1995). "Mechanisms of iron-induced proximal tubule injury in rat remnant kidney." Am J Physiol 269(2 Pt 2): F218-24.

Harris, K. P., S. Klahr, et al. (1993). "Obstructive nephropathy: from mechanical disturbance to immune activation?" Exp Nephrol 1(3): 198-204.

Harris, K. P., G. F. Schreiner, et al. (1989). "Effect of leukocyte depletion on the function of the postobstructed kidney in the rat." Kidney Int 36(2): 210-5.

Harris, R. H. and J. M. Gill (1981). "Changes in glomerular filtration rate during complete ureteral obstruction in rats." Kidney Int 19(4): 603-8.

Hartsough, M. T., R. S. Frey, et al. (1996). "Altered transforming growth factor signaling in epithelial cells when ras activation is blocked." J Biol Chem 271(37): 22368-75.

Hartsough, M. T. and K. M. Mulder (1997). "Transforming growth factor-beta signaling in epithelial cells." Pharmacol Ther 75(1): 21-41.

Harvey, J. J. (1964). "An Unidentified Virus Which Causes the Rapid Production of Tumours in Mice." Nature 204: 1104-5.

Havemann, K., B. F. Pujol, et al. (2003). "In vitro transformation of monocytes and dendritic cells into endothelial like cells." Adv Exp Med Biol 522: 47-57.

Hayashida, T., M. Decaestecker, et al. (2003). "Cross-talk between ERK MAP kinase and Smad signaling pathways enhances TGF-beta-dependent responses in human mesangial cells." FASEB J 17(11): 1576-8.

He, W., C. Dai, et al. (2009). "Wnt/beta-catenin signaling promotes renal interstitial fibrosis." J Am Soc Nephrol 20(4): 765-76.

Heasman, S. J. and A. J. Ridley (2008). "Mammalian Rho GTPases: new insights into their functions from in vivo studies." Nat Rev Mol Cell Biol 9(9): 690-701.

Heino, J., R. A. Ignotz, et al. (1989). "Regulation of cell adhesion receptors by transforming growth factor-beta. Concomitant regulation of integrins that share a common beta 1 subunit." J Biol Chem 264(1): 380-8.

Helset, E., T. Sildnes, et al. (1994). "Endothelin-1 Stimulates Monocytes in vitro to Release Chemotactic Activity Identified as Interleukin-8 and Monocyte Chemotactic Protein-1." Mediators Inflamm 3(2): 155-60.

Helset, E., T. Sildnes, et al. (1993). "Endothelin-1 stimulates human monocytes in vitro to release TNF-alpha , IL-1beta and IL-6." Mediators Inflamm 2(6): 417-22.

Henderson, N. C., A. C. Mackinnon, et al. (2008). "Galectin-3 expression and secretion links macrophages to the promotion of renal fibrosis." Am J Pathol 172(2): 288-98.

Hendry, B. M., A. Khwaja, et al. (2006). "Distinct functions for Ras GTPases in the control of proliferation and apoptosis in mouse and human mesangial cells." Kidney Int 69(1): 99-104.

Henis, Y. I., J. F. Hancock, et al. (2009). "Ras acylation, compartmentalization and signaling nanoclusters (Review)." Mol Membr Biol 26(1): 80-92.

Henry, D. O., S. A. Moskalenko, et al. (2000). "Ral GTPases contribute to regulation of cyclin D1 through activation of NF-kappaB." Mol Cell Biol 20(21): 8084-92.

Herrmann, C., G. A. Martin, et al. (1995). "Quantitative analysis of the complex between p21ras and the Ras-binding domain of the human Raf-1 protein kinase." J Biol Chem 270(7): 2901-5.

Herzlinger, D. (2002). "Renal interstitial fibrosis: remembrance of things past?" J Clin Invest 110(3): 305-6.

Herzlinger, D., R. Abramson, et al. (1993). "Phenotypic conversions in renal development." J Cell Sci Suppl 17: 61-4.

Heusinger-Ribeiro, J., M. Eberlein, et al. (2001). "Expression of connective tissue growth factor in human renal fibroblasts: regulatory roles of RhoA and cAMP." J Am Soc Nephrol 12(9): 1853-61.

Himmelstein, S. I., T. M. Coffman, et al. (1990). "Atrial natriuretic peptide-induced changes in renal prostacyclin production in ureteral obstruction." Am J Physiol 258(2 Pt 2): F281-6.

Hinz, B. "The myofibroblast: paradigm for a mechanically active cell." J Biomech 43(1): 146-55.

Hirschberg, R. and S. Wang (2005). "Proteinuria and growth factors in the development of tubulointerstitial injury and scarring in kidney disease." Curr Opin Nephrol Hypertens 14(1): 43-52.

Hocher, B., C. Thone-Reineke, et al. (1997). "Endothelin-1 transgenic mice develop glomerulosclerosis, interstitial fibrosis, and renal cysts but not hypertension." J Clin Invest 99(6): 1380-9.

Hochreiter, A. E., H. Xiao, et al. (2006). "Telomerase template antagonist GRN163L disrupts telomere maintenance, tumor growth, and metastasis of breast cancer." Clin Cancer Res 12(10): 3184-92.

Holdsworth, S. R., T. J. Neale, et al. (1981). "Abrogation of macrophage-dependent injury in experimental glomerulonephritis in the rabbit. Use of an antimacrophage serum." J Clin Invest 68(3): 686-98.

Holmlund, J. T. (2003). "Applying antisense technology: Affinitak and other antisense oligonucleotides in clinical development." Ann N Y Acad Sci 1002: 244-51.

Horiguchi, K., T. Shirakihara, et al. (2009). "Role of Ras signaling in the induction of snail by transforming growth factor-beta." J Biol Chem 284(1): 245-53.

Howe, A. K. and R. L. Juliano (1998). "Distinct mechanisms mediate the initial and sustained phases of integrin-mediated activation of the Raf/MEK/mitogen-activated protein kinase cascade." J Biol Chem 273(42): 27268-74.

Hruska, K. A., G. Guo, et al. (2000). "Osteogenic protein-1 prevents renal fibrogenesis associated with ureteral obstruction." Am J Physiol Renal Physiol 279(1): F130-43.

Hu, K., L. Lin, et al. (2008). "tPA protects renal interstitial fibroblasts and myofibroblasts from apoptosis." J Am Soc Nephrol 19(3): 503-14.

Hu, K., J. Yang, et al. (2006). "Tissue-type plasminogen activator acts as a cytokine that triggers intracellular signal transduction and induces matrix metalloproteinase-9 gene expression." J Biol Chem 281(4): 2120-7.

Hu, P. P., X. Shen, et al. (1999). "The MEK pathway is required for stimulation of p21(WAF1/CIP1) by transforming growth factor-beta." J Biol Chem 274(50): 35381-7.

Hu, Q., A. Klippel, et al. (1995). "Ras-dependent induction of cellular responses by constitutively active phosphatidylinositol-3 kinase." Science 268(5207): 100-2.

Huang, X. R., A. C. Chung, et al. (2008). "Mice overexpressing latent TGF-beta1 are protected against renal fibrosis in obstructive kidney disease." Am J Physiol Renal Physiol 295(1): F118-27.

Huang, X. R., A. C. Chung, et al. (2008). "Latent TGF-beta1 protects against crescentic glomerulonephritis." J Am Soc Nephrol 19(2): 233-42.

Huber, M. A., N. Kraut, et al. (2005). "Molecular requirements for epithelial-mesenchymal transition during tumor progression." Curr Opin Cell Biol 17(5): 548-58.

Hudkins, K. L., D. G. Gilbertson, et al. (2004). "Exogenous PDGF-D is a potent mesangial cell mitogen and causes a severe mesangial proliferative glomerulopathy." J Am Soc Nephrol 15(2): 286-98.

Hughes, M. D., M. Hussain, et al. (2001). "The cellular delivery of antisense oligonucleotides and ribozymes." Drug Discov Today 6(6): 303-315.

Hugo, C., D. H. Kang, et al. (2002). "Sustained expression of thrombospondin-1 is associated with the development of glomerular and tubulointerstitial fibrosis in the remnant kidney model." Nephron 90(4): 460-70.

Hugo, C., S. J. Shankland, et al. (1998). "Thrombospondin 1 precedes and predicts the development of tubulointerstitial fibrosis in glomerular disease in the rat." Kidney Int 53(2): 302-11.

Hultstrom, M., S. Leh, et al. (2008). "Upregulation of tissue inhibitor of metalloproteases-1 (TIMP-1) and procollagen-N-peptidase in hypertension-induced renal damage." Nephrol Dial Transplant 23(3): 896-903.

Humphreys, B. D., S. L. Lin, et al. "Fate tracing reveals the pericyte and not epithelial origin of myofibroblasts in kidney fibrosis." Am J Pathol 176(1): 85-97.

Hvistendahl, J. J., T. S. Pedersen, et al. (1996). "Renal hemodynamic response to gradated ureter obstruction in the pig." Nephron 74(1): 168-74.

Hwang, I., E. Y. Seo, et al. (2009). "Wnt/beta-catenin signaling: a novel target for therapeutic intervention of fibrotic kidney disease." Arch Pharm Res 32(12): 1653-62.

Hwang, M., H. J. Kim, et al. (2006). "TGF-beta1 siRNA suppresses the tubulointerstitial fibrosis in the kidney of ureteral obstruction." Exp Mol Pathol 81(1): 48-54.

Ignotz, R. A., T. Endo, et al. (1987). "Regulation of fibronectin and type I collagen mRNA levels by transforming growth factor-beta." J Biol Chem 262(14): 6443-6.

Ignotz, R. A. and J. Massague (1986). "Transforming growth factor-beta stimulates the expression of fibronectin and collagen and their incorporation into the extracellular matrix." J Biol Chem 261(9): 4337-45.

Ignotz, R. A. and J. Massague (1987). "Cell adhesion protein receptors as targets for transforming growth factor-beta action." Cell 51(2): 189-97.

Iimura, O., H. Takahashi, et al. (2004). "Effect of ureteral obstruction on matrix metalloproteinase-2 in rat renal cortex." Clin Exp Nephrol 8(3): 223-9.

Ikegami, T., Y. Zhang, et al. (2007). "Liver fibrosis: possible involvement of EMT." Cells Tissues Organs 185(1-3): 213-21.

Imai, E., Y. Akagi, et al. (1997). "Molecular intervention with antisense oligodeoxynucleotides (ODNs) in nephrology." Nephrol Dial Transplant 12(11): 2213-5.

Imai, E., Y. Akagi, et al. (1998). "Towards gene therapy for renal diseases." Nephrologie 19(7): 397-402.

Imai, E. and Y. Isaka (1998). "Strategies of gene transfer to the kidney." Kidney Int 53(2): 264-72.

Imai, E., Y. Isaka, et al. (1998). "Gene transfer and kidney disease." J Nephrol 11(1): 16-9.

Imasawa, T., Y. Utsunomiya, et al. (2001). "The potential of bone marrow-derived cells to differentiate to glomerular mesangial cells." J Am Soc Nephrol 12(7): 1401-9.

Ina, K., H. Kitamura, et al. (2002). "Transformation of interstitial fibroblasts and tubulointerstitial fibrosis in diabetic nephropathy." Med Electron Microsc 35(2): 87-95.

Inoue, T., D. Plieth, et al. (2005). "Antibodies against macrophages that overlap in specificity with fibroblasts." Kidney Int 67(6): 2488-93.

Isaka, Y., Y. Akagi, et al. (1998). "The HVJ liposome method." Exp Nephrol 6(2): 144-7.

Isaka, Y., M. Tsujie, et al. (2000). "Transforming growth factor-beta 1 antisense oligodeoxynucleotides block interstitial fibrosis in unilateral ureteral obstruction." Kidney Int 58(5): 1885-92.

IsakaTsujie, M., Y. Isaka, et al. (2001). "Electroporation-mediated gene transfer that targets glomeruli." J Am Soc Nephrol 12(5): 949-54.

Isbel, N. M., P. A. Hill, et al. (2001). "Tubules are the major site of M-CSF production in experimental kidney disease: correlation with local macrophage proliferation." Kidney Int 60(2): 614-25.

Ishidoya, S., J. Morrissey, et al. (1996). "Delayed treatment with enalapril halts tubulointerstitial fibrosis in rats with obstructive nephropathy." Kidney Int 49(4): 1110-9.

Ishidoya, S., J. Morrissey, et al. (1995). "Angiotensin II receptor antagonist ameliorates renal tubulointerstitial fibrosis caused by unilateral ureteral obstruction." Kidney Int 47(5): 1285-94.
Ivanova, G., A. Arzumanov, et al. (2007). "Comparative studies of tricyclo-DNA- and LNA-containing oligonucleotides as inhibitors of HIV-1 gene expression." Nucleosides Nucleotides Nucleic Acids 26(6-7): 747-50.

Iwano, M., A. Fischer, et al. (2001). "Conditional abatement of tissue fibrosis using nucleoside analogs to selectively corrupt DNA replication in transgenic fibroblasts." Mol Ther 3(2): 149-59.

Iwano, M., D. Plieth, et al. (2002). "Evidence that fibroblasts derive from epithelium during tissue fibrosis." J Clin Invest 110(3): 341-50.

Jabs, D. A. and P. D. Griffiths (2002). "Fomivirsen for the treatment of cytomegalovirus retinitis." Am J Ophthalmol 133(4): 552-6.

Jackson, J. H., C. G. Cochrane, et al. (1990). "Farnesol modification of Kirsten-ras exon 4B protein is essential for transformation." Proc Natl Acad Sci U S A 87(8): 3042-6.

Jackson, J. H., J. W. Li, et al. (1994). "Polylysine domain of K-ras 4B protein is crucial for malignant transformation." Proc Natl Acad Sci U S A 91(26): 12730-4.

Jafar, T. H., P. C. Stark, et al. (2001). "Proteinuria as a modifiable risk factor for the progression of non-diabetic renal disease." Kidney Int 60(3): 1131-40.

Jaffe, A. B. and A. Hall (2002). "Rho GTPases in transformation and metastasis." Adv Cancer Res 84: 57-80.

Jain, R., P. W. Shaul, et al. (2007). "Endothelin-1 induces alveolar epithelial-mesenchymal transition through endothelin type A receptor-mediated production of TGF-beta1." Am J Respir Cell Mol Biol 37(1): 38-47.

Jain, S., G. R. Bicknell, et al. (2000). "Molecular changes in extracellular matrix turnover after renal ischaemia-reperfusion injury." Br J Surg 87(9): 1188-92.

Jakobisiak, M. and J. Golab (2003). "Potential antitumor effects of statins (Review)." Int J Oncol 23(4): 1055-69.

Janda, E., K. Lehmann, et al. (2002). "Ras and TGF[beta] cooperatively regulate epithelial cell plasticity and metastasis: dissection of Ras signaling pathways." J Cell Biol 156(2): 299-313.

Janknecht, R., W. H. Ernst, et al. (1995). "SAP1a is a nuclear target of signaling cascades involving ERKs." Oncogene 10(6): 1209-16.

Janowski, B. A., K. Kaihatsu, et al. (2005). "Inhibiting transcription of chromosomal DNA with antigene peptide nucleic acids." Nat Chem Biol 1(4): 210-5.

Jason, T. L., J. Koropatnick, et al. (2004). "Toxicology of antisense therapeutics." Toxicol Appl Pharmacol 201(1): 66-83.

Jaumot, M. and J. F. Hancock (2001). "Protein phosphatases 1 and 2A promote Raf-1 activation by regulating 14-3-3 interactions." Oncogene 20(30): 3949-58.

Jaumot, M., J. Yan, et al. (2002). "The linker domain of the Ha-Ras hypervariable region regulates interactions with exchange factors, Raf-1 and phosphoinositide 3-kinase." J Biol Chem 277(1): 272-8.

Jiang, H., J. Q. Luo, et al. (1995). "Involvement of Ral GTPase in v-Src-induced phospholipase D activation." Nature 378(6555): 409-12.

Jinde, K., D. J. Nikolic-Paterson, et al. (2001). "Tubular phenotypic change in progressive tubulointerstitial fibrosis in human glomerulonephritis." Am J Kidney Dis 38(4): 761-9.

Johnson, D. W., H. J. Saunders, et al. (1998). "Paracrine stimulation of human renal fibroblasts by proximal tubule cells." Kidney Int 54(3): 747-57.

Johnson, L., D. Greenbaum, et al. (1997). "K-ras is an essential gene in the mouse with partial functional overlap with N-ras." Genes Dev 11(19): 2468-81.

Johnson, T. S., M. Fisher, et al. (2007). "Transglutaminase inhibition reduces fibrosis and preserves function in experimental chronic kidney disease." J Am Soc Nephrol 18(12): 3078-88.

Johnson, T. S., N. J. Skill, et al. (1999). "Transglutaminase transcription and antigen translocation in experimental renal scarring." J Am Soc Nephrol 10(10): 2146-57.

Jullien-Flores, V., O. Dorseuil, et al. (1995). "Bridging Ral GTPase to Rho pathways. RLIP76, a Ral effector with CDC42/Rac GTPase-activating protein activity." J Biol Chem 270(38): 22473-7.

Kaissling, B. and M. Le Hir (2008). "The renal cortical interstitium: morphological and functional aspects." Histochem Cell Biol 130(2): 247-62.

Kalluri, R. and M. Zeisberg (2006). "Fibroblasts in cancer." Nat Rev Cancer 6(5): 392-401.

Kanalas, J. J. and U. Hopfer (1997). "Effect of TGF-beta 1 and TNF-alpha on the plasminogen system of rat proximal tubular epithelial cells." J Am Soc Nephrol 8(2): 184-92.

Kaneto, H., J. Morrissey, et al. (1993). "Increased expression of TGF-beta 1 mRNA in the obstructed kidney of rats with unilateral ureteral ligation." Kidney Int 44(2): 313-21.

Kaneto, H., H. Ohtani, et al. (1999). "Increased expression of TGF-beta1 but not of its receptors contributes to human obstructive nephropathy." Kidney Int 56(6): 2137-46.

Kang, D. H., A. H. Joly, et al. (2001). "Impaired angiogenesis in the remnant kidney model: I. Potential role of vascular endothelial growth factor and thrombospondin-1." J Am Soc Nephrol 12(7): 1434-47.

Kapeller, R. and L. C. Cantley (1994). "Phosphatidylinositol 3-kinase." Bioessays 16(8): 565-76.

Kelly, D. J., A. J. Cox, et al. (2002). "Attenuation of tubular apoptosis by blockade of the renin-angiotensin system in diabetic Ren-2 rats." Kidney Int 61(1): 31-9.

Kerkhoff, E. and U. R. Rapp (1998). "High-intensity Raf signals convert mitotic cell cycling into cellular growth." Cancer Res 58(8): 1636-40.

Khan, S., R. P. Cleveland, et al. (1999). "Hypoxia induces renal tubular epithelial cell apoptosis in chronic renal disease." Lab Invest 79(9): 1089-99.

Khan, S. B., H. T. Cook, et al. (2005). "Antibody blockade of TNF-alpha reduces inflammation and scarring in experimental crescentic glomerulonephritis." Kidney Int 67(5): 1812-20.

Khwaja, A., M. E. Dockrell, et al. (2006). "Prenylation is not necessary for endogenous Ras activation in non-malignant cells." J Cell Biochem 97(2): 412-22.

Khwaja, A., P. Rodriguez-Viciana, et al. (1997). "Matrix adhesion and Ras transformation both activate a phosphoinositide 3-OH kinase and protein kinase B/Akt cellular survival pathway." EMBO J 16(10): 2783-93.

Khwaja, A., C. C. Sharpe, et al. (2005). "The inhibition of human mesangial cell proliferation by S-trans, trans-farnesylthiosalicylic acid." Kidney Int 68(2): 474-86.

Kikuchi, A., S. D. Demo, et al. (1994). "ralGDS family members interact with the effector loop of ras p21." Mol Cell Biol 14(11): 7483-91.

Kim, E., P. Ambroziak, et al. (1999). "Disruption of the mouse Rce1 gene results in defective Ras processing and mislocalization of Ras within cells." J Biol Chem 274(13): 8383-90.

Kim, H., T. Oda, et al. (2001). "TIMP-1 deficiency does not attenuate interstitial fibrosis in obstructive nephropathy." J Am Soc Nephrol 12(4): 736-48.

Kim, K. K., Y. Wei, et al. (2009). "Epithelial cell alpha3beta1 integrin links beta-catenin and Smad signaling to promote myofibroblast formation and pulmonary fibrosis." J Clin Invest 119(1): 213-24.

King, A. J., H. Sun, et al. (1998). "The protein kinase Pak3 positively regulates Raf-1 activity through phosphorylation of serine 338." Nature 396(6707): 180-3.

King, A. J., R. S. Wireman, et al. (2001). "Phosphorylation site specificity of the Pak-mediated regulation of Raf-1 and cooperativity with Src." FEBS Lett 497(1): 6-14.

Kipari, T., J. F. Cailhier, et al. (2006). "Nitric oxide is an important mediator of renal tubular epithelial cell death in vitro and in murine experimental hydronephrosis." Am J Pathol 169(2): 388-99.

Kipari, T. and J. Hughes (2002). "Macrophage-mediated renal cell death." Kidney Int 61(2): 760-1.

Kirsten, W. H. and L. A. Mayer (1967). "Morphologic responses to a murine erythroblastosis virus." J Natl Cancer Inst 39(2): 311-35.

Kivinen, L. and M. Laiho (1999). "Ras- and mitogen-activated protein kinase kinase-dependent and -independent pathways in p21Cip1/Waf1 induction by fibroblast growth factor-2, platelet-derived growth factor, and transforming growth factor-beta1." Cell Growth Differ 10(9): 621-8.

Klahr, S. (2003). "The bone morphogenetic proteins (BMPs). Their role in renal fibrosis and renal function." J Nephrol 16(2): 179-85.

Klahr, S. and J. Morrissey (1998). "Angiotensin II and gene expression in the kidney." Am J Kidney Dis 31(1): 171-6.

Klahr, S. and J. Morrissey (2003). "Obstructive nephropathy and renal fibrosis: The role of bone morphogenic protein-7 and hepatocyte growth factor." Kidney Int Suppl(87): S105-12.

Klahr, S. and J. J. Morrissey (2000). "The role of vasoactive compounds, growth factors and cytokines in the progression of renal disease." Kidney Int Suppl 75: S7-14.

Klein, S., A. Bikfalvi, et al. (1996). "Integrin regulation by endogenous expression of 18-kDa fibroblast growth factor-2." J Biol Chem 271(37): 22583-90.

Klein, S., A. R. de Fougerolles, et al. (2002). "Alpha 5 beta 1 integrin activates an NF-kappa B-dependent program of gene expression important for angiogenesis and inflammation." Mol Cell Biol 22(16): 5912-22.

Kliem, V., R. J. Johnson, et al. (1996). "Mechanisms involved in the pathogenesis of tubulointerstitial fibrosis in 5/6-nephrectomized rats." Kidney Int 49(3): 666-78.

Kluth, D. C. (2007). "Pro-resolution properties of macrophages in renal injury." Kidney Int 72(3): 234-6.

Knapp, J. E. and D. Liu (2004). "Hydrodynamic delivery of DNA." Methods Mol Biol 245: 245-50.

Knecht, A., L. G. Fine, et al. (1991). "Fibroblasts of rabbit kidney in culture. II. Paracrine stimulation of papillary fibroblasts by PDGF." Am J Physiol 261(2 Pt 2): F292-9.

Kobayashi, N., S. Nakano, et al. (2002). "Involvement of Rho-kinase pathway for angiotensin II-induced plasminogen activator inhibitor-1 gene expression and cardiovascular remodeling in hypertensive rats." J Pharmacol Exp Ther 301(2): 459-66.

Kocher, H. M., J. Moorhead, et al. (2003). "Expression of Ras GTPases in normal kidney and in glomerulonephritis." Nephrol Dial Transplant 18(11): 2284-92.

Kocher, H. M., R. Senkus, et al. (2005). "Subcellular distribution of Ras GTPase isoforms in normal human kidney." Nephrol Dial Transplant 20(5): 886-91.

Kodaki, T., R. Woscholski, et al. (1994). "The activation of phosphatidylinositol 3-kinase by Ras." Curr Biol 4(9): 798-806.

Koera, K., K. Nakamura, et al. (1997). "K-ras is essential for the development of the mouse embryo." Oncogene 15(10): 1151-9.

Koesters, R., B. Kaissling, et al. (2010) "Tubular overexpression of transforming growth factor-beta1 induces autophagy and fibrosis but not mesenchymal transition of renal epithelial cells." Am J Pathol 177(2): 632-43.

Kolch, W. (2000). "Meaningful relationships: the regulation of the Ras/Raf/MEK/ERK pathway by protein interactions." Biochem J 351 Pt 2: 289-305.

Kolch, W., G. Heidecker, et al. (1991). "Raf-1 protein kinase is required for growth of induced NIH/3T3 cells." Nature 349(6308): 426-8.

Kothapalli, D. and G. R. Grotendorst (2000). "CTGF modulates cell cycle progression in cAMP-arrested NRK fibroblasts." J Cell Physiol 182(1): 119-26.

Krasilnikov, M. A. (2000). "Phosphatidylinositol-3 kinase dependent pathways: the role in control of cell growth, survival, and malignant transformation." Biochemistry (Mosc) 65(1): 59-67.

Krieg, A. M. (2006). "Therapeutic potential of Toll-like receptor 9 activation." Nat Rev Drug Discov 5(6): 471-84.

Kretzschmar, M., J. Doody, et al. (1999). "A mechanism of repression of TGFbeta/ Smad signaling by oncogenic Ras." Genes Dev 13(7): 804-16.

Kretzschmar, M. and J. Massague (1998). "SMADs: mediators and regulators of TGF-beta signaling." Curr Opin Genet Dev 8(1): 103-11.

Kubicek, M., M. Pacher, et al. (2002). "Dephosphorylation of Ser-259 regulates Raf-1 membrane association." J Biol Chem 277(10): 7913-9.

Kuncio, G. S., E. G. Neilson, et al. (1991). "Mechanisms of tubulointerstitial fibrosis." Kidney Int 39(3): 550-6.

Kurreck, J. (2003). "Antisense technologies. Improvement through novel chemical modifications." Eur J Biochem 270(8): 1628-44.

Kushibiki, T., N. Nagata-Nakajima, et al. (2006). "Enhanced anti-fibrotic activity of plasmid DNA expressing small interference RNA for TGF-beta type II receptor for a mouse model of obstructive nephropathy by cationized gelatin prepared from different amine compounds." J Control Release 110(3): 610-7.

Kuwabara, K., S. Ogawa, et al. (1995). "Hypoxia-mediated induction of acidic/basic fibroblast growth factor and platelet-derived growth factor in mononuclear phagocytes stimulates growth of hypoxic endothelial cells." Proc Natl Acad Sci U S A 92(10): 4606-10.

Laezza, C., G. Mazziotti, et al. (2006). "HMG-CoA reductase inhibitors inhibit rat propylthiouracil-induced goiter by modulating the ras-MAPK pathway." J Mol Med 84(11): 967-73.

Lahsnig, C., M. Mikula, et al. (2009). "ILEI requires oncogenic Ras for the epithelial to mesenchymal transition of hepatocytes and liver carcinoma progression." Oncogene 28(5): 638-50.

Lai, K. N., J. C. Leung, et al. (2007). "Interaction between proximal tubular epithelial cells and infiltrating monocytes/T cells in the proteinuric state." Kidney Int 71(6): 526-38.

Laiho, M., O. Saksela, et al. (1987). "Transforming growth factor-beta induction of type-1 plasminogen activator inhibitor. Pericellular deposition and sensitivity to exogenous urokinase." J Biol Chem 262(36): 17467-74.

Lan, H. Y., H. Mitsuhashi, et al. (1997). "Macrophage apoptosis in rat crescentic glomerulonephritis." Am J Pathol 151(2): 531-8.

Lan, H. Y., W. Mu, et al. (2003). "Inhibition of renal fibrosis by gene transfer of inducible Smad7 using ultrasound-microbubble system in rat UUO model." J Am Soc Nephrol 14(6): 1535-48.

Lan, H. Y., D. J. Nikolic-Paterson, et al. (1995). "Local macrophage proliferation in the progression of glomerular and tubulointerstitial injury in rat anti-GBM glomerulonephritis." Kidney Int 48(3): 753-60.

Lang, H. and D. M. Fekete (2001). "Lineage analysis in the chicken inner ear shows differences in clonal dispersion for epithelial, neuronal, and mesenchymal cells." Dev Biol 234(1): 120-37.

Lange-Sperandio, B., F. Cachat, et al. (2002). "Selectins mediate macrophage infiltration in obstructive nephropathy in newborn mice." Kidney Int 61(2): 516-24.

Le Hir, M., I. Hegyi, et al. (2005). "Characterization of renal interstitial fibroblast-specific protein 1/S100A4-positive cells in healthy and inflamed rodent kidneys." Histochem Cell Biol 123(4-5): 335-46.

Leask, A., A. Holmes, et al. (2003). "Connective tissue growth factor gene regulation. Requirements for its induction by transforming growth factor-beta 2 in fibroblasts." J Biol Chem 278(15): 13008-15.

Lee, S., S. Huen, et al. (2011) "Distinct macrophage phenotypes contribute to kidney injury and repair." J Am Soc Nephrol 22(2): 317-26.

Leevers, S. J., H. F. Paterson, et al. (1994). "Requirement for Ras in Raf activation is overcome by targeting Raf to the plasma membrane." Nature 369(6479): 411-4.

Lelongt, B., S. Bengatta, et al. (2001). "Matrix metalloproteinase 9 protects mice from anti-glomerular basement membrane nephritis through its fibrinolytic activity." J Exp Med 193(7): 793-802.

Lelongt, B., G. Trugnan, et al. (1997). "Matrix metalloproteinases MMP2 and MMP9 are produced in early stages of kidney morphogenesis but only MMP9 is required for renal organogenesis in vitro." J Cell Biol 136(6): 1363-73.

Leon, J., I. Guerrero, et al. (1987). "Differential expression of the ras gene family in mice." Mol Cell Biol 7(4): 1535-40.

Levin, A. A. (1999). "A review of the issues in the pharmacokinetics and toxicology of phosphorothioate antisense oligonucleotides." Biochim Biophys Acta 1489(1): 69-84.

Li, C., C. W. Yang, et al. (2004). "Pravastatin treatment attenuates interstitial inflammation and fibrosis in a rat model of chronic cyclosporine-induced nephropathy." Am J Physiol Renal Physiol 286(1): F46-57.

Li, J., J. A. Deane, et al. (2007). "The contribution of bone marrow-derived cells to the development of renal interstitial fibrosis." Stem Cells 25(3): 697-706.

Li, J. H., W. Wang, et al. (2004). "Advanced glycation end products induce tubular epithelial-myofibroblast transition through the RAGE-ERK1/2 MAP kinase signaling pathway." Am J Pathol 164(4): 1389-97.

Li, L., P. Truong, et al. (2007). "Renal and bone marrow cells fuse after renal ischemic injury." J Am Soc Nephrol 18(12): 3067-77.

Li, L., D. Zepeda-Orozco, et al. (2010) "Autophagy is a component of epithelial cell fate in obstructive uropathy." Am J Pathol 176(4): 1767-78.

Li, S., P. Janosch, et al. (1995). "Regulation of Raf-1 kinase activity by the 14-3-3 family of proteins." EMBO J 14(4): 685-96.

Li, Y., C. Dai, et al. (2007). "PINCH-1 promotes tubular epithelial-to-mesenchymal transition by interacting with integrin-linked kinase." J Am Soc Nephrol 18(9): 2534-43.

Li, Y., Y. S. Kang, et al. (2008). "Epithelial-to-mesenchymal transition is a potential pathway leading to podocyte dysfunction and proteinuria." Am J Pathol 172(2): 299-308.

Li, Y., X. Tan, et al. (2009). "Inhibition of integrin-linked kinase attenuates renal interstitial fibrosis." J Am Soc Nephrol 20(9): 1907-18.

Li, Y., J. Yang, et al. (2003). "Role for integrin-linked kinase in mediating tubular epithelial to mesenchymal transition and renal interstitial fibrogenesis." J Clin Invest 112(4): 503-16.

Liapis, H., M. Nag, et al. (1994). "Effects of experimental ureteral obstruction on platelet-derived growth factor-A and type I procollagen expression in fetal metanephric kidneys." Pediatr Nephrol 8(5): 548-54.

Lin, F. (2008). "Renal repair: role of bone marrow stem cells." Pediatr Nephrol 23(6): 851-61.

Lin, F., A. Moran, et al. (2005). "Intrarenal cells, not bone marrow-derived cells, are the major source for regeneration in postischemic kidney." J Clin Invest 115(7): 1756-64.

Lin, J., S. R. Patel, et al. (2005). "Kielin/chordin-like protein, a novel enhancer of BMP signaling, attenuates renal fibrotic disease." Nat Med 11(4): 387-93.

Lin, R. Y., K. M. Sullivan, et al. (1995). "Exogenous transforming growth factor-beta amplifies its own expression and induces scar formation in a model of human fetal skin repair." Ann Surg 222(2): 146-54.

Lin, S. L., A. P. Castano, et al. (2009). "Bone marrow Ly6Chigh monocytes are selectively recruited to injured kidney and differentiate into functionally distinct populations." J Immunol 183(10): 6733-43.

Lin, S. L., T. Kisseleva, et al. (2008). "Pericytes and perivascular fibroblasts are the primary source of collagen-producing cells in obstructive fibrosis of the kidney." Am J Pathol 173(6): 1617-27.

Lin, S. L., B. Li, et al. "Macrophage Wnt7b is critical for kidney repair and regeneration." Proc Natl Acad Sci U S A 107(9): 4194-9.

Liu, Y. (2004). "Epithelial to mesenchymal transition in renal fibrogenesis: pathologic significance, molecular mechanism, and therapeutic intervention." J Am Soc Nephrol 15(1): 1-12.

Liu, Y., H. Miyoshi, et al. (2006). "Encapsulated ultrasound microbubbles: therapeutic application in drug/gene delivery." J Control Release 114(1): 89-99.

Lloyd, C. M., A. W. Minto, et al. (1997). "RANTES and monocyte chemoattractant protein-1 (MCP-1) play an important role in the inflammatory phase of crescentic nephritis, but only MCP-1 is involved in crescent formation and interstitial fibrosis." J Exp Med 185(7): 1371-80.

Loke, S. L., C. A. Stein, et al. (1989). "Characterization of oligonucleotide transport into living cells." Proc Natl Acad Sci U S A 86(10): 3474-8.

Lorusso, P. M., A. A. Adjei, et al. (2005). "Phase I and pharmacodynamic study of the oral MEK inhibitor CI-1040 in patients with advanced malignancies." J Clin Oncol 23(23): 5281-93.

Lu, A., F. Tebar, et al. (2009). "A clathrin-dependent pathway leads to KRas signaling on late endosomes en route to lysosomes." J Cell Biol 184(6): 863-79.

Luo, G. H., Y. P. Lu, et al. (2008). "Inhibition of connective tissue growth factor by small interfering RNA prevents renal fibrosis in rats undergoing chronic allograft nephropathy." Transplant Proc 40(7): 2365-9.

Luo, Z., B. Diaz, et al. (1997). "An intact Raf zinc finger is required for optimal binding to processed Ras and for ras-dependent Raf activation in situ." Mol Cell Biol 17(1): 46-53.

Luo, Z. J., X. F. Zhang, et al. (1995). "Identification of the 14.3.3 zeta domains important for self-association and Raf binding." J Biol Chem 270(40): 23681-7.

Luttrell, D. K. and L. M. Luttrell (2003). "Signaling in time and space: G protein-coupled receptors and mitogen-activated protein kinases." Assay Drug Dev Technol 1(2): 327-38.

Luttrell, L. M. (2002). "Activation and targeting of mitogen-activated protein kinases by G-protein-coupled receptors." Can J Physiol Pharmacol 80(5): 375-82.

Luttrell, L. M. (2003). "'Location, location, location': activation and targeting of MAP kinases by G protein-coupled receptors." J Mol Endocrinol 30(2): 117-26.

Luttrell, L. M., Y. Daaka, et al. (1997). "G protein-coupled receptors mediate two functionally distinct pathways of tyrosine phosphorylation in rat 1a fibroblasts. Shc phosphorylation and receptor endocytosis correlate with activation of Erk kinases." J Biol Chem 272(50): 31648-56.

Luttrell, L. M., T. van Biesen, et al. (1997). "G-protein-coupled receptors and their regulation: activation of the MAP kinase signaling pathway by G-protein-coupled receptors." Adv Second Messenger Phosphoprotein Res 31: 263-77.

Lygoe, K. A., J. T. Norman, et al. (2004). "AlphaV integrins play an important role in myofibroblast differentiation." Wound Repair Regen 12(4): 461-70.

Lyons, J. F., S. Wilhelm, et al. (2001). "Discovery of a novel Raf kinase inhibitor." Endocr Relat Cancer 8(3): 219-25.

Ma, C. and N. Chegini (1999). "Regulation of matrix metalloproteinases (MMPs) and their tissue inhibitors in human myometrial smooth muscle cells by TGF-beta1." Mol Hum Reprod 5(10): 950-4.

Ma, F. Y., J. Liu, et al. (2009). "Targeting renal macrophage accumulation via c-fms kinase reduces tubular apoptosis but fails to modify progressive fibrosis in the obstructed rat kidney." Am J Physiol Renal Physiol 296(1): F177-85.

Ma, L. J., H. Yang, et al. (2003). "Transforming growth factor-beta-dependent and -independent pathways of induction of tubulointerstitial fibrosis in beta6(-/-) mice." Am J Pathol **163**(4): 1261-73.

Mackay, D. J. and A. Hall (1998). "Rho GTPases." J Biol Chem 273(33): 20685-8.

Mackensen-Haen, S., A. Bohle, et al. (1992). "The consequences for renal function of widening of the interstitium and changes in the tubular epithelium of the renal cortex and outer medulla in various renal diseases." Clin Nephrol 37(2): 70-7.

Magee, A. I., L. Gutierrez, et al. (1989). "Targeting of oncoproteins to membranes by fatty acylation." J Cell Sci Suppl 11: 149-60.

Magee, T. and M. C. Seabra (2005). "Fatty acylation and prenylation of proteins: what's hot in fat." Curr Opin Cell Biol 17(2): 190-6.

Makkinje, A., D. A. Quinn, et al. (2000). "Gene 33/Mig-6, a transcriptionally inducible adapter protein that binds GTP-Cdc42 and activates SAPK/JNK. A potential marker transcript for chronic pathologic conditions, such as diabetic nephropathy. Possible role in the response to persistent stress." J Biol Chem 275(23): 17838-47.

Marais, R., Y. Light, et al. (1995). "Ras recruits Raf-1 to the plasma membrane for activation by tyrosine phosphorylation." EMBO J 14(13): 3136-45.

Marastoni, S., G. Ligresti, et al. (2008). "Extracellular matrix: a matter of life and death." Connect Tissue Res 49(3): 203-6.

Marciano, D., G. Ben-Baruch, et al. (1995). "Farnesyl derivatives of rigid carboxylic acids-inhibitors of ras-dependent cell growth." J Med Chem 38(8): 1267-72.

Marshall, M. S. (1993). "The effector interactions of p21ras." Trends Biochem Sci 18(7): 250-4.

Marshall, M. S., L. J. Davis, et al. (1991). "Identification of amino acid residues required for Ras p21 target activation." Mol Cell Biol 11(8): 3997-4004.

Martin, G. A., D. Viskochil, et al. (1990). "The GAP-related domain of the neurofibromatosis type 1 gene product interacts with ras p21." Cell 63(4): 843-9.

Martinez, F. O., A. Sica, et al. (2008). "Macrophage activation and polarization." Front Biosci 13: 453-61.

Martinez-Salgado, C., I. Fuentes-Calvo, et al. (2006). "Involvement of H- and N-Ras isoforms in transforming growth factor-beta1-induced proliferation and in collagen and fibronectin synthesis." Exp Cell Res 312(11): 2093-106.

Mason, C. S., C. J. Springer, et al. (1999). "Serine and tyrosine phosphorylations cooperate in Raf-1, but not B-Raf activation." EMBO J 18(8): 2137-48.

Massague, J. (1998). "TGF-beta signal transduction." Annu Rev Biochem 67: 753-91.

Massague, J. and F. Weis-Garcia (1996). "Serine/threonine kinase receptors: mediators of transforming growth factor beta family signals." Cancer Surv 27: 41-64.

Masszi, A., C. Di Ciano, et al. (2003). "Central role for Rho in TGF-beta1-induced alpha-smooth muscle actin expression during epithelial-mesenchymal transition." Am J Physiol Renal Physiol 284(5): F911-24.

Masterson, R., K. Kelynack, et al. (2006). "Effect of inhibition of farnesylation and geranylgeranylation on renal fibrogenesis in vitro." Nephron Exp Nephrol 102(1): e19-29.

Matsuo, S., J. M. Lopez-Guisa, et al. (2005). "Multifunctionality of PAI-1 in fibrogenesis: evidence from obstructive nephropathy in PAI-1-overexpressing mice." Kidney Int 67(6): 2221-38.

McCormick, F., G. A. Martin, et al. (1991). "Regulation of ras p21 by GTPase activating proteins." Cold Spring Harb Symp Quant Biol 56: 237-41.

McGlade, J., B. Brunkhorst, et al. (1993). "The N-terminal region of GAP regulates cytoskeletal structure and cell adhesion." EMBO J 12(8): 3073-81.

McKay, M. M. and D. K. Morrison (2007). "Integrating signals from RTKs to ERK/MAPK." Oncogene 26(22): 3113-21.

McMillan, J. I., J. W. Riordan, et al. (1996). "Characterization of a glomerular epithelial cell metalloproteinase as matrix metalloproteinase-9 with enhanced expression in a model of membranous nephropathy." J Clin Invest 97(4): 1094-101.

Medema, R. H., W. L. de Laat, et al. (1992). "GTPase-activating protein SH2-SH3 domains induce gene expression in a Ras-dependent fashion." Mol Cell Biol 12(8): 3425-30.

Menke, J., Y. Iwata, et al. (2009). "CSF-1 signals directly to renal tubular epithelial cells to mediate repair in mice." J Clin Invest 119(8): 2330-42.

Mezzano, S. A., M. A. Droguett, et al. (2000). "Overexpression of chemokines, fibrogenic cytokines, and myofibroblasts in human membranous nephropathy." Kidney Int 57(1): 147-58.

Mezzano, S. A., M. Ruiz-Ortega, et al. (2001). "Angiotensin II and renal fibrosis." Hypertension 38(3 Pt 2): 635-8.

Miao, L., Y. Dai, et al. (2002). "Mechanism of RhoA/Rho kinase activation in endothelin-1- induced contraction in rabbit basilar artery." Am J Physiol Heart Circ Physiol 283(3): H983-9.

Miao, W., L. Eichelberger, et al. (1996). "p120 Ras GTPase-activating protein interacts with Ras-GTP through specific conserved residues." J Biol Chem 271(26): 15322-9.

Milburn, M. V., L. Tong, et al. (1990). "Molecular switch for signal transduction: structural differences between active and inactive forms of protooncogenic ras proteins." Science 247(4945): 939-45.

Minden, A., A. Lin, et al. (1994). "Differential activation of ERK and JNK mitogen-activated protein kinases by Raf-1 and MEKK." Science 266(5191): 1719-23.

Mitch, W. E., M. Walser, et al. (1976). "A simple method of estimating progression of chronic renal failure." Lancet 2(7999): 1326-8.

Mitin, N. Y., M. B. Ramocki, et al. (2004). "Identification and characterization of rain, a novel Ras-interacting protein with a unique subcellular localization." J Biol Chem 279(21): 22353-61.

Miyajima, A., T. Asano, et al. (2001). "Tranilast ameliorates renal tubular damage in unilateral ureteral obstruction." J Urol 165(5): 1714-8.

Miyazono, K. (2009). "Transforming growth factor-beta signaling in epithelial-mesenchymal transition and progression of cancer." Proc Jpn Acad Ser B Phys Biol Sci 85(8): 314-23.

Mizui, M., Y. Isaka, et al. (2004). "Electroporation-mediated HGF gene transfer ameliorated cyclosporine nephrotoxicity." Kidney Int 65(6): 2041-53.

Mizuno, S., T. Kurosawa, et al. (1998). "Hepatocyte growth factor prevents renal fibrosis and dysfunction in a mouse model of chronic renal disease." J Clin Invest 101(9): 1827-34.

Mizuno, S., K. Matsumoto, et al. (2001). "Hepatocyte growth factor suppresses interstitial fibrosis in a mouse model of obstructive nephropathy." Kidney Int 59(4): 1304-14.

Mizuno, S. and T. Nakamura (2004). "Suppressions of chronic glomerular injuries and TGF-beta 1 production by HGF in attenuation of murine diabetic nephropathy." Am J Physiol Renal Physiol 286(1): F134-43.

Moeller, S., S. Gioberge, et al. (2002). "ESRD patients in 2001: global overview of patients, treatment modalities and development trends." Nephrol Dial Transplant 17(12): 2071-6.

Monia, B. P. (1997). "First- and second-generation antisense inhibitors targeted to human c-raf kinase: in vitro and in vivo studies." Anticancer Drug Des 12(5): 327-39.

Monia, B. P., J. F. Johnston, et al. (1996). "Antitumor activity of a phosphorothioate antisense oligodeoxynucleotide targeted against C-raf kinase." Nat Med 2(6): 668-75.

Mor, A., G. Keren, et al. (2008). "N-Ras or K-Ras inhibition increases the number and enhances the function of Foxp3 regulatory T cells." Eur J Immunol 38(6): 1493-502.

Mor, A., Y. Kloog, et al. (2009). "Ras inhibition increases the frequency and function of regulatory T cells and attenuates type-1 diabetes in non-obese diabetic mice." Eur J Pharmacol 616(1-3): 301-5.

Moreno-Bueno, G., H. Peinado, et al. (2009). "The morphological and molecular features of the epithelial-to-mesenchymal transition." Nat Protoc 4(11): 1591-613.

Moridaira, K., J. Morrissey, et al. (2003). "ACE inhibition increases expression of the ETB receptor in kidneys of mice with unilateral obstruction." Am J Physiol Renal Physiol 284(1): F209-17.

Morigi, M., D. Macconi, et al. (2002). "Protein overload-induced NF-kappaB activation in proximal tubular cells requires H(2)O(2) through a PKC-dependent pathway." J Am Soc Nephrol 13(5): 1179-89.

Morrison, A. R., F. Thornton, et al. (1981). "Thromboxane A2 is the major arachidonic acid metabolite of human cortical hydronephrotic tissue." Prostaglandins 21(3): 471-81.

Morrison, D. K. (2001). "KSR: a MAPK scaffold of the Ras pathway?" J Cell Sci 114(Pt 9): 1609-12.

Morrissey, J., K. Hruska, et al. (2002). "Bone morphogenetic protein-7 improves renal fibrosis and accelerates the return of renal function." J Am Soc Nephrol 13 Suppl 1: S14-21.

Mosser, D. M. and J. P. Edwards (2008). "Exploring the full spectrum of macrophage activation." Nat Rev Immunol 8(12): 958-69.

Mulder, K. M. (2000). "Role of Ras and Mapks in TGFbeta signaling." Cytokine Growth Factor Rev 11(1-2): 23-35.

Mulder, K. M. and S. L. Morris (1992). "Activation of p21ras by transforming growth factor beta in epithelial cells." J Biol Chem 267(8): 5029-31.

Muller, G. A. and H. P. Rodemann (1991). "Characterization of human renal fibroblasts in health and disease: I. Immunophenotyping of cultured tubular epithelial cells and fibroblasts derived from kidneys with histologically proven interstitial fibrosis." Am J Kidney Dis 17(6): 680-3.

Muller, G. A., M. Zeisberg, et al. (2000). "The importance of tubulointerstitial damage in progressive renal disease." Nephrol Dial Transplant 15 Suppl 6: 76-7.

Muller, R., D. J. Slamon, et al. (1983). "Transcription of c-onc genes c-rasKi and c-fms during mouse development." Mol Cell Biol 3(6): 1062-9.

Munger, J. S., X. Huang, et al. (1999). "The integrin alpha v beta 6 binds and activates latent TGF beta 1: a mechanism for regulating pulmonary inflammation and fibrosis." Cell **96**(3): 319-28.

Murai, H., M. Ikeda, et al. (1997). "Characterization of Ral GDP dissociation stimulator-like (RGL) activities to regulate c-fos promoter and the GDP/GTP exchange of Ral." J Biol Chem 272(16): 10483-90.

Murdoch, C., A. Giannoudis, et al. (2004). "Mechanisms regulating the recruitment of macrophages into hypoxic areas of tumors and other ischemic tissues." Blood 104(8): 2224-34.

Murdoch, C., A. Giannoudis, et al. (2004). "Mechanisms regulating the recruitment of macrophages into hypoxic areas of tumors and other ischemic tissues." Blood 104(8): 2224-34.

Murdoch, C., M. Muthana, et al. (2005). "Hypoxia regulates macrophage functions in inflammation." J Immunol 175(10): 6257-63.

Murphy, F. R., R. Issa, et al. (2002). "Inhibition of apoptosis of activated hepatic stellate cells by tissue inhibitor of metalloproteinase-1 is mediated via effects on matrix metalloproteinase inhibition: implications for reversibility of liver fibrosis." J Biol Chem 277(13): 11069-76.

Mustoe, T. A., G. F. Pierce, et al. (1987). "Accelerated healing of incisional wounds in rats induced by transforming growth factor-beta." Science 237(4820): 1333-6.

Nagase, H., R. Visse, et al. (2006). "Structure and function of matrix metalloproteinases and TIMPs." Cardiovasc Res 69(3): 562-73.

Nagatoya, K., T. Moriyama, et al. (2002). "Y-27632 prevents tubulointerstitial fibrosis in mouse kidneys with unilateral ureteral obstruction." Kidney Int 61(5): 1684-95.

Nakagawa, T., H. Y. Lan, et al. (2004). "Differential regulation of VEGF by TGF-beta and hypoxia in rat proximal tubular cells." Am J Physiol Renal Physiol 287(4): F658-64.

Nakamura, S., I. Nakamura, et al. (2000). "Plasminogen activator inhibitor-1 expression is regulated by the angiotensin type 1 receptor in vivo." Kidney Int 58(1): 251-9.

Nangaku, M. (2006). "Chronic hypoxia and tubulointerstitial injury: a final common pathway to end-stage renal failure." J Am Soc Nephrol 17(1): 17-25.

Nankivell, B. J., R. A. Boadle, et al. (1992). "Iron accumulation in human chronic renal disease." Am J Kidney Dis 20(6): 580-4.

Napoli, C., C. Lemieux, et al. (1990). "Introduction of a Chimeric Chalcone Synthase Gene into Petunia Results in Reversible Co-Suppression of Homologous Genes in trans." Plant Cell 2(4): 279-289.

Nassar, N., G. Horn, et al. (1995). "The 2.2 A crystal structure of the Ras-binding domain of the serine/threonine kinase c-Raf1 in complex with Rap1A and a GTP analogue." Nature 375(6532): 554-60.

Nath, K. A. (1992). "Tubulointerstitial changes as a major determinant in the progression of renal damage." Am J Kidney Dis 20(1): 1-17.

Nath, K. A. (1996). "Reshaping the interstitium by platelet-derived growth factor. Implications for progressive renal disease." Am J Pathol 148(4): 1031-6.

Navar, L. G. and P. G. Baer (1970). "Renal autoregulatory and glomerular filtration responses to gradated ureteral obstruction." Nephron 7(4): 301-16.

Nee, L. E., T. McMorrow, et al. (2004). "TNF-alpha and IL-1beta-mediated regulation of MMP-9 and TIMP-1 in renal proximal tubular cells." Kidney Int 66(4): 1376-86.

Ng, Y. Y., J. M. Fan, et al. (1999). "Glomerular epithelial-myofibroblast transdifferentiation in the evolution of glomerular crescent formation." Nephrol Dial Transplant 14(12): 2860-72.

Ng, Y. Y., T. P. Huang, et al. (1998). "Tubular epithelial-myofibroblast transdifferentiation in progressive tubulointerstitial fibrosis in 5/6 nephrectomized rats." Kidney Int 54(3): 864-76.

Nishida, M., H. Fujinaka, et al. (2002). "Absence of angiotensin II type 1 receptor in bone marrow-derived cells is detrimental in the evolution of renal fibrosis." J Clin Invest 110(12): 1859-68.

Nishida, M., Y. Okumura, et al. (2005). "Adoptive transfer of macrophages ameliorates renal fibrosis in mice." Biochem Biophys Res Commun 332(1): 11-6.

Nishitani, Y., M. Iwano, et al. (2005). "Fibroblast-specific protein 1 is a specific prognostic marker for renal survival in patients with IgAN." Kidney Int 68(3): 1078-85.

Noble, N. A., J. R. Harper, et al. (1992). "In vivo interactions of TGF-beta and extracellular matrix." Prog Growth Factor Res 4(4): 369-82.

Norman, J. T. and L. G. Fine (1999). "Progressive renal disease: fibroblasts, extracellular matrix, and integrins." Exp Nephrol 7(2): 167-77.

Norman, J. T., C. Orphanides, et al. (1999). "Hypoxia-induced changes in extracellular matrix metabolism in renal cells." Exp Nephrol 7(5-6): 463-9.

Nunes, I., J. Munger, et al. (1998). "Structure and activation of the large latent transforming growth factor-Beta complex." J Am Optom Assoc 69(10): 643-8.

Oda, T., Y. O. Jung, et al. (2001). "PAI-1 deficiency attenuates the fibrogenic response to ureteral obstruction." Kidney Int 60(2): 587-96.

Ogbureke, K. U. and L. W. Fisher (2005). "Renal expression of SIBLING proteins and their partner matrix metalloproteinases (MMPs)." Kidney Int 68(1): 155-66.

Okado, T., Y. Terada, et al. (2002). "Smad7 mediates transforming growth factor-beta-induced apoptosis in mesangial cells." Kidney Int 62(4): 1178-86.

Okunishi, K., M. Dohi, et al. (2005). "A novel role of hepatocyte growth factor as an immune regulator through suppressing dendritic cell function." J Immunol 175(7): 4745-53.

Oldfield, M. D., L. A. Bach, et al. (2001). "Advanced glycation end products cause epithelial-myofibroblast transdifferentiation via the receptor for advanced glycation end products (RAGE)." J Clin Invest 108(12): 1853-63.

Oliver, J. A., J. Barasch, et al. (2002). "Metanephric mesenchyme contains embryonic renal stem cells." Am J Physiol Renal Physiol 283(4): F799-809.

Olmeda, D., M. Jorda, et al. (2007). "Snail silencing effectively suppresses tumour growth and invasiveness." Oncogene 26(13): 1862-74.

Orphanides, C., L. G. Fine, et al. (1997). "Hypoxia stimulates proximal tubular cell matrix production via a TGF-beta1-independent mechanism." Kidney Int 52(3): 637-47.

Otto, J. C., E. Kim, et al. (1999). "Cloning and characterization of a mammalian prenyl protein-specific protease." J Biol Chem 274(13): 8379-82.

Ovchinnikov, D. A. (2008). "Macrophages in the embryo and beyond: much more than just giant phagocytes." Genesis 46(9): 447-62.

Overall, C. M., J. L. Wrana, et al. (1989). "Independent regulation of collagenase, 72-kDa progelatinase, and metalloendoproteinase inhibitor expression in human fibroblasts by transforming growth factor-beta." J Biol Chem 264(3): 1860-9.

Parada, L. F., C. J. Tabin, et al. (1982). "Human EJ bladder carcinoma oncogene is homologue of Harvey sarcoma virus ras gene." Nature 297(5866): 474-8.

Patel, S., K. I. Takagi, et al. (2005). "RhoGTPase activation is a key step in renal epithelial mesenchymal transdifferentiation." J Am Soc Nephrol 16(7): 1977-84.

Patil, S. D., D. G. Rhodes, et al. (2005). "DNA-based therapeutics and DNA delivery systems: a comprehensive review." Aaps J 7(1): E61-77.

Peinado, H., D. Olmeda, et al. (2007). "Snail, Zeb and bHLH factors in tumour progression: an alliance against the epithelial phenotype?" Nat Rev Cancer 7(6): 415-28.

Perico, N., I. Codreanu, et al. (2005). "Prevention of progression and remission/regression strategies for chronic renal diseases: can we do better now than five years ago?" Kidney Int Suppl(98): S21-4.

Peterson, J. C., S. Adler, et al. (1995). "Blood pressure control, proteinuria, and the progression of renal disease. The Modification of Diet in Renal Disease Study." Ann Intern Med 123(10): 754-62.

Phanish, M. K., N. A. Wahab, et al. (2006). "The differential role of Smad2 and Smad3 in the regulation of pro-fibrotic TGFbeta1 responses in human proximal-tubule epithelial cells." Biochem J 393(Pt 2): 601-7.

Phanish, M. K., N. A. Wahab, et al. (2005). "TGF-beta1-induced connective tissue growth factor (CCN2) expression in human renal proximal tubule epithelial cells requires Ras/MEK/ERK and Smad signalling." Nephron Exp Nephrol 100(4): e156-65.

Pichler, R. H., C. Hugo, et al. (1996). "SPARC is expressed in renal interstitial fibrosis and in renal vascular injury." Kidney Int 50(6): 1978-89.

Pille, J. Y., H. Li, et al. (2006). "Intravenous delivery of anti-RhoA small interfering RNA loaded in nanoparticles of chitosan in mice: safety and efficacy in xenografted aggressive breast cancer." Hum Gene Ther 17(10): 1019-26.

Plowman, S. J., D. J. Williamson, et al. (2003). "While K-ras is essential for mouse development, expression of the K-ras 4A splice variant is dispensable." Mol Cell Biol 23(24): 9245-50.

Polakis, P. and F. McCormick (1993). "Structural requirements for the interaction of p21ras with GAP, exchange factors, and its biological effector target." J Biol Chem 268(13): 9157-60.

Potenza, N., C. Vecchione, et al. (2005). "Replacement of K-Ras with H-Ras supports normal embryonic development despite inducing cardiovascular pathology in adult mice." EMBO Rep 6(5): 432-7.

Poulsom, R., S. J. Forbes, et al. (2001). "Bone marrow contributes to renal parenchymal turnover and regeneration." J Pathol 195(2): 229-35.

Pozzi, A., K. K. Wary, et al. (1998). "Integrin alpha1beta1 mediates a unique collagen-dependent proliferation pathway in vivo." J Cell Biol 142(2): 587-94.

Pozzi, A. and R. Zent (2003). "Integrins: sensors of extracellular matrix and modulators of cell function." Nephron Exp Nephrol 94(3): e77-84.

Prior, I. A. and J. F. Hancock (2001). "Compartmentalization of Ras proteins." J Cell Sci 114(Pt 9): 1603-8.

Prior, I. A., A. Harding, et al. (2001). "GTP-dependent segregation of H-ras from lipid rafts is required for biological activity." Nat Cell Biol 3(4): 368-75.

Prior, I. A., C. Muncke, et al. (2003). "Direct visualization of Ras proteins in spatially distinct cell surface microdomains." J Cell Biol 160(2): 165-70.

Provoost, A. P. and J. C. Molenaar (1981). "Renal function during and after a temporary complete unilateral ureter obstruction in rats." Invest Urol 18(4): 242-6.

Pulkkinen, K., S. Murugan, et al. (2008). "Wnt signaling in kidney development and disease." Organogenesis 4(2): 55-9.

Purkerson, M. L. and S. Klahr (1989). "Prior inhibition of vasoconstrictors normalizes GFR in postobstructed kidneys." Kidney Int 35(6): 1305-14.

Qi, W., X. Chen, et al. (2006). "The renal cortical fibroblast in renal tubulointerstitial fibrosis." Int J Biochem Cell Biol 38(1): 1-5.

Quilliam, L. A., M. M. Hisaka, et al. (1996). "Involvement of the switch 2 domain of Ras in its interaction with guanine nucleotide exchange factors." J Biol Chem 271(19): 11076-82.

Rae, F., K. Woods, et al. (2007). "Characterisation and trophic functions of murine embryonic macrophages based upon the use of a Csf1r-EGFP transgene reporter." Dev Biol 308(1): 232-46.

Ramos, J. W. (2008). "The regulation of extracellular signal-regulated kinase (ERK) in mammalian cells." Int J Biochem Cell Biol 40(12): 2707-19.

Rangan, G. K., Y. Wang, et al. (1999). "Inhibition of nuclear factor-kappaB activation reduces cortical tubulointerstitial injury in proteinuric rats." Kidney Int 56(1): 118-34.

Rappaport, J., B. Hanss, et al. (1995). "Transport of phosphorothioate oligonucleotides in kidney: implications for molecular therapy." Kidney Int 47(5): 1462-9.

Rastaldi, M. P., F. Ferrario, et al. (2002). "Epithelial-mesenchymal transition of tubular epithelial cells in human renal biopsies." Kidney Int 62(1): 137-46.

Regnier, V., A. Tahiri, et al. (2000). "Electroporation-mediated delivery of 3'-protected phosphodiester oligodeoxynucleotides to the skin." J Control Release 67(2-3): 337-46.

Reich, S. J., J. Fosnot, et al. (2003). "Small interfering RNA (siRNA) targeting VEGF effectively inhibits ocular neovascularization in a mouse model." Mol Vis 9: 210-6.

Reif, K., C. D. Nobes, et al. (1996). "Phosphatidylinositol 3-kinase signals activate a selective subset of Rac/Rho-dependent effector pathways." Curr Biol 6(11): 1445-55.

Reif, S., B. Weis, et al. (1999). "The Ras antagonist, farnesylthiosalicylic acid (FTS), inhibits experimentally-induced liver cirrhosis in rats." J Hepatol 31(6): 1053-61.

Remuzzi, G., C. Chiurchiu, et al. (2004). "Proteinuria predicting outcome in renal disease: nondiabetic nephropathies (REIN)." Kidney Int Suppl(92): S90-6.

Rerolle, J. P., A. Hertig, et al. (2000). "Plasminogen activator inhibitor type 1 is a potential target in renal fibrogenesis." Kidney Int 58(5): 1841-50.

Ricardo, S. D., H. van Goor, et al. (2008). "Macrophage diversity in renal injury and repair." J Clin Invest 118(11): 3522-30.

Ridley, A. J. (1995). "Rho-related proteins: actin cytoskeleton and cell cycle." Curr Opin Genet Dev 5(1): 24-30.

Riely, G. J., M. L. Johnson, et al. "A phase II trial of Salirasib in patients with lung adenocarcinomas with KRAS mutations." J Thorac Oncol 6(8): 1435-7.

Robinson, M. J. and M. H. Cobb (1997). "Mitogen-activated protein kinase pathways." Curr Opin Cell Biol 9(2): 180-6.

Roberts, J., E. Palma, et al. (2006). "Efficient and persistent splice switching by systemically delivered LNA oligonucleotides in mice." Mol Ther 14(4): 471-5.

Rodriguez-Pena, A. B., M. T. Grande, et al. (2008). "Activation of Erk1/2 and Akt following unilateral ureteral obstruction." Kidney Int 74(2): 196-209.

Rodriguez-Viciana, P., P. H. Warne, et al. (1994). "Phosphatidylinositol-3-OH kinase as a direct target of Ras." Nature 370(6490): 527-32.

Rogers, K. K., T. S. Jou, et al. (2003). "The Rho family of small GTPases is involved in epithelial cystogenesis and tubulogenesis." Kidney Int 63(5): 1632-44.

Rosenbaum, J., S. Blazejewski, et al. (1995). "Fibroblast growth factor 2 and transforming growth factor beta 1 interactions in human liver myofibroblasts." Gastroenterology 109(6): 1986-96.

Ross, R., N. B. Everett, et al. (1970). "Wound healing and collagen formation. VI. The origin of the wound fibroblast studied in parabiosis." J Cell Biol 44(3): 645-54.

Rotblat, B., I. A. Prior, et al. (2004). "Three separable domains regulate GTP-dependent association of H-ras with the plasma membrane." Mol Cell Biol 24(15): 6799-810.

Roufosse, C., G. Bou-Gharios, et al. (2006). "Bone marrow-derived cells do not contribute significantly to collagen I synthesis in a murine model of renal fibrosis." J Am Soc Nephrol 17(3): 775-82.

Roy, M. O., R. Leventis, et al. (2000). "Mutational and biochemical analysis of plasma membrane targeting mediated by the farnesylated, polybasic carboxy terminus of K-ras4B." Biochemistry 39(28): 8298-307.

Roy, S., R. Luetterforst, et al. (1999). "Dominant-negative caveolin inhibits H-Ras function by disrupting cholesterol-rich plasma membrane domains." Nat Cell Biol 1(2): 98-105.

Roy, S., B. Wyse, et al. (2002). "H-Ras signaling and K-Ras signaling are differentially dependent on endocytosis." Mol Cell Biol 22(14): 5128-40.

Roy-Chaudhury, P., G. Hillis, et al. (1997). "Importance of the tubulointerstitium in human glomerulonephritis. II. Distribution of integrin chains beta 1, alpha 1 to 6 and alpha V." Kidney Int 52(1): 103-10.

Rudin, C. M., J. Holmlund, et al. (2001). "Phase I Trial of ISIS 5132, an antisense oligonucleotide inhibitor of c-raf-1, administered by 24-hour weekly infusion to patients with advanced cancer." Clin Cancer Res 7(5): 1214-20.

Rudin, C. M., J. L. Marshall, et al. (2004). "Delivery of a liposomal c-raf-1 antisense oligonucleotide by weekly bolus dosing in patients with advanced solid tumors: a phase I study." Clin Cancer Res 10(21): 7244-51.

Ruiz-Ortega, M. and J. Egido (1997). "Angiotensin II modulates cell growth-related events and synthesis of matrix proteins in renal interstitial fibroblasts." Kidney Int 52(6): 1497-510.

Russell, M., C. A. Lange-Carter, et al. (1995). "Direct interaction between Ras and the kinase domain of mitogen-activated protein kinase kinase kinase (MEKK1)." J Biol Chem 270(20): 11757-60.

Russo, L. M., E. del Re, et al. (2007). "Evidence for a role of transforming growth factor (TGF)-beta1 in the induction of postglomerular albuminuria in diabetic nephropathy: amelioration by soluble TGF-beta type II receptor." Diabetes 56(2): 380-8.

Rutherford, W. E., J. Blondin, et al. (1977). "Chronic progressive renal disease: rate of change of serum creatinine concentration." Kidney Int 11(1): 62-70.

Sabbatini, M., A. Pisani, et al. (2004). "Atorvastatin improves the course of ischemic acute renal failure in aging rats." J Am Soc Nephrol 15(4): 901-9.

Safina, A. F., A. E. Varga, et al. (2009). "Ras alters epithelial-mesenchymal transition in response to TGFbeta by reducing actin fibers and cell-matrix adhesion." Cell Cycle 8(2): 284-98.

Sakai, N., K. Furuichi, et al. (2010) "Fibrocytes are involved in the pathogenesis of human chronic kidney disease." Hum Pathol 41(5): 672-8.

Sampson, N. S., S. T. Ryan, et al. (2001). "Global gene expression analysis reveals a role for the alpha 1 integrin in renal pathogenesis." J Biol Chem 276(36): 34182-8.

Sands, H., L. J. Gorey-Feret, et al. (1994). "Biodistribution and metabolism of internally 3H-labeled oligonucleotides. I. Comparison of a phosphodiester and a phosphorothioate." Mol Pharmacol 45(5): 932-43.

Santini, D., S. Galluzzo, et al. "Should oncologists be aware in their clinical practice of KRAS molecular analysis?" J Clin Oncol 29(8): e206-7; author reply e208-9.

Santos, E. and A. R. Nebreda (1989). "Structural and functional properties of ras proteins." FASEB J 3(10): 2151-63.

Satoh, M., N. Kashihara, et al. (2001). "Renal interstitial fibrosis is reduced in angiotensin II type 1a receptor-deficient mice." J Am Soc Nephrol 12(2): 317-25.

Schaber, M. D., V. M. Garsky, et al. (1989). "Ras interaction with the GTPase-activating protein (GAP)." Proteins 6(3): 306-15.

Scheffler, J. E., D. S. Waugh, et al. (1994). "Characterization of a 78-residue fragment of c-Raf-1 that comprises a minimal binding domain for the interaction with Ras-GTP." J Biol Chem 269(35): 22340-6.

Scheffzek, K., M. R. Ahmadian, et al. (1997). "The Ras-RasGAP complex: structural basis for GTPase activation and its loss in oncogenic Ras mutants." Science 277(5324): 333-8.

Scheffzek, K., A. Lautwein, et al. (1996). "Crystal structure of the GTPase-activating domain of human p120GAP and implications for the interaction with Ras." Nature 384(6609): 591-6.

Scheidegger, K. J., S. Butler, et al. (1997). "Angiotensin II increases macrophage-mediated modification of low density lipoprotein via a lipoxygenase-dependent pathway." J Biol Chem 272(34): 21609-15.

Schlaepfer, D. D., S. K. Hanks, et al. (1994). "Integrin-mediated signal transduction linked to Ras pathway by GRB2 binding to focal adhesion kinase." Nature 372(6508): 786-91.

Schlaepfer, D. D. and T. Hunter (1996). "Evidence for in vivo phosphorylation of the Grb2 SH2-domain binding site on focal adhesion kinase by Src-family protein-tyrosine kinases." Mol Cell Biol 16(10): 5623-33.

Schreiner, G. F., K. P. Harris, et al. (1988). "Immunological aspects of acute ureteral obstruction: immune cell infiltrate in the kidney." Kidney Int 34(4): 487-93.

Schwartz, J. C., S. T. Younger, et al. (2008). "Antisense transcripts are targets for activating small RNAs." Nat Struct Mol Biol 15(8): 842-8.

Scolnick, E. M., E. Rands, et al. (1973). "Studies on the nucleic acid sequences of Kirsten sarcoma virus: a model for formation of a mammalian RNA-containing sarcoma virus." J Virol 12(3): 458-63.

Seccia, T. M., C. Maniero, et al. (2008). "Role of angiotensin II, endothelin-1 and L-type calcium channel in the development of glomerular, tubulointerstitial and perivascular fibrosis." J Hypertens 26(10): 2022-9.

Sermon, B. A., P. N. Lowe, et al. (1998). "The importance of two conserved arginine residues for catalysis by the ras GTPase-activating protein, neurofibromin." J Biol Chem 273(16): 9480-5.

Seron, D., E. Alexopoulos, et al. (1990). "Number of interstitial capillary cross-sections assessed by monoclonal antibodies: relation to interstitial damage." Nephrol Dial Transplant 5(10): 889-93.

Shah, M., D. M. Foreman, et al. (1995). "Neutralisation of TGF-beta 1 and TGF-beta 2 or exogenous addition of TGF-beta 3 to cutaneous rat wounds reduces scarring." J Cell Sci 108 (Pt 3): 985-1002.

Shao, D. D., R. Suresh, et al. (2008). "Pivotal Advance: Th-1 cytokines inhibit, and Th-2 cytokines promote fibrocyte differentiation." J Leukoc Biol 83(6): 1323-33.

Sharpe, C. C., M. E. Dockrell, et al. (2000). "Role of Ras isoforms in the stimulated proliferation of human renal fibroblasts in primary culture." J Am Soc Nephrol 11(9): 1600-6.

Sharpe, C. C., M. E. Dockrell, et al. (1999). "Evidence of a role for Ki-Ras in the stimulated proliferation of renal fibroblasts." J Am Soc Nephrol 10(6): 1186-92.

Shields, J. M., K. Pruitt, et al. (2000). "Understanding Ras: 'it ain't over 'til it's over'." Trends Cell Biol 10(4): 147-54.

Shihab, F. S., W. M. Bennett, et al. (2002). "Pirfenidone treatment decreases transforming growth factor-beta1 and matrix proteins and ameliorates fibrosis in chronic cyclosporine nephrotoxicity." Am J Transplant 2(2): 111-9.

Shimizu, H., Y. Hori, et al. "siRNA-based therapy ameliorates glomerulonephritis." J Am Soc Nephrol 21(4): 622-33.

Shimizu, K., M. Goldfarb, et al. (1983). "Isolation and preliminary characterization of the transforming gene of a human neuroblastoma cell line." Proc Natl Acad Sci U S A 80(2): 383-7.

Shimizu, K., M. Goldfarb, et al. (1983). "Three human transforming genes are related to the viral ras oncogenes." Proc Natl Acad Sci U S A 80(8): 2112-6.

Shinozaki, M., S. Kawara, et al. (1997). "Induction of subcutaneous tissue fibrosis in newborn mice by transforming growth factor beta--simultaneous application with basic fibroblast growth factor causes persistent fibrosis." Biochem Biophys Res Commun 240(2): 292-7.

Shirouzu, M., H. Koide, et al. (1994). "Mutations that abolish the ability of Ha-Ras to associate with Raf-1." Oncogene 9(8): 2153-7.

Siegel, P. M. and J. Massague (2003). "Cytostatic and apoptotic actions of TGF-beta in homeostasis and cancer." Nat Rev Cancer 3(11): 807-21.

Sigal, I. S., J. B. Gibbs, et al. (1986). "Identification of effector residues and a neutralizing epitope of Ha-ras-encoded p21." Proc Natl Acad Sci U S A 83(13): 4725-9.

Skorski, T., C. Szczylik, et al. (1992). "Growth factor-dependent inhibition of normal hematopoiesis by N-ras antisense oligodeoxynucleotides." J Exp Med 175(3): 743-50.

Sledz, C. A., M. Holko, et al. (2003). "Activation of the interferon system by short-interfering RNAs." Nat Cell Biol 5(9): 834-9.

Sledz, C. A. and B. R. Williams (2004). "RNA interference and double-stranded-RNA-activated pathways." Biochem Soc Trans 32(Pt 6): 952-6.

Smith, M. R., S. J. DeGudicibus, et al. (1986). "Requirement for c-ras proteins during viral oncogene transformation." Nature 320(6062): 540-3.

Smotrys, J. E. and M. E. Linder (2004). "Palmitoylation of intracellular signaling proteins: regulation and function." Annu Rev Biochem 73: 559-87.

Socha, M. J., M. Manhiani, et al. (2007). "Secreted protein acidic and rich in cysteine deficiency ameliorates renal inflammation and fibrosis in angiotensin hypertension." Am J Pathol 171(4): 1104-12.

Sorrell, J. M. and A. I. Caplan (2009). "Fibroblasts-a diverse population at the center of it all." Int Rev Cell Mol Biol 276: 161-214.

Soutschek, J., A. Akinc, et al. (2004). "Therapeutic silencing of an endogenous gene by systemic administration of modified siRNAs." Nature 432(7014): 173-8.

Stadler, W. M. (2005). "Targeted agents for the treatment of advanced renal cell carcinoma." Cancer 104(11): 2323-33.

Stephenson, M. L. and P. C. Zamecnik (1978). "Inhibition of Rous sarcoma viral RNA translation by a specific oligodeoxyribonucleotide." Proc Natl Acad Sci U S A 75(1): 285-8.

Stevenson, J. P., K. S. Yao, et al. (1999). "Phase I clinical/pharmacokinetic and pharmacodynamic trial of the c-raf-1 antisense oligonucleotide ISIS 5132 (CGP 69846A)." J Clin Oncol 17(7): 2227-36.

Stokoe, D., S. G. Macdonald, et al. (1994). "Activation of Raf as a result of recruitment to the plasma membrane." Science 264(5164): 1463-7.

Stratton, R., V. Rajkumar, et al. (2002). "Prostacyclin derivatives prevent the fibrotic response to TGF-beta by inhibiting the Ras/MEK/ERK pathway." FASEB J 16(14): 1949-51.

Strumberg, D., H. Richly, et al. (2005). "Phase I clinical and pharmacokinetic study of the Novel Raf kinase and vascular endothelial growth factor receptor inhibitor BAY 43-9006 in patients with advanced refractory solid tumors." J Clin Oncol 23(5): 965-72.

Strutz, F. and G. A. Muller (1995). "On the progression of chronic renal disease." Nephron 69(4): 371-9.

Strutz, F., H. Okada, et al. (1995). "Identification and characterization of a fibroblast marker: FSP1." J Cell Biol 130(2): 393-405.

Strutz, F., M. Zeisberg, et al. (2000). "Basic fibroblast growth factor expression is increased in human renal fibrogenesis and may mediate autocrine fibroblast proliferation." Kidney Int 57(4): 1521-38.

Strutz, F., M. Zeisberg, et al. (2001). "TGF-beta 1 induces proliferation in human renal fibroblasts via induction of basic fibroblast growth factor (FGF-2)." Kidney Int 59(2): 579-92.

Strutz, F., M. Zeisberg, et al. (2002). "Role of basic fibroblast growth factor-2 in epithelial-mesenchymal transformation." Kidney Int 61(5): 1714-28.

Sugimoto, H., G. Grahovac, et al. (2007). "Renal fibrosis and glomerulosclerosis in a new mouse model of diabetic nephropathy and its regression by bone morphogenic protein-7 and advanced glycation end product inhibitors." Diabetes 56(7): 1825-33.

Sullivan, K. M., H. P. Lorenz, et al. (1995). "A model of scarless human fetal wound repair is deficient in transforming growth factor beta." J Pediatr Surg 30(2): 198-202; discussion 202-3.

Sundaram, M. V. (2006). "RTK/Ras/MAPK signaling." WormBook: 1-19.

Sunderkotter, C., T. Nikolic, et al. (2004). "Subpopulations of mouse blood monocytes differ in maturation stage and inflammatory response." J Immunol 172(7): 4410-7.

Surendran, K., S. Schiavi, et al. (2005). "Wnt-dependent beta-catenin signaling is activated after unilateral ureteral obstruction, and recombinant secreted frizzled-

related protein 4 alters the progression of renal fibrosis." J Am Soc Nephrol 16(8): 2373-84.

Suzuki, D., M. Miyazaki, et al. (1997). "In situ hybridization studies of matrix metalloproteinase-3, tissue inhibitor of metalloproteinase-1 and type IV collagen in diabetic nephropathy." Kidney Int 52(1): 111-9.

Svensson, A. W., P. J. Casey, et al. (2006). "Genetic and pharmacologic analyses of the role of Icmt in Ras membrane association and function." Methods Enzymol 407: 144-59.

Takabatake, Y., Y. Isaka, et al. (2005). "Exploring RNA interference as a therapeutic strategy for renal disease." Gene Ther 12(12): 965-73.

Taneda, S., K. L. Hudkins, et al. (2003). "Obstructive uropathy in mice and humans: potential role for PDGF-D in the progression of tubulointerstitial injury." J Am Soc Nephrol 14(10): 2544-55.

Taneda, S., J. W. Pippin, et al. (2003). "Amelioration of diabetic nephropathy in SPARC-null mice." J Am Soc Nephrol 14(4): 968-80.

Tang, S., J. C. Leung, et al. (2003). "Albumin stimulates interleukin-8 expression in proximal tubular epithelial cells in vitro and in vivo." J Clin Invest 111(4): 515-27.

Tang, W. H., H. Friess, et al. (1998). "Activation of the serine proteinase system in chronic kidney rejection." Transplantation 65(12): 1628-34.

Tang, W. W., T. R. Ulich, et al. (1996). "Platelet-derived growth factor-BB induces renal tubulointerstitial myofibroblast formation and tubulointerstitial fibrosis." Am J Pathol 148(4): 1169-80.

Taniguchi, Y., N. Yorioka, et al. (1997). "Localization of hepatocyte growth factor and tubulointerstitial lesions in IgA nephropathy." Am J Nephrol 17(5): 413-6.

Temsamani, J., G. S. Pari, et al. (1997). "Antisense approach for the treatment of cytomegalovirus infection." Expert Opin Investig Drugs 6(9): 1157-67.

Terai, K. and M. Matsuda (2005). "Ras binding opens c-Raf to expose the docking site for mitogen-activated protein kinase kinase." EMBO Rep 6(3): 251-5.

Tesch, G. H., S. Maifert, et al. (1999). "Monocyte chemoattractant protein 1-dependent leukocytic infiltrates are responsible for autoimmune disease in MRL-Fas(lpr) mice." J Exp Med 190(12): 1813-24.

Tesch, G. H., D. J. Nikolic-Paterson, et al. (1998). "Rat mesangial cells express macrophage migration inhibitory factor in vitro and in vivo." J Am Soc Nephrol 9(3): 417-24.

Tesch, G. H., A. Schwarting, et al. (1999). "Monocyte chemoattractant protein-1 promotes macrophage-mediated tubular injury, but not glomerular injury, in nephrotoxic serum nephritis." J Clin Invest 103(1): 73-80.

Therrien, M., N. R. Michaud, et al. (1996). "KSR modulates signal propagation within the MAPK cascade." Genes Dev 10(21): 2684-95.

Thiery, J. P. (2003). "Epithelial-mesenchymal transitions in development and pathologies." Curr Opin Cell Biol 15(6): 740-6.

Thissen, J. A., J. M. Gross, et al. (1997). "Prenylation-dependent association of Ki-Ras with microtubules. Evidence for a role in subcellular trafficking." J Biol Chem 272(48): 30362-70.

Thorgeirsson, S. S. and J. W. Grisham (2006). "Hematopoietic cells as hepatocyte stem cells: a critical review of the evidence." Hepatology 43(1): 2-8.

Tillman, L. G., R. S. Geary, et al. (2008). "Oral delivery of antisense oligonucleotides in man." J Pharm Sci 97(1): 225-36.

Tomasek, J. J., G. Gabbiani, et al. (2002). "Myofibroblasts and mechano-regulation of connective tissue remodelling." Nat Rev Mol Cell Biol 3(5): 349-63.

Tomooka, S., W. A. Border, et al. (1992). "Glomerular matrix accumulation is linked to inhibition of the plasmin protease system." Kidney Int 42(6): 1462-9.

Trahey, M. and F. McCormick (1987). "A cytoplasmic protein stimulates normal N-ras p21 GTPase, but does not affect oncogenic mutants." Science 238(4826): 542-5.

Traynor, K. (2002). "Antisense drugs progressing through product pipelines." Am J Health Syst Pharm 59(21): 2046-7.

Trebicka, J., M. Hennenberg, et al. (2007). "Atorvastatin lowers portal pressure in cirrhotic rats by inhibition of RhoA/Rho-kinase and activation of endothelial nitric oxide synthase." Hepatology 46(1): 242-53.

Trevillian, P., H. Paul, et al. (2004). "alpha(v)beta(6) Integrin expression in diseased and transplanted kidneys." Kidney Int **66**(4): 1423-33.

Truong, L. D., Y. J. Choi, et al. (2001). "Renal cell apoptosis in chronic obstructive uropathy: the roles of caspases." Kidney Int 60(3): 924-34.

Truong, L. D., G. Petrusevska, et al. (1996). "Cell apoptosis and proliferation in experimental chronic obstructive uropathy." Kidney Int 50(1): 200-7.

Tse, J. C. and R. Kalluri (2007). "Mechanisms of metastasis: epithelial-to-mesenchymal transition and contribution of tumor microenvironment." J Cell Biochem 101(4): 816-29.

Tzivion, G., Z. Luo, et al. (1998). "A dimeric 14-3-3 protein is an essential cofactor for Raf kinase activity." Nature 394(6688): 88-92.

Uchio, K., M. Graham, et al. (2004). "Down-regulation of connective tissue growth factor and type I collagen mRNA expression by connective tissue growth factor antisense oligonucleotide during experimental liver fibrosis." Wound Repair Regen 12(1): 60-6.

Uchio-Yamada, K., N. Manabe, et al. (2005). "Decreased expression of matrix metalloproteinases and tissue inhibitors of metalloproteinase in the kidneys of hereditary nephrotic (ICGN) mice." J Vet Med Sci 67(1): 35-41.

Umanoff, H., W. Edelmann, et al. (1995). "The murine N-ras gene is not essential for growth and development." Proc Natl Acad Sci U S A 92(5): 1709-13.

van der Geer, P., T. Hunter, et al. (1994). "Receptor protein-tyrosine kinases and their signal transduction pathways." Annu Rev Cell Biol 10: 251-337.

Vaughan, E. D., Jr., J. H. Shenasky, 2nd, et al. (1971). "Mechanism of acute hemodynamic response to ureteral occlusion." Invest Urol 9(2): 109-18.

Vignery, A. (2005). "Macrophage fusion: are somatic and cancer cells possible partners?" Trends Cell Biol 15(4): 188-93.

Voice, J. K., R. L. Klemke, et al. (1999). "Four human ras homologs differ in their abilities to activate Raf-1, induce transformation, and stimulate cell motility." J Biol Chem 274(24): 17164-70.

Vrtovsnik, F., S. Couette, et al. (1997). "Lovastatin-induced inhibition of renal epithelial tubular cell proliferation involves a p21ras activated, AP-1-dependent pathway." Kidney Int 52(4): 1016-27.

Wada, T., N. Sakai, et al. (2007). "Fibrocytes: a new insight into kidney fibrosis." Kidney Int 72(3): 269-73.

Walton, G., R. Buttyan, et al. (1992). "Renal growth factor expression during the early phase of experimental hydronephrosis." J Urol 148(2 Pt 2): 510-4.

Wang, J. H., B. M. Hendry, et al. (2008). "Silencing genes in the kidney: antisense or RNA interference?" Nephrol Dial Transplant 23(7): 2115-8.

Wang, S., M. de Caestecker, et al. (2006). "Renal bone morphogenetic protein-7 protects against diabetic nephropathy." J Am Soc Nephrol 17(9): 2504-12.

Wang, S., M. Denichilo, et al. (2001). "Connective tissue growth factor in tubulointerstitial injury of diabetic nephropathy." Kidney Int 60(1): 96-105.

Wang, S., G. M. Mitu, et al. (2008). "Osmotic polyuria: an overlooked mechanism in diabetic nephropathy." Nephrol Dial Transplant 23(7): 2167-72.

Wang, S. N. and R. Hirschberg (1999). "Tubular epithelial cell activation and interstitial fibrosis. The role of glomerular ultrafiltration of growth factors in the nephrotic syndrome and diabetic nephropathy." Nephrol Dial Transplant 14(9): 2072-4.

Wang, S. N., J. Lapage, et al. (1999). "Glomerular ultrafiltration and apical tubular action of IGF-I, TGF-beta, and HGF in nephrotic syndrome." Kidney Int 56(4): 1247-51.

Wang, Y., J. Chen, et al. (1997). "Induction of monocyte chemoattractant protein-1 in proximal tubule cells by urinary protein." J Am Soc Nephrol 8(10): 1537-45.

Wang, Y., Y. P. Wang, et al. (2007). "Ex vivo programmed macrophages ameliorate experimental chronic inflammatory renal disease." Kidney Int 72(3): 290-9.

Warne, P. H., P. R. Viciana, et al. (1993). "Direct interaction of Ras and the amino-terminal region of Raf-1 in vitro." Nature 364(6435): 352-5.

Watts, K. L. and M. A. Spiteri (2004). "Connective tissue growth factor expression and induction by transforming growth factor-beta is abrogated by simvastatin via a Rho signaling mechanism." Am J Physiol Lung Cell Mol Physiol 287(6): L1323-32.

Weber, J. D., D. M. Raben, et al. (1997). "Sustained activation of extracellular-signal-regulated kinase 1 (ERK1) is required for the continued expression of cyclin D1 in G1 phase." Biochem J 326 (Pt 1): 61-8.

White, D. P., P. T. Caswell, et al. (2007). "alpha v beta3 and alpha5beta1 integrin recycling pathways dictate downstream Rho kinase signaling to regulate persistent cell migration." J Cell Biol 177(3): 515-25.

Whyte, D. B., P. Kirschmeier, et al. (1997). "K- and N-Ras are geranylgeranylated in cells treated with farnesyl protein transferase inhibitors." J Biol Chem 272(22): 14459-64.

Wiggins, R., M. Goyal, et al. (1993). "Vascular adventitial cell expression of collagen I messenger ribonucleic acid in anti-glomerular basement membrane antibody-induced crescentic nephritis in the rabbit. A cellular source for interstitial collagen synthesis in inflammatory renal disease." Lab Invest 68(5): 557-65.

Willenbring, H., A. S. Bailey, et al. (2004). "Myelomonocytic cells are sufficient for therapeutic cell fusion in liver." Nat Med 10(7): 744-8.

Williams, S. A. and J. S. Buzby (2000). "Cell-specific optimization of phosphorothioate antisense oligodeoxynucleotide delivery by cationic lipids." Methods Enzymol 313: 388-97.

Willumsen, B. M., A. Christensen, et al. (1984). "The p21 ras C-terminus is required for transformation and membrane association." Nature 310(5978): 583-6.

Wilson, D. R. (1972). "Micropuncture study of chronic obstructive nephropathy before and after release of obstruction." Kidney Int 2(3): 119-30.

Wilson, H. M., N. E. Haites, et al. (1996). "Interleukin-1 beta up-regulates the plasminogen activator/plasmin system in human mesangial cells." Kidney Int 49(4): 1097-104.

Wilson, H. M., F. J. Reid, et al. (1995). "Transforming growth factor beta (TGF-beta) regulates the matrix-associated plasminogen activator inhibitor 1 (PAI-1) in glomerular mesangial and epithelial cells." Exp Nephrol 3(2): 141-2.

Wilson, H. M., D. Walbaum, et al. (2004). "Macrophages and the kidney." Curr Opin Nephrol Hypertens 13(3): 285-90.

Winkler, J., M. Stessl, et al. "Off-target effects related to the phosphorothioate modification of nucleic acids." ChemMedChem 5(8): 1344-52.

Wittinghofer, A. and E. F. Pai (1991). "The structure of Ras protein: a model for a universal molecular switch." Trends Biochem Sci 16(10): 382-7.

Wittinghofer, A., K. Scheffzek, et al. (1997). "The interaction of Ras with GTPase-activating proteins." FEBS Lett 410(1): 63-7.

Wittinghofer, F. (1998). "Ras signalling. Caught in the act of the switch-on." Nature 394(6691): 317, 319-20.

Wolf, G., S. Aberle, et al. (1993). "TNF alpha induces expression of the chemoattractant cytokine RANTES in cultured mouse mesangial cells." Kidney Int 44(4): 795-804.

Wolf, G., R. Kalluri, et al. (1999). "Angiotensin II induces alpha3(IV) collagen expression in cultured murine proximal tubular cells." Proc Assoc Am Physicians 111(4): 357-64.

Woods, D., D. Parry, et al. (1997). "Raf-induced proliferation or cell cycle arrest is determined by the level of Raf activity with arrest mediated by p21Cip1." Mol Cell Biol 17(9): 5598-611.

Wright, L. P. and M. R. Philips (2006). "Thematic review series: lipid posttranslational modifications. CAAX modification and membrane targeting of Ras." J Lipid Res 47(5): 883-91.

Wu, L. L., A. Cox, et al. (1997). "Transforming growth factor beta 1 and renal injury following subtotal nephrectomy in the rat: role of the renin-angiotensin system." Kidney Int 51(5): 1553-67.

Wynn, T. A. (2004). "Fibrotic disease and the T(H)1/T(H)2 paradigm." Nat Rev Immunol 4(8): 583-94.

Wynn, T. A. (2007). "Common and unique mechanisms regulate fibrosis in various fibroproliferative diseases." J Clin Invest 117(3): 524-9.

Wynn, T. A. (2008). "Cellular and molecular mechanisms of fibrosis." J Pathol 214(2): 199-210.

Xiang, X., M. Zang, et al. (2002). "Phosphorylation of 338SSYY341 regulates specific interaction between Raf-1 and MEK1." J Biol Chem 277(47): 44996-5003.

Xie, L., B. K. Law, et al. (2004). "Activation of the Erk pathway is required for TGF-beta1-induced EMT in vitro." Neoplasia 6(5): 603-10.

Xu, D. and J. M. Kyriakis (2003). "Phosphatidylinositol 3'-kinase-dependent activation of renal mesangial cell Ki-Ras and ERK by advanced glycation end products." J Biol Chem 278(41): 39349-55.

Xue, L., J. H. Murray, et al. (2000). "The Ras/phosphatidylinositol 3-kinase and Ras/ERK pathways function as independent survival modules each of which inhibits a distinct apoptotic signaling pathway in sympathetic neurons." J Biol Chem 275(12): 8817-24.

Yamada, M., S. Katsuma, et al. (2005). "Inhibition of protein kinase CK2 prevents the progression of glomerulonephritis." Proc Natl Acad Sci U S A 102(21): 7736-41.

Yan, J., S. Roy, et al. (1998). "Ras isoforms vary in their ability to activate Raf-1 and phosphoinositide 3-kinase." J Biol Chem 273(37): 24052-6.

Yang, B., A. M. El Nahas, et al. (2001). "Caspase-3 and apoptosis in experimental chronic renal scarring." Kidney Int 60(5): 1765-76.

Yang, B., T. S. Johnson, et al. (2001). "Expression of apoptosis-related genes and proteins in experimental chronic renal scarring." J Am Soc Nephrol 12(2): 275-88.

Yang, J., C. Dai, et al. (2003). "Hepatocyte growth factor suppresses renal interstitial myofibroblast activation and intercepts Smad signal transduction." Am J Pathol 163(2): 621-32.

Yang, J., C. Dai, et al. (2005). "A novel mechanism by which hepatocyte growth factor blocks tubular epithelial to mesenchymal transition." J Am Soc Nephrol 16(1): 68-78.

Yang, J. and Y. Liu (2001). "Dissection of key events in tubular epithelial to myofibroblast transition and its implications in renal interstitial fibrosis." Am J Pathol 159(4): 1465-75.

Yang, J. and Y. Liu (2002). "Blockage of tubular epithelial to myofibroblast transition by hepatocyte growth factor prevents renal interstitial fibrosis." J Am Soc Nephrol 13(1): 96-107.

Yang, J., R. W. Shultz, et al. (2002). "Disruption of tissue-type plasminogen activator gene in mice reduces renal interstitial fibrosis in obstructive nephropathy." J Clin Invest 110(10): 1525-38.

Yang, N., L. L. Wu, et al. (1998). "Local macrophage and myofibroblast proliferation in progressive renal injury in the rat remnant kidney." Nephrol Dial Transplant 13(8): 1967-74.

Yard, B. A., E. Chorianopoulos, et al. (2001). "Regulation of endothelin-1 and transforming growth factor-beta1 production in cultured proximal tubular cells by albumin and heparan sulphate glycosaminoglycans." Nephrol Dial Transplant 16(9): 1769-75.

Yarger, W. E., D. D. Schocken, et al. (1980). "Obstructive nephropathy in the rat: possible roles for the renin-angiotensin system, prostaglandins, and thromboxanes in postobstructive renal function." J Clin Invest 65(2): 400-12.

Yazawa, H., T. Murakami, et al. (2006). "Hydrodynamics-based gene delivery of naked DNA encoding fetal liver kinase-1 gene effectively suppresses the growth of pre-existing tumors." Cancer Gene Ther 13(11): 993-1001.

Yee, K. L., V. M. Weaver, et al. (2008). "Integrin-mediated signalling through the MAP-kinase pathway." IET Syst Biol 2(1): 8-15.

Yen, T. H., M. R. Alison, et al. (2007). "The cellular origin and proliferative status of regenerating renal parenchyma after mercuric chloride damage and erythropoietin treatment." Cell Prolif 40(2): 143-56.

Yilmaz, M. and G. Christofori (2009). "EMT, the cytoskeleton, and cancer cell invasion." Cancer Metastasis Rev.

Yokoi, H., M. Mukoyama, et al. (2004). "Reduction in connective tissue growth factor by antisense treatment ameliorates renal tubulointerstitial fibrosis." J Am Soc Nephrol 15(6): 1430-40.

Yokoi, H., M. Mukoyama, et al. (2002). "Role of connective tissue growth factor in fibronectin expression and tubulointerstitial fibrosis." Am J Physiol Renal Physiol 282(5): F933-42.

Yokoi, H., A. Sugawara, et al. (2001). "Role of connective tissue growth factor in profibrotic action of transforming growth factor-beta: a potential target for preventing renal fibrosis." Am J Kidney Dis 38(4 Suppl 1): S134-8.

Yokota, N., M. O'Donnell, et al. (2003). "Protective effect of HMG-CoA reductase inhibitor on experimental renal ischemia-reperfusion injury." Am J Nephrol 23(1): 13-7.

Yordy, J. S. and R. C. Muise-Helmericks (2000). "Signal transduction and the Ets family of transcription factors." Oncogene 19(55): 6503-13.

Yu, C., R. Gong, et al. (2007). "Long-term, high-dosage candesartan suppresses inflammation and injury in chronic kidney disease: nonhemodynamic renal protection." J Am Soc Nephrol 18(3): 750-9.

Yu, Q. and I. Stamenkovic (2000). "Cell surface-localized matrix metalloproteinase-9 proteolytically activates TGF-beta and promotes tumor invasion and angiogenesis." Genes Dev 14(2): 163-76.

Yu, X. Q., L. L. Wu, et al. (2000). "Osteopontin expression in progressive renal injury in remnant kidney: role of angiotensin II." Kidney Int 58(4): 1469-80.

Yue, J., R. S. Frey, et al. (1999). "Cross-talk between the Smad1 and Ras/MEK signaling pathways for TGFbeta." Oncogene 18(11): 2033-7.

Zamore, P. D. (2002). "Ancient pathways programmed by small RNAs." Science 296(5571): 1265-9.

Zang, M., C. Hayne, et al. (2002). "Interaction between active Pak1 and Raf-1 is necessary for phosphorylation and activation of Raf-1." J Biol Chem 277(6): 4395-405.

Zavadil, J. (2009). "New TGF-beta and Ras crosstalk in EMT." Cell Cycle 8(2): 184.

Zeisberg, E. M., S. E. Potenta, et al. (2008). "Fibroblasts in kidney fibrosis emerge via endothelial-to-mesenchymal transition." J Am Soc Nephrol 19(12): 2282-7.

Zeisberg, M. and J. S. Duffield "Resolved: EMT produces fibroblasts in the kidney." J Am Soc Nephrol 21(8): 1247-53.

Zeisberg, M., J. Hanai, et al. (2003). "BMP-7 counteracts TGF-beta1-induced epithelial-to-mesenchymal transition and reverses chronic renal injury." Nat Med 9(7): 964-8.

Zeisberg, M. and R. Kalluri (2008). "Reversal of experimental renal fibrosis by BMP7 provides insights into novel therapeutic strategies for chronic kidney disease." Pediatr Nephrol 23(9): 1395-8.

Zeisberg, M. and E. G. Neilson (2009). "Biomarkers for epithelial-mesenchymal transitions." J Clin Invest 119(6): 1429-37.

Zeisberg, M., A. A. Shah, et al. (2005). "Bone morphogenic protein-7 induces mesenchymal to epithelial transition in adult renal fibroblasts and facilitates regeneration of injured kidney." J Biol Chem 280(9): 8094-100.

Zeisberg, M., F. Strutz, et al. (2000). "Role of fibroblast activation in inducing interstitial fibrosis." J Nephrol 13 Suppl 3: S111-20.

Zeisberg, M., C. Yang, et al. (2007). "Fibroblasts derive from hepatocytes in liver fibrosis via epithelial to mesenchymal transition." J Biol Chem 282(32): 23337-47.

Zeng, R., Y. Yao, et al. (2008). "Biliverdin reductase mediates hypoxia-induced EMT via PI3-kinase and Akt." J Am Soc Nephrol 19(2): 380-7.

Zhang, C., X. Meng, et al. (2004). "Connective tissue growth factor regulates the key events in tubular epithelial to myofibroblast transition in vitro." Cell Biol Int 28(12): 863-73.

Zhang, F. L. and P. J. Casey (1996). "Protein prenylation: molecular mechanisms and functional consequences." Annu Rev Biochem 65: 241-69.

Zhang, G., K. A. Kernan, et al. (2007). "Plasmin(ogen) promotes renal interstitial fibrosis by promoting epithelial-to-mesenchymal transition: role of plasmin-activated signals." J Am Soc Nephrol 18(3): 846-59.

Zhang, G., H. Kim, et al. (2003). "Urokinase receptor deficiency accelerates renal fibrosis in obstructive nephropathy." J Am Soc Nephrol 14(5): 1254-71.

Zhang, Q. L. and D. Rothenbacher (2008). "Prevalence of chronic kidney disease in population-based studies: systematic review." BMC Public Health 8: 117.

Zhao, Y., D. Glesne, et al. (2003). "A human peripheral blood monocyte-derived subset acts as pluripotent stem cells." Proc Natl Acad Sci U S A 100(5): 2426-31.

Zheng, H., J. McKay, et al. (2007). "H-Ras does not need COP I- or COP II-dependent vesicular transport to reach the plasma membrane." J Biol Chem 282(35): 25760-8.

Zhou, W., J. E. Marsh, et al. (2001). "Intrarenal synthesis of complement." Kidney Int 59(4): 1227-35.

Zoja, C., A. Benigni, et al. (1999). "Protein overload activates proximal tubular cells to release vasoactive and inflammatory mediators." Exp Nephrol 7(5-6): 420-8.

Zoja, C., R. Donadelli, et al. (1998). "Protein overload stimulates RANTES production by proximal tubular cells depending on NF-kappa B activation." Kidney Int 53(6): 1608-15.

Zoja, C., M. Morigi, et al. (1995). "Proximal tubular cell synthesis and secretion of endothelin-1 on challenge with albumin and other proteins." Am J Kidney Dis 26(6): 934-41.

Publications arising from this thesis

2012: Wang JH, Newbury LJ, Knisely AS, Monia B, Hendry BM, Sharpe CC. 'Antisense knockdown of kras inhibits fibrosis in a rat model of unilateral ureteric obstruction.' *Am J Pathol. 2012 Jan;180(1):82-90. Epub 2011 Nov 7.*

2011: Denby L, Ramdas V, McBride MW, Wang J, Robinson H, McClure J, Crawford W, Lu R, Hillyard DZ, Khanin R, Agami R, Dominiczak AF, Sharpe CC, Baker AH. 'miR-21 and miR-214 are consistently modulated during renal injury in rodent models.' *Am J Pathol. 2011 Aug;179(2):661-72. Epub 2011 May 31.*

2008: Wang JH, Hendry BM, Sharpe CC. Editorial Comment: 'Silencing genes in the kidney: antisense or RNA interference?'. *Nephrology, Dialysis, Transplantation 2008 23(7): 2115-2118.*

The American Journal of Pathology, Vol. 180, No. 1, January 2012

DOI: 10.1016/j.ajpath.2011.09.036

Cardiovascular, Pulmonary, and Renal Pathology

Antisense Knockdown of Kras Inhibits Fibrosis in a Rat Model of Unilateral Ureteric Obstruction

Jia-Hui Wang,* Lucy J. Newbury,* A.S. Knisely,† Brett Monia,‡ Bruce M. Hendry,* and Claire C. Sharpe*

From the Department of Renal Medicine and the Institute of Liver Studies,† King's College Hospital, London, United Kingdom; and ISIS Pharmaceuticals,‡ Carlsbad, California*

Tubulointerstitial fibrosis is the hallmark of chronic kidney disease and is characterized by an increase in the number and activity of interstitial fibroblasts and by excessive matrix deposition. Ras is an intracellular signaling molecule involved in cell proliferation and differentiation. It has recently been implicated in the pathogenesis of renal fibrosis. Of the three different isoforms of Ras (Kirsten, Harvey, and Neural), we previously demonstrated that the Kirsten isoform is key in the control of renal fibroblast proliferation *in vitro*. In this study, we used gene therapy in the form of antisense oligonucleotides (ASOs) specifically to silence *Kras* (alias *Ki-ras*) expression in a rat model of renal fibrosis caused by unilateral ureteric obstruction. We demonstrate that renal *Kras* expression increases by 70% in this model compared with sham-operated animals and that treatment with ASOs can reduce total renal Kras by >90% to levels well below basal. This silencing is associated with a dramatic inhibition of interstitial fibrosis, a fivefold reduction in α-smooth muscle actin expression, and a 2.4-fold reduction in collagen I deposition. This inhibition was observed despite histologic evidence of marked interstitial inflammation. These findings demonstrate that silencing *Kras* expression can markedly inhibit renal fibrosis. This strategy should be considered as a new potential therapeutic avenue. ***(Am J Pathol 2012, 180: 82–90; DOI: 10.1016/j.ajpath.2011.09.036)***

Chronic kidney disease is a large and expanding problem worldwide. Whatever the initiating insult, the presence of progressive chronic kidney disease is associated with scarring of the tubulointerstitial compartment. Interstitial myofibroblasts are responsible for the laying down of extracellular matrix,[1] and although sparse in the normal kidney, after injury they increase in number via several potential mechanisms, such as proliferation, pericyte and fibrocyte differentiation and migration, and epithelial to mesenchymal transition.[2,3] Although complex, the many fibrogenic cell signals and phases of fibrosis are clearly described.[4] Despite this large body of knowledge, there is still no effective, fibrosis-specific therapeutic agent that has been adopted into clinical practice.

Ras monomeric GTPases are transduction molecules in many extracellular signaling pathways that regulate cell proliferation, survival, and differentiation.[5] Although Ras family species are, to date, of particular interest in oncology,[6] we and others have accumulated a substantial amount of evidence for a role for the Ras monomeric GTPases in the pathogenesis of renal disease and in epithelial to mesenchymal transition. Ras family members are downstream convergence points for signal cascades mediated by many cell surface receptors with ligands expressed in renal injury, such as transforming growth factor β, platelet-derived growth factor, angiotensin II, and epidermal growth factor, allowing transduction of signal to downstream profibrotic effectors. As such, they may be an important potential target for treating the fibrosis of chronic kidney disease.[7–14]

Recently, Bechtel et al[15] demonstrated a direct link between Ras activation and renal fibrogenesis. They showed that hypermethylation of *RASAL1* in fibrotic kidneys results in decreased expression of the Ras inhibitory

Supported in part by the National Institute for Health Research, UK (clinician scientist award DHCS/G121/33 to C.C.S.), and Kidney Research UK (project grant RP37/1/05 to C.C.S. and clinical training fellowship TF10/2006 to J.-H.W.). ISIS Pharmaceuticals, which designs and develops antisense oligonucleotides as potential therapeutic agents, provided the oligonucleotides used in this study free of charge.

Accepted for publication September 26, 2011.

Disclosure: B.M. is an employee of ISIS Pharmaceuticals.

Supplemental material for this article can be found at *http://ajp.amjpathol.org* or at doi: 10.1016/j.ajpath.2011.09.036.

Address reprint requests to Claire C. Sharpe, F.R.C.P., Ph.D., Department of Renal Medicine, King's College London, 10 Cutcombe Rd., London SE5 9RJ, UK. E-mail: Claire.sharpe@kcl.ac.uk.

protein RASAL1. This correlates with an increase in Ras activity and a subsequent increase in fibrosis in several murine models of renal fibrosis. The group concluded that hyperactive Ras contributes to fibroblast activation and fibrosis and that the antifibrotic capacity of Ras inhibitors should be further explored.

There are three separate isoforms of Ras: Kirsten (Kras; alias Ki-Ras), Harvey (Hras; alias Ha-Ras), and Neural (Nras; alias N-Ras). Although the isoforms are 85% homologous, they differ in their C-terminal 24 amino acids, a "hypervariable region" of the molecule. This region confers on each isoform distinct characteristics with respect to cell localization and function.[16,17] Our group previously demonstrated that Kras is the predominantly expressed isoform in human renal fibroblasts and that knockdown of this isoform by antisense oligonucleotides (ASOs) results in significant inhibition of fibroblast proliferation.[18,19] In this study, we investigated whether silencing of *Kras* (alias *Ki-ras*) expression using ASOs is antifibrotic in a rat model of unilateral ureteric obstruction (UUO).

Materials and Methods

Oligonucleotides

ASOs were designed and produced by ISIS Pharmaceuticals, Carlsbad, California. They are 20-nucleotide, fully phosphorothioate "gapmers." The five sugar residues on each end are 2′-O-methoxy-ethyl modified. The central 10 sugars are deoxyribonucleotides. All pyrimidine bases are 5-methyl substituted (T and me5-C). The oligonucleotide sequences were as follows: ASO 1, 5′-ATTCACATGACTATACACCT-3′; ASO 2, 5′-CACACTTATTCCCTACTAGG-3′; SO 1, 5′-ATTAACACGCCTACATACTT-3′; SO 2, 5′-CCCACTAAATCCGTTCTATG-3′; CO 1, 5′-TCAGTAATAGCCCCACATGG-3′; and CO 2, 5′-CCTTCCCTGAAGGTTCCTCC-3′. CO 1 was used for *in vitro* experiments because this was the control used in a previous *in vitro* study.[18] CO 2 is a standard control oligonucleotide used by ISIS Pharmaceuticals for *in vivo* work and was used for the initial *in vivo* experiments. SO 1 and SO 2 were subsequently designed for this project and are scrambles of ASO 1 and ASO 2, respectively.

Primary Culture and Cell Lines

Primary rat fibroblasts were cultured as previously described.[18] Briefly, rat kidneys were decapsulated in sterile ice-cold HBSS. Cortices were removed and fragmented under sterile conditions. This tissue was digested in a 1-mg/mL solution of collagenase type IV (Sigma-Aldrich Co. Ltd., Dorset, UK) and incubated in a water bath at 37°C for 30 minutes. The digestion process was terminated by the addition of ice-cold 2% fetal calf serum (Sigma-Aldrich Co. Ltd.)/HBSS solution. The digest was then passed through a 100-μm sieve, and the filtrate was centrifuged at 200 $\times$ *g* for 5 minutes at 4°C to pellet cellular material. This material was then washed in HBSS and resuspended in 30 mL of a 50% Percoll solution (Sigma-Aldrich Co. Ltd.) and centrifuged at 4°C at 30,000 $\times$ *g* for 30 minutes. The top band in the gradient obtained contained the fibroblast fraction, which was harvested and cultured in Dulbecco's modified Eagle's medium Ham's F-12 (Gibco BRL, Life Technologies, Paisley, UK) supplemented with 10% fetal calf serum.

Normal adult rat fibroblast cells (NRK-49F) were obtained from the European Collection of Cell Cultures (6101301) and cultured in Dulbecco's modified Eagle's medium supplemented with penicillin (100 IU/mL), streptomycin (100 μg/mL), amphotericin (2.5 μg/mL), and 10% fetal calf serum.

Semiquantitative RT-PCR

Total cellular RNA was extracted using a Qiagen RNeasy minikit (Qiagen, Crawley, UK). Promega's Access RT-PCR kit (Promega, Southampton, UK) was used for semiquantitative RT-PCR analysis of sample RNA. The primer pairs targeting Kras and β-actin in the rat had the following forward and reverse sequences, respectively: Kras, 5′-AGAGTGCCTTGACGATACAGC-3′ and 5′-TCCCTCATTGCACTGTACTCC-3′; β-actin, 5′-CCCACACTGTGCCCATC-3′ and 5′-TGATCCACATCTGCTGGA-3′. Samples were amplified for 22 cycles of PCR, and the products were separated on a 1.5% agarose gel.

In Vitro *Transfection of Oligonucleotides*

Oligonucleotides were diluted with Opti-MEM (Gibco BRL) to form a 10-μmol/L stock. Cells were grown to a confluence of 50% to 70% and were washed with PBS before transfection. Oligonucleotides were transfected into cells using Lipofectin (Gibco BRL), a cationic liposomal system. Lipofectin, 1.25 μL, was used per 100 nmol/L oligonucleotide per 100 μL of final transfection volume. The final concentration of oligonucleotides used for transfection was 200 nmol/L. Cells were transfected for 6 to 12 hours before the transfection medium was removed and replaced with normal culture medium.

UUO Model

All the experimental procedures were approved under provisions of the Animals (Scientific Procedures) Act 1986 and were performed under license number PPL 70/6054. UUO was caused in adult male Wistar rats. After a midline incision was made, the left ureter was isolated and ligated with two 6/0 silk ties. The abdomen was closed, and buprenorphine (30 μg/kg) was administered subcutaneously. Any first dose of treatment (oligonucleotide or vehicle) was also administered subcutaneously at this point. Animals undergoing the sham procedure underwent a full laparotomy and manipulation of the ureter without ligation. All the animals were sacrificed on day 16 after UUO.

Administration of Oligonucleotides in Vivo

ASOs and control oligonucleotides were administered by subcutaneous injection in either the nape of the neck or a

rear limb. Variation of injection points prevented cumulative tissue damage. All oligonucleotides were dissolved in sterile water and administered on alternate days at a dose of 12.5 mg/kg.

RNA Retrieval from Tissue

RNA was retrieved from tissue using the Qiagen RNeasy minikit. The sample (30 mg) was initially homogenized in 600 μL of guanidine-thiocyanate lysis buffer (supplied) using a potter homogenizer. This suspension was then transferred to a QIAshredder (Qiagen), and the manufacturer's protocol was followed. Isolated RNA was quantified, and its purity was established using absorbance spectroscopy.

Quantitative PCR

Reverse transcription of total RNA was performed using the Omniscript reverse transcription kit (Qiagen) according to the manufacturer's protocol. The TaqMan sequence detection system (Applied Biosystems, Carlsbad, CA) was used, and quantitative PCR (qPCR) was performed using the ABI Prism 7900HT machine (Applied Biosystems). Abundance of target-gene transcript was quantified relative to the endogenous control glyceraldehyde-3-phosphate dehydrogenase. Target and endogenous control levels for each sample were measured in triplicate. TaqMan gene expression assays and TaqMan master mix were purchased from Applied Biosystems.

Histologic Analysis

Tissue was fixed in buffered formalin for 24 hours, embedded in paraffin, cut into 4-μm-thick sections, and picked up onto glass slides (plain or polylysine coated). Sections were stained with H&E.

Special Stains

Sections stained using the picro-Mallory trichrome (PMT) and picrosirius red (PSR) techniques were used to assess fibrosis. PSR-stained sections were viewed under cross-polarized light and under bright light. The degree of cortical fibrosis was scored by a consultant renal histopathologist in a randomized and blinded manner.

Immunostaining

Sections mounted on polylysine-coated slides were deparaffinized after baking at 40°C overnight. Antigen retrieval was performed by pressure cooking in citrate buffer (pH 6) as required. Antibodies used were directed against aquaporin 1 (AB2219; Millipore, Billerica, MA), aquaporin 2 (AB3066; Millipore), modified oligonucleotides (supplied by ISIS Pharmaceuticals, rabbit polyclonal), α-smooth muscle actin (α-SMA) (A2547; Sigma-Aldrich Co. Ltd.), collagen I (AB755P; Millipore), Ki-67 (NCL-L-KI67-MM1; Novocastra, Newcastle on Tyne, UK), ED-1 (MCA341R; Serotec, Kidlington, UK), and FSP-1 (S100A4) (A5114; Dako, Ely, UK). Detection was achieved by a peroxidase substrate kit using a synthetic dextran backbone polymer and diaminobenzidine [Dako EnVision detection system (K5007), Dako]. Sections were assessed after hematoxylin counterstaining. For α-SMA and ED-1, slides were scored by measurement of staining intensity and area using Nikon NIS-Elements (basic research) software (Nikon, London, UK). Slides were scored in a blinded manner based on five random cortical views per section at $\times$200 magnification. Staining for collagen 1 was scored by a consultant renal histopathologist in a randomized and blinded manner. Staining for Ki-67 and FSP-1 was scored in a blinded manner using light microscopy at $\times$200 magnification. Ten random fields of cortex were evaluated, with assignment of cells to glomerular, tubular, or interstitial compartments.

Western Blot Analysis

Western blot analysis was performed using antibodies against α-SMA (A2547; Sigma-Aldrich Co. Ltd.) and pan-Ras (OP40; Merck, Darmstadt, Germany). Glyceraldehyde-3-phosphate dehydrogenase (MAB374; Millipore) was used as a loading control for α-SMA blots.

Immunoprecipitation

Due to a relatively low abundance of Ras within the cell, Ras protein was concentrated from crude protein lysates using immunoprecipitation; 0.5 mg of protein was used. All the volumes were normalized to 1 mL with PBSTDS [1$\times$ PBS, 1% Triton X-100 (Roche Diagnostics GmbH, Mannheim, Germany), 0.5% sodium deoxycholate, 0.1% SDS, 0.5 μg/mL of leupeptin, 1.0 μg/mL of pepstatin, 1.0 mmol/L EDTA, and phenylmethylsulfonyl fluoride 0.2 mmol/L]. Anti-Ras–agarose conjugate, 15 μL (OP01A; Merck), was added per milliliter volume, and all the samples were incubated, under rotation, at 4°C overnight. Samples were then washed and separated by SDS-PAGE for analysis.

Statistical Analysis

Statistical analysis of data was performed using GraphPad Prism version 4 software (GraphPad Software Inc., La Jolla, CA). When comparing two sets of data, an unpaired Student's *t*-test was used. For group data, analysis of variance testing was initially performed. Bonferroni adjustment was then used to correct for multiple testing.

Results

ASOs Reduce Kras *Expression* in Vitro

ASOs consist of single strands of 20-22mer oligonucleotides that are complementary to their target mRNA sequence. Binding of ASOs to target induces RNase H and subsequent target mRNA hydrolysis, thereby effecting "gene silencing." Oligonucleotides administered systemically are filtered at the glomerulus and are rapidly taken

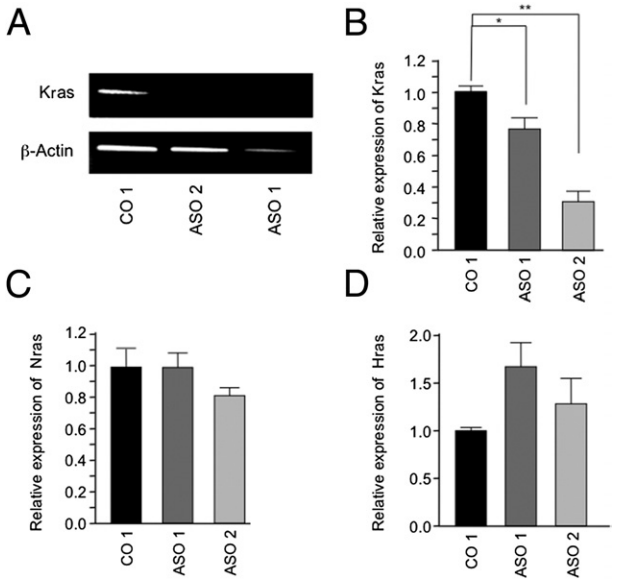

Figure 1. ASOs reduce *Kras* expression *in vitro*. **A:** Primary culture rat renal fibroblasts were transfected with 200 nmol/L control oligonucleotide (CO 2) or antisense oligonucleotides (ASO 1 and ASO 2). After 24 hours, the cells were lysed, and extracted mRNA was subjected to semiquantitative RT-PCR for Kras. β-actin primers were used to detect this housekeeping gene. **B–D:** NRK-49F cells were transfected with 200 nmol/L control oligonucleotide (CO 2) or antisense oligonucleotides (ASO 1 and ASO 2). After 24 hours, the cells were lysed, and extracted mRNA was subjected to RT-qPCR for Kras, Nras, and Hras as indicated. $n = 3$ separate experiments. Error bars are SEM. $^*P < 0.05$, $^{**}P < 0.001$.

up by tubular epithelial cells. Thus, they are an attractive therapeutic option when considering potential therapies for renal disease.[20]

Oligonucleotides ISIS 104440 (ASO 1) and ISIS 104419 (ASO 2) target the Kirsten isoform of Ras in the rat. Four separate control oligonucleotides were used in this study. All the oligonucleotides, control and antisense, were 20-mer in length. Control oligonucleotide 15167 (CO 1) targets the HIV promoter sequence but has no recognized target in the rat. Control oligonucleotide 141923 (CO 2) also has no recognized target in the rat. Control oligonucleotides 417230 (SO 1) and 417226 (SO 2) are scrambled sequences of ASO 1 and ASO 2, respectively.

Oligonucleotides were initially evaluated for specificity and efficacy *in vitro* using primary rat renal fibroblasts in culture. After transfection, RNA was extracted, and semiquantitative PCR was used to demonstrate knockdown of *Kras* expression by transfection with ASO 1 and ASO 2 compared with CO 1 (Figure 1A). For further validation, normal rat kidney cells [NRK-49F, European Collection of Cell Cultures (86101301)] were transfected with ASO 1 and ASO 2. Both oligonucleotides significantly reduced expression of Kras mRNA by 23% and 69%, respectively, compared with CO 1 as assessed by RT-qPCR, with no significant knockdown of either the Nras or Hras isoforms (Figure 1, B–D). However, a nonsignificant trend toward up-regulation of the latter isoform was noted, with an increase in expression of 68% for ASO 1 and 44% for ASO 2.

ASOs Reduce Kras *Expression* in Vivo

Oligonucleotides were administered subcutaneously to adult male Wistar rats on alternate days at a dose of 12.5 mg/kg for 6 days. Sequential sections of renal tissue were immunostained for aquaporin 1 to label proximal convoluted tubules, for aquaporin 2 to label distal convoluted tubules and collecting ducts, and with an anti-oligonucleotide antibody to localize oligonucleotide deposition. Figure 2A illustrates that oligonucleotide is deposited in proximal convoluted tubules only, with no staining apparent in either the glomeruli or distal convoluted tubules and collecting ducts. RT-qPCR analysis of renal tissue demonstrated oligonucleotide effects reflecting those seen *in vitro*. No significant difference was seen between CO 2– and vehicle-only–treated groups regarding *Kras* expression. However, 12% and 66% knockdown of Kras mRNA expression was seen in the ASO 1 and ASO 2

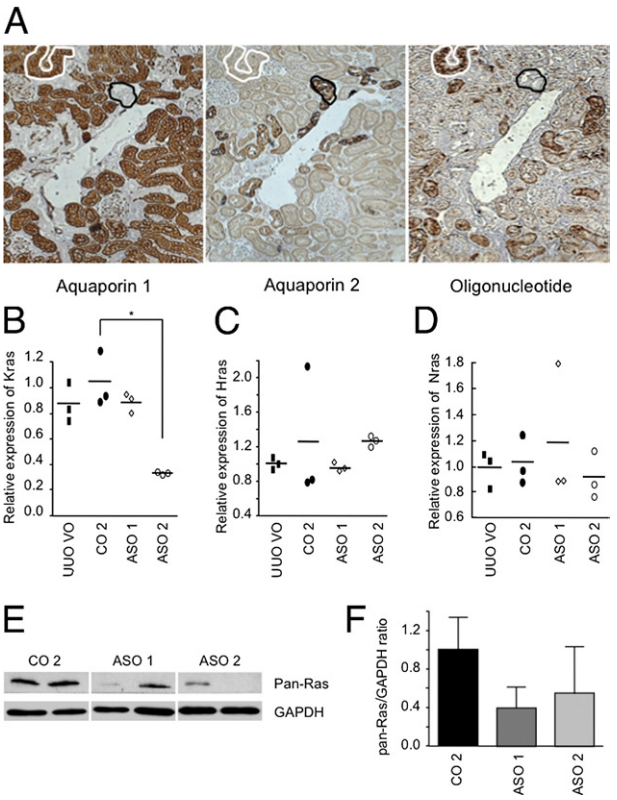

Figure 2. ASOs reduce *Kras* expression *in vivo*. Control or antisense oligonucleotides were administered to Wistar rats subcutaneously on alternate days at a dose of 12.5 mg/kg over 6 days (three doses). **A:** Sequential sections were obtained from a single rat kidney and were immunostained for aquaporin 1, aquaporin 2, and oligonucleotide deposits as labeled. The corresponding proximal convoluted tubule in each section is outlined in white, and the corresponding distal convoluted tubule and collecting duct in each section is outlined in black. mRNA and total protein were extracted from whole renal tissue after sacrifice. **B–D:** mRNA was subjected to RT-qPCR for Kras, Hras, and Nras as indicated ($n = 3$ animals). **E** and **F:** Pan-Ras was immunoprecipitated from a 0.5-mg aliquot of all protein extracted from whole kidney tissue. The precipitate was then subjected to Western blot analysis for total pan-Ras. To demonstrate equality of protein content among samples studied, glyceraldehyde-3-phosphate dehydrogenase (GAPDH) also was quantitated, by Western blot analysis, in cell lysates after pan-Ras immunoprecipitation. The blot is representative of three similar experiments. Error bars are SEM. $^*P < 0.001$. VO, vehicle only.

groups, respectively. No significant difference for any group was seen regarding *Hras* and *Nras* expression (Figure 2, B–D). Although modest effects were seen in Kras mRNA expression after ASO treatment, these were translated into decreases in total Ras protein expression by 60% in the ASO 1– and 44% in the ASO 2–treated groups compared with the CO 2 control group (Figure 2, E and F).

Kras *and* Nras *Expression Is Increased in UUO*

UUO was caused in male Wistar rats as described previously herein. Renal tissue from obstructed kidneys, contralateral nonobstructed kidneys, and the kidneys of sham-operated animals was analyzed for Ras mRNA levels. This analysis demonstrated increases in *Kras* and *Nras* expression by 70% and 80%, respectively, in obstructed kidneys compared with in the contralateral kidneys or kidneys from sham-operated rats (Figure 3). No significant difference in *Hras* expression among groups was found.

Kras ASOs Reduce Kras *mRNA Expression in UUO*

Administration of Kras ASOs greatly reduced *Kras* expression in obstructed kidneys in a rat model of UUO compared with renal tissue retrieved from UUO vehicle-only and UUO control oligonucleotide–treated groups. ASO 1 reduced Kras mRNA levels by 61% and 56% compared with the scrambled oligonucleotides SO 1 and SO 2, respectively, whereas ASO 2 reduced expression by 97% compared with both these scrambled controls ($P < 0.01$). No statistically significant change in either *N-* or *Hras* mRNA levels was found in either ASO group. Administration of SO 1 or SO 2 resulted in a trend toward increased expression of all isoforms of *ras,* but only the rise in *Nras* in the SO 1–treated group was statistically significant ($P < 0.01$) (Figure 4). Administration of Kras ASOs did not affect gross phenotypic appearance or behavior of the animals or have a significant effect on growth or weight gain (see Supplemental Figure S1 at *http://ajp.amjpathol.org*).

Kras ASOs Inhibit Fibrosis in UUO

Sixteen days of UUO resulted in macroscopic, histologic, and molecular evidence of obstructive nephropathy and fibrosis. Compared with renal tissue from sham-operated animals, obstructed kidneys had dilated tubules, flattened tubular epithelial cells, greatly increased interstitial volumes, and prominent inflammatory infiltrates. Fibrosis was markedly increased, with evidence of substantial myofibroblastic and macrophage activity as reflected by an increase in α-SMA expression and ED-1–positive cells (Figures 5 and 6). The degree of interstitial fibrosis was determined by staining with PMT and PSR, and collagen I deposition was stained directly using specific antibodies (Figure 5A). ASOs were scored against CO 2 and SO 1 or SO 2 by a consultant histopathologist blinded to

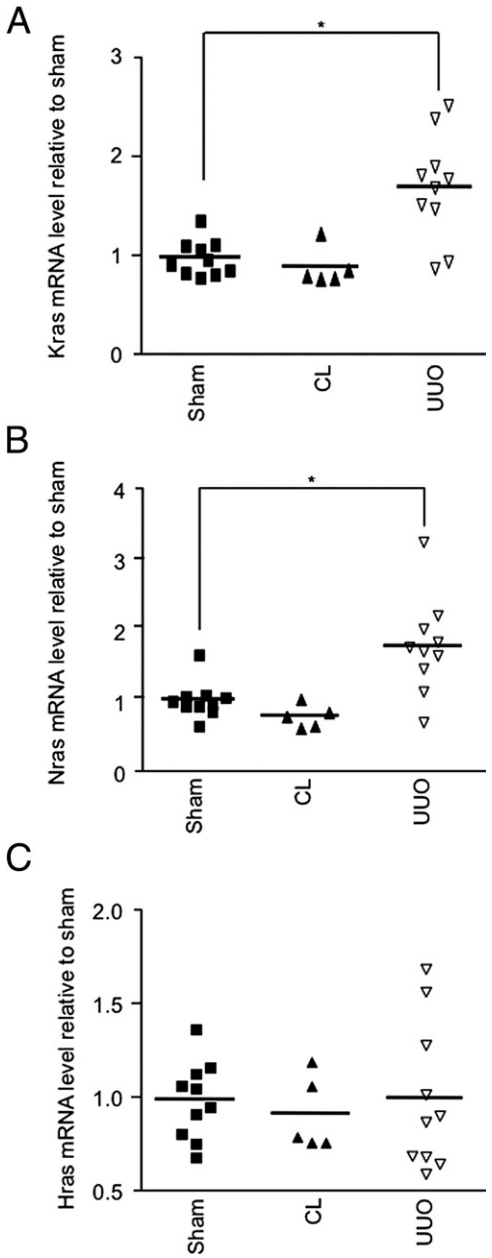

Figure 3. *Kras* expression is increased in UUO. UUO was caused in male Wistar rats. mRNA was extracted from renal tissue from obstructed kidneys, contralateral kidneys (CL), nonobstructed kidneys, and kidneys from sham-operated animals. Each sample ($n = 5$ to 10) underwent RT-qPCR for Kras, Hras, and Nras. Expression of each gene was compared; glyceraldehyde-3-phosphate dehydrogenase served as an internal control. *$P < 0.001$.

treatment. Percentage fibrosis scores as derived from PMT- and PSR-stained sections were averaged to provide an overall mean percentage fibrosis score (Figure 5B). This demonstrated an increase in the interstitial fibrosis score in vehicle-only–treated UUO models to 61.9% compared with the control sham-operated kidney group baseline fibrosis score of 5.8%. No significant difference in fibrosis was observed after administration of CO 2, with a mean observed fibrosis score of 67% in this group. Although the administration of SO 1 and SO 2 reduced fibrosis scores to 40.1% and 36.6%, respec-

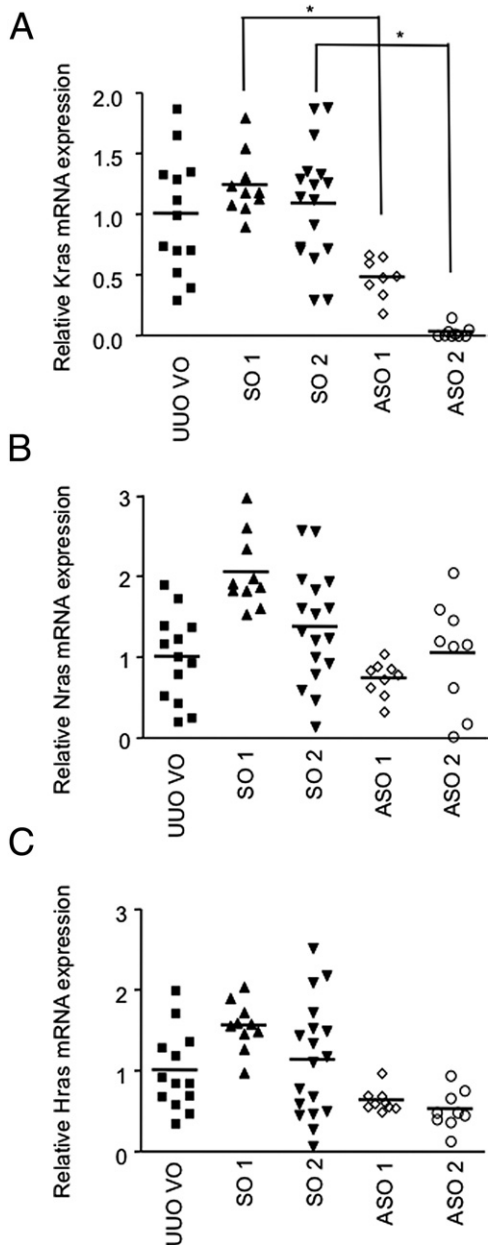

Figure 4. Kras ASOs reduce Kras mRNA levels in UUO. After 16 days of UUO, mRNA was extracted from whole renal tissue from obstructed kidneys and subjected to RT-qPCR for Kras (**A**), Nras (**B**), and Hras (**C**). $n = 10$ to 13 animals; each result is a mean of triplicate measures. $^*P < 0.001$. VO, vehicle only.

tively, the administration of active Kras ASOs additionally reduced fibrosis, with ASO 1 reducing the fibrosis score to 17% ($P < 0.001$) and ASO 2 reducing it to 20.3% ($P < 0.01$).

Collagen I deposition was observed to increase from 9% in sham-operated kidneys to 50% in vehicle-treated obstructed kidneys. Administration of CO 2 did not significantly affect this finding (collagen I deposition score, 40%). However, administration of ASO 1 and ASO 2 reduced the collagen deposition score to 18.4% and 17%, respectively ($P < 0.05$ for both), compared with CO 2 (Figure 5C).

Kras ASOs Inhibit α-SMA Expression While Increasing Inflammation in UUO

α-SMA is a well-recognized marker of myofibroblast activity. Figure 6A shows tissue sections stained for α-SMA from sham and UUO models, with quantified results shown in Figure 6B. Expression of this protein rose from 1% to 44.5% of the total area after 16 days of UUO. This was not significantly altered by the administration of CO 2 (53%) but was reduced to 21% and 32% by SO 1 and SO 2, respectively. Marked edema was also present. Administration of ASO 1 and ASO 2, however, further reduced the expression of α-SMA to 3.9% and 20%, respectively, in the presence of similar levels of edema. To quantify α-SMA expression further, Western blot analysis for α-SMA was performed on protein extracted from renal tissue. This demonstrated a large up-regulation in protein expression after UUO that was not affected by the administration of control oligonucleotides (Figure 6, C and D). However, ASO 1– and ASO 2–treated groups exhibited a marked decrease in α-SMA expression that almost,

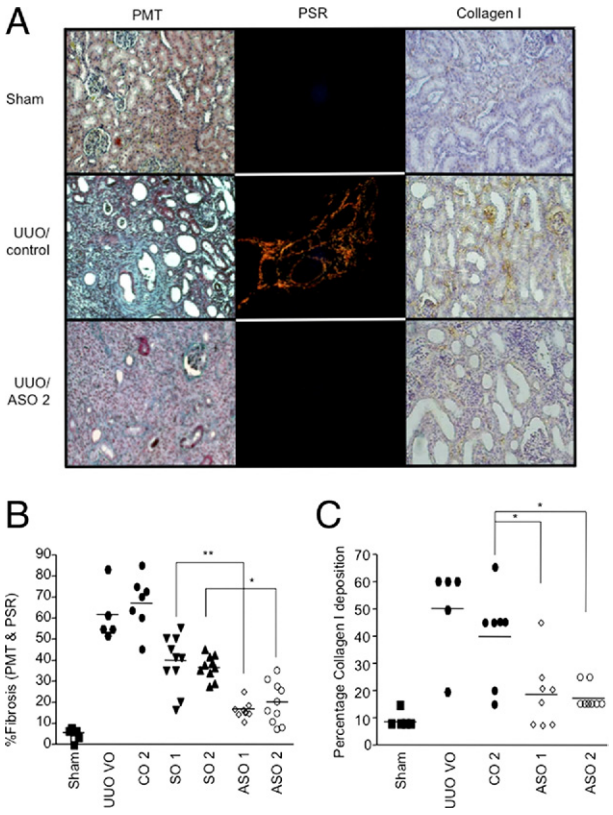

Figure 5. Kras ASOs inhibit fibrosis in UUO. **A:** Tissue sections were fixed and stained with PMT or PSR or were immunostained for collagen I as indicated. UUO/control indicates SO 2 oligonucleotide for PMT and PSR and CO 2 for collagen I. The PSR sections were viewed under cross-polarized light. Images shown are representative. Original magnification, ×100 for all images. **B:** Each animal was assigned a mean fibrosis score by averaging the percentage of fibrosis observed with PMT and the percentage of fibrosis observed with PSR. This score is plotted against the treatment the animal received as indicated. **C:** For each animal, the percentage of collagen deposition was scored by a consultant histopathologist as described in *Materials and Methods* and is plotted against the treatment the animal received as indicated. $n = 5$ to 10 animals. $^*P < 0.05$. VO, vehicle only.

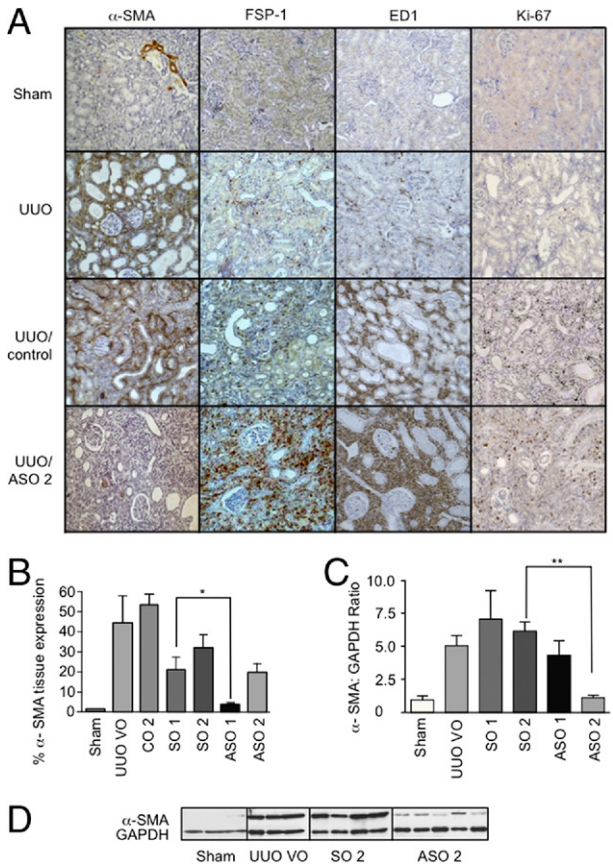

Figure 6. Kras ASOs inhibit α-SMA expression despite increased interstitial cell numbers in UUO. Oligonucleotides were administered subcutaneously to adult male Wistar rats on alternate days at a dose of 12.5 mg/kg across 16 days after UUO or a sham operation. The animals were then sacrificed **A:** Tissue sections were fixed and immunostained for α-SMA, FSP-1, ED-1, or Ki-67 as indicated. Images shown are representative. Original magnification, ×100 for all images. **B:** Five random cortical views per section were scored in a blinded manner by measuring staining intensity and area using Nikon NIS-Elements (basic research) software. The results are plotted as percentage of α-SMA tissue expression against the individual treatments as indicated. n = 5 to 10 animals. **C:** Total protein was extracted from whole renal tissue and underwent Western blot analysis for α-SMA. **D:** Densitometry was performed, and α-SMA/glyceraldehyde-3-phosphate dehydrogenase (GAPDH) density ratios are plotted against each treatment as indicated. n = 3 to 5 animals. Error bars are SEM. $^{*}P < 0.05$, $^{**}P < 0.001$. VO, vehicle only.

in the latter group, reverted to basal levels (as expressed in sham-operated animals).

Renal tissue from sham-operated and obstructed kidneys was also stained for FSP-1 expression (Figure 6A). The discrete nature of staining allowed for stained cells to be categorized as glomerular, tubular, or interstitial. As expected, staining for FSP-1 was minimal in all compartments in sham-operated kidneys. Obstruction led to a nonsignificant rise in tubular expression of FSP-1 (data not shown) and to an increase in interstitial expression from 4 FSP-1–positive cells per view to 28 FSP-1–positive cells per view ($P < 0.05$) (Figure 7A). Administration of oligonucleotides, either control or ASO, did not significantly alter FSP-1 expression in either glomerular or tubular compartments compared with the vehicle-only group (data not shown). Although interstitial expression of FSP-1 increased on administration of scrambled oligonucleotides and Kras ASOs compared with administration of vehicle-only UUO, the increase was significant only on administration of ASO 1 ($P < 0.001$).

Measurement of intensity and area of ED-1 antibody staining (against the macrophage marker CD 68) using Nikon NIS-Elements (basic research) software clarified the nature of the increased interstitial infiltrate (Figures 6 and 7B). Sham-operated samples revealed few macrophages per view (<1% of the total area). As expected,

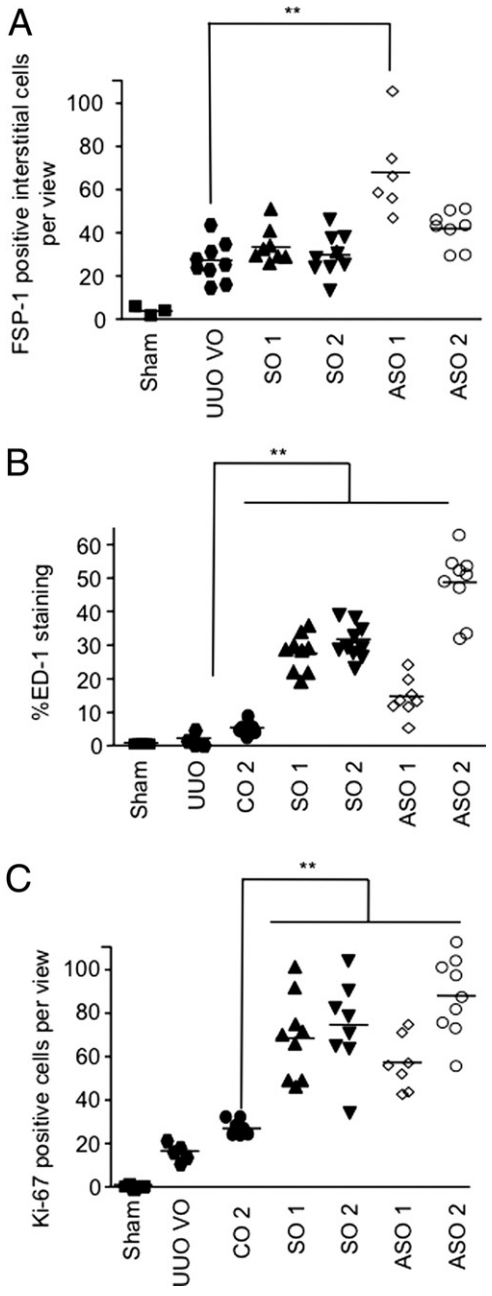

Figure 7. ASOs increase inflammation in UUO. Tissue sections were immunostained for FSP-1 (**A**), ED-1 (**B**), and Ki-67 (**C**). For ED-1 staining, five random cortical views per section were scored in a blinded manner by measurement of staining intensity and area using Nikon NIS-Elements (basic research) software. The results are plotted as percentage of ED-1 tissue expression. For Ki-67 and FSP-1 staining, cells that marked were counted by two people in a blinded manner (light microscopy; original magnification, ×200) in 10 random fields of cortex. n = 5 to 10 animals. $^{**}P < 0.001$. VO, vehicle only.

obstruction resulted in an increase in ED-1 staining to 2.4%, reflecting the inflammatory infiltration associated with UUO. The administration of CO 2 led to a doubling of ED-1 staining (5.5%). However, ED-1 staining further increased significantly with the administration of scrambled and antisense oligonucleotides. SO 1 and SO 2 administration increased ED-1 staining to 28% and 32%, respectively ($P < 0.001$). Administration of ASO 1 increased ED-1 staining to 15%, but administration of ASO 2 resulted in a more substantial increase to 49% ($P < 0.001$).

Ras is known to play a central role in cell proliferation. Our previous work has demonstrated that Kras knockdown reduces stimulated proliferation in renal fibroblasts.[18,19] Kidney sections were, therefore, stained for Ki-67, a marker of actively dividing cells. In the interstitial compartment, Ki-67 expression was increased by 2.5-fold to fourfold in the SO 1–, SO 2–, ASO 1–, and ASO 2–treated groups compared with the CO 2–treated group ($P < 0.01$) (Figures 6 and 7C).

Oligonucleotides also Target Other Tissues

Two hours after systemic administration, the highest concentrations of oligonucleotides are found in the liver and kidneys.[21] RT-qPCR analysis of hepatic tissue produced results comparable with those obtained from the kidney. Both SO 1 and SO 2 administration resulted in an increase in Kras hepatic mRNA levels compared with the vehicle-only–treated UUO group. Administration of ASO 1 and ASO 2 reduced *Kras* hepatic expression by 67% and 82%, respectively, compared with their paired, base-matched scrambled oligonucleotides (see Supplemental Figure S2B at *http://ajp.amjpathol.org*). Oligonucleotide deposits could also be detected in other tissues, including heart and muscle, although less than in liver and kidney (see Supplemental Figure S2A at *http://ajp.amjpathol.org*). Despite this widespread uptake of oligonucleotide, wound healing did not differ, either clinically or histologically, between vehicle-treated animals and those treated with ASOs (see Supplemental Figure S2C at *http://ajp.amjpathol.org*).

In H&E-stained hepatic tissue, we found mild to moderate inflammation in both lobule and portal tract on administration of oligonucleotide, with ASO 2 causing more inflammation than ASO 1. Architecture was normal (see Supplemental Figure S3A at *http://ajp.amjpathol.org*). Similarly, mild inflammation was noted in the heart tissue stained for ED-1 from oligonucleotide-treated animals, with ASO 2 being the most inflammatory oligonucleotide (see Supplemental Figure S3, B and C, at *http://ajp.amjpathol.org*).

Discussion

In this study, we demonstrated that a single isoform of *ras* can be specifically targeted *in vitro* and *in vivo* using ASOs. Ras is a key signaling molecule pivotal to control of cell growth and differentiation in many cell types. Our previous work highlighted Kras as the predominant isoform in renal fibroblasts. This isoform is, therefore, a desirable target to maximize the effect on the kidney while minimizing other tissue involvement. Binding of the ASO to target mRNA results not only in steric inhibition of translation by the ribosomal complex but also, and more important, in the induction of RNase H, which cleaves the 3′-O-P-bond of the RNA molecule. This mechanism of action theoretically provides 100% specificity for the target gene, an unachievable goal for most conventional pharmacologic agents. In addition, parenterally administered ASO accumulates principally in the kidneys, with a kidney/plasma concentration ratio of 80:1 after 2 hours.[21]

Although we and other researchers have been investigating the role of Ras in renal fibrosis for some years, Ras has become a more pertinent target recently. RASAL1, a Ras GTPase activating protein and, hence, a Ras inhibitor, has been found to be down-regulated in fibroblasts from fibrotic kidneys and not in fibroblasts from nonfibrotic kidneys as a result of hypermethylation of its parent gene. Hypermethylation results in reduced *RASAL1* gene transcription and, hence, in Ras activation.[15] This phenomenon is also present in colonic neoplasms, where decreased RASAL1 expression was noted in more advanced tumors expressing wild-type Kras.[22]

In this study, we demonstrated that parenteral administration of ASOs targeting *Kras* can significantly inhibit the onset of fibrosis in a model of UUO as measured by PMT, PSR, collagen I deposition, and α-SMA expression. This inhibition is achieved despite an increase in the observed interstitial inflammation demonstrated in the kidneys of treated animals. This inflammation is not specific to the Kras ASOs as it seems to be the same for the scrambled control oligonucleotides. The nonstoichiometric control oligonucleotide (CO 2) caused significantly less inflammation, suggesting that this phenomenon is probably not sequence related but instead depends on relative nucleotide compositions of each oligonucleotide. We also stained the samples for FSP-1 as an assumed marker for interstitial fibroblasts. Although expression of FSP-1 increased with UUO, unlike α-SMA, it increased further in scrambled oligonucleotide–treated and ASO-treated kidneys. FSP-1 is expressed by interstitial fibroblasts, but it is also expressed by inflammatory cells. This expression probably overwhelmed any reduction in fibroblast numbers in this study.[23] Although we did not specifically characterize the nature of the inflammatory reaction, we did demonstrate that it contained both macrophages and actively dividing cells likely not to be of the macrophage inflammatory lineage. Whether these inflammatory cells or increased numbers of interstitial fibroblasts cause increased *Kras* and *Nras* expression in UUO is unclear. Administration of the Kras ASOs did, however, reduce total kidney *Kras* expression well below values seen in UUO alone, despite increased inflammation in the treated groups.

Although the kidneys are preferentially targeted by small oligonucleotides, they also deposit in other tissues throughout the body, including the liver and, to a lesser degree, the heart and striated muscle. We noted a moderate reduction in *Kras* expression in the livers of ASO-treated animals and an associated mild inflammation in

the liver and heart, suggesting a widespread oligonucleotide-related inflammatory reaction. This caused no significant architectural disturbance or evidence of fibrosis. Neither did any treated animal exhibit outward signs of ill health, gaining weight at the same rate as untreated animals with UUO.

In conclusion, we demonstrated that targeting *Kras* with ASOs can prevent the onset of fibrosis in a rat model of unilateral obstruction, even in the presence of significant inflammation. New ASO design techniques promise to produce noninflammatory ASOs, which may be used in future studies.

Chronic inflammation is generally thought, in clinical medicine, to inevitably lead to irreversible fibrosis. The dissociation between inflammation and fibrosis demonstrated herein suggests that this may not always be so. If fibrosis can be inhibited while the initial insult resulting in inflammation is either removed or controlled, irreversible scarring of the kidney may be avoided. Although further study is called for, we believe that ASOs targeting *Kras* represent a first step in developing a true "antifibrotic" therapy, one that in the future may prevent renal fibrosis.

Acknowledgments

We thank the late Dr. Neelanjana Dutt, who contributed substantially to this work with her expertise in renal histopathology.

References

1. Norman JT, Fine LG: Progressive renal disease: fibroblasts, extracellular matrix, and integrins. Exp Nephrol 1999, 7:167–177
2. Iwano M, Plieth D, Danoff TM, Xue C, Okada H, Neilson EG: Evidence that fibroblasts derive from epithelium during tissue fibrosis. J Clin Invest 2002, 110:341–350
3. Lin SL, Kisseleva T, Brenner DA, Duffield JS: Pericytes and perivascular fibroblasts are the primary source of collagen-producing cells in obstructive fibrosis of the kidney. Am J Pathol 2008, 173:1617–1627
4. Eddy AA: Molecular basis of renal fibrosis. Pediatr Nephrol 2000, 15:290–301
5. Wittinghofer A, Scheffzek K, Ahmadian MR: The interaction of Ras with GTPase-activating proteins. FEBS Lett 1997, 410:63–67
6. Bos JL: ras oncogenes in human cancer: a review. Cancer Res 1989, 49:4682–4689
7. Clarke HC, Kocher HM, Khwaja A, Kloog Y, Cook HT, Hendry BM: Ras antagonist farnesylthiosalicylic acid (FTS) reduces glomerular cellular proliferation and macrophage number in rat thy-1 nephritis. J Am Soc Nephrol 2003, 14:848–854
8. Dockrell ME, Phanish MK, Hendry BM: Tgf-β auto-induction and connective tissue growth factor expression in human renal tubule epithelial cells requires N-ras. Nephron Exp Nephrol 2009, 112:e71–e79
9. Grande MT, Fuentes-Calvo I, Arevalo M, Heredia F, Santos E, Martinez-Salgado C, Rodriguez-Puyol D, Nieto MA, Lopez-Novoa JM: Deletion of H-Ras decreases renal fibrosis and myofibroblast activation following ureteral obstruction in mice. Kidney Int 2010, 77:509–518
10. Janda E, Lehmann K, Killisch I, Jechlinger M, Herzig M, Downward J, Beug H, Grunert S: Ras and TGFβ cooperatively regulate epithelial cell plasticity and metastasis: dissection of Ras signaling pathways. J Cell Biol 2002, 156:299–313
11. Kocher HM, Moorhead J, Sharpe CC, Dockrell ME, Al-Nawab M, Hendry BM: Expression of Ras GTPases in normal kidney and in glomerulonephritis. Nephrol Dial Transplant 2003, 18:2284–2292
12. Lahsnig C, Mikula M, Petz M, Zulehner G, Schneller D, van Zijl F, Huber H, Csiszar A, Beug H, Mikulits W: ILEI requires oncogenic Ras for the epithelial to mesenchymal transition of hepatocytes and liver carcinoma progression. Oncogene 2009, 28:638–650
13. Martinez-Salgado C, Fuentes-Calvo I, Garcia-Cenador B, Santos E, Lopez-Novoa JM: Involvement of H- and N-Ras isoforms in transforming growth factor-β1-induced proliferation and in collagen and fibronectin synthesis. Exp Cell Res 2006, 312:2093–2106
14. Rodriguez-Pena AB, Grande MT, Eleno N, Arevalo M, Guerrero C, Santos E, Lopez-Novoa JM: Activation of Erk1/2 and Akt following unilateral ureteral obstruction. Kidney Int 2008, 74:196–209
15. Bechtel W, McGoohan S, Zeisberg EM, Muller GA, Kalbacher H, Salant DJ, Muller CA, Kalluri R, Zeisberg M: Methylation determines fibroblast activation and fibrogenesis in the kidney. Nat Med 2010, 16:544–550
16. Johnson L, Greenbaum D, Cichowski K, Mercer K, Murphy E, Schmitt E, Bronson RT, Umanoff H, Edelmann W, Kucherlapati R, Jacks T: K-ras is an essential gene in the mouse with partial functional overlap with N-ras. Genes Dev 1997, 11:2468–2481
17. Santos E, Nebreda AR: Structural and functional properties of ras proteins. FASEB J 1989, 3:2151–2163
18. Sharpe CC, Dockrell ME, Noor MI, Monia BP, Hendry BM: Role of Ras isoforms in the stimulated proliferation of human renal fibroblasts in primary culture. J Am Soc Nephrol 2000, 11:1600–1606
19. Sharpe CC, Dockrell ME, Scott R, Noor MI, Cowsert LM, Monia BP, Hendry BM: Evidence of a role for Ki-Ras in the stimulated proliferation of renal fibroblasts. J Am Soc Nephrol 1999, 10:1186–1192
20. Wang JH, Hendry BM, Sharpe CC: Silencing genes in the kidney: antisense or RNA interference? Nephrol Dial Transplant 2008, 23:2115–2118
21. Sands H, Gorey-Feret LJ, Cocuzza AJ, Hobbs FW, Chidester D, Trainor GL: Biodistribution and metabolism of internally 3H-labeled oligonucleotides, I: comparison of a phosphodiester and a phosphorothioate. Mol Pharmacol 1994, 45:932–943
22. Ohta M, Seto M, Ijichi H, Miyabayashi K, Kudo Y, Mohri D, Asaoka Y, Tada M, Tanaka Y, Ikenoue T, Kanai F, Kawabe T, Omata M: Decreased expression of the RAS-GTPase activating protein RASAL1 is associated with colorectal tumor progression. Gastroenterology 2009, 136:206–216
23. Le Hir M, Hegyi I, Cueni-Loffing D, Loffing J, Kaissling B: Characterization of renal interstitial fibroblast-specific protein 1/S100A4-positive cells in healthy and inflamed rodent kidneys. Histochem Cell Biol 2005, 123:335–346

The American Journal of Pathology, Vol. 179, No. 2, August 2011

DOI: 10.1016/j.ajpath.2011.04.021

Cardiovascular, Pulmonary, and Renal Pathology

miR-21 and miR-214 Are Consistently Modulated during Renal Injury in Rodent Models

Laura Denby,* Vasudev Ramdas,* Martin W. McBride,* Joe Wang,† Hollie Robinson,* John McClure,* Wendy Crawford,* Ruifang Lu,* Dianne Z. Hillyard,* Raya Khanin,‡ Reuven Agami,§ Anna F. Dominiczak,* Claire C. Sharpe,† and Andrew H. Baker*

From the BHF Glasgow Cardiovascular Research Centre, Glasgow, United Kingdom; the Department of Renal Medicine,† The Rayne Institute, King's College London, London, United Kingdom; the Department of Statistics,‡ University of Glasgow, Glasgow, United Kingdom; and the Division of Gene Regulation,§ The Netherlands Cancer Institute, Amsterdam, The Netherlands*

Transforming growth factor (TGF)-β is one of the main fibrogenic cytokines that drives the pathophysiology of progressive renal scarring. MicroRNAs (miRNAs) are endogenous non-coding RNAs that post-transcriptionally regulate gene expression. We examined the role of TGF-β–induced expression of miR-21, miRNAs in cell culture models and miRNA expression in relevant models of renal disease. *In vitro*, TGF-β changed expression of miR-21, miR-214, and miR-145 in rat mesangial cells (CRL-2753) and miR-214, miR-21, miR-30c, miR-200b, and miR-200c during induction of epithelial-mesenchymal transition in rat tubular epithelial cells (NRK52E). miR-214 expression was robustly modulated in both cell types, whereas in tubular epithelial cells miR-21 was increased and miR-200b and miR-200c were decreased by 58% and 48%, respectively, in response to TGF-β. TGF-β receptor-1 was found to be a target of miR-200b/c and was downregulated after overexpression of miR-200c. To assess the differential expression of these miRNAs *in vivo*, we used the anti-Thy1.1 mesangial glomerulonephritis model and the unilateral ureteral obstruction model in which TGF-β plays a role and also a genetic model of hypertension, the stroke-prone spontaneously hypertensive rat with and without salt loading. The expressions of miR-214 and miR-21 were significantly increased in all *in vivo* models, showing a possible miRNA signature of renal damage despite differing causes. *(Am J Pathol 2011, 179:661–672; DOI: 10.1016/j.ajpath.2011.04.021)*

Transforming growth factor (TGF)-β is a critically important mediator of pathophysiological events in renal disease.[1,2] Many types of glomerular diseases, including IgA nephropathy and lupus nephritis are characterized by mesangial cell proliferation,[3] mesangial matrix expansion, and alterations in extracellular turnover and composition. In the chronic anti-Thy1.1 model of glomerulonephritis, proliferation of mesangial cells is followed by the production of extracellular matrix, leading to chronic glomerulosclerosis and eventually interstitial fibrosis. Tubulo-interstitial fibrosis is the common end point of most progressive kidney diseases and results in loss of renal function. The model of unilateral ureteral obstruction (UUO) has been widely used as an animal model of tubulo-interstitial disease that is characterized by a mononuclear cell infiltration followed by fibroblast proliferation, increased extracellular matrix deposition, and tubule atrophy. These common processes of fibrosis and sclerosis are known to be driven primarily by TGF-β along with a host of other cytokines and growth factors. It is probable therefore that these pathologic processes involve interrelated and complex molecular pathways in which microRNAs (miRNAs) may play an important regulatory role.

In humans, decreased renal function is often a complication of essential hypertension, and hypertension is one of the most common causes of end-stage renal disease in the United States.[4] A rat genetic model of essential hypertension the stroke-prone, spontaneously hypertensive rat (SHRSP) also develops renal damage with age.[5,6] The damage observed is typically vascular smooth muscle hyperplasia and tubule atrophy and/or dilation.[5] Furthermore, in humans salt sensitivity is common in persons with essen-

Supported by Kidney Research UK, British Heart Foundation Chair, and Programe Grants (RG/09/005/27915 and BHFRG/07/005/23633) and by a pump priming grant from the Integrative Mammalian Biology Initiative at the University of Glasgow.

Accepted for publication April 29, 2011.

Supplemental material for this article can be found at *http://ajp.amjapthol.org* or at doi: 10.1016/j.ajpath.2011.04.021.

Address reprint requests to Andrew H. Baker, Ph.D., BHF Glasgow Cardiovascular Research Centre, Institute of Cardiovascular and Medical Sciences, College of Medicine, Veterinary Medicine and Life Sciences, University of Glasgow, Glasgow, G12 8TA United Kingdom. E-mail: andrew.h.baker@glasgow.ac.uk.

tial hypertension, and, when SHRSPs are challenged with salt, this increases their systolic blood pressure [not observed in Wistar-Kyoto (WKY) rats] and induces further renal damage compared with WKY rats.[7]

miRNAs are endogenous non-coding RNAs that are ~22 nucleotides in length and can have structural, enzymatic, and regulatory functions.[8] miRNAs act within the RNA-induced silencing complex[9] and can down-regulate gene expression by binding to the 3′-untranslated region (UTR) of the mRNA which results in either productive translational repression or target degradation. miRNAs are fundamental in development and are expressed in a tissue-specific manner.[10–12] However, they have now been found to play a role in the pathophysiology of many diverse diseases, including cancer,[13,14] vascular proliferative disease,[15] and cardiac hypertrophy.[16] It is clear that many genes contain miRNA binding sequences within their 3′-UTR, and a single miRNA can "hit" multiple genes and influence many pathways.[8] With respect to the kidneys, a number of studies of miRNA expression have been conducted.[17–22] They have been shown to be fundamentally important in the kidney by several studies.[19–21] For example, targeted knockout of DICER, a protein important in miRNA biogenesis, selectively in podocytes leads to severe proteinuria.[2,19–22] These animals had marked abnormalities in the glomerulus, including foot process effacement, mesangial expansion, and glomerulosclerosis, which ultimately lead to animal death. From those studies it appears that several miRNAs are important for normal kidney homeostasis; miR-30a was found to be lost in podocytes of DICER knockout mice compared with controls[20] and in mutant glomeruli where mature miRNAs were knocked out targets of the miR-30 family were enriched in the up-regulated genes.[19]

Several miRNAs have also been shown to have specific localization within the kidney. With the use of locked nucleic acid (LNA)—immunostaining in the normal kidney it has been shown that miR-23b, miR-24, and miR-26a show a pan glomerular localization[20,21]; miR-145 is found in mesangial cells[20] and vascular smooth muscle cells[20]; miR-10a and miR-30c are reported to be tubular specific[20,21]; and miR-126 is detected in the glomerular and peritubular endothelial cells.[20] Furthermore, an integrated study of miRNAs and gene targets found several miRNAs differentially regulated, miR-21, miR-31, miR-128, miR-147, and miR-217, in polycystic kidney disease[17]; however, the role of these differentially expressed miRNAs in polycystic kidney disease has yet to be shown *in vivo*.

TGF-β has been shown to stimulate a set of miRNAs.[18,22,23] miR-192 and miR-377 are up-regulated in mouse[18,22] and human[18,22] mesangial cells *in vitro* in response to TGF-β and also *in vivo* in mouse diabetic models.[18,22] Analysis of the targets has shown that miR-192 targets SIP1[18] and miR-377 targets p21-activated kinase and superoxide dismutase,[22] which results in an increase in collagen and fibronectin, respectively. In contrast TGF-β–stimulated epithelial-mesenchymal transition (EMT) results in loss of the miR-200 family,[24–26] and an increase in expression targets the E-cadherin repressors ZEB1 and ZEB2.[24–26]

Because miRNAs have been shown to be essential in kidney homeostasis, we sought to assign a specific role for TGF-β in modulation of miRNAs in cell culture and *in vivo* with respect to renal pathology. We therefore focused our analysis on a subset of miRNAs with potential relevance in this setting (miR-21, miR-214, miR-192, miR-26b, miR-145, miR-24, miR-30c, and miR-200b/c). We used two *in vitro* models to assess TGF-β stimulation of rat mesangial cells and induction of EMT in rat kidney tubular epithelial cells. We then investigated the expression of these miRNAs in the chronic anti-Thy1.1 model of glomerulonephritis, the UUO model of interstitial fibrosis, and a rat genetic model of hypertension, the SHRSP.

Materials and Methods

In Vitro *Analysis of miRNA*

Rat mesangial cells (CRL-2753) and rat tubular epithelial cells (NRK52E) were cultured according to American Type Culture Collection (ATCC; Manassas, VA) instructions. Cells were serum starved for 48 hours (0.2% fetal calf serum) before stimulation with 10 ng/mL TGF-β(R&D Systems, Minneapolis, MN). Total RNA was extracted from the cells at 24, 48, 72, and 96 hours after stimulation with the use of miRNeasy kit (Qiagen, Inc., Valencia, CA) following the manufacturer's instructions, treated with the Turbo DNase (Ambion, Austin TX), to eliminate genomic DNA contamination, and quantified with the use of the NanoDrop ND-1000 Spectrophotometer (Nano-Drop Technologies, Wilmington, DE).

In Vitro *Analysis of EMT*

NRK52E cells were plated in 6-well plates at 8×10^4 cells per well. Cells were serum starved for 48 hours (0.2% fetal calf serum) before stimulation with 10 ng/mL TGF-β (R&D Systems). Total RNA and protein were extracted at 24, 48, 72, and 96 hours after stimulation. RNA was extracted and treated as before. Immunocytochemistry was performed with α-smooth muscle actin (α-SMA; 1:500; Abcam, Cambridge, MA) and goat anti-mouse Alexa Fluro 546 secondary antibody (Invitrogen, Paisley, UK) with DAPI Prolong Gold mounting media (Invitrogen). Protein was quantified, and 50 μg was fractionated on 7.5% (for E-cadherin) and 10% (for α-SMA) SDS polyacrylamide gels. Proteins were transferred onto nitrocellulose membranes and probed for E-cadherin (1:2000; BD Biosciences, San Jose, CA) and α-SMA (1:500; Abcam) antibodies. Membranes were exposed with the use of enhanced chemiluminescence ECL (GE Healthcare, Chalfont St Giles, Buckingham, UK) and developed using the X-OMAT 100 (Kodak, Rochester, NY).

TGF-β Inhibition Experiments

TGF-β inhibition experiments were performed with commercially available TGF-β receptor-1 (TGFβR1; Alk5) inhibitors A-83-01 and AB525339 (Tocris Bioscience, Bristol, UK) at a concentration of 1 μmol/L. NRK52E cells were

plated at 8×10^4 cells per well. Cells were serum starved for 48 hours (0.2% fetal calf serum) before adding either inhibitor or dimethyl sulfoxide (DMSO; vehicle control) for 1 hour before stimulation with 10 ng/mL TGF-β (R&D Systems). RNA was extracted and treated as before.

Manipulation of miR-200c Levels

NRK52E cells (ATCC) were plated in 6-well plates at 1×10^5 cells per well. Cells were transfected with cytomegalovirus–pri-miR-200c plasmid with the use of 2 μg of DNA/3 μL of lipofectamine per well. Lipofectamine:DNA complex was left on the cells for 5 hours, then supplemented with 20% serum containing media. Twenty-four hours later the cells were washed with PBS, and cells were replenished with fresh serum-free media. After 48 hours serum-starving cells were stimulated with TGF-β (10 ng/mL) and left for 72 hours. Total RNA was extracted as described above, and miR-200c levels were quantified.

Manipulation of miR-21 and miR-214 Levels

Lentiviral vectors were produced by triple transient transfection of HEK293T cells with a packaging plasmid (pCMVΔ8.74), a plasmid encoding the envelope of vesicular stomatitis virus (kind gift from Adrian J. Thrasher, London, UK), and the expression plasmid, using polyethylenimine (Sigma-Aldrich, St Louis, MO) as previously described.[27] Lentiviral titers were ascertained by TaqMan real-time quantitative PCR (qPCR) as previously described.[28] To overexpress the miR-21 and miR-214 the precursor (pre)–miRNA sequences were obtained from miRBase (*http://microrna.sanger.ac.uk*), codon-optimized, and manufactured by GeneArt (Regensburg, Germany) and subsequently cloned into the *Hin*DIII-*Eco*RV sites of pcDNA3.1 (Invitrogen). As the *Xho*I and *Bam*H1 restriction sites were maintained, the pre-miR sequence was cloned directly into the pLNT/SFFV-MCS plasmid (kind gift from Adrian J. Thrasher, London, UK) to obtain the construct pLNT/SFFV-pre-miR.

Reverse Transcription of miRNA

After quantification of DNase-treated RNA, miRNA reverse transcription was performed with stem-loop reverse transcription primers according to the TaqMan MicroRNA Assay protocol (Applied Biosystems, Foster City, CA). Each reaction contained 5 ng of extracted total RNA and 50 nmol/L stem-looped reverse transcription primer, specific for each miRNA. cDNA synthesis was performed on 1 μg of total RNA with the use of reverse transcription reagents (Applied Biosystems) following the manufacturer's protocol.

miRNA and Gene Expression

Real-time qPCR was performed. The amplification step was performed with specific Taqman miRNA probe or for gene expression inventoried gene expression-specific primers (Applied Biosystems) on the Applied Biosystems 7900 HT real-time PCR system following the manufacturer's instructions. U87 was used as an endogenous control for the miRNA expression, and rat glyceraldehyde-3-phosphate dehydrogenase (GAPDH) was used as an endogenous control for gene expression. Results are shown as RQ $\pm$ RQ max, calculated with SD.

Northern Blotting

Total RNA was extracted from cells or rat tissues with the use of miRNeasy Mini kit (Qiagen, Dorking, Surrey, UK). Three to 10 μg of total RNA was resolved in a 15% tris-boric acid-EDTA and urea denaturing gel (Invitrogen), transferred onto Hyband-NX membrane (GE Healthcare). After 1-ethyl-3-[3-dimethylaminopropyl]carbodiimide hydrochloride (EDC) cross-linking, membranes were hybridized with 5′-DIG–labeled LNA Mercury probes (Exiqon, Vedbaek, Denmark) at 40°C (miR-21 probe) or 55°C (miR-214 probe and U6) overnight. After post-hybridization washes, membranes were incubated with anti-DIG-AP antibody (1:5000; Roche, Burgess Hill, UK) in 1% blocking reagents (Roche), and signals were detected with CDP-Star (Sigma-Aldrich) according to the manufacturer's instructions.

Prediction of Potential miRNA Targets

A list of targets for miR-21 and miR-214 was obtained through searching 3′-UTR sequences of rat mRNAs for the seeds of miRNAs. Rat mRNAs were downloaded from the USCS Genome Browser (*http://genome.ucsc.edu*). For each 3′-UTR, a number of seeds, its flanking nucleotides, and position were recorded.[29,30] Each list of potential targets was screened with specific criteria, including high number of seeds, small distance between seeds, intersection between the two miRNAs, and physiological function of the targets.[29,30]

Animal Models

All protocols and surgical procedures were approved by the local animal care committee. Animal experiments were in accordance with the Animals Scientific Procedures Act UK 1986.

Induction of Mesangial Proliferative Glomerulonephritis

Male WKY rats (Harlan, Wyton, UK) (7 to 12 weeks old) were used throughout. All protocols and surgical procedures were approved by the local animal care committee. Animals were age matched at sacrifice to minimize age-related differences in miRNA expression. For the induction of mesangial proliferative glomerulonephritis rats were intravenously infused with 2 mg/kg ER4. For the three-injection protocol the ER4 was infused three times, 1 week apart. After sacrifice, kidneys were removed, and portions were fixed in 10% formalin or snap frozen and stored at -80°C.

Histologic scoring was adapted from Tomita et al[31] and was performed blind with 50 glomeruli and surround-

ing tubules scored per section. Glomerular damage was scored from 0 to 4, with 0 being 0% to 4% glomerular lesion, mesangial matrix expansion; 1 being 5% to 24%; 2 being 25% to 49%; 3 being 50% to 74%; and 4 being >75%. Interstitial lesions were counted as tubular dilation, tubular trophy, basophilia, interstitial inflammation, and fibrosis and were scored from 0 to 4, with 0 being no lesion, 1 being <5%, 2 being 5% to 24%, 3 being 25% to 49%, and 4 being ≥50%.

Unilateral Ureteral Obstruction

Male Wistar rats weighing 200 g were used. Each rat was initially placed in an induction chamber and exposed to 4% isoflurane and oxygen at a flow rate of 4 L/minute. Once anesthetized, the rat was transferred to a heated mat with continued administration of isoflurane at 2% to 2.5%. A midline incision was made with aseptic technique, and the left kidney was exposed. The left ureter was isolated by blunt dissection, and two 6-0 silk ligatures were tied around it. The incision was re-sutured, and buprenorphine was administered subcutaneously at a dose of 30 μg/kg. As a control, a sham operation was performed, including a laparotomy and handling of the ureter, only it was not ligated. All rats were sacrificed on postoperative day 16. After sacrifice, kidneys were removed, and portions were fixed in 10% formalin or snap frozen and stored at −80°C.

Genetic Rat Model of Hypertension

Inbred colonies of SHRSP and WKY rats have been developed and maintained at the University of Glasgow since 1991, as described previously.[32] For salt-loading experiments, at 18 weeks of age, rats were given a salt challenge (1% NaCl in drinking water) for 3 weeks. All animals were sacrificed at 21 weeks. After sacrifice, kidneys were removed, snap frozen, and stored at −80°C.

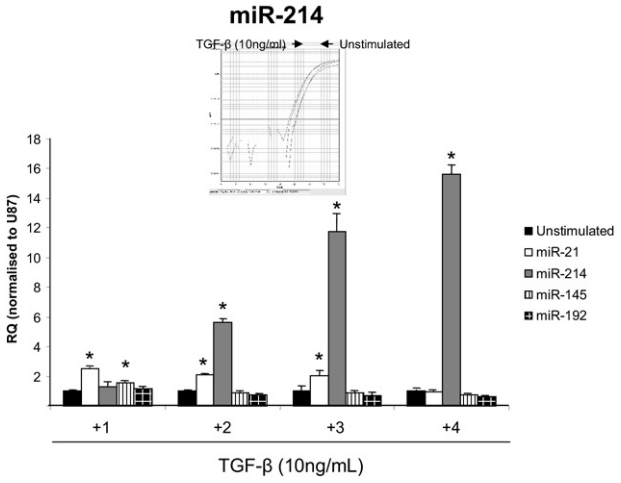

Figure 1. Effect of TGF-β on microRNA expression in cultured rat mesangial cells. Rat mesangial cells (CRL-2573; RMCs) were stimulated with 10 ng/mL rTGF-β (R&D Systems) over a 4-day time course. RNA was harvested from the cells by miReasy kit (Qiagen), and miRNA expression was measured by specific miRNA Taqman probes (Applied Biosystems) and normalized to U87. RQ ± RQ max. $^*P < 0.05$ versus unstimulated time-matched controls. **Inset** is a representative Taqman amplification curve from one unstimulated versus a TGF-β sample; $N = 3$.

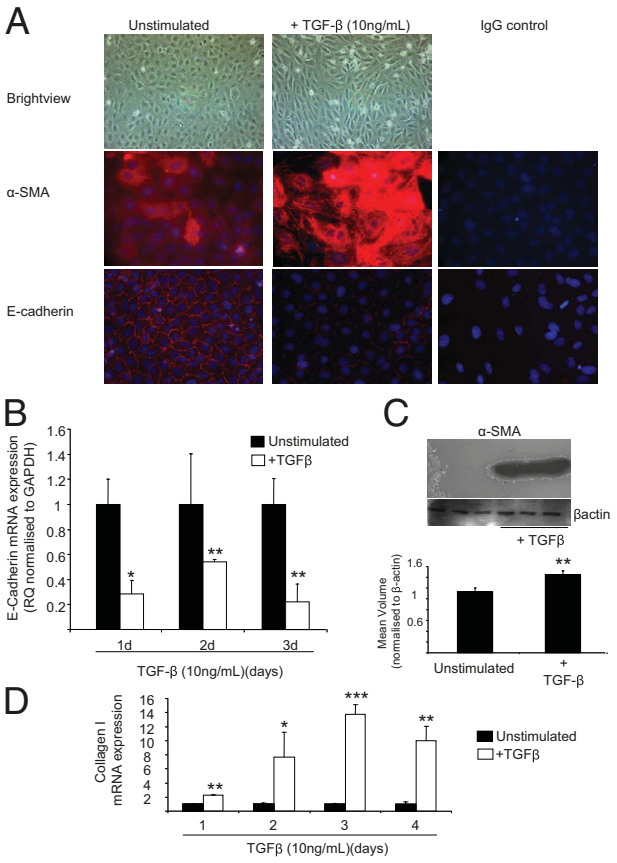

Figure 2. TGF-β–induced EMT in cultured rat tubular epithelial cells. Rat tubular epithelial cells (NRK52E; NRK) were stimulated with 10 ng/mL rTGF-β (R&D Systems) over a 4-day time course. **A:** Immunocytochemistry for α-SMA and E-cadherin expression in unstimulated and TGF-β–stimulated cells (5 days); original magnification, ×40. **B:** E-cadherin gene expression. Total RNA was extracted with the miRNeasy kit (Qiagen), and E-cadherin expression was measured by specific rat Taqman probes (Applied Biosystems) and normalized to rat GAPDH. RQ ± RQ max. $^*P < 0.05$ and $^{**}P < 0.01$ versus unstimulated time-matched controls. **C:** α-SMA protein expression in cells undergoing EMT. Western blot analysis of cell lysates probed for α-SMA and β-actin as a loading control. Images underwent densitometry. Mean volume ± SD. $^{**}P < 0.01$. **D:** Gene expression of collagen 1 in unstimulated and TGF-β–stimulated cells. RQ ± RQ max. $^*P < 0.05$, $^{**}P < 0.01$, and $^{***}P < 0.001$ compared with unstimulated time-matched control cells.

Statistical Analysis

All *in vitro* experiments were performed in triplicate on three separate occasions. All *in vivo* work was conducted in groups of four to six. A standard Student's *t*-test was used to designate significant differences between control and other groups.

Results

TGF-β Induces Changes in miRNA Profiles in Renal Cells in Vitro

We first investigated the expression of miRNAs modulated by TGF-β in the rat mesangial cell line CRL-2573

and tubular epithelial cell line NRK52E. Both were stimulated with rTGF-β (10 ng/mL) and assessed for individual miRNA levels compared with no stimulation. The response of mesangial cells to TGF-β stimulation was to significantly proliferate to levels similar to that seen after incubation in growth media (see Supplemental Figure S1A at *http://ajp.amjpathol.org*). We also found significant increase in the gene expression of TGF-β and TGFβ-R1 (see Supplemental Figure S1, B and C, at *http://ajp.amjpathol.org*), showing that cellular levels of TGF-β were increased after stimulation. Notably, in the mesangial cell line miR-214 was significantly up-regulated 2 days after stimulation ($P < 0.01$) and remained elevated for the time course with the peak expression of ~16-fold increase at 4 days after stimulation when evaluated in a detailed time course (Figure 1). miR-21 expression showed a sustained significant increase ~twofold from day 1 to day 3 before dropping to levels below that expressed in time-matched control cells (Figure 1). No increase in miR-192 was observed (Figure 1), which is in contrast to previous reports.[18,22] This suggests that miR-192 may be differentially regulated or expressed in rat mesangial cells as assessed by real-time qPCR. Interestingly, miR-145 was significantly elevated 24 hours after stimulation before returning to unstimulated levels (Figure 1).

In tubular epithelial cells, TGF-β stimulation resulted in EMT, characterized by loss of E-cadherin expression, gain of α-SMA expression and increased collagen production (Figure 2, A–D). In response to TGF-β stimulation the NRK52E (NRK) cells also increased the expression of both TGF-β and TGF-βR1 gene expression (see Supplemental Figure S2 at *http://ajp.amjpathol.org*). TGF-β stimulation of the NRK cells resulted in miR-200b and miR-200c being significantly down-regulated by day 4 of TGF-β stimulation, with miR-200b and miR-200c being reduced 58% and 48%, respectively, compared with time-matched unstimulated controls (Figure 3). miR-192 was not significantly different over the time course (Figure 3), but miR-30c had a significant decrease in expression 24 hours after TGF-β stimulation, which remained for the time course. However, and similar to data obtained in the mesangial cells, miR-214 and miR-21 were significantly up-regulated over the time course in the NRK cells (Figure 3). To further examine miR-21 and miR-214 expression we performed Northern blot analyses and found that over the 5-day time course stimulation of NRK cells with TGF-β resulted in increased expression of the mature miR-21 and miR-214 (see Supplemental Figure S3 at *http://ajp.amjpathol.org*). Interestingly, when the precursors of the miRs are examined, there is increased expression of pre-miR-21 after stimulation of cells with TGF-β (see Supplemental Figure S3 at *http://ajp.amjpathol.org*). In contrast no pre-miR-214 could be detected, but there was very high expression of primary (pri)–miR-214 expressed in NRK cells at all time points in both unstimulated and stimulated cells (see Supplemental Figure S3 at *http://ajp.amjpathol.org*).

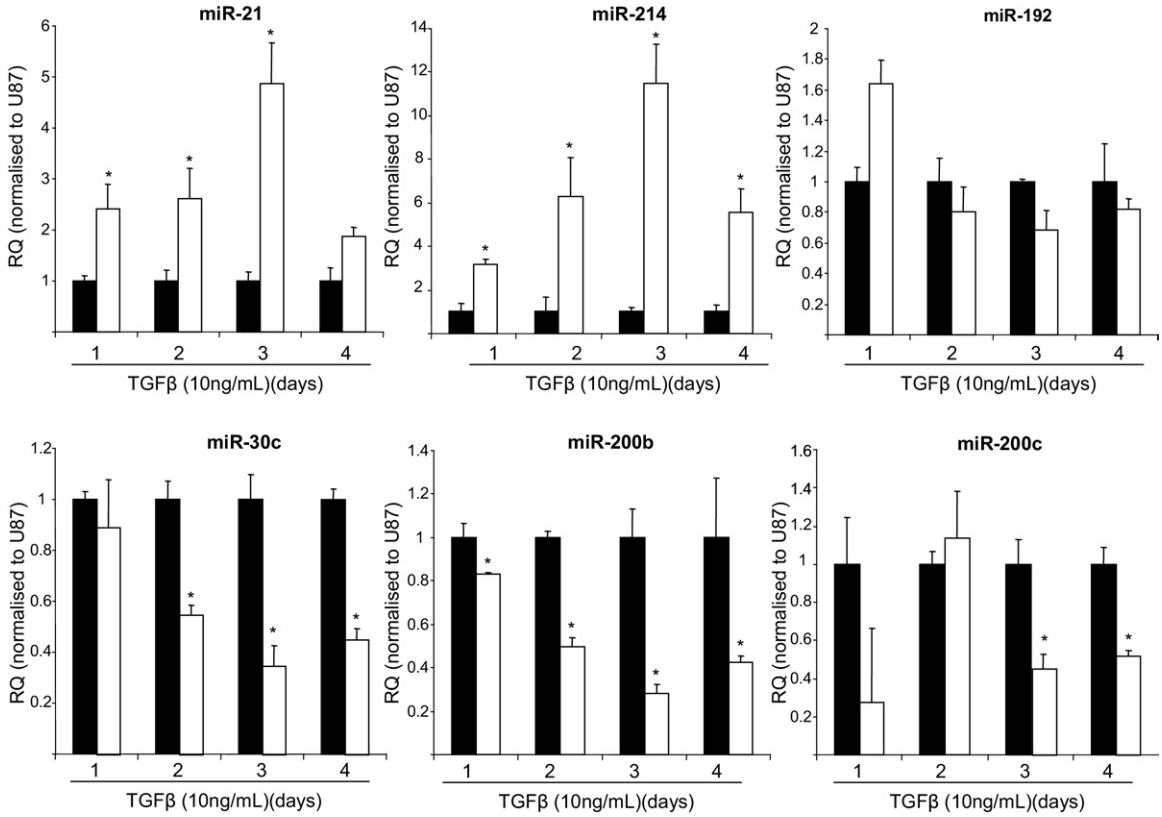

Figure 3. miRNA expression in tubular epithelial cells undergoing EMT. Rat tubular epithelial cells (NRK52E; NRK) were stimulated with 10 ng/mL rTGF-β (R&D Systems) over a 4-day time course. RNA was harvested from the cells by miReasy kit (Qiagen), and miRNA expression was measured by specific miRNA Taqman probes (Applied Biosystems) and normalized to U87. Each graph represents an individual miRNA. RQ ± RQ max. *$P < 0.05$ compared with unstimulated time-matched control cells.

To examine whether TGF-β directly affected the expression of miR-21 and miR-214, we sought to block TGF-β signaling with the use of TGF-βR1 signaling inhibitors (SB525339 and A-83-01). Both inhibitors block downstream activation of the TGF-β signaling cascade, but they allow binding of TGF-β to TGFRII.[33] With the use of the rat tubular epithelial cells, we serum starved the cells for 48 hours then treated the cells with SB525339, A-83-01, or DMSO (vehicle control) for 1 hour before stimulating the cells with TGF-β (10 ng/mL) for 4 days. As expected cells treated with DMSO had a significant increase in miR-21 and miR-214 expressions in response to TGF-β stimulation, which was abolished by both inhibitors (see Supplemental Figure S4A at *http://ajp.amjpathol.org*). Similarly, the TGF-βRI inhibitors also blocked the loss of the miR-200 family and other TGF-β–modulated miRNAs in these cells (see Supplemental Figure S4B at *http://ajp.amjpathol.org*). The inhibitor A-83-01 has previously been shown to block EMT induced by TGF-β,[34] and we found that both inhibitors prevented the loss of E-cadherin expression and increased in expression of α-SMA and collagen 1a, observed when the cells undergo EMT (see Supplemental Figure S4C at *http://ajp.amjpathol.org*).

To examine the effects of miR-21 and miR-214 alone, we constructed lentiviruses expressing pre-miR-21 (LNT-miR-21) and pre-miR-214 (LNT-miR-214) to allow overexpression of each miRNA and performed experiments in culture in the absence of TGF-β. Infection of rat tubular epithelial cells with LNT-miR-21 resulted in an increase of mature miR-21 expression by ~3.5-fold compared with uninfected cells or LNT-egfp–infected cells (Figure 4A). Infection with LNT-miR-214 resulted in a significant increase of ~400-fold in the levels of mature miR-214 (Figure 4B). The effect of overexpressing either miR-21 or miR-214 was to induce a change in EMT-associated markers E-cadherin, α-SMA, and collagen I, similar to that observed when these cells undergo EMT in response to TGF-β (Figure 4C). In summary, our *in vitro* data show that TGF-β modulates the expression of several miRNAs in both cell types (miR-214, miR-21, miR-30c, miR-200b, and miR 200c).

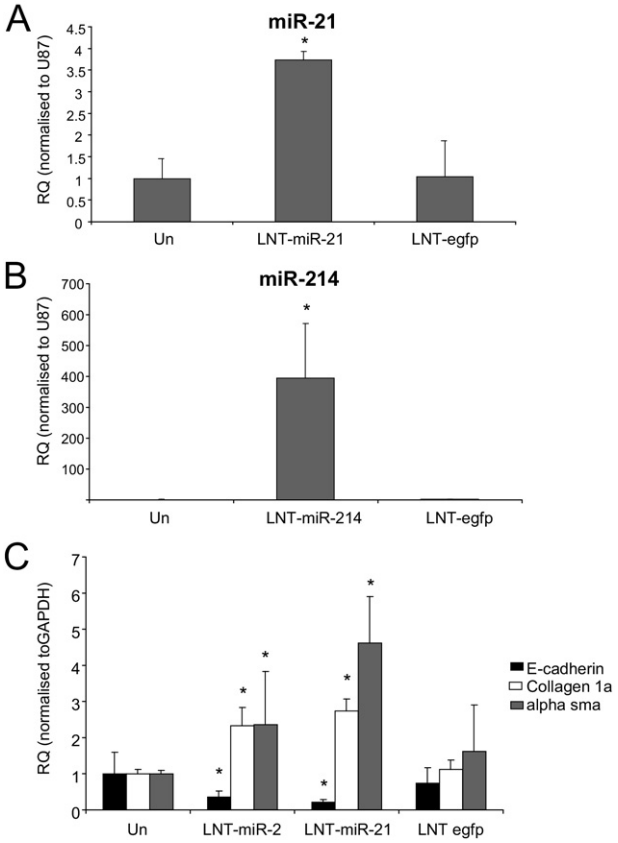

Figure 4. Effect of miR-21 and miR-214 overexpression on rat tubular epithelial cells. NRK52E cells were infected with Lenti-(LNT) miR-21, LNT-miR-214, or LNT-egfp at a multiplicity of infection of 5 for 24 hours. Cells were then serum starved for 2 days and then cultured for 4 days in serum-free media. RNA was harvested from the cells by miReasy kit (Qiagen), and miRNA expression was measured by specific miRNA Taqman probes (Applied Biosystems) and normalized to U87. Gene expression was measured with the use of gene-specific probes (rat) and normalized to GAPDH. **A:** Expression of miR-21 by LNT-miR-21. RQ ± RQ max. **B:** Expression of miR-214 by LNT-miR-214. RQ ± RQ max. **C:** Modulation of EMT-associated genes by LNT-miR-21, LNT-miR-214, and LNT-egfp. RQ ± RQ max. Un, unifected. $^*P < 0.05$ versus Un.

TGFβR1 Is a Target for miR-200c and Is Modulated by Dynamic Changes in miR-200c Levels

We examined the potential targets of miR-200b/c (because these share the same seed sequence). The 3′-UTR sequences of rat mRNAs for the seeds of miRNAs (nucleotides 2 to 7) that we were interested in were downloaded from the USCS Genome Browser and were searched for potential targets.[18,24] Interestingly, when a search of targets of miR-200b/c was performed, many other targets along with ZEB1 and ZEB2[24–26] were found (see Supplemental Table S1 at *http://ajp.amjpathol.org*). This list included TGFβR1, which has six seeds for miR-200b/c within its 3′-UTR, one of which is a 7mer-m8 (position 746) and another a 7mer-1A (position 3755) (see Supplemental Table S1 at *http://ajp.amjpathol.org*; Figure 5A). To investigate whether the miR-200b/c members regulate the expression of TGFβR1 we initially used the *in vitro* model of TGF-β–stimulated EMT in rat tubular epithelial cells. We used plasmid-based transfection to overexpress miR-200c. miR-21 and miR-200b were used as controls because TGF-β induced miR-21 expression and reduced miR-200b expression (Figure 3). In cells transfected with pri-miR-200c, stimulation with TGF-β resulted in the same pattern, an increase in miR-21 (2.7-fold increase) and a 64% decrease in miR-200c expression (Figure 5B). When EMT markers were examined, overexpression of pri-miR-200c resulted in a significant decrease in α-SMA and collagen I after stimulation with TGF-β, which was similar to that observed before.[26] Stimulation with TGF-β resulted in a marked reduction in miR-200c (75%) and a significant induction of TGFβ-R1 ($P < 0.05$; Figure 5B). Overexpression of pri-miR-200c resulted in an approximate sevenfold increase in miR-200c expression and a marked inhibition (~48%) of TGFβR1 expression (Figure 5). Therefore, the changes in miRNA associated with TGF-β are reflected in changes in TGFβR1.

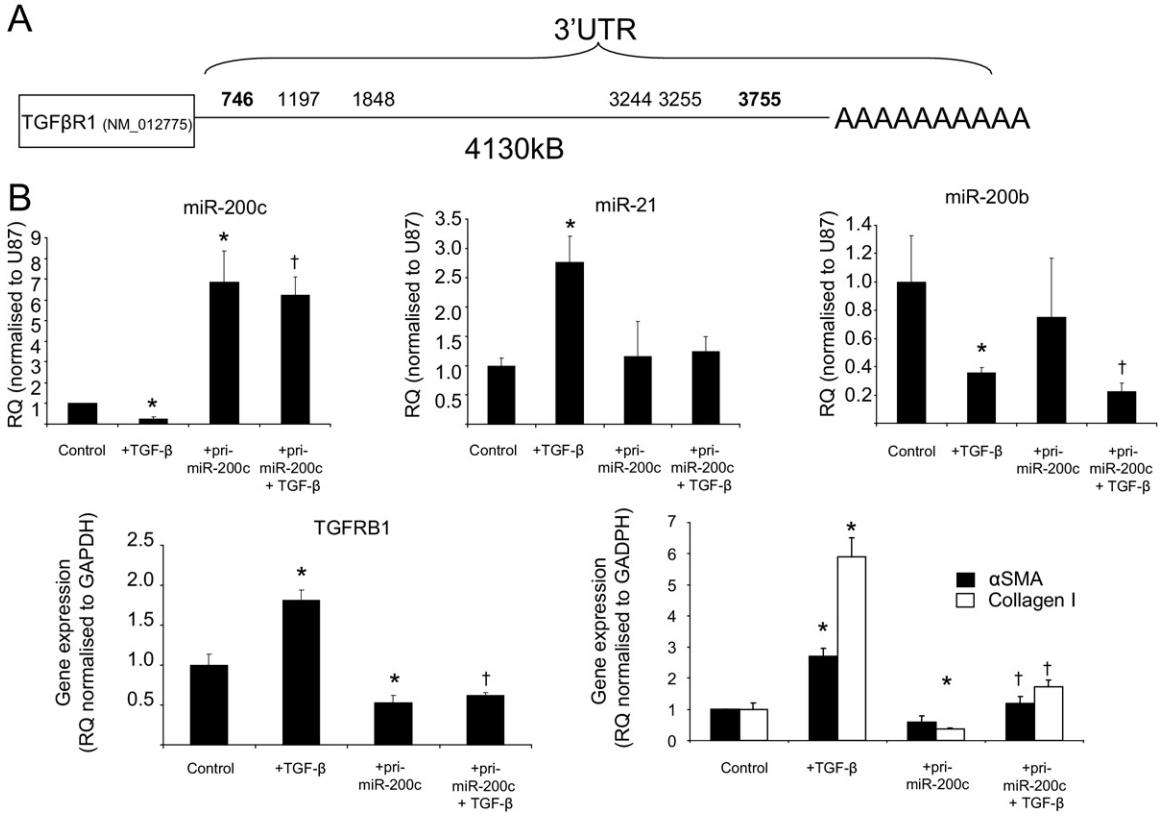

Figure 5. Effect of manipulation of miR-200c on TGFβ-R1 gene expression. **A:** Schematic diagram of 3′-UTR of rat TGFβR1 and miRNA seed sequence matches (nucleotide 2 to 7) for miR-200b/c. **B:** NRK52E cells were transfected with a plasmid containing cytomegalovirus promoter-driven pri-miR-200c by lipofectamine 2000 (2 μg of DNA:3 μl of lipofectamine), serum starved for 48 hours, and then stimulated with TGF-β. Total RNA was extracted with the miRNeasy kit (Qiagen), and miRNA expression was measured by specific miRNA Taqman probes (Applied Biosystems) and normalized to U87. TGF-βR1, α-SMA, and collagen I expressions were measured by specific rat gene expression probes (Applied Biosystems) and normalized to GAPDH (rat). RQ ± RQ max. $^{*}P < 0.05$ versus control cells and $^{\dagger}P < 0.05$ compared with control cells stimulated with TGF-β.

Correlation of miRNA Modulation in Vitro *in Models of Renal Disease* in Vivo

To address whether miRNAs are modulated during the development of glomerulonephritis, we used the rat anti-Thy1.1 model of mesangial proliferative glomerulonephritis, which is self-limiting and has a well-characterized progression.[35] We induced mesangial proliferative glomerulonephritis in WKY rats, and after sacrifice histologic evaluation was performed to look at glomerular and tubular lesions. A single administration of ER4 resulted in mild glomerular damage (Table 1), which was resolved by 14 days (data not shown). Kidneys from these animals had limited glomerular lesions that featured global or segmental mesangial proliferation (Table 1; Figure 6A). Multiple administration of the ER4 protocol induced more severe histologic changes with ~50% of glomeruli affected and some evidence of tubular damage in the form of tubular atrophy (Table 1 and Figure 6A). To quantify temporal changes in miRNA we sacrificed a further group of animals 14 days after final administration of ER4, which histologically appeared similar to those sacrificed at 7 days with the glomerular and tubular scores remaining similar (Table 1).

We performed TaqMan analysis for miRNA expression in animals that received three injections and sacrificed at 7 days but also in the second group which were sacrificed at 14 days and compared this with age-matched control animals (Figure 6B). miR-21 and miR-214 expression was significantly increased at 7 and 14 days compared with controls (Figure 6B). No other miRs tested in the *in vitro* setting showed altered expression in this pathological setting (Figure 6B). Because we have demonstrated *in vitro* that TGF-β was stimulating expression of miR-21 and miR-214, we sought to evaluate the levels of

Table 1. Histologic Evaluation of Kidney Damage in Anti-Thy1.1 Animals

Group	Glomerular score	Tubular score	Total
Control	0.25	0.25	0.5
1 × ER4, 7 days	1	0.5	1.5
3 × ER4, 7 days	2	2	4
3 × ER4, 14 days	2.1	1.3	3.4

Histologic scoring of animals used in this study. Scoring was adapted from Tomita et al.[29] Scoring was performed blind ($N = 4$ to 6 animals per group) with 50 glomeruli and surrounding tubules scored per section. Glomerular damage was scored from 0 to 4, with 0 being 0% to 4% glomerular lesion, mesangial matrix expansion; 1 being 5% to 24%; 2 being 25% to 49%; 3 being 50% to 74%; and 4 being >75%. Interstitial lesions were counted as tubular dilation, tubular trophy, basophilia, interstitial inflammation, and fibrosis and scored from 0 to 4, with 0 being no lesion; 1 being <5%, 2 being 5% to 24%, 3 being 25% to 49%, and 4 being ≥50%.

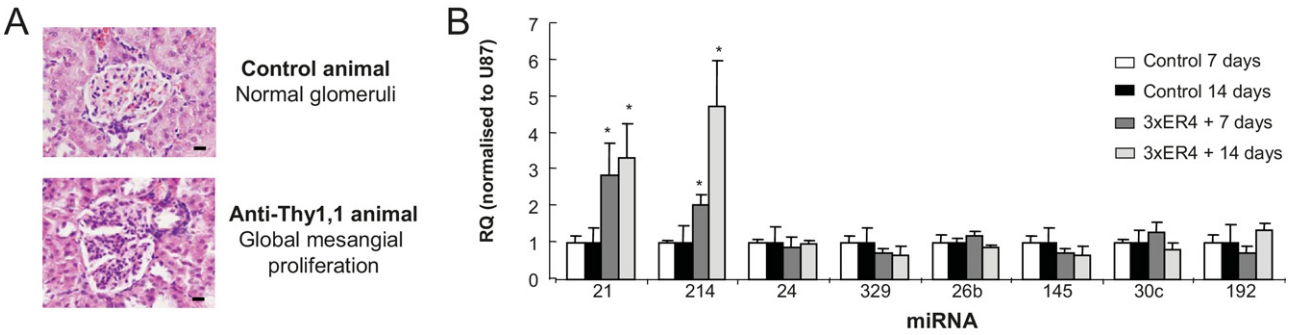

Figure 6. Validation of miRNA expression after induction of mesangial proliferative glomerulonephritis. Validation of miRNAs expressed in animals sacrificed 7 and 14 days after three ER4 injections 1 week apart compared with age-matched controls. **A:** Representative histology of normal glomeruli from control animals and the global mesangial proliferation observed in glomeruli in kidneys from animals that received three ER4 injections. **B:** miRNA expression measured by specific miRNA Taqman probes (Applied Biosystems) and normalized to U87. RQ ± RQ max. $^*P < 0.05$ versus age-matched control animals ($N = 4$ to 6).

TGF-β expression in this animal model. We found that at 7 days and 14 days after injection of the third ER4 there was a significant increase in TGF-β but no change in TGFβRI expression (see Supplemental Figure S5 at *http://ajp.amjpathol.org*).

Similarly to the chronic glomerulonephritis model, TGF-β is the main profibrotic mediator in the UUO model.[36] To examine miRNA expression in the UUO model, we performed a time course. Histologic evaluation of tissue taken from animals sacrificed at 16 days after surgery showed moderate interstitial fibrosis (Figure 7A) and a high level of α-SMA staining in the interstitium (Figure 7A; see also Supplemental Figure S6 at *http://ajp.amjpathol.org*), suggestive of a large increase in the number of active myofibroblasts but not the origin. Because EMT is reported to contribute to the fibroblast population in this model,[37] we examined the expression of a panel of markers known to be indicative of the EMT process. E-cadherin loss is an integral component of EMT in our *in vitro* model; yet, the effects of pathological insults *in vivo* on E-cadherin regulation and association with EMT are less clear. Therefore, we examined E-cadherin gene expression and found that it was up-regulated at this time point along with matrix metalloproteinase 2 and matrix metalloproteinase 14 (see Supplemental Figure S6 at *http://ajp.amjpathol.org*). We wanted to detail how TGF-β expression in the kidney was changing in this model, so we preformed real-time qPCR and found that within 3 days of surgery the level of TGF-β expression was significantly increased to ~3.5-fold that of sham-operated animals (Figure 7B). Furthermore, the level of expression increased further when examined at 7 and 14 days after surgery. This confirmed that in the kidneys of UUO animals the levels of TGF-β have increased (Figure 7B). On the basis of our *in vitro* model results, we assessed the expression levels of a panel of miRNAs in whole kidney extracts from UUO and sham-operated animals at 16 days. In similarity with the anti-Thy1.1 animals miR-21 and miR-214 were significantly up-regulated (sixfold for miR-21 and 2.5-fold for miR-214) (Figure 7C). miR-200b was found to be decreased in the UUO kidneys compared with controls; in addition, several other miRNAs were also found to be significantly down-regulated, miR-192, miR-329, miR-24, miR-26b, and miR-30c (Figure 7C). TGFβ-R1 was also found to be up-regulated at the gene expression level, which correlates with members of the miR-200 family being down-regulated (see Supplemental Figure S6 at *http://ajp.amjpathol.org*). To examine what happened to miR-21 and miR-214 expression over time in this model we examined their expression and found that miR-21 expression had doubled within 3 days and continued to increase over time (Figure 7D). miR-214 expression was also significantly increased but only significantly from 7 days after surgery when miR-214 expression was ~2.5-fold higher than that observed in sham-operated animals. The levels of miR-214 were then sustained for the time course (Figure 7D). Because we had observed previously in the *in vitro* models differences in the precursors of the miR-21 and miR-214 we performed Northern blot analyses on kidney RNA extracted from the animals 7 days after surgery (Figure 7E) that we had also demonstrated had significantly increased TGF-β expression (Figure 7B). For miR-21 the primary form of miR was present in all samples but the precursor form was only present in the UUO samples (Figure 7E). Mature miR-21 could be detected in all samples but was expressed higher in the UUO samples (Figure 7E). In contrast, similar levels of pre- and pri-miR-214 were present in both UUO and sham-operated animals. However, the mature miR-214 levels were increased significantly only in the UUO animals (Figure 7E).

Because the causes of these two renal diseases are different but TGF-β plays a role, we examined the expression of miR-21 and miR-214 in the SHRSP rat to identify if there is a common miRNA signature in the renal pathological process. We assessed the expression of miR-21 and miR-214 alongside miR-30c, miR-192, and miR-145. The expression of the miRs was assessed in 21-week SHRSP rats with established hypertension (systolic blood pressure > 170 mmHg)[5] and compared with that observed in age-matched normotensive reference strain WKY rats (systolic blood pressure < 125 mmHg).[5] Both miR-21 (~2.25-fold increased) and miR-214 (~threefold increased) were significantly increased when SHRSP animals were compared with the reference strain (WKY) with no change in the other miRs examined (Figure 8). However, when young 5-week-old animals that are not hypertensive were assessed for miR-21 and miR-214,

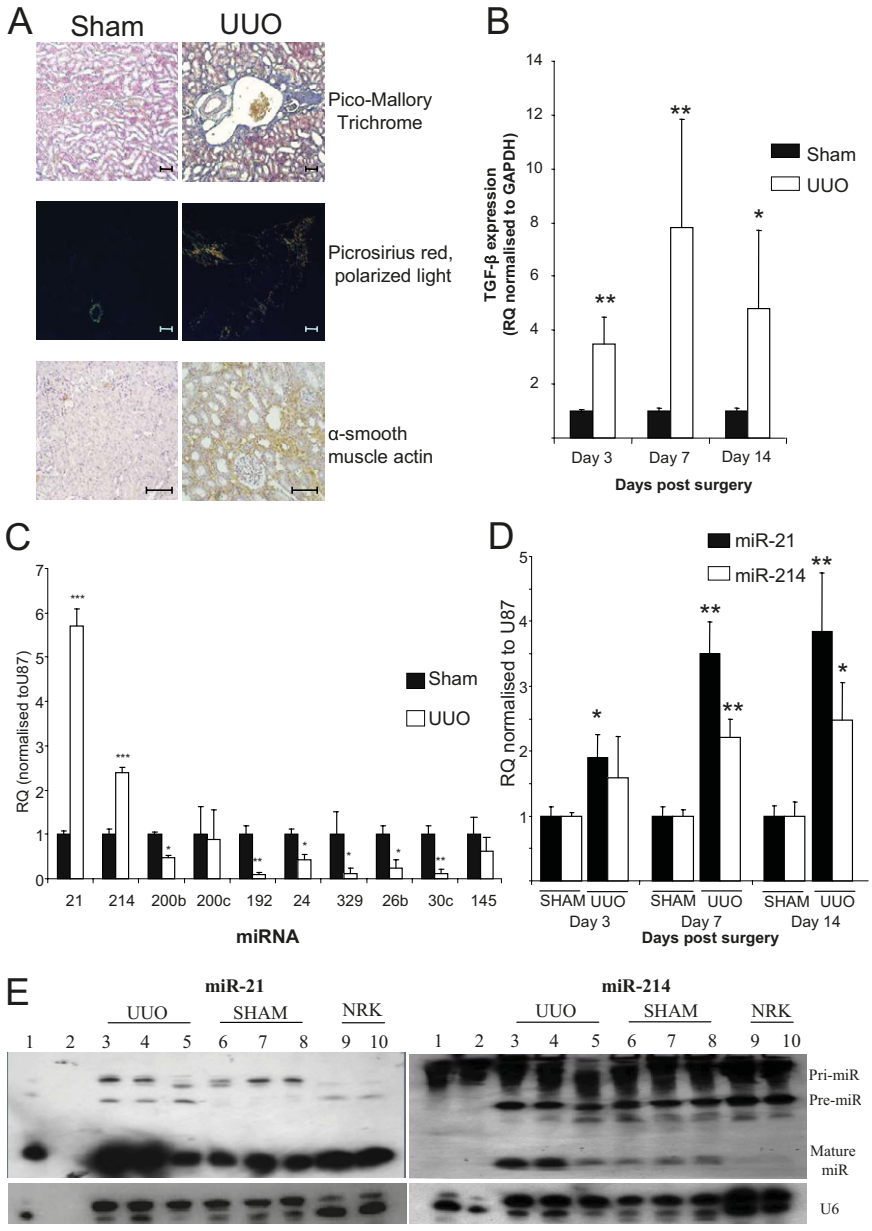

Figure 7. miRNA expression after UUO. **A:** Histologic analysis of kidneys from sham and UUO animals for tubulo-interstitial fibrosis by Pico-Mallory Trichrome and Picro Sirius red (viewed under cross-polarized light) and α-SMA staining 16 days after surgery. Scale bars: 100 μm. **B:** TGF-β gene expression in animals undergoing UUO. Total kidney RNA was extracted with the use of the miRNeasy kit (Qiagen), and TGF-β gene expression was measured by specific rat TGF-β gene expression probe (Applied Biosystems) and normalized to GAPDH (rat). RQ ± RQ max. $^{*}P < 0.05$ and $^{**}P < 0.01$. **C:** miRNA expression in kidneys of sham or UUO animals was measured by specific miRNA Taqman probes (Applied Biosystems) and normalized to U87. RQ ± RQ max. $^{*}P < 0.05$, $^{**}P < 0.01$, and $^{***}P < 0.001$ compared with sham animals ($N = 5$). **D:** miR-21 and miR-214 expression in UUO animals over time. Total RNA was extracted with the use of the miRNeasy kit (Qiagen), and miRNA expression was measured by specific miRNA Taqman probes (Applied Biosystems) and normalized to U87. RQ ± RQ max. $^{*}P < 0.05$ and $^{**}P < 0.01$ versus age-matched control sham-operated animals ($N = 3$). **E:** miR-21 and miR-214 expression in kidney tissue 7 days after surgery. Northern blot analyses were performed on total kidney RNA extracted with the use of the miRNeasy kit (Qiagen) of tissue from UUO and sham-operated animals at 7 days after surgery and probed with 5′-DIG–labeled LNA Mercury probes (Exiqon) rat miRNA for miR-21 and miR-214. U6 was used as a loading control (Exiquon). Lane 1 indicates HeLa cells; lane 2, RNA ladder; lanes 3 to 5, UUO RNA; lanes 6 to 8, SHAM RNA; and lanes 9 and 10, NRK52E (NRK) control RNA.

there was no difference (data not shown), indicating that these miRs are not altered before the onset of hypertension or renal damage. Interestingly, the expression of these miRs was further increased in the SHRSP when they were challenged with salt (1%), with miR-21 levels increasing ~14-fold and miR-214 levels increasing by fourfold. Surprisingly, in the WKY rats that are not salt sensitive and do not have any renal insufficiency, salt loading significantly increased miR-21 expression by six times compared with age-matched normal WKY rats. The salt challenge also resulted in miR-30c and miR-192 being significantly increased in both WKY and SHRSP rats, and miR-145 only being increased in SHRSP. Because we found increases in miR-21 and miR-214 in the SHRSP compared with the WKY rats and under salt loading, we investigated whether an increase in TGF-β is associated with this increase. We therefore measured the level of mRNA for TGF-β and TGFβRI in tissues and observed that TGF-β was significantly increased in the SHRSP rats compared with the WKY rats and further increased under salt loading (see Supplemental Figure S7 at *http://ajp.amjpathol.org*). Furthermore, TGFβRI was also increased under salt loading, suggesting an increase in TGF-β signaling (see Supplemental Figure S7 at *http://ajp.amjpathol.org*).

Discussion

miRNAs have recently been shown to be dysregulated in many diseases and are thought to contribute to the pathophysiology of the distinct disease such as cancer and myocardial infarction. Previously, miR-192 and miR-377 have been highlighted as being regulated by TGF-β in mesangial cells and in the diabetic kidney. Here, we

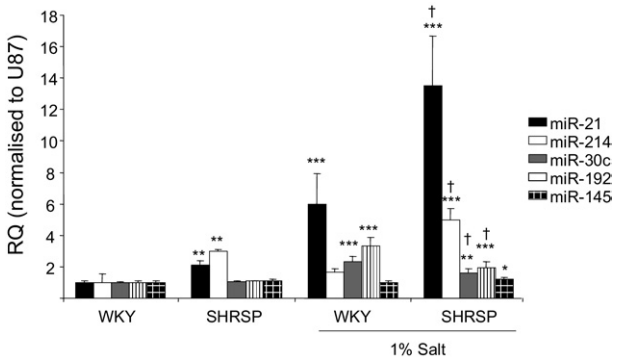

Figure 8. miRNA expression in genetic model of hypertension, the SHRSP. miRNA expression in kidneys of 21-week-old male WKY, SHRSP rats with and without salt loading (1%) was measured by specific miRNA Taqman probes (Applied Biosystems) and normalized to U87. RQ ± RQ max. $^{*}P < 0.05$, $^{**}P < 0.01$, and $^{***}P < 0.001$ compared with WKY expression levels; $^{\dagger}P < 0.05$ compared with SHRSP expression levels.

establish that the expression of miR-214 and miR-21 are also regulated by TGF-β. We demonstrate in this study that TGF-β–induced EMT in a rat tubular epithelial cell line was blocked by small molecule inhibitors of TGF-β signaling. Induction of miR-21 and miR-214 was also inhibited by these agents. Furthermore, overexpression of either miR-214 or miR-21 in the absence of TGF-β–induced EMT-like changes in culture with associated changes in E-cadherin, α-SMA, and collagen expression. This underpins an important role for these two miRNAs in TGF-β signaling-induced EMT *in vitro*. To underline the importance of miR-21 and miR-214, both were significantly increased in two models of renal disease *in vivo* in which TGF-β plays a role in the pathophysiology but also in a rat model of genetic hypertension shown to have predominately vascular renal damage. Interestingly, when these animals were challenged with high salt both WKY and SHRSP animals showed an increase in miR-21, whereas miR-214 was only increased further in the salt-loaded SHRSP animals. Furthermore, because neither miRNA has differential expression in non-hypertensive 5-week-old SHRSP animals, the change in these miRNAs illustrates a role in the pathophysiology of hypertension in this model. The effect of salt loading on WKY miR-21 expression was surprising, but together with the data from the SHRSP on miR-21 and miR-214 it indicates that other pathways beyond TGF-β also probably regulate these miRNAs. Taken together this study shows that the overexpression of both miR-21 and miR-214 represents a common signature for renal damage unrelated to its cause. To further support this a recent study found that miR-214 is increased in monocytes of patients with chronic kidney disease.[38]

miR-21 overexpression has been shown in mesangial cells stimulated with glucose (to mimic diabetic nephropathy) to protect the cells from proliferation by the down-regulation of PTEN, which was verified as a target of miR-21 in this context.[39] miR-21 is frequently found up-regulated in response to stress. In cardiac fibrosis the source of miR-21 has been found to be cardiac fibroblasts.[40] miR-214 has been found to be up-regulated in epithelial ovarian carcinomas.[41] Furthermore, PTEN has also been confirmed as a target of miR-214, and in human ovarian cancer cells an increase in miR-214 induces cell survival and cisplatin resistance via targeting the PTEN/Akt pathway.[41] miR-214 has been shown to be activated by TWIST-1 through an E-box promoter element[42] and may be involved in the development of specific neural cell populations; therefore, because TWIST activation is a key event in EMT, it may be through this pathway that miR-214 expression is increased in the tubular epithelial cells. However, TGF-β can also drive cells toward apoptosis, so it is also possible that miR-214 may mediate the switch between these two cell fates.

In mesangial cells, miR-145 expression was also measured, because it has been shown to be a mesangial cell marker,[20] and it was rapidly increased in response to TGF-β but returned to normal levels within 24 hours of TGF-β stimulation. miR-145 has been shown to act as a tumor suppressor[43] and to prevent proliferation of smooth muscle cells,[44] and, because mesangial cells are specialized smooth muscle cells, the increase in miR-145 may be a protective mechanism.

miR-30c expression was lost in the UUO kidney; previously, it has been shown to be essential for normal kidney homoeostasis and targets several genes of importance in structure and function of the kidney. It has a tubular expression within the kidney, and whether the loss of miR-30c was an initiating factor or as a result of the widespread tubular damage would need to be investigated further.

In similarity to other studies, stimulation of the rat tubular epithelial cell line with TGF-β resulted in EMT and a loss of the expression of the miR-200 family members miR-200b and miR-200c. Elegant studies have previously shown that miR-200 family overexpression prevents EMT induced by TGF-β by binding to their targets ZEB1 and ZEB2, which are transcriptional repressors of E-cadherin.[24–26] Loss of the miR-200 family results in an increase in ZEB1 and ZEB2 expression and loss of E-cadherin and subsequent induction of EMT.[24–26] In the UUO animals, miR-200b was significantly down-regulated; this could be an indicator that EMT is occurring in this model and contributing to the myofibroblast cell number. However, E-cadherin expression was up-regulated in this model at this time point (see Supplemental Figure S6 at *http://ajp.amjpathol.org*), which has been reported before[45] and is in contrast to what was observed in the *in vitro* model in which E-cadherin was down-regulated. Target analysis of miR-200b and miR-200c found that TGFβR1 was a target for these miRNAs with six seed matches in the rat. This study shows that TGFβR1 is a target of the miR-200 family and suggests the miR-200 family are important regulators of TGF-β signaling, being able to influence multiple parts of the signaling pathway. In the UUO model in which EMT of tubular epithelial cells has been reported to occur[37] and contribute to the myofibroblast population, we wanted to examine the expression of miR-200b and miR-200c. In animals 16 days after UUO, the expression of miR-200b was significantly down-regulated, and miR-200c was reduced. This may further suggest that the loss of the miR-200 family is pathophysiologically important in tubule-interstitial fibrosis, especially

because miR-200b has been shown to have a tubular location within the kidney.[20]

This study for the first time shows that miR-21 and miR-214 may represent a miRNA signature of renal damage and both these miRNAs can be regulated by TGF-β in a cell-specific manner.

Acknowledgments

We thank Bruce Hendry for critical appraisal of the manuscript. We also thank Angela McIllhoney, Nicola Britton, and Gregor Aitchison for technical assistance.

References

1. Bottinger EP, Bitzer M: TGF-{beta} signaling in renal disease. J Am Soc Nephrol 2002, 13:2600–2610
2. Liu Y: Renal fibrosis: new insights into the pathogenesis and therapeutics. Kidney Int 2006, 69:213–217
3. Schlondorff D: The glomerular mesangial cell: an expanding role for a specialized pericyte. FASEB J 1987, 1:272–281
4. Whelton PK, Klag MJ: Hypertension as a risk factor for renal disease. Review of clinical and epidemiological evidence. Hypertension 1989, 13:I19–I27
5. Koh-Tan HH, Graham D, Hamilton CA, Nicoll G, Fields L, McBride MW, Young B, Dominiczak AF: Renal and vascular glutathione S-transferase mu is not affected by pharmacological intervention to reduce systolic blood pressure. J Hypertens 2009, 27:1575–1584
6. Obata J, Nakamura T, Takano H, Naito A, Kimura H, Yoshida Y, Shimizu F, Guo DF, Inagami T: Increased gene expression of components of the renin-angiotensin system in glomeruli of genetically hypertensive rats. J Hypertens 2000, 18:1247–1255
7. Graham D, McBride MW, Gaasenbeek M, Gilday K, Beattie E, Miller WH, McClure JD, Polke JM, Montezano A, Touyz RM, Dominiczak AF: Candidate genes that determine response to salt in the stroke-prone spontaneously hypertensive rat: congenic analysis. Hypertension 2007, 50:1134–1141
8. Ambros V: The functions of animal microRNAs. Nature 2004, 431: 350–355
9. Gregory RI, Chendrimada TP, Cooch N, Shiekhattar R: Human RISC couples microRNA biogenesis and posttranscriptional gene silencing. Cell 2005, 123:631–640
10. Chang S, Johnston RJ, Frokjaer-Jensen C, Lockery S, Hobert O: MicroRNAs act sequentially and asymmetrically to control chemosensory laterality in the nematode. Nature 2004, 430:785–789
11. Johnston RJ, Hobert O: A microRNA controlling left/right neuronal asymmetry in Caenorhabditis elegans. Nature 2003, 426:845–849
12. Lee RC, Feinbaum RL, Ambros V: The C. elegans heterochronic gene lin-4 encodes small RNAs with antisense complementarity to lin-14. Cell 1993, 75:843–854
13. Huang Q, Gumireddy K, Schrier M, le Sage C, Nagel R, Nair S, Egan DA, Li A, Huang G, Klein-Szanto AJ, Gimotty PA, Katsaros D, Coukos G, Zhang L, Pure E, Agami R: The microRNAs miR-373 and miR-520c promote tumour invasion and metastasis. Nat Cell Biol 2008, 10:202–210
14. Ma L, Teruya-Feldstein J, Weinberg RA: Tumour invasion and metastasis initiated by microRNA-10b in breast cancer. Nature 2007, 449: 682–688
15. Ji R, Cheng Y, Yue J, Yang J, Liu X, Chen H, Dean DB, Zhang C: MicroRNA expression signature and antisense-mediated depletion reveal an essential role of microRNA in vascular neointimal lesion formation. Circ Res 2007, 100:1579–1588
16. Care A, Catalucci D, Felicetti F, Bonci D, Addario A, Gallo P, Bang M-L, Segnalini P, Gu Y, Dalton ND, Elia L, Latronico MVG, Hoydal M, Autore C, Russo MA, Dorn GW, Ellingsen O, Ruiz-Lozano P, Peterson KL, Croce CM, Peschle C, Condorelli G: MicroRNA-133 controls cardiac hypertrophy. Nat Med 2007, 13:613–618
17. Pandey P, Brors B, Srivastava PK, Bott A, Boehn SN, Groene HJ, Gretz N: Microarray-based approach identifies microRNAs and their target functional patterns in polycystic kidney disease. BMC Genomics 2008, 9:624
18. Kato M, Zhang J, Wang M, Lanting L, Yuan H, Rossi JJ, Natarajan R: MicroRNA-192 in diabetic kidney glomeruli and its function in TGF-beta-induced collagen expression via inhibition of E-box repressors. Proc Natl Acad Sci U S A 2007, 104:3432–3437
19. Shi S, Yu L, Chiu C, Sun Y, Chen J, Khitrov G, Merkenschlager M, Holzman LB, Zhang W, Mundel P, Bottinger EP: Podocyte-selective deletion of dicer induces proteinuria and glomerulosclerosis. J Am Soc Nephrol 2008, 19:2159–2169
20. Harvey SJ, Jarad G, Cunningham J, Goldberg S, Schermer B, Harfe BD, McManus MT, Benzing T, Miner JH: Podocyte-specific deletion of dicer alters cytoskeletal dynamics and causes glomerular disease. J Am Soc Nephrol 2008, 19:2150–2158
21. Ho J, Ng KH, Rosen S, Dostal A, Gregory RI, Kreidberg JA: Podocyte-specific loss of functional microRNAs leads to rapid glomerular and tubular injury. J Am Soc Nephrol 2008, 19:2069–2075
22. Wang Q, Wang Y, Minto AW, Wang J, Shi Q, Li X, Quigg RJ: MicroRNA-377 is up-regulated and can lead to increased fibronectin production in diabetic nephropathy. FASEB J 2008, 22:4126–4135
23. Zavadil J, Narasimhan M, Blumenberg M, Schneider RJ: Transforming growth factor-beta and microRNA: mRNA regulatory networks in epithelial plasticity. Cells Tissues Organs 2007, 185:157–161
24. Park SM, Gaur AB, Lengyel E, Peter ME: The miR-200 family determines the epithelial phenotype of cancer cells by targeting the E-cadherin repressors ZEB1 and ZEB2. Genes Dev 2008, 22:894–907
25. Burk U, Schubert J, Wellner U, Schmalhofer O, Vincan E, Spaderna S, Brabletz T: A reciprocal repression between ZEB1 and members of the miR-200 family promotes EMT and invasion in cancer cells. EMBO Rep 2008, 9:582–589
26. Gregory PA, Bert AG, Paterson EL, Barry SC, Tsykin A, Farshid G, Vadas MA, Khew-Goodall Y, Goodall GJ: The miR-200 family and miR-205 regulate epithelial to mesenchymal transition by targeting ZEB1 and SIP1. Nat Cell Biol 2008, 10:593–601
27. Demaison C, Parsley K, Brouns G, Scherr M, Battmer K, Kinnon C, Grez M, Thrasher AJ: High-level transduction and gene expression in hematopoietic repopulating cells using a human immunodeficiency virus type 1-based lentiviral vector containing an internal spleen focus forming virus promoter. Hum Gene Ther 2002, 13:803–813
28. Butler SL, Hansen MS, Bushman FD: A quantitative assay for HIV DNA integration in vivo. Nat Med 2001, 7:631–634
29. Khanin R, Vinciotti V: Computational modeling of post-transcriptional gene regulation by microRNAs. J Comput Biol 2008, 15:305–316
30. Selbach M, Schwanhausser B, Thierfelder N, Fang Z, Khanin R, Rajewsky N: Widespread changes in protein synthesis induced by microRNAs. Nature 2008, 455:58–63
31. Tomita M, Sogabe H, Nakazato S, Nakatsuji S, Noto T, Hamada K, Kawachi H, Shimizu F, Matsuo M, Mutoh S: Monoclonal antibody 1-22-3-induced glomerulonephritis in uninephrectomized rats as a model of progressive renal failure. Nephrol Dial Transplant 2005, 20:2358–2367
32. Davidson AO, Schork N, Jaques BC, Kelman AW, Sutcliffe RG, Reid JL, Dominiczak AF: Blood pressure in genetically hypertensive rats. Influence of the Y chromosome. Hypertension 1995, 26:452–459
33. Rosenbloom J, Castro SV, Jimenez SA: Narrative review: fibrotic diseases: cellular and molecular mechanisms and novel therapies. Ann Intern Med 152:159–166
34. Tojo M, Hamashima Y, Hanyu A, Kajimoto T, Saitoh M, Miyazono K, Node M, Imamura T: The ALK-5 inhibitor A-83-01 inhibits Smad signaling and epithelial-to-mesenchymal transition by transforming growth factor-beta. Cancer Sci 2005, 96:791–800
35. Bagchus W, Hoedemaeker P, Rozing J, Bakker W: Glomerulonephritis induced by monoclonal anti-Thy 1.1 antibodies. A sequential histological and ultrastructural study in the rat. Lab Invest 1986, 55:680–687
36. Kaneto H, Morrissey J, Klahr S: Increased expression of TGF-[beta]1 mRNA in the obstructed kidney of rats with unilateral ureteral ligation. Kidney Int 1993, 44:313–321
37. Iwano M, Plieth D, Danoff T, Xue C, Okada H, Neilson E: Evidence that fibroblasts derive from epithelium during tissue fibrosis. J Clin Invest 2002, 110:341–350
38. Li LM, Hou DX, Guo YL, Yang JW, Liu Y, Zhang CY, Zen K: Role of microRNA-214-targeting phosphatase and tensin homolog in advanced glycation end product-induced apoptosis delay in monocytes. J Immunol 186:2552–2560

39. Zhang Z, Peng H, Chen J, Chen X, Han F, Xu X, He X, Yan N: MicroRNA-21 protects from mesangial cell proliferation induced by diabetic nephropathy in db/db mice. FEBS Lett 2009, 583:2009–2014
40. Thum T, Catalucci D, Bauersachs J: MicroRNAs: novel regulators in cardiac development and disease. Cardiovasc Res 2008, 79:562–570
41. Yang H, Kong W, He L, Zhao J-J, O'Donnell JD, Wang J, Wenham RM, Coppola D, Kruk PA, Nicosia SV, Cheng JQ: MicroRNA expression profiling in human ovarian cancer: miR-214 induces cell survival and cisplatin resistance by targeting PTEN. Cancer Res 2008, 68:425–433
42. Lee Y-B, Bantounas I, Lee D-Y, Phylactou L, Caldwell MA, Uney JB: Twist-1 regulates the miR-199a/214 cluster during development. Nucl Acids Res 2009, 37:123–128
43. La Rocca G, Badin M, Shi B, Xu SQ, Deangelis T, Sepp-Lorenzinoi L, Baserga R: Mechanism of growth inhibition by microRNA 145: the role of the IGF-I receptor signaling pathway. J Cellular Physiol 2009, 220:485–491
44. Cordes KR, Sheehy NT, White MP, Berry EC, Morton SU, Muth AN, Lee T-H, Miano JM, Ivey KN, Srivastava D: miR-145 and miR-143 regulate smooth muscle cell fate and plasticity. Nature 2009, 460: 705–710
45. Docherty NG, Calvo IF, Quinlan MR, Perez-Barriocanal F, McGuire BB, Fitzpatrick JM, Watson RWG: Increased E-cadherin expression in the ligated kidney following unilateral ureteric obstruction. Kidney Int 2008, 75:205–213

NDT Advance Access published March 7, 2008

Nephrol Dial Transplant (2008) 1 of 4
doi: 10.1093/ndt/gfn095

NDT
Nephrology Dialysis Transplantation

Editorial Comment

Silencing genes in the kidney: antisense or RNA interference?

Jia-Hui Wang, Bruce M Hendry and Claire C Sharpe

Department of Renal Medicine, King's College London School of Medicine, London, UK

Keywords: antisense; gene therapy; siRNA

Introduction

Targeting genes in disease has long been a sought-after holy grail, with the concept of gene therapy promising a magic bullet for single gene mutation or deletion disorders. Replacing deficient or non-functional genes with the active form has proven more difficult to achieve than originally hoped. However, a subset of gene therapy termed 'gene silencing' is being developed, which is altogether more promising. By utilizing the unique nature of gene-sequence specificity, complementary or antisense molecules can be designed to 'seek and destroy' target mRNAs for specific proteins known to be pivotal in the pathogenesis of various disease processes. Two strategies have been employed to silence genes; the first involves the use of single-stranded antisense oligodeoxynucleotides (ASO) and the second uses double-stranded short-interfering RNA molecules (siRNA) otherwise known as RNA interference (RNAi).

Antisense oligodeoxynucleotides (ASO)

With the recent publication by Tillman *et al*. in the *Journal of Pharmaceutical Sciences* of the first demonstration of oral delivery of ASO in man [1] comes the possibility of this form of gene therapy becoming part of the normal repertoire of therapeutic options open to the physician in the mid- to long-term future. Zamecnick and Stephenson were the first to recognize the potential of ASO in 1978 when studying inhibition of Rous sarcoma virus replication [2]. Since then, antisense technology has developed into a powerful research tool and has begun to make its mark in the world of clinical therapy.

ASO consist of a single strand of 12–22 oligodeoxynucleotides which are complementary to the target mRNA sequence [3]. Binding of the ASO to target mRNA results in steric inhibition of translation by the ribosomal complex but more importantly the induction of RNase H, which cleaves the 3′-O-P-bond of the RNA molecule (Figure 1). This mechanism of action theoretically provides 100% specificity for the target gene, an unachievable goal for most conventional pharmacological agents.

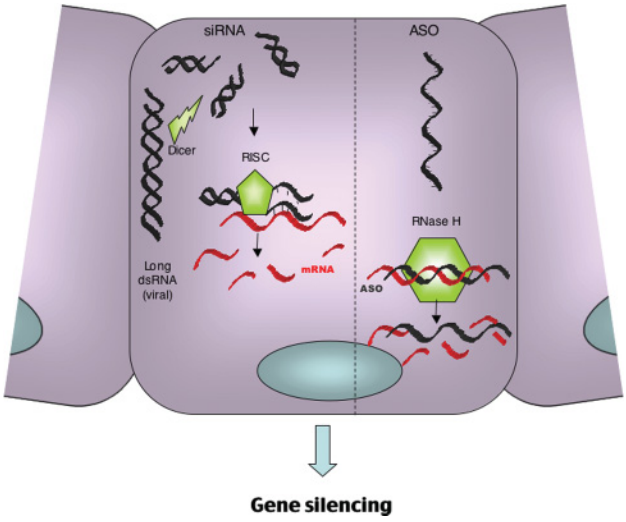

Fig. 1. The mechanism of action of ASO versus RNA interference.

Since the 1970s, ASO have been used widely as research tools used to investigate mechanisms of disease pathogenesis *in vitro*, particularly in the field of nephrology. For example, Zhang *et al*. used a connective tissue growth factor (CTGF) ASO to examine the role of this molecule during epithelial-mesenchymal transition (EMT) in proximal tubular epithelial cells [4], whilst we have employed ASO to discern the individual functions of the isoforms of the Ras monomeric GTPase in human renal fibroblast proliferation [5].

The use of ASO to target the kidney *in vivo* has been both challenging and highly rewarding. Unmodified, single-stranded oligonucleotides are rapidly broken down in serum by endogenous nucleases greatly limiting cellular uptake. To overcome this, ASO have a modification of the phosphate backbone whereby non-bridging oxygen molecules are replaced by sulphur molecules, greatly enhancing resistance to nuclease activity. These phosphorothioate ASO have a half-life in serum in the region of 10 h (in comparison to 30–60 min of unmodified forms) and,

Correspondence and offprint requests to: Claire Sharpe, Department of Renal Medicine, King's College London School of Medicine, London, UK. Tel: +44-020-7848-5693/0491; Fax: +44-020-7848-0515; E-mail: claire.sharpe@kcl.ac.uk

following parenteral administration, have a systemic bioavailability as high as 90% [6]. Further modifications of the sugar–phosphate backbone of the oligonucleotides can be made to increase their stability and RNA affinity without compromising binding selectivity. Among the available sites for modification, the furanose 2′-position has been demonstrated to offer several advantages [7]. Unfortunately, complete 2′-O-modification of the molecule results in the loss of its ability to activate RNase H. This has led to the development of chimeric oligonucleotides that are formed by combining 2′-O-modified oligonucleotides with regions of 2′-deoxy phosphorothioates. The resulting second-generation ASO both support RNase H activity and demonstrate enhanced nuclease resistance and RNA affinity. Following parenteral administration, these ASO distribute to all peripheral tissues with the highest accumulation being in the liver and kidneys, which have a concentration ratio to plasma of 20:1 and 80:1 respectively after 2 h [8]. Within the kidney, ASO are filtered freely by the glomerulus and reabsorbed by proximal tubule epithelial cells [9] making antisense technology a very attractive tool for the investigation and possibly treatment of renal disease. Cheng *et al*. were amongst the first to use these tools in an animal model of renal disease. They administered ASO to intracellular adhesion molecule 1 (ICAM-1) intravenously via the tail vein in a mouse model of unilateral ureteric obstruction (UUO) and found a decrease in inflammatory infiltration and extracellular matrix [10]. Similarly, Chen *et al*. demonstrated ICAM-1 ASO to be very effective in inhibiting the ICAM-1-dependent mechanism of graft infiltration and tissue damage involved in allograft rejection, ischaemic-reperfusion injury and cyclosporin-induced nephrotoxicity [11]. Other renal disease-associated proteins have subsequently been targeted using parenteral ASO, such as connective tissue growth factor (CTGF) [12,13], casein kinase II [14] and TGF-β. Isaka *et al*. modified the delivery of ASO to target interstitial fibroblasts. They developed an artificial viral envelope (AVE) containing anionic liposomes and proteins from the haemagglutinating virus of Japan (HVJ). The net negative charge on the ASO/AVE complex allows for selective transfection of renal interstitial fibroblasts to the exclusion of proximal tubular cells. Using retrograde ureteric administration, Isaka successfully targeted interstitial fibroblasts with ASO to TGF-β1, in a model of UUO. The ASO-treated obstructed kidneys expressed less collagen I and α-smooth muscle actin and had less interstitial fibrosis [15,16].

Although some animal studies have shown that ASO infusions may lead to complement cascade activation [17,18], these effects appear to be both dose dependent and related to the rate of administration. Subsequent clinical studies using lower doses of ASO have reported minimal toxic effects. Furthermore, subsequent generations of ASO have lower toxicity profiles [19]. Therefore, there has been much interest in pushing forward ASO for clinical therapy. Although currently there is only one ASO licensed for clinical use, Formivirsen (Vitravene®) for AIDS-related CMV retinitis, numerous others are in Phase 2 of clinical development such as ASO to ApoB-100 for the treatment of hypercholesterolaemia, ASO to ICAM-1 in ulcerative colitis and many others (see http://www.isispharm.com).

Short-interfering RNA

In 1990, Richard Jorgensen's plant biology group was the first to note the effects of administration of specific RNA molecules on gene expression [20]. Their attempt to enhance the purple pigmentation in petunias by overexpression of the appropriate transcript paradoxically resulted in the flowers losing their colouring. This phenomenon was termed 'cosuppression', though the mechanism of action was not determined until 1998. In their landmark paper, Fire and Mello showed that sequence-specific gene knockdown was possible by microinjection of synthetic double-stranded RNA (dsRNA) in the nematode *Caenorhabditis elegans* [21]. Furthermore, they showed that the use of dsRNA was over 10 times more potent than either sense or antisense RNA alone, that gene silencing was possible on administration of only a few molecules of dsRNA and that this effect may be passed on to first-generation progeny. The term 'RNA interference' was applied to their findings and they were awarded the Nobel Prize for Medicine in October 2006.

The mechanism employed by RNAi is thought to be a defensive mechanism against the abnormal presence of double-stranded viral RNA. It is different to that used by ASO and has been conserved over time and is common to all eukaryotes [22]. The process involves initial long dsRNA cleavage by the enzyme Dicer RNase III into short RNA duplexes of 21–23 nucleotides, which are then incorporated into a ribonucleoprotein–endonuclease complex termed 'RNA Induced Silencing Complex' (RISC). The siRNA is then unwound and the antisense strand directs the complex to target the specific endogenous RNA sequence. The target RNA transcript is then bound and degraded by the endonuclease activity of RISC (Figure 1). There was an initial reluctance to transfer these findings to mammalian cells since exposure to long strands of dsRNA results in non-specific degradation of all mRNA and inhibition of all protein synthesis. However, Tuschl's group subsequently demonstrated that short-interfering RNA (21-nt) against reporter genes in various mammalian cell lines specifically reduced expression up to 25-fold [23]. Since this time, short-interfering RNA (siRNA) technology has been used widely as a highly specific and powerful tool for the *in vitro* study of gene function. Its specific mechanism of action makes target site identification and oligo design easier than for ASO as the secondary RNA structure is not an obstacle. *In vitro*, the duration of knockdown is similar to that of second-generation ASO but the potency maybe significantly greater. Although both siRNA and ASO are highly specific for their target genes, siRNA may induce 'off target' effects. This can occur when non-targeted mRNA species share significant homology (>11 bases) with either the sense or antisense strand of the siRNA molecule. Additionally, it has been demonstrated that partial homology (as little as 6–7 bases) between either of the siRNA strands and the 3′ untranslated regions can cause knockdown of many genes within a cell. This mechanism parallels that employed by micro RNA (miRNA) molecules, which are naturally occurring, endogenous gene-regulatory molecules [24,25] and its effects can be difficult to predict.

The major challenge for the use of siRNA, however, is transferring the technology to the *in vivo* setting. Though these molecules have a biodistribution profile similar to ASO with preferential accumulation in the liver and kidney, they do not readily cross the cell membrane due to their large molecular mass (twice that of single-stranded ASO) and a high negative charge. Unmodified, they have a half-life in serum of a few seconds to a few minutes and are thus rapidly degraded before reaching their target tissues [26] and hence any potency advantage over ASO that they have *in vitro* is lost. In addition, they can stimulate systemic inflammatory responses by inducing interferon-mediated pathways (though this may be related to the concurrent use of vectors [27]) or by containing newly identified 'danger motifs' that bind to certain Toll-like receptors [28]. Local tissue delivery to organs such as the eye and lungs, avoiding a systemic phase, has proven successful in some circumstances and phase 1 trials are taking place into the use of VEGF siRNA in macular degeneration [29,30]. Systemic delivery however remains problematic. In order to increase siRNA delivery to less accessible tissues, researchers have used a variety of different techniques. Hamar *et al*. used hydrodynamic (large volume and high pressure) injection to deliver siRNA to target the pro-apoptotic protein, Fas in a murine model of acute renal ischaemia-reperfusion injury and were able to demonstrate reduced Fas expression and reduced tubular apoptosis, atrophy and hyaline damage [31]. Alternatively, Hwang *et al*. injected a short hairpin-RNA-expressing plasmid vector targeting TGF-β1 in a single dose under low pressure, through the renal artery in a mouse model of UUO and demonstrated that collagen I expression in the interstitium was significantly reduced, at least until Day 7 [32]. Similarly, Takabatake *et al*. injected TGF-β1 siRNA via the renal artery in a rat model of Anti-Thy-1 glomerulonephritis but required the addition of electroporation to achieve a reduction in the expression of TGF-β1 in glomeruli compared to the contralateral kidney by Day 4 [33].

Although these methods have proven successful in animal models, it is difficult to see how they can be translated into a clinical setting. Some groups have followed the lessons learnt from ASO development and have made modifications, such as the addition of a cholesterol moiety or the incorporation of 2′-O-methyl (2′OMe) uridine or guanosine nucleosides into one strand of the siRNA duplex to extend half-life and reduce toxicity [34]. These modifications may yet prove successful in advancing siRNA technology into a therapeutic setting.

Conclusion

Targeting of specific disease-causing genes using 'antisense' mechanisms is highly attractive, particularly for the kidney. Although, over 30 years from the original discovery, there is still only one licensed ASO in clinical use, much of the slow progress has been due to the necessary development of pharmacological modifications to improve ASO efficacy and safety. These next-generation molecules are safe, highly specific and powerful medicines with the potential for both systemic and oral delivery and many are moving forward to the clinical setting at an accelerating pace. RNA interference still has some way to go before drugs utilizing this technology reach the same level of preclinical and clinical applications. Though currently they appear most promising for local, non-systemic applications, hopefully with new advances in systemic drug delivery, problems of administration will be overcome and they will eventually add to the growing repertoire of gene silencing therapeutics in the future.

Acknowledgements. J.H.W. is supported by a Clinical Training Fellowship from Kidney Research UK. C.C.S. is supported by a Clinician Scientist Award from the UK Department of Health.

Conflict of interest statement. None declared.

References

1. Tillman LG, Geary RS, Hardee GE. Oral delivery of antisense oligonucleotides in man. *J Pharm Sci* 2008; 97: 225–236
2. Stephenson ML, Zamecnik PC. Inhibition of Rous sarcoma viral RNA translation by a specific oligodeoxyribonucleotide. *Proc Natl Acad Sci USA* 1978; 75: 285–288
3. Loke SL, Stein CA, Zhang XH *et al*. Characterization of oligonucleotide transport into living cells. *Proc Natl Acad Sci USA* 1989; 86: 3474–3478
4. Zhang C, Meng X, Zhu Z *et al*. Connective tissue growth factor regulates the key events in tubular epithelial to myofibroblast transition *in vitro*. *Cell Biol Int* 2004; 28: 863–873
5. Sharpe CC, Dockrell ME, Noor MI *et al*. Role of Ras isoforms in the stimulated proliferation of human renal fibroblasts in primary culture. *J Am Soc Nephrol* 2000; 11: 1600–1606
6. Crooke ST, Bennett CF. Progress in antisense oligonucleotide therapeutics. *Annu Rev Pharmacol Toxicol* 1996; 36: 107–129
7. Tereshko V, Portmann S, Tay EC *et al*. Correlating structure and stability of DNA duplexes with incorporated 2′-O-modified RNA analogues. *Biochemistry* 1998; 37: 10626–10634
8. Sands H, Gorey-Feret LJ, Cocuzza AJ *et al*. Biodistribution and metabolism of internally 3H-labeled oligonucleotides: I. Comparison of a phosphodiester and a phosphorothioate. *Mol Pharmacol* 1994; 45: 932–943
9. Rappaport J, Hanss B, Kopp JB *et al*. Transport of phosphorothioate oligonucleotides in kidney: implications for molecular therapy. *Kidney Int* 1995; 47: 1462–1469
10. Cheng QL, Chen XM, Li F *et al*. Effects of ICAM-1 antisense oligonucleotide on the tubulointerstitium in mice with unilateral ureteral obstruction. *Kidney Int* 2000; 57: 183–190
11. Chen W, Langer RM, Janczewska S *et al*. Methoxyethyl-modified intercellular adhesion molecule-1 antisense phosphorothiateoligonucleotides inhibit allograft rejection, ischemic-reperfusion injury, and cyclosporine-induced nephrotoxicity. *Transplantation* 2005; 79: 401–408
12. Guha M, Xu ZG, Tung D *et al*. Specific down-regulation of connective tissue growth factor attenuates progression of nephropathy in mouse models of type 1 and type 2 diabetes. *Faseb J* 2007; 21: 3355–3368
13. Yokoi H, Mukoyama M, Nagae T *et al*. Reduction in connective tissue growth factor by antisense treatment ameliorates renal tubulointerstitial fibrosis. *J Am Soc Nephrol* 2004; 15: 1430–1440
14. Yamada M, Katsuma S, Adachi T *et al*. Inhibition of protein kinase CK2 prevents the progression of glomerulonephritis. *Proc Natl Acad Sci USA* 2005; 102: 7736–7741
15. Isaka Y, Akagi Y, Kaneda Y *et al*. The HVJ liposome method. *Exp Nephrol* 1998; 6: 144–147
16. Isaka Y, Tsujie M, Ando Y *et al*. Transforming growth factor-beta 1 antisense oligodeoxynucleotides block interstitial fibrosis in unilateral ureteral obstruction. *Kidney Int* 2000; 58: 1885–1892

17. Farman CA, Kornbrust DJ. Oligodeoxynucleotide studies in primates: antisense and immune stimulatory indications. *Toxicol Pathol* 2003; 31(Suppl): 119–122
18. Levin AA. A review of the issues in the pharmacokinetics and toxicology of phosphorothioate antisense oligonucleotides. *Biochim Biophys Acta* 1999; 1489: 69–84
19. Jason TL, Koropatnick J, Berg RW. Toxicology of antisense therapeutics. *Toxicol Appl Pharmacol* 2004; 201: 66–83
20. Napoli C, Lemieux C, Jorgensen R. Introduction of a Chimeric Chalcone Synthase gene into Petunia results in reversible co-suppression of homologous genes in trans. *Plant Cell* 1990; 2: 279–289
21. Fire A, Xu S, Montgomery MK *et al*. Potent and specific genetic interference by double-stranded RNA in Caenorhabditis elegans. *Nature* 1998; 391: 806–811
22. Zamore PD. Ancient pathways programmed by small RNAs. *Science* 2002; 296: 1265–1269
23. Elbashir SM, Harborth J, Lendeckel W *et al*. Duplexes of 21-nucleotide RNAs mediate RNA interference in cultured mammalian cells. *Nature* 2001; 411: 494–498
24. Aagaard L, Rossi JJ. RNAi therapeutics: principles, prospects and challenges. *Adv Drug Deliv Rev* 2007; 59: 75–86
25. Birmingham A, Anderson EM, Reynolds A *et al*. 3′ UTR seed matches, but not overall identity, are associated with RNAi off-targets. *Nat Methods* 2006; 3: 199–204
26. Layzer JM, McCaffrey AP, Tanner AK *et al*. *In vivo* activity of nuclease-resistant siRNAs. *RNA* 2004; 10: 766–771
27. Ma Z, Li J, He F *et al*. Cationic lipids enhance siRNA-mediated interferon response in mice. *Biochem Biophys Res Commun* 2005; 330: 755–759
28. Hornung V, Guenthner-Biller M, Bourquin C *et al*. Sequence-specific potent induction of IFN-alpha by short interfering RNA in plasmacytoid dendritic cells through TLR7. *Nat Med* 2005; 11: 263–270
29. Bitko V, Musiyenko A, Shulyayeva O *et al*. Inhibition of respiratory viruses by nasally administered siRNA. *Nat Med* 2005; 11: 50–55
30. Reich SJ, Fosnot J, Kuroki A *et al*. Small interfering RNA (siRNA) targeting VEGF effectively inhibits ocular neovascularization in a mouse model. *Mol Vis* 2003; 9: 210–216
31. Hamar P, Song E, Kokeny G *et al*. Small interfering RNA targeting Fas protects mice against renal ischemia-reperfusion injury. *Proc Natl Acad Sci USA* 2004; 101: 14883–14888
32. Hwang M, Kim HJ, Noh HJ *et al*. TGF-beta1 siRNA suppresses the tubulointerstitial fibrosis in the kidney of ureteral obstruction. *Exp Mol Pathol* 2006; 81: 48–54
33. Takabatake Y, Isaka Y, Mizui M *et al*. Exploring RNA interference as a therapeutic strategy for renal disease. *Gene Ther* 2005; 12: 965–973
34. Judge AD, Bola G, Lee AC *et al*. Design of noninflammatory synthetic siRNA mediating potent gene silencing *in vivo*. *Mol Ther* 2006; 13: 494–505

Received for publication: 12.12.07
Accepted in revised form: 30.1.08